National Research Council Canada

Conseil national de recherches Canada

NRC · CNRC

Canadian Journal of Fisheries and Aquatic Sciences

Journal canadien des sciences halieutiques et aquatiques

http://www.nrc.ca/cisti/journals

ISSN 0706-652X / CJFSDX 56(12) 2229–2507 (1999)

The *Canadian Journal of Fisheries and Aquatic Sciences*, previously published as *Contributions to Canadian Biology* 1901–1925, *Contributions to Canadian Biology and Fisheries* 1926–1934, *Journal of the Biological Board of Canada* 1934–1937, and *Journal of the Fisheries Research Board of Canada* 1938–1979, is issued monthly to form annual volumes of 12 numbers plus supplements.

Editorial policy: The Journal publishes original research articles, perspectives (syntheses, critiques, re-evaluations), discussions (comment and reply), and rapid communications. Manuscripts may concern cells, organisms, populations, communities, ecosystems, or processes that affect aquatic systems. They may cover a range of disciplines including biology and ecology of marine and freshwater organisms, limnology, oceanography, physiology, toxicology, genetics, economics, disease, and management. Preference will be given to manuscripts that emphasize understanding of observed phenomena and interpretation of experimental results. The Journal encourages papers that lead from clearly stated purpose or rationale and from testable hypotheses, concepts, or questions to identifiable conclusions or syntheses. Such papers may amplify, modify, question, or redirect accumulated knowledge embodied in contemporary perceptions of a particular state of aquatic sciences. The Journal discourages papers that are essentially descriptive, except in emerging disciplines; have only site-specific or local applications (a certain year, place, taxon, chemical compound, etc.); only confirm previously established principles; or apply standard techniques without breaking new methodological ground.

Manuscripts for publication should be submitted to the Editors, Canadian Journal of Fisheries and Aquatic Sciences, Department of Zoology, University of Guelph, Guelph, ON N1G 2W1, Canada (519-824-4120 ext. 2646; fax: 519-767-9798; e-mail: cjfas@uoguelph.ca).

Submissions in either English or French are acceptable. The information must be original, that is, not copyrighted, published, or submitted elsewhere except in abstract form or unless by written consent of the Editor. NRC accepts no responsibility for statements or opinions expressed by a contributor. Acceptance of an advertisement, announcement, or other material does not imply endorsement by either the *Journal*'s Editors or NRC. The use of proprietary names does not imply endorsement of the product or company.

Correspondence concerning accepted manuscripts and corrected proofs should be sent to NRC Research Press, National Research Council of Canada, Ottawa, ON K1A 0R6, Canada.

Instructions to Authors are published once a year in the first issue of each volume. Copies are available from NRC Research Press or from our Web site. The **Publication Policy** of NRC Research Press is also available at our Web site:
http://www.nrc.ca/cisti/journals/rj.html

Microfilm: Issues from 1934 through the current volume can be purchased on 16- or 35-mm microfilm. Photocopies of individual articles or issues can be purchased from University Microfilms International, 330 North Zeeb Road, Ann Arbor, MI 48106, U.S.A.

U.S. periodical postage paid at Champlain, N.Y., and at additional mailing offices. Attention U.S. POSTMASTER: Send address changes to **Canadian Journal of Fisheries and Aquatic Sciences**, c/o USACAN Media Distribution Center, P.O. Box 2888, Plattsburg, NY 12901, U.S.A.

Publié sans interruption depuis 1901, le *Journal canadien des sciences halieutiques et aquatiques* a paru sous plusieurs titres : *Contributions to Canadian Biology* 1901–1925, *Contributions to Canadian Biology and Fisheries* 1926–1934, *Journal of the Biological Board of Canada* 1934–1937, et *Journal of the Fisheries Research Board of Canada* 1938–1979. Le *Journal* paraît tous les mois, formant ainsi un volume de 12 numéros, et offre en plus jusqu'à deux suppléments par année.

Politique éditoriale : On publie, dans le Journal, des articles rendant compte de recherche originale, des perspectives (synthèses, critiques et réévaluations), des discussions (commentaires et réponses) et des communications rapides. Les documents peuvent porter sur les cellules, organismes, populations, communautés, écosystèmes ou processus qui affectent les systèmes aquatiques. Ils peuvent relever de divers domaines y compris la biologie et l'écologie des organismes marins et d'eau douce, la limnologie, l'océanographie, la physiologie, la toxicologie, la génétique, l'économie, la pathologie et la gestion. On accorde la préséance aux articles qui contribuent à la compréhension de phénomènes observés et à l'interprétation de résultats expérimentaux. On invite les auteurs à soumettre des articles ayant des objectifs précis ou relevant d'hypothèses, de concepts ou de questions vérifiables et se terminant par de solides conclusions ou d'utiles synthèses. Ces articles enrichissent, changent, mettent en question ou réorientent les connaissances acquises sur divers aspects des sciences aquatiques. On décourage toutefois la soumission d'articles simplement descriptifs (à moins qu'il ne s'agisse de nouvelles disciplines), d'application très limitée (applicables à une seule année, une seule région ou un seul taxon, portant sur un unique composé chimique, etc.); d'articles qui ne font que reprendre les principes énoncés dans des articles précédents; et d'articles rendant compte de l'application de normes sans gain de méthodologie.

Les auteurs voudront adresser leurs **manuscrits** aux directeurs scientifiques, Journal canadien des sciences halieutiques et aquatiques, Département de Zoologie, University of Guelph, Guelph, ON N1G 2W1, Canada (519-824-4120 poste. 2646; télécopieur : 519-767-9798; adresse électronique : cjfas@uoguelph.ca).

Les contributions peuvent être en anglais ou en français. Elles doivent être originales, c.-à.-d. qu'elles ne doivent pas avoir fait l'objet d'un copyright, avoir été publiées ou soumises ailleurs, sauf sous forme abrégée ou avec le consentement du rédacteur. Le CNRC ne se tient en aucune façon responsable des opinions exprimées par un collaborateur ou des déclarations qui pourrait faire ce dernier. La publication d'annonces publicitaires, d'avis et autres n'implique pas l'endossement de leur contenu par les directeurs du *Journal* ou du CNRC. L'utilisation des noms de marques de commerce ne signifie aucunement une sanction du produit en question ou de la compagnie qui le fabrique.

La correspondance ayant trait aux manuscrits acceptés et les **épreuves corrigés** doivent être envoyées aux Presses scientifiques du CNRC, Conseil national de recherches du Canada, Ottawa, ON K1A 0R6, Canada.

Recommandations aux auteurs sont publiés une fois par année dans le premier numéro de chaque volume. Des copies, ainsi que la **Politique de publication**, sont disponibles auprès des Presses scientifiques du CNRC ou au site Web :
http://www.nrc.ca/cisti/journals/rj.html

Microfilms : On peut acheter sur microfilms de 16 ou 35 mm tous les numéros depuis 1934. Des photocopies d'articles ou de numéros individuels sont aussi en vente auprès de University Microfilms International, 330 North Zeeb Road, Ann Arbor, MI 48106, É.-U.

This journal is indexed or abstracted in / Ce journal est signalé ou résumé dans
ABSEARCH, Aquatic Sciences and Fisheries Abstracts, Biological Abstracts, Biological & Agricultural Index, CAB Abstracts, Chemical Abstracts, Current Contents, Elsevier BIOBASE, Environmental Abstracts, Environmental Periodicals Bibliography, GEOBASE, GeoRef, Life Sciences Collection, Meteorological and Geoastrophysical Abstracts, Oceanic Abstracts, PASCAL Database, and Science Citation Index.

Volume 56, Number 12, December 1999

Canadian Journal of Fisheries and Aquatic Sciences

Published by the National Research Council of Canada

Volume 56, numéro 12, décembre 1999

Journal canadien des sciences halieutiques et aquatiques

Publié par le Conseil national de recherches du Canada

Editors / directeurs scientifiques John C. Roff and Moira M. Ferguson

Assistant to the Editors / adjointe aux directeurs scientifiques **Holly Foster**

Associate Editors / directeurs scientifique associés

D. Boisclair, *Université de Montréal*
U. Borgmann, *Environment Canada, Burlington*
S.E. Campana, *DFO/MPO, Dartmouth*
D.G. Dixon, *University of Waterloo*
A.E. Dizon, *National Marine Fisheries Service, La Jolla, Calif.*
J.J. Dodson, *Université Laval*
J.A. Downing, *Iowa State University*
K.T. Frank, *DFO/MPO, Dartmouth*
D.F. Houlihan, *University of Aberdeen, Aberdeen, Scotland*
F.A. Huntingford, *University of Glasgow*
J.A. Hutchings, *Dalhousie University*
G.S. Jamieson, *DFO/MPO, Nanaimo*
B. Jonsson, *Norwegian Institute for Nature Research, Oslo, Norway*
L. Legendre, *Université Laval*
D.M. Mason, *Purdue University, West Lafayette, Ind.*
A. Mazumder, *University of Victoria*
D.L. Parrish, *Vermont Cooperative Fish and Wildlife Research Unit (USGS/BRD), University of Vermont*
P. Pepin, *DFO/MPO, St. John's*
R.M. Peterman, *Simon Fraser University*
E.E. Prepas, *University of Alberta*
T.M. Powell, *University of California, Berkeley, Calif.*
T.J. Quinn II, *University of Alaska–Fairbanks, Juneau, Alaska*
T.P. Quinn, *University of Washington*
R.D. Robarts, *Environment Canada, Saskatoon*
B. Sainte-Marie, *DFO/MPO, Mont-Joli*
P.F. Sale, *University of Windsor*
D.W. Schindler, *University of Alberta*
S.J. Smith, *DFO/MPO, Dartmouth*
W.G. Sprules, *University of Toronto*
R.J. Thompson, *Memorial University of Newfoundland*
C.J. Walters, *University of British Columbia*
R.D. Ward, *CSIRO Division of Fisheries, Australia*
C.M. Wood, *McMaster University*
B. de Young, *Memorial University of Newfoundland*

NRC Research Press / Presses scientifiques du CNRC

Editor-in-chief / directeur général **Bruce P. Dancik**

Assistant Editor-in-chief / directeur général adjoint **Iain F.P. Taylor**

Journals Program / Programme des revues

(Fax / télécopieur : 613-952-7656; e-mail / adresse électronique : research.journals@nrc.ca;
URL: http://www.nrc.ca/cisti/journals/)

Director / directrice **Aldyth Holmes**

Business Manager / gestionnaire des affaires **Paul McClymont**

Managing Editor / rédactrice administrative **Cecily M. Pearson (613-993-9099)**

Publication Officer / agente de publication **Jennifer McColl**

Advertising / annonces publicitaires **Judy Heyman (613-993-0151)**

Reprints / tirés à part **Roxanne Landriault (613-990-2254)**

Subscriptions / abonnements **Helen Goulet (613-993-9084)**

© National Research Council of Canada 1999. World rights reserved.
No part of this publication may be reproduced, stored, or transmitted in any form or by any means, without the written permission of the publisher, except as stated below.

The National Research Council of Canada grants **permission*** to individuals to make single copies of articles for personal use. Any person may reproduce short excerpts from articles in the journal for any purpose that respects the moral rights of authors, provided that the source is fully acknowledged. As a courtesy, the consent of authors of such material should be obtained directly from the author.

Authorization to reproduce items for other than personal use, as stated above, is granted by the National Research Council of Canada provided that the copyright fee of $7.00 per copy is paid directly to CANCOPY, One Yonge Street, Suite 1900, Toronto, ON M5E 1E5, Canada.

*The above permission does not extend to other kinds of copying, such as copying for general distribution, for advertising, or promotional purposes, for creating new collective works, or for resale. For such copying, arrangements must be made with the publisher, National Research Council of Canada, Ottawa, ON K1A 0R6, Canada.

© Conseil national de recherches du Canada 1999. Tous droits réservés.
Il est interdit de reproduire, de sauvegarder ou de transmettre quelque partie de la présente publication dans quelque format ou de quelque façon sans le consentement écrit de l'éditeur, à l'exception des conditions suivantes.

Le Conseil national de recherches du Canada accorde aux particuliers le droit de faire des copies individuelles pour leur usage personnel. Toute personne peut reproduire de courts extraits des articles de la Revue pour autant que les droits moraux de l'auteur soient respectés et que la mention de provenance soit clairement indiquée. Il est de convenance de demander le consentement de l'auteur avant de faire mention de son travail.

On obtiendra l'autorisation de reproduire des articles à d'autres fins que l'usage personnel (tel qu'on l'a décrit ci-dessus) auprès du Conseil national de recherches du Canada pour autant que des redevances de droits d'auteurs de 7,00 $/copie soient versées au CANCOPY, 1, rue Yonge, bureau 1900, Toronto, ON M5E 1E5, Canada.

*La permission ci-dessus ne s'applique pas à la reproduction à grande échelle, telle que la reproduction aux fins de distribution générale, publicitaire ou promotionnelle, de compilation de nouveaux ouvrages collectifs ou de revente. Dans de tels cas, il faudra ratifier une entente particulière avec l'éditeur, le Conseil national de recherches du Canada, Ottawa, ON K1A 0R6, Canada.

Subscription information

The *Canadian Journal of Fisheries and Aquatic Sciences* (ISSN 0706-652X) is published monthly by the National Research Council of Canada. 1999 annual subscription rates (second class postage) for Canada are $578CAN institutional and $182CAN personal, for US & foreign $578US institutional and $182US personal. For air mail add $150US to foreign rate. Canadian customers please include 7% GST (business no. 12149 1807 RT 0275). Subscriptions are entered for the calendar year. Remittances should be made payable to the Receiver General for Canada credit NRC. Price for regular single issues: institutional, $75.00; personal, $25.00. Supplements will be priced separately. Special rates apply to members of Canadian scientific and engineering societies if they subscribe through their respective societies.

There are no refunds on cancelled subscriptions once delivery has begun. Claims for missing issues should be made within four months (N. America) or six months (outside N. America) following the date of publication. The publisher expects to supply missing issues only when losses have occurred in transit and when the reserve stock will permit. For change of address and subscription enquiries: Subscription Office, NRC Research Press, National Research Council of Canada, Ottawa, ON K1A 0R6, Canada; tel: 613-993-9084; fax: 613-952-7656; e-mail: research.journals@nrc.ca.

Microform backfiles are available from UMI, P.O. Box 1346, Ann Arbor, MI 48106-1346, U.S.A., and Micromedia Ltd., 20 Victoria St., Toronto, ON M5C 2N8, Canada.

The 1999 issues of the *Canadian Journal of Fisheries and Aquatic Sciences* are available on the Web. Pricing information can be found at

http://www.nrc.ca/cisti/journals/

Renseignements sur l'abonnement

Journal canadien des sciences halieutiques et aquatiques (ISSN 0706-652X) est une publication mensuelle du Conseil national de recherches du Canada. Le prix de l'abonnement annuel au Canada (courrier de deuxième classe) est de 578 $CAN pour les organismes et de 182 $CAN pour les particuliers. À l'étranger (y compris les É.-U.), le prix de l'abonnement est de 578 $US pour les organismes et de 182 $US pour les particuliers. L'expédition par avion exige des frais de 150 $US en sus du prix d'abonnement à l'étranger. Les clients du Canada doivent ajouter la TPS de 7% (numéro d'entreprise 12149 1807 RT 0275). Les abonnements sont pour l'année civile. Tout paiement doit être adressé au Receveur général du Canada, crédit du CNRC. Le prix par numéro est de 75 $ pour les organismes et de 25 $ pour les particuliers. Le prix des hors-série varie. Les membres des sociétés canadiennes de sciences et de génie bénéficient de taux préférentiels en s'abonnant via leurs sociétés respectives.

Aucun remboursement ne sera accordé ni aucune annulation acceptée une fois que les livraisons auront commencé. Les réclamations de numéros manquants devront être soumises dans les quatre mois (Amérique du Nord) ou dans les six mois (à l'extérieur de l'Amérique du Nord) suivant la date de publication. L'éditeur ne fournira de numéros manquants que si le document a été perdu pendant l'expédition et que si le stock le permet. Adressez tout changement d'adresse ou toute question quant à l'abonnement au : Bureau des abonnements, Presses scientifiques du CNRC, Conseil national de recherches Canada, Ottawa, ON K1A 0R6, Canada; téléphone : 613-993-9084; télécopieur : 613-952-7656; adresse électronique : research.journals@nrc.ca.

On peut obtenir les fichiers rétrospectifs sur **microforme** auprès de UMI, P.O. Box 1346, Ann Arbor, MI 48106-1346, É.-U., et auprès de Micromedia Ltée, 20 rue Victoria, Toronto, ON M5C 2N8, Canada.

Les numéros de 1999 de *Journal canadien des sciences halieutiques et aquatiques* sont accessibles sur le Web. On trouvera des renseignements sur les tarifs à

http://www.nrc.ca/cisti/journals/rjfr.html

RAPID COMMUNICATIONS / COMMUNICATIONS RAPIDES

Rapid and coupled phenotypic and genetic divergence in Icelandic Arctic char (*Salvelinus alpinus*)

Davíð Gíslason, Moira M. Ferguson, Skúli Skúlason, and Sigurður S. Snorrason

Abstract: Resource polymorphism has been proposed as an important phase of diversification and speciation in vertebrates. Studies of fish in young lakes of the Northern Hemisphere indicate variably advanced cases of adaptive trophic diversification. We have previously proposed a scheme describing this variation in terms of a gradient of resource-based polymorphic traits, emphasizing flexible behaviour in early phases and morphological divergence in more advanced phases. Here, we present data on Arctic char (*Salvelinus alpinus*) in Icelandic lakes exhibiting a variable degree of phenotypic and genotypic segregation. We show that (*i*) the morphs are at different levels of phenotypic segregation and reproductive isolation and in one case completely reproductively isolated, (*ii*) morphs within lakes appear to be of intralacustrine origin, and (*iii*) the morphological and genetic divergence of morphs is correlated, suggesting a role for trophic adaptation as a driving force in morph segregation.

Résumé : Le polymorphisme lié aux ressources serait une phase importante de la diversification et de la spéciation chez les vertébrés. Des études sur des poissons vivant dans des lacs nouvellement formés de l'hémisphère Nord font ressortir des cas diversement poussés de diversification trophique adaptative. Nous avons déjà proposé un modèle décrivant cette variation en fonction d'un gradient de traits polymorphes liés aux ressources, qui montre un comportement flexible aux premiers stades de développement puis une divergence morphologique aux stades plus avancés. Nous soumettons ici des données sur l'omble chevalier (*Salvelinus alpinus*) de lacs d'Islande présentant un degré variable de ségrégation phénotypique et génotypique. Nous montrons : (*i*) que les formes se trouvent à différents niveaux de ségrégation phénotypique et d'isolement reproductif et que, dans un cas, elles sont complètement isolées sur le plan reproductif; (*ii*) que les formes présentes dans les lacs semblent être d'origine intralacustre; et, (*iii*) qu'il existe une corrélation entre la divergence morphologique et génétique des formes, ce qui indiquerait que l'adaptation trophique agirait comme élément moteur de la ségrégation des formes.

[Traduit par la Rédaction]

Many northern freshwater fish are undergoing rapid diversifying evolution, forming discrete resource-based morphs, populations, and possibly even new species (Schluter 1998; Skúlason et al. 1999). These fish have colonized postglacial freshwater systems where fish species diversity is generally low and novel resources are available for invading populations. Discrete sympatric morphs often occur in lakes and are segregated in habitat use and diet (Snorrason et al. 1994; Lu and Bernatchez 1999). The common pattern of divergence is the evolution of benthic and limnetic (piscivorous, planktivorous) morphs, suggesting that habitat diversity and discrete resources are important factors in the evolution of alternative forms (Skúlason et al. 1999).

The origin of sympatric morphs is of major importance for our understanding of adaptive radiation and speciation in freshwater fishes and provides opportunities to study the role of ecological factors in divergent evolution (Schluter 1998; Lu and Bernatchez 1999; Skúlason et al. 1999). This diverging evolution can take place either within lakes (intralacustrine) or in different lakes (allopatric) followed by invasion and secondary contact of the morphs (Bernatchez and Dodson 1990; Taylor and Bentzen 1993).

Understanding the role of resource polymorphism in speciation requires knowledge of its genetic basis. Various studies show that the relative contribution of genetic and environmental factors to the phenotypic differences in fishes varies within and among species. In some cases, morphological divergence is environmentally induced, and in other cases, phenotypic differences reflect underlying genetic differences (Skúlason et al. 1999).

The relationship between resource-based phenotypic segregation and the degree of genetic isolation is poorly under-

Received August 6, 1999. Accepted October 13, 1999.
J15279

D. Gíslason and M.M. Ferguson.[1] Department of Zoology, University of Guelph, Guelph, ON N1G 2W1, Canada.
S. Skúlason. Hólar College, Hólar, Hjaltadal, 551 Sauðárkrókur, Iceland.
S.S. Snorrason. Department of Biology, University of Iceland, Grensásvegur 12, 108 Reykjavík, Iceland.

[1]Author to whom all correspondence should be addressed.
e-mail: mmfergus@uoguelph.ca

© 1999 NRC Canada

Table 1. Mean fork length, sample size (*N*), and results from an analysis of five microsatellite loci in morphs of Arctic char from five Icelandic lakes.

Population	Mean fork length (cm)	*N*	HWP multilocus	H_o	F_{ST}	R_{ST}	*Ssa85*			*Str60*		
							A	HWP	*G*	*A*	HWP	*G*
Vatnshlíðarvatn			+	0.423	0.058*	0.038*	10	+	0	4	–	0
Silver	21.1	52	+	0.392			7	+		3	–	
Brown	19.9	57	+	0.452			10	+		4	–	
Stóra Viðarvatn			+	0.562	0.008	–0.011	10	–	0	6	–	0
Limnetic	21.8	71	+	0.599			10	–		6	–	
Benthivore	15.1	15	+	0.439			9	–		4	+	
Svínavatn			+	0.537			16	+		18	+	
Planktivore (pl)	22.1	54	+	0.513			14	+		16	+	
Piscivore (pi)	27.8	33	+	0.520			12	–		15	–	
Benthivore (be)	24.7	22	–	0.621			7	–		9	–	
pi:pl					0.033*	0.097*			0			0
pi:be					0.000	0.000			0			0
pl:be					0.059*	0.121*			0			0
Galtaból			+	0.348	0.321*	0.728*	6	–	0	10	+	1
Piscivore	35.2	67	–	0.417			3	–		6	–	
Benthivore	16.9	24	+	0.323			6	–		9	+	
Hólmavatn		72	–	0.299			2	–		2	–	
H_o							0.502			0.541		
No. of alleles							23			25		
Allele size range							152–210			156–224		

Note: H_o, observed heterozygosity; F_{ST}, allelic variance (*significant); R_{ST}, molecular variance (*significant); *A*, number of alleles per locus; HWP, Hardy–Weinberg proportions (+, significant deviations from HWP; ×, one allele fixed); *G*, differences in genotypic distributions between morphs (1, significant).

stood. If we assume that morphological segregation is driven by trophic adaptation, we would expect to see a positive relationship between phenotypic and genetic differentiation of morphs. The magnitude of divergence would depend on how extensively morphs in individual systems have adapted to alternative niches. Icelandic lakes offer excellent conditions to test these ideas. All Icelandic lakes were formed after the last glaciation 10 000 years ago. Even though the fish assemblages are depauperate (most often only two species), the lakes offer a variety of discrete niches for fish (Skúlason et al. 1999).

We present data on morphological and genetic differentiation in Arctic char (*Salvelinus alpinus*) from five Icelandic lakes. The lakes (Vatnshlíðarvatn, 65°30′ N, 19°40′ W; Stóra Viðarvatn, 66°14′ N, 15°50′ W; Lake Galtaból, 65°16′ N, 20°15′ W; Svínavatn, 65°32′ N, 20°00′ W; Hólmavatn, 65°45′ N, 21°40′ W (only genetic data)) are in separate watersheds located in northern, northwestern, and northeastern Iceland and differ extensively in physical attributes. Hólmavatn (vatn means "lake" in Icelandic) has one morph of Arctic char. Three of the lakes contain two putative morphs: in Vatnshlíðarvatn, silvery coloured (large benthic) and brown (small benthic) morphs; in Stóra Viðarvatn, limnetic and benthivorous morphs; and in Lake Galtaból, piscivorous and benthivorous morphs. Svínavatn has three putative morphs: piscivore, planktivore, and benthivore.

Arctic char were sampled in early August 1990 and 1995. Gillnets (mesh sizes 11–60 mm) were set overnight. Fish for analysis were sampled across the size range of the catch. Each fish was classified to morph based on shape and colouration in the field. Fish were positioned on right side with the mouth closed and the dorsal and anal fins were pinned to see their origin. A blue plastic plate was placed under the maxillary bone to observe its posterior termination. Each fish was photographed with a Minolta X-700 camera and a Minolta MD Macro 50-mm (1:3.5) lens outdoors using 100 ASA slide film. Otoliths were removed from a subsample of fish for aging. All samples were composed of fish of different ages to control for ontogenetic changes in morphology. Tissue samples were removed from the same fish for genetic analysis.

The photographic images were scanned and the digital images were measured with WinDIG version 2.5 software. Thirteen landmarks on each fish were used to calculate 16 morphometric lengths (Figs. 1*a* and 1*b*). The data were analyzed using both univariate and multivariate statistical analyses (Reist 1986) using SYSTAT or SAS 6.12. First, all characters (except fork length) were standardized by regression analysis to adjust for the size differences among putative morphs. Adjustment of size was effective in all cases except for Galtaból where we detected significant negative correlations between fork length and principal components analysis (PCA) axis 1 (PC1) and between fork length and standardized residuals for characters CW, HH, HL, LJL, SL, PCFL, and UJL (see Fig. 1 for descriptions). Size free shape variates were derived by using residuals from the common-within-groups regression line of the measured character on fork length as obtained from ANCOVA. The sexes were combined in all analyses, since morphological differences between the sexes in Icelandic Arctic char are small relative to differences between morphs (Snorrason et al. 1994). PCA was used with all 15 characters to examine variation among morphs in morphological space. The PC axes were derived from a variance–covariance matrix. ANOVA or *t* tests were

© 1999 NRC Canada

Sfo18			*Ssa20.19*			*Omy301*		
A	HWP	*G*	*A*	HWP	*G*	*A*	HWP	*G*
2	+	0	8	–	0	13	+	0
2	–		8	–		9	–	
2	+		6	–		10	–	
2	–	0	8	+	0	22	+	0
2	–		8	+		20	+	
2	–		5	+		12	–	
2	+		11	+		17	+	
2	+		10	+		15	–	
2	+		8	+		9	–	
2	–		5	–		9	–	
		0			0			1
		0			0			0
		0			0			1
1	×	0	7	+	0	4	+	1
1	×		3	–		2	–	
1	×		7	+		2	–	
1	×		5	–		8	–	
0.161			0.429			0.573		
2			15			30		
163–165			96–124			87–147		

used to determine if the morphs differed in their mean scores on PC1 and PC2. Canonical discriminant analysis (CDA) was used to compare the relative amount of differentiation among sympatric morphs, and Mahalanobis distances (D^2) were calculated to obtain quantitative estimates of morphological differentiation.

DNA was isolated from muscle or liver and variation at five microsatellite loci (*Ssa85DU*, *Str60INRA*, *Sfo18UL*, *Ssa20.19UCG*, *Omy301UoG*) was assayed (details in Gíslason 1998). Estimates of genetic polymorphism at each locus and within populations were calculated with TFPGA and GENETIX, respectively. We used three approaches to test if lakes contained genetically differentiated morphs. First, we tested for deviations from Hardy–Weinberg proportions (HWP) in all fish within a lake (morphs combined) and within morphs. Multilocus tests were based on the Markov chain methods for heterozygote deficiency in GENEPOP 3.1, and single locus tests were based on the *U* test from the same software. Second, we tested for significant differences in genotypic distributions at each locus between sympatric morphs with Fisher's exact test through 10 000 iterations by Markov chain methods in GENEPOP 3.1. All significance levels for simultaneous statistical tests were adjusted using sequential Bonferroni corrections. Third, we used ARLEQUIN to test for differentiation among morphs within lakes across all loci by using allele frequencies only (F_{ST}) and by analysis of molecular variance (R_{ST}), which accounts for the variance in allele size.

We differentiated between the allopatric and sympatric models of morph origin by first determining the affinity of sympatric morphs through cluster analysis. Genetic distances between all pairs of morphs were estimated by calculating Nei's D_A (Takezaki and Nei 1996), and these were used to construct a neighbour-joining (NJ) phenogram with the software NJBAFD. The repeatability of different clusters in the NJ phenogram was assessed through a bootstrapping analysis with the same software. Second, we determined the number of alleles confined to the morphs within single lakes (private alleles). We included data for an additional Icelandic lake, Thingvallavatn (data in Gislason 1998), to provide a more conservative test.

Both the PCA and CDA showed that the putative sympatric morphs are at variable degrees of morphological differentiation (Figs. 1*c*–1*f*). The degree of morphological differentiation ranged from small in Vatnshlíðarvatn to large in Lake Galtaból. PC1 and PC2 together accounted for between 44 and 79% of the total variation in the four lakes with more than one putative morph. Highly significant differences ($p < 0.001$) in mean scores on PC1 were detected among morphs in Vatnshlíðarvatn, Stóra Viðarvatn, and Lake Galtaból. The morphs did not differ in mean scores on PC2. The situation was more complex for the morphs in Svínavatn. The planktivorous morph from Svínavatn differed significantly ($p < 0.001$) from the other morphs in mean scores on PC1 and from the benthivorous morph in mean scores on PC2. The benthivorous and piscivorous morphs from Svínavatn did not differ. The CDA indicated that morph centroids (mean canonical scores) differed significantly in all cases as follows: Vatnshlíðarvatn, Mahalanobis distance $D^2 = 2.525$, Wilks lambda $F_{15,81} = 3.483$, $p < 0.001$; Stóra Viðarvatn, $D^2 = 10.8$, $F_{15,67} = 7.328$, $p < 0.001$; Lake Galtaból, $D^2 = 34.047$, $F_{15,62} = 29.051$, $p < 0.001$; Svínavatn: piscivorous versus benthivorous morph, $D^2 = 5.366$,

© 1999 NRC Canada

Fig. 1. (*a* and *b*) Illustration of the characters measured on the left side of Arctic char from Iceland: 1, fork length; 2, adipose fin to anal fin length; 3, adipose fin to dorsal peduncle length; 4, anal fin to dorsal peduncle length; 5, anal fin to ventral peduncle length; 6, adipose fin to ventral peduncle length; 7, caudal width; 8, pectoral fin length; 9, head length; 10, lower jaw length; 11, lower jaw to mideye line length; 12, snout length; 13, head height; 14, pectoral fin position 1; 15, pectoral fin position 2; 16, upper jaw length. (*c*–*f*) Plots of the distribution of scores for the first two principal components (PC1 and PC2) from PCA based on the variance–covariance matrix in morphs of Arctic char. The analysis is based on adjusted residuals from regression of 15 untransformed variables on fork length. Larger symbols represent the mean scores. (*c*) Vatnshlíðarvatn: ○, silver; ▽, brown; (*d*) Stóra Viðarvatn: ○, limnetic; ▽, benthic; (*e*) Lake Galtaból: ○, piscivore; ▽, benthivore; (*f*) Svínavatn: □, piscivore; ○, planktivore; ▽, benthivore.

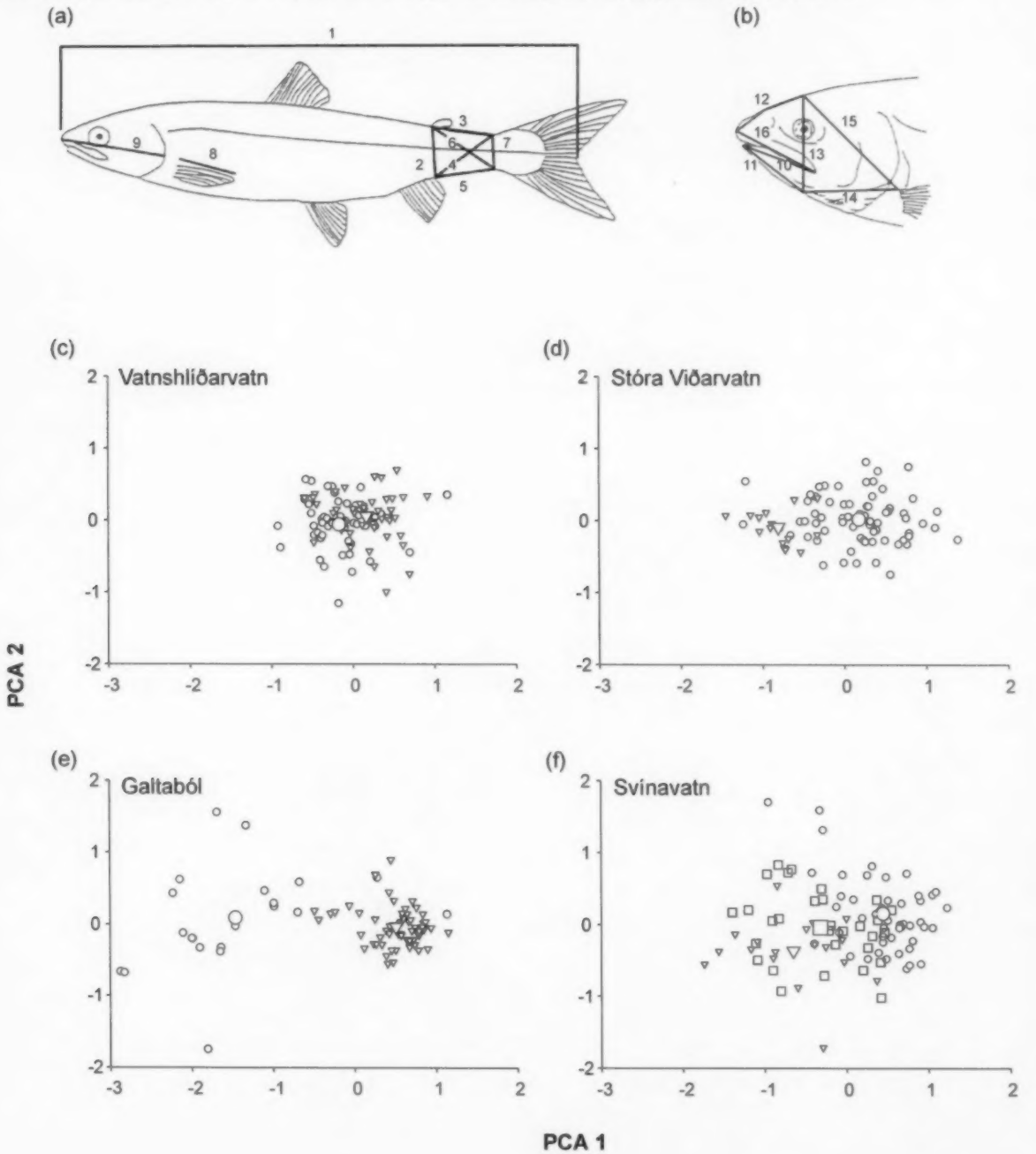

© 1999 NRC Canada

Fig. 2. Unrooted NJ phenogram showing the relationship among morphs of Arctic char from five Icelandic lakes. The phenogram is constructed using Nei's genetic distances (D_A). Numbers along branches indicate bootstrap values in percentages. Numbers in boxes at each cluster are the numbers of private alleles shared by all morphs within the respective lakes.

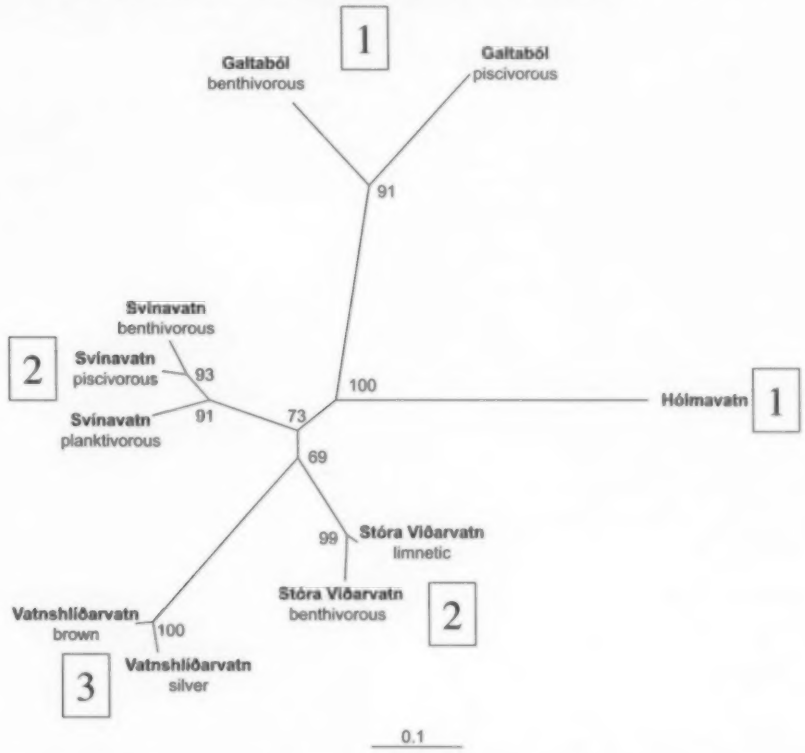

$F_{15.79} = 3.418$, $p < 0.001$; planktivorous versus piscivorous morph, $D^2 = 9.861$, $F_{15.79} = 10.309$, $p < 0.001$; planktivorous versus benthivorous morph, $D^2 = 18.438$, $F_{15.79} = 13.669$, $p < 0.001$.

Genetic analysis of the five microsatellite loci suggests a variable degree of population substructure within lakes (Table 1). This was supported by many significant deviations from HWP (heterozygote deficit) over all loci (all four multilocus tests are significant) and at individual loci (14 of 20 tests) in lakes with multiple morphs. Many significant deviations in HWP were detected within morphs both with single-locus (16 of 45) and multilocus tests (seven of nine). Interestingly, no deviations from HWP were detected in Hólmavatn, which contains a single morph.

The Arctic char morphs differed in the number of observed microsatellite alleles, genotypic frequencies, and degree of genetic differentiation (Table 1) (details in Gíslason 1998). We observed significant differences in genotypic distributions between the morphs in Lake Galtaból (two of five loci) where the morphs did not share alleles at *Omy301UoG*. In Svínavatn, the planktivorous and benthivorous morphs and the piscivorous and planktivorous morphs differed at one locus. In contrast, the morphs in Vatnshlíðarvatn and Stóra Viðarvatn and the piscivorous and benthivorous morphs in Svínavatn did not show significant differences in genotype frequencies at any locus. From 3 to 32% of allelic variance (F_{ST}) and from 3 to 72% of molecular variance (R_{ST}) within lakes was attributable to differences between morphs. Significant genetic differentiation was observed between the morphs in Lake Galtaból and Vatnshlíðarvatn and between the piscivorous and planktivorous morphs and planktivorous and benthivorous morphs in Svínavatn but not those in Stóra Viðarvatn.

The morphological and genetic data suggest that a positive association between the degree of morphological and genetic differentiation exists between pairs of sympatric morphs. The morphs in Vatnshlíðarvatn and Stóra Viðarvatn show low amounts of phenotypic and genetic divergence, while marked divergence was detected between the morphs in Lake Galtaból.

The most parsimonious explanation for the pattern of genetic differentiation in the lakes suggests that the Arctic char morphs have been formed by intralacustrine (sympatric) divergence. The morphs cluster together by lake and not with similar morphs from other lakes (Fig. 2). In all cases, bootstrap values associated with these lake clusters are very high (>90%). The clustering of morphs with lakes is compatible with a multiple invasion model if the morphs previously formed in allopatry had crossbred after secondary contact. The existence of private alleles shared by morphs within lakes (Fig. 2) and the fixation of a single allele at *Sfo18UL* in both morphs from Lake Galtaból are not consistent with this proposition (Volpe and Ferguson 1996). Furthermore, mitochondrial DNA analysis of Icelandic Arctic char (albeit

© 1999 NRC Canada

not these populations) does not support secondary contact between allopatrically derived morphs (Danzmann et al. 1991; Volpe and Ferguson 1996). The morphs are not phylogenetically distinct, which would be suggestive of long-term isolation in distinct refugia prior to secondary contact. We cannot rule out separate allopatric invasions of the different morphs until we establish that Arctic char in this study do not share private alleles with populations in adjacent watersheds.

Intralacustrine genetic and morphological divergence must have progressed rapidly among the populations that colonized these lakes. The maximum age of the lakes is about 10 000 years, so we are observing the effect of adaptive evolution over a maximum of 3000 generations in a natural system.

In conclusion, our data suggest that rapid diversification is occurring among Arctic char populations. Resource-based phenotypic segregation, which is positively correlated with the degree of reproductive isolation, ranges from very low to complete. This finding suggests the importance of ecological factors for diversifying evolution and speciation. At early stages, phenotypic divergence may be promoted by phenotypic plasticity and (or) genetic polymorphism but later substantiated by greater specialization of morphs and reduced gene flow among them (Skúlason et al. 1999). This suggests that resource polymorphism is an important step in sympatric divergence in lake fishes.

Acknowledgements

We thank Robert McLaughlin, David Noakes, Beren Robinson, and Sarah Rosloski for helpful comments on previous versions of the manuscript, Sveinn Kári Valdimarsson and Bjarni Jónsson for field assistance, Hilmar Malmquist, Kym Hartley, the Institute of Freshwater Fisheries in Iceland for help with the data collection and analysis, and Louis Bernatchez for providing manuscript preprints. This study was supported by the Natural Sciences and Engineering Research Council of Canada and by support to the University of Iceland and Hólar College from the FAIR Research and Development Programme of the European Commission.

References

Bernatchez, L., and Dodson, J.J. 1990. Allopatric origin of sympatric populations of lake whitefish (*Coregonus clupeaformis*) revealed by mitochondrial DNA restriction analysis. Evolution, **44**: 1263–1271.

Danzmann, R.G., Ferguson, M.M., Skúlason, S., Snorrason, S.S., and Noakes, D.L.G. 1991. Mitochondrial DNA diversity among four sympatric morphs of Arctic charr, *Salvelinus alpinus* L., from Thingvallavatn, Iceland. J. Fish Biol. **39**: 649–659.

Gíslason, D. 1998. Genetic and morphological variation in polymorphic Arctic charr, *Salvelinus alpinus* from Icelandic lakes. M.Sc. thesis, University of Guelph, Guelph, Ont.

Lu, G., and Bernatchez, L. 1999. Correlated trophic specialization and genetic divergence in sympatric lake whitefish ecotypes (*Coregonus clupeaformis*): support for the ecological speciation hypothesis. Evolution, **53**: 1491–1505.

Reist, J.D. 1986. An empirical evaluation of the coefficients used in residual and allometric adjustment of size covariation. Can. J. Zool. **64**: 1363–1368.

Schluter, D. 1998. Ecological causes of speciation. *In* Endless forms: species and speciation. *Edited by* D.J. Howard and S.H. Berlocher. Oxford University Press, Oxford, U.K.

Skúlason, S., Snorrason, S.S., and Jónsson, B. 1999. Sympatric morphs, populations and speciation in freshwater fish with emphasis on Arctic charr. *In* Evolution of biological diversity. *Edited by* A.E. Magurran and R. May. Oxford University Press, Oxford, U.K.

Snorrason, S.S., Skúlason, S., Jonsson, B., Malmquist, H.J., Jónasson, P.M., Sandlund, O.T., and Lindem, T. 1994. Trophic specialization in Arctic charr, *Salvelinus alpinus* (Pisces: Salmonidae): morphological divergence and ontogenetic niche shifts. Biol. J. Linn. Soc. **52**: 1–18.

Takezaki, N., and Nei, M. 1996. Genetic distances and reconstruction of phylogenetic trees from microsatellite DNA. Genetics, **144**: 389–399.

Taylor, E.B., and Bentzen, P. 1993. Evidence for multiple origin and sympatric divergence of trophic ecotypes of smelt (*Osmerus*) in northeastern North America. Evolution, **47**: 813–832.

Volpe, J.P., and Ferguson, M.M. 1996. Molecular genetic examination of the polymorphic Arctic charr *Salvelinus alpinus* of Thingvallavatn, Iceland. Mol. Ecol. **5**: 763–772.

© 1999 NRC Canada

Detecting pan-Atlantic migration in salmon (*Salmo salar*) using ^{137}Cs

Strahan Tucker, Ivano Pazzia, David Rowan, and Joseph B. Rasmussen

Abstract: ^{137}Cs is a globally dispersed radioisotope that is transferred efficiently through the food chain. There is a strong east–west gradient of ^{137}Cs in the waters of the North Atlantic due to anthropogenic inputs from Europe, with levels exceeding 10 $Bq \cdot m^{-3}$ in the Irish Sea and concentrations <1.5 $Bq \cdot m^{-3}$ in the West Atlantic. This range in values is subsequently reflected in fish, including Atlantic salmon (*Salmo salar*), caught in those waters. ^{137}Cs concentrations in adult salmon, which had returned to the Ste. Marguerite River, Canada, reflected the entire range of values seen previously across the North Atlantic. In fact, 43% of fish had concentrations characteristic of the Faroe, Norwegian, North, and Irish seas. These results are in sharp contrast with what is generally believed about the migration of salmon and suggest that their marine life history is more panoceanic than previously thought.

Résumé : Le césium-137 (^{137}Cs) est un radio-isotope omniprésent qui se transmet efficacement le long de la chaîne alimentaire. On observe dans les eaux de l'Atlantique Nord un fort gradient est-ouest du ^{137}Cs, qui est dû à des apports anthropiques provenant d'Europe, les concentrations dépassant 10 $Bq \cdot m^{-3}$ en mer d'Irlande mais étant inférieures à 1,5 $Bq \cdot m^{-3}$ dans l'Atlantique Ouest. Cette gamme de concentrations se retrouve chez les poissons, notamment le saumon atlantique (*Salmo salar*), capturés dans ces eaux. Les concentrations de ^{137}Cs chez des saumons adultes revenus à la rivière Sainte-Marguerite, au Canada, représentaient l'ensemble des valeurs observées d'une façade à l'autre de l'Atlantique Nord. En fait, 43 % des poissons présentaient des concentrations caractéristiques des eaux des îles Féroé, de la Norvège, de la mer du Nord et de la mer d'Irlande. Ces résultats contredisent nettement les idées reçues sur la migration du saumon et semblent indiquer que la phase marine est plus panocéanique qu'on ne le croyait jusque-là.

[Traduit par la Rédaction]

Total abundance of North American origin Atlantic salmon (*Salmo salar*) has recently declined to approximately 45% of average numbers from previous decades (Anonymous 1998). This has occurred despite increases in spawning escapements, high smolt production in many rivers, and reduced harvests. With the general failure of river management schemes to maintain or enhance the abundance of salmon, interest has shifted to their marine life and the variability of ocean conditions that may influence migration and survival (Bisbal and McConnaha 1998). However, progress has been limited due to the difficulty of sampling over vast distances at sea. Sources of marine mortality are poorly understood, since there is a lack of basic knowledge about the distribution of salmon in the ocean (Friedland 1998). It is generally thought that Atlantic salmon originating from North American rivers feed on the Grand Banks, in the Labrador Sea, and along the coast of Greenland, with only a small percentage (<1%) ranging as far east as Iceland and the Faroe Islands (Mills 1993). However, these are inferences based on the recapture of very few tagged individuals and information from limited surveys of salmon abundance in the North Atlantic. These results are potentially biased by small sample sizes and uneven fishing effort to recapture marked fish (Hansen and Quinn 1998). Tremendous effort is required to tag a sufficiently high number of salmon to attain a statistically satisfying number of recaptures. Recapture rates are approximately 2% on average of individuals tagged on the high seas. Thus, information derived from other tracers such as radioisotopes can provide valuable independent information that will be particularly useful, since a much larger number of fish can potentially be analyzed. In theory, information could be generated for all fish.

^{137}Cs is a nuclear fission product that is rapidly taken up by biota, transferred efficiently through the food chain, and retained with a biological half-life of several years in large fish (Rowan and Rasmussen 1994, 1996). It can easily be detected at low levels with modern gamma spectrometry (Rowan and Rasmussen 1996). There is a pronounced east–west gradient of ^{137}Cs in the waters of the North Atlantic (Aarkrog et al. 1992; Kershaw et al. 1992; IAEA 1998) due to the combined effect of the Sellafield (United Kingdom) nuclear reprocessing plant on the Irish Sea and the Chernobyl nuclear accident (Fig. 1*a*). Thus, concentrations are highest in the Irish, North, and Norwegian seas, with values ranging from 10 to 150 $Bq \cdot m^{-3}$, whereas on the Grand Banks and Labrador Sea, concentrations are <1.5 $Bq \cdot m^{-3}$. This range is subsequently reflected in prey items of salmon. In aquatic food webs, ^{137}Cs bioconcentrates in phytoplankton, approximately 10- to 1000-fold over environmental concentrations, and is transferred up the food chain into

Received September 9, 1999. Accepted October 29, 1999. J15347

S. Tucker,[1] I. Pazzia, and J.B. Rasmussen. Department of Biology, McGill University, Montreal, QC H3A 1B1, and Centre de Recherche sur le Saumon Atlantique (CIRSA), Canada.
D. Rowan. Department of Radiological Health Sciences, Colorado State University, Ft. Collins, CO 80523, U.S.A.

[1]Author to whom all correspondence should be addressed. e-mail: strahant@hotmail.com

© 1999 NRC Canada

Fig. 1. (*a*) ^{137}Cs distribution (mBq·L^{-3}) in waters of the North Atlantic (Aarkrog et al. 1992; Kershaw et al. 1992; IAEA 1998). (*b*) Frequency distribution of ^{137}Cs concentrations (Bq·kg^{-1}) in 1SW (open bars) and 2SW (solid bars) Atlantic salmon from the Ste. Marguerite River, Que. Tissue samples were obtained from the heads and tails of fish caught in the sport fishery during the summers of 1995 (n = 33 (28 2SW, five 1SW)) and 1996 (n = 28 (16 2SW, 12 1SW)) and measured by gamma spectrometry. Dashed vertical lines denote the expected range in ^{137}Cs concentrations in salmon based on a mean bioaccumulation factor of 130 from waters in the North Atlantic outlined in the color bar above (water ^{137}Cs concentrations color coded as *a*). Horizontal lines denote the observed ranges in ^{137}Cs concentrations in salmon and other fish (cod, whiting, haddock, hake, mackerel, and plaice) caught in those same waters (Aarkrog et al. 1992; Kershaw et al. 1992).

(a)

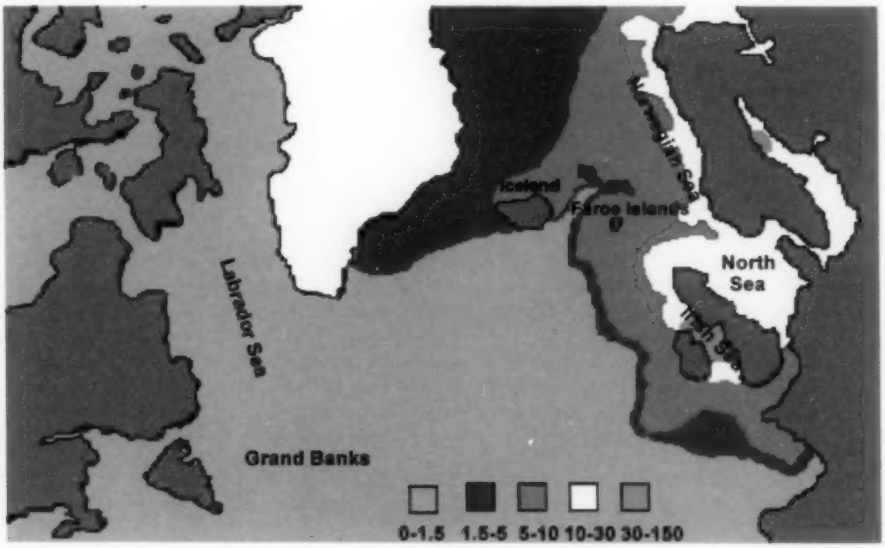

(b)

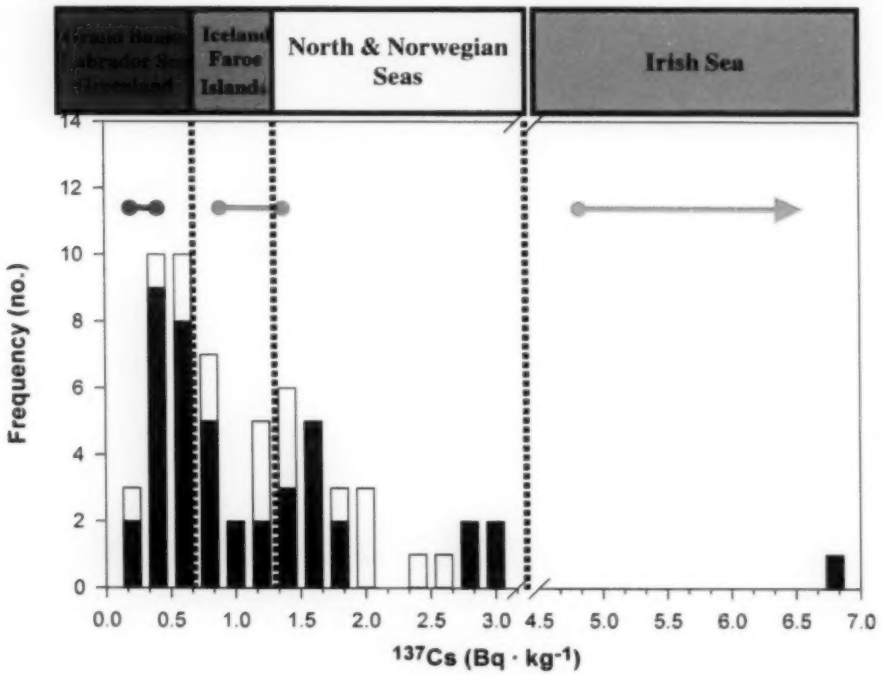

© 1999 NRC Canada

Fig. 1. (*a*) ^{137}Cs distribution ($mBq \cdot L^{-3}$) in waters of the North Atlantic (Aarkrog et al. 1992; Kershaw et al. 1992; IAEA 1998). (*b*) Frequency distribution of ^{137}Cs concentrations ($Bq \cdot kg^{-1}$) in 1SW (open bars) and 2SW (solid bars) Atlantic salmon from the Ste. Marguerite River, Que. Tissue samples were obtained from the heads and tails of fish caught in the sport fishery during the summers of 1995 (n = 33 (28 2SW, five 1SW)) and 1996 (n = 28 (16 2SW, 12 1SW)) and measured by gamma spectrometry. Dashed vertical lines denote the expected range in ^{137}Cs concentrations in salmon based on a mean bioaccumulation factor of 130 from waters in the North Atlantic outlined in the color bar above (water ^{137}Cs concentrations color coded as *a*). Horizontal lines denote the observed ranges in ^{137}Cs concentrations in salmon and other fish (cod, whiting, haddock, hake, mackerel, and plaice) caught in those same waters (Aarkrog et al. 1992; Kershaw et al. 1992).

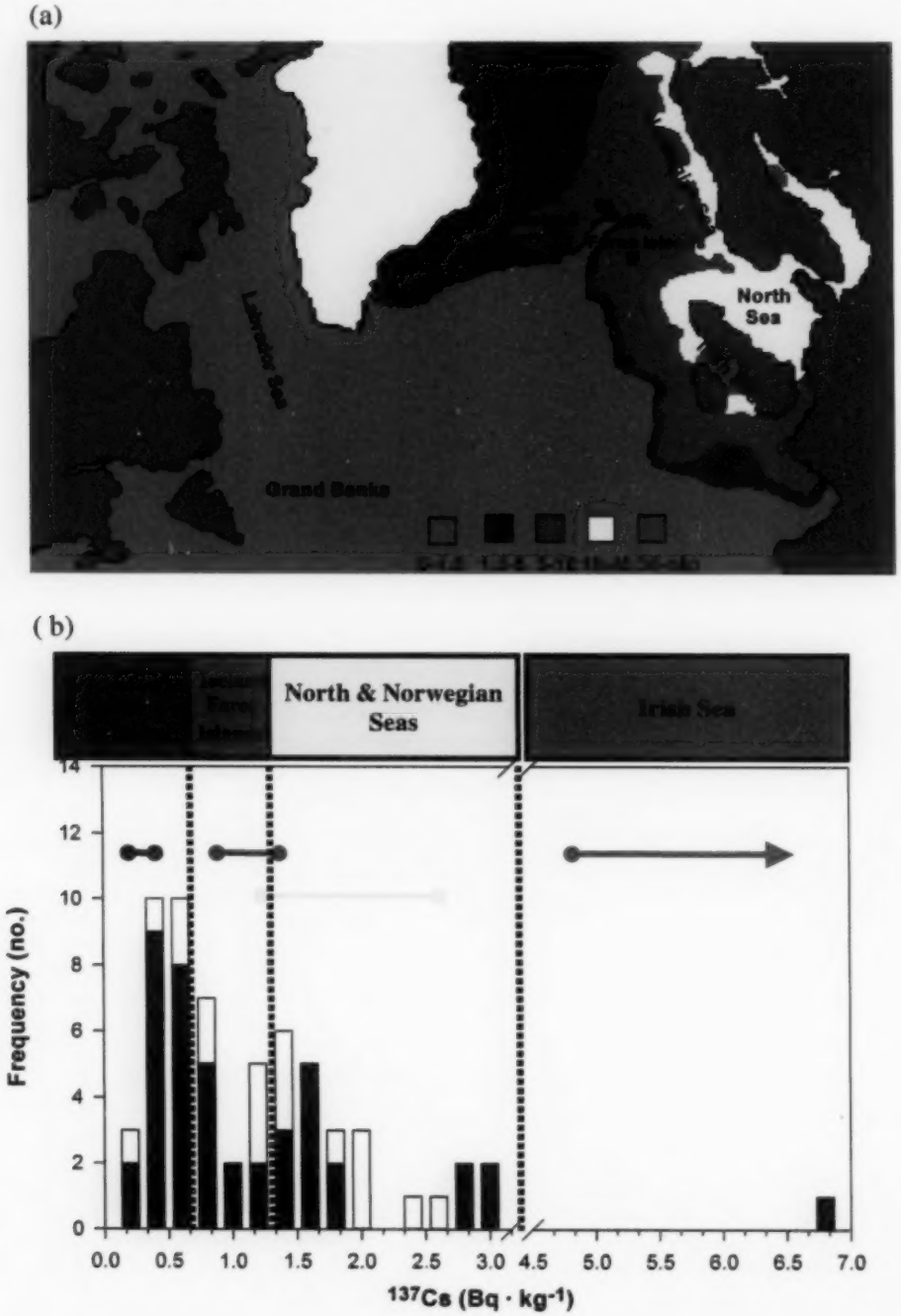

© 1999 NRC Canada

fish through ingestion with a twofold increase with each trophic level. There is therefore a general relationship between water and fish ^{137}Cs concentrations. A large, marine, piscivorous fish like salmon bioaccumulates ^{137}Cs by a factor of approximately 130 relative to seawater concentrations (Rowan and Rasmussen 1994). Thus, we can make predictions about ^{137}Cs concentrations in fish based on the observed values in the waters of the North Atlantic. Therefore, salmon that have fed exclusively in the North Sea would be expected to have ^{137}Cs concentrations of 1.3–4.0 Bq·kg^{-1}, whereas fish from the Northwest Atlantic would have concentrations of 0.15–0.65 Bq·kg^{-1}. Salmon that have spent all their marine life feeding in the vicinity of Iceland or the Faroe Islands would be expected to have concentrations of 0.65–1.3 Bq·kg^{-1}, whereas salmon from the Irish sea would have levels exceeding 4.5 Bq·kg^{-1}. These expectations are consistent with the results of marine monitoring surveys of piscivorous fish (Fig. 1*b*), including salmon, carried out by agencies in Denmark and Great Britain (Aarkrog et al. 1992; Kershaw et al. 1992). The ^{137}Cs concentrations in fish from different regions of the North Atlantic are discrete and match concentrations of ^{137}Cs in water in a predictable fashion.

Based on our present ideas on migration patterns of salmon, most returning North American fish would be expected to have levels from 0.15 to 0.65 Bq·kg^{-1}, with only a few specimens reaching 1 Bq·kg^{-1}. Our observed range of ^{137}Cs values for returning two-sea-winter (2SW) and 1SW salmon from the Ste. Marguerite River, Quebec, caught during the summers of 1995 and 1996 was very different from what we expected, as there was a 66-fold difference in ^{137}Cs levels (0.10–6.6 Bq·kg^{-1}) (Table 1). This range would suggest that these salmon had consumed prey with different ^{137}Cs levels and subsequently fed in different areas of the ocean. As mentioned previously, the bioaccumulation of ^{137}Cs has been reviewed explicitly (Rowan and Rasmussen 1994) and applied extensively to obtain consumption rates for all types of fish, including salmonids (e.g., Rowan and Rasmussen 1996; Tucker and Rasmussen 1999). We can therefore generate some expectations about the range in levels for fish feeding on the same or different prey as well. The maximum range in ^{137}Cs observed previously for salmonids within closed freshwater systems (same prey contamination levels) is a 14-fold difference (Table 1). This within-system variation in ^{137}Cs integrates large differences in consumption rates, as well as different trophic levels, among different age-classes, life history variants, and sex of fish (Rowan and Rasmussen 1996; Tucker and Rasmussen 1999). Among freshwater systems, however, the same salmonid species have very different ^{137}Cs levels. For example, lake trout (*Salvelinus namaycush*) vary 50-fold in ^{137}Cs concentrations amongst lakes (Table 1). This is not due to widely different consumption rates or trophic positions, but rather to differences in ^{137}Cs levels in water and subsequently in prey (Rowan and Rasmussen 1994). All else being equal, a 10-fold difference in consumption will result in approximately a 10-fold difference in ^{137}Cs body concentration. Therefore, if fish had all been feeding on the same prey ^{137}Cs, say 0.10 Bq·kg^{-1} from the Northwest Atlantic, it would require a 60-fold difference in consumption rates among fish to obtain the range observed for our salmon. Considering that these fish have similar growth rates (same

Table 1. Mean ^{137}Cs concentrations for different salmonids and their prey from various systems.

Species	System	Mean (±SD) ^{137}Cs (Bq·kg^{-1})	^{137}Cs range (Bq·kg^{-1})	Maximum/ minimum	^{137}Cs in diet (Bq·kg^{-1})	Reference
Atlantic salmon (*Salmo salar*)	Atlantic Ocean	1.14±1.03	0.10–6.62	66.2	—	Present study
Arctic grayling (*Thymallus arcticus*)	Reservoir: Joe Wright	0.21±0.04	0.16–0.30	1.9	—	D. Rowan (unpublished data)
Atlantic salmon: juvenile	Stream: Xavier	10.19±2.45	4.89–16.17	3.3	5.0	Tucker and Rasmussen 1999
Atlantic salmon: juvenile	Stream: Morin	5.35±1.39	2.37–8.95	3.8	6.0	Tucker and Rasmussen 1999
Atlantic salmon: juvenile	River: Ste. Marguerite	7.21±2.23	3.06–14.06	4.6	2.3	Tucker and Rasmussen 1999
Atlantic salmon: juvenile	Stream: Allaire	11.79±3.18	2.50–19.99	8.0	4.5	Tucker and Rasmussen 1999
Brook trout (*Salvelinus fontinalis*)	Stream: Allaire	5.63±1.33	2.95–9.94	3.4	4.5	Tucker and Rasmussen 1999
Brook trout	Stream: Xavier	5.91±1.92	1.23–9.37	7.6	5.0	Tucker and Rasmussen 1999
Brook trout	Stream: Little Beaver	0.19±0.10	0.03–0.42	13.9	0.04	D. Rowan (unpublished data)
Brown trout (*Salmo trutta*)	Stream: Little Beaver	0.14±0.07	0.06–0.31	5.1	0.04	D. Rowan (unpublished data)
Brown trout	River: La Poudre	0.13±0.03	0.08–0.19	2.3	0.08	D. Rowan (unpublished data)
Chinook salmon (*Oncorhynchus tshawytscha*)	Lake: Lake Michigan	12.88±3.35	9.56–16.43	1.7	6.2	Rowan and Rasmussen 1996
Cisco (*Coregonus artedi*)	Lake: Opeongo	4.98±1.74	2.67–12.84	4.8	2.5	I. Pazzia et al. (unpublished data)
Lake trout (*Salvelinus namaycush*)	Lake: Great Slave	6.04±1.83	1.92–10.47	5.4	3.1	Rowan and Rasmussen 1996
Lake trout	Lake: Memphramagog	1.58±0.43	0.35–2.90	8.3	0.7	M. Trudel et al. (unpublished data)
Lake trout	Lake: Opeongo	7.24±2.14	2.07–13.79	6.9	5.0	I. Pazzia et al. (unpublished data)
Lake trout	Lake: Happy Isle	6.51±3.71	2.92–16.55	5.7	1.5	I. Pazzia et al. (unpublished data)
Lake trout	Lake: Source	6.39±3.34	2.69–17.36	6.5	1.0	I. Pazzia et al. (unpublished data)
Lake whitefish (*Coregonus clupeaformis*)	River: Ottawa	8.14±1.14	6.82–9.47	1.4	1.8	Rowan and Rasmussen 1996

© 1999 NRC Canada

Table 2. ^{137}Cs concentrations in water of various zones in the North Atlantic, predicted ^{137}Cs concentrations in Atlantic salmon in those zones, the proportion of salmon observed in those ^{137}Cs ranges, and, the proportional area of the high-production continental shelf zone in the North Atlantic delineated by ^{137}Cs water concentrations.

Zone	Water ^{137}Cs ($mBq \cdot L^{-1}$)	Predicted salmon ^{137}Cs ($Bq \cdot kg^{-1}$)	Observed salmon ^{137}Cs (% total)	Area of zone (% of North Atlantic)
Grand Banks/Labrador Sea	0–1.5	0–0.20	6.6	14.5
Greenland	1.5–5	0.2–0.65	32.8	28.5
Iceland/Faroe Islands	5–10	0.65–1.3	23	29.9
North and Norwegian seas	10–30	1.3–4.0	36.1	25.1
Irish Sea	30–150	4.5+	1.6	2.0

Note: The proportion of salmon from various ^{137}Cs zones generally matches the proportional area of those feeding zones.

size range), this is highly improbable and would likely represent an excessive, and unheard of, consumption rate. Different diets would only account for a twofold difference in ^{137}Cs among trophic levels. However, salmon are considered opportunistic, generalist feeders, exploiting many different prey items (Mills 1993). Moreover, salmon caught in different regions of the Atlantic all have similar diets (Hansen and Quinn 1998), yet the ^{137}Cs values for these same prey types have been shown to be different and their distribution discrete. It is unlikely, therefore, that the 66-fold difference observed in Atlantic salmon feeding at sea could simply be obtained by feeding on prey with similar ^{137}Cs levels or by differences in feeding rate or trophic levels alone or even combined. In order to generate this range, it seems probable that fish were feeding on similar prey with different ^{137}Cs levels. Furthermore, there is a tendency in the ^{137}Cs distribution for multiple peaks (Fig. 1*b*), in contrast with the expected more uniform lognormal distribution typically observed in fish (Rowan and Rasmussen 1994). The data, then, also suggest that, individually, salmon spend most of their lives in one region, as opposed to moving about from one area to another, since the latter would bring about a smoothing effect and markedly reduce the range of variation. If prey were moving more than salmon, we would expect the range in variation to be reduced as well and more normally distributed for both our salmon and the fish surveyed at sea. Instead, we observe a range in ^{137}Cs values as might be expected from a composite sample of fish from different feeding grounds, each of which had fed most of its marine life in a single region.

The most frequently occurring values for returning salmon were in the 0.15–1.0 $Bq \cdot kg^{-1}$ range (Fig. 1*b*) expected for fish feeding in the Northwest Atlantic to the Iceland region; however, a full 43% of the fish exceeded this range, and indeed, we obtained salmon with concentrations up to 6.6 $Bq \cdot kg^{-1}$. As many as 28% of the fish had values >1.3 $Bq \cdot kg^{-1}$, consistent with fish feeding beyond Iceland. In addition, 59% of 1SW salmon had concentrations exceeding 1.3 $Bq \cdot kg^{-1}$. Thus, fish returning to the Ste. Marguerite River exhibit virtually the entire range of ^{137}Cs concentrations seen previously across the entire North Atlantic. The data suggest that salmon of North American origin are using European feeding grounds much more than previously thought, as they exhibit ^{137}Cs values distinctly characteristic of the Faroe, North, Norwegian, and Irish seas (i.e., they match the values observed for fish caught in those waters from independent sampling and monitoring).

Ocean abundance of salmon is typically greatest in the high-production continental shelf areas of the North Atlantic (Mills 1993). The proportion of salmon returning to the Ste-Marguerite from particular feeding grounds (i.e., discrete ^{137}Cs ranges) generally matches the proportional area of those feeding zones (Table 2). This would suggest, then, that salmon are proportionately distributed in the Atlantic relative to the availability of food resources. Differences were noted in the range of ^{137}Cs values among salmon of different cohorts, suggesting that migration patterns of fish from the same river might differ from year to year. For example, the range observed for 1995 1SW salmon (0.21–1.92 $Bq \cdot kg^{-1}$, mean 0.83 $Bq \cdot kg^{-1}$) was lower than the range observed for 1996 1SW salmon (0.42–2.36 $Bq \cdot kg^{-1}$, mean 1.39 $Bq \cdot kg^{-1}$). In addition, same cohort fish (i.e., 1995 1SW and 1996 2SW salmon) displayed a reduced range in ^{137}Cs concentrations (0.89 $Bq \cdot kg^{-1}$) compared with the other cohorts (1.36 $Bq \cdot kg^{-1}$). Our sample of 61 salmon cumulatively represents approximately 2% of the returning stock to the Ste. Marguerite River over 2 years. This, as opposed to the small number of fish tagged at sea that might return to individual rivers. There is thus potential to examine a far greater number of fish. Comparing variations in fish movements among years and stocks using ^{137}Cs may lead to an understanding of the broad-scale oceanic processes influencing salmon migration and survival.

While it has been previously observed, although regarded as incidental, that a few fish tagged in waters around the Faroe Islands had been recaptured in Canadian rivers (Hansen and Quinn 1998), our results imply that the marine life history of Atlantic salmon is much more panoceanic than previously imagined, as is now known to be the case for Pacific salmon (Hansen and Quinn 1998). Analogous to the results presented here, recent satellite tagging of North Atlantic bluefin tuna (*Thunnus thynnus*) questions current assumptions about migration patterns, suggesting that their distribution in the ocean is much broader than presumed (Lutcavage et al. 1999). Although only limited monitoring of salmon for ^{137}Cs has been carried out in Europe (Kershaw et al. 1992), the few fish collected show a similar pattern to the one observed here (0.18–5.3 $Bq \cdot kg^{-1}$), suggesting that fish returning to British rivers also use a wide range of feeding grounds across the North Atlantic. The implication of this pan-Atlantic marine history for the management and conservation of salmon stocks is dramatic, since it implies that salmon in most feeding grounds are of mixed origin. This, then, only emphasizes the importance of collective

© 1999 NRC Canada

management and conservation measures by all North Atlantic nations.

Acknowledgements

We thank all those who donated tissue samples of their salmon from the ZEC Ste-Marguerite and the Alcan Fishing Club, Quebec. Logistical and financial support was provided through the Centre de Recherche sur le Saumon Atlantique (CIRSA). Additional support was provided by a Natural Sciences and Engineering Research Council of Canada research grant from the Collaborative Project Program.

References

Aarkrog, A., Buch, E., Chen, Q.J., Christensen, G.C., Dahlgaard, H., Hansen, H., Holm, E., and Nielsen, S.P. 1992. Environmental radioactivity in the North Atlantic region. Annual Report Risø-R-571(EN).

Anonymous. 1998. Atlantic salmon abundance: overview for 1997. Dep. Fish. Oceans Stock Status Rep. DO-02.

Bisbal, G.A., and McConnaha, W.E. 1998. Consideration of ocean conditions in the management of salmon. Can. J. Fish. Aquat. Sci. **55**: 2178–2186.

Friedland, K.D. 1998. Ocean climate influences on critical Atlantic salmon (*Salmo salar*) life history events. Can. J. Fish. Aquat. Sci. **55**(Suppl. 1): 119–130.

Hansen, L.P., and Quinn, T.P. 1998. The marine phase of the Atlantic salmon (*Salmo salar*) life cycle, with comparisons to Pacific salmon. Can. J. Fish. Aquat. Sci. **55**(Suppl. 1): 104–118.

International Atomic Energy Agency (IAEA). 1998. Measurement and assessment of radionuclides in the marine environment. Annual Report. IAEA, Vienna, Austria.

Kershaw, P.J., Pentreath, R.J., Woodhead, D.S., and Hunt, G.J. 1992. Ministry of Agriculture, Fisheries and Food Aquatic Environment Monitoring Report 32.

Lutcavage, M.E., Brill, R.W., Skomal, G.B., Chase, B.C., and Howey, P.W. 1999. Results of pop-up satellite tagging of spawning size class fish in the Gulf of Maine: do North Atlantic bluefin tuna spawn in the mid-Atlantic? Can. J. Fish. Aquat. Sci. **56**: 173–177.

Mills, D. (*Editor*). 1993. Salmon in the sea and new enhancement strategies. Fishing News Books, Oxford, U.K.

Rowan, D.J., and Rasmussen, J.B.1994. Bioaccumulation of radiocesium by fish: the influence of physicochemical factors and trophic structure. Can. J. Fish. Aquat. Sci. **51**: 2388–2410.

Rowan, D.J., and Rasmussen, J.B.1996. Measuring the bioenergetic cost of fish activity in situ using a globally dispersed radiotracer (^{137}Cs). Can. J. Fish. Aquat. Sci. **53**: 734–745.

Tucker, S., and Rasmussen, J.B. 1999. Using ^{137}Cs to measure and compare bioenergetic budgets of juvenile Atlantic salmon (*Salmo salar*) and brook trout (*Salvelinus fontinalis*) in the field. Can. J. Fish. Aquat. Sci. **56**: 875–887.

© 1999 NRC Canada

Les métaux (Mn, Cu, Cd, Zn et Hg) des meuniers noirs (*Catostomus commersoni*) et des grands brochets (*Esox lucius*) de l'amont et de l'aval du barrage Moses-Saunders sur le fleuve Saint-Laurent près de Cornwall (Ontario) et Massena (New York)

Janick D. Lalonde, François Chapleau, Anik Brind'Amour et Lara Louise Ridgway

Résumé : Nous avons comparé les concentrations de métaux (Mn, Cu, Cd, Zn et Hg) chez les meuniers noirs (*Catostomus commersoni*) et les grands brochets (*Esox lucius*) provenant de l'amont et de l'aval du barrage hydroélectrique Moses-Saunders sur le fleuve Saint-Laurent près de Cornwall, Ontario, et de Massena, New York. Le lac Saint-Laurent, en amont du barrage, est un réservoir de 136 km^2 couvrant 90 km^2 de terres agricoles inondées en 1958, et l'aval est le lac Saint-François. Chez les grands brochets, la concentration moyenne de chaque métal dans la chair ne différait pas entre l'amont et l'aval. La concentration de Hg augmente en fonction de la longueur chez les deux populations, alors que la concentration de Zn diminue en fonction de la longueur chez les brochets de l'aval. Pour une longueur donnée, les brochets de l'aval sont plus contaminés par le Hg que les brochets de l'amont. Les meuniers noirs de l'amont du barrage contenaient, en moyenne dans leur foie, cinq fois plus de Hg et significativement plus de Mn et de Cu que ceux de l'aval. Aucune bioaccumulation de métaux n'a été observée. En se fiant aux concentrations de métaux chez les brochets, il semble que, après 37 ans, l'augmentation des concentrations de Hg qui accompagne la mise en eau d'un réservoir se soit estompé. Nous pensons que les concentrations élevées de Hg chez les meuniers de ce même lac sont le résultat de leur mode de vie qui les met en contact constant avec des sédiments qui peuvent être localement plus contaminés.

Abstract: We examined the effect of a dam on concentrations of metals (Mn, Cu, Cd, Zn, and Hg) in white sucker (*Catostomus commersoni*) and in northern pike (*Esox lucius*). Fish were caught upstream and downstream of the Moses-Saunders Power dam on the St. Lawrence River near Cornwall, Ontario, and Massena, New York. Upstream of the dam, Lake St. Lawrence is a 136-km^2 reservoir resulting from the flooding of 90 km^2 of agricultural land in 1958, and downstream is Lake St. Francis. In northern pike, no difference in the mean concentrations of metals was found between upstream and downstream fish. Hg concentrations increased with length in upstream and downstream pike, whereas Zn showed an inverse relationship with length downstream. For a particular length, Hg concentration was higher in downstream northern pike. On average, white sucker were five times more contaminated by Hg upstream than downstream. The levels of Mn and Cu were also found to be higher upstream. No bioaccumulation of metals was observed in white sucker. Based on the results obtained for the northern pike, after 37 years, it seems that the high metal concentrations observed in Lake St. Lawrence after the creation of the reservoir have now disappeared. We believe that the high level of contamination of the white suckers in this lake is linked with this species' habit of being in constant contact with the sediments, which could be locally highly contaminated.

Introduction

Au cours des dernières années, les déversements de substances organiques et inorganiques nocives dans l'environnement aquatique ont suscité un grand intérêt autant chez les chercheurs que dans le public. Parmi ces substances, les métaux ont fait l'objet de plusieurs études (Brown et Chow 1977; McFarlane et Franzin 1980; Mathers et Johanssen 1985; Pourang 1995). Ces études ont surtout tenté d'évaluer la toxicité et le caractère bioaccumulatif des métaux chez les êtres vivants (Gupta et Mathur 1983; Marcovecchio et Moreno 1993). Certaines de ces substances sont des éléments

Reçu le 21 août 1997. Accepté le 26 février 1999.
J14173

J.D. Lalonde,[1] F. Chapleau, A. Brind'Amour et L.L. Ridgway. Institut de Biologie d'Ottawa-Carleton, Département de Biologie, Université d'Ottawa, Ottawa, C.P. 450, Succursale A, ON K1N 6N5, Canada.

[1]Auteur correspondant. Courrier électronique : janick_lalonde@inrs-eau.uquebec.ca

© 1999 CNRC Canada

Tableau 1. Caractéristiques du lac Saint-Laurent, le réservoir du barrage Moses-Saunders.

Propriétaire	Hydro Ontario
Capacité lors de la construction	912 MW
Surface totale du réservoir (surface inondée)	136 km^2 (90 km^2)
Pourcentage de terre inondée	66%
Variation verticale du niveau de moyen l'eau (max.)	2,0 m (2,9 m)
Débit moyen	7720 m^3/s
Commentaire	La végétation a été partiellement enlevée lors de la mise en eau

naturels essentiels aux organismes (par ex., le manganèse, le cuivre et le zinc) alors que d'autres sont toxiques, même à de faibles doses (par ex. le cadmium et le mercure) (Wiener et Giesy 1979).

Les concentrations de mercure dans la chair des poissons augmentent chez les populations vivant dans des réservoirs nouvellement formés. Cette hausse tend à s'estomper après une trentaine d'années (Verdon et al. 1991). Ce laps de temps a été obtenu dans le cas de réservoirs situés sur le bouclier précambrien dans des zones nordiques non industrialisées (voir Potter et al. 1975; Bodaly et al. 1984; Messier et Roy 1987; Jackson 1988, 1991; Verdon et al. 1991). Ainsi, l'augmentation de la concentration de mercure dans la chair des poissons immédiatement après la mise en eau d'un réservoir est attribuée principalement à la méthylation bactérienne du Hg naturel des sols organiques et de la végétation inondée (Bodaly et al. 1984; Messier et Roy 1987; Jackson 1988, 1991; Verdon et al. 1991).

Notre étude examine les concentrations de cinq métaux (Mn, Cu, Cd, Zn, Hg) dans les tissus de poissons provenant de l'amont et de l'aval du barrage Moses-Saunders sur le fleuve Saint-Laurent près de Cornwall, Ontario, et Massena, New York. Des comparaisons intraspécifiques ont été faites chez deux espèces appartenant à autant de niveaux trophiques : un benthivore s'alimentant exclusivement d'invertébrés, le meunier noir (*Catostomus commersoni*), et un piscivore, le grand brochet (*Esox lucius*). L'objectif premier de l'étude est de vérifier s'il y a une différence de concentration de métaux entre les populations de l'amont et l'aval pour chaque espèce. Le deuxième objectif est de vérifier s'il y a bioaccumulation de métaux et de comparer, le cas échéant, les taux de bioaccumulation de l'amont et l'aval du barrage pour chaque espèce.

L'originalité de notre étude réside dans le fait que nous examinons si la dynamique des métaux traces chez les poissons des réservoirs du bouclier précambrien s'applique dans le cas d'un ouvrage hydroélectrique vieux de 37 ans construit sur un secteur fluvial qui montre un fort débit d'eau et qui est situé dans un secteur fortement industrialisé. Ce secteur a reçu, lors du vingtième siècle, un grand volume d'effluents industriels riches en métaux, le secteur fluvial en aval du barrage ayant reçu une grande proportion de ces effluents (STLRT 1994).

Matériel et méthodes

Sites et méthodes d'échantillonnage

Le lac Saint-Laurent est un réservoir de 136 km^2 qui est le résultat de l'inondation de 90 km^2 de terres agricoles lors de la mise en eau du barrage hydroélectrique Moses-Saunders en 1958 (voir tableau 1). Le réservoir est caractérisé par la présence de grandes baies peu profondes avec peu de végétation. Un peu en aval du barrage, le fleuve se subdivise en deux canaux principaux (Nord et Sud) relativement étroits qui contournent les îles de la région de Cornwall–Massena. Ces canaux se fusionnent à l'embouchure du lac Saint-François, lui-même un réservoir pour le barrage de Beauharnois (74°55′W, 45°19′N) situé plus en aval.

Des études de populations ont permis de déterminer que les meuniers noirs et les brochets provenant de l'amont et de l'aval appartiennent, respectivement, à des populations distinctes (Ridgway 1996; F. Chapleau données non publiées). Les deux populations montrent des différences significatives au niveau de la croissance. De plus, les meuniers de l'amont ont une fécondité moyenne plus basse, des oeufs ayant un plus grand diamètre, un coefficient de condition plus faible, une moyenne d'âge plus élevée et une plus grande fréquence de papillomes sur les lèvres et sur le corps (Ridgway 1996). Les brochets de l'amont ont une fécondité, un coefficient de condition et un âge moyen similaires aux brochets de l'aval mais présentent une longueur plus élevée chez les individus de 7 ans ou moins et un indice de recrutement beaucoup plus faible qu'en aval (amont : 3 brochets capturés/100 h de pêche; aval : 13 brochets capturés/100 h de pêche; F. Chapleau, données non publiées). De plus, la zone littorale des canaux en aval du barrage et dans le secteur ouest du lac Saint-François montre une plus grande biomasse de poissons et une plus grande biodiversité ichtyenne que celle du lac Saint-Laurent (Ribey 1997). Nous croyons que le faible taux de recrutement des brochets en amont expliquerait leur croissance plus rapide et ce, malgré la plus faible biomasse de poisson en l'amont. Le nombre de brochets étant beaucoup moins élevé en amont qu'en aval, il y a moins de compétition intraspécifique pour la nourriture, d'où une croissance plus rapide.

Les poissons ont été échantillonnés sur des sites répartis sur 40 km sur le fleuve Saint-Laurent (fig. 1), du parc Provincial Farran (75°00′W, 44°59′N) jusqu'à l'île Thompson (74°31′W, 45°04′N). Ce secteur du fleuve est divisé en deux régions par le barrage hydroélectrique Moses-Saunders. Neuf sites sont situés en amont du barrage, alors que 11 sites sont en aval. Quelques meuniers noirs ont également été capturés à proximité de deux frayères : le ruisseau Hoople (en amont du barrage : 74°58′W, 45°01′N) et la rivière Raisin (en aval du barrage : 74°30′W, 45°08′N). Les engins de pêche utilisés étaient : deux seines (longueur : 10 et 30 m), deux verveux (aile : 9,1 × 0,9 m; mailles : 6 mm; anneaux : 76 cm de diamètre), trois filets maillants expérimentaux (deux filets composés de huit panneaux faits de multifilaments en coton de 7,6 m (longueur) × 2,4 m (hauteur) ayant une maille étirée de 3,8, 5,1, 6,4, 7,6, 8,9, 10,2, 12,7 et 15,2 cm et un filet composé de cinq panneaux de monofilament en nylon de 7,6 m (longueur) × 1,8 m (hauteur) ayant une maille étirée de 2,5, 3,3, 4,8, 6,2 et 7,5 cm).

Les concentrations de métaux (Mn, Cu, Cd, Zn et Hg) ont été mesurées dans le foie de 48 meuniers noirs et dans la musculature épaxiale, entre la tête et la nageoire dorsale, de 50 brochets. Nous avons été contraints d'analyser le foie des meuniers noirs, parce que la chair a été utilisée lors d'une analyse de contaminants organiques (Ridgway et al. 1999). Puisque aucune analyse interspécifique n'est faite dans notre étude, le fait d'avoir analysé des tissus différents n'a pas d'impact sur nos conclusions.

Vingt-six meuniers et 11 brochets proviennent du lac Saint-Laurent (amont du barrage) alors que 22 meuniers et 39 brochets

© 1999 CNRC Canada

Fig. 1. Emplacement approximatif de la capture des meuniers noirs et des grands brochets en amont et en aval du barrage Moses-Saunder dans le fleuve Saint-Laurent.

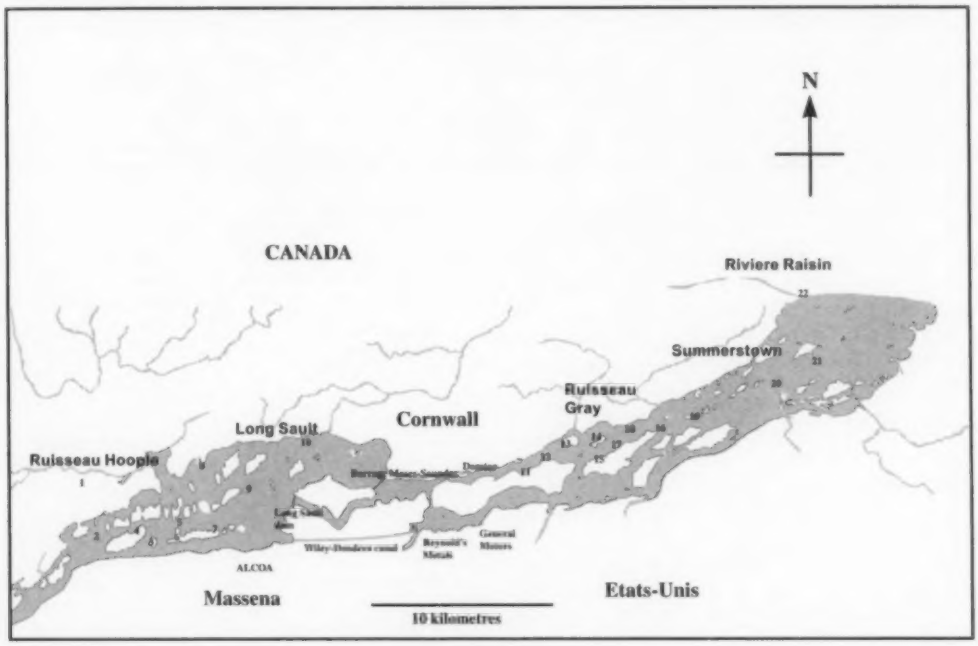

proviennent du secteur en aval du barrage (canaux et secteur ouest du lac Saint-François). Ces spécimens ont été capturés lors de la première année d'échantillonnage.

Méthodes en laboratoire

Les caractéristiques des populations de meuniers ont été déterminées par Ridgway (1996). La longueur totale (±1,0 mm) et le poids (±0,1 g) ont été mesurés pour tous les poissons. Le coefficient de condition (k) a été calculé selon la formule $k = 100\,000$ poids·longueur^{-3}. Le sexe des meuniers et des brochets a été déterminé par une inspection visuelle des gonades. L'âge des meuniers a été déterminé grâce à l'examen du plus long rayon d'une des nageoires pectorales (Ridgway 1996). L'âge des brochets a été déterminé en observant les cleithra (F. Chapleau, données non publiées). Une vérification indépendante des structures d'âge a révélé un très haut pourcentage (90%) de concordance dans la lecture de l'âge des poissons des deux espèces.

Analyse de métaux lourds

Les techniques d'extraction des métaux lourds (Mn, Cu, Cd, Zn et Hg) proviennent de documents du ministère de l'Environnement de l'Ontario (n° du document : HGBIO-E33057A, 1993 pour le Hg; et HMPNBIO-E3072A, 1993 pour le Mn, Cu, Cd et le Zn). Pour la détermination des concentrations de Mn, Cu, Cd et de Zn, 2,5 g de tissu (poids humide) ont été digérés dans l'acide nitrique (7 mL) et de l'acide perchlorique (1,5 mL) concentrés pendant 12 à 16 h dans des tubes à digestion Folin-Wu© (température maximale 130°C). Les échantillons refroidis ont été dilués pour obtenir 25 mL avec de l'eau distillée déionisée et ils ont été transférés dans des tubes de polypropylène.

Pour déterminer la concentration de Hg, 0,25 g de tissu (poids humide) a été placé dans des tubes à digestion Folin-Wu©. Un volume de 5 mL d'un mélange 4:1 d'acides (acide sulfurique – acide nitrique) a été ajouté aux tubes. Les échantillons ont été digérés sur une période de 12 à 16 h (température maximale 230°C). Les échantillons refroidis ont été dilués avec de l'eau déionisée pour obtenir un volume de 25 mL. Par la suite, ils ont été transférés dans des tubes de polypropylène.

Les concentrations de Zn ont été déterminées par absorption atomique par flamme (FAA), alors que les concentrations des autres métaux ont été établies par spectrométrie de masse utilisant un plasma inductivement couplé comme source (ICP-MS). Les concentrations de métaux lourds en $\mu g \cdot g^{-1}$ représentent la quantité de métal par gramme de poids humide du poisson. Nous avons arbitrairement utilisé la moitié de la limite de détection comme valeur empirique pour les échantillons qui contenaient des concentrations de métaux sous la limite de détection.

Trois types de blanc ont servi à vérifier la qualité des échantillons et la justesse des manipulations en laboratoire (tableau 2). Deux blancs ont été ajoutés à chaque série de digestions pour déterminer la contamination exogène. La validité ainsi que la reproductibilité de la méthode ont été vérifiées par l'analyse d'étalon certifié (Dolt-2). Finalement, un double de chaque échantillon a été analysé afin de vérifier la précision des techniques de laboratoire. La limite de détection de chaque métal est indiquée dans le tableau 2. Elle a été calculée en multipliant par trois l'écart-type obtenu lors de l'analyse de dix blancs.

Analyses statistiques

Nous avons effectué des tests de t afin de relever les différences entre les moyennes d'âge, de longueur, de poids et de coefficient de condition des deux échantillons de meuniers et de brochets qui ont servis lors de l'analyse des contaminants. Ceci a permis de vérifier si une comparaison directe des concentrations moyennes de métaux entre les deux régions était statistiquement possible.

La bioaccumulation des métaux a été vérifiée en utilisant des régressions linéaires montrant la concentration de chaque métal (variable dépendante) en fonction de paramètres biologiques (âge, longueur, poids et coefficient de condition) (variable indépendante) pour les poissons venant des deux régions. Une analyse de cova-

© 1999 CNRC Canada

Tableau 2. Limites de détection et résultats de trois types de blancs qui ont servis à vérifier la qualité des manipulations lors de la digestion des foies des meuniers noirs (*Catostomus commersoni*) et de la musculature épaxiale des grands brochets (*Esox lucius*) ainsi que lors de l'analyse de métaux.

Métaux	Limite de détection ($\mu g \cdot g^{-1}$)	Blancs $\bar{x}$ ± e.t. ($\mu g \cdot g^{-1}$)	Analyse des réplicats[a]		Valeur certifiée $\bar{x}$ ± e.t. ($\mu g \cdot g^{-1}$)	Valeur mesurée $\bar{x}$ ± e.t. ($\mu g \cdot g^{-1}$)
			N[b]	PDR[c]		
Catostomus commersoni						
Cu	0,01	0,103±0,06	7	4,1	25,8±1,1	26,0±1,7
Zn	0,2	0,820±0,20	—[d]	—	85,8±2,5	96,9±4,5
Cd	0,01	—	7	12	20,8±0,5	20,0±1,1
Mn	0,01	0,032±0,01	7	7,6	6,88±0,56	5,77±0,28
Hg	0,01	<0,005	6	3,8	1,99±0,10	1,48±0,33
Esox lucius						
Cu	0,01	6,00±2,16	5	0,7	25,8±1,1	26,8±1,1
Zn	0,2	0,08±0,02	—	—	85,8±2,5	99,1±4,3
Cd	0,01	1,22±0,49	5	5,5	20,8±0,5	19,3±0,7
Mn	0,01	2,50±0,58	5	4,8	6,88±0,56	6,01±0,31
Hg	0,01	0,06±0,05	8	5,8	1,99±0,10	1,58±0,10

Nota : Des blancs ont été analysés afin de vérifier la contamination exogène, des doubles ont été effectuées afin de s'assurer de la précision des analyses de métaux et un étalon certifié (Dolt-2) a été analysé afin de déterminer la reproductibilité.

[a]Un double représente deux échantillons du même spécimen de meunier analysés séparément.

[b]Nombre de double.

[c]PDR = $(X_1 - X_2)/[(X_1 + X_2)/2]$ où PDR est le pourcentage des différences relatives, X_1 est la concentration obtenue lors de la première analyse et X_2 celle obtenue lors de la deuxième analyse.

[d]Données non disponibles.

riance a permis de vérifier si les concentrations (comparaison des ordonnés à l'origine) et les taux de bioaccumulation de métaux traces (comparaison des pentes) étaient similaires chez les populations de l'amont et de l'aval. Les concentrations moyennes de métaux ont été comparées à l'aide d'un test de t pour les métaux qui n'étaient pas corrélés avec les paramètres biologiques.

Les conditions d'application des analyses paramétriques (distribution normale des données et homogénéité des variances) ont été vérifiées par une inspection visuelle des graphiques de données brutes et par des tests de Levene. Le seuil de rejet a été fixé à 0,05. Une correction de Bonferroni a été appliquée aux tests multiples afin de minimiser l'obtention d'une différence significative aléatoire. Les analyses ont été faites en utilisant SYSTAT 5.1© (Wilkinson 1990). Des tests de puissance ont aussi été faits sur les résultats de tests de t ne montrant pas de différences significatives (logiciel ST-Plan 4.0; distribué par le M.D. Anderson Cancer Center, University of Texas).

Sept concentrations de métaux dépassant la moyenne d'au moins un ordre de grandeur ont été éliminées des analyses parce qu'elles étaient attribuables à de la contamination lors des manipulations expérimentales. L'inclusion ou l'exclusion de ces échantillons n'a pas modifié le fait qu'un test soit significatif ou pas. Trois autres échantillons ont été perdus lors de l'analyse par spectrométrie de masse.

Résultats

Grands brochets

Puisque les brochets de l'amont étaient de plus grande taille que ceux capturés en aval, seuls les individus de grande taille (>562 mm) des deux régions ont été utilisés pour la détection des métaux. Les individus de plus de 562 mm de l'amont sont significativement plus lourds (t = 3,039; p = 0,036), ont un coefficient de condition plus élevé (t = 2,880; p = 0,032) bien qu'ils ne soient pas significativement plus longs (t = 2,529; p = 0,084; puissance = 0,66) ou plus âgés (t = 0,288; p = 1,000; puissance = 0,04) que les brochets de l'aval ayant un spectre de taille similaire (tableau 3). L'échantillon de brochets ne comprenait que des femelles. Lors de l'analyse comparative des concentrations moyennes de métaux lourds, tous les poissons capturés ont été inclus (incluant les poissons <562 mm).

La concentration de Hg augmente avec la masse et la longueur des grands brochets mais pas avec l'âge dans le Lac Saint-Laurent (tableau 5). Dans le secteur fluvial en aval du barrage, la concentration de Hg augmente avec l'âge, la masse et la longueur, alors que la concentration de Zn diminue avec la masse et la longueur mais pas avec l'âge des brochets (tableau 5).

La comparaison des droites de régression de la concentration de Hg en fonction de la longueur entre les brochets >562 mm du lac Saint-Laurent et ceux du secteur fluvial indique que les pentes ne sont pas significativement différentes (ANCOVA, F = 0,24; p = 0,628) mais que les ordonnées à l'origine sont dissemblables (F = 10,4; p = 0,003). Ainsi, un brochet d'une taille particulière (mais >562 mm) provenant de l'aval contient plus de Hg qu'un brochet de même taille provenant de l'amont (fig. 2). Les mêmes résultats sont obtenus lorsque la masse est utilisée en tant que variable indépendante dans l'analyse de régression.

Aucune différence significative n'a été décelée dans la concentration des métaux entre les deux populations de grands brochets (tableau 4). Il faut noter que la puissance de ces tests est inférieure à 0,10 pour tous les métaux, sauf pour le Zn (P = 0,44).

Finalement, il est intéressant de constater que 50% des meuniers noirs et 73% des grands brochets du lac Saint-Laurent ainsi que 5% des meuniers noirs et 59% des grands brochets du secteur fluvial dépassent la norme maximale de commercialisation (0,50 $\mu g \cdot g^{-1}$) de Hg recommandée par Santé et Bien-Être Canada (Ministère de l'Environnement et de l'Énergie 1997).

© 1999 CNRC Canada

Tableau 3. Moyennes et écarts-types ($\bar{x}$ ± e.t.) de l'âge, du poids, des longueurs totales et des coefficients de conditions des meuniers noirs (*Catostomus commersoni*) et des grands brochets (*Esox lucius*) capturés en amont et en aval du barrage Moses-Saunders sur le fleuve Saint-Laurent près de Cornwall, Ontario, et Massena, New York, et qui ont servis dans les analyses de contaminants.

	Barrage Moses-Saunders			
	Amont		Aval	
Paramètre biologique	*N*	$\bar{x}$ ± e.t.	*N*	$\bar{x}$ ± e.t.
Catostomus commersoni				
Âge (année)	26	7±1,5	22	8±2,0
Poids (g)	26	1056±259	22	1208±304
Longueur totale (mm)	26	449±34	22	473±42
k^a	26	1,15±0,12	22	1,13±0,13
Esox lucius (toutes les tailles)				
Âge (année)	11	5,2±1,8	39	4,5±2,0
Poids (g)	11	2327±793**	39	1111±543**
Longueur totale (mm)	11	706±75**	39	559±107**
k^a	11	0,638±0,060*	39	0,580±0,059*
Esox lucius (>562 mm)				
Âge (année)	11	5,2±1,8	18	5,4±1,9
Poids (g)	11	2327±793*	18	1526±474*
Longueur totale (mm)	11	706±75	18	639±59
k^a	11	0,638±0,060*	18	0,568±0,067*

Nota : Les différences significatives (test de *t*) sont indiquées par *, $0,05 > p > 0,01$; et **, $p < 0,001$. *N* représente le nombre de poissons.

[a] $k = 100\,000(\text{poids-longueur}^{-3})$.

Fig. 2. Comparaison des taux de bioaccumulation du Hg en fonction de la longueur des grands brochets (*Esox lucius*) capturés en amont (□) et aval (○) du barrage Moses-Saunders sur le fleuve Saint-Laurent près de Cornwall, Ontario, et Massena, New York. Les équations des pentes sont $y = 4,60x - 12,51$* pour les brochets de l'amont et $y = 5,26x - 14,06$* pour les brochets de l'aval. La différence significative (marquée par *) indique que les ordonnées à l'origine sont significativement différentes ($p = 0,003$). L'analyse a été effectué sur un total de 29 brochets, 11 provenant de l'amont et 18 de l'aval.

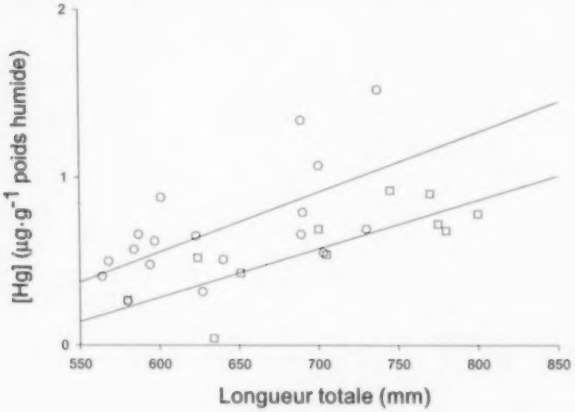

Meuniers noirs

Il n'y a pas de différences au niveau des paramètres de croissance entre les deux régions chez les meuniers noirs qui ont été analysés pour la présence de métaux. (Âge : $t = 1,592$; $p = 0,472$; longueur : $t = 2,117$; $p = 0,160$; poids : $t = 1,865$; $p = 0,276$; coefficient de condition : $t = 0,418$; $p = 1,000$ et les puissances sont 0,46, 0,55, 0,43 et 0,08 respectivement, tableau 3.)

Les meuniers mâles et femelles ont été regroupés lors des analyses statistiques, puisque aucune différence intersexuelle significative n'a été détectée dans les concentrations de métaux ($p > 0,05$ avec P (puissance) entre 0,10 et 0,25 pour tous les métaux).

Les meuniers noirs en amont du barrage semblent être plus contaminés en Cu, Mn, et Hg que ceux de l'aval (Cu : $t = 2,732$; $p = 0,045$; Mn : $t = 3,383$; $p = 0,010$; Hg : $t = 4,443$; $p = 0,001$; tableau 4). En fait, les meuniers noirs de l'amont contiennent, en moyenne, cinq fois plus de Hg. Aucune différence significative n'a été observée pour les concentrations de Cd et de Zn (Cd : $t = 0,298$; $p = 1,000$; Zn : $t = 0,266$; $p = 1,000$; tableau 4). La puissance de ces derniers tests est cependant faible ($P = 0,04$ dans les deux cas).

L'accumulation de métaux n'est pas associée avec l'âge, la longueur, le poids ni le coefficient de condition des deux populations de meuniers noirs (les résultats pour l'âge seulement sont présentés au tableau 5).

Discussion

Les brochets

L'effet de l'augmentation de la concentration en Hg qui suit la mise en eau du réservoir (Verdon et al. 1991) semble être complètement disparu chez les brochets. En effet, les brochets du réservoir montrent même une concentration en Hg plus faible que ceux vivant dans le secteur en aval du barrage. L'inégalité des ordonnées à l'origine des régressions de la concentration en Hg en fonction de la longueur

© 1999 CNRC Canada

Tableau 4. Moyennes et écarts-types ($\bar{x}$ ± e.t.) des concentrations ($\mu g \cdot g^{-1}$ de poids humide) de Cu, Zn, Cd, Mn et de Hg dans le foie de meuniers noirs (*Catostomus commersoni*) ainsi que dans la musculature épaxiale du grand brochet (*Esox lucius*) capturés en amont et aval du barrage Moses-Saunders sur le fleuve Saint-Laurent près de Cornwall, Ontario, et Massena, New York.

	Barrage Moses-Saunders			
	Amont		Aval	
Éléments	*N*	$\bar{x}$ ± e.t.	*N*	$\bar{x}$ ± e.t.
Catostomus commersoni				
Cu	24	9,772±4,598*	22	6,481±3,425*
Zn	25	0,034±0,017	22	0,033±0,011
Cd	24	0,097±0,065	21	0,102±0,059
Mn	24	1,660±0,389*	22	1,230±0,473*
Hg	25	1,056±1,217**	21	0,223±0,114**
Esox lucius				
Cu	11	23,9±11,6	39	26,2±10,8
Zn	11	5,09±1,70	39	6,26±2,03
Cd	11	0,01±0,01	39	0,01±0,05
Mn	11	0,13±0,08	39	0,15±0,09
Hg	11	0,59±0,27	39	0,55±0,30

Nota : Les différences significatives des tests de *t* sont indiquées par * (p est 0,05 et 0,010) et ** ($p < 0,001$). *N* représente le nombre de poissons.

totale indique que pour une longueur particulière, un brochet provenant de l'aval du barrage est plus contaminé qu'un brochet provenant de l'amont et ce, malgré le fait que ces derniers soient moins lourds pour le même âge. L'égalité des pentes indique un taux de bioaccumulation similaire pour les brochets plus longs que 562 mm chez les deux populations. La concentration de Hg augmente donc aussi rapidement chez les grands brochets du lac Saint-Laurent que chez les poissons de taille similaire provenant du secteur fluvial en aval. Ceci sous-entend que le taux de bioaccumulation du mercure est plus rapide chez les brochets de moins de 562 mm provenant du secteur en aval du barrage.

Comment expliquer la contamination accrue en Hg des brochets du lac Saint-François comparativement aux brochets du lac Saint-Laurent? Il est possible que cette contamination reflète le fait historique que les effluents industriels riches en métaux aient surtout été déversés en aval du barrage (STLRT 1992). Cette contamination anthropique se manifesterait particulièrement chez les espèces, comme le brochet, qui sont au sommet de la chaîne trophique.

Également, plusieurs chercheurs ont noté que le régime alimentaire des poissons joue un rôle important dans l'accumulation du Hg (Mathers et Johanssen 1985; Phillips et al. 1980; MacCrimmon et al. 1983). Une différence dans le régime alimentaire des jeunes brochets de chaque région pourraient donc expliquer les différences détectées chez les grands poissons (>562 mm). Une étude de contenus stomacaux de jeunes brochets (62 mm) pourrait éventuellement permettre de vérifier cette hypothèse. Nous savons cependant que la communauté piscicole riveraine du secteur en aval du barrage contient d'abondantes populations de perchaudes ainsi qu'une diversité plus importante d'espèces de poissons proies (Ribey 1997).

Les deux populations de brochets ne présentent pas de différences dans leurs concentrations de métaux (Cu, Mn, Cd, Zn). Cependant, la puissance de ces tests est très faible. En présumant que la variabilité des concentrations de métaux qui a été détectée est représentative, il faudrait jusqu'à 10 fois plus de spécimens pour atteindre un seuil de puissance de 0,80. Ceci implique que, pour vérifier avec plus de précision les différences de concentrations de ces métaux, il serait nécessaire d'augmenter d'autant le nombre de poissons analysés.

Le Hg est le seul métal pour lequel il y a bioaccumulation en fonction de la longueur, du poids ou de l'âge dans les deux régions. Une corrélation négative est observée entre la concentration de Zn, Mn et Cu et la longueur des brochets plus longs que 562 mm du lac Saint-François. Cette corrélation négative, observée par d'autres chercheurs (Wiener et Giesy 1979; Bohn et McElroy 1976; Giesy et Wiener 1977; Murphy et al. 1978), suggère une régulation homéostatique de ces éléments.

Les meuniers

Les meuniers noirs du réservoir sont plus contaminés en Hg, Cu, et Mn que ceux du lac Saint-François. La concentration moyenne de Hg est de cinq fois plus élevée dans le lac Saint-Laurent que dans le secteur en aval du barrage. Il est possible que l'augmentation du Hg qui suit la mise en eau d'un réservoir se fasse toujours sentir chez les meuniers. Or, ceci contredirait les résultats obtenus pour le brochet. De plus, les meuniers noirs étant à la base de la chaîne alimentaire, l'effet du réservoir devrait se dissiper plus rapidement chez ces poissons que chez les piscivores (Messier et Roy 1987). Finalement, le fort débit du fleuve Saint-Laurent suggère que le temps de résidence de l'eau dans le réservoir est court. On peut donc penser que le Hg naturel devrait être éliminé assez rapidement du réservoir (Verdon et al. 1991). Par conséquent, ceci voudrait dire que l'effet de mise en eau sur les concentrations de Hg serait probablement plus court pour le fleuve Saint-Laurent que dans le cas de barrages situés sur le bouclier précambrien. Donc, nous croyons que l'effet de la mise en eau du barrage est terminé et que les meuniers du réservoir ont une plus forte teneur en Hg pour d'autres raisons.

Les concentrations élevées de métaux chez les meuniers noirs du réservoir sont possiblement associées avec la présence de contaminants dans les sédiments. Les benthivores, tel le meunier noir, s'alimentent d'invertébrés souvent enfouis dans les sédiments. Ils sont donc constamment en contact avec ces sédiments. Si, pour des raisons inconnues, certaines zones du réservoir en amont du barrage sont particulièrement contaminées et que les meuniers montrent une certaine fidélité à un site d'alimentation, il est possible que les taux de contamination reflètent la contamination des sédiments de ces zones d'alimentation. Malheureusement, la plupart des meuniers les plus contaminés par les métaux ont été capturés près des sites de fraye (ruisseau Hoople). Les poissons ne restent que quelques jours sur le site de fraye et se dispersent par la suite dans le fleuve. On ne connaît rien des mouvements individuels des poissons hors de la saison de reproduction. Par conséquent, on ne sait pas s'il y a une certaine fidélité à une zone d'alimentation. Des études de marquage permettraient de vérifier cette hypothèse.

© 1999 CNRC Canada

Tableau 5. Régressions linéaires entre les paramètres biologiques (l'âge, la masse et la longueur) et la concentration de Cu, Zn, Cd, Mn et de Hg dans le foie de meuniers noirs (*Catostomus commersoni*) ainsi que dans la musculature épaxiale du grand brochet (*Esox lucius*) capturés en amont et aval du barrage Moses-Saunders sur le fleuve Saint-Laurent près de Cornwall, Ontario, et Massena, New York.

		Barrage Moses-Saunders					
		Amont			Aval		
Paramètres	Métaux	r^2	F	p	r^2	F	p
Catostomus commersoni							
Âge	Cu	0,04	1	0,99	0,08	1,84	0,57
	Zn	0,01	0,19	1	0	0,08	1
	Cd	0,09	2,22	0,45	0,16	3,68	0,21
	Mn	0,01	0,17	1	0,05	0,99	1
	Hg	0,06	1,37	0,76	0,13	2,93	0,31
Esox lucius							
Âge	Cu	0,06	0,59	1	0,04	1,43	0,72
	Zn	0,08	0,76	1	0,03	1,04	0,95
	Cd	0	0,04	1	0	0,16	1
	Mn	0,26	2,85	0,39	0,06	2,39	0,39
	Hg	0,35	4,93	0,15	**0,28**	14,09	<0,001
Masse	Cu	0,04	0,32	1	0,09	3,62	0,2
	Zn	0,02	0,21	1	**0,17**	**7,98**	**0,02**
	Cd	0,03	0,23	1	0,02	0,71	1
	Mn	0,17	1,58	0,73	0,06	2,46	0,38
	Hg	**0,56**	**11,39**	**0,02**	**0,38**	**22,94**	**<0,001**
Longueur	Cu	0,01	0,12	1	–0,13	5,49	0,08
	Zn	0,1	0,97	1	**–0,18**	**7,98**	**0,02**
	Cd	0,01	0,05	1	0,01	0,4	0,53
	Mn	0,01	0,11	1	–0,13	5,66	0,07
	Hg	**0,65**	**16,6**	**0,01**	**0,39**	**23,3**	**<0,001**

Nota : Les valeurs significatives (en caractères gras) indiquent la présence de bioaccumulation.

La contamination accrue de Hg retrouvée chez certains meuniers du lac Saint-Laurent pourrait également avoir comme source le lac Ontario, puisque 95% de l'eau du lac Saint-Laurent provient du lac Ontario (STLRT 1992). Potter et al. (1975) attribuent les concentrations élevées de Hg des réservoirs à la rétention accrue du Hg transporté par le courant. Ce dernier phénomène pourrait expliquer, en partie, les concentrations de contaminants plus élevées observées chez les meuniers du lac Saint-Laurent, puisque le barrage Moses-Saunders est le premier barrage important en aval du lac Ontario. Le réservoir du barrage servirait ainsi de bassin de sédimentation pour les contaminants provenant des grands lacs.

Nous n'avons pas observé de bioaccumulation de métaux chez les meuniers. La grande variabilité de nos concentrations de métaux, qui se traduit par une faible puissance de nos tests statistiques, peut expliquer l'absence de détection de bioaccumulation chez cette espèce. Heit et Klusek (1985) ont trouvé que le Cd et le Cu ne s'accumulaient pas avec l'âge chez les meuniers noirs. Ils ont aussi trouvé que le Hg s'accumulait en fonction du poids et qu'il y avait une corrélation négative entre le poids et la concentration de Zn chez ces poissons. Bendell-Young et al. (1986) et McFarlane et Franzin (1980) ont trouvé que le Cd dans le foie des meuniers s'accumulait avec l'âge. Ces derniers ont également trouvé qu'il n'y avait pas de bioaccumulation de Cu et de Hg avec l'âge. Il ne semble donc pas y avoir de consensus sur ces sujets dans la littérature.

Remerciements

Nous tenons à remercier, J. Loop et J.-M. Weber pour l'accès à leur laboratoire, J.A. Cooper, S. Ribey, L. Willard, M.D. Lemay et D. Bajurny pour leur participation lors de la capture des poissons, J. Vaive et G. Hall de la Commission Géologique du Canada pour l'analyse de détection des métaux, et C. Renaud (Musée canadien de la nature) pour la révision de cet ouvrage. Ce projet a été financé par un octroi du gouvernement fédéral (EcoRecherche : Réhabilitation de l'écosystème du Saint-Laurent) dans le cadre du Plan Vert de l'Institut de Recherche sur l'Environnement et l'Économie (Chercheur principal : Philippe Crabbé).

Bibliographie

Bendell-Young, L.I., Harvey, H.H., et Young, J.F. 1986. Accumulation of cadmium by white suckers (*Catostomus commersoni*) in relation to fish growth and lake acidification. J. Can. Sci. Halieutiques Aquat. **43** : 806–811.

Bohn, A., et McElroy, R.O. 1976. Trace metals (As, Cd, Cu, Fe and Zn) in Arctic cod, Boreogadus saida, and selected zooplancton from Strathcona Sound, northern Baffin Island. J. Fish. Res. Board Can. **33** : 2836–2840.

Bodaly, R.A., Hecky, R.E., et Fudge, R.J.P. 1984. Increases in fish mercury levels in lakes flooded by the Churchill River diversion, northern Manitoba. J. Can. Sci. Halieutiques Aquat. **41**: 682–691.

Brown, J.R., et Chow, L.Y. 1977. Heavy metal concentrations in Ontario fish. Bull. Environ. Contam. Toxicol. **17**: 190–195.

© 1999 CNRC Canada

Giesy, J.P, Jr., et Wiener, J.G. 1977. Frequency distributions of trace metal concentrations in five freshwater fishes. Trans. Am. Fish. Soc. **106** : 393–403.

Gupta, B.N., et Mathur, A.K. 1983. Toxicity of heavy metals. Indian J. Med. Sci. **37** : 236–240.

Heit, M., et Klusek, C.S. 1985. Trace element concentrations in the dorsal muscle of white suckers and brown bullheads from two acidic Adirondack lakes. Water Air Soil Pollut. **25** : 87–96.

Jackson, T.A. 1988. The mercury problem in recently formed reservoirs of northern Manitoba (Canada): effects of impoundment and other factors on the production of methyl mercury by microorganisms in sediments. J. Can. Sci. Halieutiques Aquat. **45** : 97–121.

Jackson, T.A. 1991. Biological and environmental control of mercury accumulation by fish in lakes and reservoirs of northern Manitoba, Canada. Can. J. Fish. Aquat. Sci. **48** : 2449–2470.

MacCrimmon, H.R., Wren, C.D., et Gots, B.L. 1983. Mercury uptake by lake trout Salvelinus namaycush, relative to age, growth, and diet in Tadenak Lake with comparative data from other Precambrian Shield lakes. J. Can. Sci. Halieutiques Aquat. **40** : 114–120.

Marcovecchio, J.E., et Moreno, V.J. 1993. Cadmium, zinc and total mercury levels in the tissues of several fish species from La Plata river estuary, Argentina. Environ. Monit. Assess. **25** : 119–130.

Mathers, R.A., et Johanssen, P.H. 1985. The effects of feeding ecology on mercury accumulation in walleye (*Stizostedion vitreum*) and pike (*Esox lucius*) in Lake Simcoe. Can. J. Zool. **63** : 2006–2012.

McFarlane, G.A., et Franzin, W.G. 1980. An examination of Cd, Cu, and Hg concentrations in livers of northern pike, Esox lucius, and white sucker, *Catostomus commersoni*, from five lakes near a base metal smelter at Flin Flon, Manitoba. J. Can. Sci. Halieutiques Aquat. **37** : 1573–1578.

Messier, D., et Roy, D. 1987. Concentrations en mercure chez les poissons au complexe hydroélectrique de la Grande rivière (Québec). Nat. Can. (Quebec), **114** : 357–368.

Murphy, B.R., Atchison, G.J., McIntosh, A.W., et Kolar, D.J. 1978. Cadmium and zinc content of fish from industrially contaminated lake. J. Fish. Biol. **13** : 327–335.

Phillips, G.R., Lenhart, T.E., et Gregory, R.W. 1980. Relationship between trophic position and mercury accumulation among fishes from the Tongue River Reservoir, Montana, U.S.A. Environ. Res. **22** : 73–80.

Potter, L., Kidd, D., et Strandiford, D. 1975. Mercury levels in Lake Powell. Bioamplification of mercury in man-made desert reservoirs. Environ. Sci. Technol. **9** : 41–46.

Pourang, N. 1995. Heavy metal bioaccumulation in different tissues of two fish species with regards to their feeding habits and trophic levels. Environ. Monit. Assess. **35** : 207–219.

Ribey, S.C. 1997. Characterization of litteral fish assemblages and their habitat in the St. Lawrence River near Cornwall, Ontario. M.Sc. thesis, University of Ottawa, Ottawa, Ont.

Ridgway, L.L. 1996. Population characteristics and contaminant burdens of the white sucker (*Catostomus commersoni*) from the St. Lawrence River near Cornwall, Ontario and Massena, New York. M.Sc. thesis, University of Ottawa, Ottawa, Ont.

Ridgway, L.L., Chapleau, F., Comba, M.E., et Bockus, S.M. 1999. Population characteristics and contaminant burdens of the white sucker (*Catostomus commersoni*) from the St. Lawrence River near Cornwall, Ontario, and Massena, New York. J. Great Lakes Res. Sous presse.

STLRT (St. Lawrence Rap Team). 1992. The St. Lawrence River area of concern remedial action plan for Cornwall – Lake St. Francis Area, stage 1 report : environmental conditions and problem definition. Environment Canada and Environment Ontario, Cornwall.

STLRT (St. Lawrence Rap Team). 1994. The St. Lawrence River area of concern remedial action plan for Cornwall-Lake St. Francis Area, stage 2 report: Choices for cleanup: deciding the future of a great river. Environment Canada and Environment Ontario, Cornwall.

Verdon, R., Brouard, D., Demers, C., Lalumière, R., Laperle, M., et Schetagne, R. 1991. Mercury evolution (1978–1988) in fishes of the La Grande hydroelectric complex, Québec, Canada. Water Air Soil Pollut. **56** : 405–417.

Wiener, J.G., et Giesy, J.P. 1979. Concentrations of Cd, Cu, Mn, Pb, and Zn in fishes in a highly organic softwater pond. J. Fish. Res. Board Can. **36** : 270–279.

Wilkinson, L. 1990. SYSTAT: the system for statistics. SYSTAT Inc., Evanston, Ill.

© 1999 CNRC Canada

Multiple dispersal strategies of the invasive quagga mussel (*Dreissena bugensis*) as revealed by microsatellite analysis

A.B. Wilson, K-A Naish, and E.G. Boulding

Abstract: The recent invasion of the Laurentian Great Lakes by *Dreissena polymorpha* and *Dreissena bugensis* presents a unique opportunity to study the role of high dispersal ability in the colonization success of invading species. While the dispersal of *D. polymorpha* has been characterized by several jump dispersal events, census data suggest a more gradual diffusion of *D. bugensis* from its point of introduction through the lower Great Lakes. In this study, we use six highly polymorphic microsatellite markers to investigate the present-day population genetic structure of *D. bugensis* in North America in an effort to clarify the role of multiple dispersal strategies in its colonization success. In contrast with survey data, which would suggest a gradual spread ultimately resulting in a pattern fitting a model of isolation-by-distance, the significant allelic and F_{ST} differences observed between 18 of 28 population pairs do not correlate with any simple geographic relationship. Deviations from isolation-by-distance are due, in part, to a higher gene flow between disjunct populations than that expected under a normally distributed pattern of dispersal. These results, in combination with recent reports of the quagga mussel outside its established North American range, suggest that boater-mediated jump dispersal of *D. bugensis* may be contributing to its colonization and spread in North America.

Résumé : L'invasion récente des Grands Lacs laurentiens par *Dreissena polymorpha* et *D. bugensis* constitue une occasion unique d'étudier le rôle d'une forte capacité de dispersion pour le succès de colonisation de l'espèce envahissante. Bien que la dispersion de *D. polymorpha* se soit caractérisée par plusieurs sauts, les données d'enquête montrent une diffusion plus graduelle de *D. bugensis* à partir de son point d'introduction dans les Grands Lacs inférieurs. Nous avons utilisé six marqueurs microsatellites fortement polymorphes pour étudier la structure génétique de la population actuelle de *D. bugensis* en Amérique du Nord dans le but de préciser le rôle de diverses stratégies de dispersion pour le succès de la colonisation. Au contraire des données des relevés, qui indiquent une diffusion graduelle finissant par donner une allure conforme à un modèle d'isolement par la distance, les écarts significatifs entre les allèles et les F_{ST} observés entre 18 des 28 paires de populations ne présentaient pas de corrélation avec aucune relation géographique simple. Les écarts au modèle isolement par la distance s'expliquent, du moins en partie, par un flux génétique plus élevé entre les populations isolées que celui que l'on peut prévoir conformément à un régime de répartition à distribution normale. Ces résultats, combinés à des signalements récents de moules quagga à l'extérieur de son aire de répartition établie en Amérique du Nord, portent à croire que les sauts de dispersion de *D. bugensis* favorisés par le déplacement des bateaux pourraient contribuer à sa colonisation et à sa diffusion en Amérique du Nord.

[Traduit par la Rédaction]

Introduction

Biological invasions are characterized by two key phases: the establishment of a species at a location and its subsequent radiation in space (Hastings 1996). Both the establishment of an initial population and successful naturalization of a species in its new habitat are critical to its colonization success. Theoretical ecologists have developed a number of models in an effort to clarify the relationship between demographic parameters and the rate of range expansion of introduced species (Hastings 1996). While empirical verification of these models is incomplete, existing data suggest that rare, long-distance jump dispersal events may play an important role in the spread of recent invaders (Hastings 1996).

Until recently, estimates of species spread following invasion have been limited to ecological and laboratory studies of life history parameters and survey data documenting range expansion (Hastings 1996). With the advent of highly polymorphic molecular markers, a greater understanding of the parameters underlying the spread of a natural population may be obtained, providing data on rates of gene flow between populations and clarifying secondary introductions that may have a significant impact on the population structure of an invasive species.

The quagga mussel (*Dreissena bugensis*) is native to the Dnieper drainage system in the Ukraine (Mills et al. 1996).

Received February 25, 1999. Accepted August 6, 1999. J15034

A.B. Wilson, K-A Naish, and E.G. Boulding. Department of Zoology, University of Guelph, Guelph, ON N1G 2W1, Canada.

[1]Author to whom all correspondence should be sent at the following address: Faculty of Biology, University of Konstanz, Konstanz, Germany, D-78457. e-mail: tony.wilson@uni-konstanz.de

© 1999 NRC Canada

Fig. 1. Map of *D. bugensis* sampling sites. See Table 1 for detailed information on sampling methods and locations. The encircled cross indicates the putative point of the 1989 introduction (Mills et al. 1993).

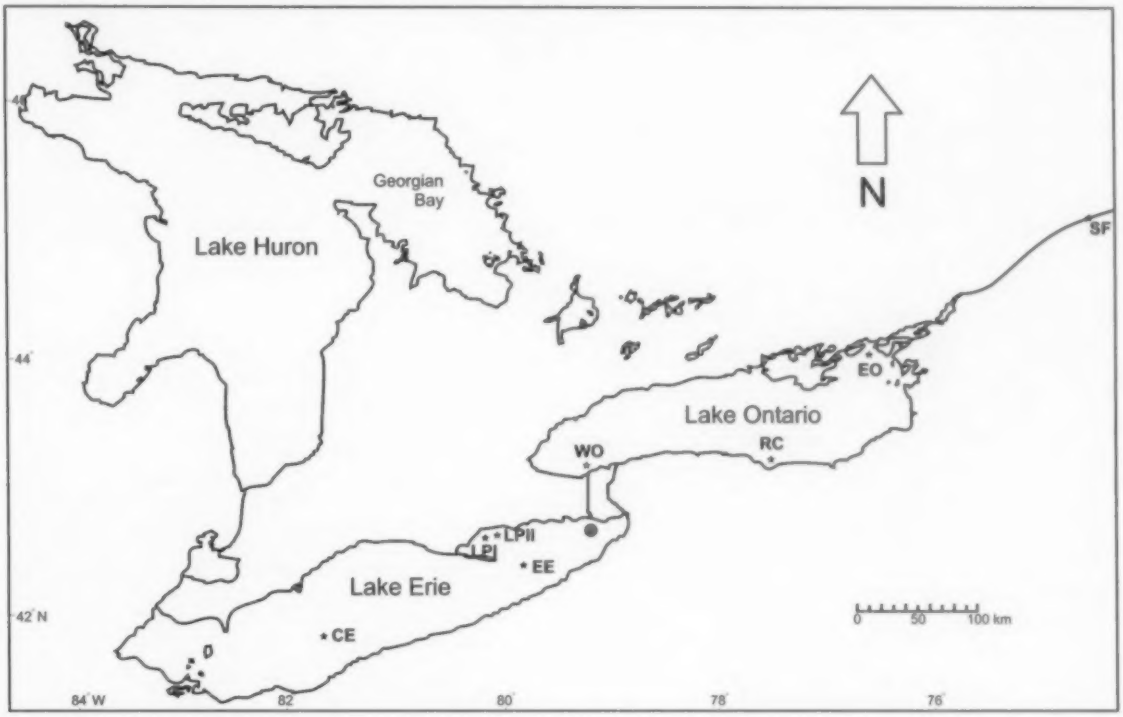

In 1989, *D. bugensis* individuals were identified in eastern Lake Erie, Canada (May and Marsden 1992; Mills et al. 1993; see Fig. 1). The quagga mussel spread rapidly following its initial colonization and by 1996 had spread through Lake Erie to Lake Ontario and the St. Lawrence River (Mills et al. 1996). Researchers have hypothesized that dreissenid mussels were introduced into the Laurentian Great Lakes following transoceanic transport of mussel larvae in the ballast water of ships (Hebert et al. 1989).

Studies on temporal variation in distribution of dreissenid mussels have benefited from an extensive survey program (U.S. Geological Survey 1997) that was established following the identification of the zebra mussel (*Dreissena polymorpha*) in Lake St. Clair, Ontario, in 1988 (Hebert et al. 1989). Census data suggest that the two dreissenid species may have colonized the Great Lakes by differing methods. While the spread of the zebra mussel has been characterized by several long-distance jump dispersal events within the Laurentian Great Lakes, the quagga mussel has exhibited a much more gradual downstream diffusion from its initial introduction in Lake Erie eastward into Lake Ontario and the St. Lawrence River (Mills et al. 1993).

Despite their apparent differential patterns of colonization, the radiation of both *D. bugensis* and *D. polymorpha* has been exceedingly rapid following their initial introduction. The quagga and zebra mussel share two notable life history characteristics that may have accelerated their colonization and spread through the Laurentian Great Lakes (Johnson and Carlton 1996). Firstly, both *D. bugensis* and *D. polymorpha* have a planktonic veliger stage, whereby free-living larvae can remain suspended in the water column for up to several weeks (Carlton 1993). During this time, larvae passively diffuse in lacustrine currents and, upon settlement, may found new populations.

Secondly, dreissenid mussels are byssate and can attach to hard substrate by producing byssal threads (Mills et al. 1996). *Dreissena* spp. have been found attached to the hulls of ships (Johnson and Carlton 1996). Movements of boats both within lakes (Johnson and Carlton 1996) and overland (Ricciardi et al. 1995) may result in the formation of new mussel populations in geographically disparate regions. Boat traffic and, to a lesser degree, birds and fish may have facilitated dispersal of the zebra mussel to upstream sites in Lake Superior, Lake Michigan, and Lake Huron from founding populations in Lake St. Clair (Carlton 1993).

While it is often difficult to directly track dispersal in aquatic environments, genetic techniques have often proven useful as indirect estimators of aquatic dispersal (Palumbi 1995; Parsons 1996). Classical population genetic models predict that geographically limited dispersal results in genetic isolation-by-distance even within large continuous populations (Wright 1946). Rousset (1997) further developed a model of isolation-by-distance using a regression approach to indirectly quantify demographic parameters such as population density and dispersal distance from genetic data.

Modelling studies by Ibrahim et al. (1996) have demonstrated that rare long-distance migration during range expansion can lead to the establishment of pocket populations in advance of the main invasion front, resulting in patterns of spatial clustering that can persist for hundreds of genera-

© 1999 NRC Canada

Table 1. *Dreissena bugensis* sampling site locations.

Sampling site	Coordinates	Depth (m)	Sampling technique	*N*	Date sampled, 1997
Central Erie (CE)	41°57.000′ N, 81°37.470′ W	10.0	Ponar grab (2)	54	October 7
Long Point Bay I (LPI)	42°42.960′ N, 80°15.084′ W	8.4	Ponar grab (3)	54	June 24
Long Point Bay II (LPII)	42°46.290′ N, 80°08.460′ W	8.4	Ponar grab (6)	54	June 22
Eastern Erie (EE)	42°30.394′ N, 79°53.798′ W	63.0	Ponar grab (2)	54	June 25
Western Ontario (WO)	43°13.471′ N, 79°16.356′ W	14.0	Ponar grab (3)	54	June 18
Rochester (RC)	43°24.500′ N, 77°53.000′ W	1.0	Shoreline	54	December 7
Eastern Ontario (EO)	44°09.020′ N, 76°38.000′ W	22.0	Ponar grab (3)	54	October 29
Lake St. Francis (SF)	45°07.140′ N, 74°21.010′ W	15.0	SCUBA	54	February 28

tions. Long-distance dispersal may have several important impacts on population genetic structure. Firstly, long-distance dispersal may lead to an upward bias in F_{ST} over that expected under normally distributed dispersal (Ibrahim et al. 1996). Secondly, a plot of isolation-by-distance regression in species that disperse over long distances should be skewed by lower differentiation at great distances (Rousset 1997). Finally, assuming that peripheral populations remain isolated in long-distance dispersers, higher inbreeding should be observed in these isolated populations (Ibrahim et al. 1996). Through an analysis of the deviation of genetic data from a model of isolation-by-distance, researchers can indirectly quantify the role of long-distance migration in range expansion of a species.

In this study, we use highly polymorphic microsatellite markers in an effort to clarify the present-day population genetic structure of the quagga mussel in the Laurentian Great Lakes. These data can serve as an indirect estimate of the dispersal of *D. bugensis* through North American waterways. As noted above, census data suggest a gradual diffusion of *D. bugensis* from its initial introduction into Lake Erie. Such a gradual diffusion should exhibit a strong fit to the isolation-by-distance model. Alternatively, departures from this model may indicate that additional dispersal mechanisms have also contributed to the range expansion of *D. bugensis*. Microsatellite markers will help to quantify this pattern of spread, clarifying the role that human-mediated dispersal vectors have played in the spread of the quagga mussel.

Materials and methods

Sample collection and microsatellite analysis

Adult *D. bugensis* were collected from a combination of nearshore and offshore habitats representing the extent of the species' range in the lower Laurentian Great Lakes (Fig. 1; Table 1). Upon collection, samples were extracted immediately or frozen at –90°C until further use. Population sample sizes were chosen following simulation study (Ruzzante 1998; Wilson 1998) in an effort to minimize statistical bias.

DNA extraction and amplification of the six microsatellite loci (*Dbug*1–6) was performed as outlined in Wilson et al. (1999). For each of the six loci, allelic ladders were constructed using a combination of polymerase chain reaction products from individual mussels. These allelic ladders were run every five lanes in each gel and helped to facilitate scoring of gels and to maintain consistency of scoring between different gel runs.

Statistical analyses

Linkage disequilibrium

Loci data were tested for genotypic disequilibrium using GENEPOP V3.1a (Raymond and Rousset 1995*a*). For the analysis, a 10 000-batch, 1000-iteration Markov chain analysis was preceded by a 10 000-step dememorization process.

Hardy–Weinberg equilibrium

Observed heterozygosities within populations were tested for departure from Hardy–Weinberg expectations using Weir and Cockerham's (1984) estimate as implemented by GENEPOP V3.1a (Raymond and Rousset 1995*a*). For loci with fewer than five alleles, an exact *P* value was calculated by a complete enumeration method, and for loci with a higher number of alleles, a 10 000-step, 1000-iteration Markov chain method (10 000 dememorization steps) was used to calculate an unbiased estimate of the *P* value.

Population differentiation

Tests for genotypic differentiation of populations are less powerful than those that assume random sampling of alleles (genic differentiation) but more appropriate when individuals exhibit nonrandom mating (Goudet et al. 1996). Both global and pairwise tests were performed, using GENEPOP V3.1a (Raymond and Rousset 1995*a*), in an effort to clarify the pattern of interpopulation differentiation. An unbiased estimate of the significance of the probability test was calculated through a 10 000-step, 1000-iteration Markov chain permutation (10 000 dememorization steps) of an R × C contingency table of allelic distribution for each population. The significance of the *P* values across the six loci was determined using Fisher's probability combination test (Raymond and Rousset 1995*b*).

Genetic distance between populations was measured by calculating F_{ST} and linearized with population divergence time via a transformation (linearized $F_{ST} = F_{ST}/(1 - F_{ST})$, Slatkin 1993) using Arlequin V1.1 (Schneider et al. 1997). The significance of these F_{ST} estimates was tested under the null hypothesis H_0 = "no difference between populations" by permuting genotypes between populations (10 000 iterations). The *P* value of the test is the proportion of permutations leading to an F_{ST} value larger or equal to that observed (Schneider et al. 1997).

Isolation-by-distance

Models of isolation-by-distance offer an empirical means to test patterns of dispersal from measures of population subdivision. Subdivided natural populations that fit a one-dimensional diffusive stepping-stone model should exhibit a strong fit to the isolation-by-distance model (Rousset 1997). Through simulation study, Rousset (1997) has found a linear relationship between $F_{ST}/(1 - F_{ST})$ and distance for one-dimensional habitats. Linearized pairwise F_{ST} estimates were plotted against the linear distance between populations. In addition to a computation of the linear regression between these two parameters, a Mantel permutation test (10 000 permutations)

© 1999 NRC Canada

Fig. 2. Allele frequency histograms for *D. bugensis* microsatellite loci.

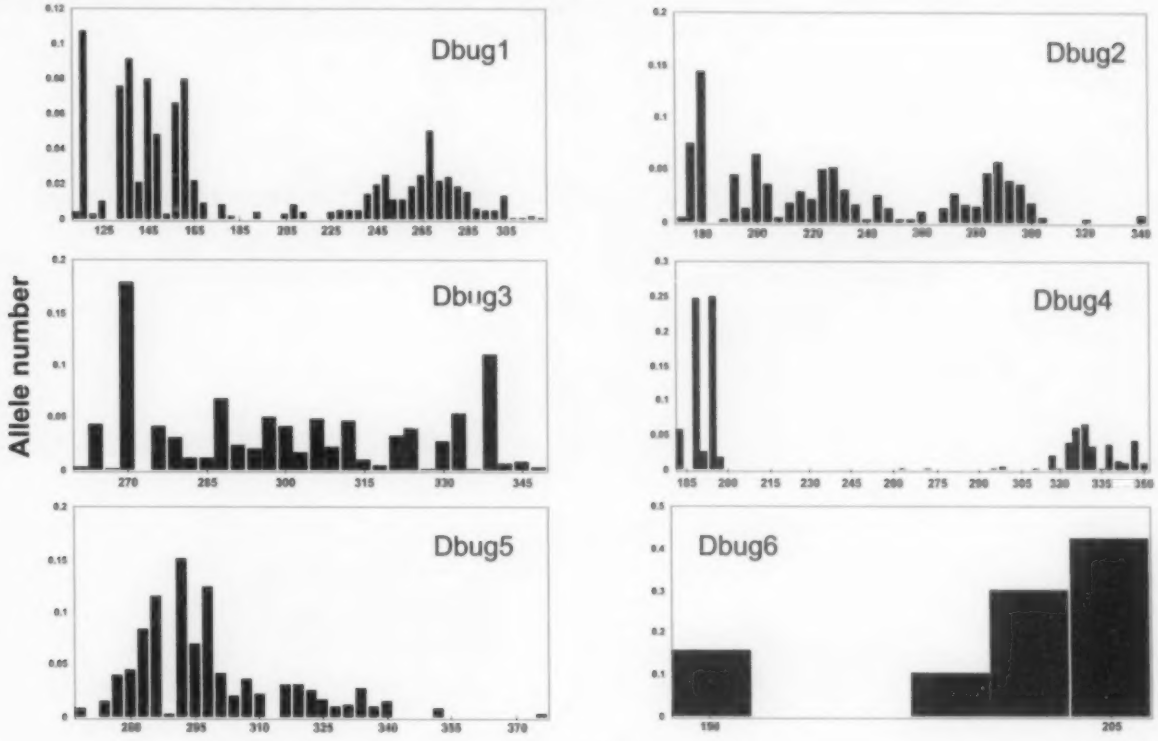

was used to test the null hypothesis H_0 = "genetic distance and geographic distance are independent" using a rank correlation coefficient calculated from the pairwise F_{ST}–distance matrix. To aid in further interpretation of overall trends of population subdivision, pairwise linearized F_{ST} estimates were also plotted versus absolute distance separating populations from a sample representing the western extent of the species' range.

Analysis of molecular variance (AMOVA)

In a further analysis of the correlation between genetic distance and topographic characteristics of the lower Great Lakes, an F_{ST}-based hierarchical AMOVA (Excoffier et al. 1992) was used to clarify the partitioning of molecular variance between three levels: variation among lakes, among populations within a lake, and among individuals within populations. Groupings were chosen in relation to putative point of introduction of *D. bugensis* (see Fig. 1).

Results

Descriptive statistics

A total of 167 alleles were observed for the six loci over eight populations (432 individuals), ranging from a low of four alleles at *Dbug*6 to a high of 44 at *Dbug*1 (Fig. 2). Allelic frequency data were plotted as a size-ranked histogram to clarify the sampling space of the allelic distribution (Fig. 2). The allelic distribution of the six microsatellites varied significantly across loci, with *Dbug*1 and *Dbug*4 exhibiting a bimodal distribution of alleles, *Dbug*5 displaying an approximately normal distribution, and *Dbug*2, *Dbug*3, and *Dbug*6 exhibiting a uniform distribution of alleles.

Linkage disequilibrium

Although exact tests for genotypic disequilibrium between microsatellite loci within populations gave five significant P values (χ^2 test, $P < 0.05$) out of 120 pairs of loci (4.17%), all values were rendered nonsignificant following sequential Bonferroni correction (Rice 1989). Global tests of linkage disequilibrium calculated from within-population data were not significant at the 5% level (χ^2 test), indicating that allelic variation at all six loci is in linkage equilibrium.

Hardy–Weinberg equilibrium

Departure from Hardy–Weinberg expectations was measured via a Markov chain permutation procedure for *Dbug*1–5 and a direct enumeration approach for *Dbug*6, which had fewer than five alleles. All six loci exhibit a significant heterozygote deficiency (χ^2 test, $P < 0.05$). The inbreeding coefficient (F_{IS}) was plotted by locus for each population (Fig. 3), graphically illustrating the departure from Hardy–Weinberg expectations.

Population differentiation

Global χ^2 tests of population differentiation indicated significant heterogeneity in gene frequencies among the eight populations ($P < 0.00001$). In an effort to further partition

© 1999 NRC Canada

Fig. 3. Hardy–Weinberg test for each locus in each *D. bugensis* population calculated using Weir and Cockerham's (1984) estimates as implemented by GENEPOP V3.1a (Raymond and Rousset 1995*a*). An asterisk indicates a significant heterozygote deficiency ($P < 0.05$). All loci exhibit a significant departure from Hardy–Weinberg equilibrium ($P < 0.00001$).

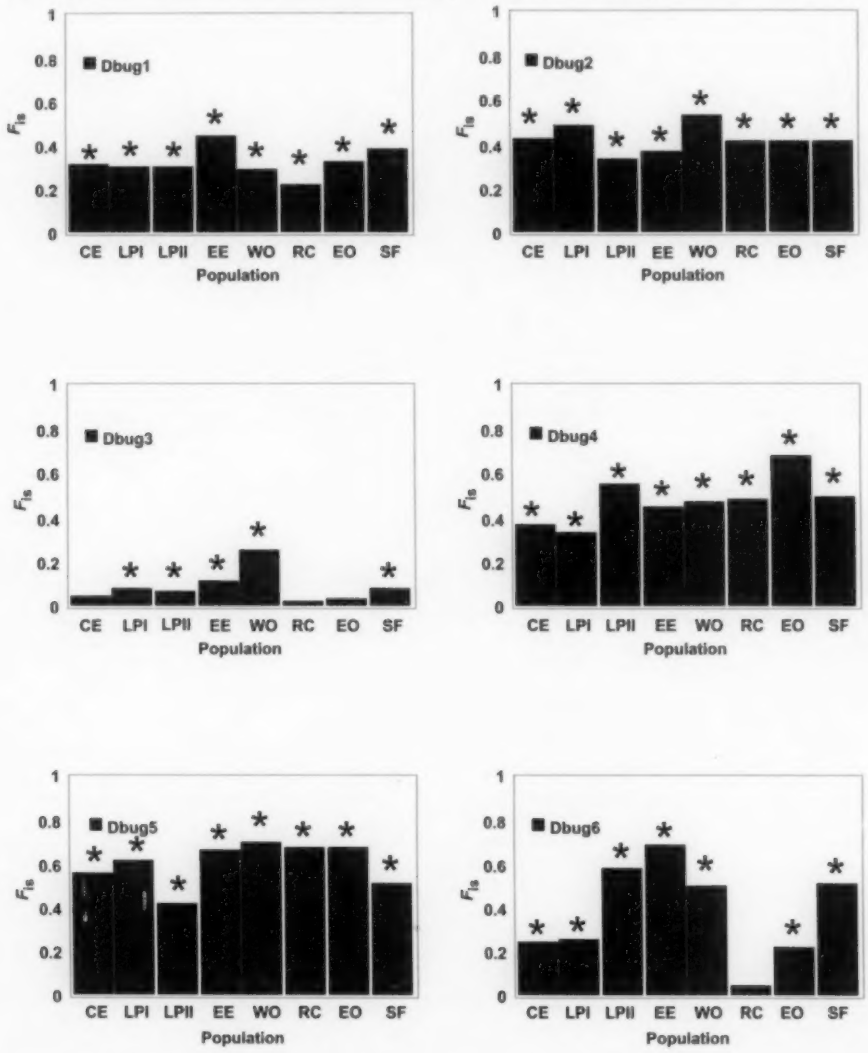

these data, pairwise estimates of genotypic differentiation were calculated (Table 2). Eighteen of 28 pairwise comparisons (75.0%) were significantly different at $P < 0.05$ (χ^2 test) following sequential Bonferroni correction (Rice 1989).

Pairwise F_{ST} estimates also showed high levels of genetic differentiation between populations (Table 3). Twenty-seven out of 28 population pairs (96.4%) were significantly differentiated on the basis of F_{ST}. While overall genetic differentiation was high, low levels of genetic differentiation were observed between several highly disjunct populations (e.g., central Erie – Lake St. Francis) under both exact tests for population differentiation and estimates based on F_{ST}.

Isolation-by-distance

While F_{ST} and exact tests of population differentiation both indicated significant differences between many populations, these differences are not correlated with the geographic distance between populations ($r^2 = 0.0344$; one-tailed Mantel test, $P = 0.32061$). The power of the significance of the regression slope (Zar 1984) was calculated to be 0.85. The high power of this test, coupled with the high P value observed, indicates that this result is not likely to be due to a type II error (i.e., falsely concluding that no significant difference occurs when, in fact, it does). These deviations from a pattern of isolation-by-distance suggest that diffusive dispersal of mussel larvae may not be the sole vector of gene flow between populations. The y-intercept of the regression line was positive and relatively large ($y = (8.818 \times 10^{-6}x) + 0.01395$), suggesting that gene flow maintained by long-distance dispersal has contributed to the poor overall fit to the isolation-by-distance model.

In an effort to clarify consistent trends contributing to the

© 1999 NRC Canada

Table 2. Fisher's exact test for genotypic differentiation: pairwise population comparisons.

Population–population	χ^2	*P* value
CE–LPI	18.951	0.0897
CE–LPII	49.326	0.0000*
CE–EE	15.617	0.2094
CE–WO	26.715	0.0085
CE–RC	69.710	0.0000*
CE–EO	43.590	0.0000*
CE–SF	16.912	0.1529
LPI–LPII	37.453	0.0002*
LPI–EE	27.296	0.0070
LPI–WO	31.517	0.0016*
LPI–RC	54.620	0.0000*
LPI–EO	41.404	0.0000*
LPI–SF	52.446	0.0000*
LPII–EE	46.171	0.0000*
LPII–WO	43.657	0.0000*
LPII–RC	29.308	0.0035*
LPII–WO	69.800	0.0000*
LPII–SF	62.704	0.0000*
EE–WO	22.172	0.0321
EE–RC	43.852	0.0000*
EE–EO	28.045	0.0054
EE–SF	19.155	0.0849
WO–RC	48.955	0.0000*
WO–EO	26.310	0.0097
WO–SF	22.523	0.0356
RC–EO	69.710	0.0000*
RC–SF	52.609	0.0000*
EO–SF	36.600	0.0003*

Note: Locus by locus pairwise *P* values were computed by GENEPOP V3.1a (Raymond and Rousset 1995*a*) and pooled using Fisher's χ^2 method for combining probabilities (Sokal and Rohlf 1981). Significance of pairwise comparisons was assessed following a sequential Bonferroni correction (Rice 1989). Global tests indicated that all loci were highly significantly differentiated among the eight populations ($P < 0.0001$). Asterisks indicate that allelic distributions are significantly different (χ^2 test, $P < 0.05$, df = 12).

deviation from isolation-by-distance, pairwise estimates of $F_{ST}/(1 - F_{ST})$ were plotted versus absolute distance (Fig. 4). Several key trends are observed over the range of the species. Firstly, and most significantly, even over short within-lake comparisons, there is no strong pattern of isolation-by-distance. Secondly, although some of the lowest levels of gene flow were detected between EO and the other sites, all populations exhibit a decrease in $F_{ST}/(1 - F_{ST})$ versus the Lake St. Francis population.

AMOVA

Populations were partitioned into two groups on the basis of their geographical relationship to the putative point of introduction of *D. bugensis* in eastern Lake Erie (see Fig. 1) in an effort to further clarify if the present-day genetic structure has been defined by historical colonization events. While significant ($P < 0.05$), less than 1% of the total genetic variation can be explained on the basis of these groupings (Table 4). These data are consistent with the isolation-by-distance test, indicating that while significant differences do exist, the current population genetic structure of *D. bugensis* in North America cannot be directly correlated with geographic distance between populations.

Discussion

The results of previous population census data (Mills et al. 1993) indicated that *D. bugensis* experienced a gradual diffusion from its initial point of introduction into Lake Erie. In contrast, the present population genetic study suggests that long-distance dispersal has also had a significant impact, maintaining gene flow between geographically disjunct populations. While significant differences were observed between many of the populations, tests of population subdivision and genotypic differentiation suggest that simple diffusion is not the sole factor underlying population structuring of the quagga mussel in the Laurentian Great Lakes. These empirical data support simulation study (Ibrahim et al. 1996), stressing the fact that the significance of long-distance dispersal must be taken into account in future theoretical estimates of species spread.

Descriptive statistics

The high number of alleles observed at five of six microsatellite loci (average allele number = 27.8 ± 7.5 alleles) allows the use of more powerful statistical tests for population structure than is possible using allozyme markers (Estoup et al. 1998). However, the overall low frequency of some of these alleles may confound analyses of population structure that place a higher significance on rare alleles (such as the private alleles method, see Slatkin 1985). While 14 putative private alleles were identified (Appendix), they are randomly distributed throughout the eight study populations and, given the low frequency at which they occur, may be present in one or more additional populations at a similar low frequency. In an effort to minimize bias associated with statistical estimators, Fisher's exact test for population differentiation and *F* statistics were chosen to estimate population structure (see Ruzzante 1998).

Distribution of alleles at each of the loci indicates that mutational modes at few, if any, of the loci fit strict stepwise mutation models. As the quagga mussel has only been present in the Laurentian Great Lakes for 8 years, the likelihood that de novo mutations have become established in North American populations appears unlikely. As the present-day allelic distribution in North American populations of *D. bugensis* may also be biased by historical founder effects, the use of F_{ST}, a more conservative estimator based on the infinite alleles model, is more appropriate than statistics that consider allelic size.

Deviation from Hardy–Weinberg equilibrium

All six loci exhibit significant heterozygote deficits, suggesting that nonrandom mating may be occurring in North American populations of *D. bugensis*. While outlying microsatellite loci may often exhibit significant heterozygote deficiencies due to differential amplification and (or) null alleles, the congruent pattern of heterozygote deficiency observed across all six loci demands a biological explanation. Three hypotheses relating to the life history of this species may help to explain this deviation. Firstly, *D.bugensis* is a

© 1999 NRC Canada

Table 3. Pairwise linearized F_{ST} estimates ($F_{ST}/(1 - F_{ST})$) (lower left) calculated by Arlequin V1.1 (Schneider et al. 1997) and distance between populations (km) (upper right) for eight study sites.

Population	CE	LPI	LPII	EE	WO	RC	EO	SF
CE	—	142	153	155	239	347	474	685
LPI	0.0059*	—	11	37	95	208	333	544
LPII	0.0089*	0.0116*	—	36	87	197	323	533
EE	0.0033	0.0150*	0.0146*	—	98	192	322	532
WO	0.0096*	0.0186*	0.0210*	0.0089*	—	115	236	446
RC	0.0097*	0.0134*	0.0117*	0.0127*	0.0189*	—	130	347
EO	0.0230*	0.0345*	0.0363*	0.0166*	0.0151*	0.0284*	—	211
SF	0.0113*	0.0305*	0.0230*	0.0058*	0.0105*	0.0182*	0.0172*	—

Note: Asterisks indicate that populations are significantly different (permutation test with sequential Bonferroni correction (Rice 1989), $P < 0.05$).

Fig. 4. Linearized F_{ST} ($F_{ST}/(1 - F_{ST})$) calculated by Arlequin V1.1 (Schneider et al. 1997) versus absolute linear distance from central Erie for each of six most westernly *D. bugensis* study populations.

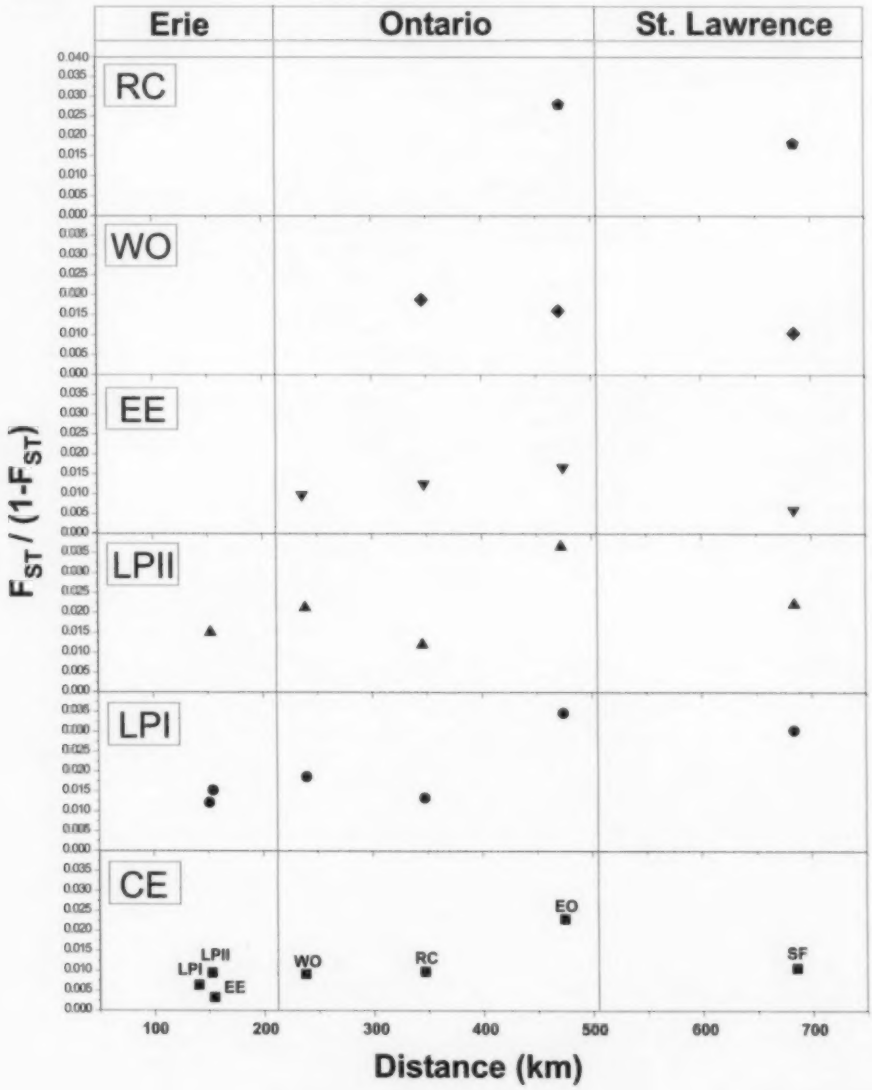

© 1999 NRC Canada

Table 4. AMOVA calculated by Arlequin V1.1 (Schneider et al. 1997).

Source of variation	df	Variance component	Percentage of variation
Among groups	1	0.00950 Va	0.39*
Among populations within groups	6	0.02526 Vb	1.03*
Among individuals within populations	424	0.86084 Vc	35.12*
Within individuals	432	1.55556 Vd	63.46*

Note: Populations were divided into two groups on the basis of location in relation to the putative point of introduction (Mills et al. 1993). Group 1: CE, LPBI, LPBII, EE; group 2: WO, RC, EO, SF. An asterisk indicates that the variance component is significant (permutation test, $P < 0.05$).

planktonic disperser. Thus, several cohorts of larvae that were spawned at different locations may settle at the same site. A genetic study of a single site, comprising several cohorts, could produce results that deviate from expected Hardy–Weinberg proportions, the homozygote excess known as the Wahlund effect (Hartl and Clark 1989).

A second explanation for the observed heterozygote deficiency is that clumps of adult mussels collected from the same site may often be half or full siblings produced by relatively few adults. Li and Hedgecock (1998) found differences in the genetic composition of oyster larvae within a single bay over an 11-day period that they attributed to temporal changes in the genetic composition of the adult population that produced the larvae. Their research highlights the fact that, as bivalves are capable of producing millions of larvae, only a few reproductive individuals may be needed to repopulate a large area.

Thirdly, heterozygote deficiencies among adult populations may arise due to selective pressures. Similarly high heterozygote deficiencies have been observed in adult populations of marine invertebrates with planktonic larvae (Singh and Green 1984; Beaumont 1991). Singh and Green (1984) hypothesized that heterozygous larvae may suffer greater mortality due to increased food requirements associated with higher growth rates, which could lead to an excess of homozygotes upon settlement. However, Haag and Garton (1995) found little support for this hypothesis in an examination of variation in allelic frequencies at a single allozyme locus during different life history stages of *D. polymorpha*. These data support the first hypothesis put forward here, that the high heterozygote deficiency that we observed at *D. bugensis* microsatellite loci may be more reasonably attributed to population-level effects than to differential mortality of larvae.

Because peripheral populations are often founded by rare, long-distance migrants, they may tend to show high levels of inbreeding within populations (Ibrahim et al. 1996). However, we did not observe the predicted pattern. No consistent population-level trends in inbreeding coefficient (F_{IS}) were observed across all six loci (Fig. 3). This may be due to the relatively continuous distribution of *D. bugensis* in the lower Great Lakes. While several peripheral populations may have originally been founded by low numbers of individuals, they may no longer be considered isolated given the present-day continuous distribution of the species in the lower Great Lakes.

High population differentiation

The F_{ST} values for *D. bugensis* ranged from 0.0033 to 0.0363 (mean = 0.016, SD = 0.0084) (Table 3). While population genetic data are limited for planktonic dispersers in freshwater systems, allozyme study has demonstrated comparable estimates of F_{ST} (in the range of 0.004–0.015) over a similar geographic range for marine species with extended planktotrophic development (Sarver and Foltz 1993; Holborn et al. 1994).

Both F_{ST} estimates and tests of population differentiation consistently demonstrate significant differences between 18 of 28 pairwise population comparisons. This high level of population differentiation does not correlate with any simple geographic relationship between populations, suggesting a complex pattern of interpopulation gene flow.

Deviations from isolation-by-distance and AMOVA

While the isolation-by-distance model is a useful tool for illuminating simple relationships between population structure and geography, it is limited in that it may be invalidated by as little as a single pairwise comparison that deviates from expectations (Rousset 1997). In this study, several geographically disjunct populations exhibit minimal population differentiation. While these major deviations from the isolation-by-distance model contribute to the poor overall fit of the genetic data to geography, a plot of pairwise F_{ST} versus absolute distance reveals a consistently higher level of gene flow between the Lake St. Francis site and all other populations than that that is expected under isolation-by-distance (Fig. 4). This congruent pattern adds additional strength to the hypothesis of long-distance dispersal of *D. bugensis*. The large positive *y*-intercept of the isolation-by-distance regression line also indicates a deviation from a normally distributed pattern of dispersal. We hypothesize that a pattern of leptokurtic dispersal (Ibrahim et al. 1996), involving a combination of rare long-distance dispersal and diffusive settlement of veliger larvae, has maintained high gene flow over long distances and contributed to a poor overall fit to the isolation-by-distance model.

The absence of any pattern of isolation-by-distance in *D. bugensis* over long distances in the present study may be due to the recent colonization of the Laurentian Great Lakes in addition to a deviation from a normally distributed pattern of dispersal. However, even when a group of populations are not at equilibrium, isolation-by-distance should remain detectable over short distances (Slatkin 1993). In the present study, no strong pattern of isolation-by-distance can be detected even over short within-lake comparisons (Fig. 4), providing additional evidence to suggest that long-distance dispersal has played a role in deviations from isolation-by-distance.

Although the AMOVA is more conservative than the isolation-by-distance test, it too indicates that the majority of the observed genetic variation cannot be explained on the basis of geography. The results of both of these tests indicate a more complex model of mussel dispersal than the diffusive radiation expected from survey data.

Significant local genetic subdivision

Studies of marine species with an extended larval stage have revealed genetic uniformity across wide distances but high levels of local genetic subdivision (Parsons 1996). Sim-

© 1999 NRC Canada

ilarly, while several disjunct populations have a similar allelic distribution and low F_{ST} in the present study, other more proximate sites, including two Long Point Bay populations (LPI and LPII, separated by only 11 km), are significantly different. These data suggest that while long-distance dissemination has had an impact on the population structure of the quagga mussel in North America, factors operating on a microgeographic level may contribute to significant genetic differences over short distances. Unfortunately, ecological study of dreissenid dispersal has been hampered by limitations in our ability to directly track larval dispersal. It is unclear how far mussel larvae may disperse in lacustrine environments and if dispersing larvae aggregate, as has been demonstrated in other bivalve species (Andrews 1979), factors that may also have a significant impact on population structuring. A recent study that investigated larval dispersal in a riverine metapopulation of *D. polymorpha* (Stoeckel et al. 1997) estimated that larvae may travel more than 300 km before settlement. While current flows vary significantly between riverine and lacustrine environments, these data may help to explain the differences observed between neighbouring populations in the present study, as larvae may travel large distances before settlement. A more detailed understanding of larval dynamics in lakes is essential to clarify the significance of random and nonrandom processes in the spread of dreissenid species.

Habitat shift: impact on future distributional modes

While the established range of the quagga mussel remains much more restricted than that of the zebra mussel, adult quagga mussels have recently been found in the Mississippi (Mills et al. 1996), Ohio (Brence and Miller 1994), and Rideau rivers (A. Martel, Canadian Museum of Nature, Ottawa, Ont., personal communication). The increased number of sightings of the quagga mussel outside the lower Great Lakes suggests an increasing dissemination of *D. bugensis*.

Dreissena bugensis was first identified in the offshore zone of Lake Erie (Mills et al. 1993) and became established quickly, presumably due to a lack of competition from the zebra mussel. While populations of *D. bugensis* grew to dominate the offshore zone (Mills et al. 1993), mussels from these areas were presumably much less likely to come into contact with boat traffic than individuals from zebra mussel populations in the nearshore zone. Boater-mediated transport of *D. polymorpha* may help to explain the more widespread distribution of the zebra mussel in North America.

Claxton (1998) and Mills et al. (1998) have suggested that *D. bugensis* may currently be displacing nearshore zebra mussels in eastern Lake Erie and on the south shore of Lake Ontario, perhaps due to a faster growth rate of the quagga mussel under resource-limited conditions (Mills et al. 1998). This pattern of competitive exclusion has also been described in eastern Europe, where *D. bugensis* has come to dominate populations of *Dreissena* at nearshore sites in several Ukrainian reservoirs (Mills et al. 1996). With the movement of quagga mussel populations into the nearshore zone, they are now much more likely to come in contact with local boat traffic. This hypothesis is consistent with recent mussel sightings (see above) and the results of the present study, which indicate high levels of gene flow between a number of disjunct populations. Although the quagga mussel may be limited by environmental factors or competitive exclusion by established zebra mussel populations, these results show that widespread dissemination of *D. bugensis* is not only possible but is presently occurring on a large scale.

Conclusions

The results of this study suggest that long-distance dispersal, possibly mediated by boater movement patterns, may be having a significant impact on quagga mussel dispersal patterns. The increased number of sightings of quagga mussels outside their established range, correlated with the recent movement of *D. bugensis* into the nearshore zone, may indicate an increased potential for the establishment of new quagga mussel populations. In contrast with these results, significant genetic differences were identified between populations separated by short distances, suggesting that microgeographic factors governing larval settlement and spread may play a role in limiting gene flow between populations.

Persistent founder effects often associated with range expansions may lead to a positive bias in genetic differentiation and a gradual decrease in within-population heterozygosity (Le Corre and Kremer 1998). These genetic consequences may be more pronounced under geographically limited dispersal than under an island model. Thus, while the present study offers an excellent snapshot view of quagga mussel population genetic structure, future work, including temporal as well as spatial variation, will help to reveal whether the present data form part of a persistent pattern of population subdivision or represent a transitory state as the system moves towards equilibrium.

As the zebra mussel became established in the Laurentian Great Lakes several years before the quagga mussel, concurrent molecular study on *D. polymorpha* (K.-A. Naish, unpublished data) may also provide an "eye to the future," illuminating what might be expected from the quagga mussel in the next 5–10 years. A comparison of quagga and zebra mussel data may help clarify large-scale patterns that have lead to the success of these molluscan invaders.

Acknowledgements

We are grateful to P.D.N. Hebert, G.L. Mackie, T.J. Crease, and three anonymous reviewers for their constructive comments on earlier drafts of this manuscript. Special thanks to W.G. Sprules, the captain and crew of the *Limnos*, and Y. Delafontaine and B. Cusson at Environment Canada in Montreal for assistance with collections. This research was funded in part by a Natural Sciences and Engineering Research Council of Canada collaborative research grant to E.G.B., P.D.N. Hebert, W.G. Sprules, and P. Yodzis and by a Natural Sciences and Engineering Research Council of Canada research grant to E.G.B. A.B.W. was partially supported by an Ontario graduate scholarship.

References

Andrews, J.D. 1979. Pelecypoda: Osteridae. *In* Reproduction of marine invertebrates. *Edited by* A.C. Giese and J.S. Pearce. Academic Press, Inc., New York.

Beaumont, A.R. 1991. Genetic studies of laboratory reared mussels, *Mytlius edulis*: heterozygote deficiencies, heterozygosity, and growth. Biol. J. Linn. Soc. **44**: 273–285.

© 1999 NRC Canada

Brence, A., and Miller, M. 1994. Quagga found in the Ohio River. *In* Zebra mussel update #21. *Edited by* C. Kraft. Gopher: //gopher.adp.wisc.edu:80/.browse/.METASGIZM/.data/.00000137.

Carlton, J.T. 1993. Dispersal mechanisms of the zebra mussel (Dreissena polymorpha). *In* Zebra mussels: biology, impacts, and control. Edited by T.F. Nalepa and D. Schloesser. Lewis Publishers, Boca Raton, Fla. pp. 677–697.

Claxton, W.T. 1998. Molecular systematics and ecology of deep and shallow water populations of *Dreissena polymorpha* and *Dreissena bugensis*. Ph.D. thesis, University of Guelph, Guelph, Ont.

Estoup, A., Rousset, F., Michalakis, Y., Cornuet, J.-M., Adriamanga, M., and Guyomard, R. 1998. Comparative analysis of microsatellite and allozyme markers: a case study investigating microgeographic differentation in brown trout (*Salmo trutta*). Mol. Ecol. **7**: 339–353.

Excoffier, L., Smouse, P.E., and Quattro, J.M. 1992. Analysis of molecular variance inferred from metric distances among DNA haplotypes: application to human mitochondrial DNA restriction data. Genetics, **131**: 479–491.

Goudet, J., Raymond, M., de Meeus, T., and Rousset, F. 1996. Testing differentiation in diploid populations. Genetics, **144**: 1933–1940.

Haag, W.R., and Garton, D.W. 1995. Variation in genotype frequencies during the life cycle of the bivalve, *Dreissena polymorpha*. Evolution, **49**: 1284–1288.

Hartl, D.L., and Clark, A.G. 1989. Principles of population genetics. Sinauer Associates, Inc., Sunderland, Mass.

Hastings, A. 1996. Models of spatial spread: is the theory complete? Ecology, **77**: 1675–1679.

Hebert, P.D.N., Muncaster, B.W., and Mackie, G.L. 1989. Ecological and genetic studies on *Dreissena polymorpha* (Pallas): a new mollusc in the Great Lakes region. Can. J. Fish. Aquat. Sci. **46**: 1587–1591.

Holborn, K., Johnson, M.S., and Black, R. 1994. Population genetics of the corallivorous gastropod *Drupella cornus* at Ningaloo Reef, Western Australia. Coral Reefs, **13**: 33–39.

Ibrahim, K., Nichols, R.A., and Hewitt, G.M. 1996. Spatial patterns of genetic variation generated by different forms of dispersal during range expansion. Heredity, **77**: 282–291.

Johnson, L.E., and Carlton, J.T. 1996. Post establishment spread in large-scale invasions: dispersal mechanisms of the zebra mussel *Dreissena polymorpha*. Ecology, **77**: 1686–1690.

Le Corre, V., and Kremer, A. 1998. Cumulative effects of founding events during colonisation on genetic diversity and differentiation in an island and stepping-stone model. J. Evol. Biol. **11**: 495–512.

Li, G., and Hedgecock, D. 1998. Genetic heterogeneity, detected by PCR-SSCP, among samples of larval Pacific oysters (*Crassostrea gigas*) supports the hypothesis of large variance in reproductive success. Can. J. Fish. Aquat. Sci. **55**: 1025–1033.

May, B., and Marsden, J.E. 1992. Genetic identification and implications of another invasive species of dreissenid mussel in the Great Lakes. Can. J. Fish. Aquat. Sci. **49**: 1501–1506.

Mills, E.L., Dermott, R.M., Roseman, E.F., Dustin, D., Mellina, E., Conn, D.B., and Spidle, A.P. 1993. Colonization, ecology, and population structure of the "quagga" mussel (Bivalvia: Dreissenidae) in the lower Great Lakes. Can. J. Fish. Aquat. Sci. **50**: 2305–2314.

Mills, E.L., Rosenberg, G., Spidle, A.P., Ludyanskiy, M., Pligin, Y., and May, M. 1996. A review of the biology and ecology of the quagga mussel (*Dreissena bugensis*), a second species of freshwater dreissenid introduced to North America. Am. Zool. **36**: 271–286.

Mills, E.L., Chrisman, J.R., Baldwin, B.S., Owens, R.W., O'Gorman, R., Howell, T., Roseman, E.F., and Raths, M.K. 1998. Recent changes in the dreissenid community and a shift toward the quagga mussel in Lake Ontario. 41st Conference of the International Assocation for Great Lakes Research, Hamilton, Ont., May 1998. International Assocation for Great Lakes Research, Ann Arbor, Mich. p. 118. (Abstr.)

Palumbi, S.R. 1995. Using genetics as an indirect estimator of larval dispersal. *In* Ecology of marine invertebrate larvae. *Edited by* L.R. McEdward. CRC Press, Inc., Boca Raton, Fla. pp. 369–387.

Parsons, K.E. 1996. The genetic effects of larval dispersal depend on spatial scale and habitat characteristics. Mar. Biol. **126**: 403–414.

Raymond, M., and Rousset, F. 1995*a*. GENEPOP (version 1.2): population genetics software for exact tests and ecumenicism. J. Hered. **83**: 239.

Raymond, M., and Rousset, F. 1995*b*. An exact test for population differentiation. Evolution, **49**: 1280–1283.

Ricciardi, A., Serrouya, R., and Whoriskey, F.G. 1995. Aerial exposure tolerance of zebra and quagga mussels (Bivalvia: Dreissenidae): implications for overland dispersal. Can. J. Fish. Aquat. Sci. **52**: 470–477.

Rice, W.R. 1989. Analyzing tables of statistical tests. Evolution, **43**: 223–225.

Rousset, F. 1997. Genetic differentiation and estimation of gene flow from *F*-statistics under isolation by distance. Genetics, **145**: 1219–1228.

Ruzzante, D.E. 1998. A comparison of several measures of genetic distance and population structure with microsatellite data: bias and sampling variance. Can. J. Fish. Aquat. Sci. **55**: 1–14.

Sarver, S.K., and Foltz, D.W. 1993. Genetic population structure of a species' complex of blue mussels (*Mytilus* spp.). Mar. Biol. **117**: 105–112.

Schneider, S., Kueffer, J.-M., Roessli, D., and Excoffier, L. 1997. Arlequin V1.1: a software for population genetic analysis. Genetics and Biometry Laboratory, University of Geneva, Geneva, Switzerland.

Singh, S.M., and Green, R.H. 1984. Excess of allozyme homozygosity in marine molluscs and its possible biological significance. Malacologia, **25**: 569–581.

Slatkin, M. 1985. Rare alleles as indicators of gene flow. Evolution, **39**: 53–65.

Slatkin, M. 1993. Isolation by distance in equilibrium and nonequilibrium populations. Evolution, **47**: 264–279.

Sokal, R.R., and Rohlf, F.J. 1981. Biometry. 2nd ed. W.H. Freeman & Co., San Francisco, Calif.

Stoeckel, J.A., Schneider, D.W., Soeken, L.A., Blodgett, K.D., and Sparks, R.E. 1997. Larval dynamics of a riverine metapopulation: implications for zebra mussel recruitment, dispersal, and control in a large-river system. J. North Am. Benthol. Soc. **16**: 586–601.

U.S. Geological Survey. 1997. National zebra mussel and aquatic nuisance species clearinghouse: United States distribution maps. http://www.nfrcg.gov/zebra.mussel.

Weir, B.S., and Cockerham, C.C. 1984. Estimating *F*-statistics for the analysis of population structure. Evolution, **38**: 1358–1370.

Wilson, A.B. 1998. Dispersal patterns of *Dreissena bugensis* in the Laurentian Great Lakes as inferred from highly polymorphic microsatellite markers. M.Sc. thesis, University of Guelph, Guelph, Ont.

Wilson, A.B., Boulding, E.G., and Naish, K.-A. 1999. Characterization of tri- and tetra-nucleotide microsatellite loci in the invasive mollusc, *Dreissena bugensis*. Mol. Ecol. **8**: 692–693.

Wright, S. 1946. Isolation by distance under diverse systems of mating. Genetics, **31**: 39–59.

Zar, J.H. 1984. Biostatistical analysis. 2nd ed. Prentice-Hall, Inc., Englewood Cliffs, N.J.

© 1999 NRC Canada

Appendix. Allele frequency data for *D. bugensis* microsatellite data.

Population	Allele											
Locus: *Dbug*1	1	2	3	4	5	6	7	8	9	10	11	12
CE-54	0.000	0.139	0.000	0.009	0.019	0.176	0.000	0.074	0.028	0.000	0.111	0.102
EE-54	0.000	0.102	0.000	0.000	0.083	0.093	0.019	0.074	0.028	0.019	0.167	0.056
LPI-54	0.000	0.140	0.010	0.000	0.030	0.100	0.030	0.100	0.020	0.000	0.060	0.080
LPII-54	0.009	0.104	0.000	0.028	0.179	0.113	0.057	0.038	0.085	0.000	0.000	0.019
WO-54	0.000	0.127	0.000	0.000	0.029	0.069	0.010	0.098	0.029	0.000	0.049	0.196
RC-54	0.000	0.132	0.000	0.047	0.132	0.047	0.057	0.085	0.123	0.009	0.019	0.009
EO-54	0.028	0.075	0.019	0.000	0.019	0.094	0.000	0.113	0.019	0.000	0.057	0.066
SF-54	0.000	0.125	0.000	0.000	0.115	0.038	0.000	0.067	0.058	0.000	0.067	0.125
	23	24	25	26	27	28	29	30	31	32	33	34
CE-54	0.000	0.000	0.037	0.019	0.028	0.000	0.000	0.009	0.037	0.028	0.028	0.009
EE-54	0.000	0.000	0.009	0.028	0.037	0.019	0.037	0.000	0.000	0.046	0.019	0.009
LPI-54	0.000	0.020	0.010	0.030	0.010	0.020	0.040	0.010	0.010	0.010	0.050	0.030
LPII-54	0.019	0.028	0.000	0.000	0.000	0.028	0.000	0.066	0.028	0.057	0.000	0.000
WO-54	0.010	0.000	0.000	0.029	0.039	0.010	0.000	0.029	0.059	0.059	0.020	0.039
RC-54	0.019	0.000	0.009	0.009	0.000	0.009	0.000	0.028	0.028	0.094	0.000	0.038
EO-54	0.000	0.000	0.038	0.019	0.009	0.009	0.019	0.000	0.028	0.085	0.009	0.047
SF-54	0.000	0.000	0.019	0.029	0.087	0.000	0.000	0.010	0.019	0.029	0.058	0.029
Locus: *Dbug*2	1	2	3	4	5	6	7	8	9	10	11	12
CE-54	0.028	0.083	0.176	0.000	0.046	0.009	0.046	0.046	0.000	0.000	0.019	0.037
EE-54	0.019	0.047	0.132	0.000	0.057	0.009	0.066	0.057	0.000	0.019	0.019	0.009
LPI-54	0.000	0.077	0.183	0.010	0.058	0.058	0.029	0.010	0.010	0.010	0.000	0.010
LPII-54	0.000	0.074	0.130	0.009	0.019	0.000	0.065	0.037	0.028	0.028	0.019	0.028
WO-54	0.000	0.077	0.096	0.000	0.077	0.010	0.058	0.077	0.010	0.019	0.029	0.029
RC-54	0.000	0.070	0.190	0.000	0.040	0.020	0.070	0.000	0.000	0.050	0.080	0.000
EO-54	0.000	0.080	0.200	0.000	0.010	0.000	0.090	0.050	0.000	0.010	0.060	0.050
SF-54	0.000	0.108	0.049	0.010	0.059	0.010	0.098	0.020	0.000	0.020	0.029	0.029
	23	24	25	26	27	28	29	30	31	32	33	34
CE-54	0.000	0.009	0.009	0.000	0.046	0.046	0.046	0.028	0.028	0.037	0.000	0.000
EE-54	0.000	0.028	0.047	0.019	0.038	0.038	0.057	0.000	0.047	0.019	0.028	0.000
LPI-54	0.000	0.010	0.010	0.019	0.000	0.077	0.087	0.077	0.038	0.029	0.000	0.010
LPII-54	0.009	0.000	0.019	0.019	0.009	0.046	0.083	0.028	0.046	0.009	0.000	0.000
WO-54	0.000	0.000	0.038	0.058	0.010	0.029	0.010	0.115	0.038	0.010	0.010	0.010
RC-54	0.000	0.010	0.020	0.000	0.010	0.040	0.070	0.050	0.030	0.010	0.000	0.010
EO-54	0.000	0.040	0.020	0.030	0.000	0.050	0.050	0.010	0.060	0.040	0.000	0.000
SF-54	0.000	0.020	0.069	0.000	0.020	0.059	0.069	0.029	0.010	0.010	0.010	0.000
Locus: *Dbug*3	1	2	3	4	5	6	7	8	9	10	11	12
CE-54	0.000	0.037	0.000	0.139	0.000	0.019	0.046	0.009	0.037	0.074	0.019	0.019
EE-54	0.000	0.009	0.000	0.113	0.000	0.047	0.028	0.000	0.028	0.113	0.009	0.038
LPI-54	0.000	0.028	0.000	0.226	0.000	0.009	0.009	0.038	0.009	0.085	0.057	0.019
LPII-54	0.010	0.087	0.010	0.077	0.010	0.048	0.019	0.019	0.019	0.038	0.019	0.029
WO-54	0.019	0.056	0.000	0.278	0.000	0.056	0.065	0.028	0.009	0.093	0.000	0.019
RC-54	0.000	0.046	0.000	0.222	0.000	0.093	0.028	0.000	0.000	0.037	0.019	0.009
EO-54	0.000	0.019	0.000	0.208	0.000	0.019	0.047	0.009	0.000	0.047	0.057	0.000
SF-54	0.000	0.074	0.009	0.167	0.000	0.056	0.019	0.009	0.000	0.065	0.028	0.037
	23	24	25	26	27	28	29	30	Genes			
CE-54	0.000	0.028	0.074	0.000	0.083	0.019	0.000	0.009	108			
EE-54	0.000	0.038	0.085	0.000	0.057	0.000	0.000	0.019	106			
LPI-54	0.000	0.000	0.057	0.000	0.123	0.000	0.028	0.000	106			
LPII-54	0.010	0.038	0.038	0.000	0.144	0.010	0.029	0.000	104			
WO-54	0.009	0.000	0.046	0.000	0.074	0.019	0.009	0.000	108			
RC-54	0.009	0.093	0.019	0.009	0.093	0.000	0.009	0.009	108			
EO-54	0.000	0.028	0.094	0.000	0.189	0.009	0.000	0.000	106			
SF-54	0.000	0.009	0.028	0.009	0.130	0.009	0.000	0.000	108			

© 1999 NRC Canada

Allele										
13	14	15	16	17	18	19	20	21	22	
0.009	0.000	0.009	0.009	0.009	0.000	0.000	0.009	0.000	0.000	
0.019	0.019	0.000	0.000	0.000	0.009	0.019	0.009	0.000	0.009	
0.040	0.000	0.010	0.000	0.010	0.000	0.000	0.020	0.000	0.020	
0.009	0.000	0.000	0.000	0.000	0.000	0.038	0.000	0.000	0.009	
0.029	0.010	0.000	0.000	0.000	0.000	0.010	0.000	0.000	0.010	
0.009	0.000	0.028	0.009	0.000	0.019	0.000	0.000	0.009	0.000	
0.057	0.028	0.028	0.000	0.000	0.000	0.000	0.000	0.028	0.000	
0.010	0.019	0.000	0.000	0.019	0.000	0.000	0.000	0.000	0.000	
35	36	37	38	39	40	41	42	43	44	Genes
0.019	0.019	0.000	0.000	0.009	0.037	0.009	0.009	0.000	0.000	108
0.028	0.009	0.000	0.000	0.000	0.028	0.000	0.000	0.009	0.000	108
0.040	0.030	0.020	0.000	0.000	0.000	0.000	0.000	0.000	0.000	100
0.019	0.038	0.000	0.019	0.009	0.000	0.000	0.000	0.000	0.000	106
0.010	0.010	0.000	0.000	0.000	0.020	0.000	0.000	0.000	0.000	102
0.000	0.019	0.000	0.009	0.000	0.000	0.000	0.000	0.000	0.000	106
0.019	0.000	0.038	0.009	0.009	0.028	0.000	0.000	0.000	0.000	106
0.019	0.010	0.000	0.010	0.019	0.000	0.000	0.000	0.010	0.010	104
13	14	15	16	17	18	19	20	21	22	
0.093	0.037	0.019	0.009	0.000	0.037	0.037	0.000	0.000	0.028	
0.085	0.057	0.028	0.019	0.009	0.019	0.019	0.009	0.000	0.000	
0.019	0.048	0.010	0.019	0.019	0.048	0.000	0.000	0.000	0.029	
0.046	0.111	0.037	0.009	0.000	0.037	0.009	0.028	0.009	0.009	
0.019	0.000	0.048	0.029	0.000	0.019	0.038	0.000	0.000	0.000	
0.070	0.020	0.020	0.030	0.010	0.030	0.020	0.000	0.020	0.000	
0.030	0.060	0.040	0.000	0.000	0.010	0.000	0.000	0.000	0.000	
0.049	0.088	0.059	0.029	0.000	0.020	0.000	0.000	0.000	0.020	
35	36	Genes								
0.000	0.000	108								
0.000	0.000	106								
0.000	0.000	104								
0.000	0.000	108								
0.000	0.038	104								
0.010	0.000	100								
0.000	0.010	100								
0.000	0.010	102								
13	14	15	16	17	18	19	20	21	22	
0.093	0.074	0.019	0.056	0.037	0.056	0.000	0.009	0.028	0.019	
0.038	0.057	0.038	0.047	0.009	0.075	0.009	0.009	0.057	0.075	
0.047	0.066	0.019	0.047	0.000	0.047	0.000	0.000	0.038	0.047	
0.048	0.019	0.048	0.029	0.029	0.048	0.029	0.010	0.029	0.058	
0.009	0.028	0.009	0.028	0.037	0.056	0.009	0.000	0.028	0.019	
0.065	0.037	0.009	0.037	0.028	0.028	0.028	0.019	0.037	0.019	
0.047	0.009	0.009	0.047	0.019	0.038	0.009	0.000	0.038	0.057	
0.065	0.056	0.000	0.102	0.028	0.037	0.009	0.000	0.019	0.037	

© 1999 NRC Canada

Appendix (*concluded*).

Population	Allele											
Locus: *Dbug4*	1	2	3	4	5	6	7	8	9	10	11	12
CE-54	0.046	0.222	0.093	0.194	0.028	0.000	0.009	0.009	0.000	0.000	0.000	0.000
EE-54	0.019	0.264	0.000	0.245	0.009	0.019	0.000	0.000	0.009	0.000	0.000	0.000
LPI-54	0.019	0.415	0.009	0.217	0.028	0.000	0.000	0.000	0.000	0.000	0.000	0.000
LPII-54	0.073	0.208	0.031	0.208	0.052	0.000	0.010	0.000	0.000	0.000	0.000	0.000
WO-54	0.148	0.194	0.000	0.296	0.009	0.000	0.000	0.000	0.000	0.000	0.028	0.000
RC-54	0.058	0.298	0.000	0.154	0.000	0.000	0.000	0.029	0.000	0.029	0.000	0.010
EO-54	0.085	0.198	0.000	0.481	0.000	0.000	0.000	0.000	0.000	0.000	0.019	0.000
SF-54	0.037	0.194	0.093	0.213	0.037	0.000	0.009	0.000	0.000	0.000	0.000	0.000
	23	24	25	26	Genes							
CE-54	0.000	0.019	0.056	0.037	108							
EE-54	0.038	0.038	0.085	0.009	106							
LPI-54	0.028	0.000	0.009	0.028	106							
LPII-54	0.021	0.010	0.031	0.000	96							
WO-54	0.019	0.000	0.037	0.000	108							
RC-54	0.000	0.019	0.048	0.000	104							
EO-54	0.019	0.009	0.009	0.000	106							
SF-54	0.000	0.000	0.083	0.019	108							
Locus: *Dbug5*	1	2	3	4	5	6	7	8	9	10	11	12
CE-54	0.000	0.041	0.020	0.000	0.051	0.153	0.010	0.143	0.071	0.143	0.051	0.010
EE-54	0.010	0.000	0.010	0.030	0.080	0.130	0.000	0.230	0.100	0.070	0.020	0.020
LPI-54	0.021	0.000	0.074	0.011	0.064	0.160	0.000	0.138	0.011	0.213	0.000	0.021
LPII-54	0.034	0.034	0.102	0.045	0.114	0.068	0.000	0.182	0.000	0.125	0.091	0.000
WO-54	0.011	0.000	0.033	0.011	0.087	0.098	0.000	0.217	0.033	0.196	0.065	0.022
RC-54	0.010	0.000	0.070	0.020	0.190	0.080	0.010	0.080	0.030	0.080	0.020	0.020
SF-54	0.000	0.010	0.051	0.031	0.020	0.092	0.010	0.143	0.112	0.061	0.112	0.010
	23	24	25	26	27	Genes						
CE-54	0.020	0.051	0.020	0.010	0.000	98						
EE-54	0.010	0.020	0.000	0.000	0.000	100						
LPI-54	0.011	0.021	0.000	0.000	0.032	94						
LPII-54	0.000	0.000	0.011	0.000	0.000	88						
WO-54	0.000	0.022	0.000	0.000	0.000	92						
RC-54	0.023	0.000	0.011	0.000	0.000	88						
EO-54	0.000	0.030	0.000	0.000	0.000	100						
SF-54	0.010	0.000	0.020	0.000	0.000	98						
Locus: *Dbug6*	1	2	3	4	Genes							
CO-54	0.148	0.148	0.343	0.361	108							
EE-54	0.194	0.102	0.435	0.269	108							
LPI-54	0.167	0.093	0.472	0.269	108							
LPII-54	0.093	0.130	0.287	0.491	108							
WO-54	0.102	0.083	0.315	0.500	108							
RC-54	0.296	0.056	0.278	0.370	108							
EO-54	0.194	0.083	0.139	0.583	108							
SF-54	0.102	0.157	0.167	0.574	108							

© 1999 NRC Canada

Allele									
13	14	15	16	17	18	19	20	21	22
0.000	0.000	0.009	0.037	0.028	0.046	0.130	0.028	0.009	0.000
0.000	0.000	0.019	0.000	0.000	0.085	0.047	0.047	0.009	0.057
0.000	0.000	0.038	0.000	0.038	0.019	0.075	0.028	0.000	0.047
0.000	0.000	0.042	0.000	0.083	0.104	0.031	0.042	0.000	0.052
0.009	0.000	0.019	0.000	0.037	0.037	0.056	0.074	0.000	0.037
0.000	0.019	0.019	0.000	0.058	0.144	0.096	0.010	0.000	0.010
0.000	0.000	0.019	0.000	0.038	0.009	0.038	0.019	0.000	0.057
0.009	0.019	0.009	0.000	0.056	0.065	0.056	0.037	0.009	0.056

13	14	15	16	17	18	19	20	21	22
0.020	0.010	0.010	0.020	0.041	0.041	0.010	0.000	0.031	0.020
0.060	0.030	0.000	0.060	0.040	0.020	0.000	0.020	0.000	0.040
0.096	0.000	0.000	0.000	0.032	0.021	0.021	0.000	0.021	0.032
0.011	0.045	0.000	0.000	0.057	0.000	0.045	0.000	0.011	0.023
0.011	0.098	0.000	0.033	0.000	0.011	0.033	0.000	0.022	0.000
0.050	0.040	0.000	0.080	0.080	0.040	0.020	0.000	0.000	0.050
0.010	0.041	0.000	0.092	0.010	0.051	0.051	0.041	0.000	0.020

© 1999 NRC Canada

Estimating the probability of exceeding elevated pH values critical to fish populations in a hypereutrophic lake

Jacob Kann and Val H. Smith

Abstract: Current eutrophication models typically are used to predict seasonal mean conditions. However, the risk of summer fish kills in hypereutrophic lakes is likely to be more closely dependent on periodic extreme events, such as potentially lethal peaks in pH driven by algal photosynthesis. In hypereutrophic Upper Klamath and Agency lakes, Oregon, peak summertime pH values frequently exceed critical levels that can reduce fish growth and survival (pH > 9.50, a likely sublethal tolerance limit for two resident endangered fish species). We developed two empirical models, one parametric and one nonparametric, that predict the likelihood of exceeding user-defined critical values of pH from concentrations of chlorophyll *a* in these lakes. Separate models were derived to incorporate seasonal dynamics and differences between the two lakes, and the behavior of these models was tested under four different critical pH scenarios. Both parametric and nonparametric models performed similarly, suggesting that management efforts to reduce chlorophyll *a* in these lakes from 200 to 100 $\mu g \cdot L^{-1}$ should decrease the probability of exceeding pH 9.5 by 45%. We suggest that this general approach potentially can be applied to the management of fish populations in other hypereutrophic lakes as well.

Résumé : Les modèles d'eutrophisation actuels sont généralement utilisés pour prévoir les conditions saisonnières moyennes. Par ailleurs, le risque d'hécatombes de poissons dans les lacs hypereutrophes en été est sans doute plus dépendant d'événements périodiques extrêmes (comme les pics de pH dus à la photosynthèse des algues et pouvant s'avérer mortels). Dans les lacs hypereutrophes Upper Klamath et Agency de l'Orégon, les valeurs pics du pH en été excèdent fréquemment les valeurs critiques pouvant réduire la croissance des poissons et nuire à leur survie (pH > 9,50, une valeur limite sans doute sublétale pour deux espèces de poisson de ces lacs). Nous avons élaboré deux modèles empiriques, l'un paramétrique et l'autre non paramétrique, afin de prévoir la probabilité de dépasser les valeurs de pH critiques définies en fonction de l'utilisateur, à partir des concentrations de chlorophylle *a* notées dans ces lacs. Des modèles distincts ont été obtenus afin d'inclure les dynamiques saisonnières et les écarts entre les deux lacs, et le comportement des modèles a été testé dans le cadre de quatre scénarios différents de pH critique. Les modèles paramétriques et non paramétriques ont donné des résultats semblables, ce qui porte à croire que les mesures de gestion visant à réduire les concentrations de chlorophylle *a* de ces lacs de 200 à 100 $\mu g \cdot L^{-1}$ devraient donner lieu à une diminution de 45% de la probabilité que le pH soit supérieur à 9,5. Nous croyons que cette démarche générale pourrait être appliquée à la gestion des populations de poisson d'autres lacs hypereutrophes.

[Traduit par la Rédaction]

Introduction

Summer algal blooms are a consistent feature of eutrophic and hypereutrophic lakes worldwide (Smith 1998). These algal blooms dramatically reduce water clarity and frequently cause taste, odor, and filtration problems in water supplies (Cooke et al. 1993). In many such lakes, poor water quality causes fish kills that can be costly (American Fisheries Society 1992) and can result in a complete restructuring of the fish community (Vanni et al. 1990). The development of an objective plan that minimizes eutrophication-related risks to fish populations in lakes requires the use of a quantitative framework that (*i*) relates fish populations to key water quality variables of concern and (*ii*) subsequently relates these key variables to manageable watershed or lake characteristics.

Quantitative approaches to the effects of water quality on fish have previously been proposed by Barica (1975) and Mericas and Malone (1984), who developed water chemistry based fish kill models. Unfortunately, the utility of these models is limited because historical records of fish kills are typically poor due to inconsistent reporting, rapid predation by avian and fish predators, settling of dead fish to benthic areas, and the difficulty in observing mortality in larval and juvenile fish. Furthermore, models based solely on fish kill probability do not account for deleterious sublethal or chronic population-level effects. An alternative approach presented here is based on (*i*) documented physiological tolerance limits for fish and (*ii*) the probability of exceeding these critical limits.

Accomplishment of (*ii*) above requires a modification of

Received January 15, 1999. Accepted August 5, 1999. J14975

J. Kann.[1] Aquatic Ecosystem Sciences, 232 Nutley Street, Ashland, OR 97520, U.S.A.
V.H. Smith. Department of Ecology and Evolutionary Biology, Haworth Hall, University of Kansas, Lawrence, KS 66045, U.S.A.

[1]Author to whom all correspondence should be addressed. e-mail: jacobkann@aol.com

© 1999 NRC Canada

traditional approaches that utilize regression-based models to relate seasonal means of a key water quality variable to its putative controlling factors (e.g., Dillon and Rigler 1974). The use of seasonal means may not be adequate when evaluating the impact of lethal or sublethal stressors, for which the frequency of extreme events is likely to be a better predictor of fish growth and survival than a simple seasonal mean. In the case of dissolved oxygen stress, Oregon Department of Environmental Quality (1994) suggested that repeated exposure to concentrations near acute levels or to chronic stress levels poses serious risks to the aquatic community. Predicting the frequency of exceeding critical tolerance limits thus may provide a valuable alternative approach to assessing eutrophication-related risk to fish populations.

Upper Klamath and Agency lakes, a system of connected lakes located in south-central Oregon, are an example of ecosystems whose fish populations have been strongly impacted by eutrophication. The shortnose sucker (*Chasmistes brevirostris*) and Lost River sucker (*Deltistes luxatus*) (Catostomidae) are endemic to the Upper Klamath River Basin but are now near extinction. Both species were listed as endangered, and water quality degradation resulting from algal blooms has been identified as a probable major factor in their declines (Williams 1988). Both species are predominantly adfluvial (spawning takes place in tributaries with rapid emigration of larvae to the lake upon hatching) and are long-lived (>25 years) and depend heavily on satisfactory lake water quality for long-term population viability. Adverse effects of eutrophication on native fishes in Upper Klamath Lake include summer fish kills (Scoppettone and Vinyard 1991) as well as a pronounced horizontal redistribution of the fish populations (Hazel 1969). Massive blooms of *Aphanizomenon flos-aquae* now occur nearly continuously from June through October (Kann 1998), causing dramatic variations in dissolved oxygen concentrations and pH. Summertime pH values typically exceed 9.50, a likely sublethal limit for the two resident fish species, and periodically exceed 10. These water quality conditions are of great concern because pH values >9.55 caused a loss of equilibrium in native *Chasmistes brevirostris* juveniles (Falter and Cech 1991). Similarly, short-term acute lethality tests (96-h LC_{50}s) indicate that mortality of juvenile *Deltistes luxatus* occurs when pH values >9.94 are reached (Saiki et al. 1999). Elevated pH is of further concern to fish populations as the frequency of sublethal and lethal concentrations of un-ionized ammonia increases with increasing pH in Upper Klamath and Agency lakes.

Based on the above evidence, pH is considered to be an important factor regulating the growth and survival of resident fish populations in Klamath and Agency lakes and is thus a major focus of water quality concern. We present here two empirical models, one parametric and one nonparametric, that can be used to predict the frequency or likelihood of exceeding critical values of photosynthetically elevated pH from chlorophyll *a* (Chl) in these lakes, and that we suggest can be used to help guide the future management of the resident fish populations in Klamath and Agency lakes. The first model uses a linear regression approach to predict the probability of exceeding defined physiological limits for fish growth or survival. The second model is based on a nonparametric cross-tabulation procedure that has been used successfully in other aspects of eutrophication modeling by Heiskary and Walker (1988) and Walker and Havens (1995).

Materials and methods

Data collection and analysis

Limnological measurements were made in Upper Klamath and Agency lakes from 1990 to 1996 as part of a long-term eutrophication monitoring program. Samples were taken biweekly or occasionally weekly during June–September and at monthly intervals (except when prevented by ice cover) for the remainder of the year; in general, 6–10 sites were sampled on each date. Depth profiles of pH, temperature, and oxygen were measured using a Hydrolab Surveyor multiparameter probe. Because the lake is polymictic and only undergoes weak and intermittent stratification, a depth-integrated water sample was taken on each date by combining a minimum of three replicate hauls of a weighted 5-cm-diameter plastic tube at each site. A portion of this sample was then analyzed for Chl and phaeophytin (Phae) (Nusch 1980).

The first 5 years of data (1990–1994) were used in model development, and the last 2 years (1995 and 1996) were used in model verification. Very strict care was taken to evaluate the data for conformity to the statistical requirements of regression analysis. The assumptions of linear regression were evaluated using residual and normal probability plots, autocorrelation of residuals, estimates of skewness and kurtosis, and Kolmogorov–Smirnov tests of fit (Kleinbaum et al. 1988; Wilkinson 1996). Chl data were transformed to their common logarithms to improve linearity and to reduce heteroscedasticity.

Regression-based probability modeling

Linear regression analyses were performed between lake-wide mean pH and Chl values using two different data subsets: (*i*) June–September lake-wide means and (*ii*) June-only lake-wide means. Only data from open-water sites in Upper Klamath Lake were used to compute lake-wide means; a separate regression analysis was performed for Agency Lake because the shallower Agency Lake typically exhibits more extreme pH and Chl fluctuations as well as differences in bloom timing (Kann 1998).

Regression modeling was also used to develop probabilistic models. When the assumptions of linear regression are met, one can assume that the distribution of the dependent variable at fixed values of the independent variable is normally distributed (Kleinbaum et al. 1988). The model's predictions can then be re-expressed as the probability of exceeding a defined value of the dependent variable (in this case, a defined critical concentration of pH). This was accomplished here by (*i*) predicting the mean value of pH (pH_{pred}) at specified Chl values from the linear regression equations, (*ii*) computing the standard error of the estimate ($S_{y|x}$, as estimated from the square root of the error or residual mean sum of squares; Kleinbaum et al. 1988), (*iii*) normalizing a chosen critical pH value (pH_{crit}, based on bioassay data) to its standard score (Z; cf. Zar 1984) using the following equation:

$$(1) \qquad Z = \frac{pH_{crit} - pH_{pred}}{S_{y|x}}$$

and then (*iv*) computing the proportion (expressed as a percentage) of the normal distribution that lies beyond the computed Z value:

$$(2) \qquad \text{Probability of } pH > pH_{crit} = 100(1 - zcf(Z))$$

where zcf denotes the standard normal cumulative distribution function (Wilkinson 1996). This procedure allowed us to calculate the probability of obtaining values greater than pH_{crit} for the observed range of Chl data.

© 1999 NRC Canada

Fig. 1. Seasonal trends in lake-wide mean pH (broken line) and Chl (solid line) in (*a*) Upper Klamath Lake and (*b*) Agency Lake, 1990–1996.

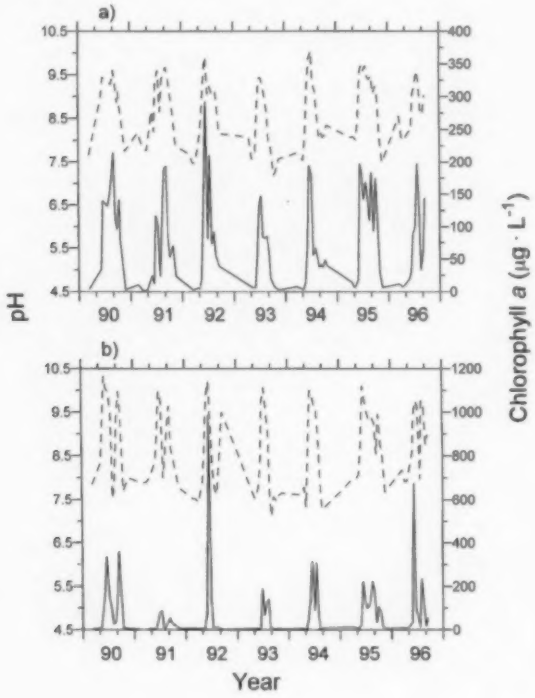

Nonparametric cross-tabulation probability modeling

The same subset of pH and Chl measurements used to develop the above models was used in development of a nonparametric model. However, instead of using lake-wide means, this analysis was performed on simultaneous paired pH and Chl measurements from individual lake sampling sites and dates. Following Heiskary and Walker (1988) and Walker and Havens (1995), the data first were ordered by ascending Chl concentration, divided into a chosen number of data intervals, and the median Chl for each interval computed. The frequency of pH observations within each interval that exceeded the chosen pH_{crit} value was computed, and this computed exceedence frequency (expressed here as a percentage of the total observations within each interval) was then plotted against the median Chl value for each interval.

In order to quantitatively describe the relationship expressed by this plot, and to make the model more useful for predictive purposes, a logistic equation was used to describe the relationship between exceedence frequency of chosen values of pH_{crit} and Chl. Equation parameters for the logistic model were estimated using Systat nonlinear regression procedures (Wilkinson 1996) using the following equation:

$$(3) \qquad \text{Frequency of pH} > pH_{crit} = \frac{pH_{\infty}}{1 + e^{(\beta_0 - (\beta_1 Chl))}}$$

where pH_{∞} is the asymptotic limit for pH_{crit}, β_0 is a location parameter for the curve, β_1 is a slope parameter, and Chl is the median Chl value of an interval. The fit was evaluated using residual plots, standard errors of the parameter estimates, and R^2 values.

Establishment of pH_{crit}

An important step in the development of both of the models outlined above is the choice of critical values of the dependent variable (in this case, pH_{crit}). Although excursions of pH beyond these critical limits only suggest a strong likelihood that a negative fish response will occur, avoidance of high-pH water masses would be a minimal behavioral response. As a result, stressed fish populations are often restricted to limited areas of tolerable water quality where food limitation and crowding may lead to negative effects on fish success, as reflected in reduced survivorship, growth, and reproduction (Beitinger 1990).

Bioassays using the two endangered fishes of the Upper Klamath system have revealed large interspecific and life stage dependent variability in short-term 96-h LC_{50} tests (Saiki et al. 1999). However, the most conservative value from these bioassays (pH = 9.94) was the lower 95% confidence limit for juvenile *Deltistes luxatus* (Saiki et al. 1999). When coupled with the pH 9.55 loss of equilibrium pH threshold observed by Falter and Cech (1991), these data suggest that pH 9.50 is a likely protective level that would encompass sublethal effects as well. These values are consistent with other studies that concluded that pH values between 9 and 10 are harmful to many fish species and that pH values >10.0 are typically lethal (e.g., Alabaster and Lloyd 1980).

In addition, behavioral, ontogenetic, and sublethal factors, along with interactions with other environmental factors such as ammonia and dissolved oxygen availability, can reduce fish success at critical pH levels lower than those derived from acute lethality tests (e.g., Bergerhouse 1992). Moreover, the fraction of total ammonia that remains in the toxic un-ionized form increases from 28 to 55% between pH 9.0 and pH 9.5 at 20°C. It was therefore decided to apply four separate values for pH_{crit} (9.00, 9.50, 9.75, and 10.00) in the analyses in order to investigate the models' behavior under a range of differing critical pH values.

Results and discussion

Simple linear regression analyses

A strong degree of covariation was evident between pH and Chl concentrations in Upper Klamath and Agency lakes when paired pH and Chl measurements from all sites and dates were plotted (Fig. 1). However, because regression statistics are biased when correlations exist between observations that are proximate in time or space, an evaluation of serial and spatial autocorrelation statistics is necessary when working with multiyear and or multisite data from a particular lake (Reckhow and Chapra 1983). In the case of Upper Klamath and Agency lakes, these measures indicated that utilizing paired pH and Chl measurements from all sites and dates was inappropriate (data not shown). It was therefore decided to develop the regression-based models utilizing only biweekly lake-wide means. Moreover, because the timing and magnitude of pH and Chl values in Agency Lake differed from those at the Upper Klamath Lake sites, the computation of lake-wide means was best achieved by performing separate analyses for the two lakes. Further analysis indicated that due to seasonal variance and the presence of outliers and extreme values in Chl (Kann 1998), these data were generally lognormally distributed so that the geometric mean provided the best estimate of lake-wide central tendency. When the goal of regression models is to make predictive or probabilistic statements regarding future conditions, it is necessary to both accurately reflect central tendency when combining spatial or temporal data for model input and ensure that the basic assumptions of linear regression

© 1999 NRC Canada

Table 1. Summary statistics for regressions of pH on Chl in Upper Klamath and Agency lakes.

Model	Parameter		Regression		
	β_0	β_1	$S_{y\cdot x}$	r^2	n
Lake-wide means, June–September dates	6.396	1.398	0.317	0.72	43
Lake-wide means, June dates only	6.809	1.260	0.165	0.95	11
Agency Lake, June–September dates	6.859	1.265	0.533	0.73	37

Note: The regression model is $pH_{pred} = \beta_0 + \beta_1(\log Chl)$; all regressions and parameter estimates were significant at $P < 0.0001$. β_0 is the intercept, β_1 is the slope, $S_{y\cdot x}$ is the standard error of the estimate, and r^2 is the coefficient of determination.

Fig. 2. Lake-wide mean pH versus Chl (log scale) during (*a*) June–September and (*b*) June only for Upper Klamath Lake and during (*c*) June–September for Agency Lake, 1990–1994. Regression lines are computed from parameters in Table 1.

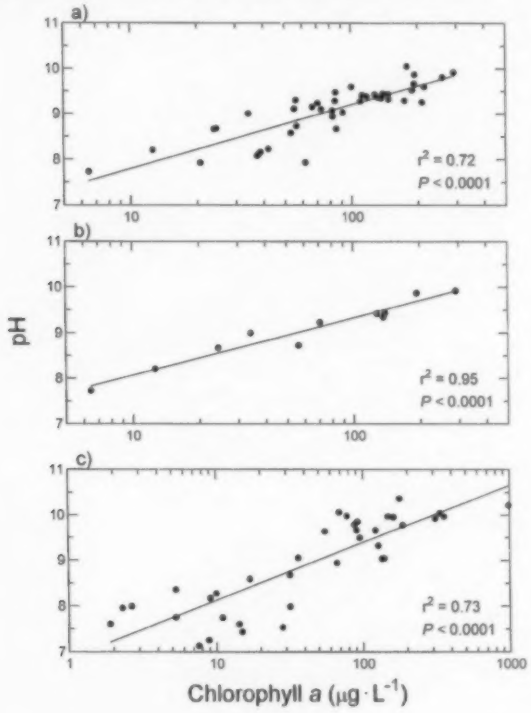

are not violated. For example, all estimates of uncertainty and probability partially rely on the computation of $S_{y\cdot x}$, which could be underestimated considerably due to sample size (n) inflation when autocorrelation is significant.

Despite the controlling effect of time of day that the sample was collected, temperature, photoinhibition, self-shading, solar irradiance (intensity and duration), and physiological state of the bloom on photosynthesis (e.g., Reynolds 1984), and therefore on subsequent elevated pH, Chl was still found to be a strong predictor of pH for all linear regression models (Table 1; Fig. 2). Seventy-two and 73% of the observed variation in pH during June–September could be explained by Chl for the lake-wide Upper Klamath Lake and Agency Lake models, respectively. A third model developed from June lake-wide means explained 95% of the observed variability in pH; despite a lower sample size ($n = 11$), there was considerably less error in the model estimate ($S_{y\cdot x} = 0.165$) for this model, when compared with the two models developed from June–September data ($S_{y\cdot x} = 0.317$). We conclude that this difference likely results from the fact that the June–September period encompasses a wide range of bloom conditions, including rapid growth and bloom collapse, and the photosynthetic elevation of pH produced per unit Chl would be expected to vary strongly with these changing physiological conditions. In contrast, June is a period of rapid algal growth and would not be affected by variability in photosynthetic performance associated with bloom collapses or senescence.

Because the concentration of Phae increases when Chl degradation occurs, it was hypothesized that the ratio of Phae to Chl (Phae/Chl) would provide a relative index of algal physiological state and could be used to account for some of the variability in pH unexplained by the simple regression models in Table 1. The addition of Phae/Chl ratio to the lake-wide June–September model produced a new predictive equation of the form

$$(4) \quad pH_{pred} = 6.800 + 1.277(\log Chl) - 0.615(Phae/Chl); \quad R^2 = 0.79,\ S_{y\cdot x} = 0.282,\ P < 0.0001.$$

This new model explained an additional 7% of the variability in pH, and $S_{y\cdot x}$ was reduced by about 11% when compared with the June–September lake-wide regression model using Chl alone. As would be expected if a high Phae/Chl ratio provides evidence for reduced photosynthetic performance, the coefficient for this term is negative, indicating a reduction in predicted pH at a given concentration of Chl as the Phae/Chl ratio increases. Moreover, the intercept and slope values of this multiple regression model are nearly identical to those of the June-only bivariate model (Table 1), indicating that when differences in algal physiological state are accounted for, pH_{pred} is similar for both June-only and June–September conditions.

Probability of exceedence analyses

The primary goal of this paper was to develop new probabilistic models that can be used to predict the frequency of exceeding critical values of water quality in these lakes, and that can be used to help guide the future management of the resident fish populations in Klamath and Agency lakes. The availability of objective pH_{crit} values based on established physiological limits for pH tolerance by fish (see Materials and methods), along with the observed relationships between algal biomass and pH in Upper Klamath and Agency lakes (Fig. 2), provided the empirical basis for a probabilistic approach to the modeling of fish success. New regression-based and cross-tabulation probability models for pH in these hypereutrophic lakes are presented below.

© 1999 NRC Canada

Fig. 3. Probability of exceeding four critical pH levels computed from the regression-based probability models developed for Upper Klamath and Agency lakes. Probability curves are computed from eq. 5 with input parameters from Table 1 (model subset descriptions for *a*, *b*, and *c* are the same as for Fig. 2). Symbols represent observed exceedence frequencies from the independent model validation data set and are plotted against mean Chl (see text for detailed explanation).

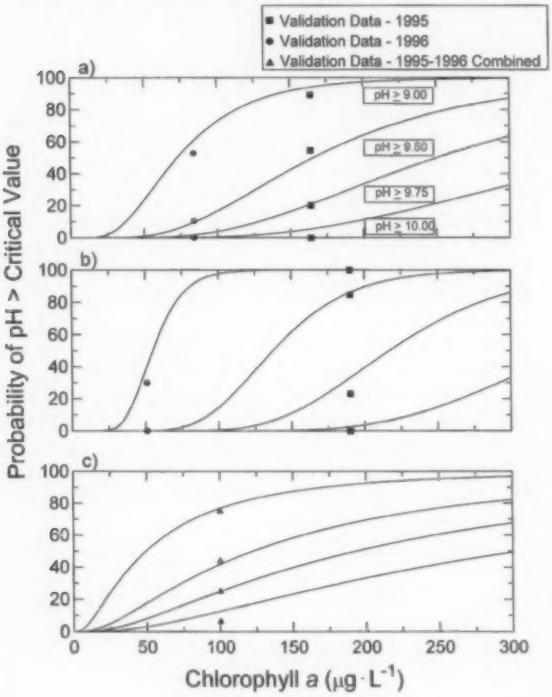

Fig. 4. Probability of exceeding pH = 9.50 at four constant levels of the Phae/Chl ratio (Phae/Chl = 0.00, 0.25, 0.50, 0.75) using the regression-based probability models developed for Upper Klamath and Agency lakes. Probability curves are computed by substituting eq. 4 for pH_{pred} in eq. 5.

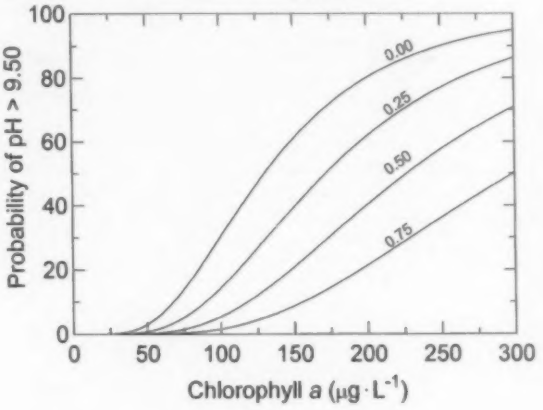

Regression-based probability model

By combining the regression equations from Table 1 with eqs. 1 and 2, the probability of exceeding the four defined pH_{crit} values was computed from the following equation:

$$\text{(5)}\quad \text{Probability of pH} > pH_{crit} = 100(1 - zcf)\left(\frac{pH_{crit} - (\beta_0 + \beta_1(\log \text{Chl}))}{S_{y1x}}\right)$$

where $\beta_0 + \beta_1(\log \text{Chl})$ equals pH_{pred} and the portion of the equation within the large parentheses equals Z. The statistical basis for this model stems from the fact that by meeting the assumptions of linear regression (hence the strict attention paid to evaluating these assumptions), one can assume that pH_i is normally distributed with mean $\beta_0 + \beta_1 Chl_i$ (where $i = 1,2,\ldots, n$) and constant variance S^2_{y1x} (Kleinbaum et al. 1988). Thus, for any value of Chl, a mean pH and its standard error can be computed, and from this method, any proportion of a normal distribution that lies beyond a defined critical pH value can be computed based on the normal probability density function.

When applied to the range of Chl data for each of the three models in Table 1, eq. 5 produces a series of probability curves for each chosen pH_{crit} value (see lines in Fig. 3). For example, Fig. 3*a* shows that for the lake-wide mean June–September model, the probability of exceeding $pH_{crit} > 9.50$ ($P(pH_{crit} > 9.50)$) is 60% at Chl = 200 μg·L^{-1}. In contrast, $P(pH_{crit} > 9.50)$ is only 18% at Chl = 100 μg·L^{-1}. For these same two Chl values, $P(pH_{crit} > 9.50)$ was 90 and 18%, respectively, using the June model (Fig. 3*b*); for the Agency Lake model, $P(pH_{crit} > 9.50)$ was 70 and 40%, respectively (Fig. 3*c*). Given the healthier physiological state of the June blooms, it is not surprising that a higher probability of exceedence is predicted per unit Chl for this model.

The apparent effects of algal physiological state on the predicted probability of exceedence for Upper Klamath Lake during June–September can be illustrated by holding the Phae/Chl ratio constant in eq. 4 and computing a series of probability curves for each Phae/Chl ratio by substituting eq. 4 for pH_{pred} in eq. 5 (Fig. 4). This plot clearly shows reduced probability of exceeding pH_{crit} as the Phae/Chl ratio increases. It is interesting to note that Phae/Chl = 0 produces results similar to the June model (Fig. 3*b*), while Phae/Chl = 0.25 produces similar results to the lake-wide mean June–September model (Fig. 3*a*).

These data also suggest that the predicted exceedence values per unit Chl are higher in Agency Lake than in Upper Klamath Lake. Because all of these empirical models are based on integrated water column Chl samples (which would capture algal cells both inside and outside the photic zone), we conclude that photosynthetic pH elevation per unit Chl may be higher in Agency Lake because its shallower mixing depth should increase the amount of time that algal cells are exposed to optimal light conditions.

Nonparametric cross-tabulation probability model

Similar probability of exceedence curves were generated using a nonparametric cross-tabulation procedure (see Materials and methods). This procedure requires no assumptions about the shape or functional form of the pH–Chl relationship (cf. Walker and Havens 1995); one simply computes exceedence frequencies for pH_{crit} values within the desig-

© 1999 NRC Canada

Table 2. Parameter estimates (±SE) and summary statistics for logistic probability models (eq. 3) of exceeding four different proposed values of pH_{crit} in Upper Klamath Lake.

pH_{crit}	pH_{∞}	β_0	β_1	$S_{y|x}$	R^2
9.00	95.6±2.185	2.878±0.274	0.052±0.005	3.001	0.99
9.50	60.3±1.901	4.694±0.400	0.040±0.004	1.899	0.99
9.75	39.7±1.970	4.970±0.923	0.033±0.007	1.879	0.99
10.00	18.0[a]	5.143±0.662	0.024±0.003	0.818	0.99

[a]Value fixed based on plot.

Fig. 5. Probability of exceeding four critical pH levels computed from the nonparametric cross-tabulation probability models developed for Upper Klamath and Agency lakes. Frequency of exceedence curves are computed from eq. 3 with input parameters from Table 2. Open circles are the observed frequencies computed within six ordered and paired pH and Chl intervals and plotted on the median Chl of each interval). Solid symbols represent observed exceedence frequencies from the independent model validation data set and are plotted against mean Chl for the June–September time period.

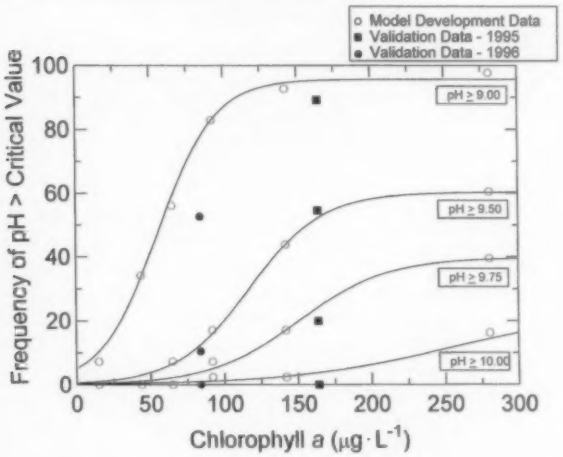

nated intervals of ordered and paired pH/Chl values. To maximize the number of observations, and to maximize the amount of spatial and temporal variance accounted for, only one model was developed that used all paired measurements from the Upper Klamath Lake subset (n = 248). This data set was divided into six intervals, with the number of samples within an interval (n_{int}) equal to 41 for intervals 1–5 and 43 for interval 6. The frequency of pH values that exceeded each of the defined pH_{crit} values within each interval was then plotted versus the median Chl value for the interval (open circles in Fig. 5). Because these six data points appeared to approximate a logistic function, the logistic equation (eq. 3; Table 2) was used to describe the apparent relationship between exceedence frequency and Chl (lines in Fig. 5). These models provided an excellent fit to the observed frequencies within the six intervals (open circles in Fig. 5). Moreover, the predictions of these models were very similar to the June–September regression-based model; the frequency of exceeding pH_{crit} = 9.5 was 59% at Chl = 200 $\mu g \cdot L^{-1}$ and 20% at Chl = 100 $\mu g \cdot L^{-1}$.

Despite the lack of parametric assumptions in development of this modeling approach, an assessment of the model sensitivity to both n_{int} and the use of an interval median (or any chosen measure of interval central tendency) to construct the exceedence plot is necessary to ensure an accurate description of the data. When n_{int} is small, one or two values within an interval can greatly alter the computed frequencies. For example, if n_{int} = 10, then for every pH value that is below or exceeds pH_{crit}, there is a 10% decrease or increase in the computed frequency within the interval. Applying this concept to model development, it is apparent that a large data set is required and that the number of intervals that the data set is divided into cannot be so great as to reduce n_{int} to an unacceptable level. However, the number of samples within an interval must be balanced against the need to have enough intervals to describe the shape of the relationship. For example, a data set could be divided into two intervals to ensure high n_{int}, but this would not allow the functional shape of the relationship to be described. When exceedence frequencies are computed for one interval (the entire data set, n_{int} = 248), two intervals (n_{int} = 124), and so on through six intervals (Fig. 6), one can evaluate model sensitivity to interval choice.

Because the plotted values (open circles in Fig. 5) are based on median Chl values of each interval, each point actually represents a range of Chl values, and the described functional shape could vary if the placement of these values along the abscissa changed due to an inappropriate description of the Chl central tendency within intervals. An evaluation of model sensitivity to this can be gained from Fig. 6, whereby each set of intervals fewer than six produced completely different median Chl values from the six-interval model, yet the frequencies associated with them were generally well described by the logistic functions. To evaluate the entire range of Chl, exceedence frequencies for the pH_{crit} value 9.50 were computed based on moving intervals (n_{int} = 41, the same as that for six intervals) of each successive set of 41 samples (1–41, 2–42, 3–43,..., 208–248) and plotted on the median Chl of each moving interval (Fig. 7). As with Fig. 6, exceedence frequencies for Chl values falling between the six independent (nonoverlapping) intervals were also relatively well described by the logistic model.

The excellent fit of the logistic equations to the observed data, and the fact that model sensitivity to both the number of intervals chosen and the use of median Chl values for intervals was minimal, provide the basis for use of the logistic functions to predict future conditions.

Model validation

While the above models provide excellent descriptions of the observed data, their predictive ability must be validated with independently derived data. Walker and Havens (1995) proposed using the binomial distribution to compute stan-

© 1999 NRC Canada

Fig. 6. Sensitivity of the frequency of exceedence models to interval choice and use of medians to represent interval central tendency. Frequency of exceedence curves are the same as those for Fig. 5 and are overlain on observed exceedence frequencies for one (entire data set, n_{int} = 248), two (n_{int} = 124), three (n_{int} = 83), four (n_{int} = 62), five (n_{int} = 50), and six intervals (n_{int} = 41), which are plotted on their respective interval medians. The symbols denote each of the four pH_{crit} models (●, pH 9.00; ▲, pH 9.50; ■, pH 9.75; ◆, pH 10.00), and the symbol labels (numbers) refer to the number of intervals. In this way, the label "1" shows up once for each model, the label "2" twice, etc., through to the label "6", which shows up six times.

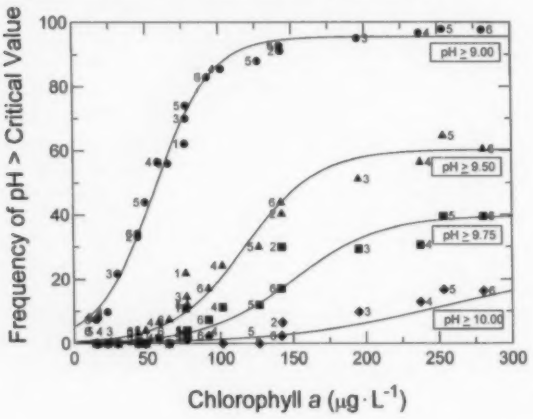

Fig. 7. Sensitivity of the modeled exceedence frequencies for pH_{crit} = 9.50 (line, same as that from Fig. 5) to the use of medians to represent interval central tendency for the entire range of Chl. Exceedence frequencies (○) were computed based on moving intervals (n_{int} = 41, same as that for the original six intervals) of each successive set of 41 samples (1–41, 2–42, 3–43,..., 208–248) and plotted on the median Chl of each moving interval. This generates frequencies for six nonoverlapping or independent intervals (×), which are the same as the original six intervals from Fig. 5.

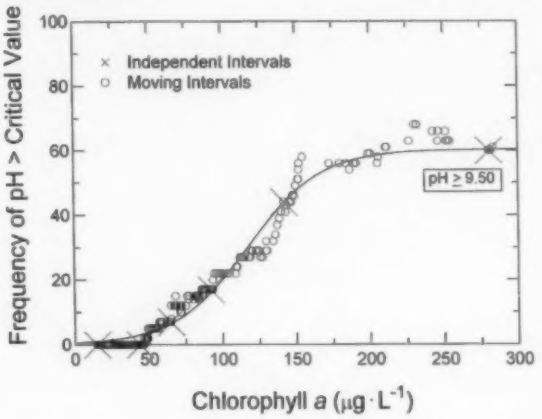

dard errors of measured frequencies within intervals for the cross-tabulation model. However, this procedure only provides an estimate of error in the descriptive model and does not serve to validate the predictive capability of the models, nor does it describe prediction uncertainty. Likewise, the nonlinear and linear regression statistics (Tables 1 and 2) are estimates of error in model fit to the observed data and also do not describe prediction uncertainty. With the multiyear database in Upper Klamath and Agency lakes, all available data were not needed to formulate the model, and the predictive ability of the models could be verified from independently derived data.

For each year of the Upper Klamath Lake 1995–1996 validation data set, the frequency of exceedence of pH_{crit} was computed as the number of observations (expressed as a percentage of the total observations) at all sites and dates within the June–September and June-only time periods that exceeded the chosen pH_{crit} values. The Agency Lake model is based on only one site; therefore, data from both years were combined to ensure an adequate sample size for validation. Exceedence frequencies were paired with the mean Chl for each of the time periods and overlain on the parametric- and nonparametric-based probability plots (Figs. 3 and 5). With the exception of the nonparametric model for pH_{crit} = 9.00, which overpredicted exceedence frequency by about 25% in 1996 (Fig. 5), both plots qualitatively indicate good prediction by all models. A quantitative measure of the predictive ability of the models was assessed by regressing predicted values from the models with observed values from the model validation data set (Fig. 8). The predictive ability of all models was highly significant ($r^2 > 0.95$, $P < 0.01$), and the predicted regression lines were not significantly different from the 1:1 relationship between observed and predicted values ($\beta_0 = 0$, $\beta_1 = 1$). After Keller (1989), a quantitative measure of the predictive ability between the regression-based and nonparametric models was assessed through F tests on the residual variability from the regression between observed and predicted values. This test showed no difference ($P > 0.10$) between the predictive ability of the two models. Despite a nearly twofold difference in June–September lake-wide mean Chl between 1995 (164 $\mu g \cdot L^{-1}$) and 1996 (84 $\mu g \cdot L^{-1}$), predicted exceedence frequencies for all pH_{crit} values were remarkably accurate for both years. Seasonal or time period mean Chl thus provides a good indication of the expected probability of exceeding various pH_{crit} values and therefore provides a good indication of the pH conditions experienced by fish both spatially and temporally at given seasonal mean algal biomass. These models clearly show that the frequency and severity of photosynthetically elevated pH events are greatly decreased as the concentration of Chl in the water column is reduced.

Practical implications

Probabilistic approaches have been used very successfully in the assessment of lake trophic state (Organization for Economic Cooperation and Development 1982; Reckhow and Chapra 1983). For example, they have been used in the trophic state classification of South African lakes (Walmsley 1984) and in the development of phosphorus criteria for Minnesota lakes (Heiskary and Walker 1988). In addition, they have been used to relate algal bloom frequency to concentrations of Chl (Havens 1994), to relate Chl to concentrations of total phosphorus (Walker and Havens 1995), and to

© 1999 NRC Canada

Fig. 8. Relationship between predicted exceedence frequency from the regression-based (●) and nonparametric (○) probability models and the observed frequency from the independent model validation data set (model subset descriptions for *a*, *b*, and *c* are the same as for Fig. 2; the broken line is the 1:1 relationship between the observed and predicted values). The regressions between the predicted and observed values were significant for all models ($r^2 > 0.95$, $P < 0.01$), and the predicted regression lines were not significantly different from the 1:1 relationship between observed and predicted values ($\beta_0 = 0$, $\beta_1 = 1$).

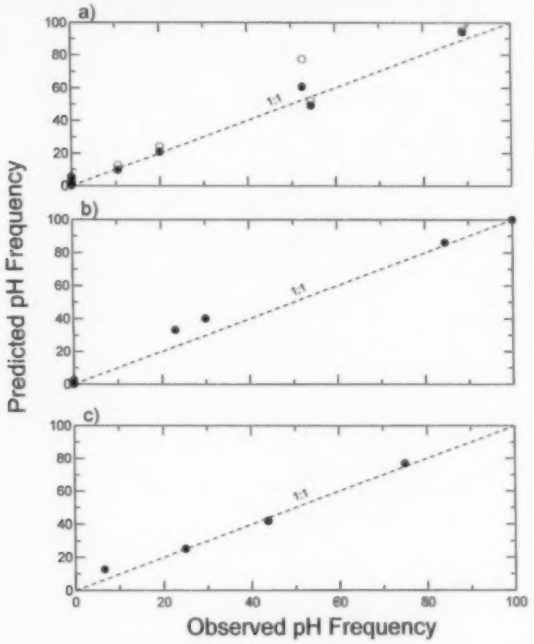

relate summer fish kill probability to total phosphorus (Mericas and Malone 1984).

We have adopted a probabilistic approach in this research because the proper management of fisheries in water systems requires not only a knowledge of the environmental conditions that result in fish kills, but also an understanding of both the lethal and sublethal responses of fish to changes in water quality. In the analysis presented here, we have recognized the importance of considering both responses. We have shown a clear relationship between algal biomass and photosynthetically elevated pH and have used parametric and nonparametric methods to evaluate the probability of exceeding critical limits for fish at varying concentrations of Chl in Upper Klamath and Agency lakes, Oregon.

In this paper, we have been strongly influenced by the work of Mericas and Malone (1984), who proposed that their probabilistic fish kill model could be linked to phosphorus loading models and that such a combined eutrophication modeling framework could be used in the objective assessment of lake management alternatives designed to minimize the risk of summer fish kills. We similarly suggest that the empirical models illustrated here (Figs. 3 and 5) can be used to help provide guidelines for the reductions in Chl that will be necessary to improve fisheries in Upper Klamath and Agency lakes. In large shallow hypereutrophic lakes with high external and internal nutrient loading, such as Upper Klamath Lake, complete reversals of eutrophication are typically not technically or economically feasible. However, Chl in general and blue-green algae in particular show substantial reductions in response to reduction in total phosphorus loading in such lakes, even when total phosphorus concentrations remain in the hypereutrophic range (>100 $\mu g \cdot L^{-1}$) after restoration (Jeppesen et al. 1991; Seip et al. 1992).

In Upper Klamath Lake, our analysis suggests that nearly a 45% reduction (72% for the June model) in the probability of exceeding pH 9.5 could be realized by reducing Chl from 200 to 100 $\mu g \cdot m^{-3}$. When linked with models that predict water column Chl concentrations from phosphorus loading, the combined models can be used as the basis for development of an objective framework to restore endangered fish populations in the Upper Klamath Lake system.

However, we emphasize that the models presented here are specific only to Upper Klamath and Agency lakes and that attempts to apply them directly to lakes of differing fertility, alkalinity, mean depth, and algal assemblages should be done with extreme caution. Rather, we suggest that lake-specific relationships between algal biomass, pH, and fish success should be developed for use in water bodies elsewhere, using approaches similar to those used here. This probability-based approach incorporates the inherent spatial and temporal variance in the independent and dependent variables and reexpresses it as the probability or frequency of stressful conditions likely to be experienced by fish. Once validated, these probability-based models permit an objective definition of the degree of water quality impairment and provide a quantitative lake management tool.

However, we also suggest that the general risk assessment approach presented here (relating a key quality parameter of concern → physiological tolerance limits → probability of exceedence of critical tolerance limits) can be more broadly applied in lake management and restoration. This procedure could equally well be applied to modeling the behavior of dissolved oxygen, whereby concentrations of Chl were linked to the frequency with which oxygen concentrations in the water column exceed known tolerance limits for fish or for other animals. Moreover, the biota in most surface waters are now being subjected to a wide variety of stressors, including toxic contaminants (Laws 1993). We suggest that the probabilistic methods used here to relate fish success, pH, and concentrations of Chl may potentially be of value in modeling the harmful effects of these other environmental stressors as well.

Acknowledgments

We particularly thank Kenneth Knight and Don Gentry for their assistance with field collections and laboratory analysis. We are also grateful to Larry Dunsmoor and Craig Bienz for suggestions and editorial comments. In addition to the very helpful comments of all anonymous reviewers, discussions with Drs. William Walker, Eugene Welch, and Kenneth Reckhow helped solidify ideas. Additional field assistance was provided by Edward Case, Bill Ehinger, Richard Barbiero, and Mark Osburn. Sharon Campbell, Mark Buettner, and the Klamath Tribes were instrumental in pro-

© 1999 NRC Canada

viding continued support for data collection through U.S. Bureau of Reclamation – Klamath Tribe Cooperative Agreements.

References

Alabaster, J.S., and Lloyd, R. 1980. Water quality criteria for freshwater fish. Butterworths, London, U.K.

American Fisheries Society. 1992. Investigation and valuation of fish kills. Spec. Publ. 24, American Fisheries Society, Bethesda, Md.

Barica, J. 1975. Summerkill risk in prairie ponds and possibilities of its prediction. J. Fish. Res. Board Can. **32**: 1283–1288.

Beitinger, T.L. 1990. Behavioral reactions for the assessment of stress in fishes. J. Gt. Lakes Res. **16**: 494–528.

Bergerhouse, D.L. 1992. Lethal effects of elevated pH and ammonia on early life stages of walleye. N. Am. J. Fish. Manage. **12**: 356–366.

Cooke, G.D., Welch, E.B., Peterson, S., and Newroth, P. 1993. Restoration and management of lakes and reservoirs. Lewis Publishers, Boca Raton, Fla.

Dillon, P.J., and Rigler, F.H. 1974. The phosphorus–chlorophyll relationship in lakes. Limnol. Oceanogr. **19**: 767–773.

Falter, M.A., and Cech, J. 1991. Maximum pH tolerance of three Klamath Basin fishes. Copeia, **4**: 1109–1111.

Havens, K.E. 1994. Relationships of annual chlorophyll *a* means, maxima and bloom frequencies and intensities in a shallow eutrophic lake (Lake Okeechobee, Florida, U.S.A.). Lake Reservoir Manage. **10**: 133–138.

Hazel, C.R. 1969. Limnology of Upper Klamath Lake, Oregon, with emphasis on benthos. Doctoral dissertation, Oregon State University, Corvallis, Oreg.

Heiskary, S.A., and Walker, W.W. 1988. Developing phosphorus criteria for Minnesota lakes. Lake Reservoir Manage. **4**: 1–9.

Jeppesen, E., Kristensen, P., Jensen, J.P., Sondergaard, M., Mortensen, E., and Lauridsen, T. 1991. Recovery resilience following a reduction in external phosphorus loading of shallow, eutrophic Danish lakes: duration, regulating factors and methods for overcoming resilience. Mem. Ist. Ital. Idrobiol. **48**: 127–148.

Kann, J. 1998. Ecology and water quality dynamics of a shallow hypereutrophic lake dominated by cyanobacteria (*Aphaniomenon flos-aquae*). Doctoral dissertation, Curriculum in Ecology, University of North Carolina, Chapel Hill, N.C.

Keller, A.A. 1989. Modeling the effects of temperature, light, and nutrients on primary productivity: an empirical and a mechanistic approach compared. Limnol. Oceanogr. **34**: 82–95.

Kleinbaum, D.G., Kupper, L.L., and Muller, K.E. 1988. Applied regression analysis and other multivariable methods. PWS-Kent Publishing, Boston, Mass.

Laws, E.A. 1993. Aquatic pollution. 3rd. ed. Wiley, New York.

Mericas, C., and Malone, R.F. 1984. A phosphorus-based fish kill response function for use with stochastic lake models. N. Am. J. Fish. Manage. **4**: 556–565.

Nusch, E.A. 1980. Comparison of different methods for chlorophyll and phaeopigment determination. Arch. Hydrobiol. Beih. **14**: 14–36.

Oregon Department of Environmental Quality. 1994. Issue paper: dissolved oxygen. 1992–1994 Water Quality Standards Review, Dissolved Oxygen Standard Subcommittee. Oregon Department of Environmental Quality, Water Quality Division, Portland, Oreg.

Organization for Economic Cooperation and Development. 1982. Eutrophication of waters: monitoring, assessment and control. Organization for Economic and Cooperative Development, Paris.

Reckhow, K.H., and Chapra, S.C. 1983. Engineering approaches for lake management. Vol. 1. Data analysis and empirical modeling. Ann Arbor Science, Butterworth Publishers, Woburn, Mass.

Reynolds, C.S. 1984. The ecology of freshwater phytoplankton. Cambridge University Press, New York.

Saiki, M.K., Monda, D.P., and Bellerud, B.L. 1999. Lethal levels of selected water quality variables to larval and juvenile Lost River and shortnose suckers. Environ. Pollut. **105**: 37–44.

Scoppettone, G.G., and Vinyard, G. 1991. Life history and management of four endangered lacustrine suckers. *In* Battle against extinction: native fish management in the American West. *Edited by* W.L. Minkchley and J.E. Deacon. University of Arizona Press, Tucson, Ariz. pp. 359–377.

Seip, K.L., Sas, H., and Vermij, S. 1992. Nutrient–chlorophyll trajectories across trophic gradients. Aquat. Sci. **54**: 58–76.

Smith, V.H. 1998. Cultural eutrophication of inland, estuarine, and coastal waters. *In* Successes, limitations and frontiers in ecosystem science. *Edited by* M.L. Pace and P.M. Groffman. Springer-Verlag, New York. pp. 7–49.

Vanni, M.J., Luecke, C., Kitchell, J.F., and Magnuson, J.J. 1990. Effects of planktivorous fish mass mortality on the plankton community of Lake Mendota Wisconsin: implications for biomanipulation. Hydrobiologia, **200/201**: 329–336.

Walker, W.W., Jr., and Havens, K.E. 1995. Relating algal bloom frequencies to phosphorus concentration in Lake Okeechobee. Lake Reservoir Manage. **11**: 77–83.

Walmsley, R.D. 1984. A chlorophyll *a* trophic status classification system for South African impoundments. J. Environ. Qual. **13**: 97–104.

Wilkinson, L. 1996. Systat 6.0 for Windows: statistics. SPSS Inc., Chicago, Ill.

Williams, J.E. 1988. Endangered and threatened wildlife and plants: determination of endangered status for the shortnose sucker and the Lost River sucker. Fed. Register, **53**(137): 27 130 – 27 134.

Zar, J.H. 1984. Biostatistical analysis. Prentice Hall, Englewood Cliffs, N.J.

© 1999 NRC Canada

Entrainment, dispersal, and settlement of scallop dredge sediment plumes: field measurements and numerical modelling

Kerry P. Black and Gregory D. Parry

Abstract: Entrainment, dispersal, and settlement of sediment plumes generated by scallop dredging were measured with an instrumented towed sled and downstream sensors during a series of experiments conducted in the main scallop grounds in Port Phillip Bay in southeastern Australia. When three 36-ha experimental plots were subjected to closely supervised, intensive dredging by commercial fishers, it was found that dredges suspend a thin layer of sediment (~0.5 cm thick) inducing initial near-bed concentrations of 2–15 $kg \cdot m^{-3}$ in a billowing turbid plume. At one field site where 30% of seabed sediment was less than 4 phi, concentrations reduced after 30 min to about 2% of the initial value and grain sizes decreased to a predominantly mud-sized sediment with a mean size of 5–6 phi. A numerical model was developed to depict plume transformations and settlement patterns. The model accurately predicted patterns of sedimentation and temporal changes to suspended sediment concentration and grain size distribution in the plume. By explicitly treating local seabed grain size, current, and water column turbulence, the model can be applied to other locations and conditions to examine suspended sediment concentrations and potential sediment-related impacts of scallop dredging.

Résumé : L'entraînement, la dispersion et le dépôt des nuages de sédiments générés par les dragues à pétoncle ont été mesurés à l'aide d'un traîneau remorqué en aval et muni d'instruments et de capteurs dans le cadre d'une série d'expériences réalisées sur les principaux fonds de pêche du pétoncle de la baie Port Phillip, du sud-est de l'Australie. Des parcelles expérimentales de 36 ha ont été soumises à un dragage intensif étroitement supervisé réalisé par des pêcheurs commerciaux. Il a été trouvé que les dragues mettaient en suspension une mince couche de sédiments (~0,5 cm d'épaisseur) donnant lieu à des concentrations de 2 à 15 $kg \cdot m^{-3}$ à proximité du lit dans la zone d'un panache trouble en rouleaux. Dans l'un des sites, où 30% des sédiments du fond étaient d'une granulométrie inférieure à 4 phi, les concentrations se trouvaient réduites après 30 min à 2% environ de la valeur initiale et la granulométrie diminuait à celle des sédiments des boues, à granulométrie moyenne de l'ordre de 5–6 phi. Un modèle numérique a été élaboré dans le but de décrire les transformations du panache et les modes de sédimentation. Le modèle prévoit de façon exacte les régimes de sédimentation et les variations temporelles de la concentration des matières en suspension et de la distribution des grains de taille différente au sein du panache. Par un traitement explicite de la granulométrie, des courants et de la turbulence de la colonne d'eau en un lieu donné, le modèle peut être appliqué à d'autres lieux et conditions pour l'examen des concentrations de matières en suspension et des effets éventuels sur les sédiments de la pêche du pétoncle à la drague.

[Traduit par la Rédaction]

Introduction

Concern about the environmental effects of fishing gear grows as progressively heavier equipment is dragged across the sea floor (Hall 1994). Fishing trawls and shellfish dredges may weigh several tonnes and direct damage may be considerable (Currie and Parry 1996). Indirect impacts may also be important, as settlement of turbid plumes may cause burial, clog respiratory surfaces, and reduce light availability. By disturbing the seabed, dredging may also release heavy metals, nutrients, or toxic algal cysts. The natural sediment bonds may be broken or differential rates of settlement may alter local grain size distributions, to the detriment of colonising organisms. While such impacts could be significant, quantitative studies of sediment disturbance by fishing gear are limited to one study of the effects of beam trawls (Churchill 1989) and a preliminary study of disturbance by scallop dredges (Black and Parry 1994).

In a typical year, scallop dredges disturb about 400 km^2 (20%) of the Port Phillip Bay seabed (Currie and Parry 1996). Previous studies have indicated that intensive scallop dredging causes a 20–30% rapid decrease in abundance of most infauna (Currie and Parry 1994, 1996, 1999) and that turbidity connected with dredging could be two to three orders of magnitude greater than that caused by storms (Black and Parry 1994).

Received July 28, 1998. Accepted July 17, 1999.
J14721

K.P. Black.[1] Centre of Excellence in Coastal Oceanography and Marine Geology, National Institute of Water and Atmospheric Research Ltd. and Department of Earth Sciences, University of Waikato, P.O. Box 11-115, Hamilton, New Zealand.
G.D. Parry. Marine and Freshwater Resources Institute, P.O. Box 144, Queenscliff, Victoria, 3225, Australia.

[1]Author to whom all correspondence should be addressed.
e-mail: k.black@niwa.cri.nz

© 1999 NRC Canada

Table 1. Mean (and SDs and number of observations *N*) grain sizes, percent mud and sand, and spring tidal currents at the field sites.

	Grain size							
	Mean				Mud content			Spring tidal
Site	mm	phi	SD (phi)	*N*	%	SD	*N*	current ($m \cdot s^{-1}$)
Dromana	0.22	2.17	0.33	3	7.2	2.2	29	−0.11
Portarlington	0.14	2.82	0.44	4	30.1	6.7	44	0.11
St. Leonards	0.09	3.43	0.16	7	15.3	5.7	120	0.20

Fig. 1. Grain size distribution at the seabed and in the plume immediately behind the dredge at (A) Dromana, (B) Portarlington, and (C) St Leonards.

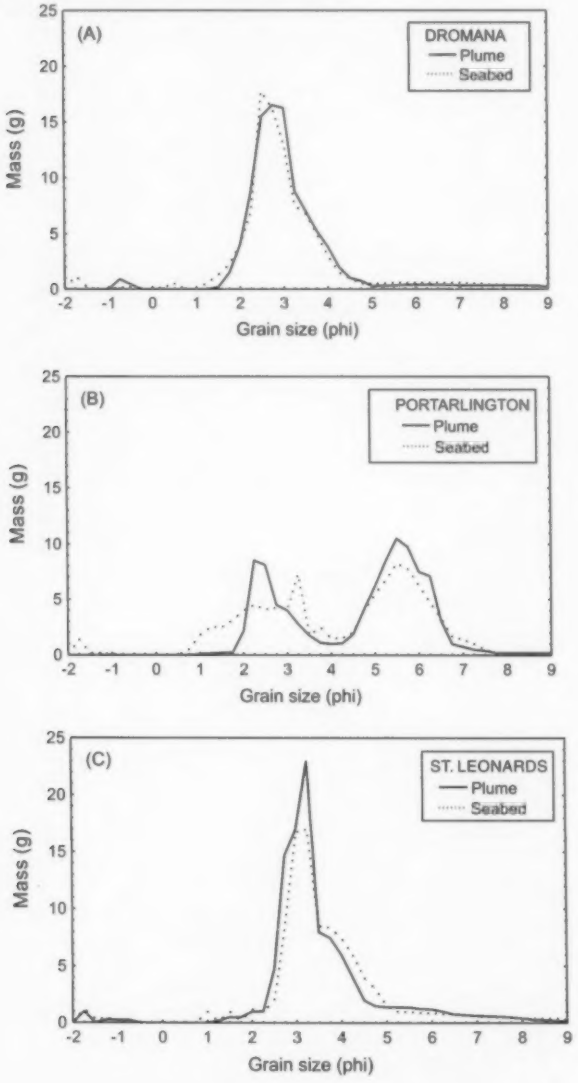

To investigate the physical impacts of dredging, measurements of plume characteristics are needed, both near and distant from the moving dredge. Measurements near the dredge indicate the extent of sediment entrainment and the conditions within the plume before plume characteristics change due to settlement of coarser particles. During the first 17 s after the passage of the dredge, an instrumented sled positioned precisely 5, 20, or 50 m behind an operating dredge recorded this entrainment phase. Measurements further from the dredge indicate the area influenced by the dredge plume. Settlement patterns and plume characteristics downstream of experimentally dredged plots were monitored up to several hours after dredging.

As the rate of change of plume characteristics depends critically on suspended sediment grain sizes, current strength, and the related water column turbulence, tests were conducted at three sites with different sediment and flow characteristics. These results were then generalised by developing a numerical model of the plume based on the principles normally used to simulate natural sediment suspension (Black and Rosenberg 1991; Black 1994; Black et al. 1995). The model was used to interpret measured sediment concentrations in the plume and to more fully examine spatial characteristics of the plume during the dispersal and settlement phase.

Materials and methods

Field site

Port Phillip Bay is a semienclosed tidal embayment linked to Bass Strait in southeastern Australia by a narrow, rocky entrance. Measurements were made at three sites in the Bay (Dromana, Portarlington, and St. Leonards), which were closed to commercial scallop dredging in 1991 when the experimentally dredged plots were monitored (Currie and Parry 1996). The sites were all 14–15 m deep, but wave intensities, tidal currents, and particularly bed sediments varied considerably between sites (Table 1; Fig. 1).

Field measurement techniques

Eighty of the 84 scallop boats licensed to fish in Port Phillip Bay use "Peninsula" dredges (Hughes 1973). The dredge is 2.7–3.3 m wide and consists of a cage 1.2 m long and 0.3 m high, which sits on two 70-mm-high skids projecting 0.5–0.6 m forward of the cage. The primary mechanism for collecting scallops and the main source of sediment disturbance is the "cutterbar," which extends across the width of the leading edge of the cage and is angled at 45° to direct scallops into the cage. The cutterbar extends to the level of the skids.

Sled experiments

A "towed sled" was developed to record plume characteristics immediately behind a moving dredge (Rosenberg et al. 1992; Black and Parry 1994). The sled supported optical backscatterance sensors (OBS) (Downing et al. 1981) that recorded turbidity at 2 Hz and electric water pumps that collected time-integrated con-

© 1999 NRC Canada

centrations over 30 s. Dredge plume behaviour was also observed using an underwater video camera mounted on the dredge and connected by cable to a surface monitor.

The OBS and pumps were attached at 0.25, 0.50, 1.12, and 2.00 m above the bed on the centreline of the sled to record vertical plume structure. To measure laterally, the four OBS sensors were mounted at 1.12 m above the bed and up to 2 m on both sides of the centreline. The combination of continuously recording turbidity sensors and water samples provided two independent estimates of suspended sediment concentrations (SSC). Pumped water samples were also analysed for grain size, and large water samples of 2.5–3.5 L were taken to minimise laboratory errors. OBS sensors are grain size sensitive (Black and Parry 1994; Black and Rosenberg 1994), and so they were calibrated in the laboratory using local plume sediments. These calibrations were later confirmed by comparing concentrations in water samples taken in situ from the plume with concentrations coming from an adjacent OBS monitor.

Dredges were operated at speeds and with tow cable lengths similar to those used by fishers: tow speeds of 4, 5, and 6 kn and tow cable length to depth ratios of 3.5:1–4.5:1. By precisely positioning the sled, measurements were made 5, 20, and 50 m behind the moving dredge. By observing floating buoys attached to the dredge and sled, and by comparing the concentrations recorded by sensors spread laterally across the plume, we confirmed that the sled was in the geometric and concentration centre of the plume during measurements.

The sand fraction in sediment samples was analysed for fall velocity and equivalent grain size in an automated settling tube, while pipette analysis was used for muds (Greilach et al. 1995). All samples were wet sieved in seawater to minimise any damage to flocs, and pipette analyses were conducted in seawater. Percent sands and muds was obtained by collecting the mud fraction on a 4-phi filter.

Large-scale experimental dredging

Large-scale experimental dredging was conducted in three plots centred within areas of 20–30 km^2. The plots were 600 × 600 m at Dromana and Portarlington and 600 × 750 m at St. Leonards (Currie and Parry 1996). After subdividing the plots into three laneways, up to seven commercial scallop boats dredged each plot by dredging laneways in succession. On average, dredges passed twice over each plot (Currie and Parry 1996). Experiments lasted 2 or 3 days and were conducted over 3 h per day when tidal currents were flowing most strongly. The downstream recording instrumentation was located perpendicular to the midpoint of the 600-m dredge path along the flow orientation direction. Dredge paths were aligned perpendicular to the currents so that the plume always encountered the recording instruments and concentrations were laterally uniform, thereby eliminating edge effects. Tabulated data from these experiments can be found in Rosenberg et al. (1992).

To examine dredge depth of penetration, divers inserted metal rings into the seabed before dredging (Black and Parry 1994). Rings were inserted between 0 and 8 cm (colour coded by insertion depth) and observers on each vessel collected the rings trapped by the dredges. To record waves, currents, and suspended sediment load, we used "SEDCAM" (Black and Parry 1994), a bottom-mounted, instrumented frame supporting two OBS turbidity sensors, a vector-averaging S4 electromagnetic current meter (InterOcean), sediment traps, and a time-lapse video recorder (Black and Parry 1994). The frame was placed 60 and 80 m downstream of the boundaries of the experimental plots at St. Leonards and Portarlington, respectively.

Sediment traps consisted of 12 transparent acrylic tubes (70 mm in diameter × 350 mm high) standing vertically in plastic crates with the entrances 0.35 m above the bed. Traps were placed 30, 60, 90, 200, and 400 m downstream of the boundary of the experimental plots, as well as at two upstream control sites. Plume travel time to the most distant trap exceeded 1 h. Vertical variation in the plume was tested using additional traps with entrance elevations at 0.5, 1.0, and 2.0 m at the Portarlington site. In all cases, traps were deployed just prior to the dredging and removed as soon as possible after dredging was completed. Upstream control traps were used to adjust the trapped masses for the small amount of natural deposition.

Results

Field measurements

Video observations of a dredge in operation showed that the sediment plume was entrained across the full width of the dredge, mostly by the cutterbar. As the dredge travelled across the irregular seabed, the cutterbar trimmed off the high regions, creating a series of billowing, turbulent pulses of sediment. Smaller sediment plumes also billowed from both skids, and while these sediments appeared to extend higher into the water column, these plumes were much narrower and smaller than those from the cutterbar. Video observations that the dredge only skimmed the surface sediment layers were consistent with the recovery of colour-coded rings during experimental dredging, which indicated that the depth of disturbance was usually less than 2 cm. The maximum depth from which a ring was recovered (6 cm) was at St. Leonards, where variation in bottom topography was greatest (Black and Parry 1994).

Sediments collected in the water samples on the towed sled from the dredge plume exhibited markedly different grain sizes at the three experimental sites (Fig. 1). However, plume sediments immediately after entrainment were very similar to the sediment distributions on the bed (Fig. 1), indicating that all fractions in the bed sediment grain size population were entrained together.

SSC decreased approximately linearly with elevation from 3.1–5.1 $kg \cdot m^{-3}$ at 0.25 m elevation to 0.1–1.1 $kg \cdot m^{-3}$ at 2 m elevation (Fig. 2A). The vertical concentration profile may therefore be described by

$$(1) \qquad C_p = C_0 (1 - z/Z_m)$$

where Z_m is the elevation where plume concentration goes to zero and is about 2.1 m. The largest near-bed SSC (C_0 = 10–15 $kg \cdot m^{-3}$) was recorded at St. Leonards, but a more representative value was about 4.5 $kg \cdot m^{-3}$ (Fig. 2A). In conjunction with the video observations, these results indicate that sediment entrained by the scallop dredge occupies a near-bed zone that is about 2.1 m high and spans the full width of the dredge (2.7–3.3 m).

Grain sizes did not change markedly with elevation, although average sizes were coarsest at 1.12 m and finest at 2 m (Fig. 2B). When averaged over all sites and levels, grain size became finer with distance behind the dredge. Mean grain size changes from 3.34 to 3.74 phi between 5 and 50 m, i.e., a 0.4-phi increase over a 15-s interval (Fig. 2D). The reduction in grain size results from preferential settling of the coarse fraction.

SSC decreased more rapidly with distance from the dredge at Dromana and St. Leonards (Fig. 2C), the two sites with the highest percentages of sand, due to the greater fall velocity of the local sand (~10 $mm \cdot s^{-1}$) compared with the finer mud (~0.3 $mm \cdot s^{-1}$). Sand falls through 2 m of water

© 1999 NRC Canada

Fig. 2. Plume characteristics in sled experiments at different study site. (A) Vertical distribution of sediment concentrations by site; (B) vertical distribution of grain sizes by site; (C) sediment concentrations behind the dredge; (D) grain sizes behind the dredge; (E) sediment concentrations behind the dredge by elevation for all sites combined; (F) grain sizes behind the dredge by elevation for all sites combined.

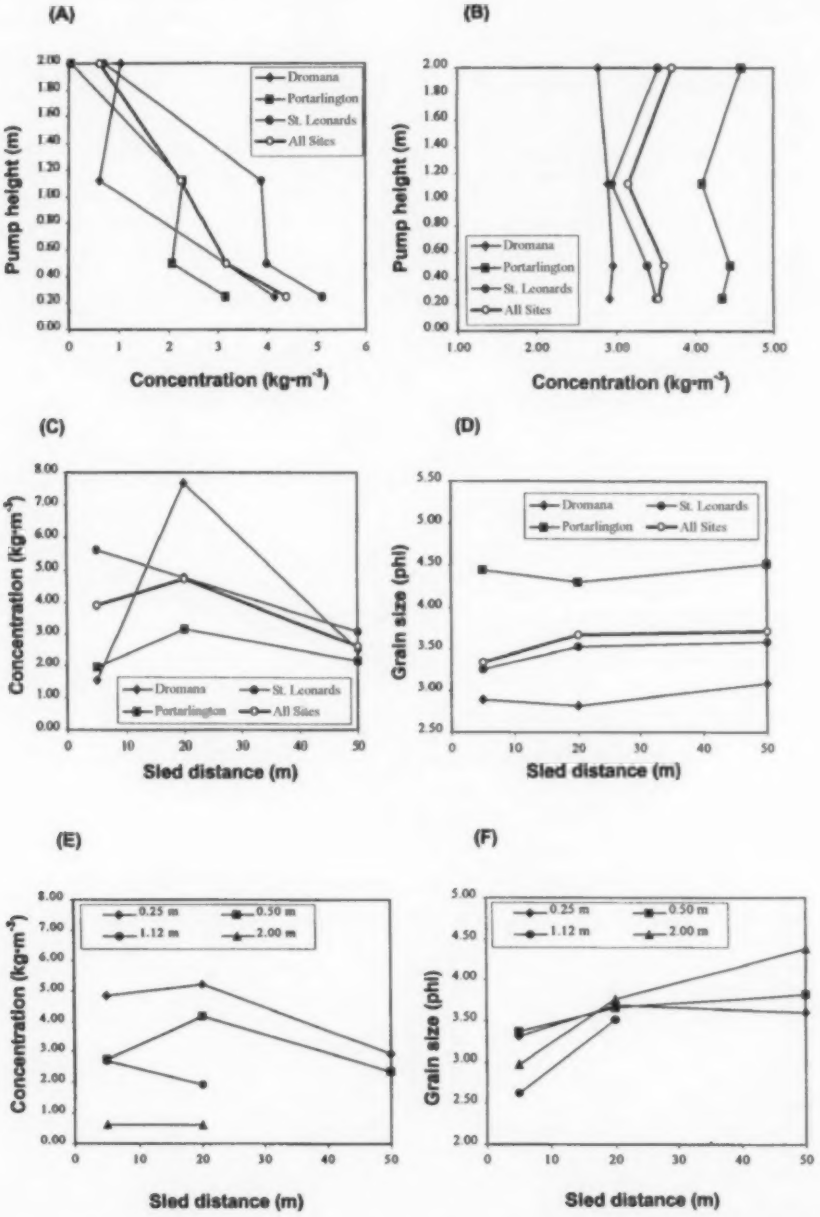

column (the initial height of the dredge plume) in about 3–4 min, while the muds would take more than 2 h to settle. When averaged over all sites and elevations, SSC was 3.91, 4.77, and 2.68 kg·m^{-3} at 5, 20, and 50 m behind the dredge, respectively (Fig. 2C). Thus, SSC was reduced by 31% in the 15 s taken by the sled to travel at 6 kn from 5 to 50 m behind the dredge.

Maximum concentration occurred 20 m behind the dredge (Fig. 2E), rather than at 5 m, particularly at the lowest two levels (Fig. 2E). This may be explained by video observations that showed that the plume was deflected upwards by the dredge, temporarily leaving a zone of lower concentration nearer the bed in its lee.

Far-field concentration recorded at the SEDCAM monitoring site at Portarlington remained relatively constant throughout each dredging experiment. However, peak con-

© 1999 NRC Canada

Fig. 3. (A) Measured peak sediment concentration versus current velocity during four experimental dredging trials at Portarlington. Average (C_T) and maximum (C_M) concentrations predicted by the numerical model for the modelled velocity are also shown. (B) Relative mass in sediment traps, both the measured values and those predicted by the numerical model, versus the inverse of elapsed time at Portarlington. To convert distance to time, the origin is taken as the downstream end of the experimental dredging plot and current velocity is 0.092 $m \cdot s^{-1}$.

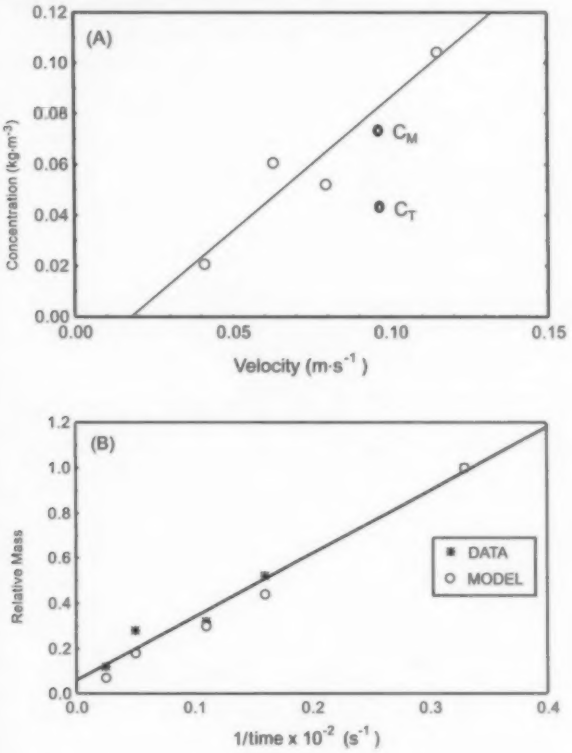

centrations C recorded during each experiment were found to be linearly correlated with plume velocity (i.e., time of travel) (r = 0.96, N = 4) (Fig. 3A). The relationship is explained by the fact that sediment has less time to settle out in faster currents, and so concentrations at a fixed distance are higher in faster flows.

Extending this analysis to examine the sedimentation rates at all sediment trap sites, we undertook a regression of "relative" mass (normalised by the mass trapped at the 30-m site) versus the inverse of elapsed plume travel time (Fig. 3B). A very high correlation coefficient of r = 0.99 (N = 5 data points) indicates that the concentration remained (linearly) inversely proportional to elapsed time, even beyond the turbidity monitoring site at 80 m, at relatively long time scales; the plume took over 1 h to reach the most distant trap. While the linear relationship held for Portarlington and Dromana, the St. Leonards measurements exhibited the strongest correlation (r = 0.99) with an exponential concentration decay of the form $C = \alpha \exp(\beta/d)$ where α = 0.056 depends on concentration at the most distant site and β = 86 is a decay constant. The constants have limited physical meaning beyond the Port Phillip Bay site, but the exponential relationship at St. Leonards was fundamentally different from the linear decay at the other two locations studied. SSC decay rate must depend on the grain size distribution. An initially rapid decay in concentration followed by a slower subsequent decay, as at St. Leonards, reflects a distribution of sediments containing a relatively high fraction of coarse material that reaches the closest traps but drops out before reaching the more distant traps.

We tested whether concentration exhibited an exponential decay with elevation above the seabed by analysing the concentrations and grain sizes in the traps deployed at four different elevations. For natural entrainment of sediment, the vertical concentration profile can be described as

$$(2) \qquad C = C_0 e^{(-z/l_s)}$$

where C_0 is the bed level concentration and l_s is a mixing length. Eddy diffusivity is then vertically uniform (Nielsen 1986) and given by

$$(3) \qquad E_s = |w_s| l_s$$

where w_s is the grain fall velocity.

At the 60-m Portarlington site, the relative mass at each elevation (normalised by the mass trapped at the 0.5-m elevation for each deployment) exhibited a high correlation (r = 0.97, N = 7 data points) with eq. 2 with l_s = 0.61 m. Thus, the initially linear concentration profile measured at the dredge evolved to be exponential in the far-field, in accordance with eq. 2. The eddy diffusivity can now be obtained with eq. 3. With l_s = 0.61 m and average $w_s = 5.8 \times 10^{-4}$ in the sediment traps, the eddy diffusivity is $E_s = 3.5 \times 10^{-4} m^2 \cdot s^{-1}$ The eddy diffusivity defines natural mixing in the water column at the site, one of the key parameters used later in the numerical description of plume settlement.

Numerical model

A Lagrangian numerical model of plume entrainment and fate was developed by modifying techniques used previously for the simulation of natural sediment transport and larval dispersal (Black and Rosenberg 1991; Benzie et al. 1994; Black 1994; Jenkins and Black 1994; Black et al. 1995, 1999). The model treats the plume as consisting of small packets of sediment that advect with the currents and mix through the water column. Because of the large difference between the settling rates of mud and sand, the model divides the packets into different grain size fractions that are treated individually. In natural conditions, sediments near the seabed can be considered as two independent components: a "sink" associated with settling material and an independent "source" being actively entrained. Special treatment was needed for the entrainment that results from the mechanical action of the dredge, but advection and settlement were treated identically to the natural process.

Lagrangian modelling techniques

In a Lagrangian model, particles (representing packets of sediment with a known grain size) are introduced with parameters C_p and V_p, which are the concentration and volume, respectively, associated with each particle. The particle mass M_p is then

© 1999 NRC Canada

(4) $M_p = C_p V_p$

Concentration within any subregion at elevation z is equal to the total mass in the subregion per unit volume. Thus:

(5) $C_z = \sum_{i=1}^{n} M_{pi}/(dxdydz)$

where n is the number of particles and dx, dy, and dz are the subregion dimensions.

Entrainment induced by the dredge was treated by releasing particles at random initial positions in a zone with dimensions given by the measured initial size of the dredge plume. Each particle was assigned a concentration C_p that, according to the field measurements, can be described by eq. 1. Thus, the near-field distribution is set by eq. 1 at the dredge, and the model then predicts the plume evolution in the mid- to far-field.

The volume assigned to each particle is

(6) $V_p = V_r / N$

where V_r is the total volume of the release region defining the initial size of the plume and N is the number of particles released. The number of particles released determines the resolution of the model, and in this paper, about 20 000 particles were used in each simulation.

Settlement of sediment was recorded as the total mass accumulated in the model cell in which a particle settled. The model cell was incremented by the particle mass, and the bed-level change ΔZ_b in the cell was then given by

(7) $\Delta Z_b = \sum_{i=1}^{N_p} M_{pi}/(\rho_s P \Delta x \Delta y)$

where ρ_s is the sediment density (2650 kg·m^{-3}) and P is the pore space correction factor that varies with grain size for a total of N_p settling particles.

Above bed level at the entrances to the elevated sediment traps, the accumulated mass (ΔM_t) at each time step (Δt) can be obtained from the mass flux falling due to gravity (a sediment flux condition) and is

(8) $\Delta M_t = -C_z A w_s \Delta t$

where A is the area of the sediment trap entrance, C_z is the concentration at the trap entrance, and w_s is the grain fall velocity. The bed-level change in a sediment trap (or in a model cell) was therefore

(9) $\Delta Z_t = -C_z w_s \Delta t/(\rho_s P)$.

At bed level, eqs. 7 and 9 give the same results, i.e., when C_z is the bed-level concentration C_0.

Because different grain sizes behave differently, the full grain size distribution was modelled by breaking the fall velocity distribution into intervals that were treated independently and simultaneously (the χ unit is defined in the formula $w_s = 2^{-\chi}$). As the muds floculate and are therefore not independent, we have used grain sizes obtained from fall velocities in seawater and that therefore incorporate the floculation effect. The concentration carried by each particle was weighted by the mass fraction contained in each interval.

The bed-level change due to sediment accumulation for a population of grain sizes then becomes

(10) $\Delta Z_t = -\sum_{m=1}^{M} C_{zm} w_{sm} \Delta t/(\rho_s P)$

where C_{zm} and w_{sm} are the concentrations and fall velocities for the mth size fraction for a total of M fractions in the full distribution.

Diffusion was modelled as a random walk in which particles move a small random distance horizontally or vertically (ΔX_n) each time step. This can be achieved numerically (Black 1994) as

(11) $\Delta X_n = R_n(6E_s\Delta t)^{0.5}$

where R_n is a random number in the uniform range (–1,1) and E_s is the lateral, longitudinal, or vertical eddy diffusivity.

In the advection stage, vertical particle position adjustments Δz were made according to the particle fall velocity as $\Delta z = -w_s \Delta t$. Similarly, a linear approximation for the horizontal advection is adopted where $\Delta x = U(z)\Delta t$ where $U(z)$ is the current velocity at elevation z. The vertical velocity profile was assumed to be logarithmic. Thus:

(12) $U(z) = 5.75u^* \log_{10}(z/z_0)$

where u^* is the friction velocity and z_0 is the roughness length. The speed at elevation z can then be obtained without knowledge of u^* as

(13) $U(z) = U_1 \log_{10}(z/z_0) / \log_{10}(z_1/z_0)$

where U_1 is the velocity measured by the current meter at elevation z_1.

Estimation of the eddy diffusivity and roughness length

While there are many alternatives for the profile of vertical eddy diffusivity (Simons et al. 1989), a vertically uniform diffusivity was adopted, as this had been used satisfactorily in previous sediment transport models (Black 1994). Local wind creates a second boundary layer at the surface, but this layer was neglected in the model because of the low near-surface sediment concentrations and light winds during the experiments. At the surface, a zero-flux boundary condition was imposed by reflecting particles back into the water column that attempted to move through the surface by diffusion.

Eddy diffusivity was assumed to be zero at levels below $z = z_0$, i.e., within one roughness length of the bed where the velocity profile is undefined. Particles reaching the seabed were considered to have settled permanently, as reentrainment was not expected in the mild weather conditions experienced during the experimental dredging. In accordance with the sediment flux boundary condition (eq. 9), diffusive random jumps that would carry a particle to the bottom were disallowed, as recommended by Black (1994).

To treat the full spread of particle sizes, the fall velocity distribution was broken into 13 fractions in one-chi bins and a total of 19 500 particles were released (1500 for each fall velocity fraction). While the number of particles was constant for each fall velocity fraction, each particle carried a

© 1999 NRC Canada

mass that was proportional to the relative mass in each fraction to simulate the natural grain size distribution.

For the dispersal and settlement simulations, particles were tracked until concentrations became negligible. With typical current speeds of 0.075 $m \cdot s^{-1}$, 10 000 s was simulated. The model time step was $\Delta t = 0.2$ s for simulations during the first 20 s after dredging and 2 s for longer simulations of sediment deposition rates. Predicted values of mass accumulation, SSC, and grain size at the elevation of the sediment traps were stored at 10-s intervals over a horizontal model region of 750 × 21 m.

Dredging occurred throughout the 600 × 600 m experimental plot along drag paths aligned perpendicular to the flow direction. As logging (GPS) position fixing was not available on the fishing boats, the distance to the recording instruments varied with each pass. To treat this variation, boat positions were randomly generated over the 600-m width of the experimental plot such that

$$(14) \quad P_b = 600R_n + D_t$$

where P_b is the total distance between the boat and trap, R_n is a uniform random number in the range (0,1), and D_t is the distance to the traps from the downstream end of the experimental plot. The randomly generated positions within the experimental plots were then used to determine the travel distance between the dredge and the trap location, and settled mass in each trap was interpolated at these locations along the modelled plume path. Total accumulation was the sum over the full grain size distribution for a total $N_d = 355$ drags.

Instantaneous concentrations and grain sizes observed down-current of the dredging depend additionally on the time interval between boat passes that determines horizontal distribution of concentration in the plume. Thus, without knowing the exact locations and timing of the vessels, the time series of plume SSC cannot be properly reconstructed. However, the average concentration and grain size at the SEDCAM monitoring site were calculated as

$$(15) \quad C_T = \sum_{i=1}^{N_d} C_{av} W_i / \sum W_i$$

where the weighting factor is $W_i = 1/P_{bi}$, where P_{bi} is the distance from the dredge to the monitoring site for the ith boat pass, and C_{av} is the concentration in the modelled plume for a single boat pass at the randomly generated distance from the trap. The same methods are used to find the average grain size D_{av} in the model plume. Only events within 380 m of the monitoring site were treated after the model indicated that plumes from more distant dredging events exhibited negligibly low concentrations. We also consider the maximum concentration $[\mathrm{Max}(C_{av})] = C_M$ when the dredge is at the downstream end of the experimental dredging plot and closest to the monitoring site. While these plume concentration parameters were examined for model validation (see below), the integrated settling flux in the sediment traps was the most accurate measure of model calibration because the boat positions were unknown.

Numerical model calibration

The numerical model was calibrated by comparing predicted sedimentation rates with sediment trap measurements at Portarlington on 20–21 November 1991. This site had the broadest spread of bed sediment grain sizes and so provided the most difficult test of the model. The period modelled was chosen because turbidity sensors were operating with the sediment traps during the experiments. In addition, weather was calm during the deployment period, and the mass trapped at the control site, which was unrelated to dredging, was less than 10% of the mass caught at the 30-m site.

The model was compared with trapped mass, rather than depth of sedimentation in the traps, to eliminate errors associated with poorly known pore space and consolidation rates. The ratio of sediment mass to depth in the traps is dependent on percent mud content and changes from about 2.0 for the sandy samples at Dromana to 0.6 for the muddiest samples at Portarlington, and so porosity would vary similarly.

The most appropriate values of roughness length and eddy diffusivity for the model were determined from previous measurements. Roughness length in similar environments has been shown to be $z_0 = 0.0007$–0.001 m (Black and Healy 1982). No comparable measurements have been made in Port Phillip Bay, but detailed calibration of a numerical hydrodynamic model of the Bay (Black et al. 1993) indicated that $z_0 = 0.0007$ m, and so we have adopted this value again.

The eddy diffusivity value was estimated from our own sediment trap data ($E_s = 3.5 \times 10^{-4}$ $m^2 \cdot s^{-1}$), while sensitivity of the model to eddy diffusivity was additionally tested using E_s values spanning three orders of magnitude. No field information was available to adequately differentiate between the eddy diffusivities in the three orthogonal directions, and so we took $E_s = E_x = E_y = E_z$ in the two horizontal and vertical directions, respectively. For simulations of small-scale larval dispersal, the same approximation was made by Benzie et al. (1994) using $E_s = 0.0015$ $m^2 \cdot s^{-1}$.

In the model, the initial vertical concentration profile was linear (eq. 1) with $C_0 = 4$ $kg \cdot m^{-3}$ and $Z_1 = 2.1$ m (Fig. 2A), and particles were released within a cuboid of dimensions $\Delta x = 3$ m (the width of the dredge), $\Delta y = 1$ m (a unit length), and $\Delta z = 2.1$ m (the initial height of the plume). Although some variation in the initial grain size vertical profile was measured (Fig. 2B), a uniform size distribution was applied because the data were insufficient to confidently define a grain size profile.

Model calibration results

The model was first calibrated against the sled measurements over the first 20 s of the plume's evolution. Predictions for Portarlington with eddy diffusivities of $E_s = 0.01$, 0.001, and 0.0001 $m^2 \cdot s^{-1}$ showed that grain size was not strongly influenced by eddy diffusivity values over the first 20 s and that all three predictions were within the range of the measurements (Fig. 4A). Concentration was more strongly influenced (Fig. 4B) and concentration decay was most similar to the field measurements with $E_s = 0.001$–0.003 $m^2 \cdot s^{-1}$ and best with $E_s = 0.0015$ $m^2 \cdot s^{-1}$, the same value as that obtained by Benzie et al. (1994) when modelling larval dispersal.

© 1999 NRC Canada

Fig. 4. Sensitivity testing with three values of eddy diffusivity at Portarlington. (A) Predicted and measured mean grain size versus time; (B) Predicted concentration versus time. Concentration is normalised by the initial value.

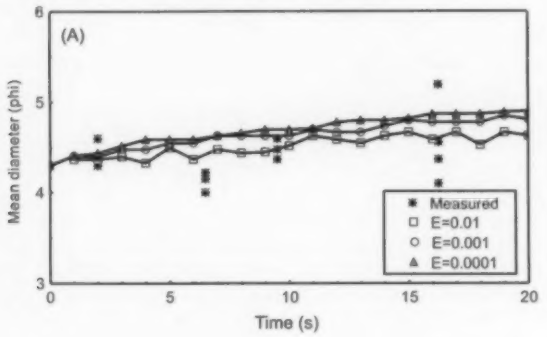

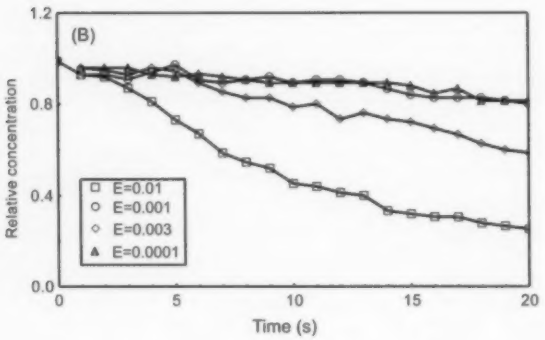

Fig. 5. Mass predicted by the numerical model versus the measured mass caught in traps at 30, 60, 90, and 200 m for Portarlington over the period 20–21 November 1991. The line of equivalence is included.

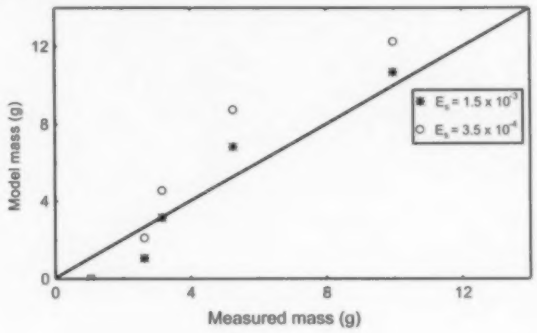

Further confirmation of the best value for E_s (0.0015 $m^2 \cdot s^{-1}$) was obtained as follows. The grain size at Portarlington reduced by 0.34 phi over the first 20 s, which was similar to the measured value of 0.4 phi averaged over all sites. During the first 20 s in the model, concentrations reduced at 0.25, 0.5, and 1.12 m by 23, 30, and 31%, respectively, and these reductions were similar to the average 31% reduction measured at these heights. Concentrations at 2 m remained steady, as depicted by the field data. Finally, using the same eddy diffusivity (E_s = 0.0015 $m^2 \cdot s^{-1}$), predictions for St. Leonards and Dromana were equally as accurate.

A long simulation of the plume over the sediment traps at Portarlington was then undertaken without changing any model parameters to validate the model. The comparison between the model prediction of accumulated mass in the sediment traps and the measured values (Fig. 5) shows that the model predicts the measurements extremely well. Indeed, the very close agreement strongly confirms model behaviour considering the many processes being treated simultaneously; the comprehensive model integrates the processes of suspension, advection, sedimentation, and the random positions of the scallop boats for 355 drags.

Using the same output data, Fig. 3B shows that the model also effectively predicts the linear change in relative mass (normalised by the sediment mass at 30 m) with the inverse of the elapsed time. Finally, the average and maximum predicted concentrations (C_T and C_M) at the monitoring site are shown with the data on Fig. 3A, and the measured concentration is close to the range of the two model values. Thus, we conclude that the numerical model effectively reproduces plume entrainment, mixing, advection, and settlement over time scales from seconds to several hours.

Model application

Potential environmental effects of a scallop dredge plume depend on SSC and settlement rates, which govern light availability and burial depths. Here, we depict sedimentation, grain size, and residual concentration in the water column for a case with typical current speed for inner Port Phillip Bay of 0.1 $m \cdot s^{-1}$ and a constant water depth of 15 m. The initial vertical concentration profile was linear with maximum concentration at the bed C_0 = 10 $kg \cdot m^{-3}$ and zero concentration at 2.1 m elevation. To depict plume behaviour as a function of seabed grain size, a very broad grain size distribution was simulated (Table 2). The first hour after entrainment was modelled, and for case 1, E_s = 0.0015 $m^2 \cdot s^{-1}$ was retained whereas high and low diffusivity (E_s = 0.015 and 0.00015 $m^2 \cdot s^{-1}$) were examined in cases 2 and 3.

Total sedimentation at the seabed, grain size within the plume, and concentration within the plume are shown in Fig. 6. Sedimentation is a maximum of 2 mm within a few metres of the dredge. Sedimentation reduces to less than 0.1 mm at 20 m behind the dredge and then reduces more slowly to 0.001 mm at 350 m (Fig. 6A). Grain size of the depositing sediment reduces very rapidly over the first 10 m (from –1 to 3 phi) as the coarse sediments fall out of suspension during the first 100 s after disturbance by the dredge (Fig. 6B). Plume sediments beyond 50 m have a mean size in the mud range (4–5 phi) out to 350 m from the dredge. The plume moved 350 m after 1 h (Fig. 6C) and spread over more than 100 m longitudinally. Plume concentration dropped to about 0.01 $kg \cdot m^{-3}$ from an initial value of 2–5 $kg \cdot m^{-3}$.

The percentage of sediment remaining in suspension with time depends predominantly on the relative proportions of each grain size fraction in the local bed sediments. Cases 2 and 3 showed that increased eddy diffusivity resulted in a minor reduction in deposition (Fig. 6A) and that depositing sediment was coarser over the first 300 m (Fig. 6B). In addi-

© 1999 NRC Canada

Table 2. Twelve grain size fractions used in the dispersal model application.

Fall velocity ($m \cdot s^{-1}$)	Size (mm)	Size (phi)
0.5000	4.8697	–2.2838
0.0500	0.3653	1.4529
0.0050	0.0838	3.5765
0.0005	0.0255	5.2944
0.2000	1.3985	–0.4839
0.0200	0.1892	2.4022
0.0020	0.0516	4.2753
0.0002	0.0161	5.9592
0.1000	0.6699	0.5780
0.0100	0.1236	3.0157
0.0010	0.0362	4.7880
0.0001	0.0114	6.4605

tion, the higher diffusivity caused sediment to mix more evenly and rapidly through the water column, away from the near-bed boundary layer, and caused the plume to disperse less along the longitudinal direction and the maximum concentration within the plume to increase (Fig. 6C). Current strength has the effect of linearly scaling the travel distance and inversely scaling deposition thickness. Increasing bed roughness length accentuates the curvature in the velocity profile near the bed, and this causes the plume to spread longitudinally, with the magnified shear in the boundary layer.

Discussion

A multiparameter model was developed to simulate and examine the sediment plume in the lee of scallop dredges. Sensitivity tests were undertaken, and it was found that the best values for the constants in the model obtained by calibration were realistic for natural water bodies. In particular, the adopted roughness length was taken from previous calibrated hydrodynamic model simulations of Port Phillip Bay (Black et al. 1993), and the best eddy diffusivity is close to the value found by Benzie et al. (1994) when simulating mixing of crown-of-thorns starfish larvae over coral reefs. The E_s value is also close to that adopted by Black et al. (1999) for simulation of sediment transport in Manukau Harbour in New Zealand. All other parameters in the model were initial conditions measured directly and therefore required no adjustment. As such, the model is able to effectively simulate plume dynamics, and, conversely, the key processes responsible for plume transformation and advection have been fully accounted for.

The sled measurements provided the essential initial conditions by recording concentrations in the formative stage of the plume's evolution. Integration of eq. 1 through the depth with $Z_m = 2.1$ m and $C_0 = 4.5$ kg·m^{-3} gives a total suspended mass per square metre of bed of 4.73 kg. With a pore space correction of 0.65 and adopting a quartz density of 2650 kg·m^{-3}, this mass would occupy a bed layer thickness of 2.8 mm prior to suspension. Thus, the dredge appears to disturb only a thin layer of bed sediments. Indeed, video observations indicate that, where the seabed is uneven, dredges principally trim off the high points. The low recovery rate of

Fig. 6. Plume behaviour with distance from the entraining dredge for three values of eddy diffusivity. (A) Mean bed-level accretion; (B) mean grain size in the plume; (C) mean concentration in the plume. The three curves show the effect of varying vertical eddy diffusivity from 0.00015 to 0.015 m^2·s^{-1}.

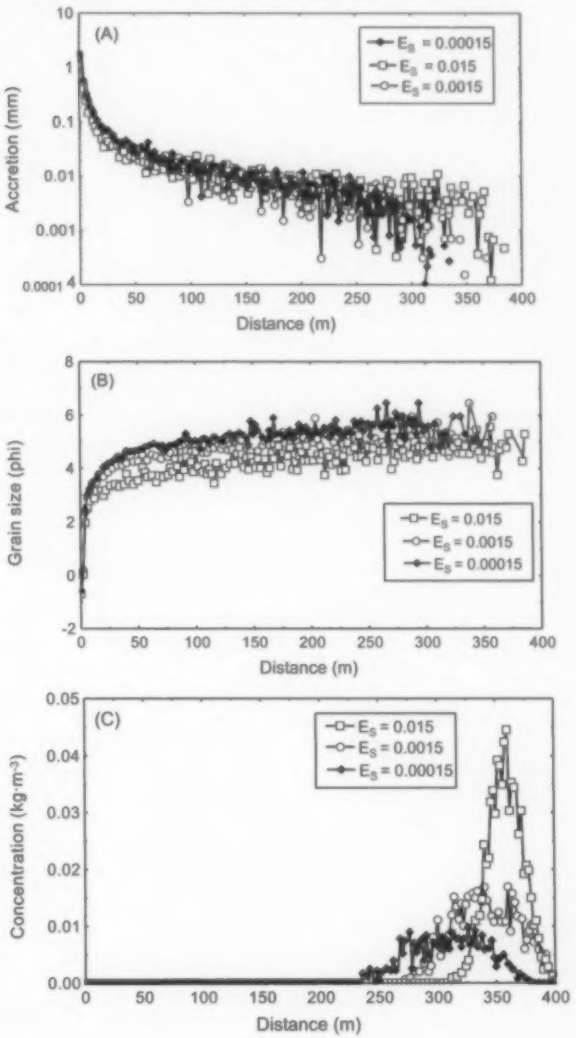

depth rings inserted more than 2 cm below bed level also indicated that dredges usually disturb only a thin layer.

Measured concentrations 5 m behind the dredge were within a factor of 1.5 for the three sites (Fig. 2A). Thus, depth of disturbance was not strongly dependent on the nature of the sediment at normal operating speeds of 6 kn. However, during the sled experiments, it was noted that the dredge often bogged at slow towing speeds of 4 and 5 kn at Portarlington. The dredge was presumably digging into the bed sediments at slow speed, but travelling across the seabed with limited penetration at the most common dredging speed of 6 kn. Slow vessel speeds and longer cable lengths increased the likelihood of becoming bogged, but sediments

© 1999 NRC Canada

also influenced dredge operation because bogging was rare except at Portarlington, the muddiest site. Thus, the operation of the dredge, particularly with respect to boat speed, can critically affect depth of penetration and net sediment entrainment, leading to the possibility that the environmental impacts of different dredge types and operational techniques may be classified in terms of the plume concentrations. This would provide a quantitative measure to assess dredge design at commonly used speeds and tow cable lengths.

An environmental impact of scallop dredging may arise from a local physical change that directly impacts on biota. Intense dredging was found to reduce biota by 20–30% (Currie and Parry 1996). Elevated turbidity may also cause far-field impacts on seagrass or reef communities. At Portarlington, about 98% of the sediment in the plume fell back to the seabed within the first 30 min, and sedimentation occurred even more rapidly at other sites where grain sizes were coarser. However, a plume with low concentration and fine grain size may be present for several hours, e.g., after 30 min at Portarlington, the plume was found to consist of fine sediments with grain sizes less than 5 phi (0.03 mm), and the residual constituents can take much longer to settle. The long settlement times indicate that seagrass beds around Port Phillip Bay may be impacted by muds from the dredging whereas suspended sand impacts are negligible, as the seagrass and scallop beds are mostly separated by more than a few hundred metres.

The major impact on seagrass is associated with reduction in light, rather than the direct presence of the sediments, and muds are more effective scatterers of light than sands for a given concentration. Concentrations in the sediment plume in the first 20 s are two to three orders of magnitude higher than natural concentrations (Black and Parry 1994), but SSC is equivalent to natural levels in large storms after about 9 min, and about 98% of the sediment in the plume had deposited within 30 min at Portarlington. Water column SSC was therefore equivalent to natural conditions within this time frame of order 30 min. Thus, while the present studies indicate that turbidity could induce far-field effects, especially in sensitive environments such as seagrass or reefs, it seems unlikely that sediment concentrations more than 100 m from a single dredge would significantly impact on seagrass communities or reefs, as sedimentation rates are equivalent to background levels after storms at this distance in the slow current speeds around Port Phillip Bay. Regions more than 100 m from dredging may be impacted where currents are higher or where several boats are dredging simultaneously. The impacts of muds on light attenuation depend on the relationship between sediment concentration and photosynthetically active radiation, and this was not measured in the study.

Changes to the character of the local sediments due to winnowing of the fines may affect colonisation success of some biota. Fines travel much further after entrainment than the rapidly settling sands. Thus, changes to the composition of bed sediments may occur, as scallop dredging may lead to a loss of fine material from dredging sites. Dredging will also break natural sediment bonds (cohesiveness and biological bonding), causing increased likelihood of renewed suspension during natural storms. However, further measurements are required to determine the quantitative importance and duration of any loss of sediment cohesion caused by dredging.

Vertical stratification, weather (through local wind waves, wind-induced shear, and turbulence), and tidal current intensities mostly determine eddy diffusivity at any coastal site. In turn, the settlement rates of plume sediments are dependent on eddy diffusivity, water depth, and grain size. The high-quality calibration of the numerical model demonstrated that knowledge of these factors is sufficient to specify the behaviour of a scallop dredge plume.

Acknowledgments

We thank the Victorian scallop industry whose assistance was vital to the success of this study. Field support was provided by John Barry, Anna Bos, Lauren Brown, Tom Budd, Dave Byer, David Currie, Mark Ferrier, Rhonda Flint, David Forbes, Ross Haughton, Matt Hoskins, Andy Longmore, Bob Metcalfe, Geoff Nicholson, and Tony Sheehan. Mike Forsyth analysed the sediment samples. We also thank David Hatton who assisted with data analyses and David Ball who undertook the final report layout.

References

Benzie, J.A.H., Black, K.P., Moran, P.J., and Dixon, P. 1994. Small-scale dispersion of eggs and sperm of the crown-of-thorns starfish (*Acanthaster planci* L.) in a shallow coral reef habitat. Biol. Bull. **186**: 153–167.

Black, K.P. 1994. Suspended sediment load during an asymmetric wave cycle over a plane bed. Coastal Eng. **23**: 95–114.

Black, K.P., and Healy, T.R. 1982. Sediment transport investigations in a New Zealand tidal inlet. *In* Proceedings of the Eighteenth Coastal Engineering Conference, November 14–19, 1982, Cape Town, Republic of South Africa. *Edited by* B.L. Edge. American Society of Civil Engineers, New York. pp. 2436–2457.

Black, K.P., and Parry, G.D. 1994. Sediment transport rates and sediment disturbance due to scallop dredging in Port Phillip Bay. Mem. Queensl. Mus. **36**: 327–341.

Black, K.P., and Rosenberg, M.A. 1991. Suspended load at three time scales. *In* Coastal Sediments '91. Proceedings of a Specialty Conference on Quantitative Approaches to Coastal Sediment Processes, June 25–27, 1991, Seattle, Wash. *Edited by* N.C. Kraus, K.J. Gingerich, and D.L. Kriebel. Waterway, Port, Coastal, and Ocean Division, American Society of Civil Engineers, New York. pp. 313–327.

Black, K.P., and Rosenberg, M.A. 1994. Suspended sand measurements in a turbulent environment: field comparison of optical and pump sampling techniques. Coastal Eng. **24**: 137–150.

Black, K.P., Hatton, D.N., and Rosenberg, M.A. 1993. Dynamics of a large bay and ocean strait in Southern Australia. J. Coastal Res. **9**: 509–538.

Black, K.P., Gorman, R.M., and Symonds, G. 1995. Sediment transport near the break point associated with cross-shore gradients in vertical eddy diffusivity. Coastal Eng. **26**: 153–175.

Black, K., Green, M., Healy, T., Bell, R., Oldman, J., and Hume, T. 1999. Lagrangian modelling techniques simulating wave and sediment dynamics determining sand-body equilibria. *In* Computerized modeling of sedimentary systems. *Edited by* J. Harff, W. Lemke, and K. Stattegger. Elsevier, Holland. pp. 3–21.

Churchill, J.H. 1989. The effect of commercial trawling on sediment resuspension and transport over the Middle Atlantic Bight continental shelf. Continental Shelf Res. **9**: 841–864.

© 1999 NRC Canada

Currie, D.R., and Parry, G.D. 1994. The impact of scallop dredging on a soft sediment community using multivariate techniques. Mem. Queensl. Mus. **36**: 315–326.

Currie, D.R., and Parry, G.D. 1996. The effects of scallop dredging on a soft sediment community: a large-scale experimental study. Mar. Ecol. Prog. Ser. **134**: 131–150.

Currie, D.R., and Parry, G.D. 1999. Impacts and efficiency of scallop dredging on different soft substrates. Can. J. Fish. Aquat. Sci. **56**: 539–550.

Downing, J.P., Sternberg, R.W., and Lister, C.R.B. 1981. New instrumentation for the investigation of sediment suspension processes in the shallow marine environment. Mar. Geol. **42**: 19–34.

Greilach, P., Black, K.P., Parry, G.D., and Forsyth, M. 1995. Scallop dredging and sedimentation in Port Phillip Bay. Vol. 2. Sediment analyses. Victorian Inst. Mar. Sci. Working Pap. No. 29.

Hall, S. 1994. Physical disturbance and marine benthic communities: life in unconsolidated sediments. Ocean. Mar. Biol. Annu. Rev. **32**: 179–239.

Hughes, W.D. 1973. Operational tests of Victorian scallop boats. Aust. Fish. **33**: 14–16.

Jenkins, G.P., and Black, K.P. 1994. Temporal variability in settlement of a coastal fish (*Sillaginodes punctata*) determined by low-frequency hydrodynamics. Limnol. Oceanogr. **39**: 1744–1754.

Nielsen, P. 1986. Suspended sediment concentrations under waves. Coastal Eng. **10**: 23–31.

Rosenberg, M., Black, K., and Parry, G. 1992. Scallop dredging and sedimentation in Port Phillip Bay. Vol. 1. Sediment and hydrodynamic measurements: field data collection and analysis. Victorian Inst. Mar. Sci. Working Pap. No. 24.

Simons, R.R., Kyriacou, A.G., and Black, K.P. 1989. Predicting wave–current interactions at Mallacoota Bay. 9th Australian Coastal Engineering Conference, Adelaide. Institution of Professional Engineers, Canberra, Australia. pp. 297–301.

© 1999 NRC Canada

Evaluation of the flood-pulse concept based on statistical models of growth of selected fishes of the Upper Mississippi River system

Steve Gutreuter, Andrew D. Bartels, Kevin Irons, and Mark B. Sandheinrich

Abstract: The flood-pulse concept (FPC) states that annual inundation is the principal force responsible for productivity and biotic interactions in river–floodplain systems. Somatic growth is one component of production, and we hypothesized that, if the FPC applies, growth of fishes that use the moving littoral zone should differ among years with differing flood pattern, whereas nonlittoral fishes would show no such response. Growth of largemouth bass (*Micropterus salmoides*) and bluegill (*Lepomis macrochirus*), species that exploit littoral resources, increased during a year having an unusual warm-season flood in the Upper Mississippi River system and was reduced during low-water years. Growth of white bass (*Morone chrysops*), which do not rely heavily on the littoral zone, did not differ significantly between the extreme-flood and low-water years. Patterns of growth of black crappie (*Pomoxis nigromaculatus*), which have intermediate dependence on the moving littoral zone, were somewhat ambiguous. These results are consistent with the hypothesis that the FPC applies, at least under certain conditions, to this temperate river system. Our results can also provide an important basis from which to assess some costs and benefits of water level management strategies in large regulated temperate rivers.

Résumé : Selon le concept des poussées de crue (PC), les inondations annuelles constituent la principale force à l'origine de la productivité et des interactions biotiques dans les systèmes cours d'eau – plaine inondable. La croissance somatique est l'une des composantes de la production et nous avons formulé l'hypothèse que si le concept de la PC s'appliquait, la croissance des poissons qui utilisent la zone littorale changeante devait différer d'une année à l'autre en fonction du régime des crues tandis que celle des autres poissons ne devrait pas présenter une telle réaction. La croissance de l'achigan à grande bouche, *Micropterus salmoides*, et du crapet arlequin *Lepomis macrochirus*, qui exploitent les ressources du littoral, a été plus importante au cours d'une année où la crue de saison chaude du haut Mississipi a été plus importante que la normale tandis qu'elle a été réduite pendant les années de faible étiage. La croissance du bar blanc *Morone chrysops*, qui n'utilise pas beaucoup la zone littorale, ne présentait pas de différence significative entre les années où la crue ou l'étiage avaient été extrêmes. L'allure de la croissance de la marigane noire, *Pomoxis nigromaculatus*, dont la dépendance envers la zone littorale changeante est intermédiaire, n'était pas nette. Ces résultats corroborent l'hypothèse des effets du concept des poussées de crue, du moins dans certaines conditions, dans ce bassin de zone tempérée. Nos résultats pourraient s'avérer très utiles pour l'évaluation de certains coûts et avantages des stratégies de gestion des niveaux de l'eau dans les importants cours d'eau de zone tempérée faisant l'objet d'une régularisation.

[Traduit par la Rédaction]

Introduction

The flood-pulse concept (FPC) states that annual inundation is "the principal driving force responsible for the existence, productivity, and interactions of the major biota in river–floodplain systems" (Junk et al. 1989). Rivers seem to be more productive than lakes (Randall et al. 1995), and the FPC may partly explain this difference. The FPC is predicated on the idea that major floodplain biota are adapted to sequester energy redistributed by predictable annual flooding. The FPC requires species and communities that efficiently exploit the moving littoral "aquatic/terrestrial transition zone"

Received March 26, 1999. Accepted August 10, 1999.
J15084

S. Gutreuter.[1] U.S. Geological Survey, Upper Midwest Environmental Sciences Center, 2630 Fanta Reed Road, La Crosse, WI 54603, U.S.A.
A.D. Bartels. Wisconsin Department of Natural Resources, Long Term Resource Monitoring Field Station, 575 Lester Avenue, Onalaska, WI 54650, U.S.A.
K. Irons. Illinois Natural History Survey, Long Term Resource Monitoring Field Station, 704 N. Schrader Avenue, Havana, IL 62644, U.S.A.
M.B. Sandheinrich. River Studies Center, Department of Biology and Microbiology, University of Wisconsin-La Crosse, La Crosse, WI 54601, U.S.A.

[1]Author to whom all correspondence should be addressed. e-mail: steve_gutreuter@usgs.gov

© 1999 NRC Canada

Fig. 1. Upper Mississippi River system showing Pool 8 of the Mississippi River and the La Grange Pool of the Illinois River.

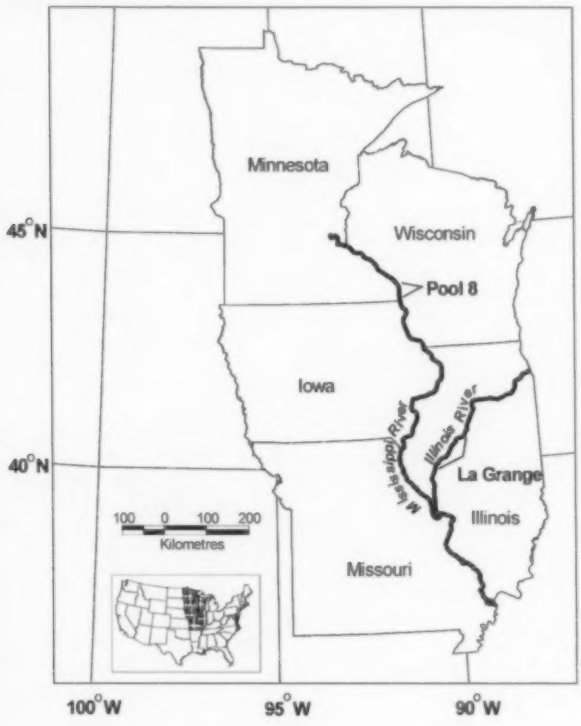

(Junk et al. 1989). The FPC is far too broad and general to be tested as a single hypothesis because of the complexity of production processes in complicated food webs. Rather, it is best viewed as a descriptive concept (Johnson et al. 1995) and relies for evidence on observations on many features of floodplain ecosystems.

Study of the predictions and consequences of the FPC is important because it is one of only two unifying concepts for ecological function of large floodplain rivers (Johnson et al. 1995) and because of interest in restoring the natural flood pulse and otherwise manipulating water levels in some regulated rivers (Lubinski et al. 1991; Bayley 1995; Sparks 1995). Information on likely biological responses to flood pulses is needed by resource managers in developing water level management strategies.

Analyses of growth are attractive for initial examinations of the FPC. Growth is one component of production, and the instantaneous rate of growth can be interpreted as the ratio of production to mean biomass (Ricker 1975). Somatic growth is more easily measured than mean biomass, particularly for fishes of large rivers where quantitative sampling is particularly difficult. Growth is also a familiar process, so that the ramifications of changes in growth are easily conveyed.

Few studies have examined growth of fishes in large floodplain rivers for associations with fluctuations in water level or consistency with the FPC, and there is apparent inconsistency among some of those studies. Welcomme (1979) consolidated two studies of growth of three species of cichlids from the tropical Kafue River of Zambia; measures of age- and sex-specific growth generally tended to be positively correlated with a flood index and negatively correlated with the degree of drawdown. However, Dudley (1979) studied age-specific growth rates of two species of cichlids in the Kafue floodplain before and after construction and operation of the Kafue Gorge Dam, which altered the annual flood regime. Dudley (1979) did not detect any change in annual growth that could be associated with the altered hydrograph but noted that Lee's phenomenon, resulting from back-calculating growth up to 8 years in the past, clouded interpretation of growth patterns. In contrast, Bayley (1988) found that short-term growth of certain omnivorous fishes of the Amazon basin of Brazil was greater during the rising-water season than during the dry season. This increased growth was correlated with the rate of water level rise and was attributed to the increased availability of food. The growth of detritivorous fishes did not increase, which indicated the importance of trophic position to manifestations of the FPC. Rutherford et al. (1995) examined growth of four species of fish from the channelized and leveed Lower Mississippi River of the temperate southern United States. They did not observe patterns in annual growth of age-0 and age-1 fish that could be attributed to the extent of inundation and concluded that those patterns "did not conform to predictions of the flood-pulse concept." In total, these four studies of growth of fishes in large tropical and temperate floodplain rivers do not present compelling evidence for the FPC. However, with the exceptions of the study of Bayley (1988), all contained methodological features or inconsistencies that complicate interpretation.

Our main objective was to examine annual growth data for consistency with a hypothesis derived from the FPC of river ecology. We hypothesized that selected fishes should be able to convert energy redistributed by flooding into measurable increments of somatic growth and that this capability should differ among species and among sizes within a species. This task required development of statistical models that isolate environmental effects from ontogenic effects, and that was a secondary objective.

Materials and methods

Study areas

We studied annual growth of fishes in two impounded segments of the Upper Mississippi River system, which we define as the Mississippi River from St. Anthony Falls to the confluence of the Ohio River and navigable portions of certain tributaries, including the Illinois River (Fig. 1). Fremling et al. (1989) described the fisheries and history of modifications to the Mississippi River. Navigation Pool 8 of the Mississippi River lies between Minnesota and Wisconsin 1093–1131 km upstream of the mouth of the confluence with the Ohio River (Fig. 1). The floodplain in Pool 8 had an area of 19 068 ha, of which 40% was open water and 10% was in agriculture (Laustrup and Lowenberg 1994). There were no agricultural levees in the floodplain of Pool 8. The central floodplain was urban (La Crosse, Wis.), but there otherwise existed extensive areas of floodplain forest and wetlands. Contiguous (to the main channel) backwaters constituted 31% of the total aquatic area in Pool 8. The La Grange Pool of the Illinois River lies 138–254 km upriver of the confluence with the Mississippi River (Fig. 1). This portion of the Illinois River flows through a wide low-gradient floodplain formed by an ancient course of the Mississippi River. The floodplain in the La Grange Pool had an area of 105 244 ha, of

© 1999 NRC Canada

Table 1. Sample sizes for measurements of annual growth increments from four species captured from Pool 8 of the Mississippi River (P8) and the La Grange Pool of the Illinois River (LG).

		Year					
Species	Location	1989	1991	1992	1993	1994	Total
Largemouth bass	LG			64	207	244	515
Bluegill	P8	96	59	91	59		305
	LG				48	54	102
Black crappie	P8	158	73	85	43		360
	LG				70	64	134
White bass	LG				84	43	127

Fig. 2. Smoothed (by cubic spline) mean monthly average water surface elevations above mean sea level (○, 1989; +, 1991; ×, 1992; ●, 1993; ◇, 1994) for (*a*) Pool 8 of the Mississippi River and (*b*) the La Grange Pool of the Illinois River. The shaded areas are the interquartile range (25–50th percentile mean monthly elevation) for the period 1934–1994 in Pool 8 and 1973–1994 in the La Grange Pool.

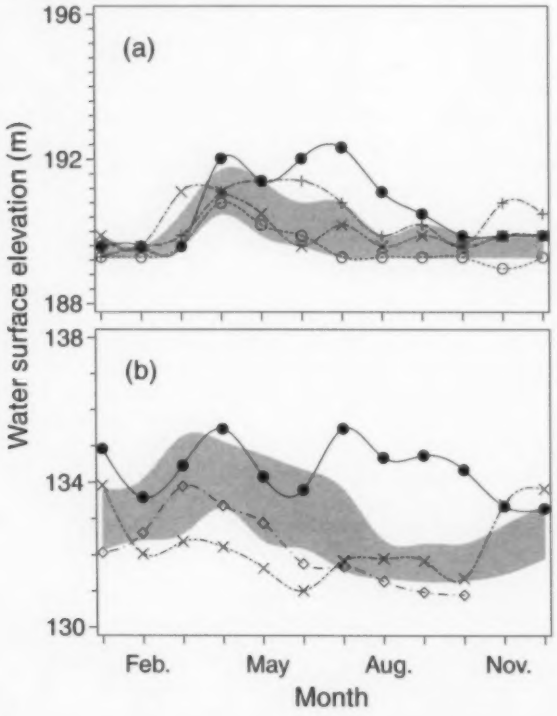

which 16% was open water and 60% was agricultural land isolated by levees (Laustrup and Lowenberg 1994). However, 52% of the total aquatic area consisted of contiguous backwaters, and there persisted a substantial aquatic–terrestrial transition zone.

We studied annual growth of fishes accrued during 1989 and 1991–1993 in Pool 8 and during 1992–1994 in the La Grange Pool. Rainfall patterns differed among these years and resulted in marked differences in the hydrographs (Fig. 2) that permitted our search for growth effects that were consonant with the FPC. In the Upper Midwest of the United States, 1989 was a drought year and water levels remained relatively low in Pool 8 (Fig. 2). Water levels also remained low from April through October of 1994 in the La Grange Pool. A major flood occurred in the Upper Mississippi River system during 1993 that was particularly unusual in that it lagged the typical spring flood pulse by several months and peaked during midsummer. Because metabolic rates are temperature dependent, the flood of 1993 offered an unusual opportunity to observe any direct growth effects that might have resulted from inundation of terrestrial areas and any increased production of aquatic food resources fueled by increased nutrient cycling. Although the 1993 flood was atypical in this respect, this unusual opportunity for study was also relevant to assessment of potential effects of various strategies of water level management.

This was an observational study in which we could not isolate effects of flooding from other confounding variables. In particular, hydrographic measurements and weather are interrelated because flooding is caused by regional precipitation. Temperature may be the most problematic confounding feature of weather because it affects metabolism and growth. There were some differences in mean monthly water temperatures among some years (Fig. 3), but the relative temperature differences between high- and low-water years were small and inconsistent from April through October compared with the differences in water surface elevation.

Growth data

We studied annual growth increments of bluegill (*Lepomis macrochirus*), largemouth bass (*Micropterus salmoides*), black crappie (*Pomoxis nigromaculatus*), and white bass (*Morone chrysops*) during several years (Table 1). These are warmwater species in that optimum temperatures for growth are from 24 to 30°C, and their growing season is approximately April–October in the midwestern United States. Bluegill and largemouth bass show a strong affinity to littoral areas (Pflieger 1975), particularly when feeding. Early life stages of both bluegill and largemouth bass feed primarily on zooplankton, but intermediate-sized individuals shift to consumption of aquatic macroinvertebrates (Pflieger 1975), and largemouth bass quickly become piscivorous (Olson 1996). Black crappie inhabit lacustrine backwaters of the Upper Mississippi River system but tend to feed in midwater away from the terrestrial edge, consuming zooplankton, planktonic macroinvertebrates, and fish (Becker 1983). In the Upper Mississippi River system, white bass are most abundant in tailwaters below locks and dams, channel borders, and other riverine aquatic areas (Fremling et al. 1989). Early life stages feed on zooplankton but become piscivorous with increasing size (Becker 1983). Therefore, bluegill and largemouth bass have the greatest, and white bass have the least, affinity to the moving floodplain littoral zone. A priori, we expected to observe the strongest effect of flooding on growth of small to intermediate-sized bluegill and largemouth bass and the weakest response from white bass.

Data from Pool 8 consisted of measurements of fish total length (Fig. 4) and annual growth increments from the foci to the anterior margins of scales that were collected during routine monitoring surveys conducted by the Long Term Resource Monitoring Program (Gutreuter et al. 1995). Impressions of scales were pressed onto 2-mm-thick transparent acetate sheets with a heated hydraulic press. Data from the La Grange Pool consisted of measurements of fish total length (Fig. 4) and annuli from sagittal otoliths from

© 1999 NRC Canada

Fig. 3. Smoothed (by cubic spline) mean monthly average water temperatures (○, 1989; +, 1991; ×, 1992; ●, 1993; ◇, 1994) for (*a*) Pool 8 of the Mississippi River and (*b*) the La Grange Pool of the Illinois River.

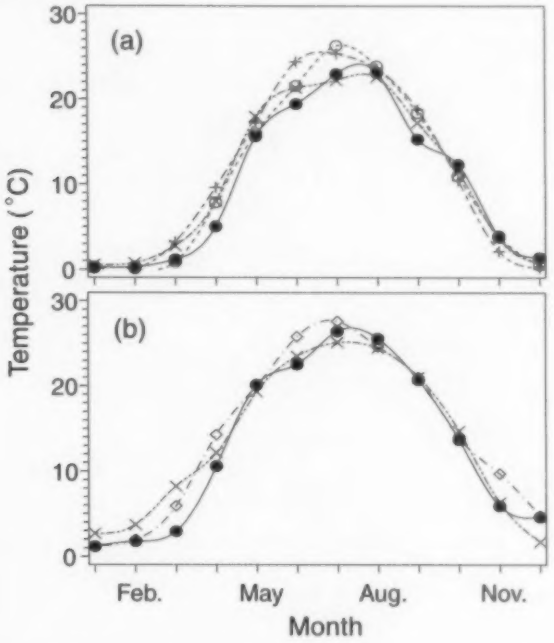

bluegill, black crappie, and white bass collected during Long Term Resource Monitoring Program surveys and from largemouth bass collected by Raibley et al. (1997). We measured annual increments from whole otoliths, except for large largemouth bass, from which a mixture of whole otoliths and transverse sections were measured. A stereoscope combined with an Optimus optical imaging system was used to make all annular measurements (± 1 μm). We used measurements from only the most recent complete growth year to minimize biases imparted by size-selective mortality (Gutreuter 1987). The primary data consisted of the measurements of scale and otolith radii from the foci to the start of the growth year and lengths of growth increments (distances between annuli) accrued during the growth year for individual fish. We based our analyses on these primary data by assuming that the radii and increments on scales and otoliths are surrogates for initial total body lengths and annual length increments, respectively (Weisberg and Frie 1987). However, the mixture of measurements of whole and transverse sections of otoliths from our largemouth bass does not conform to a single scale of measurement, and we therefore used linear scale-proportional hypothesis back calculations (Francis 1990) to estimate initial total lengths and annual length increments and used these as our primary data for this species.

It is difficult to assess the practical importance of growth differences resulting from measurements of scale or otolith increments and radii. Therefore, for display purposes only, we fitted models to scale-proportional hypothesis back-calculated initial total lengths and annual length increments and here present graphs of those fits for interpretation of our test results. Back calculation is a projection or transformation of pattern from one measurement scale to another and it did not alter the general pattern evident in the otolith or scale measurements.

Statistical models

We required statistical models of growth that were consonant with conventional theory and included an effect for the annual flood regime. Flooding can be quantified by any combination of discharge, rate of rise, amplitude, variance, duration, and many other hydrographic features. For simplicity, we viewed flooding as the composite of these factors and used simple annual effects as their surrogates in our models.

Fig. 4. Maximum total lengths at times of capture of (*a*) bluegill from Pool 8 of the Upper Mississippi River, (*b*) bluegill from the La Grange Pool of the Illinois River, (*c*) black crappie from Pool 8, (*d*) black crappie from the La Grange Pool, (*e*) largemouth bass from the La Grange Pool, and (*f*) white bass from the La Grange Pool.

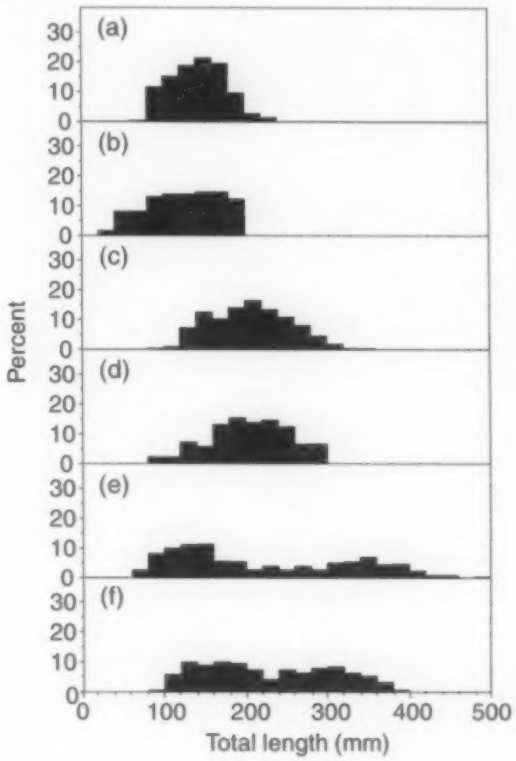

Traditional models of fish growth are predicated on functional relationships between growth rate and body size (Ricker 1979). Size-related patterns in fish growth are created by ontogenic niche shifts (Osenberg et al. 1988), associations between predator size and prey size (Werner 1979), and size-related patterns of prey availability (Mills et al. 1989). Therefore, to detect any differences in annual growth rates that might be attributable to effects of the annual hydrograph, we required statistical models that include both annual effects and the effects of body size.

For description of our models, we refer to both the back-calculated total length and length increments and scale radii and scale increments as initial lengths L at the start of the growth year and annual length increments ΔL, respectively. To model the relationship between annual ΔL and L at the start of the growth year, we built upon the function given by

$$(1) \qquad \frac{\Delta L}{\Delta t} = \beta_0 + \beta_1 L + \beta_2 L \log L$$

where Δt is the growth interval and β_0, β_1, and β_2 are parameters.

© 1999 NRC Canada

Setting $\beta_0 = 0$ and taking the limit as $\Delta t \downarrow 0$, eq. 1 becomes the differential form of the Gompertz growth function (Ricker 1979), and we henceforth refer to terms containing $L \log L$ as Gompertz terms. Equation 1 also reduces to the differential form of the Pütter (von Bertalanffy) growth model by setting $\beta_2 = 0$ and taking the limit as $\Delta t \downarrow 0$. Therefore, eq. 1 encompasses these two traditional growth models and offers a commensurate degree of flexibility. In this study, $\Delta t = 1$ year and is henceforth suppressed from our notation. To incorporate the possibility of annual environmental effects on growth, we extended eq. 1 to formulate the linear predictor function η_{ij} (McCullagh and Nelder 1989) for the ith fish during the jth growth year given by

$$(2) \quad \eta_{ij} = \beta_0 + \beta_{0j} + \beta_1 L_{ij} + \beta_{1j} L_{ij} + \beta_2 L_{ij} \log L_{ij} + \beta_{2j} L_{ij} \log L_{ij}$$

where β_{0j} is the main effect of year j, β_{1j} is effect of the jth year on the linear effect of L (year × length interaction), and β_{2j} is the effect of year j on the Gompertz term. Equation 2 can be viewed as a generalization of analysis of covariance that allows both linear and nonlinear responses over L that are not necessarily identical among years. We can achieve additional flexibility in the growth response by defining mean annual growth in length $\mu_{\Delta L} = g^{-1}(\eta)$ where $g(\cdot)$ is called the link function (McCullagh and Nelder 1989). For the identity link, $\mu_{\Delta L} = \eta$, and for the log link, $\mu_{\Delta L} = e^{\eta}$. Examinations of deviance residuals were used to guide the choice of link function and to confirm the adequacy of eq. 2 for particular data. We used the identity link unless specified otherwise.

For growth rates, variance is an increasing function of the mean (Francis 1990; Gutreuter and Childress 1990). We accommodated this feature of the data by modeling the variance of ΔL given L as a power function given by

$$(3) \quad \mathrm{Var}(\Delta L) = \sigma^2 \mu_{\Delta L}^{\theta}$$

where θ is a parameter for heteroscedasticity. For $\theta = 0$, the variance of growth increments is independent of the mean and constant at σ^2.

Given the mean response function $\mu_{\Delta L}$ and variance function (eq. 3), we fitted three statistical models of annual growth. We used three models to reduce the chance that our results were artifacts of a particular model choice. All three models assume distributions in the exponential family (McCullagh and Nelder 1989) and can be fitted via available software. Generally, the models produced very similar results and we based our graphical displays on model 1 (below) because θ was estimated in that model rather than assumed.

Model 1

For model 1, we assumed that annual length increments were conditionally, on year and initial length, normally distributed having mean $\mu_{\Delta L} = \eta$ and variance given by eq. 3. We fitted this model with generalized least-squares estimation, which consists of (*i*) obtaining a preliminary estimate of the parameter vector $\beta = (\beta_0, \ldots, \beta_{2j})^T$ from eq. 2, where β^T denotes the transpose of β, by using ordinary least-squares estimation, (*ii*) estimating θ via weighted nonlinear least squares from absolute values of the residuals and the estimates of $\mu_{\Delta L}$ from step *i*, (*iii*) obtaining a revised estimate of β by using weighted least squares with estimated weights $\hat{\mu}_{\Delta L}^{-\hat{\theta}}$, and (*iv*) repeating steps *ii* and *iii* until the error sums of squares converge, which usually occurs within six iterations (Carroll et al. 1988). This algorithm is easily implemented with most statistical computing packages. We tested for differences among years in the overall growth response by using F tests of the null hypothesis $\beta_{ij} = \beta_{ij'} = 0$ for all $i = 0,\ldots,2$ and $j \neq j'$, which states that the mean growth responses are identical for all years.

Model 2

For model 2, we assumed that annual length increments followed an unnamed distribution from the exponential family characterized by $\theta = 1$ and having σ^2 as a free dispersion parameter. By analogy to a discrete random variable, this distribution is equivalent to a Poisson-like distribution with extra-Poisson variation given by σ^2. We fitted model 2 with extended quasilikelihood estimation (McCullagh and Nelder 1989). Despite the exotic distribution, this model is easier to fit than model 1 but requires access to software having generalized linear models capability such as GLIM, SAS, or S-Plus; we used the SAS GENMOD (SAS Institute, Inc. 1997) procedure. We tested for among-year differences in the overall growth response by using approximate quasilikelihood ratio tests of the null hypothesis $\beta_{ij} = \beta_{ij'} = 0$ for all $i = 0,\ldots,2$ and $j \neq j'$.

Model 3

For model 3, we assumed that annual length increments follow a gamma distribution, which implies the constraint $\theta = 2$. We fitted model 3 with maximum likelihood estimation implemented through the SAS GENMOD procedure, but any software for generalized linear models will suffice. We tested for among-year differences in the overall growth response by using likelihood ratio χ^2 tests (McCullagh and Nelder 1989) of the null hypothesis $\beta_{ij} = \beta_{ij'} = 0$ for all $i = 0,\ldots,2$ and $j \neq j'$.

Results

Species with strong affinities to the moving littoral zone

Overall patterns of mean annual growth in length of largemouth bass from the La Grange Pool of the Illinois River differed significantly between the typical year (1992) and both the extreme flood year (1993: models 1 and 2, $P < 0.01$; model 3, $P = 0.04$) and the low-water year (1994: all $P \leq 0.01$), and our results do not appear to be an artifact of model choice. The magnitude of the difference in growth between the flood year and the low-water year was substantial for some sizes. For example, this difference was about 73% of 1994 growth for a 150-mm-long largemouth bass. For 50- to 350-mm largemouth bass, growth tended to be greater during 1993 than during the other two years (Fig. 5). Mean length increments of 50- to 350-mm largemouth bass tended to be least, and were inflected differently, during 1994 (Fig. 5) when water levels tended to be lowest during the latter portion of the growing season (Fig. 2). Growth of age-0 largemouth bass, which start the growth year near 0 mm total length, showed no distinct pattern among years. The apparent differences in growth for the longest largemouth bass might be an artifact of the small number of these large fish in our sample and the fact that our growth response function accommodated only one inflection. The parameter estimates and standard errors (Appendix) strongly indicate the importance of the Gompertz terms and the annual effects to overall model fit. The generalized least-squares estimate of θ, the variance function parameter, lies between the assumed values for models 2 and 3 and indicates strong heteroscedasticity.

Patterns of mean annual growth of bluegill differed among years in Pool 8 of the Mississippi River based on all three models. Growth differed significantly between the 1993 flood year and the more typical years of 1991–1992 combined and also between 1989 and 1991–1992 combined in all three models ($P < 0.01$). The growing season during 1989 was characterized by mild drought, and water elevations

© 1999 NRC Canada

Fig. 5. Model fit to total length increment data from largemouth bass captured from the La Grange Pool of the Illinois River. The growing season during 1993 was characterized by extreme persistent flooding and during 1994 was characterized by low water levels (Fig. 2).

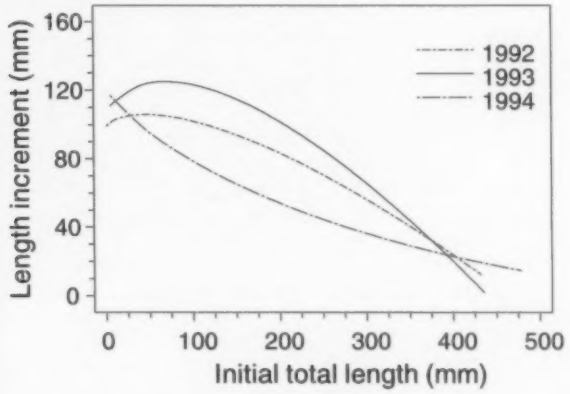

Fig. 6. Model fit for bluegills captured from (*a*) Pool 8 of the Mississippi River and (*b*) the La Grange Pool of the Illinois River.

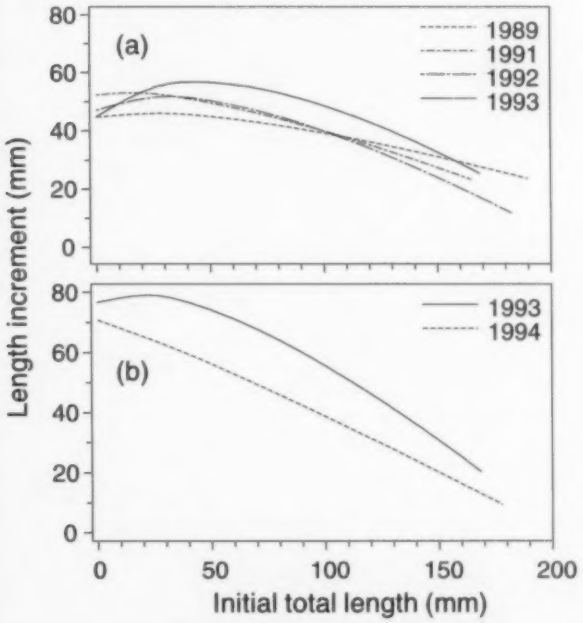

tended to be low (Fig. 2). Again, the overall significance of growth patterns cannot be explained by differences in model assumptions and is therefore likely real. Mean annual growth of 25- to 100-mm bluegill from Pool 8 was greatest during 1993 and least during 1989 (Fig. 6). Growth patterns were generally similar during the two more typical years of 1991 and 1992.

In the La Grange Pool of the Illinois River, annual growth of bluegill differed significantly based on all three models ($P < 0.01$). Again, mean growth was greater during the flood year than during the low-water year (Fig. 6). The relative magnitude of the growth differences was, for some sizes, substantial. For example, the growth difference between the flood year (1993) and the low-water year (1994) was about 43% of 1994 growth for 100-mm bluegill.

Fig. 7. Model fit for black crappie captured from (*a*) Pool 8 of the Mississippi River and (*b*) the La Grange Pool of the Illinois River.

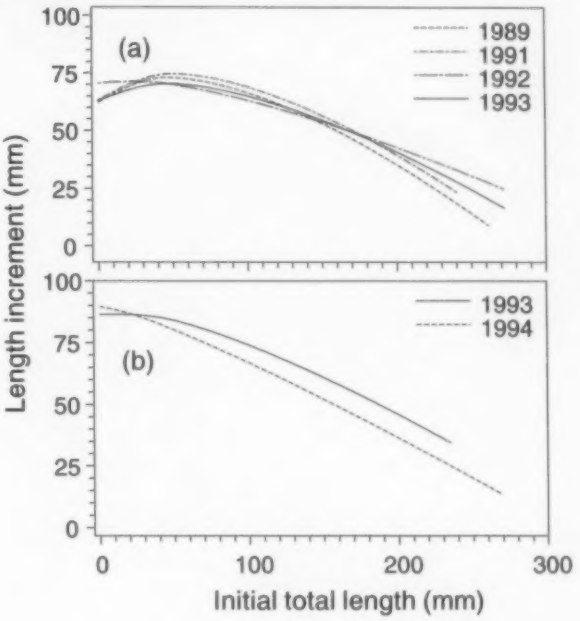

Species with weaker affinities to the moving littoral zone

Overall patterns of mean annual growth of black crappie from Pool 8 of the Mississippi River differed significantly between 1993 and 1991–1992 combined and between 1989 and 1991–1992 combined based on all three models ($P < 0.01$) except for the test for 1993 versus 1991–1992 combined from model 3 ($P = 0.21$). Therefore, conclusions about the difference between growth during 1993 and 1991–1992 combined are somewhat sensitive to model choice. Further, features of the data that produce those test results do not include a clear difference in growth over any broad size range that might be ecologically interpretable (Fig. 7). Overall patterns of mean growth of black crappie from the La Grange Pool of the Illinois River differed significantly between the 1993 flood year and the 1994 low-water year based on all three models ($P < 0.01$). Black crappie between 50 and 200 mm long grew only 5–25% faster during 1993 than during 1994 (Fig. 7).

Overall patterns in mean annual growth of white bass from the La Grange Pool of the Illinois River did not differ significantly between 1993 and 1994 based on any of the three models (all $P > 0.40$). The annual mean growth curves for the two years are relatively similar and intertwined (Fig. 8). In contrast with bluegill and largemouth bass, white bass from 100 to 150 mm grew only 14–25% faster during 1993 than during 1994. Our sample size for white bass was greater than that for bluegill from the La Grange Pool (Ta-

© 1999 NRC Canada

Fig. 8. Model fit for white bass captured from the La Grange Pool of the Illinois River.

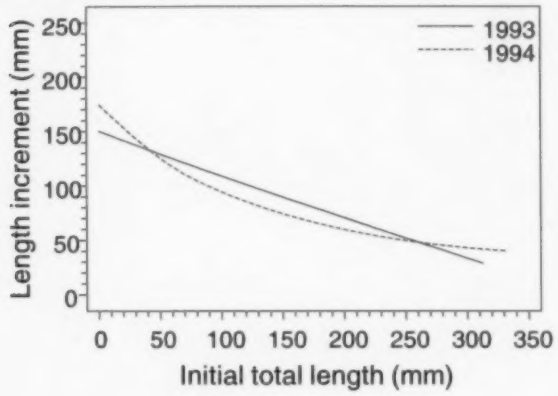

ble 1), and standard errors for the year-effects parameters were somewhat larger (Appendix). Therefore, this lack of a statistically significant growth difference is unlikely to merely be an artifact of insufficient statistical power but is more likely the result of the combination of a small annual effect and relatively large variability in growth.

Discussion

Our results were consistent with those of Bayley (1988) and suggest that some fishes of the temperate Upper Mississippi River system can, at least sometimes, show growth responses consistent with the FPC. Bayley (1988) examined short-term (about 2 weeks) growth in mass obtained from modal progressions of mean weights from pooled seine samples of mostly juveniles of 12 species of fish from the floodplain of the Rio Solimões near Manaus, Brazil. Bayley (1988) based statistical models of effects of hydrological changes on a linearized discrete-time form of the allometric growth model of Parker and Larkin (1959). Short-term growth of all species combined was 60% faster during the rising-water period than during the falling-water period. Growth increments of juvenile detritivores were not correlated with hydrological season, whereas those of omnivores were. Further, growth of omnivores was positively correlated with the rate of water level increase during the rising-water season but seemed independent of the rate of decrease during the falling-water season. These results suggest that, for these fishes of the Amazon basin, growth responses differ with trophic position, and those for the omnivores are consistent with the FPC.

Rutherford et al. (1995) examined annual growth of blue catfish (*Ictalurus furcatus*) (ages 0 and 1), channel catfish (*Ictalurus punctatus*) (age 0), and freshwater drum (*Aplodinotus grunniens*) and gizzard shad (*Dorosoma cepedianum*) (ages 0–2) captured near channel training structures between 669 and 883 km upriver of the mouth of the Mississippi River. Rutherford et al. (1995) hypothesized that if river–floodplain relationships in the temperate Lower Mississippi River are consistent with observations from the tropics (e.g., Bayley 1988), annual growth of these species should be correlated with discharge and overbank flooding. They used an ad hoc analysis of variance model of age-specific (cf. size-specific) growth and correlations with physicochemical variables to examine their hypothesis. Annual growth of these cohorts was not positively correlated with total hectares inundated, but rather, growth of blue catfish, channel catfish, and gizzard shad was correlated with the length of the growing season. From this, Rutherford et al. (1995) concluded their observations "did not conform to predictions of the flood-pulse concept," although they also recognized that reduction of the extent of the former floodplain might influence growth. Channel-alignment and flood-control strategies have reduced the area of the floodplain of the Lower Mississippi River by more than 90%; most of the former floodplain is presently in agriculture and isolated from the channel by levees, and floodplain lakes have been isolated (Fremling et al. 1989). We conclude that the study of Rutherford et al. (1995) constitutes a negative result that is nonetheless consistent with the FPC if only because the Lower Mississippi River is no longer an ecologically functional floodplain river in the sense of Junk et al. (1989), and the FPC applies to relatively rare pristine river–floodplain systems (Johnson et al. 1995).

We believe that our observations, coupled with those of Rutherford et al. (1995), help complete a more coherent picture of the applicability of the FPC to the Mississippi River system and perhaps other regulated temperate rivers. We have demonstrated that some species with high affinity to the moving littoral zone of the Upper Mississippi River system have potential to manifest a growth response that is consistent with the FPC. The strength of that response is mediated by body size in response to ontogenic niche shifts. Bluegill and largemouth bass exploit the moving littoral zone and, in our study, showed strong growth responses during an extreme flood. Black crappie exhibited an ambiguous response during the flood year, which we believe is due to their weak affinity for the aquatic–terrestrial transition zone. Finally, the more lotic white bass showed no immediate growth response that was consistent with the FPC. The ability to observe a growth response consistent with the FPC likely depends on the degree to which a particular species exploits the moving littoral zone, trophic position, the amount and quality of flooded terrestrial area, water temperature during flooding, and the efficiency of the statistical analysis.

The 1993 flood of the Upper Mississippi River system was unusual in that the flood crest lagged the typical flood crest by 3–5 months and occurred during midsummer when water temperatures, and therefore metabolic rates of fish, were high. Therefore, we cannot address whether growth responses to seasonal flooding are a frequent or important determinant of biological production in this system or in other large temperate rivers. Only examination of growth responses over many years and in many temperate floodplain rivers can provide data to resolve that remaining question. Further, development of a better understanding of biological production in large rivers will also require measurement of food web dynamics and trophic processes. In contrast, our data simply but clearly suggest that there is potential, under the conditions that we observed for some sizes of certain species, for a substantial growth response that is consistent

© 1999 NRC Canada

with the FPC. Even this limited result has important implications for management of temperate floodplain rivers.

The use of water level management strategies is gaining acceptance (Lubinski et al. 1991; Sparks 1995). Particular actions might have different effects on different ecosystem components. For example, experimental water level drawdowns designed to consolidate sediments and stimulate the growth of submersed and emergent macrophytes are being conducted in some areas of the Upper Mississippi River. Our results suggest that midsummer drawdowns might result in reduced growth of some littoral fishes. Conversely, artificial flooding might stimulate growth of some fishes. Our purpose here is not to comment on the merits of particular water level management strategies, but rather to suggest that some strategies might produce unintended costs and benefits. We are confident that careful evaluation of experimental water level management strategies will help managers assess and document the various costs and benefits and help scientists better understand the applicability and utility of the FPC for large temperate rivers.

Finally, our statistical modeling approach was central to our ability to detect growth responses consistent with the FPC. Our size-structured approach relied on conventional theory of growth, which allowed us to construct models with relatively few parameters and reasonable assumptions about variance that made efficient use of the data. For example, our model for largemouth bass in the La Grange Pool of the Illinois River required only 10 parameters to model effects of three years and a range of sizes that contained 10 age-classes. In contrast, an analysis of variance approach, analogous to that used by Rutherford et al. (1995), including the effects of year, age, and year × age interactions could have required as many as 29 parameters, and reasonable variance assumptions would not have been met. We gained efficiency in two ways. First, estimation of fewer parameters provides increased statistical power by leaving more degrees of freedom for error. Second, adequate modeling of variance is critical to efficient estimation of the mean response (Davidian and Carroll 1987). Our approach to the analysis of growth rates is not limited to our specific inquiry but can be extended to observational studies and controlled experiments that include random effects and repeated measurements from experimental units (Wolfinger and O'Connell 1993).

Acknowledgments

This study is a contribution of the Long Term Resource Monitoring Program of the Upper Mississippi River system, which is a cooperative effort of the U.S. Army Corps of Engineers, U.S. Fish and Wildlife Service, U.S. Geological Survey, and the States of Illinois, Iowa, Minnesota, Missouri, and Wisconsin. Partial financial and administrative support was provided by the University of Wisconsin-La Crosse, Illinois Natural History Survey, and the U.S. Geological Survey. The data from Pool 8 were part of a Master of Science thesis by A.D.B. produced under the guidance of S.G. and M.B.S. We thank the many people who contributed to the data collection and processing and particularly Paul Raibley, T. Matt O'Hara, Steve Skemp, Kristi Jackson, and Shaun Hyde. We particularly thank K. Douglas Blodgett, Barry L. Johnson, Brent C. Knights, William B. Richardson, R.I.C.C. Francis, and an anonymous reviewer for helpful comments.

References

Bayley, P.B. 1988. Factors affecting growth rates of young tropical floodplain fishes: seasonality and density-dependence. Environ. Biol. Fishes, **21**: 127–142.

Bayley, P.B. 1995. Understanding large river–floodplain ecosystems. BioScience, **45**: 153–158.

Becker, G.C. 1983. Fishes of Wisconsin. University of Wisconsin Press, Madison, Wis.

Carroll, R.J., Wu, C.F., and Ruppert, D. 1988. The effect of estimating weights in weighted least squares. J. Am. Stat. Assoc. **83**: 1045–1054.

Davidian, M., and Carroll, R.J. 1987. Variance function estimation. J. Am. Stat. Assoc. **82**: 1079–1091.

Dudley, R.G. 1979. Changes in growth and size distribution of *Saratherodon macrochir* and *Saratherodon andersoni* from the Kafue Floodplain, Zambia, since construction of the Kafue Gorge Dam. J. Fish Biol. **14**: 205–223.

Francis, R.I.C.C. 1990. Back-calculation of fish length: a critical review. J. Fish Biol. **36**: 883–902.

Fremling, C.R., Rasmussen, J.L., Sparks, R.E., Cobb, S.P., Bryan, C.F., and Claflin, T.O. 1989. Mississippi River fisheries: a case history. *In* Proceedings of the International Large River Symposium. *Edited by* D.P. Dodge. Can. Spec. Publ. Fish. Aquat. Sci. No. 106. pp. 309–351.

Gutreuter, S. 1987. Considerations for estimation and interpretation of annual growth rates. *In* Age and growth of fish. *Edited by* R.C. Summerfelt and G.E. Hall. Iowa State University Press, Ames, Iowa. pp. 115–126.

Gutreuter, S., and Childress, W.M. 1990. Evaluation of condition indices for estimation of growth of largemouth bass and white crappie. N. Am. J. Fish. Manage. **10**: 434–441.

Gutreuter, S., Burkhardt, R., and Lubinski, K.S. 1995. Long Term Resource Monitoring Program procedures: fish monitoring. Program Rep. 95-P002-1. National Biological Service, Environmental Management Technical Center, Onalaska, Wis.

Johnson, B.L., Richardson, W.B., and Naimo, T.J. 1995. Past, present, and future concepts in large river ecology. BioScience, **45**: 134–141.

Junk, W.L., Bayley, P.B., and Sparks, R.E. 1989. The flood pulse concept in river–floodplain systems. *In* Proceedings of the International Large River Symposium. *Edited by* D.P. Dodge. Can. Spec. Publ. Fish. Aquat. Sci. No. 106. pp. 110–127.

Laustrup, M.S., and Lowenberg, C.D. 1994. Development of a systemic land cover/land use database for the Upper Mississippi River system derived from Landsat Thematic Mapper satellite data. Tech. Rep. 94-T001. U.S. Geological Survey Environmental Management Technical Center, Onalaska, Wis.

Lubinski, K.S., Carmody, G., Wilcox, D., and Drazkowski, B. 1991. Development of water level regulation strategies for fish and wildlife, Upper Mississippi River system. Regul. Rivers: Res. Manage. **6**: 117–124.

McCullagh, P., and Nelder, J.A. 1989. Generalized linear models. Chapman and Hall, London, U.K.

Mills, E.L., Pol, M.V., Sherman, R.E., and Culver, T.B. 1989. Interrelationships between prey body size and growth of age-0 yellow perch. Trans. Am. Fish. Soc. **118**: 1–10.

Olson, M.H. 1996. Ontogenic niche shifts in largemouth bass: variability and consequences for first-year growth. Ecology, **77**: 179–190.

Osenberg, C.W., Werner, E.E., Mittelbach, G.G., and Hall, D.J. 1988. Growth patterns in bluegill (*Lepomis macrochirus*) and

© 1999 NRC Canada

pumpkinseed (*L. gibbosus*) sunfish: environmental variation and the importance of ontogenic niche shifts. Can. J. Fish. Aquat. Sci. **45**: 17–26.

Parker, R.R., and Larkin, P.A. 1959. A concept of growth in fishes. J. Fish. Res. Board Can. **16**: 721–745.

Pflieger, W.L. 1975. The fishes of Missouri. Missouri Department of Conservation, Jefferson City, Mo.

Raibley, P.T., O'Hara, T.M., Irons, K.S., Blodgett, K.D., and Sparks, R.E. 1997. Largemouth bass size distributions under varying annual hydrological regimes in the Illinois River. Trans. Am. Fish. Soc. **126**: 850–856.

Randall, R.G., Kelso, J.R.M., and Minns, C.K. 1995. Fish production in freshwaters: are rivers more productive than lakes? Can. J. Fish. Aquat. Sci. **52**: 631–643.

Ricker, W.E. 1975. Computation and interpretation of biological statistics of fish populations. Bull. Fish. Res. Board Can. No. 191.

Ricker, W.E. 1979. Growth rates and models. *In* Fish physiology. Vol. 8. *Edited by* W.S. Hoar, J.D. Randall, and J.R. Brett. Academic Press, New York. pp. 677–743.

Rutherford, D.A., Kelso, W.E., Bryan, C.F., and Constant, G.C. 1995. Influence of physicochemical characteristics on annual growth increments of four fishes from the Lower Mississippi River. Trans. Am. Fish. Soc. **124**: 687–697.

SAS Institute, Inc. 1997. SAS/STAT software: changes and enhancements through release 6.12. SAS Institute, Inc., Cary, N.C.

Sparks, R.E. 1995. Need for ecosystem management of large rivers and their floodplains. BioScience, **45**: 168–182.

Weisberg, S., and Frie, R.V. 1987. Linear models for the growth of fish. *In* Age and growth of fish. *Edited by* R.C. Summerfelt and G.E. Hall. Iowa State University Press, Ames, Iowa. pp. 127–143.

Welcomme, R.L. 1979. Fisheries ecology of floodplain rivers. Longman, London, U.K.

Werner, E.E. 1979. Niche partitioning by food size in fish communities. *In* Predator–prey systems in fisheries management. *Edited by* H. Clepper. Sport Fishing Institute, Washington, D.C. pp. 311–322.

Wolfinger, R., and O'Connell, M. 1993. Generalized linear mixed models: a pseudo-likelihood approach. J. Stat. Comput. Simul. **48**: 233–243.

Appendix. Parameter estimates (SE in parentheses) for the growth rate response function given by eq. 2 fitted to three statistical models assuming different variance functions and response distributions.

	Parameter												
Model	β_0	$\beta_{0,1}$	$\beta_{0,2}$	$\beta_{0,3}$	β_1	$\beta_{1,1}$	$\beta_{1,2}$	$\beta_{1,3}$	β_2	$\beta_{2,1}$	$\beta_{2,2}$	$\beta_{2,3}$	θ
Largemouth bass, La Grange Pool, Illinois River													
1	123.063	–20.405	–8.58		–1.073	1.779	2.361		0.137	–0.288	–0.392		1.282
	(3.587)	(8.199)	(4.839)		(0.143)	(0.330)	(0.252)		(0.005)	(0.055)	(0.042)		(0.112)
2[a]	4.820	–0.288	–0.106		–0.007	0.031	0.032		0.005	–0.005	–0.005		1[b]
	(0.028)	(0.079)	(0.039)		(0.002)	(0.005)	(0.004)		(0.001)	(0.001)	(0.001)		
3	122.304	–17.163	–6.740		–1.018	1.525	1.926		0.128	–0.247	–0.317		2[b]
	(4.280)	(10.563)	(5.896)		(0.131)	(0.371)	(0.218)		(0.021)	(0.058)	(0.035)		
Bluegill, Pool 8, Mississippi River													
1	–1.944	1.011	1.457	0.981	2.719	–1.015	–1.198	–0.874	–1.313	0.451	0.555	0.412	0.794
	(0.298)	(0.420)	(0.430)	(0.380)	(0.272)	(0.362)	(0.388)	(0.344)	(0.135)	(0.182)	(0.189)	(0.169)	(0.240)
2	–1.947	1.028	1.458	1.010	2.717	–1.028	–1.197	–0.902	–1.309	0.456	0.552	0.425	1[b]
	(0.295)	(0.407)	(0.429)	(0.374)	(0.268)	(0.350)	(0.386)	(0.338)	(0.131)	(0.173)	(0.186)	(0.163)	
3	–1.994	1.125	1.474	1.146	2.747	–1.112	–1.208	–1.033	–1.314	0.493	0.552	0.487	2[b]
	(0.323)	(0.409)	(0.450)	(0.400)	(0.305)	(0.367)	(0.415)	(0.373)	(0.146)	(0.177)	(0.196)	(0.177)	
Bluegill, La Grange Pool, Illinois River													
1	1.955	–0.177			–0.583	0.296			0.112	–0.153			1.158
	(0.261)	(0.450)			(0.220)	(0.400)			(0.116)	(0.216)			(0.334)
2	1.945	–0.178			–0.574	0.298			0.108	–0.154			1[b]
	(0.262)	(0.446)			(0.224)	(0.400)			(0.119)	(0.216)			
3	2.016	–0.169			–0.637	0.285			0.141	–1.146			2[b]
	(0.256)	(0.463)			(0.197)	(0.393)			(0.098)	(0.206)			
Black crappie, Pool 8, Mississippi River													
1	0.034	–0.569	–0.622	–0.322	1.223	0.384	0.503	–0.182	–0.567	–0.200	–0.264	0.059	1.246
	(0.399)	(0.426)	(0.459)	(0.452)	(0.263)	(0.287)	(0.320)	(0.310)	(0.106)	(0.118)	(0.135)	(0.128)	(0.204)
2	–0.012	–0.539	–0.587	0.356	1.261	0.368	0.476	–0.207	–0.585	–0.194	–0.252	0.070	1[b]
	(0.417)	(0.446)	(0.477)	(0.469)	(0.270)	(0.295)	(0.327)	(0.318)	(0.108)	(0.120)	(0.137)	(0.130)	
3[a]	0.088	–0.080	0.018	0.220	0.743	0.174	0.083	–0.249	–0.417	–0.130	–0.080	0.111	2[b]
	(0.113)	(0.120)	(0.125)	(0.122)	(0.136)	(0.149)	(0.162)	(0.155)	(0.064)	(0.072)	(0.081)	(0.075)	
Black crappie, La Grange Pool, Illinois River													
1	3.388	–0.505			–1.301	0.443			0.422	–0.187			0.631
	(0.237)	(0.324)			(0.165)	(0.257)			(0.076)	(0.127)			(0.278)

© 1999 NRC Canada

Appendix (*concluded*).

Model	Parameter												
	β_0	$\beta_{0,1}$	$\beta_{0,2}$	$\beta_{0,3}$	β_1	$\beta_{1,1}$	$\beta_{1,2}$	$\beta_{1,3}$	β_2	$\beta_{2,1}$	$\beta_{2,2}$	$\beta_{2,3}$	θ
2	3.327	–0.447			–1.255	0.400			0.401	–0.167			1[b]
	(0.255)	(0.344)			(0.173)	(0.264)			(0.077)	(0.128)			
3	3.171	–0.298			–1.146	0.298			0.351	–0.122			2[b]
	(0.305)	(0.403)			(0.193)	(0.285)			(0.083)	(0.132)			
White bass, La Grange Pool, Illinois River													
1	5.366	–1.020			–2.113	0.795			0.738	–0.357			0.787
	(0.792)	(0.850)			(0.472)	(0.550)			(0.197)	(0.237)			(0.186)
2	5.324	–0.934			–2.087	0.728			0.727	–0.328			1[b]
	(0.843)	(0.886)			(0.499)	(0.553)			(0.207)	(0.234)			
3[a]	1.924	–0.753			–0.718	0.655			0.174	–0.308			2[b]
	(0.514)	(0.582)			(0.333)	(0.423)			(0.147)	(0.192)			

© 1999 NRC Canada

Population processes responsible for larger-fish-upstream distribution patterns of Arctic grayling (*Thymallus arcticus*) in interior Alaskan runoff rivers

Nicholas F. Hughes

Abstract: During the summer months, Arctic grayling (*Thymallus arcticus*) in Alaskan streams adopt a larger-older-fish-upstream distribution pattern. In this paper, I analyse data from two large interior Alaskan rivers to determine how population processes maintain this size and age gradient. These analyses support the hypothesis that age-phased recruitment and growth-dependent movement are primarily responsible for this distribution pattern. Age-phased recruitment describes the way that the mean age of fish recruiting to a reach increases upstream, from ages 0–1 in the lower river to ages 3–7 in the headwaters. This process begins with the concentration of spawning fish, and the resultant fry, in the lower reaches of the river. Downstream movement during the first year of life further concentrates young fish in the lower river. Over time, the distribution of this cohort broadens steadily as individuals move further upstream, so that fish recruiting to headwater reaches are 3–7 years old. This process contributes to both size and age gradients. Growth-dependent movement magnifies the size gradient by sorting fast-growing fish into the upper river and slow-growing fish into the lower river. This sorting results from the fact that individuals making long-distance upstream movements tend to have grown particularly rapidly that year, while individuals making long-distance downstream movements tend to have grown especially slowly that year. I rejected the hypothesis that age and size gradients are the result of whole-stream gradients in growth or mortality acting on a sedentary population. However, there was some evidence that fish did grow more slowly in the lowest 40 km of one river, although this made only a minor contribution to the size gradient and growth rates were remarkably constant for the next 120 km. There was no suggestion that spatial variation in mortality rate contributes towards the size or age gradient, but natural and sampling variability could have obscured small but significant differences between reaches.

Résumé : Pendant les mois d'été, le profil de répartition de l'ombre arctique (*Thymallus arcticus*) des cours d'eau de l'Alaska est tel qu'on trouve des poissons plus âgés et de plus grande taille vers l'amont. Dans le présent document, j'analyse les données de deux grands cours d'eau intérieurs de l'Alaska afin d'établir de quelle manière les processus démographiques conservent ce gradient selon la taille et l'âge. Ces analyses appuient l'hypothèse selon laquelle le recrutement par groupe d'âge et le déplacement selon la taille sont les principaux responsables de ce profil de répartition. Le recrutement selon l'âge décrit la façon dont l'âge moyen des poissons recrutés dans un tronçon en amont passe de l'âge 0–1 dans le cours inférieur aux âges de 3–7 dans le cours supérieur. Ce processus commence par la concentration des géniteurs, et des alevins produits, dans les tronçons inférieurs du cours d'eau. Le déplacement en aval au cours de la première année concentre encore plus les jeunes poissons dans le cours inférieur. Avec le temps, la distribution de cette cohorte s'élargit régulièrement à mesure que les individus remontent, de sorte que les poissons recrutés dans les tronçons du cours supérieur sont âgés de 3 à 7 ans. Ce processus contribue aux gradients selon la taille et selon l'âge. Le déplacement selon la croissance amplifie le gradient selon la taille, en concentrant les poissons à croissance rapide dans le cours supérieur, et les poissons à croissance lente dans le cours inférieur. Cette répartition est attribuable au fait que les individus qui ont parcouru de grandes distances en amont se sont développés particulièrement rapidement cette année-là, tandis que ceux qui ont effectué de long parcours en aval se sont développés particulièrement lentement pendant la même période. J'ai rejeté l'hypothèse selon laquelle les gradients selon l'âge et la taille découlent de gradients de croissance ou de mortalité visant l'ensemble du cours d'eau et qui agissent sur une population sédentaire. Toutefois, certaines indications ont montré que la croissance des poissons avait été plus lente dans les derniers 40 km d'un cours d'eau, même si cela ne contribue que de façon minime au gradient de tailles et les taux de croissance étaient remarquablement constants dans les 120 km suivants. Rien n'indique que la variation spatiale du taux de mortalité contribue au gradient selon la taille ou selon l'âge, mais la variabilité naturelle et celle des échantillons auraient pu masquer des différences petites mais importantes entre les tronçons.

[Traduit par la Rédaction]

Received June 2, 1997. Accepted March 10, 1999.
J14037

N.F. Hughes. School of Fisheries and Ocean Sciences, University of Alaska-Fairbanks, Fairbanks, Alaska 99775-97220, U.S.A.
e-mail: ffnfh@uaf.edu

© 1999 NRC Canada

Introduction

During the summer feeding period, Arctic grayling (*Thymallus arcticus*) in Alaskan streams and brown trout (*Salmo trutta*) in some New Zealand streams adopt a larger-older-fish-upstream distribution pattern (Tack 1974; Hughes and Reynolds 1994; Jellyman and Graynoth 1994; Hughes 1998). The way in which population processes maintain these size and age gradients from one year to the next is poorly documented. One possibility is that most young fish recruit to downstream reaches and move further upstream as they grow older and larger (Tack 1980). I term this idea the "age-phased recruitment hypothesis." Another possibility is that fast-growing fish tend to move upstream, while slow-growing fish move downstream, an idea I call the "growth-dependent movement hypothesis." The processes described by these two movement-centered hypotheses could occur simultaneously.

A movement-free explanation is that the larger-older-fish-upstream distribution pattern is produced by whole-stream gradients in growth and mortality acting on a sedentary population. This appears to be true for Japanese river sculpin (*Cottus hangiongensis*) (Goto 1989) and Trinidadian guppies (*Poecilia reticulata*) (Reznick and Endler 1982). This could be called the "static population with growth and mortality gradients hypothesis" and would be the most acceptable explanation if you shared the traditional opinion that stream fish live out most of their lives in a short section of stream (e.g., Miller 1957; Gerking 1959; but see Gowan et al. 1994).

In this paper, I test these three hypotheses using data on Arctic grayling collected from two interior Alaskan rivers. To test the age-phased recruitment hypothesis, I evaluated the evidence that young fish recruit to the lower river and move to reaches progressively further upstream as they grow older and larger. To test the growth-dependent movement hypothesis, I looked for the expected correlation between upstream movement and rapid growth. To test the static population with growth and mortality gradients hypothesis, I looked for the predicted decrease in mortality rates and (or) an increase in growth rate with the progression upstream. Finally, I review the evidence suggesting that the same processes responsible for size gradients of Arctic grayling also produce the larger-fish-upstream patterns shown by New Zealand brown trout and the smaller-fish-upstream pattern that can be inferred for brown trout in European rivers (Solomon and Templeton 1976; Milner et al. 1978; Baglinière et al. 1989; Maisse and Baglinière 1990; Bembo et al. 1993).

Methods

Study area

The Goodpaster and Chena rivers are two large runoff tributaries of the turbid glacier-fed Tanana River, a major tributary of the Yukon River (Fig. 1). The Goodpaster River flows about 200 km from source to mouth, while the Chena River flows about 260 km. Arctic grayling in these rivers spend 6–7 months a year overwintering under the ice, spawn immediately after breakup, and then migrate to summer feeding areas. It is during the summer that fish adopt the larger-older-fish-upstream distribution pattern that I discuss in this paper. These size and age gradients are stable from one year to the next (Tack 1974, 1975), provided that there are no major changes in the size and age structure of the population as a whole (Hughes and Reynolds 1994).

Data sources

Goodpaster River

Most analyses of the Goodpaster River were based on data collected by Tack (1974), who estimated population parameters from data collected during three complete passes over the length of the river (a total of 185 km, from within 15 km of the source to the mouth), in June, July, and August 1973. Fish in the upper river were captured with hook and line, and fish in the middle and lower river were captured using an electrofishing boat. Tack (1974) also made observations on the distribution and size of fry along the length of the river during the course of the summer. The number of fish larger than 150 mm fork length that he handled during the season was about 3140 in the lower section (river km 0–53), 880 in the middle section (river km 53–98), and 630 in the upper section (river km 98–185) for a total of 4650 fish. Fork length was measured and scales collected from each fish handled.

I also used length–frequency data collected by the Alaska Department of Fish and Game from the lower Goodpaster River during the spawning season (May) and the summer feeding period (August) in 1995 and 1996. I employed length-at-age data from scales sampled in May 1995 and 1996 and for samples collected in August over a 6-year period between 1988 and 1993. May sample sizes totalled 4165 fish, of which 1912 were aged, August sample sizes in 1995 and 1996 totalled 1255 fish, and August sample sizes over the period 1988–1993 totalled 4400 fish, all of which were aged (W.P. Ridder, Alaska Department of Fish and Game, unpublished data). Fish were captured using an electrofishing boat.

Chena River

Most analyses for the Chena River were based on data collected from the lower 140 km of the river during July and August between 1987 and 1995 by the Alaska Department of Fish and Game using an electrofishing boat (R.A. Clark, Alaska Department of Fish and Game, unpublished data). To get a complete picture of the whole-stream distribution pattern in 1992, I also obtained length and scale samples from 683 fish from the upper Chena River (river km 140–240) by sampling with hook and line during late August and early September.

The data collection protocol for the lower 140 km of the Chena River changed between 1987 and 1995. From 1987 to 1990, fish were sampled by electrofishing four 3.2-km sections of the lower 72 km of the river and in a single large section extending from 72 to 140 km upstream from the mouth. Both banks of each section in the lower 72 km were electrofished three to five times, while both banks of the large upper section were fished twice. The fork length of each fish was measured, scales were sampled for age determination, and fish larger than 150 mm fork length were tagged with individually numbered Floy FD-67 internal anchor tags. During these three years, the location of fish capture was categorized into sections about 16 km long, so the resolution on fish movements from recaptures was fairly low. From 1990 onwards, this resolution was improved by categorizing fish into sections 5 km or less in length. From 1991 to 1993 the coverage was also improved by electrofishing the entire 140-km section. However, only fish captured during the first of two passes along the river were individually tagged. The same procedure was continued in 1994–1995, except that fish were no longer individually marked.

Additional data on the distribution of small fish in the Chena River were provided by Tack's (1971) electrofishing surveys between 34 and 126 km upstream of the mouth. Tack's (1971) boat used alternating current, which was more effective at sampling age 1 and 2 fish than the direct-current boat that was used during the 1987–1995 period. Seining surveys by Holmes (1984) provided data on changes in the abundance of age 0+ fish along the lower 120 km of the river, and direct observations of the distribution of young-of-the-year in the Chena River and its major tributaries were made by Tack (1975) and Hallberg (1978).

© 1999 NRC Canada

Fig. 1. Map of the study area showing reach divisions on the Chena and Goodpaster rivers.

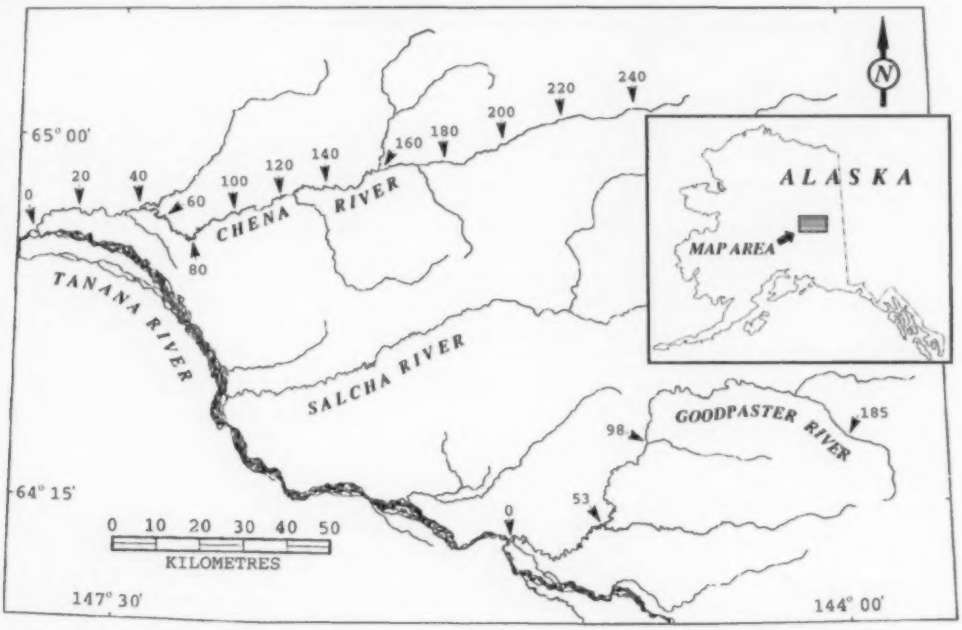

Data analysis

Most of my analyses of data from the Goodpaster River were based on the information that Tack presented in his 1974 report rather than on the original data. For this reason, I used Tack's (1974) division of the river into upper, middle, and lower sections, which are naturally delimited by major tributaries (Fig. 1). For the Chena River, I based my analyses on the raw data. I divided the lower 240 km of the river into 12 reaches, each 20 km long, pairing these to form six 40-km reaches for analysis of whole-river trends in growth rate (Fig. 1).

Size and age gradients

The first step of my analysis was to characterize the size and age gradients of Arctic grayling in the Chena and Goodpaster rivers. To determine the length composition of fish captured from each 20-km reach of the Chena River in 1992, I simply tabulated the fork lengths of all the fish in the catch that were larger than 150 mm. Tack (1974) used the same method to determine the length composition in the three sections of the Goodpaster River. I estimated the age composition of fish captured from each 20-km reach of the Chena River in 1992 using Ketchen's method (Ricker 1975), deriving confidence intervals (CIs) for estimates of mean age using bootstrap procedures (Press et al. 1988). Tack (1974) estimated the age composition of fish in the lower, middle, and upper Goodpaster River by reading scales from 100 randomly sampled fish from each reach.

Spatial patterns of spawning and recruitment

To examine the extent to which spatial patterns in recruitment maintain the size gradient, I tried to determine the way in which age 0+ fry are distributed along the length of the river and the way that the distribution of a cohort changes as its members grow older and larger.

I used two approaches to determine fry distribution. First, I analysed information on the distribution of spawners because fry will initially be most abundant in areas where spawners congregate. Because fish that feed in the upper river are thought to spawn in downstream reaches (W.P. Ridder, personal communication), I compared length–frequency data collected from the lower Goodpaster River during the spawning season (May 1995–1996) and the summer feeding period (July and August 1995–1996). Large spawning fish should be abundant during spring but scarce by summer. To search for corroborative evidence that fish spawning in the lower river did, in fact, subsequently migrate to feed in the upper river, I compared the length-at-age of fish captured in the lower Goodpaster River during May (1995–1996) and August (1988–1993). If length-at-age for large fish in the lower river falls between May and August, this will support the idea that spawners in the lower river summer in the upper river. This inference is possible because length-at-age is a marker for summer feeding location, with fish that summer in the upper river (or nearby spring-fed creeks) being particularly large for their age (W.P. Ridder, personal communication; also see below). My second approach to characterizing fry distribution was analysis of seining surveys (Holmes 1984) and visual observations of free-living fish (Tack 1974, 1975; Hallberg 1978).

My analysis of the distribution of age 1 and 2 fish is based on Tack's (1971) electrofishing survey of five reaches of the Chena River between 34 and 126 km from the mouth. Tack's (1971) length–frequency histograms show two clear modes, corresponding to these two age-classes. The size range 70–139 mm encompasses age 1 fish and the size range 140–179 encompasses age 2 fish in late June 1970. By counting the fish in each of these two modes, I determined how the relative abundance of these two age-classes changed with the progression upstream.

Once fish reached age 3, they were adequately sampled by the electrofishing boat and hook-and-line gear and I was able to infer distribution patterns of fish age 3 and older directly from the samples collected with these gear types.

Growth and related movements

To determine whether there was a whole-stream gradient in growth rate on the Chena River, I used two methods. First, I used scale-aged fish to fit von Bertalanffy growth curves for all six 40-

© 1999 NRC Canada

km reaches using Beverton's method (Ricker 1975) and all scale-aged fish captured between 1991 and 1995. Sample sizes were as follows: river km 0–39, 3347; river km 40–79, 2819; river km 80–119, 2497; river km 120–159, 1888; river km 160–199, 292; river km 200–239, 176, Total sample size was 11 019 fish.

In the second approach, I used mark–recapture data to fit von Bertalanffy growth curves for the four most downstream 40-km reaches using a Walford plot as described by Ricker (1975). I seeded the Walford line with the mean length at age 2 for all scale-aged fish caught in the lower 160 km of the river between 1991 and 1995 (181 mm, 95% CI ± 0.6 mm, n = 1709). I calculated CIs on mean length-at-age using bootstrap procedures (Press et al. 1988). This analysis used fish that were marked and recaptured in the same reach between 1987 and 1994. Sample sizes were as follows: river km 0–39, 299; river km 40–79, 376; river km 80–119, 366; river km 120–159, 257. Total sample size was 1298 fish.

To check for correlations between movement and growth, I compared the annual growth increment of fish that moved upstream at least 10 km with the growth increment of fish that moved less than 10 km, or downstream at least 10 km. I used data from fish captured in two consecutive years between 1987 and 1995, restricting the analysis to fish of known age, which confined their movements to the section between river km 40 and 140. This protocol controlled for both reach and age effects on growth rate because growth was remarkably constant within this 100-km section (see below) and it was possible to divide the sample into six age-classes for analysis. Sample sizes for fish 2–7 years old were as follows: moving down, 4, 10, 23, 13, 2, and 4; staying put, 14, 40, 152, 74, 26, and 24; moving up, 1, 15, 15, 19, 7, and 2. Total sample size was 445 fish. I tested for a correlation between movement direction and growth using the sign test (Conover 1980), which has the advantage of being almost assumption free and is also more conservative than alternative tests.

Mortality rates

To see if mortality rates increased upstream, I used mark–recapture data to estimate annual mortality rates for each 20-km reach in the lower 140 km of the Chena River. These calculations were based on the number of fish marked in a reach in two successive years and the number of these two batches of fish recaptured in later years through 1995 (in any reach). I obtained estimates for 1991–1992 and 1992–1993 using Ricker's (1975) large-sample formula. I restricted this analysis to fish that were larger than 200 mm to reduce bias from the rapidly increasing probability of capture with fish size, which occurs between 150 and 200 mm, particularly in the lower 80 km of the river (unpublished analyses). This precaution reduces this source of bias but will not eliminate it because the probability of capture continues to rise for fish larger than 200 mm, at least in the reach between river km 80 and 140. These changes in capture probability will bias estimates of mortality downwards. I used linear regression to test for a relationship between mortality rate and distance upstream.

Gear selectivity

One primary concern in these analyses is the possibility that differences in the size selectivity of electrofishing and hook-and-line sampling could have biased the results. This potential exists because fish in the lower sections of both the Goodpaster and Chena rivers were captured with an electrofishing boat, while fish in the upper sections were captured with hook and line. However, there is reason to believe that differences in gear selectivity have not affected the analyses and inferences that I have made in this paper because there is evidence that the size selectivity of the two gears is rather similar. For example, mean lengths (± 95% CIs) of fish captured by electrofishing and hook and line in the nearby Delta Clearwater River were 296 mm (± 3.2, n = 1226) and 290 mm (±2.9, n = 1102), respectively (Ridder 1984). Although this difference is statistically significant, it is too small (6 mm) to influence the analyses in this paper.

Fig. 2. Change in mean length of Arctic grayling along the length of the Chena and Goodpaster rivers; 95% CIs on mean length are available for the Chena River only.

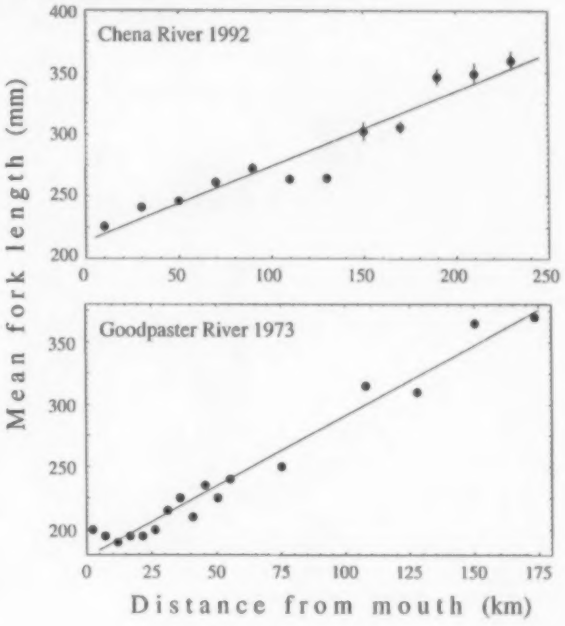

Results

Size and age gradients

Both the Goodpaster and Chena rivers had pronounced larger-fish-upstream size gradients. Mean length increased by 180 mm along the length of the Goodpaster River and 135 mm along the length of the Chena River (Fig. 2). The statistics for a linear regression of mean length on distance upstream were $p < 0.001$ and $R^2 = 0.97$ for the Goodpaster River and $p < 0.001$ and $R^2 = 0.92$ for the Chena River. Mean length near the mouth was lower on the Goodpaster River (180 mm) than on the Chena River (225 mm), but mean fish length in the headwaters was similar in both rivers, 360–370 mm.

An age gradient parallels the size gradient. In the Chena River during 1992, the mean age of fish sampled increased from less than 4 years old in the lower river to between 6.5 and 7 years old in the headwaters (linear regression, $p < 0.001$, $R^2 = 0.74$). In the Goodpaster River during 1973, the mean age of fish was 3.4 years old in the lower river, 4.2 years old in the middle river, and 6.5 years old in the upper river. This gradient reflects a loose age segregation along the length of the river (Fig. 3).

Spatial patterns of spawning and recruitment

Evidence from the Goodpaster River shows that mature fish concentrate in the lower river to spawn and then leave to summer in upstream reaches or nearby spring-fed creeks. This is demonstrated by the change in the length–frequency

© 1999 NRC Canada

Fig. 3. Age–frequency distributions of fish captured in the upper, middle, and lower reaches of the Goodpaster and Chena rivers. Section boundaries on the Goodpaster River were 0–53 km (lower), 53–98 km (middle), and 98–185 km (upper). Data for the Chena River are from the lower (river km 0–20), middle (river km 120–140), and uppermost (river km 220–240) study reaches.

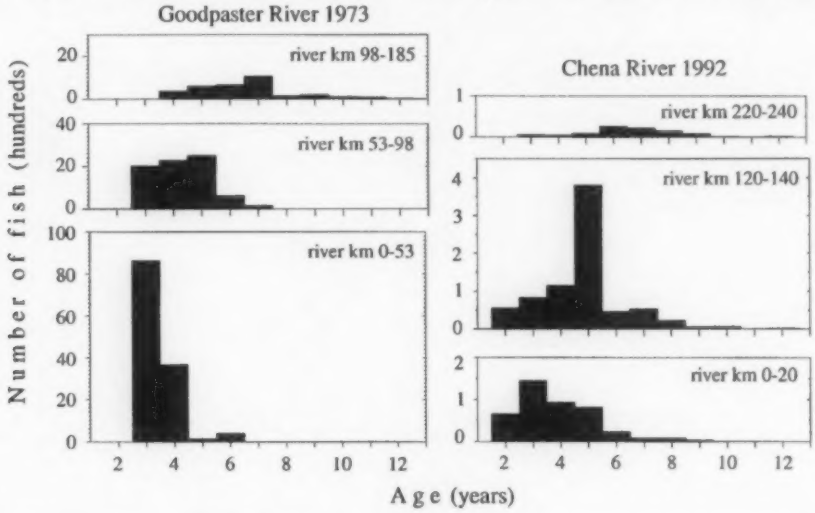

Fig. 4. Length–frequency distributions of fish captured in the lower 53 km of the Goodpaster River during the spawning season in May and the summer feeding period in August. Data from 1995 and 1996 are pooled.

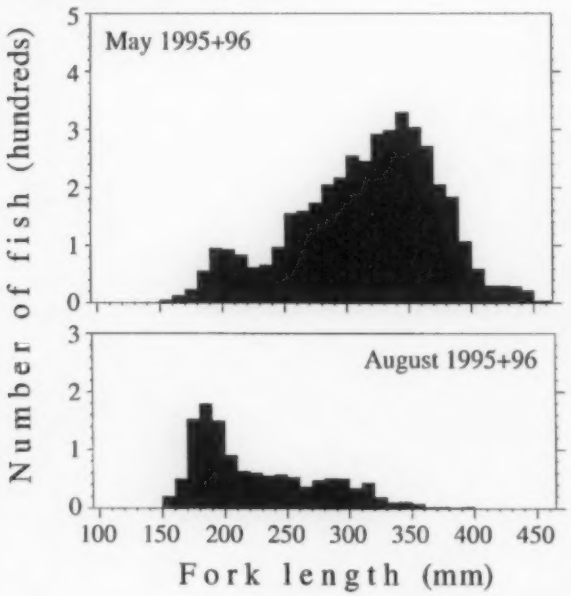

distribution of fish between spawning and feeding periods (Fig. 4); large fish are abundant in the spawning period and virtually disappear by August. The large fish present in the lower river in May have been observed defending spawning territories (W.P. Ridder, personal communication).

Supporting evidence that fish spawn in the lower river and summer in the upper river or nearby spring-fed creeks is provided by the decrease in mean length-at-age of mature individuals in the lower river between May and August (Table 1). This shows that fish large for their age present in May must have left by August, while fish small for their age stayed behind. The only place that such fish large for their age are found during August is the upper reaches of these rivers or nearby spring-fed creeks. W.P. Ridder (personal communication) has also documented these patterns of movement directly with recaptures of tagged fish.

Although spawning is concentrated in the lower reaches, it occurs all along the river. This is demonstrated by the presence of young fry all the way to the headwaters of both the Goodpaster and Chena rivers (Tack 1974, 1975; Hallberg 1978; N.F. Hughes, personal observation). Spawning occurs progressively later with the progression upstream and can extend into late June (Hallberg 1978). As a result of this, fry size decreases upstream, probably due to a later hatching date and cooler than optimal temperatures for growth in upstream reaches (Tack 1974, 1975). Seining surveys of fry abundance by Holmes (1984) confirm this picture of fry distribution in the Chena River. Catch-per-unit-effort (fry per ten 30-m seine hauls) decreased rapidly with the progression upstream from 60.4 fish between river km 0 and 42 to 27.7 fish between river km 42 and 108 and to 3.5 fish between river km 108 and 159.

Age 1 fish appear to be even more concentrated in the lower river than age 0+ fry, probably as a result of downstream movement during the first year of life. This accumulation of age 1 fish in the lower river is demonstrated by electrofishing samples, which reveal a rapid decrease in abundance with the progression upstream (Tack 1971) (Table 2). The absence of the age 2, and even age 3, age-classes in samples from the upper river (Fig. 3) also suggests that fish move down from the headwaters during their first year of life.

The tendency of fish to concentrate in downstream reaches appears to end in the second summer and is followed by an upstream extension of the cohort's distribution.

© 1999 NRC Canada

Table 1. Mean length-at-age and 95% CIs for fish caught in the lower 58 km of the Goodpaster River in May 1995–1996 (n = 1912 fish) and August 1988–1993 (n = 4400 fish), and change in mean length-at-age between May and August.

Age (years)	Mean May 1995–1996 length (mm)	Mean August 1988–1993 length (mm)	Change in length (mm)
2	169±4	180±2	11
3	199±3	217±1	18
4	237±3	249±1	12
5	268±2	272±2	4
6	302±2	298±1	–4
7	326±2	310±3	–16
8	347±3	326±5	–21
9	359±3	342±10	–17
10	378±4	360±10	–18
11	388±5	376±33	–12
12	424±12	391	–33

Table 2. Change in the relative abundance of age 1 and 2 Arctic grayling in electrofishing boat catches between river km 40 and 126 on the Chena River in late June 1970 (Tack 1971) with 95% CIs.

	Relative abundance			
	Age 1+		Age 2+	
River km	%	95% CI	%	95% CI
34–40	28	23–34	59	52–66
40–50	14	12–17	72	68–76
50–89	2	1–3	34	30–38
89–101	3	1–4	45	40–49
101–126	3	2–4	44	41–47

Note: The abundance of each age-class is expressed as a percentage of the number of fish in that age-class and older. Abundances are approximate because age composition was estimated from modes in Tack's (1971) length–frequency data, with fish 70–139 mm being classified as age 1 and fish 140–179 mm being classified as age 2.

As a result, age 2 fish are more uniformly distributed than age 1 fish in the lower and middle reaches of the Chena River (Tack 1971) (Table 2). As a result of this behavior, the age of fish recruiting to a reach increases with the progression upstream. For example, fish recruiting to the lower reaches of the Goodpaster River are presumably less than 3 years old, while fish recruiting to the middle reaches are 3–5 years old, and fish recruiting to the upper reaches are 4–7 years old (Fig. 3). The picture in the Chena River is similar, with the modal ages of fish in the downstream (river km 0–19), midriver (river km 120–140), and headwater (river km 220–240) reaches increasing from 3 to 5 to 6 years old, respectively (Fig. 3). This suggests that recruits are age 3 or less in the lower river, age 5 or less in the middle river, and ages 3–6 in the upper river.

Growth and related movements

The two methods that I used to fit growth curves give very different pictures of the way that growth rate varies with the progression upstream. Scale-based curves are "stacked," showing a steady increase in length-at-age with the progression upstream (Fig. 5). If taken at face value, this would provide strong evidence that a growth gradient makes an important contribution to the size gradient. A 3-year-old fish

Fig. 5. Scale-age based von Bertalanffy growth curves for six 40-km sections of the Chena River; 95% CIs on mean length-at-age are shown.

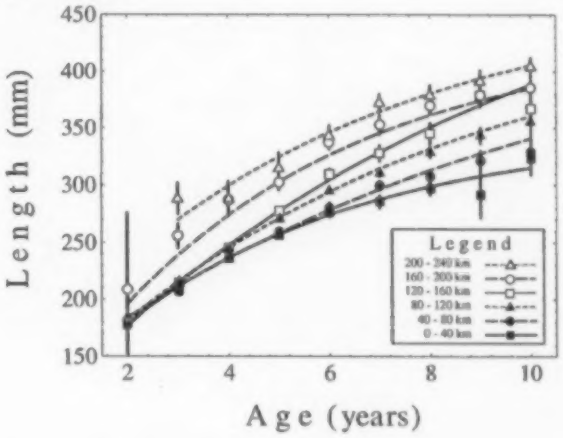

was about 20% longer in in the headwaters than near the mouth (288 versus 237 mm), while a 10-year-old fish was about 25% longer (405 versus 325 mm).

However, a very different picture is given by mark–recapture based growth curves. These show that although in situ growth is slowest in the lower 40 km, it is almost constant over the next three reaches, which span 120 km (Fig. 6). Mean length at age 10 in the lowest 40 km of the river was a substantial 26 mm less (8%) than in the middle reaches, but curves for the two middle reaches are virtually superimposed, with mean length-at-age differing by less than 1 mm. Mean lengths-at-age for the upstream reach differ from these two curves by only 4 mm (1.4%) at age 10. In fact the combined range spanned by CIs for the upper three curves was only 14 mm, or 4% of the mean length of an age 10 fish.

The contradiction between scale- and recapture-based growth curves is resolved by the fact that fast-growing individuals move upstream, while slower-growing fish stay put or move downstream (sign test, $p < 0.01$) (Fig. 7). This pattern of movement will sort fast-growing fish into upstream reaches and slow-growing fish into downstream reaches. As a consequence the length-at-age determined from scales could increase upstream, without there having to be an increase in growth rate with the progression upstream. The difference in growth between fish that move up and those that move down is quite large; 3-year-old fish that move up have an annual length increment about 45% larger than those moving downstream.

Closer examination of the scale-based growth curves (Fig. 5) tends to support this interpretation. The slope of the curves for the upper 80 km of the river is actually *less* than that of the curves for the lower 80 km, particularly for larger fish, and the high elevation of the two upper curves results from the fact that the age 2–5 fish recruiting to these reaches are very large for their age. Both of these observations are consistent with the hypothesis that upstream movement by fast-growing fish is responsible for the stacking of the scale-based growth curves, not spatial variation in in situ growth rates.

© 1999 NRC Canada

Fig. 6. Recapture-based von Bertalanffy growth curves for four 40-km sections of the Chena River; 95% CIs on mean length-at-age are shown.

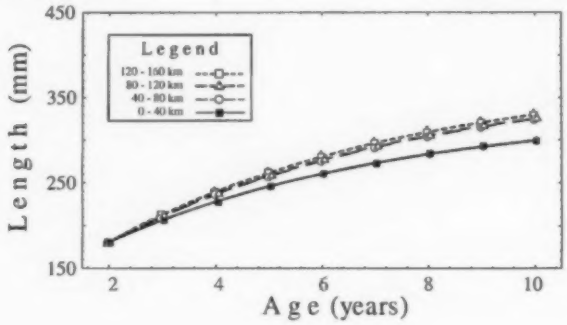

Fig. 7. Relationship between the growth increment of a fish in a given year and its movement behavior based on known-age fish between 2 and 7 years old; 95% CIs are shown except for age 2 fish that moved upstream, which are represented by a single fish.

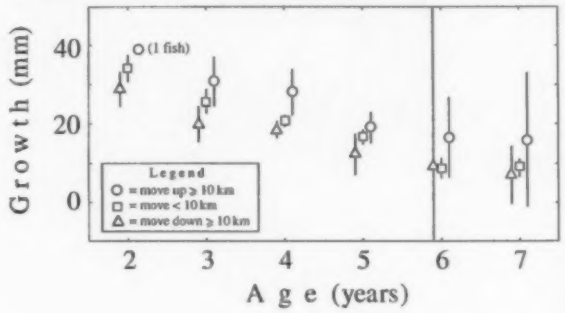

Mortality rates

My analyses revealed no evidence that differences in mortality rates between reaches made any contribution to the size gradient. Regressions relating mortality rates to the distance upstream for fish larger than 200 mm were nonsignificant for both 1991–1992 (p = 0.6, R^2 = 0.06) and 1992–1993 (p = 0.5, R^2 = 0.05). In 1992, this nonsignificant trend was positive, while in 1993, it was negative. The low R^2 values for these regressions and fact that the p values are near 0.5 in both cases provide little reason to suspect that mortaliy rate changes with the progression upstream. Estimated annual mortality rates and 95% CIs for all reaches combined were 33 ± 8% for 1991–1992 and 13 ± 14% for 1992–1993.

Discussion

My analyses revealed that two processes are almost entirely responsible for the pronounced size and age gradients of Arctic grayling in the Goodpaster and Chena rivers: age-phased recruitment and growth-dependent movement. Slower growth rates in the lower 40 km of the Chena River may also make a small but significant contribution to the size gradient. I found no evidence that spatial variations in mortality rate contributed towards these gradients.

These results provided strong corroboration for Tack's (1980) idea that most young fish recruit to downstream reaches and then move to feeding positions further upstream as they grow older and larger. I have termed this idea the "age-phased recruitment hypothesis." According to this hypothesis the size and age gradients of Arctic grayling are the result of a single population distributing itself along the entire length of the river (200–260 km in the current study).

The existence of growth-dependent movement was also supported, and this process magnifies the size gradient produced by age-phased recruitment because it sorts fast-growing fish into the upper river and slow-growing fish into the lower river. The effect of this magnification was considerable because, as a result, the large fish that inhabit the upper Chena River are about 80 mm bigger than fish of the same age from the lower river (Fig. 5), accounting for more than half of the 135 mm spanned by the size gradient.

The results of my analyses did not fit with the static population with growth and mortality gradients hypothesis. In fact, this hypothesis could have been rejected in its pure form simply by looking at the age structure of fish in downstream and headwater reaches (Fig. 3). Figure 3 shows that mature fish are virtually absent from the downstream reaches, while immature fish are practically absent from the headwaters, demonstrating that fish movement must knit the population together along the entire length of the river. This result is not consistent with the old idea that stream fish are inherently sedentary (Miller 1957; Gerking 1959). It does support the revised view that fish movement in stream salmonid populations is much more important than previously believed (Gowan et al. 1994).

However, the data did show that growth rates are lower in the downstream 40 km of the Chena River than further upstream (Fig. 6), although there is strong evidence that growth rates are practically constant for the next 120 km (Fig. 6). This result shows that spatial variation in growth does contribute towards the size gradient but that this process is less important than age-phased recruitment or growth-dependent movement. Unfortunately, there were no data to estimate recapture-based growth curves for the upper 80 km of the river; these might have given a clearer picture of the importance of spatial variation in growth rates.

I found no suggestion that spatial variations in mortality rates contribute towards the size and age gradients. However, it is possible that sampling and natural variability obscured small but significant differences.

Evidence suggests that the processes responsible for size and age gradients of Arctic grayling are also responsible for the same pattern in New Zealand brown trout streams (Jellyman and Graynoth 1994) and the smaller-fish-upstream patterns that can be inferred for brown trout in European rivers (Solomon and Templeton 1976; Milner et al. 1978; Baglinière et al. 1989; Maisse and Baglinière 1990; Bembo et al. 1993).

Age-phased recruitment underlies both older- and younger-fish-upstream distribution patterns of brown trout but operates in different directions. For example, the mean age of fish recruiting to a reach increases upstream in some New Zealand streams (Jellyman and Graynoth 1994), while the reverse pattern occurs in European rivers (Solomon and

© 1999 NRC Canada

Templeton 1976; Milner et al. 1978; Baglinière et al. 1989; Maisse and Baglinière 1990; Bembo et al. 1993). The required patterns of directed movement are documented or inferred in all these studies.

Growth-dependent movement appears to be a new discovery, but I believe that this process may also contribute towards both larger- and smaller-fish-upstream size gradients of brown trout. This hypothesis would be consistent with the way in which mean length-at-age increases upstream in the Wairau and Oreti rivers in New Zealand (Jellyman and Graynoth 1994). In European studies the opposite pattern of *decreasing* mean length-at-age upstream has been found in several rivers (Hunt and Jones 1972; Jonsson and Sandlund 1979; Bembo et al. 1993) and is usually interpreted to be result of a decrease in in situ growth with the progression upstream (e.g., Bembo et al. 1993). However, I would argue that growth-dependent movement may be responsible for these results, with fast-growing fish tending to move downstream. Mark–recapture studies and investigations of the relationship between movement and growth are needed to test this prediction.

Acknowledgements

The analyses in this paper would have been impossible without the massive amount of work performed over the years by biologists associated with Arctic grayling research at the Alaska Department of Fish and Game. I am extremely grateful to these biologists for giving me access to data and sharing their ideas. In particular, I would like to thank Steve Tack, Jerry Hallberg, Rocky Holmes, Bob Clark, Bill Ridder, and Doug Fleming. Dr. John Clark and Bob Clark arranged financial support from the Alaska Department of Fish and Game for me to sample Arctic grayling on the East Fork of the Chena River, and Bill Ridder was especially helpful during the preparation of this paper. I would also like to thank Drs. Jackie LaPerriere and Jim Reynolds at the Alaska Cooperative Fish and Wildlife Research Unit for all their support over the years. Nora Kelly provided first rate field assistance and company while sampling fish on the East Fork of the Chena River. Drs. C. Gowan and R. McLaughlin provided helpful reviews.

References

Baglinière, J.L., Maisse, G., Lebail, P.Y., and Nihouarn, A. 1989. Population dynamics of brown trout, *Salmo trutta* L., in a tributary in Brittany (France): spawning and juveniles. J. Fish Biol. **34**: 97–110.

Bembo, D.G., Beverton, R.J.H., Weightman, A.J., and Cresswell, R.C. 1993. Distribution, growth, and movement of River Usk brown trout (*Salmo trutta*). J. Fish Biol. **43**: 45–52.

Conover, W.J. 1980. Practical nonparametric statistics. John Wiley & Sons, New York.

Gerking, S.D.1959. The restricted movement of fish populations. Biol. Rev. Camb. Philos. Soc. **34**: 221–242.

Goto, A. 1989. Growth differences in males of the river-sculpin *Cottus hangiongensis* along a river course, a correlate of life-history variation. Environ. Biol. Fishes, **24**: 241–249.

Gowan, C., Young, M.K., Fausch, K.D., and Riley, S.C. 1994. Restricted movement in resident stream salmonids: a paradigm lost? Can. J. Fish. Aquat. Sci. **51**: 2626–2637.

Hallberg, J.E. 1978. Distribution, abundance, and natural history of the Arctic grayling in the Tanana River drainage. Alaska Department of Fish and Game, Federal Aid in Fish Restoration, Annual Performance Report, 1977–1978. Project F-9-10, 19 (R-1).

Holmes, R.A. 1984. Population structure and dynamics of the Arctic grayling, with emphasis on heavily fished stocks. Alaska Department of Fish and Game, Federal Aid in Fish Restoration, Annual Performance Report, 1983–1984. Project F-9-16, 25 (R-1).

Hughes, N.F. 1998. A model of habitat selection by drift-feeding stream salmonids at different scales. Ecology, **79**: 281–294.

Hughes, N.F., and Reynolds, J.B. 1994. Why do Arctic grayling (*Thymallus arcticus*) get bigger as you go upstream? Can. J. Fish. Aquat. Sci. **51**: 2154–2163.

Hunt, P.C., and Jones, J.W. 1972. Trout in Llyn Alaw, North Wales. II. Growth. J. Fish Biol. **4**: 409–424.

Jellyman, D.J., and Graynoth, E. 1994. Headwater trout fisheries in New Zealand. New Zealand Freshwater Research Reports, NIWA Freshwater, Christchurch, New Zealand.

Jonsson, B., and Sanderlund, O.T. 1979. Environmental factors and life histories of isolated stocks of brown trout (*Salmo trutta* m. *fario*) in Sore Osa river system, Norway. Environ. Biol. Fishes, **4**: 43–54.

Maisse, G., and Baglinière, J.L. 1990. The biology of brown trout, *Salmo trutta* L., in the River Scorff, Brittany: a synthesis of studies from 1973 to 1984. Aquacult. Fish. Manage. **21**: 95–106.

Miller, R.B. 1957. Permanence and size of home territory in stream-dwelling cutthroat trout. J. Fish. Res. Board Can. **14**: 687–691.

Milner, N.J., Gee, A.S., and Hemsworth, R.J. 1978. The production of brown trout, *Salmo trutta*, in tributaries of the Upper Wye, Wales. J. Fish Biol. **13**: 599–612.

Press, W.H., Flannery, B.P., Teukolski, S.A., and Vetterling, W.T. 1988. Numerical recipes in C. Cambridge University Press, Cambridge, U.K.

Reznick, D., and Endler, J.A. 1982. The impact of predation on life history evolution in Trinidadian guppies (*Poecilia reticulata*). Evolution, **36**: 160–177.

Ricker, W.E. 1975. Computation and interpretation of biological statistics of fish populations. Bull. Fish. Res. Board Can. No. 191.

Ridder, W.P. 1984. The life history and population dynamics of exploited stocks of Arctic grayling associated with the Delta and Richardson Clearwater rivers. Alaska Department of Fish and Game, Federal Aid in Fish Restoration, Annual Report of Progress, 1983–1984. Project F-9-16, 25(G-III-G).

Solomon, D.J., and Templeton, R.G. 1976. Movements of brown trout *Salmo trutta* L. in a chalk stream. J. Fish Biol. **9**: 411–423.

Tack, S.L. 1971. Distribution, abundance, and natural history of the Arctic grayling in the Tanana River drainage. Alaska Department of Fish and Game, Federal Aid in Fish Restoration, Annual Performance Report, 1970–1971. Project F-9-3, 12 (R-1).

Tack, S.L. 1974. Distribution, abundance, and natural history of the Arctic grayling in the Tanana River drainage. Alaska Department of Fish and Game, Federal Aid in Fish Restoration, Annual Performance Report, 1973–1974. Project F-9-6, 15 (R-1).

Tack, S.L. 1975. Distribution, abundance, and natural history of the Arctic grayling in the Tanana River drainage. Alaska Department of Fish and Game, Federal Aid in Fish Restoration, Annual Performance Report, 1974–1975. Project F-9-7, 16 (R-1).

Tack, S.L. 1980. Migrations and distributions of Arctic grayling *Thymallus arcticus* (Pallas) in interior and arctic Alaska. Alaska Department of Fish and Game, Federal Aid in Fish Restoration, Annual Performance Report, 1979–1980. Project F-9-12, 21 (R-1).

© 1999 NRC Canada

Destructive grazing, epiphytism, and disease: the dynamics of sea urchin – kelp interactions in Nova Scotia

Robert E. Scheibling, Allan W. Hennigar, and Toby Balch

Abstract: We measured the rate of advance of urchin (*Strongylocentrotus droebachiensis*) feeding aggregations (fronts) as they destructively grazed kelp beds (*Laminaria longicruris*) at both a wave-exposed site and a sheltered site in Nova Scotia over 3.5 years. The grazing fronts were composed of high densities of large adults (up to 98 and 70 per 0.25 m^2 at the exposed and sheltered sites, respectively). Urchins in the recently formed barrens, or in adjacent kelp beds, occurred at much lower densities and consisted mainly of juveniles. The fronts moved onshore into shallower water at each site, but their rate of advance varied markedly between sites and over time at each site, ranging from 0 to 4 m·month^{-1}. The rate of advance of a front was related to the biomass of urchins; fronts did not advance below a threshold biomass of ~2 kg·m^{-2}. Infestations of kelp by an epiphytic bryozoan (*Membranipora membranacea*) caused marked reductions in kelp canopy cover and biomass during winter, but the canopy regenerated through recruitment of juvenile sporophytes in spring. A localized outbreak of disease decimated *S. droebachiensis* at the exposed site in 1993, which enabled kelp to recolonize the barrens. Surviving urchins gradually reaggregated and resumed destructive grazing after ~1.5 years. A recurrence of disease in 1995 eliminated urchins at both sites and terminated the transition from kelp beds to barrens on a coastal scale. Our findings have important implications for the management of the urchin fishery, which targets grazing fronts for harvesting.

Résumé : Nous avons mesuré la vitesse d'avancement de concentrations (fronts) d'alimentation d'oursins (*Strongylocentrotus droebachiensis*) à mesure qu'ils broutaient de façon destructive les laminaires (*Laminaria longicruris*) dans un site exposé et un site non exposé à la houle de la Nouvelle-Écosse, au cours d'une période de 3,5 années. Les fronts d'oursins brouteurs étaient composés de fortes concentrations de gros adultes (jusqu'à 98 et 70 par 0,25 m^2 dans, respectivement, les sites exposé et non exposé). Les oursins des zones récemment dénudées, ou se trouvant dans des concentrations de laminaires voisines, s'y trouvaient à des densités beaucoup plus faibles et étaient surtout des juvéniles. Les fronts se déplaçaient dans des eaux moins profondes en direction de la côte à chacun des sites, mais la vitesse d'avancement variait de façon marquée entre les sites et en fonction du temps, allant de 0 à 4 m·mois^{-1}. La vitesse d'avancement d'un front était fonction de la biomasse des oursins : les fronts n'avançaient pas en deçà d'une biomasse seuil de 2 kg·m^{-2} environ. Les infestations des laminaires par un bryozoaire épiphyte (*Membranipora membranacea*) donnait lieu à de fortes réductions de la couverture et de la biomasse des laminaires en hiver, mais le couvert se régénérait par le recrutement de sporophytes juvéniles au printemps. Une épidémie localisée a décimé les *S. droebachiensis* du site exposé en 1993, ce qui a permis aux laminaires de recoloniser les zones dénudées. Les oursins survivants se sont graduellement regroupés et ont recommencé à brouter de façon destructive après 1,5 an environ. La réapparition de la maladie en 1995 a fait disparaître les oursins aux deux sites et mis fin à la transformation des zones à laminaires en zones dénudées à la grandeur de la côte. Nos résultats ont d'importantes incidences pour la gestion de la pêche des oursins, qui cible les fronts de broutage.

[Traduit par la Rédaction]

Introduction

Kelp beds (forests) are among the most productive communities of temperate coasts worldwide (Mann 1982). The high productivity and large standing biomass of kelps and associated macroalgae support large numbers of fish and invertebrates, which utilize the kelp as both a food resource and habitat (Dayton 1985). Among the numerous grazers that inhabit kelp beds, the pivotal role of urchins in determining community structure and stability is well recognized. Destructive grazing by urchins, which results in less productive, coralline algal-dominated assemblages termed "barrens," has been documented on a global scale in a variety of kelp habitats (Harrold and Pearse 1987). Because urchins can persist in barrens and prevent recolonization by kelps, destructive grazing can cause large-scale shifts in community state (Mann 1977).

Off the Atlantic coast of Nova Scotia, destructive grazing of kelp by the green sea urchin *Strongylocentrotus droebachiensis* is a recurrent phenomenon. The process is initiated when urchins form dense feeding aggregations that

Received April 29, 1999. Accepted July 29, 1999.
J15124

R.E. Scheibling,[1] A.W. Hennigar, and T. Balch.
Department of Biology, Dalhousie University, Halifax, NS B3H 4J1, Canada.

[1]Author to whom all correspondence should be addressed.
e-mail: rescheib@is.dal.ca

© 1999 NRC Canada

move as "fronts" through a kelp bed, consuming all erect macroalgae in their path. This was first documented in St. Margaret's Bay in the early 1970s (Breen and Mann 1976*a*, 1976*b*), and surveys in 1979 reported urchin barrens, presumably the result of previous episodes of destructive grazing, along ~500 km (straight-line distance) of coast (Wharton and Mann 1981). In the early 1980s, recurrent outbreaks of disease caused mass mortalities of urchins in the shallow (<25 m) subtidal zone throughout this range (Miller 1985*a*; Scheibling 1986). Release from grazing pressure enabled the reestablishment of kelp beds by the mid-1980s (Scheibling 1986; Johnson and Mann 1988). However, increasing densities of *S. droebachiensis* in this zone precipitated another wave of destructive grazing and the system began to shift back to the barrens state in the early 1990s (Scheibling et al. 1994).

Because the loss of kelp is associated with major changes in habitat structure and productivity in the coastal zone, understanding the dynamics of urchin–kelp interactions, and the biotic and physical factors regulating these interactions, is particularly relevant to the management of the inshore fisheries. American lobster (*Homarus americanus*), the most valuable invertebrate species in eastern Canada and the Gulf of Maine, has been implicated as a controlling predator of urchins (Mann 1977; Hagen and Mann 1992; but see Miller 1985*b*; Elner and Vadas 1990), and urchins were viewed as pests because their grazing activity reduced kelp bed habitat utilized by lobster (Wharton and Mann 1981; Bologna and Steneck 1993). In recent years, however, the roe fishery for *S. droebachiensis* in this region has expanded rapidly, transforming urchins into a valuable resource (Hatcher and Hatcher 1997). Commercial fishing for urchins, and their crustacean and fish predators, can have important direct and indirect effects on the dynamics of the coastal ecosystem (Vadas and Steneck 1995; Scheibling 1996).

Natural or anthropogenic disturbances can facilitate invasion of a community by introduced species, which in turn may alter the disturbance regime of the disrupted community (Mack and Antonio 1998). An epiphytic bryozoan (*Membranipora membranacea*) that infests kelps causing fragmentation and loss of fronds (Dixon et al. 1981) has recently invaded the Gulf of Maine (Berman et al. 1992) and Atlantic coast of Nova Scotia. Unlike destructive grazing, this loss of canopy cover is temporary, since recruitment by juvenile kelps can regenerate a kelp bed (Lambert et al. 1992). However, the coincidence of bryozoan infestation and high urchin densities may have synergistic effects that accelerate the destruction of kelp beds.

In this study, we examine ecological interactions that regulate the mode and tempo of transition between alternative states of the rocky subtidal community through detailed monitoring of two contrasting sites in Nova Scotia. Over a 3.5-year period, we recorded massive losses of kelp biomass because of recent destructive grazing by *S. droebachiensis* and epiphytism by *M. membranacea* and recovery of kelp beds following mass mortalities of urchins from disease. In particular, we focus on the composition and behaviour of grazing fronts to provide new insights into their formation and the dynamics of urchin population outbreaks. We also examine the implications of our findings for the management of a sustainable urchin fishery.

Materials and methods

Study sites

We selected two sites to represent contrasting types of kelp bed habitat with different hydrodynamic regimes: Little Duck Island (44°22′N, 64°11′W), off an exposed headland at the mouth of Mahone Bay, and Mill Cove (44°35′N, 64°3′W) in St. Margaret's Bay, a large semiprotected embayment. Our main study area at each site ranged from 5 to 10 m depth (below mean lower low water (MLLW)). The substratum at Little Duck Island is characterized by broad ridges of heavily grooved basaltic bedrock; at Mill Cove, it consists of granitic boulders of varying sizes and outcrops of bedrock pavement. At the beginning of our study, a dense aggregation (front) of *S. droebachiensis* was moving onshore at each site, destructively grazing kelp beds and creating barren grounds in their wake. The kelp bed at Little Duck Island was composed mainly of the phenotype of *Laminaria longicruris* associated with high water movement: short stipes and small, narrow fronds with highly fluted edges (Gerard and Mann 1979). Other kelp species (*Laminaria digitata* and *Alaria esculenta*) were rare in the study area but common in a shallow wave-swept zone near the island. The kelp bed at Mill Cove consisted almost exclusively of the phenotype of *L. longicruris* associated with sheltered habitats: long stipes and long, broad, and thin fronds. The kelp beds extended shoreward to the intertidal zone at both sites forming a near complete cover of the substratum, while cobble and gravel beds occurred along the deeper offshore margins of the rocky barrens.

Dynamics of urchin fronts

A sampling grid was established at each site in June 1992 with reference to four fixed position markers (steel eyebolts anchored in concrete blocks) placed in the barren grounds 10–12 m from the urchin front and spaced at 10-m intervals (Fig. 1). These were used as benchmarks to map the leading edge of the urchin front. We used a plastic measuring tape and a compass to record the polar coordinates (10-cm and 5° accuracy) of three positions along the front with reference to each of the four benchmarks: the perpendicular distance from the benchmark to the front and the distances at 20° to either side of the perpendicular. This gave a total of 12 positions along the leading edge of the front (or offshore border of the macroalgal bed) that were recorded at 1- to 3-month intervals between June 1992 and August 1995. In August 1993, we established a second series of benchmarks at Little Duck Island that was placed ~20 m along the onshore bearing from the first series (Fig. 1) to reduce the distance between the front and the benchmarks (which increased with destructive grazing of the kelp). In June 1994, we reverted to the original benchmarks at Little Duck Island, as the macroalgal bed had expanded offshore by this time. In December 1994, we used a third set of benchmarks ~10 m along the onshore bearing from the second series, as the macroalgae receded again (Fig. 1). In April 1995, we extended the study area at Little Duck Island to encompass a second site (B) with an active grazing front that was ~50 m west of the original site (A) and at 5 m depth. Two position markers were placed in the barrens ~10 m from the front and 10 m apart. We mapped the leading edge of the front at site B in the same way as at site A. At Mill Cove, we located a second set of benchmarks in July 1994 that were ~10 m along the onshore bearing from the first series and closer to the receding kelp bed (Fig. 1).

We estimated the rate of advance of the urchin front as the average distance between successive positions on the leading edge based on the three measurements taken from each benchmark. For the measurements at 20° to either side of the perpendicular, the perpendicular distance between successive positions was calculated trigonometrically. The three measurements were averaged for each

© 1999 NRC Canada

Fig. 1. Sequential maps of the study grids at Little Duck Island and Mill Cove showing the changing boundary between the kelp bed (shaded) and barrens at selected sampling dates between June 1992 and August 1995. Numbered points show locations of different series of benchmarks within the grid at each site (see Materials and methods). Depth ranges from 5 to 8 m across the grid (from 60 to 0 m along the onshore axis) at Little Duck Island and from 6 to 10 m at Mill Cove.

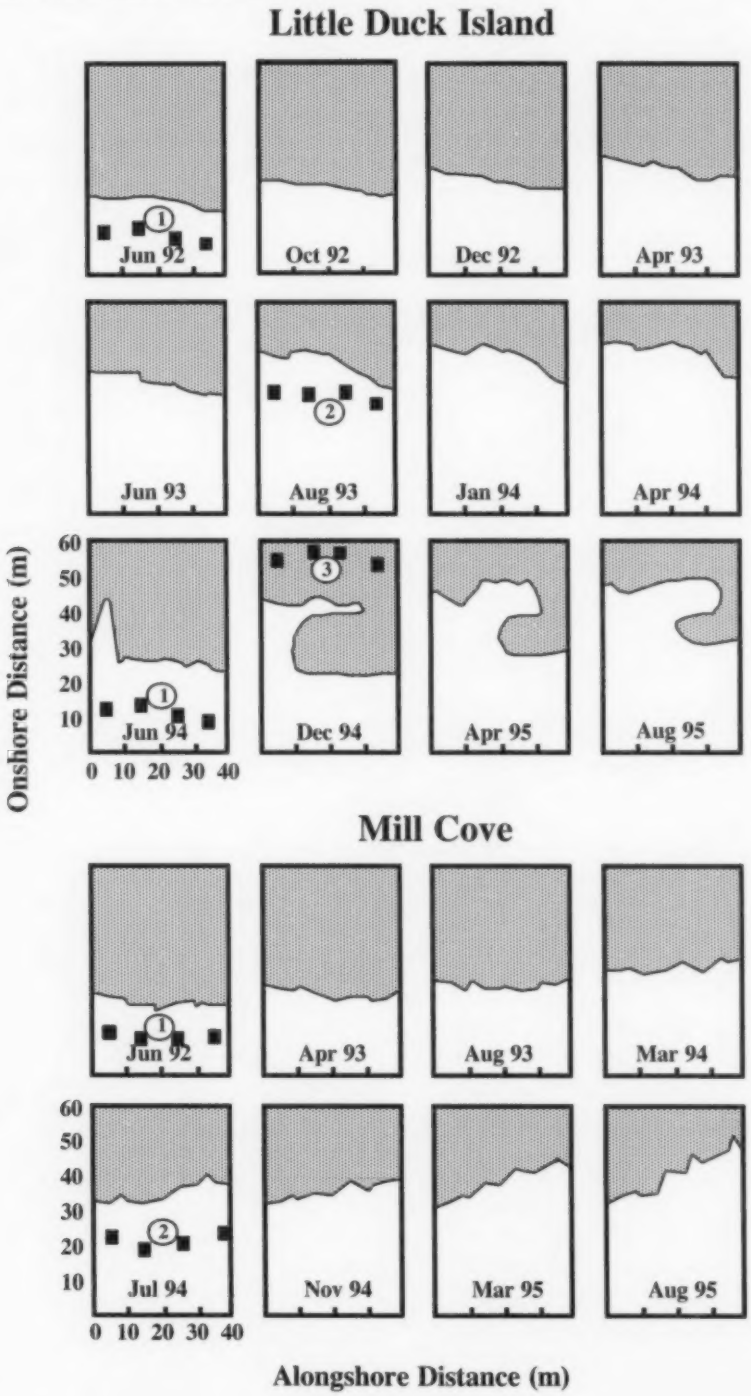

© 1999 NRC Canada

benchmark, and the grand mean for the four benchmarks was used to estimate the rate of advance of the front for each sampling interval.

On each mapping date at each site, we measured urchin density across the front in a series of contiguous 0.5 × 0.5 m (0.25 m^2) quadrats along four transects. The transects extended for ~10 m (2–4 m between June and October 1992) along the perpendicular (offshore) distance from the kelp bed (~1 m into the kelp bed from the leading edge of the front) towards the nearest benchmark in the barrens. To estimate the mean density of urchins in the front, we averaged the densities for each transect in two to four contiguous quadrats within 1–2 m from the edge of the kelp bed (usually those with the highest numbers of urchins) and then calculated the grand mean for the four transects. Crevices, undersides of cobbles and boulders, algal turf, and holdfasts of kelp were carefully searched for small and cryptic urchins.

Density and biomass of macroalgae and urchins

To compare interannually the abundance of macroalgae in the kelp bed and urchins in the barrens, we sampled 10 quadrats of 1 m^2 randomly positioned along a belt transect of 4 × 50 m (200 m^2) that extended alongshore (i.e., parallel to the series of benchmarks) in each habitat and at each site. The transects in the kelp bed were located 5–10 m into the bed from the offshore border. The initial kelp bed transect in June–July 1992 was ~15 m along the onshore bearing from the original series of benchmarks (Fig. 1). In September–October 1993 and July–August 1994 and 1995, we located another kelp bed transect (because the kelp in the initial transect had been destructively grazed) ~40 and 30 m onshore from the original series of benchmarks at Little Duck Island and Mill Cove, respectively (Fig. 1). The location of the second transect was staggered by ~4 m each year to preclude overlap of sampling areas among years. We manually collected large, canopy-forming macroalgae (kelps and *Desmarestia* spp.) from each quadrat and placed them in separate net bags. All specimens from alternate quadrats were counted and the drained fresh weight of each species (all specimens pooled) was recorded for each quadrat using a spring balance (25-g accuracy for wet weight >500 g).

The initial transects in the barrens were located 5–10 m from the offshore border of the kelp bed in June–July 1992 (~5 m along the onshore bearing from the original series of benchmarks; Fig. 1). The same general area was sampled in subsequent years, but transect locations were staggered as described above. In September–October 1993, we sampled an additional three transects in the barrens to establish a parallel series of transects that were ~5, 15 (initial transect), 25, and 35 m offshore of the border of the kelp bed at that time. Urchins were collected and counted in each quadrat in both the kelp bed and barrens transects, and horizontal test diameter of each specimen (in alternate quadrats when urchins were abundant) was measured with vernier calipers (0.1-mm accuracy). In spring (March–May) and autumn (September–November) each year, urchins along the front at each site were collected in 10–20 haphazardly positioned quadrats of 0.25 m^2 for measurement of test diameter.

We estimated the biomass (fresh weight) of urchins by converting the test diameter (D, millimetres) to wet weight (W, grams) using the regression equation ($r^2 = 0.995$) $\ln W = 2.81 \times \ln D - 7.0$. This regression was based on a pooled sample of 424 urchins from both sites (211 from Little Duck Island, 213 from Mill Cove) ranging in diameter from 15 to 53 mm; preliminary analyses showed no significant differences in regression parameters between habitats or sites. We estimated the biomass density of urchins by first determining the proportion of urchins in each 5-mm size-class in a sample and multiplying that by the mean density of urchins in that sample to estimate the numerical density of each size-class. We then multiplied the density of each size-class by the biomass of an individual at the midpoint of the respective size-class (estimated from the regression equation given above) to estimate the biomass density of each size-class. The average biomass density of the sample was then estimated by summing the biomass density over all size-classes.

Algal recolonization after urchin mass mortality

To monitor the recolonization of the barrens by macroalgae after a mass mortality of urchins in October 1993, and the subsequent reformation of grazing fronts, we measured macroalgal cover and urchin density along four transects of 50 m length in June, September, and November 1994 and April 1995 at Little Duck Island. The transects extended from each of the original benchmarks along the onshore bearing towards and into the kelp bed (except in November 1994 when only one transect was sampled due to inclement weather). Because the position of the offshore border of the kelp bed during this period differed markedly between the eastern and western halves of the sampling grid (Fig. 1), data were averaged for the two easternmost transects and the two westernmost transects, respectively, after aligning each pair of transects with reference to the kelp bed border. A similar series of transects was run at Mill Cove in November 1994 and March and June 1995. Data were averaged for all four transects (after alignment with reference to the kelp bed border) for the first two sampling dates. We videorecorded macroalgal cover along a 1 × 50 m belt transect, delineated by a weighted line graduated in metres, with a diver-held video camera (Sony CCD-V801 Hi-8 video camera recorder in an Amphibico housing). A 1-m-wide framer attached to the camera housing was used to keep the camera 0.6 m above the seabed and centred on the transect line. The videotapes were analyzed with a videocassette recorder (Sony EV-S900 VCR) and colour monitor (Sony KV-20EXR2). We measured the percentage cover of kelps (*L. longicruris*, *L. digitata*, *A. esculenta*, *Saccorhiza dermatodea*), large plumose brown algae (*Desmarestia* spp.), branching and filamentous understory algae, and articulated coralline algae (*Corallina officinalis*) by freezing frames of contiguous 1-m^2 quadrats on videotape, projecting 100 regularly spaced points onto the screen, and counting the number of points overlying each algal type. We hand-counted urchins in 0.25-m^2 quadrats placed at 1-m intervals along the entire transect (or for 10 m around the barrens–kelp bed border in November 1994 and March 1995 at Mill Cove only).

Results

Density and size structure of urchin fronts

At the start of our study in June 1992, *S. droebachiensis* at Little Duck Island were aggregated in an extremely dense grazing front along the offshore border of the kelp bed. Peak densities within 1–2 m of the bed (averaged over four transects) ranged from 52 to 98·0.25 m^{-2} between June 1992 and September 1993 (Fig. 2). The urchins were piled on top of one another in three-dimensional aggregations that were typically three or four animals deep. These aggregations were 1–2 m wide and continuous over more than 200 m of seabed (which we surveyed by diving). Densities at the front were lowest in August 1992 and July 1993 when urchins shifted from three-dimensional aggregations to closely packed two-dimensional clusters that carpeted the bottom. This resulted in a broadening of the front in summer (e.g., July 1993) (Fig. 2), but dense three-dimensional aggregations were reestablished within 1 or 2 months. Urchins along the leading edge of the front climbed up the stipes and blades of kelp, weighing down the plants, which were rapidly consumed by the aggregation. Partially eaten kelp stipes and understory turfs left in the wake of the front were consumed by trailing urchins.

© 1999 NRC Canada

Fig. 2. Density of urchins in successive quadrats along 2- to 10-m transects extending from the kelp bed (shaded) into the barrens and perpendicular to the interface between habitats at selected sampling dates between June 1992 and August 1995 at Little Duck Island and Mill Cove. Data are means ± SE for quadrats (n = 4) at each 0.5-m interval relative to the edge of the kelp bed (shaded).

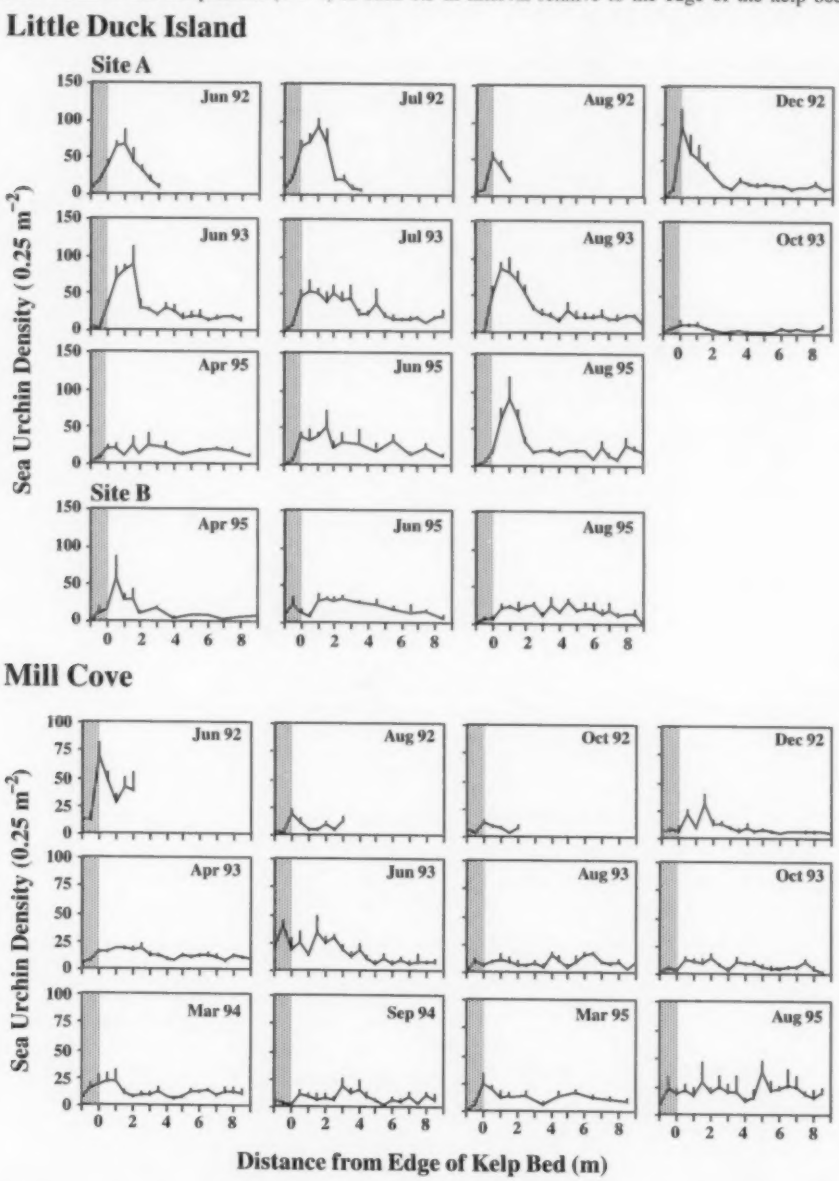

The front at Little Duck Island was composed almost exclusively of large adults with an approximately normal size distribution about a mean test diameter ranging from 38 to 51 mm (Fig. 3). Urchins at the front were consistently larger than those in either the barrens or the kelp bed within 5–10 m of the front, where size distributions were skewed by a preponderance of juveniles with modal sizes of 10–15 (1992–1994) or 5–10 mm (1995) (Fig. 3).

The front at Mill Cove was much less dense than that at Little Duck Island, consisting of clusters of urchins (rather than a continuous three-dimensional aggregation) along the offshore border of the kelp bed. Urchin density at the front was high at the start of our study (up to 70·0.25 m^{-2} in June 1992) but subsequently decreased to between 10 and 40·0.25 m^{-2}. Aside from temporary increases in urchin density in December 1992 and June 1993, a distinct front was not evident during the rest of our study at Mill Cove (Fig. 2). Because of low currents at Mill Cove, the kelp fronds were prostrate on the sea bed. Urchins along the border of the kelp bed often formed two-dimensional feeding aggregations on these fronds; in June 1992, they also were observed climbing up the stipes to graze. As at Little Duck Island,

© 1999 NRC Canada

Fig. 3. Size frequency distributions (horizontal test diameter) of urchins in the kelp bed (5–10 m from the front), the urchin front, and the barrens (5–10 m from the front in all years and 25 and 35 m from the front in 1993) at Little Duck Island (site A) and Mill Cove. Data are means ± SD based on random samples of individuals measured in July–August (1992, 1994, 1995) or September–October (1993), except for the front at Little Duck Island in 1994 and 1995 (measured in March–April at site B).

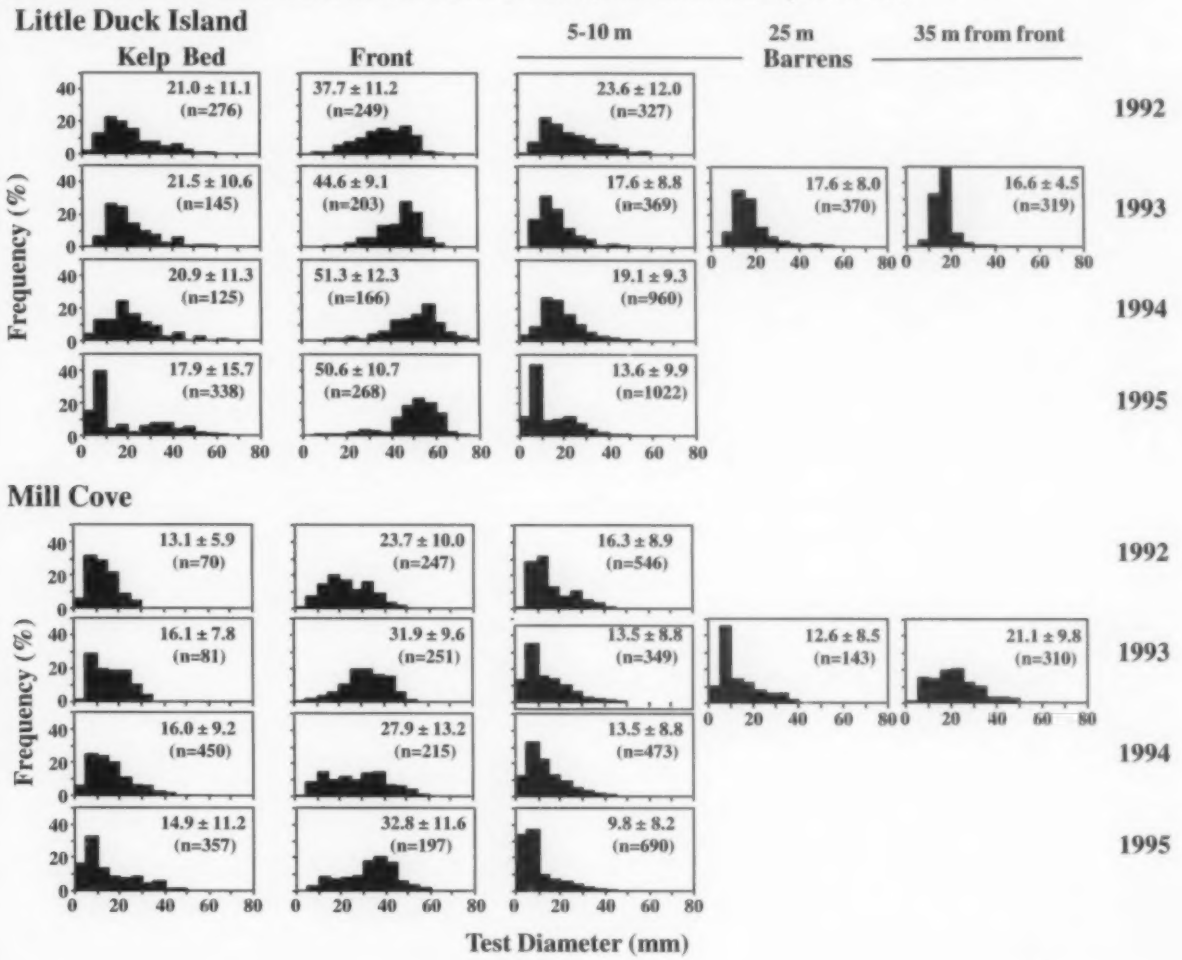

urchins in the front at Mill Cove were consistently larger (mean test diameter 24–32 mm) than those in the barrens or the kelp bed within 5–10 m of the front, where the modal diameter was generally 5–10 mm (Fig. 3). The mean diameter of urchins in each habitat was consistently smaller at Mill Cove than at Little Duck Island (Fig. 3).

Destructive grazing of kelp beds

At both sites, the urchin front advanced as a relatively linear feature, with small convolutions of the leading edge arising as the animals encountered topographical irregularities (e.g., boulders, ridges, sandy depressions) that altered their rate of advance (Fig. 1). Few urchins infiltrated the kelp bed in advance of the main aggregation, resulting in a discrete boundary at the leading edge of the front between the kelp bed and newly formed barrens (Fig. 2). At Little Duck Island, the rate of advance of the front varied markedly between June 1992 and September 1993: it peaked at 3–4 m·month^{-1} in June of each year, declined to ~1 m·month^{-1} by August, and remained low throughout the autumn and winter (Fig. 4*a*). At Mill Cove, the advance of the front was much slower, usually <1 m·month^{-1} and negligible (or not detectable over measurement error) in late summer each year (Fig. 4*a*). Regression analysis showed no significant relationship between the rate of advance of the front and urchin density (Fig. 4*b*) at Little Duck Island between June 1992 and September 1993 ($F_{[1,7]}$ = 2.41, P = 0.165), although decreases in the rate of advance in August 1992 and July 1993 were associated with a shift from three- to two-dimensional aggregation and concomitant decreases in urchin density. There also was no significant relationship between front advance and urchin density at Mill Cove throughout the study period ($F_{[1,18]}$ = 0.425, P = 0.52).

The kelp bed at Little Duck Island consisted primarily of a dense canopy of *L. longicruris* (Fig. 5*b*). Large plumose brown algae (*Desmarestia viridis* and *Desmarestia aculeata*)

© 1999 NRC Canada

Fig. 4. (*a*) Rate of advance of urchin fronts in successive sampling intervals between June 1992 and August 1995 at Little Duck Island and Mill Cove. Data are means ± SE (n = 4, except from April to August 1995 when n = 2 at site A (western half of the study grid) and site B, Little Duck Island). (*b*) Density of urchins in the front and barrens between June 1992 and October 1995 at Little Duck Island and Mill Cove. Data are means ± SE for grand means based on averages of three or four quadrats of 0.25 m^2 in the front and 68–72 quadrats in the barrens, averaged over four transects, except for the front at Little Duck Island (sites A and B) in 1995, where grand means are based on two transects.

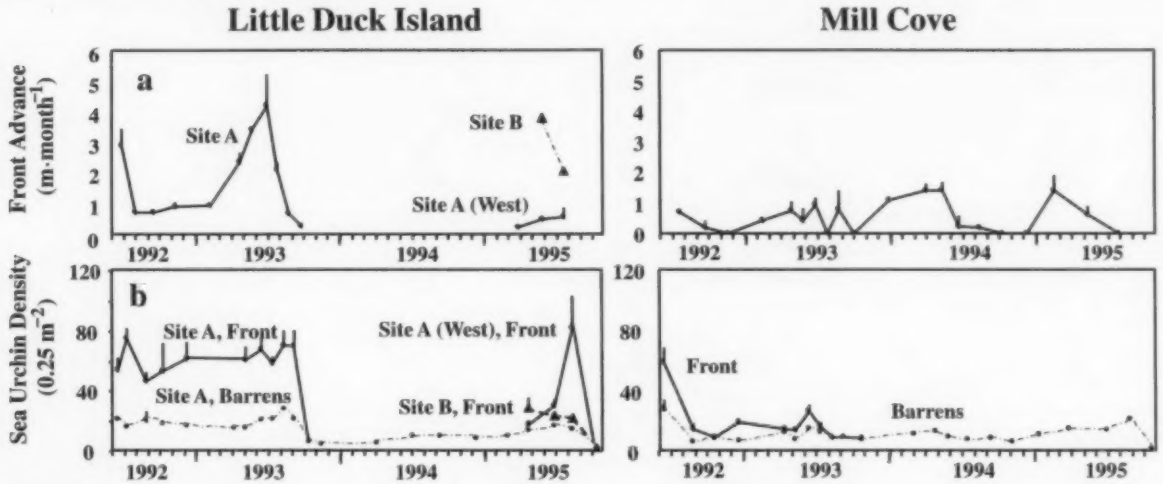

Fig. 5. (*a*) Biomass of total canopy macroalgae (total bar) as the dominant species *L. longicruris* (light shading) and other macroalgae (mainly *Desmarestia viridis* and *D. aculeata*) (open) at Little Duck Island, and *L. longicruris* (dark shading) at Mill Cove, and (*b*) density of *L. longicruris* at Little Duck Island (light shading) and Mill Cove (dark shading) between 1992 and 1995. Data are means ± SD based on 10 randomly positioned 1-m^2 quadrats sampled in kelp beds in July–August (1992, 1994, 1995) or September–October (1993).

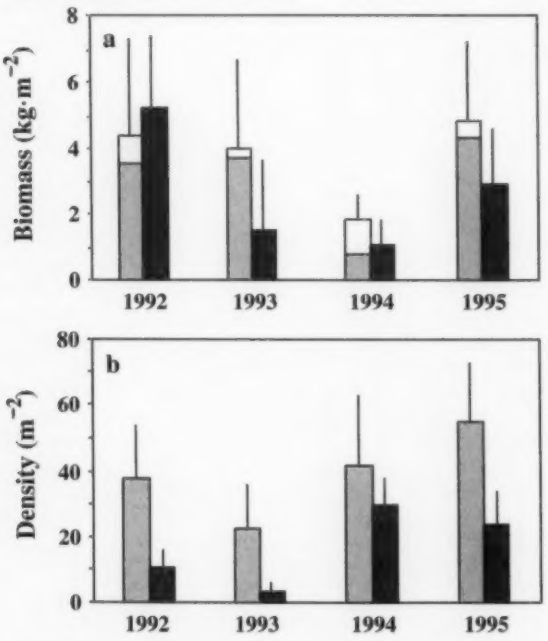

and an annual kelp (*S. dermatodea*) occurred sporadically in the bed, particularly in metre-scale gaps in the kelp canopy. The understory comprised turfs of articulated coralline algae (*Corallina officinalis*) and various foliose and filamentous red algae (e.g., *Ceramium rubrum*, *Ptilota serrata*, *Plumaria plumosa*, *Chondrus crispus*, *Palmaria palmata*). The grazing rate per metre along the urchin front at Little Duck Island, estimated by multiplying the rate of advance of the front over a sampling interval (Fig. 4*a*) by the average biomass (fresh weight) of macroalgae in the kelp bed (4.1 kg·m^{-2}, based on pooled samples from transects in 1992 and 1993, n = 20; Fig. 5*a*), ranged from 2.7 (August–September 1992) to 17.1 kg·m^{-1}·$month^{-1}$ (June–July 1993). During the first year of our study (June 1992 to June 1993), the front advanced 16.5 m (Figs. 2 and 5*a*), giving an annual grazing rate of 67.7 kg·m^{-1}. Individual grazing rates, estimated by dividing monthly grazing rate of the front by the average density of urchins at the front in the corresponding sampling interval (Fig. 4*b*), ranged from 13.5 to 67.9 g·$month^{-1}$.

The kelp bed at Mill Cove was almost exclusively *L. longicruris* with lower densities of larger plants than those at Little Duck Island (Fig. 5*b*). The understory turf was similar to that at Little Duck Island but less luxuriant. The estimated grazing rate per metre of urchin front at Mill Cove in 1992–1993, based on the macroalgal biomass measured in 1992 (5.2 kg·m^{-2}, n = 10; Fig. 5*a*) because the kelp bed had begun to erode by October 1993 (see Defoliation and recolonization of kelp beds), ranged from ~0 (November 1992) to 4.9 kg·m^{-1}·$month^{-1}$ (June 1993) and was 24.4 kg·m^{-1} (corresponding to an advance of 4.7 m) during the first year of study. Estimated individual grazing rates ranged from ~0 to 61.3 g·$month^{-1}$ during this period.

The uniformly low rate of advance at Mill Cove was related to both the smaller size and the lower density of ur-

© 1999 NRC Canada

Fig. 6. Relationship between rate of advance of the urchin front (see Fig. 4*a*) relative to urchin biomass at the front for pooled data from Little Duck Island (sites A and B) and Mill Cove, 1992–1995. Biomass is estimated from mean density of urchins at the front (see Fig. 4*b*) based on the size frequency distribution of urchins (see Fig. 3) and a regression equation relating fresh weight to test diameter (see Materials and methods).

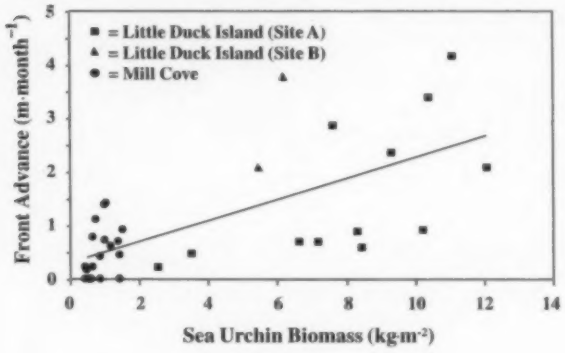

chins at Mill Cove compared with Little Duck Island, which resulted in a lower biomass density at the former site. A linear regression based on pooled samples from both sites (excluding the period between October 1993 and May 1995 after the mass mortality of urchins at Little Duck Island) showed a significant positive relationship ($F_{[1,32]} = 26.01$, $P < 0.001$) between the rate of advance of the front (R, metres per month) and estimates of urchin biomass density (W, kilograms wet weight) given by the equation ($r^2 = 0.431$) $R = 0.775 \times W + 0.325$ (Fig. 6).

At Little Duck Island, destructive grazing was arrested in autumn 1993 when urchin density was reduced to <10·0.25 m^{-2} along the front and <5·0.25 m^{-2} in the adjacent barrens by an outbreak of disease (Figs. 3 and 5*b*). Most urchins exhibited characteristic symptoms of an amoebic infection (paramoebiasis, Jones et al. 1985) in early September, and by mid-October, there were masses of dead and moribund urchins on the seabed. Urchin densities at Little Duck Island remained low over the next year and grazing of the kelp bed effectively ceased. Although a few urchins at Mill Cove exhibited symptoms of disease in September 1993, there was no evidence of significant mortality, nor did we observe a decline in density in October 1993 (Figs. 2 and 4*b*).

Urchins in the barrens

At Little Duck Island, the density of urchins in the barrens directly in the wake of the front (within 10 m of the kelp bed border) was markedly lower than that in the front (Fig. 2) and relatively constant between June 1992 and September 1993, with mean density ranging from 14 to 27·0.25 m^{-2} (Fig. 4*b*). In a series of alongshore transects in September 1993, urchin density did not vary significantly between 5 and 25 m from the edge of the kelp bed (6–7 m depth) but decreased significantly in the cobble bed at the offshore boundary of the site (35 m from the edge, 8 m depth) (one-way ANOVA, log-transformed data: $F_{[3,36]} = 6.53$, $P = 0.001$; Student–Newman–Keuls test: $P < 0.05$). Urchins in the front at that time were about three times more abundant

Fig. 7. Urchin density and biomass at 5- to 10-m intervals in an offshore direction from the kelp bed (shaded), across the front, and into the barrens at Little Duck Island and Mill Cove in September–October 1993. Data are means ± SD for urchin density based on 10 quadrats of 1 m^2 randomly sampled along 50-m transects running alongshore in the kelp bed and barrens and 12–16 quadrats of 0.25 m^2 along the front. Biomass is estimated from mean density of urchins at the front (see Fig. 4*b*) based on the size frequency distribution of urchins (see Fig. 3) and a regression equation relating fresh weight to test diameter (see Materials and methods).

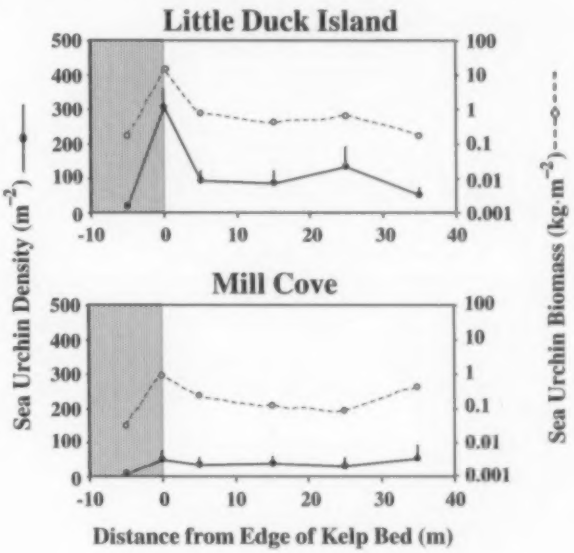

than those in the barrens and about six times more abundant than those in the cobble bed (Fig. 7). The mean size of urchins was similar between transects in the rocky barrens (test diameter 17.6 mm) but decreased in the cobble bed (16.6 mm), where few individuals exceeded 25 mm (Fig. 3). The distribution of urchin biomass paralleled that of density across the sampling gradient (Fig. 7), although the variation in biomass was even more pronounced (ranging from one to two orders of magnitude) because of the large size of urchins at the front (Fig. 3). Urchins were relatively rare (<5·0.25 m^{-2}) and generally small in the kelp bed (Figs. 3 and 7).

Urchins exhibited a similar pattern of distribution at Mill Cove as at Little Duck Island, although densities were generally much lower (Figs. 2 and 7). Densities in the wake of the front and within 10 m of the kelp were usually <15·0.25 m^{-2} (Fig. 2). Transects in October 1993 showed that urchin density in the barrens at Mill Cove did not vary significantly between 5 and 35 m from the edge of the kelp bed (7–10 m depth) (one-way ANOVA, log-transformed data: $F_{[3,36]} = 1.41$, $P = 0.256$). As at Little Duck Island, the size distribution of urchins across most of the barrens at Mill Cove was fairly constant (mean diameter ~13 mm), although the proportion of small juveniles (<10 mm) was lower in the deepest transect (mean diameter 21 mm) (Fig. 3). The larger average size of urchins in the deeper region resulted in an

© 1999 NRC Canada

Fig. 8. Density of urchins and cover of the canopy-forming and other (understorey and ephemeral species) macroalgae in successive quadrats of 0.25 m^2 (urchin density) and 1 m^2 (algal cover) along 50-m transects running offshore from the kelp bed and into the barrens at selected sampling dates at Little Duck Island. Data are means (±SE for density) for quadrats (n = 2) at 1-m intervals relative to the edge of the kelp bed based on two transects in each half of the study grid (one transect in November in the eastern half).

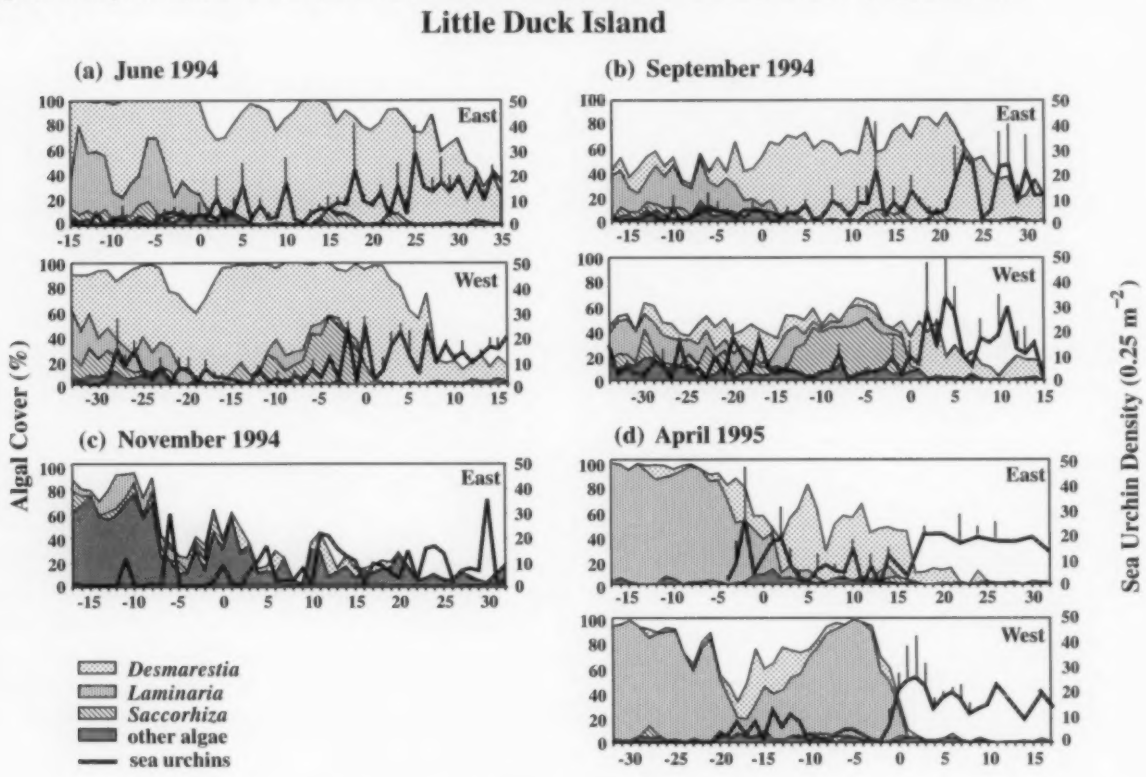

increase in biomass relative to the shallower barrens (Fig. 7). On a diving survey to 22 m depth in July 1994, we observed very few urchins on the gravel and silt bottom deeper than 15 m.

The size distribution of urchins in the barrens at both Little Duck Island and Mill Cove was relatively stable between 1992 and 1994, but a large increase in the abundance of small juveniles resulted in a marked drop in mean size by August 1995 (Fig. 3). The increase in mean density of urchins in the barrens at both sites between June and August 1995 (Figs. 2 and 4*b*) reflected our increased detection of these recruits from a major settlement pulse in July 1994 (T. Balch and R.E. Scheibling, unpublished data).

Defoliation and recolonization of kelp beds

In September 1993, colonies of *M. membranacea*, an epiphytic bryozoan, expanded rapidly on kelp fronds at Little Duck Island and Mill Cove. Fronds heavily encrusted with bryozoa became brittle and friable and were fragmented by strong wave action during late autumn and winter. By mid-November 1993, the once luxuriant kelp beds at both sites were reduced to stands of stipes (which eventually died and rotted), resulting in a major loss of kelp biomass and canopy cover.

The loss of the kelp canopy at Little Duck Island over the winter in 1993–1994 facilitated recruitment, during the following spring, of juvenile sporophytes of *L. longicruris*, which are normally light limited under a healthy canopy. By June 1994, the mean density of kelp recruits was ~80·m^{-2} in the kelp bed (R.E. Scheibling and A. Shaw, unpublished data). The cover of two other canopy-forming species (that usually are restricted to gaps in the *Laminaria* canopy), *D. viridis* and *S. dermatodea*, also expanded rapidly in summer 1994. By June 1994, *D. viridis* covered 60–100% of the previously barren area within 30 m of the border of the kelp bed (Fig. 8*a*). *Desmarestia viridis* and *S. dermatodea* are both annuals and began to die back in autumn (Fig. 8*b*). By November 1994, the cover of both species was generally <5% (Fig. 8*c*).

The rapid growth of the young kelp plants resulted in the offshore expansion of the kelp bed at Little Duck Island in 1994. By June, a large patch of *L. longicruris* and *S. dermatodea* had become established in the former barrens in the western half of the study grid (Fig. 8*a*), which by De-

© 1999 NRC Canada

Fig. 9. Density of urchins and cover of the canopy-forming and other (understorey and ephemeral species) macroalgae in successive quadrats of 0.25 m^2 (urchin density) and 1 m^2 (algal cover) along 35- to 50-m transects running offshore from the kelp bed and into the barrens at selected sampling dates at Mill Cove. Data are means (±SE for density) for quadrats (n = 2) at 1-m intervals relative to the edge of the kelp bed based on four transects for November 1994 and March 1995. Data for individual transects are given for June 1995.

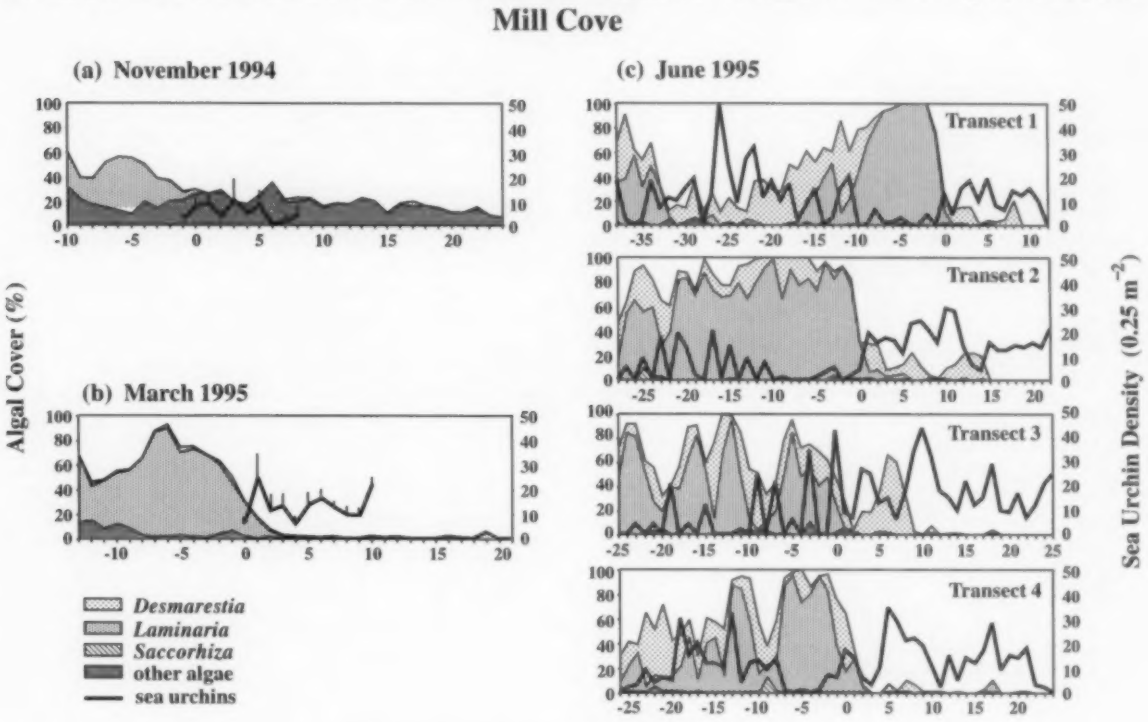

cember extended the lower boundary of the bed close to its location at the start of the study in June 1992 (Figs. 1 and 8*b*). In the eastern half of the grid, however, the boundary of the kelp bed expanded only a few metres offshore during 1994 (Fig. 1). A recurrent outbreak of *M. membranacea* in October–November 1994 further reduced the canopy cover during that winter, but to a lesser extent than the previous year. By April 1995, a luxuriant kelp canopy had regenerated at Little Duck Island (Figs. 5 and 8*d*).

At Mill Cove, the death of large but less dense kelp plants created expansive gaps in the canopy that were subsequently colonized by *D. viridis* and its perennial congener *D. aculeata* (Fig. 9*c*). Urchins infiltrating the kelp bed had created large barren patches by June 1995 (Fig. 9*c*). In spring and summer 1994–1995, a film of diatoms and filamentous algae covered much of barrens (particularly in the shallower parts), but this disappeared over winter (Figs. 9*a* and 9*b*).

Reaggregation of urchins and resumption of destructive grazing

After the mass mortality of *S. droebachiensis* at Little Duck Island in 1993, the distribution of remaining urchins shifted offshore. By June 1994, densities were low (generally <20·0.25 m^{-2}) in the area blanketed by *D. viridis* but increased towards the deeper barrens where algal cover was lower (Fig. 8*a*). By April 1995, urchins began to reaggregate at the border of the kelp bed, particularly along the arm of recently recruited kelp in the western half of the study grid, where a front had reformed (Fig. 8*d*). This front advanced at a rate of ~0.5 m·$month^{-1}$ between April and August 1995 (Fig. 4*a*), reducing the arm of new kelp (Fig. 1). In April 1995, we located another grazing front (site B) that advanced at a faster rate than the front in our study grid (site A) ~50 m away: 3.8 m·$month^{-1}$ between April and June and 2.1 m·$month^{-1}$ between June and August 1995 (Fig. 4*a*). Although the mean density of urchins in the front at site B (22–28·0.25 m^{-2}) was generally lower than that at site A (up to 82·0.25 m^{-2}) (Fig. 4*b*), urchins were larger (Fig. 3), and the density of kelp plants was lower (personal observations) at site B, which may account for the greater rate of advance of the front there.

At Mill Cove, small aggregations of urchins formed along the border of the kelp bed in March 1994 and 1995, but in both years, these weak fronts dispersed within 1 or 2 months (Fig. 2). Although the highest rates of advance of the front were recorded in spring 1994 and 1995 (1.4 m·$month^{-1}$; (Fig. 4*a*), algal consumption rates per metre of front were actually lower at these times (2.1 and 4.1 kg·m^{-1}·$month^{-1}$, respectively) than in the first year of our study (up to

© 1999 NRC Canada

4.9 $kg \cdot m^{-1} \cdot month^{-1}$) because of the lower biomass of *L. longicruris* after the bryozoan outbreak in 1993 (Fig. 5*a*).

In September 1995, a recurrence of disease virtually eliminated *S. droebachiensis* at both of our sites (Fig. 4*b*). Analysis of tissue samples from urchins collected at Little Duck Island confirmed the cause of the epizootic as paramoebiasis (Scheibling and Hennigar 1997).

Discussion

Formation of urchin fronts

Large-scale destructive grazing of *Laminaria* beds by *S. droebachiensis* was previously documented off Nova Scotia in the 1970s by K.H. Mann and co-workers (reviewed by Mann 1977). In a pioneering study of the kelp beds in St. Margaret's Bay in 1968, Mann (1972) observed that urchins generally occurred at low densities and fed on drift algae at the base of the canopy. However, in a few areas (including Mill Cove), he described "holes" in the kelp canopy, tens of metres in diameter, where urchins were abundant and grazed the kelp. These gaps expanded and coalesced, and by 1973, an estimated 70% of the kelp along 15 km of coast had been destroyed. Breen and Mann (1976*a*, 1976*b*) described high-density fronts of large urchins advancing through the kelp beds, similar to those that we observed in the early 1990s.

Bernstein et al. (1981, 1983) proposed that an increase in urchin density within kelp beds, presumably because of a reduction in predation pressure, results in the formation of aggregations that triggers destructive grazing. However, the grazing fronts that we observed did not originate within kelp beds, as suggested by these and other authors (Mann 1977; Hagen 1983). Rather, the beds were attacked along their offshore bounds as urchins moved onshore from deeper regions. We also observed the onshore migration of grazing fronts in other areas along the Atlantic coast of Nova Scotia, and this pattern has been corroborated by a number of commercial urchin harvesters. Hjörleifsson et al. (1995) described a similar pattern of aggregation of *S. droebachiensis* along the lower edge of a kelp forest (*Laminaria hyperborea*) and onshore advance of a dense grazing front in a fjord in northern Iceland.

Based on these observations, we propose an alternative explanation for the formation of destructive grazing aggregations in Nova Scotia. After mass mortalities of *S. droebachiensis* by disease, urchins that survive in deeper, colder waters (Scheibling 1984) begin to migrate into the shallower, recently established kelp beds. These migrations may be driven by chemical cues emanating from the plants: chemoreception experiments have shown that *S. droebachiensis* is strongly attracted to kelp (Mann et al. 1984). As urchins encounter a kelp bed, their movement decreases as they begin feeding on the plants. This results in increasing urchin densities along the edge of the bed and a grazing front forms. Time-lapse video records at Little Duck Island showed that urchins at the front moved little and spent most of their time grazing on kelp, whereas those in the barrens undertook more extensive, random movements (R.E Scheibling and A.W. Hennigar, unpublished data). Similarly, studies with tagged urchins (*Strongylocentrotus franciscanus*) in California have shown that individuals at the edge of a kelp forest move much less than those in the barrens (Mattison et al. 1977).

Density and size thresholds for destructive grazing

Breen and Mann (1976*a*, 1976*b*) postulated that a threshold biomass of *S. droebachiensis* was required for destructive grazing. This threshold is related to the ability of urchins to weigh down kelp fronds so that they can be entirely consumed. (Normally, wave-induced movement of the kelp limits the ability of individual urchins to climb onto fronds and effectively graze.) They found a positive relationship between urchin biomass at the edge of the kelp bed (ranging from 0.5 to 15 $kg \cdot m^{-2}$) and the rate of kelp bed recession (0–1.75 $m \cdot month^{-1}$) and a threshold biomass for destructive grazing of ~2 $kg \cdot m^{-2}$. We found a similar relationship at Little Duck Island where urchin biomass at the front was generally well above the postulated threshold level (Fig. 6), ranging from 6.6 to 12.1 $kg \cdot m^{-2}$ before the mass mortality in 1993 (site A) and from 2.5 to 8.5 $kg \cdot m^{-2}$ after fronts had reformed in spring–summer 1995 (sites A and B). At Mill Cove, urchin biomass was consistently below the threshold proposed by Breen and Mann (1976*a*, 1976*b*), ranging from 0.4 to 1.5 $kg \cdot m^{-2}$ throughout our study (Fig. 6). Nevertheless, a slow recession of the kelp bed occurred, although there was little or no advance of the front in autumn each year when densities of adult urchins usually were low.

The difference in threshold levels for destructive grazing between Little Duck Island and Mill Cove probably reflects differences in wave action, which can limit urchin feeding rate (Lissner 1983; Kawamata 1998). At Little Duck Island, where wave action is generally strong, fronds of *L. longicruris* are tossed back and forth in the surge. In contrast, because wave action is lower at Mill Cove, kelp fronds often lie along the bottom and are accessible to individuals or small clusters of urchins. Under calm conditions, urchins also can climb the kelp stipes with little risk of dislodgment. Therefore, the decrease in wave action with depth may enable the formation of fronts by a gradual accumulation of individuals, even in wave-exposed areas such as Little Duck Island.

Urchins in fronts are almost exclusively large adults, generally >30 mm in test diameter (also see Breen and Mann 1976*a*; Bernstein et al. 1981). At these sizes, *S. droebachiensis* typically forages in the open on attached plants if they are available. Smaller urchins (which comprise most of the population in the barrens) usually are cryptic, sheltering in crevices and on the undersides of rocks to avoid predators (Himmelman 1986; Scheibling and Hamm 1991). The characteristic size structure of the front probably develops as large, actively foraging urchins encounter the kelp bed. Large size is also advantageous in weighing down the kelp fronds and facilitating consumption of whole plants (Kawamata 1998). Thus, there probably is a body size threshold below which destructive grazing will not occur, such that a population consisting mainly of juveniles (<20 mm) may be unable to consume kelp. Meidel and Scheibling (1998*a*) showed that the difference in size distribution of urchins between the front and the barrens was related to differences in both age structure and growth rate. At both Little Duck Island and Mill Cove, urchins in fronts were older

© 1999 NRC Canada

(median age 6 and 5 years, respectively) than those in barrens (3 and 2 years, respectively); urchins also grew faster in fronts and kelp beds than in barrens (Meidel and Scheibling 1998*a*).

Urchins within the kelp bed, like those in the barrens, were small and cryptic. They typically occurred at low densities and in small aggregations under boulders. There was no evidence of destructive grazing of *L. longicruris* within the kelp bed throughout most of our study. However, following a major reduction in the kelp at Mill Cove, due to repeated outbreaks of *M. membranacea*, adult urchins began to infiltrate the kelp bed in 1995, creating barren patches similar to those observed by Mann (1972).

Rate of advance of urchin fronts

The rate of advance of the front at Little Duck Island peaked around midsummer but declined sharply in late summer and remained low over autumn and winter. Seasonal changes in feeding rates, possibly related to the reproductive cycle, may account for seasonal variation in the rate of advance of the front. In a concurrent study at Little Duck Island, Meidel and Scheibling (1998*b*) found that the feeding rate of urchins decreased in late summer and increased in spring (directly after spawning). A similar pattern has been observed in other studies of *S. droebachiensis* (Keats et al. 1983; Himmelman and Nédélec 1990). Individual feeding rates on macroalgae, estimated for periods of greatest advance of the fronts at Little Duck Island and Mill Cove (~2 g·day^{-1}), were consistent with those measured in laboratory studies where adult *S. droebachiensis* were fed kelp ad libidum (Minor and Scheibling 1997; Meidel and Scheibling 1999).

Strong wave surge also can influence the rate of destructive grazing when it inhibits the foraging activity of urchins. In oscillating-flow-tank experiments, Kawamata (1998) showed that the feeding rate (on kelp) of *Strongylocentrotus nudus* virtually ceased at water velocities of 0.3–0.4 m·s^{-1} and that the urchins could hardly move at 0.7 m·s^{-1}. Peak velocities during storms readily exceed these limits in the barrens at Little Duck Island (>1 m·s^{-1}, T. Balch and R.E. Scheibling, unpublished data). Wave surge also has a "whiplash" effect on kelp that can prevent urchins from climbing up kelp fronds to feed (Velimirov and Griffiths 1979). Wave action is strongest in winter, particularly at Little Duck Island, which may partly account for the low rate of advance of the front at that time. In August 1995, during a period of heavy swell generated by Hurricane Felix in the North Atlantic, we observed urchins in two-dimensional clusters along the front at Little Duck Island (sites A and B). These urchins were previously in three-dimensional aggregations during a calmer period in June 1995, suggesting that they deaggregated in response to increased wave surge. This behavioural change was associated with a broadening of the front (particularly at site B, which was shallower) and a reduction in its rate of advance. Since urchins in two-dimensional clusters can attach firmly to the rock substratum, probably even more so than isolated individuals (Garnick 1978), this may be a behavioural adaptation against wave dislodgment. Urchins also avoid dislodgment by taking refuge in sheltered microhabitats (Harrold and Reed 1985), and we observed many individuals packed into crevices during periods of strong wave action.

The rate of advance of a grazing front is directly related to the density and body size of urchins (which together determine biomass) and inversely related to the density or biomass of plants in the kelp bed. Thus, the larger size of urchins and smaller biomass of kelp at Little Duck Island, compared with Mill Cove, at the start of our study in June 1992 (when urchin densities were comparable between sites) likely account for the higher rate of advance of the front at Little Duck Island. Similarly, differences between locations (sites A and B) at Little Duck Island were related to differences in both the size and biomass of urchins and the density of kelp plants.

The maximum rates of advance of urchin fronts measured during our study (4.2 and 1.4 m·month^{-1} at Little Duck Island and Mill Cove, respectively) are consistent with those recorded previously in St. Margaret's Bay (1.8 m·month^{-1}, Breen and Mann 1976*a*, 1976*b*) and more recently in an Icelandic fjord (2 m·month^{-1}, Hjörleifsson et al. 1995). Given these grazing rates and a rough estimate of the average width of rocky subtidal habitat suitable for kelp (366 m, Moore and Miller 1983), we estimate that destructive grazing of the rocky subtidal zone, in the absence of urchin fishing or natural disturbances such as disease or bryozoan outbreaks, would take between 7 and 22 years. In St. Margaret's Bay, urchins took at least 6 years (1968–1973) to destroy kelp throughout the bay (Breen and Mann 1976*b*). Thus, it seems reasonable to propose that the transition from kelp beds to barrens on a coastal scale would take about a decade.

Defoliation and recolonization of kelp beds

In the Northwest Atlantic, the bryozoan *M. membranacea* was first recorded in the Gulf of Maine in 1987, where it became the dominant epiphyte on laminarian kelps within 2 years (Berman et al. 1992). We observed small colonies of *M. membranacea* on kelp at the start of our study in 1992, but it was not until the following year that a heavy growth of bryozoa resulted in a major loss of canopy at both of our sites (this study; R.E. Scheibling and A. Shaw, unpublished data). Similar defoliation events have been reported in the Gulf of Maine (Lambert et al. 1992) and the Northeast Pacific (Dixon et al. 1981). Bryozoan-mediated defoliation of kelp beds could augment or accelerate destructive grazing by urchins. This did not occur at Little Duck Island because of a coincident mass mortality of urchins in autumn 1993. Rather, recruitment of *Laminaria* sporelings regenerated and extended the kelp bed by summer 1994. At Mill Cove, where there was little mortality of urchins in autumn 1993, the pronounced reduction in kelp density probably facilitated a gradual infiltration of the kelp bed by urchins, thereby increasing the rate of kelp destruction. Bryozoan infestations also could hasten the demise of kelp beds by promoting population growth of urchins. Urchins incidentally consume *M. membranacea* while grazing on kelp, and this protein supplement results in increased rates of growth and reproduction (Nestler and Harris 1994). Fragmentation of heavily encrusted fronds by wave action also may enhance the nutrition of urchins in the barrens through increased production of kelp detritus.

Disease is the only known mechanism for the large-scale shift in community state from urchin-dominated barrens to

© 1999 NRC Canada

kelp beds (Scheibling 1986), although the occurrence of this transition depends on the severity of an epizootic, which, in turn, is directly related to sea temperature (Scheibling and Hennigar 1997). Thus, the lower incidence of urchin mortality at Mill Cove than at Little Duck Island in September 1993 was probably related to lower bottom temperatures at Mill Cove, which limited transmission and progression of the disease (Scheibling and Hennigar 1997). In 1995, both sites experienced a protracted period of high temperatures, which culminated in nearly complete mortality of urchins. Partial or localized mortalities of urchins may not reduce numbers below a threshold that enables extensive recolonization of kelp. Threshold densities of urchins required to maintain a barrens appear to be much lower than those required for destructive grazing of kelp (this study; Bernstein et al. 1981; Leinaas and Christie 1996). As we observed at Little Duck Island, even when populations are decimated by disease, urchins can reaggregate to form fronts and resume destructive grazing.

The epizootic that decimated the urchin population at Little Duck Island in 1993 arrested destructive grazing and enabled recolonization of recently formed barrens by macroalgae. The succession that we observed in 1994 was similar to that previously reported after urchin mass mortalities in Nova Scotia (Scheibling 1986; Johnson and Mann 1988) and Norway (Leinaas and Christie 1996). Opportunistic annuals, mainly *D. viridis* and *S. dermatodea*, were the first canopy-forming species to appear, but these were replaced within a year by *L. longicruris*, the competitive dominant (Johnson and Mann 1988). Interestingly, the surviving urchins at Little Duck Island appeared to migrate away from the edge of the kelp bed, where a dense cover of *D. viridis* had developed by summer 1994, into deeper regions with less macroalgae. Although *S. droebachiensis* can feed on *D. viridis*, it is a nonpreferred species (Lemire and Himmelman 1996) containing chemical compounds that render it unpalatable to urchins (Anderson and Velimerov 1982). As *D. viridis* eventually died back in winter, urchins reaggregated along the border of the kelp bed to form a front by spring 1995, but this second wave of destructive grazing was terminated by a recurrence of disease in September that eliminated urchins at both of our study sites and over ~130 km of coast (Scheibling and Hennigar 1997). This widespread demise of urchins led to the reestablishment of kelp beds at both sites by summer 1998 (R.E. Scheibling and T. Balch, unpublished data) and presumably throughout the disease-affected area.

Implications for the management of coastal resources

Previous consideration of the economic implications of community dynamics in the rocky subtidal zone off Nova Scotia has focussed primarily on the losses of primary productivity and habitat structure that result from destructive grazing of kelp beds by urchins (Mann 1977; Pringle et al. 1982). Wharton and Mann (1981) argued that the shift in the subtidal ecosystem from luxuriant kelp beds to urchin barrens contributes to declining yields of commercially important species such as lobsters (but see also Elner and Campbell 1987). Concern about the stability of barrens has prompted research into urchin eradication procedures designed to promote the reestablishment of kelp beds, including the use of quicklime and pathogenic agents (reviewed by Scheibling 1988). In the early 1990s, however, the urchin roe fishery in eastern Canada expanded rapidly (Hatcher and Hatcher 1997), dramatically altering the economic importance of *S. droebachiensis* from a pest species to a valuable commodity. The challenge facing fisheries managers today is conservation of urchin stocks, not their destruction.

Our empirical observations are relevant to understanding the impact of the urchin fishery on community dynamics because fishing mortality has a similar effect on urchin populations, and hence on community structure, as natural occurrences of disease. The fishery targets areas of high urchin density, primarily grazing fronts, in the shallow subtidal zone where urchins are harvested by scuba diving. Intensive harvesting of fronts can remove enough large urchins to enable the regrowth of kelp along the margins of a bed (personal observations). Thus, like disease, fishing can arrest the destruction of kelp beds and allow regeneration of macroalgae that are important food resources for urchins. Judicious harvesting procedures that leave sufficient numbers of urchins to allow fronts to reform after the fishing season, or rotate harvested areas on an annual basis, may enable stocks to be fished at a sustainable level and maintain the system in a transitional state. This underscores the key difference between fishing and disease: fishing pressure can be regulated to limit the intensity or frequency of urchin mortality, whereas outbreaks of disease appear to be related to uncontrollable stochastic events (Scheibling and Hennigar 1997).

Future studies that address the urchin density dependence of destructive grazing and kelp recolonization could provide important insights for development of sustainable harvesting and ranching procedures for an urchin fishery. Experimental fishing of grazing fronts, designed to reduce densities to specified levels and monitor responses of both urchins and algae, would be a particularly effective approach. As the roe fishery expands, human predation will become increasingly more important in regulating urchin numbers and the dynamics of kelp beds. However, given the history of recurrent outbreaks of disease in this system, the fishery along the Atlantic coast of Nova Scotia is destined to periodically crash, making it a "boom or bust" venture.

Acknowledgments

We thank Tony Carlson, Ian Dempsey, Tony Henderson, Sean Lothian, Doug Mackey, Susanne Meidel, Eric Scheibling, Lara Scheibling, Alyson Shaw, and Paul Winger for assistance with field work or sample processing and Lenny Mosher for allowing us to use his wharf. We also thank Anna Metaxas for help with statistical analysis and graphics and for critically reviewing various drafts of the manuscript. The work was supported by an NSERC research grant and an NSERC/DFO Science Subvention Program grant to RES.

References

Anderson, R.J., and Velimerov, B. 1982. An experimental investigation of the palatability of kelp bed algae to the sea urchin *Parechinus angulosus* Leske. Mar. Ecol. **3**: 357–373.

© 1999 NRC Canada

Berman, J., Harris, L., Lambert, W., Buttrick, M., and Dufresne, M. 1992. Recent invasions of the Gulf of Maine: three contrasting ecological histories. Conserv. Biol. **6**: 435–442.

Bernstein, B.B., Williams, B.E., and Mann, K.H. 1981. The role of behavioural responses to predators in modifying urchins' (*Strongylocentrotus droebachiensis*) destructive grazing and seasonal foraging patterns. Mar. Biol. **63**: 39–49.

Bernstein, B.B., Schroeter, S.C., and Mann, K.H. 1983. Sea urchin (*Strongylocentrotus droebachiensis*) aggregating behaviour investigated by a subtidal multifactorial experiment. Can. J. Fish. Aquat. Sci. **40**: 1975–1986.

Bologna, P.A.X., and Steneck, R.S. 1993. Kelp beds as habitat for American lobster *Homarus americanus*. Mar. Ecol. Prog. Ser. **100**: 127–134.

Breen, P.A., and Mann, K.H. 1976*a*. Changing lobster abundance and the destruction of kelp beds by sea urchins. Mar. Biol. **34**: 137–142.

Breen, P.A., and Mann, K.H. 1976*b*. Destructive grazing of kelp by sea urchins in eastern Canada. J. Fish. Res. Board Can. **33**: 1278–1283.

Dayton, P.K. 1985. Ecology of kelp communities. Annu. Rev. Ecol. Syst. **16**: 215–245.

Dixon, J., Schroeter, S.C., and Kestendiek, J. 1981. Effects of the encrusting bryozoan, *Membranipora membranacea*, on the loss of blades and fronds by the giant kelp, *Macrocystis pyrifera* (Laminariales). J. Phycol. **133**: 125–134.

Elner, R.W., and Campbell, A. 1987. Natural diets of lobster *Homarus americanus* from barren ground and macroalgal habitats off southwestern Nova Scotia, Canada. Mar. Ecol. Prog. Ser. **37**: 131–140.

Elner, R.W., and Vadas, R.L.S. 1990. Inference in ecology: the sea urchin phenomenon in the northwestern Atlantic. Am. Nat. **136**: 108–125.

Garnick, E. 1978. Behavioural ecology of *Strongylocentrotus droebachiensis* (Müller) (Echinodermata: Echinoidea). Aggregating behaviour and chemotaxis. Oecologia, **37**: 77–84.

Gerard, V.A., and Mann, K.H. 1979. Growth and production of *Laminaria longicruris* (Phaeophyta) populations exposed to different intensities of water movement. J. Phycol. **15**: 33–41.

Hagen, N.T. 1983. Destructive grazing of kelp beds by sea urchins in Vestfjorden, northern Norway. Sarsia, **68**: 177–190.

Hagen, N.T., and Mann, K.H. 1992. Functional response of the predators American lobster *Homarus americanus* (Milne-Edwards) and Atlantic wolffish *Anarhichas lupas* (L.) to increasing numbers of the green sea urchin *Strongylocentrotus droebachiensis* (Müller). J. Exp. Mar. Biol. Ecol. **159**: 89–112.

Harrold, C., and Pearse, J.S. 1987. The ecological role of echinoderms in kelp forests. *In* Echinoderm studies 2. *Edited by* M. Jangoux and J.M. Lawrence. A.A. Balkema, Rotterdam, The Netherlands. pp. 137–233.

Harrold, C., and Reed, D.C. 1985. Food availability, sea urchin grazing, and kelp forest community structure. Ecology, **66**: 1160–1169.

Hatcher, B.G., and Hatcher, A.I. 1997. Research directions and management options for sea urchin culture in Nova Scotia. Bull. Aquacult. Assoc. Can. **97**: 62–65.

Himmelman, J.H. 1986. Population biology of green sea urchins on rocky barrens. Mar. Ecol. Prog. Ser. **33**: 295–306.

Himmelman, J.H., and Nédélec, H. 1990. Urchin foraging and algal survival strategies in intensely grazed communities in eastern Canada. Can. J. Fish. Aquat. Sci. **47**: 1011–1026.

Hjörleifsson, E., Kaasa, Ö., and Gunnarsson, K. 1995. Grazing of kelp by green sea urchin in Eyjafjöerdur, North Iceland. *In* Ecology of fjords and coastal waters. *Edited by* H.R. Skjoldal, C. Hopkins, K.E. Erikstad, and H.P. Leinaas. Elsevier Science B.V., Amsterdam, The Netherlands. pp. 593–597, 623.

Johnson, C.R., and Mann, K.H. 1988. Diversity, patterns of adaptation, and stability of Nova Scotian kelp beds. Ecol. Monogr. **58**: 129–154.

Jones, G.M., Hebda, A.I., Scheibling, R.E., and Miller, R.J. 1985. Histopathology of disease causing mass mortality of sea urchins (*Strongylocentrofus droebachiensis*) in Nova Scotia. J. Invert. Pathol. **71**: 559–565.

Kawamata, S. 1998. Effect of wave-induced oscillatory flow on grazing by a subtidal sea urchin *Strongylocentrotus nudus* (A. Agassiz). J. Exp. Mar. Biol. Ecol. **224**: 31–48.

Keats, D.M., Steele, D.H., and South, G.R. 1983. Food relations and short term aquaculture potential of the green sea urchins (*Strongylocentrotus droebachiensis*) in Newfoundland. Tech. Rep. Memorial Univ. Nfld. Mar. Sci. Res. Lab. **24**: 1–24.

Lambert, W.J., Levin, P.S., and Berman, J. 1992. Changes in the structure of a New England (U.S.A.) kelp bed: the effects of an introduced species? Mar. Ecol. Prog. Ser. **88**: 303–307.

Leinaas, H.P., and Christie, H. 1996. Effects of removing sea urchins (*Strongylocentrotus droebachiensis*): stability of the barren state and succession of kelp forest recovery in the east Atlantic. Oecologia, **105**: 524–536.

Lemire, M., and Himmelman, J.H. 1996. Relation of food preference to fitness for the green sea urchin, *Strongylocentrotus droebachiensis*. Mar. Biol. **127**: 73–78.

Lissner, A.L. 1983. Relationship of water motion to the shallow water distribution and morphology of two species of sea urchin. J. Mar. Res. **41**: 691–709.

Mack, M.C., and D'Antonio, C.M. 1998. Impacts of biological invasions on disturbance regimes. Trends Ecol. Evol. **13**: 195–198.

Mann, K.H. 1972. Ecological energetics of the seaweed zone in a marine bay on the Atlantic coast of Canada. I. Zonation and biomass of seaweeds. Mar. Biol. **12**: 1–10.

Mann, K.H. 1977. Destruction of kelp-beds by sea urchins: a cyclical phenomenon or irreversible degradation? Helgol. Wiss. Meeresunters. **30**: 455–467.

Mann, K.H. 1982. Ecology of coastal waters, a systems approach. Studies in ecology. Blackwell Scientific Publications, Oxford, U.K.

Mann, K.H., Wright, J.L.C., Welsford, B.E., and Hatfield, E. 1984. Responses of the sea urchin *Strongylocentrotus droebachiensis* (O.F. Müller) to water-borne stimuli from potential predators and potential food algae. J. Exp. Mar. Biol. Ecol. **79**: 233–244.

Mattison, J.E., Trent, J.D., Shanks, A.L., Akin, T.B., and Pearse, J.S. 1977. Movement and feeding activity of red sea urchins (*Strongylocentrotus franciscanus*) adjacent to a kelp forest. Mar. Biol. **39**: 25–30.

Meidel, S.K., and Scheibling, R.E. 1998*a*. Size and age structure of the sea urchin *Strongylocentrotus droebachiensis* in different habitats. *In* Echinoderms: San Francisco. *Edited by* R. Mooi and M. Telford. A.A. Balkema, Rotterdam, The Netherlands. pp. 737–742.

Meidel, S.K., and Scheibling, R.E. 1998*b*. Annual reproductive cycle of the green sea urchin, *Strongylocentrotus droebachiensis*, in differing habitats in Nova Scotia, Canada. Mar. Biol. **131**: 461–478.

Meidel, S.K., and Scheibling, R.E. 1999. Effects of food type and ration on maturation and growth of the sea urchin *Strongylocentrotus droebachiensis*. Mar. Biol. **134**: 155–166.

Miller, R.J. 1985*a*. Succession in sea urchin and seaweed abundance in Nova Scotia, Canada. Mar. Biol. **84**: 275–286.

Miller, R.J. 1985*b*. Seaweeds, sea urchins, and lobsters: a reappraisal. Can. J. Fish. Aquat. Sci. **42**: 2061–2072.

© 1999 NRC Canada

Minor, M.A., and Scheibling, R.E. 1997. Effects of food ration and feeding regime on growth and reproduction of the sea urchin *Strongylocentrotus droebachiensis*. Mar. Biol. **129**: 159–167.

Moore, D.S., and Miller, R.J. 1983. Recovery of macroalgae following widespread sea urchin mass mortality with a description of the nearshore hard-bottom habitat on the Atlantic coast of Nova Scotia. Can. Tech. Rep. Fish. Aquat. Sci. No. 1230.

Nestler, E.C., and Harris, L.G. 1994. The importance of omnivory in *Strongylocentrotus droebachiensis* (Müller) in the Gulf of Maine. *In* Echinoderms through time. *Edited by* B. David, A. Guille, J.-P. Feral, and M. Roux. A.A. Balkema, Rotterdam, The Netherlands. pp. 813–818.

Pringle, J.D., Sharp, G.J., and Caddy, J.F. 1982. Interactions in kelp bed ecosystems in the northwest Atlantic: review of a workshop. *In* Multispecies approaches to fisheries management advice. *Edited by* M.C. Mercer. Can. Spec. Publ. Fish. Aquat. Sci. No. 59. pp. 108–115.

Scheibling, R.E. 1984. Echinoids, epizootics and ecological stability in the rocky subtidal off Nova Scotia, Canada. Helgol. Meeresunters. **37**: 233–242.

Scheibling, R.E. 1986. Increased macroalgal abundance following mass mortalities of sea urchins (*Strongylocentrotus droebachiensis*) along the Atlantic coast of Nova Scotia. Oecologia, **68**: 186–198.

Scheibling, R.E. 1988. Microbial control of sea urchins: Achilles' heel or Pandora's box? *In* Echinoderm biology. *Edited by* R.D. Burke, P.V. Mladenov, P. Lambert, and R.L. Parsley. A.A. Balkema, Rotterdam, The Netherlands. pp. 745–754.

Scheibling, R.E. 1996. The role of predation in regulating sea urchin populations in eastern Canada. Oceanol. Acta, **19**: 421–430.

Scheibling, R.E., and Hamm, J. 1991. Interactions between sea urchins (*Strongylocentrotus droebachiensis*) and their predators in field and laboratory experiments. Mar. Biol. **110**: 105–116.

Scheibling, R.E., and Hennigar, A.W. 1997. Recurrent outbreaks of disease in sea urchins *Strongylocentrotus droebachiensis* in Nova Scotia: evidence for a link with large-scale meteorologic and oceanographic events. Mar. Ecol. Prog. Ser. **152**: 155–165.

Scheibling, R.E., Hennigar, A.W., and Balch, T. 1994. The dynamics of destructive grazing of kelp beds by sea urchins in Nova Scotia. *In* Echinoderms through time. *Edited by* B. David, A. Guille, J.-P. Feral, and M. Roux. A.A. Balkema, Rotterdam, The Netherlands. p. 871.

Vadas, R.L., and Steneck, R.S. 1995. Overfishing and inferences in kelp – sea urchin interactions. *In* Ecology of fjords and coastal waters. *Edited by* H.R. Skjoldal, C. Hopkins, K.E. Erikstad, and H.P. Leinaas. Elsevier Science B.V., Amsterdam, The Netherlands. pp. 509–524.

Velimirov, B., and Griffiths, C.L. 1979. Wave-induced kelp movement and its importance for community structure. Bot. Mar. **22**: 169–172.

Wharton, W.G., and Mann, K.H. 1981. Relationship between destructive grazing by the sea urchin, *Strongylocentrotus droebachiensis*, and the abundance of American lobster, *Homarus americanus*, on the Atlantic coast of Nova Scotia. Can. J. Fish. Aquat. Sci. **38**: 1339–1349.

© 1999 NRC Canada

Sperm competition and fertilization success in Atlantic cod (*Gadus morhua*): effect of sire size and condition factor on gamete quality

Ana Rakitin, Moira M. Ferguson, and Edward A. Trippel

Abstract: Sperm competition experiments were conducted to test the null hypothesis that sperm quality is not affected by male body size in Atlantic cod (*Gadus morhua*). Genetic markers (allozymes) were used to determine the proportion of larvae sired by pairs of males when their sperm was combined with eggs of a single female simultaneously. Significant differences in fertilization success between males were not explained by differences in body size. Fertilization success was positively associated with male condition factor (K) and with spermatozoa density in each male's semen when equal volumes of semen from each male were used. Male K was positively associated with male fertilization success when the volume of semen used from each male was adjusted to add approximately equal numbers of spermatozoa from each male. The relative fertilization success of males varied depending on which female was the egg donor, suggesting that female "choice" at the gamete level may be occurring in cod.

Résumé : Des expériences sur la compétition entre les spermatozoïdes ont été effectuées afin de tester l'hypothèse nulle selon laquelle la qualité du sperme n'est pas affectée par la taille des mâles de la morue de l'Atlantique (*Gadus morhua*). Des marqueurs génétiques (allozymes) ont été utilisés pour déterminer les proportions relatives de larve produites par des paires de mâles lorsque leur sperme était mélangé simultanément à des oeufs provenant d'une même femelle. Des écarts appréciables du succès de la fécondation de chacun des mâles n'étaient pas expliqués par les écarts de taille. Le succès de la fécondation présentait une corrélation positive avec le facteur de condition des mâles (K) et la densité des spermatozoïdes de chacun des mâles lorsque des volumes égaux de laitance étaient utilisés. Le facteur K des mâles présentait une corrélation positive avec le succès de la fécondation lorsque le volume de laitance de chacun des mâles était corrigé de façon à obtenir un nombre approximativement égal de spermatozoïdes pour chacun des mâles. Le succès relatif de la fécondation par les mâles variait en fonction de la femelle, ce qui porte à croire que, chez la morue, la femelle pourrait exercer un certain « choix » au niveau des gamètes.

[Traduit par la Rédaction]

Introduction

Mating competition in fishes usually occurs among males and may take the form of either competition for the access to females or competition of spermatozoa for the fertilization of eggs. Simultaneous spawning, resulting in sperm competition, is probably the most common form of intrasexual competition in fish (Taborsky 1994). The relative importance of competition for the access to females and sperm competition in male reproductive success depends on the spawning system of the species.

Atlantic cod (*Gadus morhua*) are pelagic spawners with external fertilization and no parental care. During the reproductive season, cod form large aggregations on the spawning grounds (e.g., Rose 1993; Morgan and Trippel 1996). Males and females release their gametes synchronously and fertilization occurs in the water. Gametes remain viable in the water for a long time compared with other fish species. Cod eggs can be fertilized and produce normal embryos after being in the water for up to 6 h (Davenport et al. 1981; Kjørsvik and Lønning 1983). Spermatozoa are motile for 16 min on average (Westin and Nissling 1991) and retain about 50% of their initial fertilization capacity after 60 min in the water (Trippel and Morgan 1994*a*). Aggression among males, courtship, and pair formation have been described for cod spawning in captivity (Brawn 1961; Hutchings et al. 1999). The communal spawning, external fertilization, and longevity of gametes favour the occurrence of sperm competition. However, pair spawning would temper the importance of sperm competition in determining the reproductive success of males.

In fish, larger, older males (potentially with more reproductive experience) generally spawn more often with females when males compete aggressively for females. Brawn's (1961) observations and Hutchings et al.'s (1999) results support this generality in cod. Therefore, if pair spawning is the dominant reproductive tactic in cod, large males should have higher fertilization success than smaller males. However, if group spawning is the prevalent form of zygote production, the relative reproductive success of males should depend on the quantity and quality of sperm produced by different males.

In fish species where males display two alternative, size-

Received July 22, 1998. Accepted August 12, 1999.
J14704

A. Rakitin and M.M. Ferguson.[1] Department of Zoology, University of Guelph, Guelph, ON N1G 2W1, Canada.
E.A. Trippel. Department of Fisheries and Oceans, Biological Station, St. Andrews, NB E0G 2X0, Canada.

[1]Author to whom all correspondence should be addressed.
e-mail: mmfergus@uoguelph.ca

© 1999 NRC Canada

dependent reproductive strategies, the testes of small subordinate males are relatively larger than those of large dominant males (e.g., review by Taborsky 1994). In some fish, younger and smaller first-time spawner males produce sperm of better quality (e.g., Zuromska and Markowska 1984), with longer motility duration than large repeat-spawner males (e.g., Daye and Glebe 1984; de Fraipont et al. 1993; Warner et al. 1995). Small male cod do not have relatively larger testes, and in Baltic cod the maximum gonadosomatic index (the ratio of gonad weight to body weight) increases with each year of spawning (Sorokin 1960). Trippel and Neilson (1992) found no difference in fertilization rate between small, first-spawner and large, repeat-spawner male cod using sperm from one male to fertilize eggs from one female. However, the results may be different in a sperm competition situation (e.g., see Gile and Ferguson (1995) for rainbow trout (*Oncorhynchus mykiss*)).

The decreasing abundance of large cod in the Northwest Atlantic has presumably resulted in a decrease in sperm density in spawning aggregations. Because sperm density is an important factor determining fertilization success in pelagic spawners (e.g., Levitan et al. 1991), the final effect may be an overall reduction in zygote production. This effect could be aggravated if smaller and younger fish produce low-quality sperm.

We tested the null hypothesis that body size does not influence sperm quality (i.e., fertilization success) in male Atlantic cod. Additional objectives were to assess the importance of sperm motility, sperm density, and sire condition factor on fertilization success and to test whether male fertilization success was affected by the female through gamete interaction. We used allozyme loci as genetic markers to estimate the proportion of larvae sired by each of two males, differing in body size, when sperm from both males was simultaneously combined with eggs of a single female (i.e., in a sperm competition situation).

Materials and methods

Parental fish and collection of tissue and gametes

Adult male and female Atlantic cod, captured in the Bay of Fundy, were maintained at the St. Andrews Biological Station (New Brunswick, Canada) in outdoor tanks supplied with flowing seawater (salinity ~30‰) and fed a mixed diet of herring, squid, and shrimp. The experiments were conducted during the cod spawning seasons (January–April) of 1994 and 1996. Water temperature in the tanks ranged between 3 and 5°C and fish were not fed during the experiments.

Fish were measured (total length, L, to the nearest centimetre and body weight, *W*, to the nearest 50 g) at the beginning of each experiment (February 18, 1994, and January 17, 1996). Fulton's condition factor (K) was calculated for each fish as $K = W/L^3 \times 100$. The K was chosen, rather than other indicators of condition, because it has been used in studies on cod reproduction (e.g., Kjesbu 1989; Trippel and Neilson 1992) and the assumption of isometric growth ($W = aL^b$, with $b = 3$) is met for the study population. A linear regression of log L on log W was calculated using data from 124 cod (L range = 50–87 cm) from the St. Andrews Biological Station broodstock, measured on January 17 and 18, 1996. The slope was 3.01 (95% CI = 2.82–3.21) and K was not correlated with L ($r = 0.0002$).

Tissue samples (anal or caudal fin clips) were collected and stored in liquid nitrogen until they were used to determine parental genotypes at potential genetic marker loci.

Gametes were collected by hand stripping as described in Rakitin et al. (1999). No attempt was made to collect all the semen from every male. The gametes of each fish were collected in separate containers and kept covered on crushed ice until utilization. Semen samples contaminated with urine were not used.

Sperm density and motility estimation

Spermatocrit (percentage of packed cellular material in semen after centrifugation) was used to estimate spermatozoa density because it has been shown to be a reliable indicator of sperm density in cod (Rakitin et al. 1999). Spermatocrit was measured in triplicate for each semen sample as described in Rakitin et al. (1999).

The percentage of motile spermatozoa was estimated in duplicate for each semen sample. An aliquot of 0.2 mL of semen was diluted in 100 mL of seawater (water temperature 4–8°C) and a drop of this dilution was placed on the centre of a hemacytometer grid, already situated on a microscope stage. Sperm were videotaped at 400× magnification for 60 s. The percentage of spermatozoa moving forward was estimated from the videotapes.

Experimental matings and incubation and sampling of progeny

An experimental mating consisted of the in vitro combination of gametes of specific parental fish. Gametes were combined in glass beakers filled with filtered and UV-sterilized seawater at 4°C. Three types of matings were conducted during the experiments.

(*i*) Equal volume of sperm competition (EVSC) mating: 0.2 mL of semen from each of 2 males differing in body size were combined in 100 mL of seawater to obtain a semen–seawater dilution of 1:250). A 1:250 semen–water dilution was used because it results in nearly 100% fertilized eggs (Trippel and Neilson 1992) and sperm competition should occur when spermatozoa are not limiting. About 400 eggs from a single female were immediately added to the semen mixture. The gametes were gently swirled, and after 1 min the excess sperm were drained by pouring the mixture through a mesh that retained the eggs. The eggs were rinsed and placed in a different glass container with clean seawater for incubation.

(*ii*) Equal density of sperm competition (EDSC) mating: this followed the same procedure as the EVSC mating, except in this case the volume of semen from each of the two competing males was adjusted according to the density of spermatozoa (spermatocrit), so that approximately equal numbers of spermatozoa from each male were used. The total volume of semen from the two males added to 100 mL of seawater was 0.4 mL.

(*iii*) Control mating: 0.2 mL of semen from one male in 50 mL of seawater was combined with eggs from the same female and batch used in the corresponding sperm competition mating.

All matings were done in triplicate. Embryos were incubated at 4°C with each replicate in a separate labelled beaker. To prevent bacterial and (or) fungal infection, about 30–60 mg penicillin-G·L^{-1} and 50–100 mg streptomycin sulphate·L^{-1} were added and the water was replaced periodically. Nevertheless, early embryo mortality was high in some cases, which led to the exclusion of a replicate from the calculation of results in some matings.

Fertilization success was determined 10–30 h after fertilization (at 4°C the first cell division occurs 6–10 h after fertilization, unpublished observations) by counting at 30× magnification the number of embryos showing cleavage. Those not showing cell cleavage were considered unfertilized, and either oversized (presumably overripe) or deformed eggs were excluded from the count.

Hatching occurred 20–25 days after fertilization. The number of hatched larvae was recorded for each replicate and the hatching success estimated (only in experiment 1, see below) as the ratio of

© 1999 NRC Canada

hatched larvae to fertilized eggs. At yolk sac consumption (5–10 days after hatching), larvae from each replicate were stored in either liquid nitrogen or at –60°C until the genetic analysis.

Genetic analysis: Mendelian inheritance and paternity determination

Three allozyme loci that were polymorphic in the parents and could be reliably scored in the larvae with cellulose acetate gel protein electrophoresis (Hebert and Beaton 1989) were used as markers. The loci were isocitrate dehydrogenase (*IDH-1*, EC 1.1.1.42), lactate dehydrogenase (*LDH-B*, EC 1.1.1.27), and phosphoglucomutase (*PGM-1*, EC 5.4.2.2). Locus and allele designation was after Grant and Ståhl (1988).

The progeny from the control matings of experiment 1 were used to test whether the genetic markers were segregating according to Mendelian proportions and whether a particular genotype at a marker locus was associated with early larval survival.

Experiments

Experiment 1 (1994)

The purpose of this experiment was to assess the effect of male body size, sperm density, and sperm motility on male fertilization success and to determine whether the genetic markers used to determine larval paternity segregated according to Mendelian expectations (a prerequisite to making inferences about male fertilization success).

Three females and eight males (L = 55–72 cm, W = 1950–4650 g) (Table 1) were used in 10 sets of matings, conducted on 4 days of the 1994 spawning season. Each mating set consisted of an EVSC mating and one control mating for each competing male. One control mating was done for each male on a given day, even if the same male was used in more than one sperm competition mating that day. All matings were performed within 4 h of gamete collection. Sperm motility was estimated only in mating sets 4–10.

In each mating set, the two competing males differed in size and in one allele at a genetic marker locus (i.e., the marking was incomplete) (Tables 1 and 2). Therefore, only some of the larvae could be unambiguously assigned to one sire based on their genotype. Thus the proportion of larvae sired by each male was estimated assuming Mendelian ratios. This assumption is valid based on the test of Mendelian inheritance conducted on progeny from control matings (see Results). All parental males and females were either homozygous for the most frequent allele (*100/100*) or heterozygous at the marker locus. Hence, in all the mating sets, one of the males was heterozygous and the other was homozygous (*100/100*). The female was heterozygous in three mating sets and homozygous in seven at the genetic marker locus used to determine paternity of larvae. In the mating sets where the female was homozygous, all the heterozygous larvae plus an equal number of homozygous larvae were assigned to the heterozygous male and the rest of the progeny were assumed to be sired by the homozygous male. When the female was heterozygous, only the larvae homozygous for the least frequent allele could be unambiguously assigned to the heterozygous male. According to Mendelian proportions, these larvae should represent one fourth of the total progeny of this male; therefore, an equal number of homozygous larvae for the common allele (*100/100*) plus twice that number of heterozygous larvae were assigned to the same male. The remaining larvae were assigned to the homozygous male.

Experiment 2 (1996)

Experiment 2 was designed based on the results of experiment 1. The objectives of this experiment were to (*i*) confirm the lack of effect of male size on fertilization success suggested by experiment 1, (*ii*) single out the effects of sperm density and male K on fertilization success, and (*iii*) assess whether male fertilization success was independent of female.

Table 1. Total lengths (L), initial weights (W_0), Fulton's K, and genotypes at three marker loci in female and male Atlantic cod used in the two experiments (see text for further details).

				Genetic marker		
Fish	L (cm)	W_0 (g)	K	*IDH-1*	*LDH-B*	*PGM-1*
Experiment 1 (1994)						
♀3	64	3250	1.24	*100/100*	*100/100*	*100/100*
♀5	64	4650	1.77	*100/100*	*100/70*	*100/100*
♀6	61	2600	1.15	*100/100*	*100/100*	*100/100*
♂2	59	1950	0.95	*100/100*	*100/100*	*100/100*
♂3	71	2950	0.82	*100/100*	*100/70*	*100/100*
♂5	55	1950	1.17	*100/140*	*100/70*	*100/100*
♂10	65	3300	1.20	*100/100*	*100/70*	*100/100*
♂11	66	3150	1.10	*100/100*	*100/70*	*100/100*
♂12	62	2950	1.23	*100/100*	*100/70*	*100/100*
♂15	60	2300	1.07	*100/100*	*100/100*	*100/85*
♂16	72	4400	1.18	*100/100*	*100/100*	*100/100*
Experiment 2 (1996)						
♀a	62	3100	1.30		*100/100*	
♀b	63	3800	1.52		*100/100*	
♂20	63	3650	1.46		*100/100*	
♂22	74	5000	1.23		*100/100*	
♂23	63	2800	1.12		*100/100*	
♂24	86	6850	1.08		*100/100*	
♂25	59	2600	1.27		*100/100*	
♂26	68	4100	1.30		*100/100*	
♂31	84	6100	1.03		*70/70*	
♂32	62	3100	1.30		*70/70*	
♂33	63	2600	1.04		*70/70*	
♂34	65	3150	1.15		*70/70*	

Two females and 10 males (L = 59–84 cm, W = 2600–6850 g) (Table 1) were used in 12 mating sets conducted on four different days during the 1996 spawning season. Each mating set consisted of an EVSC mating, an EDSC mating, and one control mating for each competing male. As with experiment 1, one control mating was conducted for each male on a given day. Fertilization but not hatching success was determined (because embryos produced by different males did not differ in hatching success in experiment 1; see Results). Larvae from control matings were not preserved because the Mendelian inheritance of genetic markers was tested in experiment 1. Sperm motility was not determined in experiment 2 because it showed no effect on fertilization success in experiment 1. All matings were performed within 6 h of gamete collection.

In each mating set, the two competing males differed in size and K and were homozygous for a different allele at the genetic marker locus (i.e., the marking was complete) (Tables 1 and 3), while both females were homozygous for the common allele (*100/100*). Therefore, the proportion of larvae sired by each male was determined directly and unambiguously by the progeny genotype because the two males did not share alleles.

The EDSC matings of six of the 12 mating sets were used to test whether male fertilization success was affected by the female used: mating sets 1, 10, and 11 used eggs from ♀a and mating sets 6, 4, and 8 used the same male pairs respectively, but eggs from ♀b (Table 3).

Statistical analysis

Log-likelihood ratio tests were used to analyze all genotype frequency data. A heterogeneity goodness-of-fit G test (Sokal and

© 1999 NRC Canada

Table 2. Results from 10 mating sets in 1994 (experiment 1) involving combinations of gametes from a female and two male Atlantic cod differing in body size.

					Control mating		EVSC mating			
Set (date)	Dam	Sire	mot%	*S*%	P_{fert}	P_{hatch}	*n*	P_{sired}	G_P	G_H
1 (17 Feb.)	♀3	♂3		24.5	0.67	0.66	99 (2)	0.25	17.5	27.93
		♂5		85.5	0.65	0.70		0.75	***	***
2 (22 Feb.)	♀5	♂11		51	0.31	0.47	47 (2)	0.52	0.19	1.64
		♂15		67.5	0.31	0.58		0.48		
3 (22 Feb.)	♀5	♂16		49	0.29	0.50	100 (3)	0.38	0.24	46.57
		♂12		60	0.30	0.46		0.62		***
4 (8 Mar.)	♀5	♂3	90	18	0.895	0.56	147 (3)	0.27	31.7	0.87
		♂2	90	55	0.83	0.60		0.73	***	
5 (8 Mar.)	♀5	♂11	60	65			150 (3)	0.63	7.77	35.45
		♂2	90	55				0.37	*	***
6 (30 Mar.)	♀6	♂10	80	74.7	0.65	0.87	72 (2)	0.56	0.89	0.01
		♂15	80	83.7	0.68	0.60		0.44		
7 (30 Mar.)	♀6	♂2	80	34.3	0.60	0.64	145 (2)	0.32	18.32	1.38
		♂5	90	98	0.66	0.72		0.68	***	
8 (30 Mar.)	♀6	♂15	80	83.7			98 (2)	0.54	2.01	0.28
		♂5	90	98				0.46		
9 (30 Mar.)	♀6	♂10	80	74.7			159 (2)	0.62	6.9	0.89
		♂2	80	34.3				0.38	**	
10 (30 Mar.)	♀6	♂16	70	64.5	0.56	0.58	93 (3)	0.49	0.10	3.46
		♂5	90	98				0.51		

Note: The larger male is listed first. mot%, sperm motility; *S*%, spermatocrit. Control mating: P_{fert}, fertilization success; P_{hatch}, hatching success. EVSC (equal volume sperm competition) mating: *n*, number of larvae genotyped with number of replicates in parentheses; P_{sired}, mean (of two or three replicates) proportion of larvae sired by each competing male; G_P, pooled *G* statistic; G_H, heterogeneity *G* statistic; df = 1 for G_P and df = 2 for G_H. Significance level: $^*P < 0.05$, $^{**}P < 0.01$, $^{***}P < 0.001$.

Rohlf 1981) was used in all matings to assess whether replicates were homogeneous. The replicates were pooled if the heterogeneity *G* statistic (G_H) was not significant. The pooled *G* statistic (G_P) was then used in goodness-of-fit tests (*i*) in the control matings to compare the observed proportions of larvae by genotype with the expected Mendelian proportions and (*ii*) in the sperm competition matings (of experiments 1 and 2) to compare the proportion of larvae sired by the two males with the expected 1:1 if the two males did not differ in fertilization success.

Tests of independence (2 × 2 contingency tables) using the *G* statistic (Sokal and Rohlf 1981) were used in experiment 2 to assess (*i*) whether male fertilization success was independent of sperm density (factor 1 = male, with two categories: large or small; factor 2 = sperm density, with two categories: unequal in EVSC or equal in EDSC) and (*b*) whether the proportions of larvae sired by each of two competing males were independent of which female was used as egg donor (factor 1 = male, large or small; factor 2 = ♀a or ♀b).

The fertilization and hatching success of the progeny from the males in control matings were compared by *t* test on arcsine square root transformed percent fertilization and percent hatching data. Mean fertilization success and hatching success in the control matings and the mean proportion of larvae sired by each of the two males in the sperm competition matings were calculated on arcsine square root transformed proportions in each replicate and then back-transformed.

Results

Mendelian inheritance of genetic markers

The analysis of 895 larvae from 10 families from control matings of experiment 1 showed that genotypic frequencies at any of the three loci tested did not deviate significantly from expected Mendelian ratios ($P >> 0.05$ in all cases).

Experiment 1. Effect of male body size and sperm motility on fertilization success

The control matings showed a significant difference in fertilization success between the two males in only one mating set (set 10, between ♂16 and ♂5). Within a batch of eggs, there was no difference in hatching success among males. However, large differences in fertilization and hatching success were observed among egg batches of the same and different females (Table 2).

Males differed in the proportion of larvae sired in sperm competition matings. In three of the 10 mating sets the replicates of sperm competition matings revealed heterogeneous results (i.e., a significant G_H) (Table 2). Three of the remaining seven mating sets (where G_H was not significant) showed a significant difference in the proportion of larvae sired between the two males (Table 2). In two of these cases (mating sets 4 and 7) the small males were more successful than the large males, and in mating set 9 the large male sired a larger proportion of larvae. In all three cases the male that sired the largest proportion of the larvae had a 2.2–3.4 times higher spermatocrit and a 1.16- to 1.26-fold greater *K* than the male with lower fertilization success. Sperm motility had no evident effect on fertilization success. In all the semen samples analyzed, between 60 and 90% of the spermatozoa were motile during the first minute of activation (Table 2). In mating sets 4 and 9, both males had similar sperm motility but differed significantly in proportion of larvae sired. Con-

© 1999 NRC Canada

Table 3. Results from 12 mating sets conducted in 1996 (experiment 2) involving combinations of gametes from a female and two male Atlantic cod differing in body size.

				Control	EVSC mating				EDSC mating				
Set (date)	Dam	Sire	S%	P_{fert}	n	P_{sired}	G_P	G_H	n	P_{sired}	G_P	G_H	$G_{2\times2}$
1 (9 Feb.)	♀a	♂24	52	0.89	144 (3)	0.37	9.10	5.13	142 (3)	0.34	13.86	15.86	
		♂32	56	0.87		0.63	**			0.66	***	***	
2 (9 Feb.)	♀a	♂24	52		144 (3)	0.35	11.26	12.7	144 (3)	0.53	0.44	2.74	
		♂33	63	0.85		0.65	***	**		0.47			
3 (9 Feb.)	♀a	♂24			144 (3)	0.38	8.10	1.81	143 (3)	0.32	18.6	5.57	1.14
		♂34	64	0.81		0.62	**			0.68	***		
4 (15 Feb.)	♀b	♂22	51	0.86	144 (3)	0.23	42.22	6.15	143 (3)	0.30	23.4	5.24	
		♂32	67	0.89		0.77	***	*		0.70	***		
5 (15 Feb.)	♀b	♂31	84	0.90	144 (3)	0.45	1.36	0.22	142 (3)	0.37	10.29	2.41	2.15
		♂25	57	0.91		0.55				0.63	**		
6 (15 Feb.)	♀b	♂24	44	0.92	96 (2)	0.47	0.38	1.05	131 (3)	0.61	6.47	4.42	4.51
		♂32				0.53				0.39	*		*
7 (15 Feb.)	♀b	♂26	52	0.90	144 (3)	0.33	17.73	0.44	144 (3)	0.44	1.78	0.39	4.25
		♂32				0.67	***			0.56			*
8 (22 Feb.)	♀b	♂31	88	0.70	108 (3)	0.42	6.32	0.59	150 (3)	0.27	33.97	1.41	3.7
		♂23	51	0.72		0.59	*			0.74	***		
9 (22 Feb.)	♀b	♂31			137 (3)	0.18	62.78	0.10	124 (3)	0.06	112.6	0.46	7.76
		♂20	54	0.70		0.82	***			0.94	***		**
10 (29 Feb.)	♀a	♂22	52	0.77	144 (3)	0.43	2.79	8.48	144 (3)	0.52	0.25	4.20	
		♂32	80	0.78		0.57		*		0.48			
11 (29 Feb.)	♀a	♂31	92	0.77	108 (2)	0.59	3.73	0.61	120 (3)	0.43	2.14	0.20	5.76
		♂23	48	0.80		0.41				0.57			*
12 (29 Feb.)	♀a	♂22			98 (2)	0.56	1.50	0.00					
		♂34	51	0.78		0.44							

Note: The larger male is listed first. S%, spermatocrit for each male and date. Control mating: P_{fert}, fertilization success. EVSC (equal volume sperm competition mating) and EDSC (equal density sperm competition mating): n, number of larvae genotyped with number of replicates in parentheses; P_{sired}, mean (of two or three replicates) proportion of larvae sired by each competing male; G_P, pooled G statistic; G_H, heterogeneity G statistic; $G_{2\times2}$, test of independence G statistic. df = 1 for G_P, df = 2 for G_H, and df = 1 for $G_{2\times2}$. Significance level: $^*P < 0.05$, $^{**}P < 0.01$, $^{***}P < 0.001$.

versely, in mating set 10, males differed in sperm motility but not in fertilization success.

Experiment 2. Effect of male body size, K, and sperm density on fertilization success

The control fertilizations revealed no statistical differences in fertilization success among males within a batch of eggs (Table 3). Analogously to experiment 1, egg batches differed in fertilization success.

In the EVSC matings, the replicates were heterogeneous in three out of the 12 mating sets (Table 3). A significant difference in the number of larvae sired by the large and small males was observed in five of the nine mating sets with homogeneous replicates, and in all five cases the small male was the most successful (Table 3). These differences in fertilization success could not be explained by a difference in sperm density because in three mating sets (sets 1, 3, and 7) the small male had a spermatocrit only 1.08–1.29 times higher than the large male, and in the other two mating sets (sets 8 and 9) the large male had a much higher spermatocrit (1.73 and 1.63 times, respectively) than the small male (Table 3). Furthermore, in mating set 11 the large male had 1.92 times higher spermatocrit than the small male, but no difference in fertilization success was observed. Nevertheless, male relative fertilization success was not independent of sperm density, as shown by the results of independence tests (2 × 2 contingency tables, male × sperm density). These tests were conducted on pooled data of the seven mating sets for which G_H was not significant in both EVSC and EDSC matings. The relative proportion of larvae sired by each male differed significantly between the EVSC and the EDSC matings of a set in four (and marginally significantly in one) of the seven mating sets (Table 3). The change in proportion of larvae sired by a male after equalizing sperm densities was in all cases an increase in fertilization success for the male with the lowest spermatocrit and a decrease in fertilization success for the male with the highest spermatocrit.

In EDSC matings the replicates were heterogeneous in one mating set (Table 3). In mating set 12 the difference in spermatocrit between the two males was only 2%, and hence, an EDSC mating was not conducted in this set. Males differed significantly in the proportion of larvae sired in six of the 10 remaining mating sets. In five of these sets the most successful male was smaller and had greater K than the least successful male (Table 3). In mating set 6 the small male had greater K, but the large male sired most larvae.

The proportion of larvae sired by each of two competing males depended on which female was used as egg donor. Mating sets 1, 10, and 11 used eggs from ♀a and mating sets 6, 4, and 8 used the same male pairs, respectively, but eggs from ♀b. In mating set 1 the EDSC mating showed a significant G_H, rendering the comparison of results with mating set

© 1999 NRC Canada

6 unreliable. The two pairs of mating sets that allowed the comparison showed a significant interaction between males and females (mating sets 10 and 4 contingency $G = 14.50$, df = 1, $P < 0.001$; mating sets 11 and 8 contingency $G = 8.23$, df = 1, $P < 0.005$) (Fig. 1). The ♂32 attained a significantly higher fertilization success than ♂22 in mating set 4 with ♀b. However, there was no significant difference between the same two males when eggs from ♀a were used in mating set 10, 2 weeks later. The ♂31 had a low fertilization success with eggs from ♀b in mating set 8 (and also in mating sets 9 and 5, competing against different males). However, in mating set 11, ♂31 had a fertilization success comparable with that of ♂23, suggesting that a positive interaction between the sperm of ♂31 and the eggs of ♀a existed (♂23 was not used in another mating with ♀a to test for a potential negative interaction).

Fig. 1. Mean proportion of larvae sired by two pairs of males (♂22–♂32 and ♂31–♂23) competing for the fertilization of eggs from single females in equal-density sperm competition matings using eggs from two females (♀a in mating sets 10 and 11 and ♀b in mating sets 4 and 8). The vertical lines represent the 95% CI limits. Proportions were arcsine transformed and the mean and 95% confidence interval calculated and back-transformed.

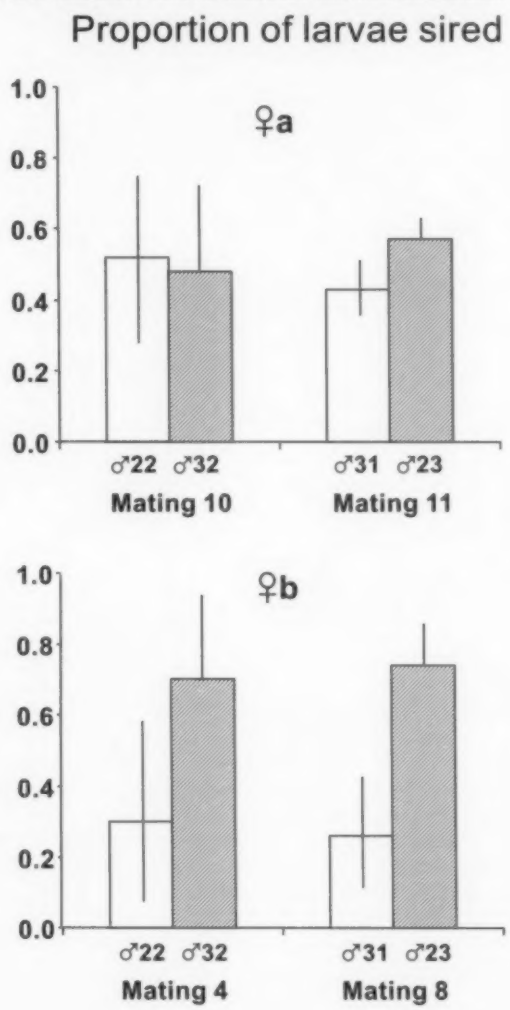

Discussion

Male Atlantic cod may show large differences in reproductive success as a result of sperm competition. Males with similar fertilization success in single pair matings differed significantly when sperm from two males was simultaneously used to fertilize eggs of a single female. Therefore, sperm competition appears to be a more sensitive experimental procedure to detect differences in sperm quality among males than single pair matings (i.e., fertilizing eggs with the sperm of one male at a time and then comparing fertilization success among males).

Genetic markers and larval survival

Differences between males in the proportion of larvae sired were not due to differential survival of embryos with specific marker genotypes. Although Mork and Sundnes (1985) observed that juvenile cod heterozygous at *LDH-3* survived longer than homozygous individuals, this effect was not evident in the present study. Survival of embryos and larvae from the control matings was not favoured by any particular genotype. There was no difference in hatching success among embryos produced by different males, and the observed frequency of genotypes in the progeny did not depart significantly from the expected proportions according to Mendelian segregation. Therefore the observed differences in proportion of larvae sired by the two competing males were due to a difference in fertilization success, i.e., in sperm quality of males rather than differential survival of progeny.

Sperm quality and male size

The null hypothesis that large and small males do not differ in sperm quality could not be rejected. There was no consistent effect of sire size on fertilization success. Although the smaller male sired the majority of larvae in most cases when males differed significantly in fertilization success, in all of these cases the small male also had a greater K, suggesting that K rather than body size affected sperm quality (see below). These results are in agreement with Trippel and Neilson's (1992) and Trippel and Morgan's (1994*b*) conclusion that neither age, body size, nor reproductive experience determines sperm quality in cod. However, male body size, age, and (or) reproductive experience affect sperm quality in other fish species (e.g., Daye and Glebe 1984; de Fraipont et al. 1993).

Sperm motility and fertilization success

Sperm motility did not explain the differences in fertilization success among males. In experiment 1, males with identical sperm motility differed significantly in fertilization success (e.g., mating sets 4 and 9), and males that differed in sperm motility attained similar fertilization success (e.g., mating set 10). The high sperm density during the experimental matings may impair the correlation between sperm motility and fertilization success. For instance, Moccia and Munkittrick (1987) found that sperm motility became an im-

© 1999 NRC Canada

portant factor determining fertilization success in rainbow trout only at low sperm concentrations or near the critical ratio of spermatozoa to eggs. Sperm motility duration also failed to explain differences in fertilization success among male brown trout (*Salmo trutta*) (Goryczko and Tomasik 1975). Neither percentage of motile sperm nor sperm swimming velocity was correlated with fertilization success in single pair matings in cod (Trippel and Neilson 1992). Trippel and Neilson (1992) argued that the swimming velocity of cod spermatozoa (average 0.15 mm/min, maximum 2 mm/min) was trivial relative to the egg size (circumference ~4.5 mm). Differences in swimming velocity might only be important if two spermatozoa arrive at the micropyle simultaneously.

A possible explanation for the lack of correlation between estimated sperm motility in water and fertilization success is that patterns of spermatozoa motility are different in water than in the proximity of the micropyle. Sperm motility enhancement substances are present in the micropylar region of the egg chorion of fish (Gilkey 1981). The presence of ovarian fluid and (or) egg enhanced both the duration and velocity of sperm motility in cod (Litvak and Trippel 1998). In herring, spermatozoa were almost immotile in seawater and became motile only when in contact with substances found in the micropyle (Yanagimachi et al. 1992). This suggests that estimating spermatozoa motility in the absence of eggs may not be an accurate indicator of sperm motility during fertilization in some fish species.

Sperm density and fertilization success

Results from the EVSC matings of experiment 1 suggest that both spermatocrit (sperm density) and male *K* affect the fertilization success of males. In the three matings where males differed significantly in the proportion of larvae sired, the most successful male had a much higher (2.2–3.4 times) sperm density than the other male. The difference in number of larvae sired appeared to be proportional to the difference in sperm density between the two males. However, sperm density did not show a clear effect on fertilization success in the EVSC matings of experiment 2. This may be because the differences in sperm density between the two males in this experiment never exceeded 1.9 times. Furthermore, significant differences in fertilization success were still evident when the numbers of spermatozoa were equalized for the two males, i.e., in the EDSC matings. Nevertheless, male fertilization success was not independent of sperm density, as equalizing sperm densities between males did significantly modify the results of the sperm competition matings in four mating sets. Similarly, equalizing sperm concentrations caused a significant change in the males' relative fertilization success in rainbow trout (Gile and Ferguson 1995).

Concentration of spermatozoa is an important factor determining fertilization success in aquatic animals with external fertilization, yet only when percent fertilization is assessed at a range of dilutions differing by one or more orders of magnitude (e.g., Rosenthal et al. 1988; Levitan et al. 1991 and cited therein). In our study the maximum difference in sperm concentration between males was less than one order of magnitude (only 3.5-fold in mating set 1 of experiment 1, where the two competing males had spermatocrits of 24.5 and 85.5).

Male *K* and sperm quality

Both experiments suggest that male *K* may be an indicator of sperm quality in cod. In the three mating sets of experiment 1 showing significant differences in fertilization success between males, the most successful male had a greater *K* and also a higher spermatocrit than the least successful male. In experiment 2, sperm density was controlled for in the EDSC matings. In five of the six EDSC matings showing significant differences between males, the most successful male had a greater *K* than the other male, suggesting that sire *K* is a potentially critical factor determining sperm fertilization potency. This conclusion may be tempered by the fact that males were reused in different mating sets. Further research should address the specific physiological mechanisms underlying the correlation between *K* and sperm fertilization potency.

Male–female gamete interaction

Female "choice" at the gamete level (specific egg–sperm interaction) may be occurring in cod. A significant male × female interaction was found in both pairs of mating sets from experiment 2 used to test the effect of female on male fertilization success.

An alternative explanation for the significant differences in the relative fertilization success of a pair of males with different females could be a temporal variation in the sperm quality of specific males. The pairs of mating sets used to test for male × female interaction were by necessity (availability of ova from females with appropriate marker genotypes) produced on different days. For instance, the semen of ♂22 and ♂32 was combined with the eggs of ♀b and ♀a 2 weeks apart (mating sets 4 and 10). Since not all males initiate spermiation simultaneously, individuals could be at different stages of spermiation on a given day. Variation in stage of spermiation (and sperm ageing) could then affect fertilization success. Sperm ageing involves the process of deterioration of sperm during the spawning season (e.g., decrease in sperm motility duration in Atlantic halibut (*Hippoglossus hippoglossus*), Methven and Crim 1991). In addition, the seasonal variation in sperm quality may be related to the degree of gonadal depletion (i.e., proportion of sperm released) rather than to the day of spawning season. Munkittrick and Moccia (1987) noted that late in the spawning season, sperm motility was highest in fish that were stripped fewer times.

The marked reduction in the proportion of offspring sired by ♂32 in mating set 10 compared with mating set 4 (Fig. 1) could potentially be explained by declining sperm quality. The relatively high spermatocrit of ♂32 during mating set 10 (80%) (Table 3) may indicate that this male was near the end of spermiation (Rakitin et al. 1999), and hence, the quality of his sperm could have been declining. Conversely, ♂22 had an intermediate to low spermatocrit (52%), suggesting that this male was not reaching gonadal depletion, possibly accounting for his increased success in mating set 10. However, temporal variation in sperm quality cannot explain the significant interaction observed in mating sets 8 and 11 (Fig. 1). The ♂31 experienced a relatively higher success in mating set 11 despite having a very high spermatocrit (92%). The occurrence of female choice at the gamete level can only be confirmed by additional experimentation using mat-

© 1999 NRC Canada

ings conducted on a single day and males with comparable spermatocrits.

Female selection of sperm has been demonstrated in plants and in some animals (ascidians and lizards, Wirtz 1997). Existing knowledge suggests that a mechanism for egg and sperm compatibility or recognition is possible in fish. Scanning electron microscopy observations of fertilization in medaka (*Oryzias latipes*) revealed that spermatozoa attached with the apical tip to a specific site in the micropylar canal of eggs (Onitake and Iwamatsu 1986). Sperm-specific antigens necessary for fertilization were detected on the surface of rainbow trout spermatozoa. These antigens were not species specific, but the number of antigenic sites varied among individual fish (Beck et al. 1992). Furthermore, a gamete-specific mate selection mechanism may have adaptive significance (Peterson 1988).

Implications for fishery management

Our results confirm Trippel and Neilson's (1992) conclusion that there is no need to adjust spawning stock reproductive potential estimations by the variation of sperm quality with male age or size. However, male *K* may determine fertilization success. Whether the effect of male *K* found in the artificial setting of this study will be significant in the wild remains to be investigated. The results of the present study suggest that male *K* should be factored into the stock–recruitment and population reproductive success calculations for Atlantic cod.

Acknowledgements

We thank the staff of the St. Andrews Biological Station for their assistance. Comments received from two anonymous reviewers helped to improve the manuscript. This work was supported by funds from the DFO/NSERC Science Subvention Program and the NSERC Research Grants Program.

References

Beck, J.C., Flucher, K.D., Beck, C.F., and Cloud, J.G. 1992. Sperm surface antigen required for fertility: identification on spermatozoa of rainbow trout by use of monoclonal antibodies. Trans. Am. Fish. Soc. **121**: 333–339.

Brawn, V.M. 1961. Reproductive behaviour of the cod (*Gadus callarias* L.). Behaviour, **18**: 177–197.

Davenport, J., Lønning, S., and Kjørsvik, E. 1981. Osmotic and structural changes during early development of eggs and larvae of the cod, *Gadus morhua* L. J. Fish Biol. **19**: 317–331.

Daye, P.G., and Glebe, B.D. 1984. Fertilization success and sperm motility of Atlantic salmon (*Salmo salar* L.) in acidified water. Aquaculture, **43**: 307–312.

de Fraipont, M., Fitzgerald, G.J., and Guderley, H. 1993. Age-related differences in reproductive tactics in the three-spined stickleback, *Gasterosteus aculeatus*. Anim. Behav. **46**: 961–968.

Gile, S.R., and Ferguson, M.M. 1995. Factors affecting male potency in pooled gamete crosses of rainbow trout, *Oncorhynchus mykiss*. Environ. Biol. Fishes, **42**: 267–275.

Gilkey, J.C. 1981. Mechanisms of fertilization in fishes. Am. Zool. **21**: 359–375.

Goryczko, K., and Tomasik, L. 1975. An influence of males on the viability and fertilisation degree of trout eggs. Acta Ichthyol. Pisc. **5**: 3–12.

Grant, W.S., and Ståhl, G. 1988. Description of electrophoretic loci in Atlantic cod, *Gadus morhua*, and comparison with Pacific cod, *Gadus macrocephalus*. Hereditas, **108**: 27–36.

Hebert, P.D.N., and Beaton, M.J. 1989. Methodologies for allozyme analysis using cellulose acetate electrophoresis: a practical handbook. Helena Laboratories, Beaumont, Tex.

Hutchings, J.A., Bishop, T.D., and McGegor-Shaw, C.R. 1999. Spawning behaviour of Atlantic cod, *Gadus morhua*: evidence of mate competition and mate choice in a broadcast spawner. Can. J. Fish. Aquat. Sci. **56**: 97–104.

Kjesbu, O.S. 1989. The spawning activity of cod, *Gadus morhua* L. J. Fish Biol. **34**: 195–206.

Kjørsvik, E., and Lønning, S. 1983. Effects of egg quality on normal fertilization and early development of the cod, *Gadus morhua* L. J. Fish Biol. **23**: 1–12.

Levitan, D.R., Sewell, M.A., and Chia, F.S. 1991. Kinetics of fertilization in the sea urchin *Strongylocentrotus franciscanus*: interaction of gamete dilution, age and contact time. Biol. Bull. **181**: 371–378.

Litvak, M.K., and Trippel, E.A. 1998. Sperm motility patterns of Atlantic cod (*Gadus morhua*) in relation to salinity: effects of ovarian fluid and egg presence. Can. J. Fish. Aquat. Sci. **55**: 1871–1877.

Methven, D.A., and Crim, L.W. 1991. Seasonal changes in spermatocrit, plasma sex steroids and motility of sperm from Atlantic halibut (*Hippoglossus hippoglossus*). *In* Proceedings of the Fourth International Symposium on the Reproductive Physiology of Fish. *Edited by* A.P. Scott, J.P. Sumpter, D.E. Kime, and M.S. Rolfe. Fish. Symp. 91, Sheffield, U.K.

Moccia, R.D., and Munkittrick, K.R. 1987. Relationship between the fertilization of rainbow trout (*Salmo gairdneri*) eggs and the motility of spermatozoa. Theriogenology, **27**: 679–688.

Morgan, M.J., and Trippel, E.A. 1996. Skewed sex ratios in spawning shoals of Atlantic cod (*Gadus morhua*). ICES J. Mar. Sci. **53**: 820–826.

Mork, J., and Sundnes, G. 1985. 0-Group cod (*Gadus morhua*) in captivity: differential survival of certain genotypes. Helgol. Meeresunters. **39**: 63–70.

Munkittrick, K.R., and Moccia, R.D. 1987. Seasonal changes in the quality of rainbow trout (*Salmo gairdneri*) semen: effect of a delay in stripping on spermatocrit, motility, volume and seminal plasma constituents. Aquaculture, **64**: 147–156.

Onitake, K., and Iwamatsu, T. 1986. Early response of the egg to sperm stimulation in the medaka, *Oryzias latipes*. *In* Proceedings of the Fifty-seventh Annual Meeting of the Zoological Society of Japan. Fukuoka Zool. Sci. **3**: 1044.

Peterson, K.H. 1988. Egg reaction to sperm: a proposed mechanism. Evol. Theor. **8**: 397–401.

Rakitin, A., Ferguson, M.M., and Trippel, E.A. 1999. Spermatocrit, spermatozoa density and size in Atlantic cod (*Gadus morhua*): correlation and variation during the spawning season. Aquaculture, **170**: 349–358.

Rose, G.A. 1993. Cod spawning on a migration highway in the north-west Atlantic. Nature (Lond.), **366**: 458–461.

Rosenthal, H., Klumpp, D., and Willfuhr, J. 1988. Influence of sperm density and contact time on herring egg fertilization. J. Appl. Ichthyol. **4**: 79–86.

Sokal, R.R., and Rholf, F.J. 1981. Biometry. The principles and practice of statistics in biological research. 2nd ed. W.H. Freeman and Company, New York.

© 1999 NRC Canada

Sorokin, V.P. 1960. Polovoi tsycl i spermatogenez u treski. Tr. PINRO, **12**: 71–87.

Taborsky, M. 1994. Sneakers, satellites, and helpers: parasitic and cooperative behavior in fish reproduction. Adv. Stud. Behav. **23**: 1–100.

Trippel, E.A., and Morgan, M.J. 1994*a*. Sperm longevity in the Atlantic cod (*Gadus morhua*). Copeia, **1994**: 1025–1029.

Trippel, E.A., and Morgan, M.J. 1994*b*. Age specific paternal influences on reproductive success of Atlantic cod (*Gadus morhua* L.) from the Grand Banks, Newfoundland. ICES Mar. Sci. Symp. **198**: 414–422.

Trippel, E.A., and Neilson, J.D. 1992. Fertility and sperm quality of virgin and repeat-spawning Atlantic cod (*Gadus morhua*) and associated hatching success. Can. J. Fish. Aquat. Sci. **49**: 2118–2127.

Warner, R.R., Shapiro, D.Y., Marcananto, A., and Petersen, C.W. 1995. Sexual conflict: males with highest mating success convey the lowest fertilization benefits to females. Proc. R. Soc. Lond. Ser. B, Biol. Sci. **262**: 135–139.

Westin, L., and Nissling, A. 1991. Effects of salinity on spermatozoa motility, percentage of fertilized eggs and egg development of Baltic cod (*Gadus morhua*), and implications for cod stock fluctuations in the Baltic. Mar. Biol. **108**: 5–9.

Wirtz, P. 1997. Sperm selection by females. Trends Ecol. Evol. **12**: 172–173.

Yanagimachi, R., Cherr, G.N., Pillai, M.C., and Baldwin, J.D. 1992. Factors controlling sperm entry into the micropyles of salmonid and herring eggs. Dev. Growth Differ. **34**: 447–461.

Zuromska, H., and Markowska, J. 1984. The effect of sexual products quality on offspring survival and quality in tench (*Tinca tinca* L.). Pol. Arch. Hydrobiol. **31**: 287–313.

© 1999 NRC Canada

Timing of the metamorphic molt of the American lobster (*Homarus americanus*) is governed by a population-based, photoperiodically entrained daily rhythm

S.L. Waddy and D.E. Aiken

Abstract: The metamorphic molt of the American lobster (*Homarus americanus*) occurs in the form of a population-based, recurring daily rhythm that is photoperiodically entrained. Molting occurs predominantly in the scotophase (dark period) at temperatures of 11, 15, and 20°C and in both normal and reversed photoperiod cycles. Molting is arrhythmic in larvae reared in continuous illumination (LL), but when larvae reared in LL are transferred to cyclic photoperiod conditions (LD 12:12), the rhythm is reinstated in a stepwise manner over 3 days. When larvae are transferred from LD 12:12 to LL, the molting rhythm continues for 3 days before dampening. The rhythm appears to be phase-set by the onset of darkness: similar proportions of larvae (79–89%) reared in scotophase lengths of 6, 10, and 12 h molted in the 12-h period following lights-off. The results demonstrate that the synchrony of the metamorphic molt with the scotophase is not fortuitous and suggest that the molting rhythm may result from a gated event under the influence of an endogenous pacemaker.

Résumé : La mue métamorphique du homard d'Amérique (*Homarus americanus*) se fait à l'échelle de la population et selon un rythme quotidien dépendant de la photopériode. La mue se produit surtout pendant la scotophase (période d'obscurité) à des températures de 11, 15 et 20°C et pendant des cycles de photopériode normaux ou inversés. La mue est arythmique chez les larves élevées sous éclairage continu (LL) mais lorsque des larves élevées en condition LL sont placées dans des conditions de photopériode cyclique (LO 12:12) le rythme est rétabli par étapes au cours d'une période de trois jours. Lorsque des larves passent de conditions LO 12:12 en conditions LL, le rythme de la mue se poursuit pendant trois jours avant de s'atténuer. Le rythme semble être mis en phase par l'apparition de l'obscurité : des proportions semblables de larves (79 à 89%) élevées à des périodes d'obscurité de 6, 10 et 12 h muent au cours des 12 h suivant la fin de l'éclairement. Les résultats obtenus montrent que le synchronisme de la mue métamorphique avec la scotophase n'est pas dû au hasard et indique que le rythme de mue peut résulter d'un événement périodique soumis à l'influence d'un générateur de rythme endogène.

[Traduit par la Rédaction]

Introduction

The dramatic increase in commercial landings of the American lobster (*Homarus americanus*) that occurred in the early 1990s focused attention on how little is known about the early life history of this species and the factors that influence survival during the planktonic stages (Fisheries Resource Conservation Council 1995; Fogarty 1995). While it is assumed that larval survival is controlled primarily by food, temperature, and predation (Sastry 1983; Ennis 1995), little is known of the mechanisms involved.

Some of the most intriguing and widespread survival mechanisms in arthropods are the innate behavioral and physiological rhythms temporally linked to daily, lunar, tidal, and annual geophysical cycles. A wide variety of endogenous rhythms have been identified in crustaceans, and considerable work has been conducted on behaviors and physiological functions that occur as circadian or tidal rhythms (DeCoursey 1983; Forward 1987, 1988; Aréchiga et al. 1993; Palmer 1995).

Rhythms with an endogenous component can occur in populations as well as in individuals. Examples of population-based daily rhythms include the hatching, molting, pupation, and adult emergence rhythms of insects and the larval release rhythms of some crustaceans (Beck 1980; Forward 1987). Developmental rhythms are precisely timed and synchronized within populations, and the synchrony is often "gated," a timing mechanism that restricts the event to a specific time of the day. Much of what is known of gated rhythms comes from research on insect eclosion rhythms. Gated synchrony results in a "rhythm" in the population, even though each insect emerges only once, that is endogenously controlled and has the characteristics of a circadian rhythm (Brady 1979; Beck 1980). Regardless of when development is completed, the event occurs only when the endogenous timer reaches the permissive gate. If development is completed after the timer has passed the gate, the event is

Received April 9, 1999. Accepted August 18, 1999.
J15101

S.L. Waddy[1] **and D.E. Aiken.** Department of Fisheries and Oceans, Aquaculture Division, Biological Station, St. Andrews, NB E0G 2X0, Canada.

[1]Author to whom all correspondence should be addressed.
e-mail: waddys@mar.dfo-mpo.gc.ca

© 1999 NRC Canada

delayed until the following day. Timing a developmental event such as emergence or molting to a specific time of the day is thought to have developed as a means of overwhelming predators or mitigating the animal's vulnerability to predation during critical periods (Brady 1979).

Less is known about developmental rhythms in crustaceans. Although endogenous larval release rhythms are widespread (Forward 1987; Morgan and Christy 1995), the endogenous control mechanisms are not well understood and appear to vary between species (for a review, see Forward 1987). In the American lobster, the maternal female appears to control the time of larval release (Ennis 1975), while in some crabs, the time of release is controlled by the developing embryos (Forward 1987). In the European lobster (*Homarus gammarus*) and the shore crab (*Carcinus maenas*), it is not clear whether the endogenous component originates with the maternal female or the larva, or whether both have a role (Ennis 1973; Zeng and Naylor 1997).

Evidence is increasing that molting rhythms may also be common in crustaceans. The metamorphic molt of the American lobster occurs in the scotophase[2] (Eagles et al. 1986; Waddy et al. 1990), and Fernandez et al. (1994) recently reported that Dungeness crab (*Cancer magister*) megalopae molt during the scotophase, apparently under endogenous control. Molting in the shore crab *C. maenas* appears to be timed by an endogenous tidal rhythm (Abello et al. 1997; Zeng et al. 1997). In this paper, we report on studies that extend our earlier observation that the metamorphic molt of American lobsters occurs during the scotophase and test the hypothesis that molting occurs as a population rhythm that is entrained by photoperiod and controlled endogenously.

Methods

Larval rearing

Ovigerous American lobsters were obtained from Passamaquoddy Bay in New Brunswick, Canada, and were held at local seawater temperature (varying from 0 to 13°C seasonally) and photoperiod (45°N) after capture. To schedule hatching, the lobsters were transferred to a temperature of 20°C at the required time as determined from the eye index of the attached embryos (Perkins 1972; Aiken and Waddy 1985).

Lobster larvae were reared in 40-L planktonkreisels enclosed in light-proof cabinets (Aiken et al. 1981). Seawater (salinity 28–31‰) was filtered through sand, degassed, and supplied from a common reservoir. Except for experiment 7, larvae were reared at a seawater temperature of 20 ± 1.0°C. The kreisels were stocked at 08:00 with either 200, 500, or 1000 sibling first-stage larvae that had hatched the previous evening (except in experiment 4 where the kreisels were stocked at dusk, immediately after the larvae had hatched). In almost all cases, the six kreisels used in each trial were stocked with sibling larvae hatched on a single day. When there were insufficient larvae to stock all six kreisels at once, the balance of the kreisels were stocked the following day.

Larvae were fed San Francisco Bay brand frozen adult brine shrimp (*Artemia*) that were thawed and introduced into the kreisels through light-proof tubes in the cabinets at 08:00, 12:00, and 16:00 daily. During the first larval stage, a total of 50 mL of brine shrimp was provided each day for every 1000 larvae stocked. The quantity of brine shrimp was gradually reduced to 20 mL·day^{-1} over the course of the development period to reflect the progressive reduction in the number of larvae due to mortality and the harvesting of fourth-stage postlarvae (detailed feeding schedule given in Aiken and Waddy 1989).

Light sources were Westinghouse 15-W F15T8/CW fluorescent bulbs suspended 30 cm above the water surface in each cabinet. The bulbs, which produced major peaks at 440 and 580 nm, were encased in a clear acrylic sheet to reduce condensation. A sheet of opaque plastic was placed between the bulb and acrylic sheet to reduce light intensity; a narrow slit cut in the sheet admitted 0.31 and 0.15 W·m^{-2} at 440 and 580 nm, respectively, at the water surface. Light intensity was measured with a Li-Cor model IL700 radiometer/photometer and photoperiod cycles were controlled with Intermatic T-109 time clocks.

Data collection and analysis

To determine when molting occurred relative to the photoperiod cycle, newly metamorphosed fourth-stage postlarvae were harvested from the kreisels twice daily: immediately after the lights came on and just before the lights went out. In experiment 3, harvesting continued at specified intervals during the photophase. Developing larvae were checked daily at the appropriate time, and harvesting began on the day that the first molts occurred and continued until five or fewer larvae were molting each day. It was easy to recognize and harvest the newly molted postlarval lobsters because their appearance and behavior were very different from those of the premetamorphic third-stage larvae (Charmantier et al. 1991). Comparisons of the proportions molting were made using either a z test or a χ^2 analysis of contingency tables. The Yates correction factor was used with all z tests and 2 × 2 contingency tables. Tests were performed with SigmaStat statistical software (SPSS Inc., Chicago, Ill.).

Experiments

Experiment 1. Normal and reversed photoperiod cycle (N = 12 000)

Larvae were reared in one of two LD 12:12 photoperiod regimes: dark from 19:00 to 07:00 (normal cycle) or from 07:00 to 19:00 (reversed cycle). Two trials were conducted (in June and July) and there were three replicates of each treatment in each trial (1000 larvae per replicate).

Experiment 2. Time of year and scotophse length (N = 26 000)

Larvae were reared in one of three scotophase lengths (10, 12, or 14 h) in trials conducted in January, March, April, June, July, and August. In most cases, each treatment in each of the trials was replicated (200, 500, or 1000 larvae in each replicate).

Experiment 3. Lights-off stimulus (N = 12 000)

In the first trial (3*a*), larvae were reared in scotophase lengths of 3, 6, and 10 h. Newly metamorphosed postlarvae were harvested immediately after lights-on and just prior to lights-off. In addition, the postlarvae in the 3-h scotophase group were harvested 6 and 10 h after lights-off (3 and 7 h after lights-on), and those in the 6-h scotophase group were harvested 10 h after lights-off (4 h after lights-on). In the second trial (3*b*), larvae were reared in scotophase lengths of 3, 6, and 12 h, and postlarvae were harvested immediately after lights-on and just prior to lights-off. The postlarvae in the 3-h scotophase were also harvested 6, 10, and 12 h after lights-off, and the 6-h scotophase group was also harvested 10 and 12 h after lights-off. The two trials were conducted in June (3*a*) and July (3*b*), and within each trial there were two replicates of each treatment (1000 larvae per replicate).

[2]The diel photoperiod cycle is composed of a photophase, or light period, and a scotophase, or dark period (Beck 1980).

© 1999 NRC Canada

Fig. 1. Diel timing of the metamorphic molt in American lobster larvae reared in June at 20°C in an LD 12:12 photoperiod cycle (experiment 1). Significantly more larvae molted in the scotophase (solid bars) than in the photophase (open bars) ($p < 0.001$).

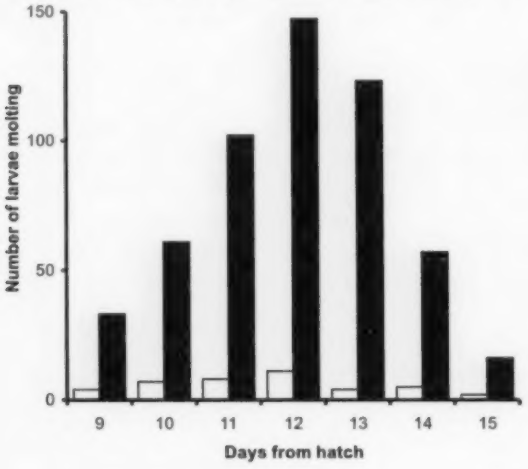

Fig. 2. Diel timing of the metamorphic molt in American lobster larvae reared in June at 20°C in normal (N = 2 922) and reversed (N = 2 678) LD 12:12 photoperiod cycles (experiment 1). The lights were on from 07:00 to 19:00 in the normal photoperiod cycle and from 19:00 to 07:00 in the reversed cycle. The timing of the molt was phase-shifted in larvae reared in the reversed cycle, and the proportion molting in the dark in the reversed and normal cycles was similar (93.1 ± 1.2 versus 89.9 ± 0.9%, $p > 0.05$). In both photoperiod regimes, significantly more larvae molted in the scotophase (solid bars) than in the photophase (open bars) ($p < 0.001$).

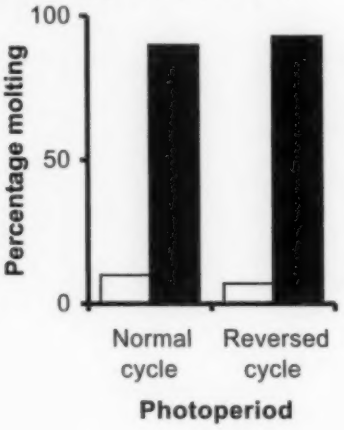

Experiment 4. Continuous illumination (LL) (N = 12 000)

Larvae were reared in either LD 12:12 or LL in two trials conducted in March and April. Newly hatched larvae were stocked into the kreisels in the evening immediately after hatching. There were three replicates of each treatment within each trial (1000 larvae per replicate).

Experiment 5. LD 12:12 followed by LL beginning on day 4, 7, or 10 (N = 6000)

In a trial conducted in May, larvae were reared initially at LD 12:12 and the light regime was switched to LL on day 4, 7, or 10. There were two replicates of each treatment (1000 larvae per replicate).

Experiment 6. LL followed by LD 12:12 beginning on day 5 or 10 (N = 6000)

In a trial conducted in April, larvae were reared under LL until day 5 or 10 when the photoperiod was changed to LD 12:12. Control kreisels remained under LL throughout the experiment. There were two replicates of each treatment (1000 larvae per replicate).

Experiment 7. Temperature (N = 5400)

Two trials were conducted at a seawater temperature of 15°C and a photoperiod of LD 12:12 in April and June (six replicates in each trial, 200 larvae per replicate). A third trial was conducted in July at a temperature of 11°C and a photoperiod of LD 12:12 (six replicates, 500 larvae per replicate).

Results

Experiment 1. Normal and reversed photoperiod cycle

Larvae reared in both the normal and reversed photoperiod cycles molted predominantly in the scotophase ($p < 0.001$) (Figs. 1 and 2). There was no significant difference in the proportion molting in the scotophase in the normal and reversed cycles (90 ± 0.9 and 93 ± 1.2%, $p > 0.05$) (Fig. 2).

Experiment 2. Time of year and scotophase length

Regardless of the time of year (January–August) or length of the scotophase (10, 12, or 14 h), larvae molted predominantly ($p < 0.01$) during the scotophase (63–97%) (Table 1). In the March and April trials, there were no significant differences in the proportion molting in the three scotophase lengths ($p > 0.05$). In June, significantly fewer larvae molted in the dark in the 10-h scotophase than in either the 12- or 14-h scotophase (86 versus 96 and 97%, $p < 0.01$). In July, there was a significant difference between the proportion molting in the 10- and 12-h groups (72 versus 90%, $p < 0.05$), but the trials were conducted in different years, so a comparison is not valid. Within the 10-h scotophase groups, the proportion molting in the dark was significantly lower in July and August than in April and June (72 and 75 versus 86 and 90%, $p < 0.05$). In the 12-h scotophase groups, significantly fewer larvae molted in the scotophase in August than in trials conducted between January and July (63 versus 86–96%, $p < 0.05$).

Experiment 3. Lights-off stimulus

In all groups (LD 21:3, 18:6, 14:10, and 12:12), both the proportion molting in the scotophase and the proportion molting within 12 h of the lights-off signal were significantly greater ($p < 0.001$) than would be expected if molting was occurring randomly throughout the day (Table 2). In the LD 21:3 and 18:6 groups, similar proportions molted within 6 h of the lights-off signal (53 and 56%, $p > 0.05$), even though the length of the scotophase of one group was twice that of the other. Similarly, in the LD 18:6, 14:10, and 12:12 groups, similar proportions molted within 10 h (78 and 79%,

© 1999 NRC Canada

Table 1. Effect of time of year and scotophase length on proportion (±SEM) of third-stage American lobster larvae molting in the scotophase.

	Scotophase length (h)						
	10		12		14		
Month	*N*	% molting in the scotophase	*N*	% molting in the scotophase	*N*	% molting in the scotophase	Mean (%)
January			1582	88±0.5			88
March			1498	86±0.7	1062	84±1.2	86
April	524	90	1255	92±1.4	980	89±1.1	90
June	953	86±1.0	1101	96±1.1	998	97±0.9	93
July	1007	72±1.3	986	90±0.6			81
August	1091	75±0.9	304	63±1.0			69
Mean		81		86		90	

Note: Statistical comparisons: in all months and in all photoperiod regimes, significantly more larvae molted in the scotophase than in the photophase ($p < 0.05$); in the LD 14:10 groups, the proportion molting in the scotophase in July and August was significantly lower than in June ($p < 0.05$); in the LD 12:12 groups, the proportion molting in the scotophase in August was significantly lower than in the other months ($p < 0.05$).

Table 2. Relationship between the lights-off signal and the timing of the metamorphic molt in American lobster larvae reared at 20°C in four scotophase lengths.

Hours after lights-off signal	Percentage of larvae molting at intervals following lights-off			
	LD 21:3 (*N* = 1821)	LD 18:6 (*N* = 2331)	LD 14:10 (*N* = 1024)	LD 12:12 (*N* = 992)
3	23.1±1.2	—	—	—
6	52.7±1.6	55.6±1.4	—	—
10	62.4±0.9*	77.6±1.3	78.9±1.1	—
12	72.4±1.0*	79.7±0.7	87.6±1.2	88.7±1.5

Note: Numbers in the columns are the proportions of larvae that molted within specified intervals following lights-off. The percentages shown in each column are cumulative. Statistical comparisons: the only significant differences in the proportions molting at each time interval following the lights-off signal (rows) were in the LD 21:3 group (significantly different groups ($p < 0.05$) are marked with an asterisk).

Table 3. Effect of LL on the timing of the metamorphic molt in American lobster larvae (data are percentages).

		Time of molt	
		Subjective day (07:00–19:00)	Subjective night (19:00–07:00)
Trial 1, March	Replicate 1 (*N* = 502)	55	45
	Replicate 2 (*N* = 487)	70*	30
	Replicate 3 (*N* = 576)	52	48
	Control LD 12:12 (*N* = 1522)	11	89
Trial 2, April	Replicate 1 (*N* = 543)	58	42
	Replicate 2 (*N* = 561)	62*	38
	Replicate 3 (*N* = 520)	51	49
	Control LD 12:12 (*N* = 1599)	5	95

Note: In some groups, there was no difference in the proportion molting during the subjective day and night; in others, significantly more larvae molted during the subjective day than during the subjective night. Statistical comparisons: LL replicates with a significantly greater proportion of larvae molting during the subjective day than during the subjective night are marked with an asterisk ($p < 0.001$); significantly more larvae molted in the scotophase in the control LD12:12 groups than molted in the subjective scotophase in the LL groups ($p < 0.001$).

$p > 0.05$) and 12 h (79, 88, and 89%, $p > 0.05$) of the lights-off signal. Although the response of the LD 21:3 group to the lights-off signal followed the same trend as that of the other groups (62 and 72% molted within 10 and 12 h of lights-off, respectively), the proportions molting within these time periods were significantly lower ($p < 0.05$) than in the groups exposed to longer scotophases.

Experiment 4. LL

Results varied in larvae exposed to LL (Table 3). In some trials, significantly more larvae molted during the subjective day (07:00–19:00) than during the subjective night (19:00–07:00) (58–70 versus 30–42%, $p < 0.05$). In other trials, there was no significant difference in the proportions molting during the subjective day and night (51–55 versus 45–49%, $p > 0.05$). In the control groups (LD 12:12), 89 and 95% of the larvae molted during the scotophase, significantly more than in the LL groups ($p < 0.001$).

Experiment 5. LD 12:12 followed by LL beginning on day 4, 7, or 10

There were no significant differences in the proportions

© 1999 NRC Canada

Fig. 3. Response of American lobster larvae reared at 20°C to LL. Larvae were reared initially in cyclic photoperiod conditions (LD 12:12) and then exposed to LL beginning on day 4, 7, or 10 of development (the metamorphic molt occurred on days 11–15; the results of day 15 are not shown but the molting times were similar in the three groups and not significantly different from those on day 14, $p > 0.05$). Larvae exposed to LL on day 4 or 7 molted throughout the day, with similar proportions molting during the subjective day and night ($p > 0.05$). Larvae transferred to LL on the day before molting began (day 10 group) molted rhythmically for 3 days before the rhythm dampened (significantly greater proportions molted during the subjective night, $p < 0.001$). On days 14 and 15, there was no significant difference in the proportion molting during the subjective night and day ($p > 0.05$), and the timing of the molt was similar to that in the groups transferred to LL on days 4 and 7 ($p > 0.05$).

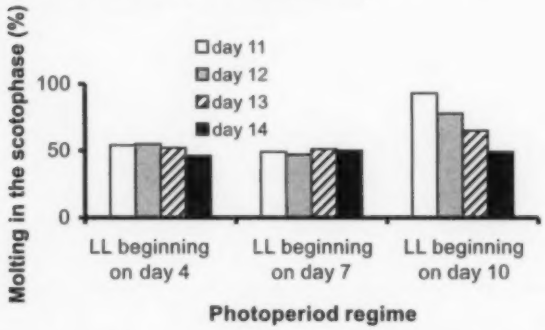

molting during the subjective day (44–52%) and subjective night (48–56%) in the groups transferred to LL on days 4 and 7 ($p > 0.05$) (Fig. 3). However, there was a significant difference in the time of molting between two subsets of the larvae transferred to LL on day 10, the day before the molting period began. Larvae that molted within 3 days of transfer to LL molted predominantly during the subjective night (73%, $p < 0.001$), while there was no rhythm in molting in those exposed to LL for 4–6 days before molting began (49% molted in the subjective photophase and 51% in the subjective scotophase, $p > 0.05$).

Experiment 6. LL followed by LD 12:12 beginning on day 5 or 10

Significantly fewer larvae in the control group (LL) molted in the subjective scotophase than in the groups that were reared initially at LL and then exposed to LD 12:12 beginning on day 5 or 10 of development (37 versus 78 and 98%, $p < 0.001$) (Fig. 4). More larvae in the group transferred to LD 12:12 on day 5 molted in the scotophase than larvae in the group exposed to LL until day 10 (78 versus 98%, $p < 0.01$). In the larvae transferred to LD 12:12 on day 10, the proportion molting in the dark increased significantly ($p < 0.001$) with time spent under cyclic conditions: only 42% of the larvae molting on day 11 molted in the dark, 70% of those molting on day 12 molted in the dark, and 98% of those molting on days 13 and 14 molted in the dark.

Experiment 7. Temperature

At both 11 and 15°C, significantly more larvae molted in the scotophase than in the photophase (70 ± 1.3 and 71 ± 0.9 versus 29 and 30%, $p < 0.001$). There was no significant effect of temperature on the proportions molting in the scotophase ($p > 0.05$).

Fig. 4. Diel timing of the metamorphic molt in American lobster larvae reared initially in LL and transferred to cyclic photoperiod conditions (LD 12:12) on day 5 or day 10 of development. In the group maintained at LL throughout the experiment, significantly more larvae molted during the subjective day than during the subjective night ($p < 0.05$). Larvae transferred on day 5 from LL to LD 12:12 had a normal molting rhythm, with significantly more larvae molting in the scotophase than in the photophase ($p < 0.001$). In the group transferred to cyclic conditions on day 10, the day before molting began, similar proportions molted in the scotophase and photophase on day 11 ($p > 0.05$). On days 12–14, significantly more larvae molted in the scotophase than the photophase ($p < 0.01$), and the proportion molting in the scotophase was significantly greater on days 13 and 14 than on day 12 ($p < 0.01$).

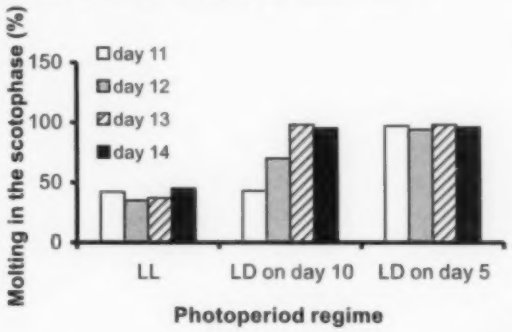

Discussion

The results from this study demonstrate that when larvae of the American lobster are reared under controlled photoperiod and temperature conditions, the metamorphic molt occurs in a well-defined rhythm during the scotophase. The rhythm is easily phase-shifted and occurs in the dark even when the photoperiod cycle is reversed so that larvae are held in the dark during the day and are exposed to illumination at night. The molting rhythm continues for 3 days after larvae are transferred from cyclic photoperiod conditions (LD 12:12) to LL and is reinstated in a stepwise manner when larvae reared in LL are transferred to cyclic conditions (LD 12:12). Molting occurs disproportionately in the dark in scotophase lengths as short as 3 h and over a range of temperatures (11, 15, and 20°C) commonly experienced by lobster larvae in nature.

The most important question when defining an apparent developmental rhythm is whether the rhythmicity results from a direct response to cyclic environmental conditions or is due to an endogenous timing mechanism. Indirect methods are used to identify the presence of an internal pacemaker and include determining whether the rhythm is free-running in the absence of cyclic environmental conditions and identifying whether an entraining (synchronizing) agent phases the internal program with the external environmental cycle (Edmunds 1983).

Our first approach to the question of whether American lobster larvae have an internal timer was to determine if lar-

© 1999 NRC Canada

vae have the ability to entrain to a photoperiod cycle out of phase with the normal cycle. Larvae were reared from hatch in either a normal LD 12:12 cycle (lights-off from 19:00 to 07:00) or a reversed LD 12:12 cycle (lights-off from 07:00 to 19:00). No significant difference was found in the proportion molting in the scotophase in the normal and reversed cycles (Fig. 2), evidence of photoperiodic entrainment of one or more of the developmental events involved in the rhythm.

To determine whether the molting rhythm is free-running under constant conditions, larvae were reared initially at LD 12:12 and then transferred to LL at various times before the molting period began. When the transfer to LL occurred the day before the onset of molting, larvae molted predominantly in the subjective scotophase on days 1, 2, and 3. The rhythm dampened rapidly, however, and by day 4, there was no significant difference in the proportion of larvae molting during the subjective day and night (Fig. 3). When larvae were transferred from LD 12:12 to LL 4 or 7 days prior to the onset of molting, molting occurred arrhythmically and there was no significant difference in the proportion molting during the subjective day and night. Larvae reared from hatch under LL had variable molting times. In some groups, significantly more larvae molted between the hours of 07:00 and 19:00 than between 19:00 and 07:00, while in other groups, there was no difference in the proportion molting during the subjective day and night (Fig. 4; Table 3).

The graded response of lobster larvae that experience a switch from continuous light to cyclic photoperiod conditions is suggestive of an internal timer that is being reset in stepwise increments. On the first day after transfer from LL to LD 12:12, only 42% of the molts occurred in the scotophase. On the second day, the percentage of larvae molting in the scotophase increased to 70%, and on the third day, 97% of the larvae molted in the scotophase. This result, and that in which the rhythm continued for 3 days after the larvae were transferred from LD 12:12 to LL, demonstrate that the molting rhythm is not the result of a direct response to cyclic photoperiod conditions.

The diel photoperiod cycle provides at least three possible phase-setting stimuli: the lights-on stimulus, the lights-off stimulus, and the length of the intervening time interval. Phase-setting stimuli are called synchronizers, or zeitgebers, as they synchronize the internal clock of the individual with the external environment (Beck 1980), leading to the manifestation of a rhythm in the population. The time-dependent stimuli — the beginning of daylight or the beginning of night — are the most common zeitgebers (Beck 1980). The results from this study suggest that the timing of the metamorphic molt in American lobsters is phase-set in the third larval stage by the lights-off signal. Larvae reared in scotophase lengths of 6, 10, and 12 h had similar responses to the onset of darkness, despite the difference in the length of the dark phase and the timing of the lights-on signal. The various night lengths produced significant differences in the percentages molting in the scotophase, but similar proportions molted within 10 and 12 h of the lights-off signal (Table 2).

Although the rhythm in the metamorphic molt of larval American lobsters occurs at the population level, it is clear that an endogenous component is involved in the control of its timing. When dealing with population-based rhythms, it is important to distinguish between fortuitous and gated synchrony (Beck 1980). If, for example, ecdysis in lobster larvae is temporally linked to an earlier developmental event that is regulated by photoperiod, molting could occur as a result of a fortuitous rhythm. The fact that molting in third-stage lobster larvae occurs in the scotophase over a range of temperatures and when the photoperiod cycle is reversed indicates that the synchrony between the timing of the scotophase and the metamorphic molt is not fortuitous. Rather, the results suggest the synchrony is "gated" and that no matter when premolt is completed, ecdysis is held in abeyance until the endogenous timer reaches the gate (onset of darkness) that permits molting.

Gated rhythms are involved in the control of timing of insect ecdyses, with the endogenous timer advancing or delaying ecdysis depending on the insect's developmental state relative to the clock (Steel and Ampleford 1984; Truman 1984). In the tobacco hornworm (*Manduca sexta*), adult ecdysis is under circadian-gated control of the brain (Truman 1972; Ewer et al. 1997), and in *Rhodnius prolixus*, hemolymph ecdysteroid titer is under circadian control and thought to be involved in synchronizing the ecdysis rhythm with the photoperiod cycle (Ampleford and Steel 1985). In fact, ecdysis can be phase-shifted by altering the ecdysteroid titer and mimicing the effect of manipulating the LD cycle (Ampleford 1985).

Almost nothing is known about the linkages between environmental signals and the (neuro)endocrine control of ecdysis in crustaceans. However, many eyestalk neurohormones involved in physiological and behavioral functions display circadian rhythmicity of secretion and release, including some that may have a role in molting (for a review, see Aréchiga et al. 1993). The peak in the titer of some of these hormones occurs during the scotophase (Aréchiga et al. 1993), and in at least one eyestalk hormone, a burst of exocytotic activity occurs at the onset of the scotophase (for references, see Van Herp 1993).

This study has demonstrated the existence of a population-based molting rhythm in third-stage American lobster larvae that has an endogenous component and is entrained by photoperiod. It is probably significant that the scotophase and (or) the onset of the scotophase appear to be important to many rhythms in decapods. Now that the rhythm in the metamorphic molt has been identified, it could become a useful tool for studying the relationships between environmental signals and the hormonal mechanisms involved in the rhythm. Despite the implications of these results, however, additional studies are required to determine whether the metamorphic molt occurs as a gated event under the direct influence of an endogenous pacemaker or whether it occurs indirectly as the result of another gated event.

Acknowledgments

We thank Bruce Thorpe, Wilfred Young-Lai, Theresia Fawkes, and Ross Chandler for assistance with these studies. Michael Eagles provided valuable comments on an earlier draft of the manuscript.

References

Abello, P., Warman, C.G., and Naylor, E. 1997. Circatidal moult-

© 1999 NRC Canada

ing rhythm in the shore crab *Carcinus maenas*. J. Mar. Biol. Assoc. U.K. **77**: 277–280.

Aiken, D.E., and Waddy, S.L. 1985. Production of seed stock for lobster culture. Aquaculture, **44**: 103–114.

Aiken, D.E., and Waddy, S.L. 1989. Culture of the American lobster, *Homarus americanus*. *In* Cold-water aquaculture in Atlantic Canada. *Edited by* A.D. Boghen. Canadian Institute for Research on Regional Development, Moncton, N.B. pp. 78–123.

Aiken, D.E., Martin, D.J., Meisner, J.D., and Sochasky, J.B. 1981. Influence of photoperiod on survival and growth of larval American lobsters (*Homarus americanus*). J. World Maricult. Soc. **12**: 225–230.

Ampleford, E.J. 1985. Ecdysteroids influence the circadian system timing ecdysis in the insect *Rhodnius prolixus* (Hemiptera). J. Comp. Physiol. A, Sens. Neural Behav. Physiol. **157**: 699–704.

Ampleford, E.J., and Steel, C.H.J. 1985. Circadian control of a daily rhythm in hemolymph ecdysteroid titer in the insect *Rhodnius prolixus* (Hemiptera). Gen. Comp. Endocrinol. **59**: 453–459.

Aréchiga, H., Fernandez-Quiroz, F., Fernandez de Miguel, F., and Rodriguez-Sosa, L. 1993. The circadian system of crustaceans. Chronobiol. Int. **10**: 1–15.

Beck, S.D. 1980. Insect photoperiodism. 2nd ed. Academic Press, Inc., New York.

Brady, J. 1979. Biological clocks. Institute of Biology's Studies in Biology No. 104. Edward Arnold (Publishers) Ltd., London, U.K.

Charmantier, G., Charmantier-Daures, M., and Aiken, D.E. 1991. Metamorphosis of the lobster *Homarus* (Decapoda): a review. J. Crustacean Biol. **11**: 481–495.

DeCoursey, P.J. 1983. Biological timing. *In* The biology of Crustacea. Vol. 7. *Edited by* F.J. Vernberg and W.B. Vernberg. Academic Press, Inc., New York. pp. 107–162.

Eagles, M.D., Aiken, D.E., and Waddy, S.L. 1986. Influence of light and food on larval American lobsters, *Homarus americanus*. Can. J. Fish. Aquat. Sci. **43**: 2303–2310.

Edmunds, L.N. 1983. Cellular and molecular bases of biological clocks: models and mechanisms for circadian timing. Springer-Verlag, New York.

Ennis, G.P. 1973. Endogenous rhythmicity associated with larval hatching in the lobster *Homarus gammarus*. J. Mar. Biol. Assoc. U.K. **53**: 531–538.

Ennis, G.P. 1975. Observations on hatching and larval release in the lobster, *Homarus americanus*. J. Fish. Res. Board Can. **32**: 2210–2213.

Ennis, G.P. 1995. Larval and postlarval ecology. *In* Biology of the American lobster, *Homarus americanus*. *Edited by* J.R. Factor. Academic Press, San Diego, Calif. pp. 23–46.

Ewer, J., Gammie, S.C., and Truman, J.W. 1997. Control of insect ecdysis by a positive-feedback endocrine system: role of eclosion hormone and ecdysis triggering hormone. J. Exp. Biol. **200**: 869–991.

Fernandez, M., Iribarne O., and Armstrong, D. 1994. Ecdysial rhythms in megalopae and first instars of the Dungeness crab *Cancer magister*. Mar. Biol. **118**: 611–615.

Fisheries Resource Conservation Council. 1995. A conservation framework for Atlantic lobster. Report to the Minister of Fisheries and Oceans FRCC95.R.1. Supply and Services Canada, Ottawa, Ont.

Fogarty, M.J. 1995. Populations, fisheries and management. *In* Biology of the American lobster, *Homarus americanus*. *Edited by* J.R. Factor. Academic Press, San Diego, Calif. pp. 111–137.

Forward, R.B., Jr. 1987. Larval release rhythms of decapod crustaceans: an overview. Bull. Mar. Sci. **41**: 165–176.

Forward, R.B., Jr. 1988. Diel vertical migration: zooplankton photobiology and behaviour. Oceanogr. Mar. Biol. Annu. Rev. **26**: 361–393.

Morgan, S.G., and Christy, J.H. 1995. Adaptive significance of the timing of larval release by crabs. Am. Nat. **145**: 457–459.

Palmer, J.D. 1995. The biological rhythms and clocks of intertidal organisms. Oxford University Press, Inc., New York.

Perkins, H.C. 1972. Developmental rates at various temperatures of embryos of the northern lobster *Homarus americanus* Milne-Edwards. U.S. Dep. Commer. Fish. Bull. **70**: 95–99.

Sastry, A.N. 1983. Pelagic larval ecology and development. *In* The biology of Crustacea. Vol. 7 *Edited by* F.J. Vernberg and W.B. Vernberg. Academic Press, Inc., New York. pp. 213–282.

Steel, C.G.H., and Ampleford, E.J. 1984. Circadian control of haemolymph ecdysteroid titres and the ecdysis rhythm in *Rhodnius prolixus*. *In* Ciba Foundation Symposium 104. Photoperiodic regulation of insect and molluscan hormones. *Edited by* R. Porter and G.M. Collins. Pittman, London, U.K. pp. 150–162.

Truman, J.W. 1972. Physiology of insect rhythms. I. Circadian organization of the endocrine events underlying the moulting cycle of larval tobacco hornworms. J. Exp. Biol. **57**: 805–820.

Truman, J.W. 1984. Physiological aspects of two oscillators that regulate the timing of eclosion in moths. *In* Ciba Foundation Symposium 104. Photoperiodic regulation of insect and molluscan hormones. *Edited by* R. Porter and G.M. Collins. Pittman, London, U.K. pp. 222–229.

Van Herp, F. 1993. Importance of reproductive biological knowledge for the application of biotechnology in aquaculture: crustaceans as an example. J. Mar. Biotechnol. **1**: 17–20.

Waddy, S.L., Aiken, D.E., and Young-Lai, W.W. 1990. Scotophase influences timing of the metamorphic molt in larvae American lobsters (*Homarus americanus*). Am. Zool. **30**: 129A. (Abstr.)

Zeng, C.E., and Naylor, E. 1997. Rhythms of larval release in the shore crab *Carcinus maenas* (Decapoda: Brachyura). J. Mar. Biol. Assoc. U.K. **77**: 451–461.

Zeng, C.E., Naylor, E., and Abello, P. 1997. Endogenous control of timing of metamorphosis in megalopae of the shore crab *Carcinus maenas*. Mar. Biol. **128**: 299–305.

© 1999 NRC Canada

Relative importance of stream-borne particulate and dissolved phosphorus fractions to Lake Tahoe phytoplankton

Lorin K. Hatch, John E. Reuter, and Charles R. Goldman

Abstract: Algal bioassays using stream water additions from seven Lake Tahoe basin mountain creeks were used to assess short-term bioavailability of stream P to Lake Tahoe phytoplankton during the 1996 spring snowmelt. Results indicate that 75–90% of bioassay response is due to nutrients in the <0.45-μm range. Lake Tahoe phytoplankton are primarily P limited, although N colimitation has been observed during summer. Bioassay response did not correlate well with particulate P > 0.45 μm but was highly correlated with dissolved inorganic P. Dissolved organic P may also be stimulatory to Lake Tahoe phytoplankton. Bioassay response was relatively constant for each treatment during the study, due in part to a consistent diatom dominance of the phytoplankton community. The bioassay technique utilized is not sensitive enough to detect changes in land use along a single stream. Dissolved inorganic P was determined to best represent Lake Tahoe short-term (several days) stream bioavailable P at the present time. Physical bioavailability factors such as lake thermal dynamics and biological factors such as lake microbial dynamics should be addressed in addition to the chemical factors when considering lake biologically available P.

Résumé : Des essais biologiques sur des algues comportant l'exposition à de l'eau de sept ruisseaux de montagne du bassin du lac Tahoe ont été effectués afin d'évaluer la disponibilité biologique à court terme du P des cours d'eau pour le phytoplancton du lac Tahoe pendant la fonte des neiges du printemps de 1996. Les résultats obtenus montrent que de 75 à 90% de la réaction à l'essai biologique s'expliquent par la présence de matières nutritives de la gamme inférieure à 0,45 μm. Le phytoplancton du lac Tahoe est surtout limité par le phosphore (P), bien qu'une co-limitation par l'azote ait été observée en été. La réaction ne présentait pas une bonne corrélation avec le P particulaire (PP) de plus de 0,45 μm mais une forte corrélation avec le P inorganique dissous. Ce dernier pourrait aussi avoir un effet stimulateur pour le phytoplancton du lac Tahoe. La réaction était relativement constante pour chacun des traitements réalisés au cours de l'étude et cela s'explique en partie par l'uniformité de la dominance des diatomées de la communauté phytoplanctonique. La technique utilisée n'était pas suffisamment sensible pour permettre de déceler les changements de l'utilisation des terres le long d'un même cours d'eau. Le P inorganique dissous était l'élément qui représentait le mieux la disponibilité biologique à court terme (plusieurs jours) du P du lac Tahoe au moment de l'étude. D'autres facteurs de la biodisponibilité physique, tels la dynamique thermique et des facteurs biologiques, comme la dynamique microbienne du lac, devraient aussi être examinés, en plus des facteurs chimiques, au moment de l'examen du phosphore biologiquement disponible du lac.

[Traduit par la Rédaction]

Introduction

Although stream P is predominantly transported to mountain lakes in particulate form (Leonard et al. 1979; Meyer and Likens 1979; Burrus et al. 1990), not all of this P is biologically available to lake phytoplankton. Algal bioassays have been used to determine the biologically available P (BAP) content of stream water. Many studies using this technique have focused on the chemical aspect of BAP (i.e., how much of a specific P fraction is removed by algae) but not necessarily on the physical and (or) biological aspects of BAP. Physical considerations should include examining the ability of stream sediments to be transported into the lake proper, a process significantly influenced by sediment particle size. A significant portion of the P pool in stream water is located inside suspended sediment particles (occluded) and can be bound within the mineral matrix (Peters 1978; Froelich 1988; Correll 1998). Consequently, particle size is an important consideration when examining P bioavailability (Dorich et al. 1984; Broberg and Persson 1988). Occluded P associated with relatively large stream suspended sediments (i.e., sands) can quickly settle out at the stream–lake interface and become removed from the active lake P cycle (buried) for hundreds of years (Cowen and Lee 1976). Lighter particles such as silts and clays can remain suspended in the lake photic zone for significant periods of time, increasing their biological availability potential (Persson 1990). How-

Received January 7, 1999. Accepted August 18, 1999.
J14965

L.K. Hatch.[1] University of Minnesota Water Resources Center, 1518 Cleveland Avenue North, Suite 302, St. Paul, MN 55108, U.S.A.
J.E. Reuter and C.R. Goldman. University of California Tahoe Research Group, 3104 Wickson Hall, One Shields Avenue, Davis, CA 95616, U.S.A.

[1]Author to whom all correspondence should be addressed.
e-mail: hatch013@tc.umn.edu

© 1999 NRC Canada

ever, silt- and clay-sized particles can bind together in streams to form larger aggregates (Ongley et al. 1981), enhancing their potential to settle to the lake bottom quickly.

A major biological consideration when conducting algal bioassays should be whether to use a single species culture or a lake's natural phytoplankton assemblage. A single species culture may be useful when a lake and (or) several lakes are dominated by one major species. The use of a standard test organism (*Selenastrum capricornutum*) is useful to deduce the chemical nature of sediment BAP (DePinto et al. 1981; Hegemann and Keenan 1983; Ellis and Stanford 1988). The use of natural phytoplankton assemblages is useful in assessing BAP when (*i*) a complex community structure is present, (*ii*) the assemblage shifts over the course of the year, and (*iii*) management of a single lake is of concern (Schelske et al. 1978; Grobbelaar 1983; Schelske 1984; Dodds et al. 1989). These three factors are present at Lake Tahoe (California–Nevada).

Pioneering work on stream water addition bioassays that used water from undeveloped (General Creek, located within a state park) and developed (Incline Creek and the Upper Truckee River) watersheds displayed varying amounts of stimulation using Lake Tahoe phytoplankton (Goldman and Armstrong 1969). Using ^{14}C to measure productivity, the authors demonstrated that the relatively undisturbed General Creek water gave little stimulation and possible inhibition to bioassays. Incline Creek and the Upper Truckee River responses were significantly higher, with greater stimulation in late spring and summer than in winter. Similar studies concluded that the stream water of highly developed watersheds (Incline Creek, Trout Creek, Upper Truckee River) gave greater bioassay stimulation than that of lesser developed watersheds like General Creek and Ward Creek (McGauhey et al. 1971).

The nutrient dynamics of Lake Tahoe have changed significantly since the 1960s. In addition to a steady decline in clarity and an increase in lake primary productivitiy since at least 1967 (Goldman 1988), concomitant nutrient addition work has shown that the phytoplankton community shifted from N limitation to increasing P limitation in the early 1980s (Goldman et al. 1993). This shift has been attributed to enhanced atmospheric N loading (Jassby et al. 1994; Jassby et al. 1995). Since then, all monthly bioassays have shown P limitation, although N and P colimitation often occurs in summer. A recently developed total P (TP) budget has indicated that 25% of P loading to the lake is via atmospheric deposition (Reuter et al. 1998).

The objective of this study is to characterize the short-term bioavailability of stream P to Lake Tahoe phytoplankton. Initial insight into the physical component of BAP was gained by examining particle size effects on biological response; stream-to-iake transport models were not addressed. A comprehensive assessment of BAP in Tahoe streams is also needed to determine if stream BAP varies with location in the Tahoe basin (due to varying distributions of granitic and volcanic parent materials). Stream water volume additions and particle size treatments were conducted on seven streams from March to August 1996 to address spatiotemporal variability in the quantity and quality of stream P in the Tahoe basin. Finally, the ability of algal bioassays to assess land use impacts within a given subwatershed was tested. A subset of the experiments examined the stimulatory qualities of stream water collected both above and below human development in the Incline Creek and Upper Truckee River watersheds.

Methods

Study site

Ultraoligotrophic Lake Tahoe is located 30 km southwest of Reno, Nevada, at the crest of the Sierra Nevada range (Fig. 1). The lake has two thirds of its area in California and one third of its area in Nevada. With a surface elevation of 1898 m, Lake Tahoe has a mean depth of 313 m and a maximum depth of 501 m (Goldman 1974). A lake volume of 156 km^3 is largely responsible for a 700-year hydraulic retention time. The drainage area and surface areas of Lake Tahoe are 800 and 500 km^2, respectively. Slopes of 30–50% are not uncommon, as steep peaks rise quickly from the lakeshore. Soils are primarily granitic, with volcanics located primarily in the north basin (Matthews and Burnett 1971; Goldman 1974). Soils along stream channels and the lakeshore are generally alluvial wash deposits, and the most recent glaciation (11 000 years ago) occurred in the western canyons and high-elevation bowls. Mixed conifers and pure pine stands dominate the densely vegetated basin. Basin vegetation is currently secondary and tertiary growth, recovering from intensive late nineteenth century logging. Although industrial and agricultural activities are essentially absent, construction activities remain common in the Lake Tahoe basin. Sewage has been pumped out of the basin since the early 1970s.

Precipitation falls primarily as snow from November to March, resulting in a spring snowmelt runoff season that delivers about 75% of the annual stream P load to Lake Tahoe (Hatch 1997). The western slopes of the basin receive twice the annual precipitation of the eastern slopes due to a rain shadow effect. Summer–fall rainstorms occur occasionally, as do rain-on-snow events, which can deliver extremely large quantities of sediment and nutrients to the lake in a short (2–3 days) period of time. To assess the impact of spring snowmelt runoff on phytoplankton response, the stream water addition bioassay study covered the period before (March), during (May–June), and after (July–August) the 1996 snowmelt season. No major precipitation events occurred during this time period.

Field methodology and laboratory analyses

Seven creek mouth stations were chosen to encompass spatial variation in stream water quality in the Tahoe basin (Fig. 1). Geomorphic, geologic, and urban indices for these watersheds are given elsewhere (Hatch 1997). Additional sites upstream of significant human development included Incline Creek and the Upper Truckee River. Stream water samples were taken in early evening during the rising limb of the daily snowmelt hydrograph (sample dates in Table 1). Separate creek water samples were filtered through predried, preweighed 0.45-μm (defined as TSS) and 63-μm (defined as SS63) nylon filters within 2 h of collection (duplicate filters for suspended solids concentration were dried at 60°C, weighed, and dried again until a constant weight was obtained to the nearest 0.01 mg). Raw stream water, the 63-μm filtrate, and the 0.45-μm filtrate were stored at 4°C until use in the algal incubations the following day or for later chemical analyses.

Sixty litres of water from a midlake location was collected at 20 m (zone of maximum primary production; Goldman et al. 1993) the day before algal incubations began. Synoptic lake surveys indicated that primary productivity and water quality at this midlake station approximate those of other stations across the lake (including those near shore) within 10% (Goldman 1988). Water was screened through an 80-μm mesh to remove the herbivorous zooplankton and the omnivore *Mysis relicta*. In situ light intensity and

© 1999 NRC Canada

Fig. 1. Lake Tahoe basin, California–Nevada. Streams in the present study have their watersheds highlighted. Heavy lines denote the 63 watersheds and intervening areas. Developed areas are indicated by the road network. Map courtesy of the Tahoe Regional Planning Agency, Zephyr Cove, Nev.

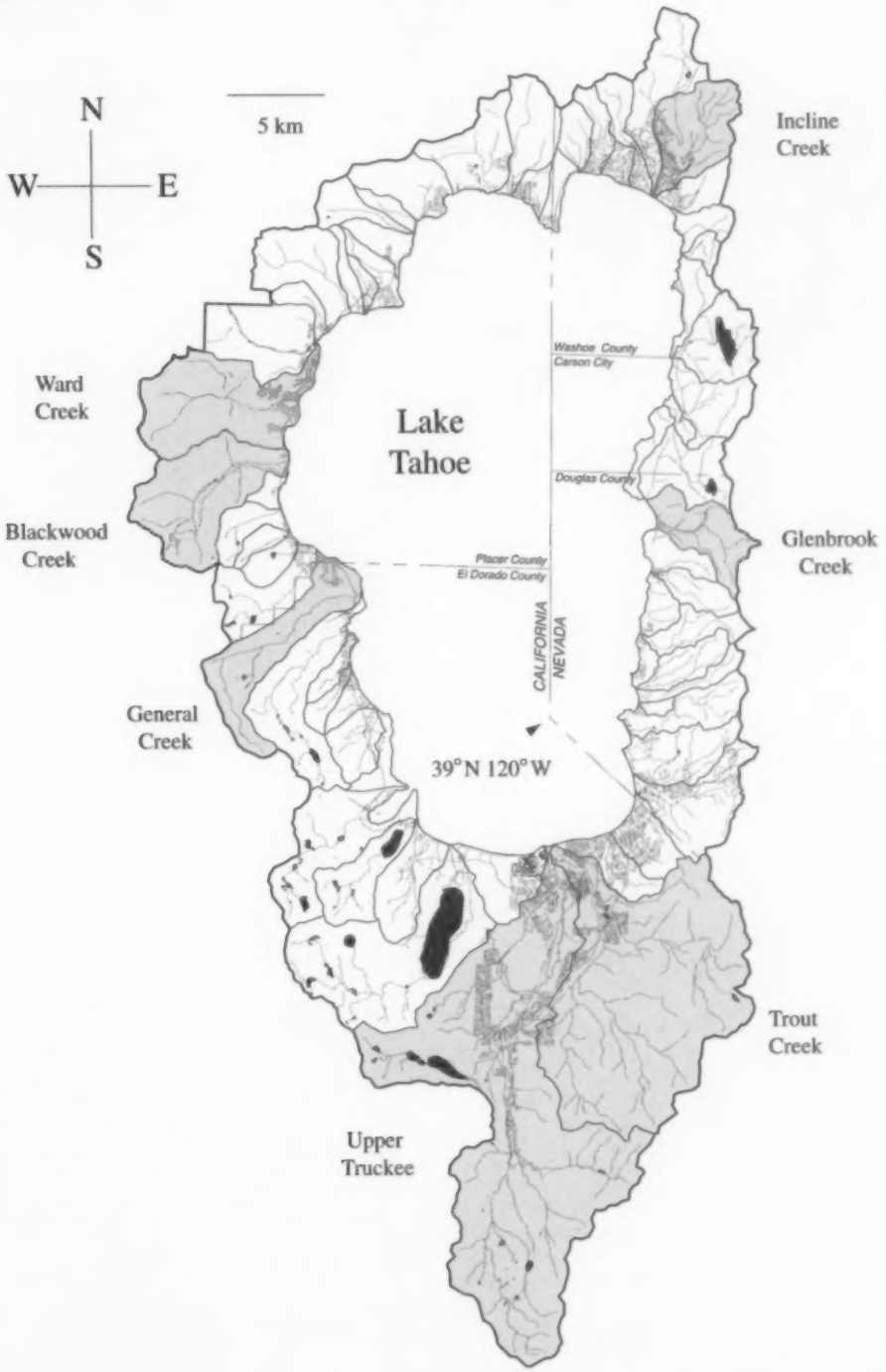

© 1999 NRC Canada

Table 1. Range of bioassay treatment response means for the 1996 streamwater addition study.

	Treatment response					
Stream	1%	2.5%	5%	10%/raw	63 µm	0.45 µm
Blackwood	107–118	112–128	125–141	132–172	142–158	130–150
General	84–113	86–123	110–152	121–146	120–144	119–128
Glenbrook	116–130	126–159	141–182	169–194	150–211	159–189
Incline	109–125	117–144	133–168	123–222	126–198	135–197
Trout	104–129	113–148	134–170	157–185	150–170	130–170
Upper Truckee	100–112	108–130	116–149	133–179	126–169	133–160
Ward	104–114	112–132	128–130	142–163	134–152	128–156

Note: Response given as (treatment mean)/(control mean). Bioassay periods 1, 3, 5, and 7: Blackwood Creek, Glenbrook Creek, Trout Creek, and Ward Creek; bioassay periods 2, 4, 6, and 8: General Creek, Incline Creek, and Upper Truckee River. Bioassay incubation start: 1 = March 28, 2 = April 15, 3 = April 29, 4 = May 13, 5 = May 27, 6 = June 12, 7 = July 16, and 8 = August 9. Percentages represent % volume stream water additions to lake water. The 10% and raw treatments are equivalent. Raw = raw stream water addition, 63 µm = 63-µm stream water filtrate addition, and 0.45 µm = 0.45-µm stream water filtrate addition (these treatments at 10% by volume).

Fig. 2. Mean response for volume addition treatments for each stream in the 1996 study. Standard errors are indicated above each bar.

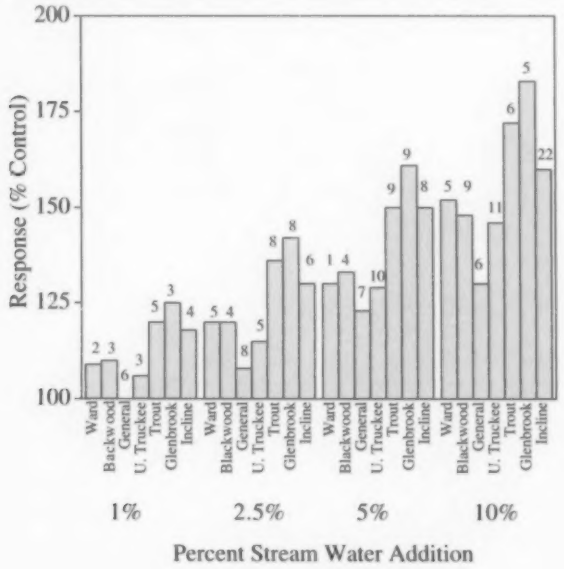

water temperature were measured and laboratory incubators were set to these ambient conditions.

The volume addition experiment utilized 1, 2.5, 5, and 10% stream water additions for all stream mouth stations. The volume addition experiment was not intended to simulate dilution by the lake proper. This experiment was exploratory to determine the minimum dilution treatment that would be able to detect differences from the controls. The particle size experiment consisted of 10% stream water additions using raw stream water, the 63-µm filtrate, and the 0.45-µm filtrate; the two upstream stations were included in addition to the seven mouth stations in this experiment. All treatments for both experiments were run in triplicate, with a triplicate set of deionized water additions to lake water serving as the control for all stations.

An identical procedure was used for a nutrient addition bioassay (i.e., laboratory reagents), which determined the type of nutrient limitation present in the lake phytoplankton community in July 1996. Lake water collection and the beginning of the 6-day incubation both occurred on July 24, 1996. Reagent-grade nutrient additions consisted of triplicate flasks for a control (lake water only), a NO_3-N addition (20 µg·L^{-1} spike), an ortho-P addition (10 µg·L^{-1} spike), and a NO_3-N plus ortho-P addition (20 µg NO_3-N·L^{-1} plus 10 µg ortho-P·L^{-1}).

Filtrations for chlorophyll *a* (1.2-µm glassfiber filter, $n = 3$) occurred at the beginning and end (day 6) of the algal incubations (frozen at –20°C). Triplicate blank filters were processed for turbidity correction. Filters were thawed and chlorophyll *a* was extracted overnight in methanol. A Turner III fluorometer fitted with a CS 2-64 filter on the emission side and a CS 5-60 filter over the excitation light (F4T5/CW) was used to determine fluorescence on the extracted chlorophyll *a* samples (Strickland and Parsons 1972; Holm-Hansen 1978). The fluorometer was calibrated with chlorophyll *a* standards prior to the beginning of the experiments, and chlorophyll *a* values were corrected for phaeopigments. In vivo fluorescence was measured at the same time that chlorophyll *a* filtrations took place on a separate sample. All incubation flasks were gently shaken daily and before chlorophyll *a* or fluorescence samples were taken. There was a strong fluorescence – chlorophyll concentration relationship for individual treatment responses for each round of stream water addition incubations ($r^2 = 0.750$, $p < 0.0001$) and creek treatment means for the entire experiment ($r^2 = 0.922$, $p < 0.0001$). Hence, all further discussion of bioassay results will pertain to day 6 fluorescence response.

Phosphorus analyses were carried out according to the ascorbic acid method of Murphy and Riley (1962), following persulfate oxidation digestion where appropriate (Menzel and Corwin 1965). Subtraction of total dissolved P (TDP) (digestible P in the 0.45-µm filtrate) from TP yields total particulate P (PP), while subtraction of soluble reactive P (SRP) (0.45-µm filtrate) from TDP yields dissolved organic P (DOP). Subtraction of DP63 (digestible P in the 63-µm filtrate) from TP yields particulate P in the sand-sized fraction (PP_{sand}, >63 µm), while subtraction of SRP63 (SRP in the 63-µm filtrate) from DP63 yields particulate P in the silt- and clay-sized fraction ($PP_{s\&c}$, >0.45 µm but <63 µm).

All analytical procedures were within quality assurance limits as established for the Tahoe Research Group Laboratory, which is a contract laboratory for the U.S. Environmental Protection Agency. Internal quality control procedures consist of biannual performance audits, system audits, and reports (Hunter 1996). External quality control procedures consist of analyzing biannual reference samples from the U.S. Geological Survey and the U.S. Environmental Protection Agency in addition to interlaboratory replicate sample comparisons.

Results

The results of the July 1996 nutrient addition bioassay (reagent-grade nutrients only, no stream water) agree with

© 1999 NRC Canada

Table 2. Mean (SE in parentheses) stream bioassay responses and P concentrations for particle size treatments.

	Treatment response			Stream concentration mean					
Stream	Raw	63 μm	0.45 μm	TP	PP	DOP	SRP	PP_{sand}	$PP_{s\&c}$
Blackwood	148 (9)	148 (4)	138 (5)	49 (29)	33 (28)	11 (2)	5 (1)	16 (15)	26 (14)
General	130 (6)	134 (5)	123 (2)	18 (6)	2 (3)	10 (2)	6 (4)	2 (0)	10 (3)
Glenbrook	183 (5)	191 (14)	172 (7)	58 (5)	27 (7)	14 (2)	17 (4)	4 (1)	21 (4)
Incline	160 (22)	153 (16)	154 (15)	76 (20)	50 (18)	14 (3)	12 (1)	39 (17)	21 (5)
Trout	172 (6)	162 (4)	154 (9)	41 (2)	20 (3)	11 (2)	10 (1)	7 (1)	24 (6)
Upper Truckee	146 (11)	143 (9)	141 (6)	34 (1)	15 (4)	13 (3)	6 (1)	9 (1)	16 (2)
Ward	152 (5)	145 (4)	140 (6)	26 (9)	9 (7)	11 (3)	6 (1)	4 (1)	19 (8)
Response	Statistic			TP	PP	DOP	SRP	PP_{sand}	$PP_{s\&c}$
Raw	r^2			0.367	0.205	0.337	0.722	0.006	0.390
	MSE			235	295	246	103	369	227
	p value			0.149	0.307	0.172	0.016	0.874	0.134
63 μm	r^2					0.352	0.817		0.230
	MSE					268	76		319
	p value					0.160	0.005		0.277
0.45 μm	r^2					0.567	0.821		
	MSE					126	52		
	p value					0.051	0.005		

Note: All sites are stream mouths. Bioassay response = (treatment mean)/(control mean). Mean (SE in parentheses) concentrations in $\mu g \cdot L^{-1}$. Regression dependent variable = bioassay response. Regressions were not performed for nutrients not wholly present in a given response treatment class. For example, the 63-μm response did not include P from sand-sized particles, so the 63-vm response was not compared with TP (which contains sand-sized particles). PP, PP_{sand}, and $PP_{s\&c}$ were determined independently and therefore may not sum as expected. See Table 1 for treatment (raw, 63 μm, 0.45 μm) definitions. PP, particulate P; DOP, dissolved organic P; SRP, soluble reactive P; PP_{sand}, particulate P >63 μm (i.e., sands); $PP_{s\&c}$, particulate P >0.45 μm and <63 μm (i.e., silts and clays).

Fig. 3. Mean response for particle size treatments for each stream in the 1996 study. Standard errors are indicated above each bar; 0.45 μm = 0.45-μm filtrate addition, 63 μm = 63-μm filtrate addition, and raw = raw stream water addition.

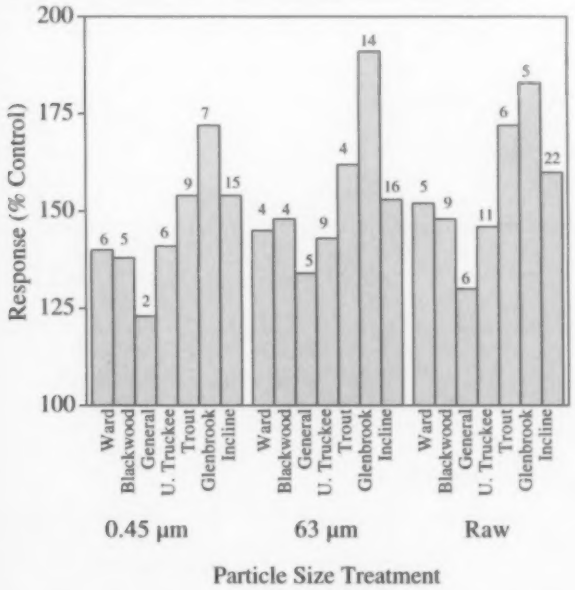

the July–August N and P colimitation results of Goldman et al. (1993), who have conducted the same method of bioassay for over 25 years. Significant growth of the control occurred, with mean fluorescence increasing by a factor of 2 over the course of the 6-day July 1996 bioassay. Mean fluorescence values were 13.67 for the controls, 14.67 for N addition, 27.33 for P addition, and 31.67 for N plus P addition. Colimitation is inferred because the fluorescence response for N plus P addition (229% of control) was higher than the sum of the individual nutrient responses (107% for N + 200% for P – 100% = 207% of the control).

The pattern of bioassay response for the volume addition treatments was relatively similar for all streams, increasing from the 1% dose to the 10% dose, with indications of lowered response per unit dose as dose increased (Fig. 2). Using Trout Creek as an example, mean response (treatment/control) increases from 120% at the 1% dose, to 136% at the 2.5% dose, to 150% at the 5% dose, and to 172% at the 10% dose. Hence, we can be assured that the 10% additions associated with the particle size treatments will yield significant responses. Statistical comparison of volume addition treatment means (shown in Fig. 2) between streams (t tests at the 0.05 level) detected significant differences, and a pattern emerged in which the clusters of Glenbrook Creek – Trout Creek – Incline Creek and Blackwood Creek – Ward Creek – Upper Truckee River – General Creek were identified. For example, the General Creek 1% dose mean was significantly different from those for Glenbrook Creek, Incline Creek, and Trout Creek but was not significantly different from those for Upper Truckee River and Ward Creek. However, this overall pattern did not yield significant differences in 33% of the comparisons (eight of 32, primarily Incline Creek at the 10% dose) for the volume addition treatments, making the validity of the stream clusters tentative at this time.

A comparison of volume addition treatments for specific doses for specific creeks between bioassays revealed few instances of increasing or decreasing trends as the year progressed (Table 1). For example, the Ward Creek 1% values were 109, 104, 114, and 109 over the entire experiment.

© 1999 NRC Canada

Table 3. Bioassay treatment responses, P concentrations, and statistical comparisons between upstream and downstream stations for the 1996 bioassay study.

	Treatment response			Stream nutrient concentration					
Site	Raw	63 μm	0.45 μm	TP	PP	DOP	SRP	PP_{sand}	$PP_{s\&c}$
Incline upstream	167 (25)	155 (23)	152 (11)	65 (12)	40 (12)	14 (3)	11 (2)	23 (8)	34 (14)
Incline downstream	160 (22)	153 (16)	154 (15)	76 (20)	50 (18)	15 (4)	12 (1)	39 (18)	21 (5)
Upper Truckee upstream	143 (8)	132 (4)	134 (6)	27 (4)	6 (2)	12 (3)	9 (4)	3 (1)	16 (3)
Upper Truckee downstream	146 (11)	143 (10)	141 (7)	34 (2)	15 (4)	13 (3)	6 (1)	9 (1)	16 (2)
	Upstream/downstream difference of means test (*t* statistic)								
Stream	Raw	63 μm	0.45 μm	TP	PP	DOP	SRP	PP_{sand}	$PP_{s\&c}$
Incline	0.21	0.07	0.11	0.47	0.47	0.23	0.55	0.83	0.65
Upper Truckee	0.22	1.07	0.79	1.71	2.23	0.28	0.82	5.37	0.00

Note: Treatment responses are mean values (SE in parentheses) from four bioassays (beginning dates: April 15, May 13, June 12, and August 9). Response = (treatment mean)/(control mean). Mean (SE in parentheses) nutrient concentrations in $\mu g \cdot L^{-1}$. For the 0.05 level of significance, $t = 2.447$. See Tables 1 and 2 for treatment and nutrient definitions.

Hunter et al. (1990) demonstrated that diatoms dominate the Lake Tahoe phytoplankton community from April to June (about 50–80% of total biomass), about the same period of the present study. This diatom dominance may help explain why bioassay response showed little seasonality for the present study. Algal nutrient requirements may remain relatively constant, due to the nutrient-scavenging efficiency of diatoms, resulting in stable bioassay responses over the study period.

SRP and to a lesser extent DOP concentrations were the only P water quality variables significantly correlated with bioassay response (Table 2), indicating that stream particle sizes >0.45 μm are not important sources of short-term BAP to Lake Tahoe phytoplankton (at least under the bioassay conditions of the present study). Linear regressions indicate that SRP concentration had the best relationship with all response classes based on low *p* and MSE values. Evidence to support SRP as readily bioavailable was also seen in the July 1996 nutrient addition bioassay in which ortho-P additions significantly stimulated growth of Lake Tahoe phytoplankton. DOP concentration can be considered significantly related to the 0.45-μm response due to a marginal *p* value of 0.051. DOP was not, however, significantly correlated with either the raw response or the 63-μm response, which more accurately reflect natural stream conditions. TP, PP, DOP, PP_{sand}, and $PP_{s\&c}$ concentrations were not significantly correlated with bioassay response at the 0.05 level.

The P nutrient pool that could be potentially available for algae increased from dissolved (0.45 μm) to silt and clay (63 μm) to sand (raw) particle sizes (Table 2). However, there were no significant differences (0.05 level) between the three particle size treatment means for any of the creeks during any of the bioassay rounds. The lack of significant differences between all particle size categories indicates that the <0.45-μm fraction of stream water contributed the majority of stimulation to phytoplankton in this study.

The relative stimulation of each particle size-class was estimated by comparison of the particle size treatment means. For example, the average response for the 0.45-μm treatment for the Upper Truckee River mouth site was 141, while the average response for the raw treatment was 146 (Fig. 3). In other words, stream water constituents <0.45 μm are responsible for 41/46 = 89% of the total response of Lake Tahoe phytoplankton to Upper Truckee River water. Similar results were found for the other streams, with 75–90% of total mean bioassay response due to stream water nutrients in the <0.45-μm fraction.

The clusters of streams shown to have similar responses for the volume addition treatments (Glenbrook Creek – Trout Creek – Incline Creek and Blackwood Creek – Ward Creek – Upper Truckee River – General Creek) were not apparent for the particle size treatments, although significant mean differeneces (*t* tests at the 0.05 level) existed. For example, the Blackwood Creek 63-μm mean was significantly different from those for General Creek, Glenbrook Creek, and Trout Creek but was not significantly different from those for Incline Creek, Upper Truckee River, and Ward Creek. Again, there is evidence to support the proposed clusters of streams, but further clarification will be necessary in future work.

There were no significant differences in algal response between undeveloped upstream and developed downstream stations on the same stream (Table 3). It has been shown previously that bioassay response is strongly correlated with stream SRP concentration (Table 2). This stream constituent was not significantly different (*t* test at the 0.05 level) between the upstream and downstream stations on Incline Creek and the Upper Truckee River (Table 3). The only significant concentration difference was PP_{sand} for the Upper Truckee River, but this constituent was not found to be correlated with bioassay response (Table 2). Thus the lack of significant difference for bioassay response between the upstream and downstream stations is likely due to the similarity of nutrient concentrations, especially SRP, for those stations.

Discussion

Determination of which portion of the nutrient load to a lake is bioavailable for phytoplankton is a fundamental concern when adopting lake and watershed management policy and when designing a monitoring program to evaluate lake response. The answer to this question needs to account for physical, chemical, and biological properties in both stream and lake water. In this discussion, we focus specifically on stream water P bioavailability to lake phytoplankton on a time scale of many days to a week.

© 1999 NRC Canada

Table 4. Mean measured instantaneous P loads ($g \cdot s^{-1}$) during the 1996 bioassay study.

Stream	TP	PP	DOP	SRP	PP_{sand}	$PP_{s\&c}$
Blackwood	327	272	42	13	138	134
General	18	3	12	3	2	1
Glenbrook	10	5	3	3	1	4
Incline	65	44	12	9	34	10
Trout	123	60	36	27	12	48
Upper Truckee	201	106	66	28	54	52
Ward	115	61	39	15	17	44

Note: Data represent means of March–August 1996 study ($n = 4$ for each stream mouth). Values were calculated as the product of discharge ($L \cdot s^{-1}$) and concentration ($\mu g \cdot L^{-1}$) and converted to grams. See Table 2 for definitions of P fractions.

Physical availability of stream water sources of BAP in Lake Tahoe (e.g., particle size distributions, temperature, water density) will constrain biological and chemical factors (microbial mineralization, phosphatase activity, particulate P desorption) relating to bioavailability. High-mass stream particulates (>63 µm) begin falling through the lake water column relatively quickly after stream momentum dissipates at the stream–lake interface. Considering that Broberg and Persson (1988) demonstrated that particles about 50 µm in size would settle at a rate of 23 $m \cdot day^{-1}$, P associated with stream sand-sized particulates would fall out of the photic zone of deep lakes before microbial mineralization or algal phosphatase activity could liberate significant quantities of BAP. Estimation of this high-mass potential BAP fraction, which may take years to come into contact with Lake Tahoe phytoplankton, is beyond the scope of this study.

Low-mass stream particulates (<63 µm) and dissolved stream P may become bioavailable on a time scale of days to weeks. This lower mass fraction of BAP consists of SRP, certain low relative molecular mass DOP compounds (unknown at this time for Tahoe streams), and desorbable PP in the <63-µm fraction (also unknown at this time for Tahoe streams). These low-mass/dissolved materials will remain suspended in the photic zone for weeks, increasing the potential for contact with phytoplankton and phytoplankton exudates. Paerl (1973) demonstrated that most microbial colonization (bacteria and fungi) of stream particulates occurs very quickly (<3 days) in the upper 75 m of Lake Tahoe. Microbial aggregation onto particles was 10 times greater on unsterilized samples than for sterilized samples, suggesting that microbial colonization of stream particulates may not only increase BAP release, but also increase settling velocities. Hence, a stream particle that was relatively low mass when it entered the lake may increase in mass very quickly due to rapid microbial colonization, resulting in a higher sedimentation rate than one might expect. This phenomenon could reduce the bioavailability of <63-µm sized stream particles in a physical sense (i.e., more rapid sedimentation out of the photic zone).

The best estimate for short-term (days to weeks) BAP loading from Lake Tahoe streams at this time is SRP loading. DOP, however, may constitute a significant portion of short-term BAP, considering its correlation with algal response (Table 2) and its contribution to stream loading (Table 4). Although P associated with stream particulates <63 µm has the potential to become bioavailable in a very short time period (Paerl 1973), the present study did not examine this potential. Long-term (weeks, months, years) estimates of Tahoe stream P bioavailability are not known. Stream PP may become BAP over time as mineralization occurs in the lake.

Annual SRP loads for Tahoe streams have been shown to range from 0.1 to nearly 1000 $kg \cdot year^{-1}$, depending primarily on the quantity of spring snowmelt runoff (Hatch 1997). These loads were also highly correlated with precipitation, basin area, basin steepness, and impermeable land coverage. About 75% of SRP loads occur during spring runoff at Tahoe (Table 5). Of the nine streams depicted in Table 5 (which contribute about 50% of the annual P stream to Lake Tahoe), the Upper Truckee River contributes the greatest SRP loads, followed by Trout Creek, Blackwood Creek, and Ward Creek.

Two groups of Tahoe streams were distinguishable from one another based on volume addition and particle size treatment bioassays: Glenbrook Creek, Incline Creek, and Trout Creek and Blackwood Creek, General Creek, Upper Truckee River, and Ward Creek (Figs. 2 and 3). These two groupings may be the result of watershed characteristics and human disturbance factors. In comparison with the other streams, Glenbrook Creek, Incline Creek, and Trout Creek as a group have a greater percentage of high-hazard land, smaller drainage densities and channel lengths, and steeper slopes (Hatch 1997). These three creeks are located on the eastern side of the Tahoe basin, which receives only 50% of the annual precipitation received on the western side due to a rain shadow effect. Trout Creek, however, most likely receives greater amounts of precipitation (as snow) due to the large percentage of area located at high elevations. Lowered precipitation amounts on the east shore may result in relatively sparse vegetation, steeper slopes, and less pronounced soil nutrient leaching in comparison with the west shore watersheds. These factors may be responsible for the higher nutrient concentrations and higher bioassay responses seen for east shore streams (Figs. 2 and 3).

The overall contribution of BAP to the lake from Glenbrook Creek and Incline Creek (along with other low discharge/load yielding east shore streams) is minimal compared with Trout Creek (Table 5). However, water quality concerns in these smaller east shore streams may be contributing to localized algal blooms (e.g., periphyton near stream mouths) and hence should not be ignored with respect to cleanup initiatives. Increasing development in these areas may result in flashier streams (i.e., higher discharge peaks) due to greater amounts of impervious surfaces. This situation would most likely create greater stream bank erosion and greater nutrient loads in the future from these relatively high-nutrient watersheds on the east shore.

The present study included stream sampling during temperature-driven snowmelt runoff and summer low-flow conditions. Sampling during different precipitation-related events (rain-on-snow or rain-on-soil), the use of more sensitive techniques (^{14}C productivity), or greater sample sizes to generate more rigorous statistical conclusions may be necessary to determine how human development impacts phytoplankton productivity through enhanced stream nutrient transport.

Many lake management plans focus on TP when consider-

© 1999 NRC Canada

Table 5. Mean 1989 to 1996 monthly SRP load (kg) for Tahoe stream mouths.

Month	Blackwood	General	Glenbrook	Incline	Trout	Upper Truckee	Ward
October	2	1	1	3	8	4	1
November	2	1	1	3	8	5	2
December	4	2	1	3	9	9	3
January	5	3	1	3	10	16	5
February	8	4	2	4	10	19	7
March	16	7	5	8	19	48	14
April	25	12	6	10	26	66	23
May	43	17	8	16	44	124	46
June	33	10	4	14	52	107	32
July	13	3	1	9	35	42	13
August	3	1	1	4	16	8	2
September	2	1	1	3	10	4	1
Sum	156	62	32	80	247	452	149

Note: Data from the Lake Tahoe Interagency Monitoring Program (Tahoe Research Group, University of California at Davis; U.S. Geological Survey, Carson City, Nev.). Annual log–log nutrient rating curves were generated for each stream and year. Monthly values were then calculated using mean daily discharge values for each stream and year. Eight monthly values (e.g., Blackwood Creek January 1989, Blackwood Creek January 1990, etc.) were then averaged.

ing reductions of external P loads. Increasing evidence indicates that watershed sources of BAP are different than TP sources (e.g., Gerdes and Kunst 1998). Hatch (1997) found that TP and PP, but not SRP or DOP, were significantly correlated eith stream alluvial deposits. Past Tahoe research and the present study suggest that if certain PP and DOP stream fractions are to become biologically available, these fractions must first (*i*) have their BAP released (e.g., by the microbial community) and then (*ii*) be situated in the locale of the lake phytoplankton (e.g., have lake thermal dynamics such that the liberated BAP will come into contact with algae in the photic zone). These factors may be lake specific; a lake at 60°N will most likely have different thermal and microbial dynamics than a lake at 10°N. Considering the enormous amounts of resources being channeled into lake restoration measures, it is in the best interests of lake managers to focus on BAP dynamics in lakes and their tributaries, not just on TP.

Future research on the bioavailability of stream P sources should focus on analytical techniques and physical/chemical stream–lake dynamics. Independent chemical determinations of the DOP and PP fractions will give a more accurate representation of these compounds for statistical analysis. Selective filtration of stream water would also allow specific particle sizes to be analyzed independently for P. High relative molecular mass organic and inorganic compounds should be examined more closely to determine mineralization rates and movement characteristics in the lake. Answers to these questions will provide a stronger understanding of how BAP is mobilized at depth and moved into the lake photic zone during mixing events. Considerations of lighter weight BAP fractions should include studies on the bioavailability of low relative molecular mass DOP compounds and the <63-μm fraction of PP. Quantification of these compounds, along with stream particle size distributions and BAP content, will help determine how short-term stream BAP compounds are delivered to and cycled within lakes.

Acknowledgements

We thank Bob Richards, Scott Hackley, and Mark Palmer of the Tahoe Research Group laboratory for field and laboratory assistance and John Hitchcock of the Tahoe Regional Planning Agency for assistance with figures. This work was supported by the U.S. Environmenta Protection Agency (R819658) Center for Ecological Health Research at the University of California at Davis. Although the information in this document has been funded wholly or in part by the U.S. Environmental Protection Agency, it may not neccessarily reflect the views of the Agency and no official endorsement should be inferred.

References

Broberg, O., and Persson, G. 1988. Particulate and dissolved phosphorus forms in freshwater: composition and analysis. Hydrobiologia, **170**: 61–90.

Burrus, D., Thomas, R., Dominik, J., and Vernet, J. 1990. Seasonal delivery of the particulate forms of phosphorus to Lake Geneva from the upper Rhone River. Aquat. Sci. **52**: 221–235.

Correll, D. 1998. The role of phosphorus in the eutrophication of receiving waters: a review. J. Environ. Qual. **27**: 261–266.

Cowen, W., and Lee, G. 1976. Phosphorus availability in particulate materials transported by urban runoff. J. Water Pollut. Control Fed. **48**: 580–591.

DePinto, J., Young, T., and Martin, S. 1981. Algal-available phosphorus in suspended sediments from lower Great Lakes tributaries. J. Gt. Lakes Res. **7**: 311–325.

Dodds, W., Johnson, K., and Priscu, J. 1989. Simultaneous nitrogen and phosphorus deficiency in natural phytoplankton assemblages: theory, empirical evidence, and implications for lake management. Lake Reservoir Manage. **5**: 21–26.

Dorich, R., Nelson, D., and Sommers, L. 1984. Algal availability of phosphorus in suspended stream sediments of varying particle size. J. Environ. Qual. **13**: 82–86.

Ellis, B., and Stanford, J. 1988. Phosphorus bioavailability of fluvial sediments determined by algal assays. Hydrobiologia, **160**: 9–18.

Froelich, P. 1988. Kinetic control of dissolved phosphate in natural rivers and estuaries: a primer on the phosphate buffer mechanism. Limnol. Oceanogr. **33**: 649–668.

Gerdes, P., and Kunst, S. 1998. Bioavailability of phosphorus as a tool for efficient P reduction schemes. Water Sci. Technol. **37**: 241–247.

© 1999 NRC Canada

Goldman, C. 1974. Eutrophication of Lake Tahoe emphasizing water quality. U.S. Environ. Prot. Agency NTIS EPA Rep. 660/3-74-034.

Goldman, C. 1988. Primary production, nutrients, and transparency during the early onset of eutrophication in ultra-oligotrophic Lake Tahoe, California–Nevada. Limnol. Oceanogr. **33**: 1321–1333.

Goldman, C., and Armstrong, R. 1969. Primary productivity studies in Lake Tahoe, California. Verh. Int. Ver. Limnol. **17**: 49–71.

Goldman, C., Jassby, A., and Hackley, S. 1993. Decadal, interannual, and seasonal variability in enrichment bioassays at Lake Tahoe, California–Nevada, U.S.A. Can. J. Fish. Aquat. Sci. **50**: 1489–1496.

Grobbelaar, J. 1983. Availability to algae of nitrogen and phosphorus adsorbed on suspended solids in turbid waters of the Amazon River. Arch. Hydrobiol. **96**: 302–316.

Hatch, L. 1997. The generation, transport, and fate of phosphorus in the Lake Tahoe ecosystem. Ph.D. thesis, University of California at Davis, Davis, Calif.

Hegemann, D., and Keenan, J. 1983. Bioassay techniques for soil-nutrient availability. Water Air Soil Pollut. **19**: 259–276.

Holm-Hansen, O. 1978. Chlorophyll *a* determination: improvements in methodology. Oikos, **30**: 438–447.

Hunter, D. 1996. Lake Tahoe Interagency Monitoring Program Water Chemistry Water Quality Control Report, January–June 1996. Tahoe Research Group, University of California at Davis, Davis, Calif.

Hunter, D., Goldman, C., and Byron, E. 1990. Changes in the phytoplankton community structure in Lake Tahoe, California–Nevada. Verh. Int. Ver. Limnol. **24**: 505–508.

Jassby, A., Reuter, J., Axler, R., Goldman, C., and Hackley, S. 1994. Atmospheric deposition of nitrogen and phosphorus in the annual nutrient load of Lake Tahoe (California–Nevada). Water Resour. Res. **30**: 2207–2216.

Jassby, A., Goldman, C., and Reuter, J. 1995. Long-term change in Lake Tahoe (California–Nevada, U.S.A.) and its relation to atmospheric deposition of algal nutrients. Arch. Hydrobiol. **135**: 1–21.

Leonard, R., Kaplan, L., Elder, J., Coats, R., and Goldman, C. 1979. Nutrient transport in surface runoff from a subalpine watershed, Lake Tahoe Basin, California. Ecol. Monogr. **49**: 281–310.

Matthews, R., and Burnett, J. 1971. Geology and land use planning in the Lake Tahoe basin. *In* Geology and geomorphology of the Lake Tahoe region: a guide for planning. Tahoe Regional Planning Agency, Zephyr Cove, Nev. pp. 5–32.

McGauhey, P., Dugan, G., and Porcella, D. 1971. Eutrophication of surface waters — Lake Tahoe. Water Pollut. Control Res. Ser. 16010 DSWO 5/71.

Menzel, D., and Corwin, N. 1965. The measurement of total phosphorus in seawater based on the liberation of organically bound fractions by persulfate oxidation. Limnol. Oceanogr. **10**: 280–282.

Meyer, J., and Likens, G. 1979. Transport and transformation of phosphorus in a forest stream ecosystem. Ecology, **60**: 1255–1269.

Murphy, J., and Riley, J. 1962. A modified single solution method for the determination of phosphate in natural waters. Anal. Chim. Acta, **27**: 31–36.

Ongley, E., Bynoe, M., and Percival, J. 1981. Physical and geochemical characteristics of suspended solids, Wilton Creek, Ontario. Can. J. Earth Sci. **18**: 1365–1379.

Paerl, H. 1973. Detritus in Lake Tahoe: structural modification by attached microflora. Science (Washington, D.C.), **180**: 496–498.

Persson, G. 1990. Utilization of phosphorus in suspended particulate matter as tested by algal bioassays. Verh. Int. Ver. Limnol. **24**: 242–246.

Peters, R. 1978. Concentrations and kinetics of phosphorus fractions in water from streams entering Lake Memphremagog. J. Fish. Res. Board Can. **35**: 315–328.

Reuter, J., Jassby, A., Marjanovic, P., Heyvaert, A., and Goldman, C. 1998. Preliminary phosphorus and nitrogen budgets for Lake Tahoe. *In* Annual Progress Report — lake clarity and watershed modeling. John Muir Institute for the Environment, University of California at Davis, Davis, Calif.

Schelske, C. 1984. In situ and natural phytoplankton assemblage bioassays. *In* Algae as ecological indicators. *Edited by* L.E. Shubert. Academic Press, London, U.K.

Schelske, C., Rothman, E., and Simmons, M. 1978. Comparison of bioassays procedures for growth-limiting nutrients in the Laurentian Great Lakes. Mitt. Int. Ver. Limnol. **21**: 65–80.

Strickland, J., and Parsons, P. 1972. A practical handbook of seawater analysis. Bull. Fish. Res. Board Can. No. 167.

© 1999 NRC Canada

Phylogeny of the lamprey genus *Lampetra* inferred from mitochondrial cytochrome *b* and ND3 gene sequences

Margaret F. Docker, John H. Youson, Richard J. Beamish, and Robert H. Devlin

Abstract: Mitochrondrial DNA analysis resolved many previously unanswered questions concerning the phylogeny of the lamprey genus *Lampetra* (comprising the subgenera *Entosphenus*, *Lethenteron*, and *Lampetra*). A total of 735 base pairs were sequenced from the cytochrome *b* and NADH dehydrogenase subunit 3 (ND3) genes in 11 lamprey species. With the exception of *L.* (*E.*) *hubbsi* from California, species of the *Entosphenus* subgenus formed a tight-knit clade that was very distinct from the other two subgenera. *Lampetra hubbsi* clustered with species of the *Lampetra* subgenus from the west coast of North America (*L. ayresii* and *L. richardsoni*) whereas species of the *Lampetra* subgenus from Atlantic drainages, namely the North American *L. aepyptera* and European *L. fluviatilis*, formed a third cluster. A fourth cluster included two species from the *Lethenteron* subgenus (*L. japonica* and *L. appendix*). Inclusion of published data from a third *Lethenteron* species, *L. zanandreai*, showed it to group with the *L.* (*L.*) *fluviatilis* lineage rather than with the other two *Lethenteron* species. Within each subgenus, members of paired and satellite species were closely related to one another (e.g., *L. japonica* and *L. appendix*) or were genetically indistinguishable (e.g., *L. ayresii* and *L. richardsoni*). Using rates of molecular evolution estimated in other fish taxa, these genetically indistinguishable species diverged less than 70 000 years ago.

Résumé : L'analyse de l'ADN mitochrondial a permis de répondre à bon nombre de questions relativement à la phylogénie du genre de lamproie *Lampetra* (englobant les sous-genres *Entosphenus*, *Lethenteron* et *Lampetra*). On a déterminé la séquence d'un total de 735 paires de bases des gènes pour la cytochrome *b* et la sous-unité 3 de la NADH déshydrogénase (ND3) chez 11 espèces de lamproie. À l'exception de *L. (E.) hubbsi* de la Californie, les espèces du sous-genre *Enthosphenus* formaient un clade cohérent très distinct de ceux des deux autres sous-genres. *Lampetra hubbsi* se rapprochait des espèces du sous-genre *Lampetra* de la côte ouest de l'Amérique du Nord (*L. ayresii* et *L. richardsoni*) tandis que les espèces du sous-genre *Lampetra* des bassins de l'Atlantique, à savoir *L. aepyptera* de l'Amérique du Nord et *L. fluviatilis* de l'Europe formaient un troisième groupe. Un quatrième groupe englobait deux espèces du sous-genre *Lethenteron* (*L. japonica* et *L. appendix*). L'ajout de données publiées pour une troisième espèce de *Lethenteron*, *L. zanandreai*, indiquait une parenté avec *L.* (*L.*) *fluviatilis* plutôt qu'avec les deux autres espèces de *Lethenteron*. Au sein de chaque sous-genre, les membres d'espèces appariées et satellites étaient fortement apparentés les uns aux autres (p. ex. *L. japonica* et *L. appendix*) ou étaient génétiquement indiscernables (p. ex. *L. ayresii* et *L. richardsoni*). L'utilisation des taux d'évolution moléculaire estimés pour d'autres taxons de poisson montre que ces espèces génétiquement indiscernables ont divergé il y a moins de 70 000 ans.

[Traduit par la Rédaction]

Introduction

Lampreys are extant representatives of the ancient vertebrate group Agnatha and are one of the oldest groups of living fishes in the fossil record, about 300 million years old (Janvier and Lund 1983). There are about 40 extant species of lampreys; four species described from the Southern Hemisphere have been placed in the families Geotriidae and Mordaciidae, while the remaining species inhabit the Northern Hemisphere. The Northern Hemisphere lampreys belong to a single family, Petromyzonidae, and have been assigned to at least six genera (Hubbs and Potter 1971; Potter 1980).

Received January 7, 1999. Accepted August 6, 1999.
J14968

M.F. Docker[1] **and R.H. Devlin.** Department of Fisheries and Oceans, West Vancouver Laboratory, 4160 Marine Dr., West Vancouver, BC V7V 1N6, Canada.
J.H. Youson. Division of Life Sciences, University of Toronto at Scarborough, 1265 Military Trail, Scarborough, ON M1C 1A4, Canada.
R.J. Beamish. Department of Fisheries and Oceans, Pacific Biological Station, Nanaimo, BC V9R 5K6, Canada.

[1]Author to whom all correspondence should be sent at the following address: Biology Program, College of Science and Management, University of Northern British Columbia, 3333 University Way, Prince George, BC V2N 4Z9, Canada.
e-mail: docker@unbc.ca

© 1999 NRC Canada

Lamprey taxonomy is problematic because, compared with bony vertebrates, there are relatively few taxon-distinctive morphological characters. Species identification and generic status have been largely based on adult dentition, as well as on differences in body proportions, number of myomeres, number and morphology of velar tentacles, and pigmentation (Hubbs and Potter 1971; Richards et al. 1982).

Adult body size, life history type, and habitat are also commonly used to distinguish between closely related taxa. All lampreys spend the first years of life as blind larvae that burrow in the silt bottoms of rivers and streams and feed on microscopic organisms. Following metamorphosis, they may remain nontrophic (nonparasitic) in their natal stream and spawn and die within 6–9 months, or they may migrate to freshwater lakes or to seawater and become trophic (parasitic). In most lamprey genera, groups of two or more species exist in which the larvae are morphologically similar but the species adopt different life history types as adults. It is generally believed that these so-called "paired species" (Zanandrea 1959) or multiple "satellite species" (Vladykov and Kott 1979*a*) are very closely related, with the nonparasitic species having evolved from a parasitic ancestor (Zanandrea 1959). Not all authorities, however, recognize life history type as a reliable indication of species differentiation (e.g., McPhail and Lindsey 1970) and consider paired or satellite species to be races or types of a single species. An objective of the current study was to determine the degree of molecular divergence between paired or satellite species.

A second objective was to use molecular data to test the evolutionary relationships among some higher lamprey taxa. A specific goal was to resolve the relationships among the 15 or more species currently assigned to the genus *Lampetra* (Potter 1980), which has controversial morphological characters (Table 1). Potter (1980) named *Entosphenus*, *Lethenteron*, and *Lampetra* as subgenera within the genus *Lampetra*, whereas other authors (e.g., Vladykov and Kott 1979*a*) classified each as distinct genera and further recognized a division between the taxa by placing *Entosphenus* into a separate subfamily from *Lampetra* and *Lethenteron*. Taxonomic questions centre on the degenerate or intermediate characteristics of several so-called relict species, nonparasitic lampreys that occur at or near the extreme southern limits of distribution of the Northern Hemisphere lampreys (Hubbs and Potter 1971). One such relict species is *Lampetra* (*Entosphenus*) *hubbsi* from California (Vladykov and Kott 1976*a*), which appears to demonstrate an intergradation of characters among the three subgenera (Table 1). Similarly, two other nonparasitic species, *Lampetra* (*Lampetra*) *aepyptera* and *Lampetra* (*Lethenteron*) *zanandreai*, possess ambiguous morphological characters (Table 1). The current study examined the evolutionary relationships among the three subgenera of *Lampetra* and evaluated the relationships of the relict species *L. hubbsi* and *L. aepyptera*.

Given the inclusiveness and overlap of lamprey morphological characters, an independent molecular data set from mitochondrial DNA sequences is used to resolve these taxonomic issues. In this study, we sequenced the entire NADH dehydrogenase subunit 3 (ND3) gene and about one third of the cytochrome *b* gene from 11 species of lampreys of the genus *Lampetra* and compared the data with published cytochrome *b* sequences from two additional *Lampetra* species (Tagliavini et al. 1994). Cytochrome *b* sequence has been used to resolve phylogenetic relationships in a variety of fish taxa (e.g., Cantatore et al. 1994), and the ND3 gene, which appears to evolve somewhat faster than cytochrome *b* (Thomas and Beckenbach 1989; McVeigh and Davidson 1991), may be useful in distinguishing among some of the more closely related paired and satellite species.

Materials and methods

Eleven lamprey species of the genus *Lampetra* were collected in Canada (British Columbia and Ontario), the United States (Oregon, California, and Tennessee), Germany, and Russia (Table 2). Species identification was confirmed morphologically in adults; ammocoetes were used only where a single species was present or where adequate larval characteristics exist to distinguish between species (Richards et al. 1982). DNA analysis was performed on two to four individuals per species or collection site. A single landlocked sea lamprey (*Petromyzon marinus*) from Ontario was collected for use as an outgroup, and cytochrome *b* and ND3 sequences were compared with those from an anadromous sea lamprey from New Hampshire (Lee and Kocher 1995). All samples were either frozen at –70°C or preserved in 95% ethanol.

In *L. japonica*, DNA was extracted from liver tissue by digesting overnight at 37°C with proteinase K in proteinase K buffer (10 mM Tris (pH 8.0), 10 mM EDTA, 1% SDS, 200 µg proteinase K/mL), cleaning with phenol–chloroform (1:1), and precipitating with NaOAc and isopropanol. In the other specimens, DNA was extracted from fin or tail clippings, which were digested for 1 h at 55°C with proteinase K and used as crude homogenates.

Polymerase chain reaction (PCR) amplification of 414 base pairs (bp) at the 5′ end of the cytochrome *b* gene used primers located in the tRNA-Glu and cytochrome *b* genes: GLUDG-L (5′-TGACTTGAARAACCAYCGTTG-3′) and CB2-H (5′-CCCTCAGAATGATATTTGTCCTCA-3′), respectively (Palumbi 1996). Since lampreys possess a large noncoding region between these two genes (Lee and Kocher 1995), the PCR product exceeded 1000 bp. Two internal primers (5′-CCATCCAACATCTCAGCWTGATGAAA-3′ (L) from Palumbi (1996) and 5′-CAAGGCTAGTTCAGTRTTAGC-3′ (H) designed from conserved regions of lamprey sequence) were used to amplify subsections of this larger fragment. The entire 351 bp of the lamprey ND3 gene were amplified with primers designed from conserved regions in the tRNA-Arg gene of other vertebrates (e.g., Thomas and Beckenbach 1989) and the tRNA-Gly gene of sea lamprey (Lee and Kocher 1995): 5′-ATGCGGATCCTTTTGAGCCGAAATCA-3′ and 5′-ACGTGAATTCTATAGTTGGGTTCCAACCA-3′, respectively.

Each 50-µL reaction contained standard PCR buffer (10 mM Tris (pH 8.3), 50 mM KCl, 1.5 mM $MgCl_2$, 0.001% gelatin), 0.2 mM dNTP, 50 pmol of each primer, and 1.25 units of *Taq* DNA polymerase (Gibco BRL, Burlington, Ont.). The reactions were run in a Perkin Elmer thermocycler (Perkin Elmer Cetus, Norwalk, Conn.) for 30 cycles consisting of denaturation at 94°C for 1 min, primer annealing at 60°C for 1 min, and extension at 72°C for 2 min; the 30 cycles were preceded by an initial denaturation for 3 min at 94°C and followed by a final 10-min 72°C extension. Negative controls, which used distilled water instead of template DNA, were included in each series of reactions to screen for possible contamination.

The PCR products were sequenced using the Cyclist DNA Sequencing Kit (Stratagene, La Jolla, Calif.) or the Sequenase PCR Product Sequencing Kit (United States Biochemical, Cleveland, Ohio); the manufacturer's instructions were followed. Given the heteroplasmic nature of the noncoding insert located at the 5′ end of cytochrome *b* (M.F. Docker, J.H. Youson, R.J. Beamish, J.M.P. Joss, T.D. Kocher, and R.H. Devlin, unpublished data), all cytochrome *b* sequencing was accomplished from the 3′ end of the

© 1999 NRC Canada

Table 1. Summary of the taxonomy of the lamprey genus *Lampetra*.

Species	Comments regarding classification	Relevant morphological characteristics[a]	Life history type and distribution
Subgenus *Lampetra*	Considered by Vladykov and co-workers as distinct genus and included in subfamily Lampetrinae with genera *Lethenteron* and *Eudontomyzon*[1]	Supraoral (SO) lamina 2 cusps; 3 inner laterals[b] with 2–3–2 cusps; infraoral (IO) lamina 7–8 cusps; posterial circumorals (posterials) absent[2]	
ayresii (river lamprey)	Initially considered synonymous with *L. fluviatilis*; described as distinct species (Vladykov and Follett 1958)	Velar tentacles 4; larger eye, longer prebrancial, and shorter branchial region relative to *L. fluviatilis*	Parasitic, anadromous; Pacific coast of North America from Skeena River, B.C., to San Francisco Bay, Calif.
richardsoni (western brook lamprey)	Derivative of *L. ayresii* (Vladykov and Follett 1965)		Nonparasitic, freshwater; Pacific drainages from B.C. to Oreg.
pacifica (Pacific brook lamprey)	Described as second nonparasitic derivative of *L. ayresii* (Vladykov 1973); now considered by American Fisheries Society to be synonymous with *L. richardsoni*[3]	Fewer myomeres and less well-developed teeth than typical *L. richardsoni*	Nonparasitic, freshwater; Columbia River basin, Oreg.; San Joachin – Sacramento River system, Calif.
fluviatilis (European river lamprey)			Parasitic, anadromous; western European watersheds of the Atlantic, Baltic, and Mediterranean; some landlocked[4]
planeri (European brook lamprey)	Derivative of *L. fluviatilis*		Nonparasitic, freshwater; similar distribution to *fluviatilis* but further inland in central and northern Europe[5]
aepyptera (least brook lamprey)	Occurs far from any parasitic *Lampetra*; perhaps derived from *L. ayresii*,[1] from *Eudontomyzon–Tetrapleurodon* type,[6] or *L. japonica*[4,7]; may bridge gap between *Lampetra* and *Lethenteron*[7]	Dentition extremely degenerate and variable; posterials absent; reduced number of myomeres[8]	Nonparasitic, freshwater; southeastern U.S. in Ohio River basin, Gulf and Atlantic plains
Subgenus *Entosphenus*	Generic status in subfamily Entosphenidae with genus *Tetrapleurodon*[1]	SO lamina 3 cusps; 4 inner laterals with 2–3–3–2 cusps; IO lamina with 5 cusps; posterials present[2]	
tridentata (Pacific lamprey)		Posterials 18 (2 bicuspid); velar tentacles 13	Parasitic, anadromous; spawns in rivers of Pacific basin from Alaska to southern Calif.
macrostoma (lake lamprey)	Derivative of *L. tridentata* (Beamish 1982); recognized as distinct species by American Fisheries Society[3]	Posterials 18 (3 bicuspid); velar tentacles 13	Parasitic, freshwater; reported only in 2 lakes on Vancouver Island, B.C.
similis (Klamath River lamprey)	Derivative of *L. tridentata* (Vladykov and Kott 1979*b*); once regarded as subspecies of *tridentata*,[9] now recognized as distinct[3]	Posterials 18 (6 bicuspid); velar tentacles 8	Parasitic, freshwater; Klamath River drainage, Calif. and Oreg.
lethophaga (Pit–Klamath brook lamprey)	Derivative of *L. tridentata* (Hubbs 1971)	Dentition more variable and degenerate than other *Entosphenus*; velar tentacles 8; adult size about 140 mm[10]	Nonparasitic, freshwater; Klamath and Pit River systems in Oreg. and Calif.
folletti	Described as second nonparasitic derivative of *L. tridentata* (Vladykov and Kott 1976*c*); considered by American Fisheries Society as synonymous with *lethophaga*[9]	Dentition more robust than typical *lethophaga*; adult size about 200 mm	Nonparasitic, freshwater; restricted to Klamath River drainage of northern Calif.

© 1999 NRC Canada

Table 1 (*concluded*).

Species	Comments regarding classification	Relevant morphological characteristics[a]	Life history type and distribution
hubbsi (Kern brook lamprey)	Presumed derivative of *L. tridentata* (Vladykov and Kott 1976*a*), although prior to canal, Kern River basin lacked connection with other *Entosphenus*; *L.* (*L.*) *pacifica* (*L. richardsoni*) only other species in canal	SO lamina 2 cusps; 4 inner laterals unicuspid; IO lamina 5 cusps; posterials about 10 (unicuspid); velar tentacles 3; reduced number of myomeres	Nonparasitic, freshwater; limited distribution in Calif. in San Joachin basin[1]; probably originated in Kern River, which now connects with San Joachin River through artificial Millerton Lake
Subgenus *Lethenteron*	Considered distinct genus in subfamily Lampetrinae with *Lampetra* and *Eudontomyzon*[1]	SO lamina 2 cusps; 3 inner laterals with 2–2–2 cusp pattern; IO lamina with >5 cusps; unicuspid posterials[6]	
japonica (Arctic lamprey)			Parasitic, anadromous; from Varangar Fjord in Europe to Pacific coast of Japan; in North America, in Alaska and northern Canada
appendix (American brook lamprey)	Synonymous with *L.* (*Le.*) *lamottenii*; designated *L. appendix* by American Fisheries Society[9]; current distribution differs from *L. japonica*, but almost certainly one of its many derivatives; considered indistinguishable from *L.* (*Le.*) *alaskense*[9]		Nonparasitic, freshwater; tributarites of Great Lakes, St. Lawrence and Mississippi River systems, and rivers tributary to the Atlantic from N.H. to N.C.
zanandreai (Po brook lamprey)	Originally *Lampetra* (Vladykov 1955), but posterials and inner lateral cusp formula suggest *Lethenteron*[4]; ancient southern relict of *L.* (*L.*) *fluviatilis*[1] or *L.* (*Le.*) *japonica*[6]	Inner laterals 2–2–2 cusp pattern; single row of minute posterials, which may sometimes be lacking or deeply embedded[11]; velar tentacles 3–5; reduced number of myomeres	Nonparasitic, freshwater; restricted to Po River drainage in northern Italy

Note: References other than original species descriptions: 1, Vladykov and Kott (1979*a*); 2, Vladykov and Kott (1976*a*); 3, Robins et al. (1991); 4, Potter (1980); 5, Hardisty (1986); 6, Hubbs and Potter (1971); 7, Bailey (1980); 8, Vladykov and Kott (1976*b*); 9, Robins et al. (1980); 10, Vladykov and Kott (1976*c*); 11, Bianco (1986).

[a]Mean or mode given.

[b]Inner laterals equivalent to lateral circumorals.

© 1999 NRC Canada

Table 2. Collection data for the lamprey species analyzed in this study.

Species	Collection site	*N*	Stage
Genus *Lampetra*			
Subgenus *Lampetra*			
ayresii	Strait of Georgia, Fraser River discharge, B.C.	2 (fr)	Juvenile
richardsoni	Cowichan River, Vancouver Island, B.C.	2 (fr)	Ammocoete
	Chemainus River, Vancouver Island, B.C.	2 (fr)	Ammocoete
fluviatilis	Elba River, Germany	2 (EtOH)	Adult
aepyptera	Cane Creek, Tenn.	2 (EtOH)	Ammocoete
Subgenus *Entosphenus*			
tridentata	Cowichan River, Vancouver Island, B.C.	2 (fr)	Ammocoete
	Chemainus River, Vancouver Island, B.C.	2 (fr)	Ammocoete
	Elk River, coastal Oreg.	4 (EtOH)	Ammocoete
macrostoma	Cowichan Lake, Vancouver Island, B.C.	2 (fr)	Juvenile
lethophaga	Pit River, Calif.	2 (fr)	Adult
	Hat Creek, Calif.	2 (fr)	Ammocoete
similis 1–3	Agency Lake, Klamath Basin, Oreg.	3 (fr)	Adult
similis 4–7	Sprague River, Klamath Basin, Oreg.	4 (fr)	Adult
similis	Merced River, Calif.	2 (fr)	Ammocoete
hubbsi	Merced River, Calif.	2 (fr)	Adult
	Kings River, Calif.	2 (fr)	Adult
Subgenus *Lethenteron*			
japonica	Kamchatka Channel, Russia	2 (EtOH)	Adult
appendix	Nolachucky River, Ont.	2 (EtOH)	Ammocoete
Genus *Petromyzon*			
marinus	Bronte Creek, Ont. (landlocked)	1 (EtOH)	Ammocoete

Note: Sample size (*N*), method of preservation (fr, frozen at –70°C; EtOH, preserved in 95% ethanol), and life cycle stage are indicated.

fragment or with the internal primers. The sequences have been deposited in GenBank with accession Nos. AF177947–AF177976.

Sequence comparisons were made on 384 bp at the 5′ end of the cytochrome *b* gene, on the entire ND3 gene, and on the combined sequences (735 bp). Using the Molecular Evolutionary Genetics Analysis (MEGA) program (version 1.01) developed by Kumar et al. (1993), genetic distances were estimated with Kimura's (1980) two-parameter distances and phylogenetic relationships were inferred from the neighbour-joining (NJ) method; support of the data set for each branch point was tested by 500 bootstrap replications. For comparison, we also carried out the maximum parsimony procedure as implemented in MEGA (branch and bound method). Published cytochrome *b* sequences from two European species, *L.* (*L*). *planeri* and *L.* (*Le.*) *zanandreai* (Tagliavini et al. 1994), were added to our data set, and the phylogenetic analyses above were repeated on the 267 bp of sequence (positions 118–384) common to all 13 species.

Results

Phylogenetic analysis

The portion of the cytochrome *b* gene sequenced had a 12-bp insert (positions 10–21) in lampreys relative to most teleosts (e.g., Cantatore et al. 1994), but there were no insertions or deletions among the lamprey species examined. The ND3 gene likewise showed no interspecific differences in length.

Intraspecific variation in the nucleotide sequence of both genes was relatively low in the current study. Cytochrome *b* and ND3 sequences were identical in eight Pacific lampreys (*L. tridentata*) from British Columbia and Oregon, and four *L. richardsoni*, *L. lethophaga*, and *L. hubbsi* likewise showed no intraspecific differences, even among sites. Both gene sequences were identical in the landlocked sea lamprey of the current study and the anadromous sea lamprey from Lee and Kocher (1995). Intraspecific sequence differences were noted, however, in two species: *L. aepyptera* (cytochrome *b*) and *L. similis* (both genes) (Table 3). *Lampetra similis* from the Merced River in California varied consistently from the Oregon specimens by a total of two or three nucleotides, but the differences among the Oregon specimens (one or two nucleotides) were not population specific. All intraspecific nucleotide substitutions were third-position transitions.

Within the *Lampetra* genus, interspecific sequence variation ranged from 0 to 9.1% in cytochrome *b* and from 0 to 12.5% in ND3 (Table 3). In both genes, there were no differences between *L. ayresii* and *L. richardsoni* and among *L. tridentata*, *L. macrostoma*, *L. lethophaga*, and *L. similis* from California. The greatest differences were observed between a haplotype of *L. similis* and *L. appendix* (cytochrome *b*) and *L. similis* and *L. hubbsi* (ND3). Comparisons between the *Lampetra* species and *P. marinus* showed variation between genera to range from 13.0 to 14.3% in cytochrome *b* and from 16.0 to 17.4% in ND3.

The cytochrome *b* and ND3 nucleotide sequences were used to estimate the phylogeny of the 11 *Lampetra* species using sea lamprey as an outgroup. Since the tree topologies obtained from each gene separately or together and those by the NJ or maximum parsimony method were almost consensus, just the phylogenetic analysis of the NJ method using the combined data is shown (Fig. 1). Only the topology of the NJ tree using the ND3 data differed slightly from Fig. 1

© 1999 NRC Canada

Table 3. Pairwise sequence differences (expressed as first/second/third codon position substitutions) in 384 bp of the lamprey cytochrome *b* gene (above the diagonal) and in the 351-bp ND3 gene (below the diagonal).

	1	2	3	4	5	6	7	8	9	10	11	12	13
Genus *Lampetra*													
Subgenus *Lampetra*													
1. *ayresii, richardsoni*	—	2/0/22	4/0/21	4/0/22	2/0/26	2/0/25	2/0/25	2/0/25	2/0/26	3/0/8	1/1/24	1/2/23	7/1/42
2. *fluviatilis*	5/1/27	—	4/0/11	4/0/12	4/0/20	4/0/21	4/0/21	4/0/21	4/0/22	5/0/26	1/1/22	1/2/23	7/1/44
3. *aepyptera* 1	9/2/24	6/1/18	—	0/0/1	6/0/23	6/0/24	6/0/24	6/0/24	6/0/25	7/0/25	5/1/25	5/2/24	11/1/39
4. *aepyptera* 2	9/2/24	6/1/18	0/0/0	—	6/0/24	6/0/25	6/0/25	6/0/25	6/0/26	7/0/26	5/1/26	5/2/25	11/1/40
Subgenus *Entosphenus*													
5. *tridentata, macrostoma, lethophaga, similis* (Calif.)	5/2/24	8/3/29	8/4/28	8/4/28	—	0/0/1	0/0/1	0/0/1	0/0/2	5/0/28	3/1/27	3/2/28	9/1/42
6. *similis* 2, 4–6	5/2/29	8/3/30	8/4/29	8/4/29	0/0/1	—	0/0/0	0/0/0	0/0/1	5/0/27	3/1/28	3/2/29	9/1/41
7. *similis* 1	5/2/30	8/3/31	8/4/30	8/4/30	0/0/2	0/0/1	—	0/0/0	0/0/1	5/0/27	3/1/28	3/2/29	9/1/41
8. *similis* 3	5/2/28	8/3/31	8/4/29	8/4/29	0/0/2	0/0/1	0/0/2	—	0/0/1	5/0/27	3/1/28	3/2/29	9/1/41
9. *similis* 7	5/2/29	8/3/30	8/4/29	8/4/29	0/0/1	0/0/0	0/0/1	0/0/1	—	5/0/28	3/1/29	3/2/30	9/1/40
10. *hubbsi*	5/2/15	6/1/28	10/2/26	10/2/26	8/4/30	8/4/31	8/4/32	8/4/32	8/4/31	—	4/1/28	4/2/27	10/1/41
Subgenus *Lethenteron*													
11. *japonica*	9/1/28	6/0/27	7/1/22	7/1/22	9/3/28	9/3/29	9/3/30	9/3/30	9/3/29	8/1/26	—	0/1/1	6/2/47
12. *appendix*	9/1/28	6/0/27	8/1/22	8/1/22	10/3/28	10/3/29	10/3/30	10/3/30	10/3/29	8/1/26	2/0/0	—	6/3/46
Genus *Petromyzon*													
13. *marinus*	10/1/48	9/2/45	15/3/43	15/3/43	13/3/45	13/3/45	13/3/46	13/3/44	13/3/45	10/3/46	12/2/42	12/2/42	—

Note: Sequences of both genes were identical in *L. ayresii* and *L. richardsoni*, as were those in *L. tridentata, L. macrostoma, L. lethophaga,* and *L. similis* from the Merced River, Calif. *Lampetra similis* 1–7 were collected in Oregon; sample sizes and collection sites are given in Table 2.

in that the *L. ayresii* and *L. hubbsi* clade clustered with the *Entosphenus* species rather than with the other *Lampetra* or *Lethenteron* species, but this difference was not reproducible at more than 50% bootstrapping. In all cases, four distinct clades were apparent: (*i*) the *Entosphenus* subgenus without *L.* (*E.*) *hubbsi*, (*ii*) *L.* (*E.*) *hubbsi* with the westcoast North American *L.* (*L.*) *ayresii* and *L.* (*L.*) *richardsoni*, (*iii*) species of the *Lampetra* subgenus from Atlantic drainages, i.e., *L. fluviatilis* and *L. aepyptera*, and (*iv*) the *Lethenteron* species *L. japonica* and *L. appendix*.

A second consensus tree (not shown) was constructed to include 267 bp of cytochrome *b* sequence from *L.* (*L.*) *planeri* and *L.* (*Le.*) *zanandreai* from Italy (Tagliavini et al. 1994). Cytochrome *b* sequence in *L. planeri* was identical to that of *L. fluviatilis* from Germany and the three European species grouped together; *L. zanandreai* did not form a clade with the other *Lethenteron* species. *Lampetra aepyptera* clustered with the three European species but with a lower bootstrap confidence limit (57%) than it did with *L. fluviatilis* in Fig. 1.

Patterns of variation in cytochrome *b* and ND3

Overall nucleotide sequence variation among lamprey species was, on average, 1.35 times greater in the ND3 gene than in the cytochrome *b* gene (Table 3). In both genes, third-position substitutions were more common than variations at first- and second-codon positions, and transition substitutions outnumbered transversions. The fraction of substitutions observed in first-, second-, and third-position sites was 13.8, 2.6, and 83.4%, respectively, in cytochrome *b* and 20.8, 5.2, and 74.1%, respectively, in ND3. In cytochrome *b*, transitions accounted for 85.2% of all substitutions but only 77.1% of substitutions in ND3. Accordingly, the frequency of nonsilent nucleotide substitutions was two to three times higher in ND3 than in cytochrome *b*, and amino acid substitutions averaged 5.1% in ND3 but only 2.0% in cytochrome *b*. However, whereas the frequency of nonsilent substitutions for a given genetic distance was relatively constant among species pairs in ND3, this value was not uniform in cytochrome *b* (Fig. 2). For example, despite a genetic distance between *L. ayresii* and *L. tridentata* nucleotide sequences of 0.079, there were no amino acid differences. Similarly, there were only two amino acid differences between either *L. ayresii* or *L. tridentata* and *P. marinus*. In contrast, all pairwise comparisons with the relict nonparasitic species (*L. aepyptera* or *L. hubbsi*) showed comparatively high rates of nonsilent substitutions, and intermediate rates were observed in pairwise comparisons with *L. appendix* (Fig. 2).

Discussion

Relict species and subgenera

Analysis of partial mitochrondrial DNA sequence permitted resolution of a number of questions concerning the phylogeny of the lamprey genus *Lampetra*. One of the clearest and most notable findings was that *L. hubbsi*, assigned to the genus *Entosphenus* by Vladykov and Kott (1976*a*) based largely on adult dentition (Table 1), appears more closely related to *L.* (*L.*) *ayresii* and *L.* (*L.*) *richardsoni* than it is to any other *Entosphenus* species. On the strength of the mito-

© 1999 NRC Canada

Fig. 1. Neighbour-joining analysis comparing species of the genus *Lampetra* using 735 bp of cytochrome *b* and ND3 sequence; *P. marinus* is the outgroup. Numbers at nodes indicate bootstrap confidence levels; life history type is indicated: P, parasitic; NP, nonparasitic; A, anadromous; FW, freshwater. Collection data are provided in Table 2; locations in which more than one site was sampled are indicated by an asterisk.

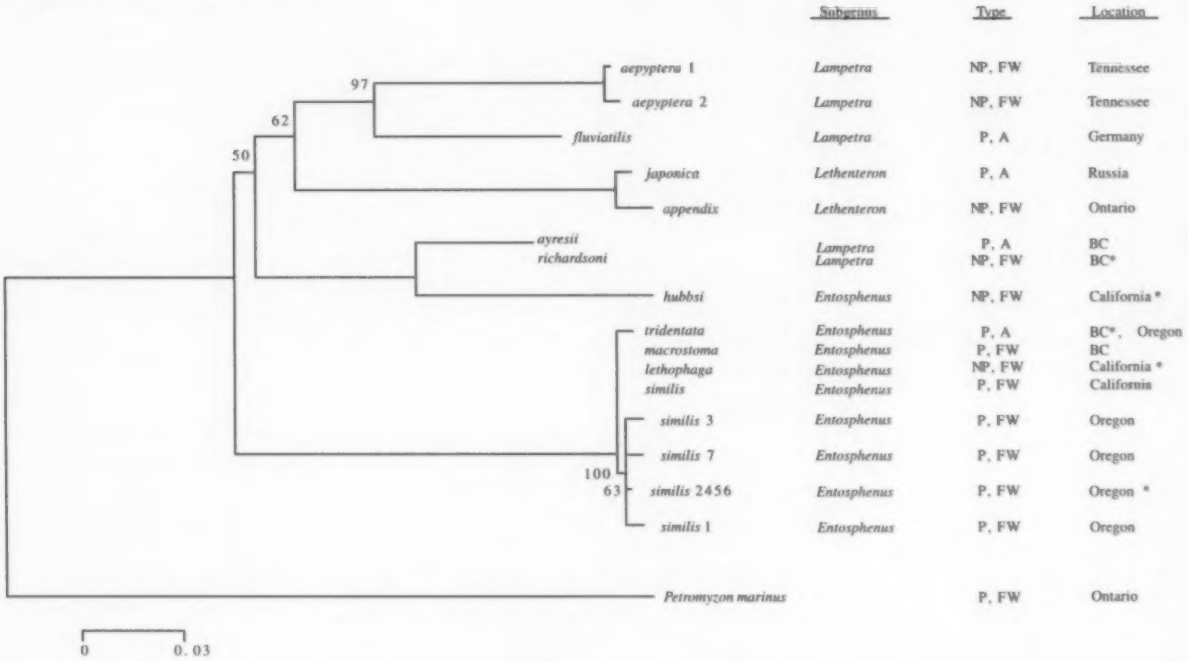

chondrial DNA data, it appears that *L. hubbsi* is a southern relict species of the *L. ayresii* lineage and should be placed in the subgenus *Lampetra*.

Also notable were the findings that two other relict species of the *Lampetra* genus, *L.* (*Le.*) *zanandreai* and *L.* (*L.*) *aepyptera*, both appear to have descended from the *L.* (*L.*) *fluviatilis* lineage. The molecular data show *L. zanandreai* to be more closely related to *L.* (*L.*) *fluviatilis* than to the two *Lethenteron* species and support its original designation as a species of *Lampetra* (Vladykov 1955). As was suggested by Vladykov and Kott (1979*a*), it appears that *L. zanandreai* descended from an *L. fluviatilis*-type ancestor, even though it is no longer sympatric with the present-day *L. fluviatilis* (Bianco 1986). *Lampetra* (*L.*) *aepyptera* likewise is no longer sympatric with any likely parasitic ancestor, and its phylogenetic position within the *Lampetra* genus has been the subject of considerable debate. Its morphological characteristics "are so poorly developed that they render its position and generic placement difficult and somewhat dubious" (Hubbs and Potter 1971), and at one time, it was placed in the "provisional and noncommittal" genus *Okkelbergia* (Hubbs and Potter 1971). Vladykov and Kott (1976*b*), however, concluded that this species displays no characteristics not found in *Lampetra*, and descent from either an *L. ayresii*-type ancestor (Vladykov and Kott 1979*a*) or an *L.* (*Le.*) *japonica*-type ancestor (Bailey 1980; Potter 1980) has been suggested, since both occur in North America. The mitochondrial DNA data are consistent with its present placement in the *Lampetra* subgenus as a nonparasitic species of considerable antiquity (Potter 1980) but suggest descent from an *L.* (*L.*) *fluviatilis*-type ancestor rather than from either North American species.

In addition to resolving these relationships within each of the *Lampetra* subgenera, the current molecular study has resolved some of the relationships among the subgenera. Potter (1980) grouped *Entosphenus*, *Lethenteron*, and *Lampetra* within a single genus largely due to the intergradation of characteristics found in *L. hubbsi*. Its bicuspid supraoral lamina and few velar tentacles are typical of *Lampetra* and *Lethenteron*, but its posterial circumorals and other features of its dentition (Table 1) resulted in its placement in *Entosphenus* (Vladykov and Kott 1976*a*). If *L. hubbsi* is removed from the *Entosphenus* taxon because of its closer genetic similarity to *L.* (*L.*) *ayresii*, however, the molecular data support the previous classifications which have held *Entosphenus* distinct from *Lampetra* and *Lethenteron*.

In contrast, the *Lampetra* and *Lethenteron* subgenera were not clearly delineated. Rather, the species assigned to these two taxa fell into three general groups and there was considerable overlap between the putative subgenera. The three groups were (*i*) the westcoast North American *Lampetra* species (including *L.* (*E.*) *hubbsi*), (*ii*) Atlantic *Lampetra* species from both North America and Europe and *L.* (*Le.*) *zanandreai*, and (*iii*) the two other *Lethenteron* species examined in the current study. It was surprising that the North American and European species of the *Lampetra* subgenus had little more genetic affinity with one another than either did with the other subgenera, since *L. ayresii* and *L. richardsoni*, respectively, were once considered North American races of *L. fluviatilis* and *L. planeri* (Hubbs and

© 1999 NRC Canada

Fig. 2. Frequency of nonsilent substitutions in the cytochrome *b* and ND3 genes of lampreys versus genetic distance for 55 intra- and inter-specific pairwise comparisons. Solid circles represent all comparisons involving the relict nonparasitic species *L. hubbsi* and *L. aepyptera*, closed triangles represent the remaining comparisons involving the nonparasitic *L. appendix*, and open triangles represent all other species comparisons.

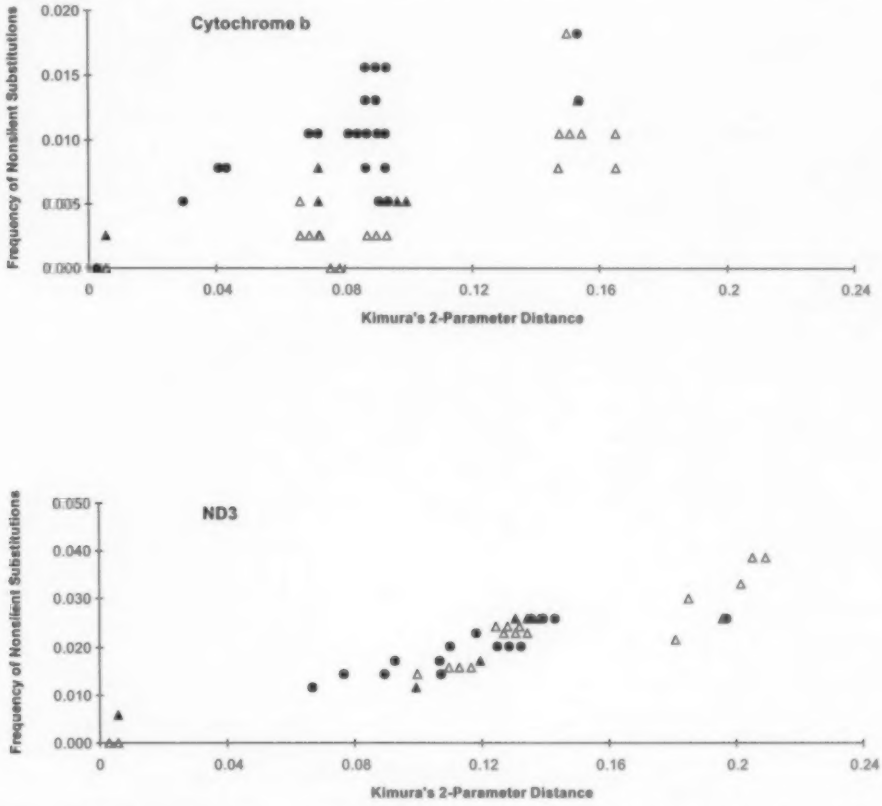

Potter 1971). The distinction between *L. ayresii* and *L. fluviatilis* was based on relatively small differences in body proportions (Table 1) whereas other morphological differences among other species seem not to be taxon distinctive. In particular, the presence of posterial circumorals does not seem to reflect a common evolutionary origin. As was discussed above, *L.* (*E.*) *hubbsi* is genetically most similar to *L.* (*L.*) *ayresii* despite the absence of posterials in the latter species. Posterials are present in most *Lethenteron* species, and like *L. hubbsi*, they are all unicuspid, but *L. hubbsi* did not cluster with these *Lethenteron* species. Likewise, *L. zanandreai* appears to be the only species with posterials in the *L. fluviatilis* lineage, and posterials may be absent in some *L. zanandreai* (Hubbs and Potter 1971; Bianco 1986). As was suggested by Bailey (1980), the presence of posterials appears to be inconsistent and unreliable in the separation of the subgenera, and given the substantial overlap between *Lampetra* and *Lethenteron*, morphologically and genetically, there appears to be little justification for the continued division. However, further clarification is needed; longer gene sequences are required from *L. zanandreai*, and more of the European and Asian representatives of the genus need to be examined. Similarly, complete resolution of the *Lampetra–Lethenteron* relationship will require examination of the *Eudontomyzon* and *Tetrapleurodon* genera. Bailey (1980) included these two taxa from Eurasia and Mexico, respectively, in the *Lampetra* genus, and the subfamily classification of Vladykov and Kott (1979*a*) that groups *Eudontomyzon* with *Lampetra* and *Lethenteron* and *Tetrapleurodon* with *Entosphenus* also implies interrelatedness of these taxa with the three subgenera of *Lampetra*. Molecular data should go a long way toward resolving these taxonomic questions.

Assuming an overall rate of mitochondrial DNA sequence divergence of 2% per million years calculated for several mammalian species (Brown et al. 1979) and used to estimate divergence times in a variety of fish taxa (see review by Billington and Hebert 1991), the three relict species are estimated to have diverged from the *L. fluviatilis* or *L. ayresii* lineages about 0.9–2.7 million years ago. Divergences among the four major clades within the *Lampetra* genus occurred about 3–5 million years ago, and the *Lampetra* and *Petromyzon* genera diverged about 9–13 million years ago, maybe more if a general trend for slower substitution rates in many fishes and other ectotherms (see Billington and Hebert 1991) is also true for lampreys. In particular, suggestions of a slower rate of nonsilent substitutions in fishes relative to birds and mammals (Thomas and Beckenbach 1989) may be true of lampreys. For example, although 28 nucleotide differences were observed in the 384 bp of cytochrome

© 1999 NRC Canada

b sequences from *L. ayresii* and *L. tridentata*, all were silent, and even relative to *P. marinus*, *L. ayresii* or *L. tridentata* cytochrome *b* showed only two amino acid substitutions. It was interesting to note, however, that cytochrome *b* amino acid sequences were less conserved in the relict species (Fig. 2). There were two amino acid differences between the closely related *L. hubbsi* and *L. ayresii* and three between *L. aepyptera* and *L. fluviatilis*. A similarly high rate of replacement substitutions in cytochrome *b* was observed in *L. zanandreai* relative to *L. planeri* (Tagliavini et al. 1994) and suggests either a relaxation of certain functional constraints in these southerly nonparasitic lampreys or directional mutation. This same trend was not seen in the ND3 gene.

Paired and satellite species

In addition to addressing the ambiguous evolutionary relationships of some of the relict nonparasitic species, molecular analysis confirmed that the hypothesized paired species are closely related and diverged from one another more recently than the relict species diverged from their parasitic ancestors. For example, the molecular data agree with the present-day consensus of morphological studies that consider *L.* (*Le.*) *appendix* to be a derivative of *L.* (*Le.*) *japonica*. The paired nature of these two species, however, was not always considered obvious: the two species are no longer sympatric (McPhail and Lindsey 1970), and Zanandrea (1961) listed *L. appendix* as one of three nonparasitic species without a paired species. The molecular data are thus consistent with this hypothesis that *L. appendix* is part of the *L. japonica* assemblage yet more divergent from *L. japonica* than most of the other nonparasitic *Lethenteron* species (e.g., *L. reissneri*; Potter 1980). Applying the above rate of 2% sequence divergence per million years (Brown et al. 1979), *L. japonica* and *L. appendix* are estimated to have diverged about 270 000 years ago. Furthermore, like the above relict species, *L. appendix* showed a relatively high rate of replacement substitutions relative to other species; of the four substitutions observed in both genes between *L. japonica* and *L. appendix*, three were nonsilent.

In contrast, the close genetic relationship between *L. planeri* and the parasitic *L. fluviatilis* was not surprising, since they have long been recognized as paired species (Hubbs and Potter 1971). Similarly, close relationships between *L. richardsoni* and *L. ayresii* and among *L. tridentata* and its presumed freshwater derivatives were expected from morphology-based taxonomies. Most members of paired and satellite species, in fact, were genetically indistinguishable from each other. Given the 735 bp sequenced in the current study, this implies divergences within the past 70 000 years. This rapid speciation is consistent with the distribution of these species and hypothesized changes in drainage patterns and river connections with glaciation. Lake Cowichan drainage patterns, for example, changed about 10 000 years ago, resulting in isolation of the *L. macrostoma* lineage from sea-run *L. tridentata* in the Strait of Georgia (Beamish 1982). In rivers east of the Baltic, *L. planeri* is also believed to have originated within the last 10 000 years (Hubbs and Potter 1971). To detect divergence times of 10 000 years or less, however, it is estimated that more than 5000 bp of the mitochondrial genome would have to be sequenced, or perhaps a more variable region such as the control region (Lee et al. 1995) would be useful.

The lack of observed genetic divergence between members of paired and satellite species is not necessarily inconsistent with each being given species designation. Meyer et al. (1990) found a 363-bp fragment of cytochrome *b* to be identical among seven species of Lake Victoria cichlids, and species designation cannot be decided on sequence differences alone, since rapid morphological differentiation resulting in distinct species may be decoupled from molecular divergence. Most lamprey taxonomies recognize life history type as a significant characteristic distinguishing between closely related species, and the different life history types appear to result in reproductive isolation. Although artificial hybridization between paired species has succeeded in producing viable larvae (e.g., Beamish and Neville 1992), interbreeding appears to be impaired by size differences between the life history types (Beamish and Neville 1992) and temporal and spatial differences in spawning (Beamish 1982).

Despite the lack of detectable differences among several species, intraspecific sequence differences were observed in *L. aepyptera* and *L. similis*. These were within the range found in other fish species (Billington and Hebert 1991), but the consistent genetic differences between populations of *L. similis* were notable. Although *L. similis* from the Merced River in California was genetically indistinguishable from *L. tridentata*, *L. similis* from the Klamath Basin of Oregon differed from them by two or three third-position transitions. This may indicate that the Merced River *L. similis* has arisen from *L. tridentata* more recently than the Oregon populations, and preliminary data suggesting that Merced River *L. similis* exhibits significant morphological and life history differences from the Oregon specimens (R.J. Beamish and J.H. Youson, unpublished data) support this hypothesis. Wide-ranging anadromous lampreys may have given rise to multiple freshwater parasitic or nonparasitic derivatives at different times, and the morphological differences observed among populations in other species (e.g., between *L. pacifica* and the now-synonymous *L. richardsoni* (Table 1), or *L. folletti* and *L. lethophaga*) may also reflect separate origins. More extensive molecular surveys will no doubt uncover more intraspecific differences and reveal the polyphyletic origins of a number of derived species.

In summary, mitochrondrial DNA sequence analysis answered several questions concerning the phylogeny of the lamprey genus *Lampetra*. *Lampetra hubbsi*, assigned to the genus *Entosphenus* largely on the basis of adult dentition, is most closely related to *L. ayresii* and should be placed in the subgenus *Lampetra*. *Lampetra* (*Le.*) *zanandreai* is genetically more similar to *L.* (*L.*) *fluviatilis* than to the other two *Lethenteron* species, and *L.* (*L.*). *aepyptera* is more closely related to *L. (L.) fluviatilis* than to the other North American species. Although there was no distinct division between the subgenera *Lampetra* and *Lethenteron*, *Entosphenus* (without *L. hubbsi*) formed a genetically separable taxon.

Acknowledgements

We thank F.W.H. Beamish, Department of Zoology, University of Guelph, Guelph, Ont., Y. Rosli, Pacific Institute of Fisheries and Oceanography, TINRO, Khabarovsk, Russia, and J.H.

© 1999 NRC Canada

Trautner, Institute of Hydrobiology and Fisheries Science, University of Hamburg, Germany, for their kind donation of samples. We also thank T.D. Kocher, Department of Zoology, University of New Hampshire, Durham, N.H., for many insightful discussions. This study was supported by a Visiting Fellowship in a Canadian Government Laboratory (M.F.D.), the National Biotechnology Strategy (R.H.D.), Department of Fisheries and Oceans grants (R.H.D. and R.J.B.), and a Department of Fisheries and Oceans/Natural Sciences and Engineering Research Council of Canada Science Subvention grant (J.H.Y.).

References

Bailey, R.M. 1980. Comments on the classification and nomenclature of lampreys — an alternative view. Can. J. Fish. Aquat. Sci. **37**: 1626–1629.

Beamish, R.J. 1982. *Lampetra macrostoma*, a new species of freshwater parasitic lamprey from the west coast of Canada. Can. J. Fish. Aquat. Sci. **39**: 736–747.

Beamish, R.J., and Neville, C-M.E. 1992. The importance of size as an isolating mechanism in lampreys. Copeia, **1992**: 191–196.

Bianco, P.G. 1986. *Lethenteron zanandreai* (Vladykov, 1955). *In* The freshwater fishes of Europe. Vol. 1. Part I. Petromyzoniformes. *Edited by* J. Holčík. AULA-Verlag, Weisbaden. pp. 237–246.

Billington, N., and Hebert, P.D.N. 1991. Mitochondrial DNA diversity in fishes and its implications for introductions. Can. J. Fish. Aquat. Sci. **48**(Suppl. 1): 80–94.

Brown, W.M., George, M., Jr., and Wilson, A.C. 1979. Rapid evolution of animal mitochondrial DNA. Proc. Natl. Acad. Sci. U.S.A. **76**: 1967–1971.

Cantatore, P., Roberti, M., Pesole, G., Ludovico, A., Milella, F., Gadaleta, M.N., and Saccone, C. 1994. Evolutionary analysis of cytochrome *b* sequences in some Perciformes: evidence for a slower rate of evolution than in mammals. J. Mol. Evol. **39**: 589–597.

Hardisty, M.W. 1986. General introduction. *In* The freshwater fishes of Europe. Vol. 1. Part I. Petromyzoniformes. *Edited by* J. Holčík. AULA-Verlag, Weisbaden. pp. 19–83.

Hubbs, C.L. 1971. *Lampetra* (*Entosphenus*) *lethophaga*, new species, the nonparasitic derivative of the Pacific lamprey. Trans. San Diego Soc. Nat. Hist. **16**: 125–164.

Hubbs, C.L., and Potter, I.C. 1971. Distribution, phylogeny and taxonomy. *In* The biology of lampreys. Vol. 1. *Edited by* M.W. Hardisty and I.C. Potter. Academic Press, London, U.K. pp. 1–65.

Janvier, P., and Lund, R. 1983. *Hardistiella montanensis* n. gen. et sp. (Petromyzontida) from the Lower Carboniferous of Montana, with remarks on the affinities of lampreys. J. Vertebr. Paleontol. **2**: 407–413.

Kimura, M. 1980. A simple method for estimating evolutionary rate of base substitutions through comparative studies of nucleotide sequences. J. Mol. Evol. **16**: 111–120.

Kumar, S., Tamura, K., and Nei, M. 1993. MEGA: Molecular Evolutionary Genetics Analysis, version 1.01. Pennsylvania State University Press, University Park, Pa.

Lee, W-J., and Kocher, T.D. 1995. Complete sequence of a sea lamprey (*Petromyzon marinus*) mitochondrial genome: early establishment of the vertebrate genome organization. Genetics, **139**: 873–887.

Lee, W-J., Conroy, J., Howell, W.H., and Kocher, T.D. 1995. Structure and evolution of teleost mitochondrial control regions. J. Mol. Evol. **41**: 54–66.

McPhail, J.D., and Lindsey, C.C. 1970. Freshwater fishes of northwestern Canada and Alaska. Bull. Fish. Res. Board Can. No. 173.

McVeigh, H.P., and Davidson, W.S. 1991. A salmonid phylogeny inferred from mitochondrial cytochrome *b* gene sequences. J. Fish Biol. **39A**: 277–282.

Meyer, A., Kocher, T.D., Basasibwaki, P., and Wilson, A.C. 1990. Monophyletic origin of Lake Victoria cichlid fishes suggested by mitochondrial DNA sequences. Nature (Lond.), **347**: 550–553.

Palumbi, S.R. 1996. Nucleic acids II: the polymerase chain reaction. *In* Molecular systematics. 2nd ed. *Edited by* D.M. Hillis, C. Moritz, and B.K. Mable. Sinauer Associates, Inc., Sunderland, Mass. pp. 205–247.

Potter, I.C. 1980. The Petromyzoniformes with particular reference to paired species. Can. J. Fish. Aquat. Sci. **37**: 1595–1615.

Richards, J.E., Beamish, R.J., and Beamish, F.W.H. 1982. Descriptions and keys for ammocoetes of lampreys from British Columbia, Canada. Can. J. Fish. Aquat. Sci. **39**: 1484–1495.

Robins, C.R., Bailey, R.M., Bond, C.E., Brooker, J.R., Lachner, E.A., Lea, R.N., and Scott, W.B. 1980. A list of common and scientific names of fishes from the United States and Canada. Am. Fish. Soc. Spec. Publ. No. 12.

Robins, C.R., Bailey, R.M., Bond, C.E., Brooker, J.R., Lachner, E.A., Lea, R.N., and Scott, W.B. 1991. Common and scientific names of fishes from the United States and Canada. Am. Fish. Soc. Spec. Publ. No. 20.

Tagliavini, J., Tizzi, R., Conterio, F., Mariottini, P., and Gandolfi, G. 1994. Mitochondrial DNA sequences in three genera of Italian lampreys. Boll. Zool. **61**: 331–333.

Thomas, W.K., and Beckenbach, A.T. 1989. Variation in salmonid mitochondrial DNA: evolutionary constraints and mechanisms of substitution. J. Mol. Evol. **29**: 233–245.

Vladykov, V.D. 1955. *Lampetra zanandreai*, a new species of lamprey from northern Italy. Copeia, **1955**: 215–223.

Vladykov, V.D. 1973. *Lampetra pacifica*, a new nonparasitic species of lamprey (Petromyzontidae) from Oregon and California. J. Fish. Res. Board Can. **30**: 205–213.

Vladykov, V.D., and Follett, W.I. 1958. Redescription of *Lampetra ayresii* (Günther) of western North America, a species of lamprey (Petromyzonidae) distinct from *Lampetra fluviatilis* (Linnaeus) of Europe. J. Fish. Res. Board Can. **15**: 47–77.

Vladykov, V.D., and Follett, W.I. 1965. *Lampetra richardsoni*, a new nonparasitic species of lamprey (Petromyzonidae) from western North America. J. Fish. Res. Board Can. **22**: 139–158.

Vladykov, V.D., and Kott, E. 1976*a*. A new nonparasitic species of lamprey of the genus *Entosphenus* Gill, 1862 (Petromyzonidae) from south central California. Bull. South. Calif. Acad. Sci. **75**: 60–67.

Vladykov, V.D., and Kott, E. 1976*b*. Is *Okkelbergia* Creaser and Hubbs, 1922 (Petromyzonidae) a distinct taxon? Can. J. Zool. **54**: 421–425.

Vladykov, V.D., and Kott, E. 1976*c*. A second nonparasitic species of *Entosphenus* Gill, 1862 (Petromyzonidae) from Klamath River system, California. Can. J. Zool. **54**: 974–989.

Vladykov, V.D., and Kott, E. 1979*a*. Satellite species among the holarctic lampreys (Petromyzonidae). Can. J. Zool. **57**: 860–867.

Vladykov, V.D., and Kott, E. 1979*b*. A new parasitic species of the holarctic lamprey genus *Entosphenus* Gill, 1862 (Petromyzonidae) from Klamath River, in California and Oregon. Can. J. Zool. **57**: 808–823.

Zanandrea, G. 1959. Speciation among lampreys. Nature (Lond.), **184**: 380.

Zanandrea, G. 1961. Studies on European lampreys. Evolution, **15**: 523–534.

© 1999 NRC Canada

Dispersal of early life stage haddock (*Melanogrammus aeglefinus*) as inferred from the spatial distribution and variability in length-at-age of juveniles

Nancy L. Shackell, Kenneth T. Frank, Brian Petrie, David Brickman, and Jennifer Shore

Abstract: In southwestern Nova Scotia, haddock (*Melanogrammus aeglefinus*) spawning is centered on Browns Bank where the variability of a partial gyre influences the distribution of eggs and larvae. An unknown proportion of each year-class is advected northward to the Bay of Fundy. We examined the variability in length at age 2 as an index of retention during early life. We assumed that early life stages that are retained in the Scotian Shelf area grow more slowly, while those that are advected into the Bay of Fundy grow more quickly. An optimization program was used to estimate the proportions of Scotian Shelf and Bay of Fundy sized components in length at age 2 bimodal frequency distributions for year-classes 1968–1993. The median proportion of Scotian Shelf sized fish was 0.89. A physical circulation model showed that the majority of particles released on Browns Bank drifted towards the Bay of Fundy. Results of the physical model and the size-based index differ partly because the former predicts the fate of passive particles, while the latter is an integrated measure of the proportion of fish retained and surviving. Survival is associated with high wind stress ($r = -0.5$, $p = 0.011$, $n = 25$) implying a higher probability of survival of those retained in the Scotian Shelf region.

Résumé : Dans le sud-ouest de la Nouvelle-Écosse, le frai de l'aiglefin (*Melanogrammus aeglefinus*) est surtout concentré sur le banc Browns où la variabilité d'une circulation partielle influe sur la distribution des oeufs et des larves. Une proportion inconnue de chaque classe d'âge est ainsi attirée en direction nord, vers la baie de Fundy. Nous avons examiné la variabilité de la longueur à l'âge 2 à titre d'indice de rétention pendant le début de la vie. Nous avons supposé que les individus des premières étapes du cycle vital retenus dans la zone de la plate-forme Scotian présentaient une croissance plus lente que ceux attirés par advection vers la baie de Fundy. Un programme d'optimisation a été appliqué à l'estimation des proportions des composantes par tailles des individus de la plate-forme Scotian et de la baie de Fundy au sein des distributions de fréquences bimodales des longueurs à l'âge 2 des classes d'âge de 1968 à 1993. La proportion médiane des poissons de la taille correspondant à celle de la plate-forme Scotian était de 0,89. Un modèle de circulation physique a montré que la majorité des particules libérées au banc Browns dérivaient en direction de la baie de Fundy. Les résultats du modèle physique et l'indice fondé sur la taille diffèrent notamment parce que le premier prévoit le devenir de particules passives tandis que le second est une mesure intégrée de la proportion des poissons retenus qui ont survécu. La survie est associée à la force élevée d'entraînement du vent $r = -0,5$; $p = 0,011$; $n = 25$), ce qui suppose une probabilité de survie plus élevée pour les individus retenus dans la région de la plate-forme Scotian.

[Traduit par la Rédaction]

Introduction

Haddock (*Melanogrammus aeglefinus*) spawn in three principal areas in the northwest Atlantic: Western Bank and Browns Bank on the Scotian Shelf (SS) and Georges Bank in the Gulf of Maine (Fig. 1). Each of these spawning areas constitutes a discrete management unit for haddock. Peak spawning on Browns Bank occurs in April–May (Hurley and Campana 1989). While there is limited spawning on some of the other offshore banks, there is no spawning in inshore areas.

The circulation and dispersion on Browns Bank have been shown to influence the distribution of haddock eggs and larvae. The circulation on Browns Bank is characterized by a year-round clockwise partial gyre, which is weakened typically by wind-forced currents. The range of residence time at 10 m is from 5 to 25 days with a 14-day average (Smith 1989). Initially, O'Boyle et al. (1984) noted that haddock larvae were retained on Browns Bank and proposed that this

Received November 25, 1998. Accepted August 25, 1999. J14920

N.L. Shackell[1] **and K.T. Frank.** Department of Fisheries and Oceans, Marine Fish Division, Bedford Institute of Oceanography, Dartmouth, NS B2Y 4A2, Canada.
B. Petrie, D. Brickman, and J. Shore. Department of Fisheries and Oceans, Ocean Sciences Division, Bedford Institute of Oceanography, Dartmouth, NS B2Y 4A2, Canada.

[1]Author to whom all correspondence should be addressed. e-mail: shackelln@mar.dfo-mpo.gc.ca

© 1999 NRC Canada

was a consequence of the gyre; larvae advected away from the bank, they hypothesized, represented population losses. In 1985, Campana et al. (1989*a*) observed that the majority of larval haddock appeared to be retained on or near Browns Bank but that a portion of the population was advected inshore. This portion may have been distributed continuously into the eastern Bay of Fundy (BoF)/Digby Neck area, although no direct observations were available to support this claim (Campana et al. 1989*a*). Campana et al. (1989*a*) proposed that the variability in the leakiness of the gyre influenced the proportion of larvae retained and subsequently the variability of year-class abundance. We undertook to develop indices that can be examined as proxies for the surviving proportion of a year-class retained in the SS region during the early life history stage.

There are no long time series of egg/larval distributions in the study area; however, we do have annual trawl surveys that provide information on juvenile (ages 1 and 2) distributions. Assuming that juveniles do not migrate, we can use the relative abundance of juveniles in the SS area as a potential "geographical" index of the proportion of a year-class retained and surviving in that area.

Because juveniles may migrate, we also developed a size-based retention/survival index. A consequence of the spatial separation of a given year-class is that two distinct growth patterns occur. Juvenile haddock sampled in the BoF in July are, on average, larger at age than haddock collected offshore on the southwestern SS (Hurley et al. 1997). This situation is not unique to haddock, as Atlantic cod (*Gadus morhua*) show a similar growth pattern between the two geographic areas (Clark and Brown 1996). Differences in growth rates may be established during the larval period because of spatial gradients in planktonic prey or predator abundance known to exist between the two areas (Frank 1988; Suthers and Frank 1990). If growth differences are generated upon settling, the greater rate of growth observed in the BoF may reflect its higher bottom temperature (Marshall 1995) and (or) its richer benthic food supply relative to offshore (Wildish et al. 1989).

Our assumption that growth differences seen at the juvenile stage are established during the early life history (either during the larval stage or at the settlement stage) is based on empirical data. Growth differences observed during the larval stage were maintained in the juvenile stage in laboratory studies (Rosenberg and Haugen 1982; Chambers et al. 1988). In juvenile/adult stages, a correlation between earlier and later weights-at-age in northern Atlantic cod has been observed in the field (Krohn and Kerr 1997).

The proportion of juveniles in a given year-class of SS size should represent the proportion that had been retained during early life in the SS area and had survived. Conversely, the proportion of juveniles in a given year-class that are of BoF size should represent the proportion that had been dispersed as eggs, larvae, or postlarvae from Browns Bank to the BoF and had survived.

In this paper, we investigate whether the spatial distribution of juveniles and (or) the variability in length-at-age of juvenile haddock in southwestern Nova Scotia can be used to infer dispersal patterns during the early life history. We present geographical and size-based retention/survival indices and hypothesize that they reflect the surviving proportion of a year-class retained on the SS during early life history. We then examine the indices in relation to survival and wind stress to address the suggestion of Campana et al. (1989*a*) of covariability in cohort survival and gyre leakiness. Finally, we compare the results of the biological indices of retention/survival with the physical retention as suggested by particle tracking using the climatological spring flow fields off southwestern Nova Scotia.

Materials and methods

Biological research vessel survey data

The SS is divided into Northwest Atlantic Fisheries Organization (NAFO) statistical divisions that form the basic fishery management units. The haddock in southwestern Nova Scotia are managed as a unit stock within NAFO Division 4X (Fig. 1). Since 1970, the Canadian Department of Fisheries and Oceans has conducted annual bottom trawl surveys on the SS. The shelf is divided into strata based on depth, and trawl samples (sets) of groundfish are taken randomly within each stratum. The sampling intensity is proportional to stratum area. There are roughly 90–120 sets per survey in NAFO Division 4X, which begins at stratum 70 and ends in the BoF (for further survey details, see Halliday and Koeller 1981). The strata representing the BoF include strata 85, 90, 91, and 95, while those representing the offshore southwestern SS include strata 70–81 (Fig. 1). These survey strata have been used to assess the status of the NAFO Division 4X haddock. Estimates of population numbers-at-age from the survey are scaled to adjust for areal differences among strata (see Hurley et al. 1997).

Geographical and size-based indices of retention/survival

Our main goal was to estimate the proportion of a given year-class that was retained near its principal spawning ground (Browns Bank, SS) during the early life history. Initially, we examined the relative proportions of age 2 haddock in the SS and BoF areas. If juveniles were sampled accurately and did not migrate, the proportion of juveniles in the SS region represented the surviving proportion that was retained there during the egg/larval/postlarval period, and we refer to that as SS_G.

Our second approach was to use the spatial size variation of age 2 haddock. The first immature age group fully available to the survey gear occurs at age 2. Ages 0 and 1 haddock are poorly sampled relative to the older ages and are not as representative of the population. Age 2 BoF juveniles are on average larger than age 2 SS juveniles. The size difference between BoF and SS varies among years (Fig. 2). Also, differences at age 2 propagate through to the older age-classes for the majority of year-classes (Hurley et al. 1997). In some years, sizes-at-age are quite distinct between the two areas and in other years are similar. However, there are no years in which mean length at age 2 of the SS haddock exceeds that of BoF haddock.

We used the growth differences to estimate the proportion of BoF-sized fish and proportion of SS-sized fish by testing for bimodality in length-at-age frequency distributions for all strata combined. For each haddock year-class from 1968 to 1993 at age 2, we compiled catch-weighted length-at-age frequency distributions to yield total population numbers-at-length-at-age matrices. Selected examples are shown in Fig. 3. The range of sizes is quite broad, about 20 cm in most cases, and the shape of the length at age 2 frequency distributions varies considerably.

A unimodal length-at-age frequency distribution represents samples of fish from a similar growth regime. Bimodality represents samples of fish from dissimilar growth regimes. If all surviving larvae were retained in the SS region, we would expect a unimodal

© 1999 NRC Canada

Fig. 1. Southwestern SS showing the SS strata (70–81) and BoF strata (85, 90, 91, 95) from bottom trawl surveys of NAFO fishery Division 4X (broken line).

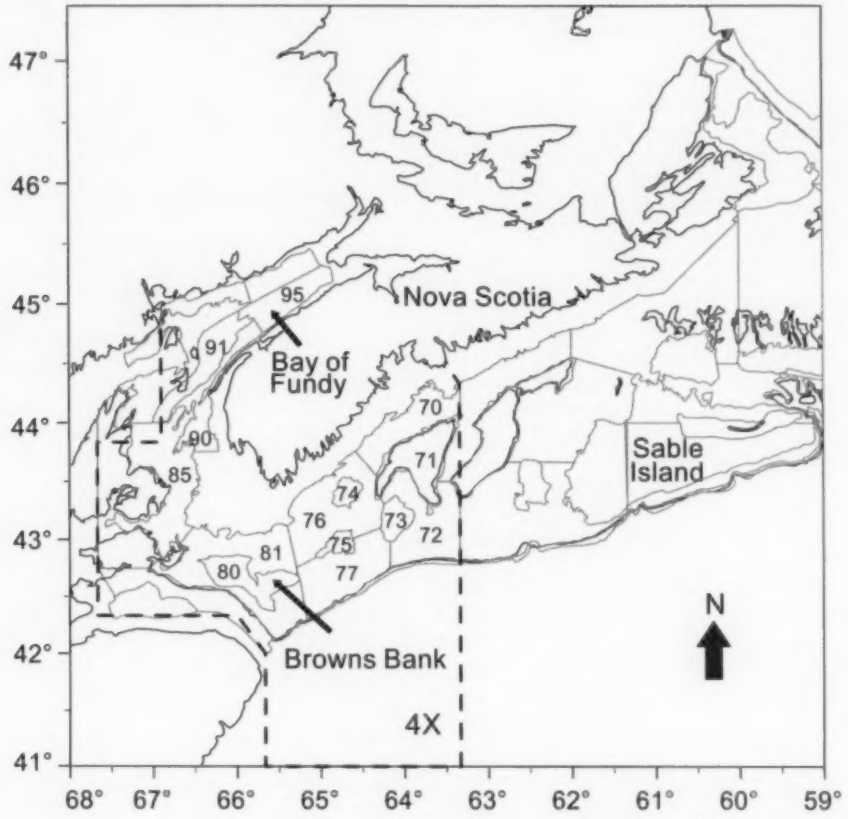

Fig. 2. Time series of mean length at age 2 estimated from research vessel surveys. Solid line, BoF; broken line, SS.

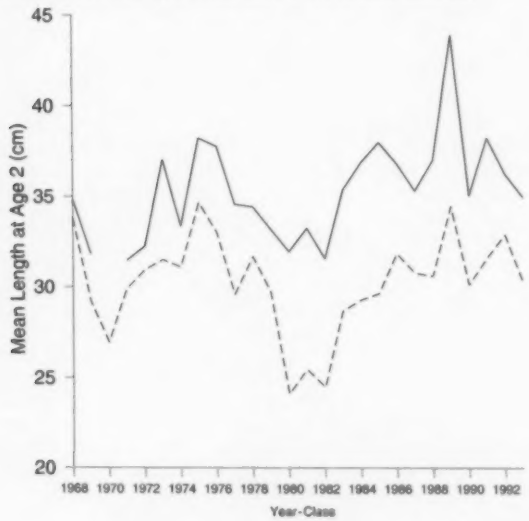

length frequency distribution and a relatively smaller mean length-at-age. If all surviving larvae were advected away from the bank region, we would expect a unimodal length frequency distribution and a relatively larger mean length-at-age. If the length-at-age frequency distribution for a given year-class was bimodal, and one of the modes corresponded to the average length-at-age of the SS and the other mode corresponded to the average length-at-age of the BoF, we inferred that the bimodality corresponded to a mixture of fish having grown up in either SS or BoF.

We created a size-based index of the surviving proportion of haddock retained in the SS region (SS_S) using "mixture analysis" (MacDonald and Pitcher 1979) in an optimization program developed by Ichthus Data Systems (59 Arkell St., Hamilton, ON L8S 1N6, Canada).

A mixed probability density function g of variable x is the sum of weighted k component densities, consisting of parameters of Gaussian distributions: proportions (π_i), means (μ_i), and variances (σ_i) where $i = 1$ to k:

$$g(x) = \pi_1 f_1(x) + \ldots + \pi_k f_k(x).$$

The goal of the mixture modelling was to determine whether the data were best fit by a bimodal versus unimodal distribution of the 4X area (both BoF and SS). For each year-class, the goal was to see whether a unimodal ($g(x) = \pi_1 f_1(x)$) or bimodal ($g(x) = \pi_1 f_1(x) + \pi_2 f_2(x)$) distribution fit the data through the use of the optimization program. A maximum mikelihood method and quasi-Newton algo-

© 1999 NRC Canada

Fig. 3. Length-at-age frequency distributions of selected year-classes. The top panels show unimodal distributions, while the middle and bottom panels show varying degrees of bimodality. Year-classes: (*a*) 1969, (*b*) 1978, (*c*), 1974, (*d*)1975, (*e*)1977, and (*f*) 1979.

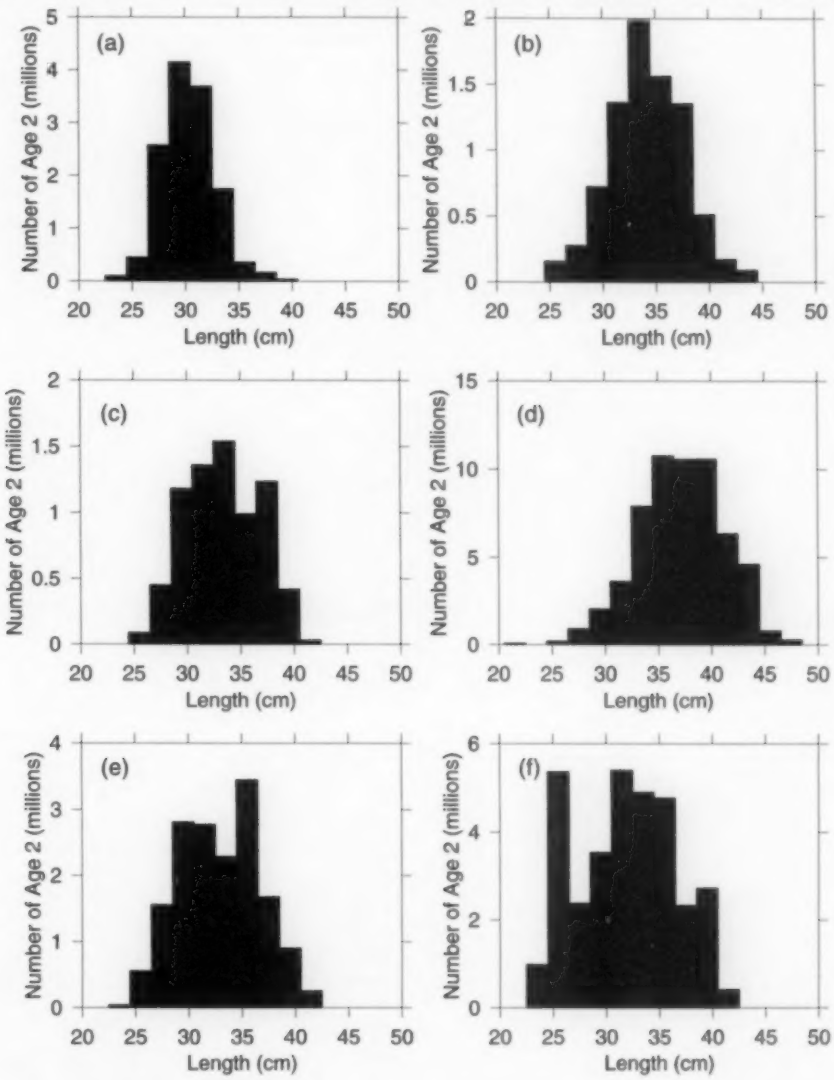

rithm were used to estimate parameters. In this optimization program, parameters are tested for goodness-of-fit based on a χ^2 approximation to the likelihood ratio test (MacDonald and Pitcher 1979). That is, a function is minimized and used as a χ^2 statistic to test for goodness-of-fit. The function is scale dependent. Larger values produce larger differences between expected and observed; therefore, the standard errors of the estimates are very small and the χ^2 statistic is inflated for very large sample sizes. Simply stated, the program does not work for very large samples. We scaled down the stratified sample sizes for each year-class by dividing through a factor of 1000 in order to be within the range suitable for the optimization program. The parameter estimates themselves did not change substantially between the original and the scaled down samples, but the standard errors of the estimates were larger in the scaled down samples.

One of our goals was to examine the relationship of the derived indices of retention/survival (SS_G and SS_S) with survival (recruitment), wind stress, and the physical oceanographic prediction of the proportion retained near the spawning area. We developed a survival index by dividing the numbers of age 1 by the spawner biomass (ages 3 and older) that produced that year-class. We used the data as derived from virtual population analysis in Hurley et al. (1997).

Wind stress was calculated using the formulation of Smith and Banke (1975) from hourly observations of wind speed and direction made at Sable Island (Fig. 1). Earlier studies indicated that the winds at Sable Island are representative of conditions over the SS (Petrie and Lively 1979; Sandstrom 1980). Scalar average monthly wind stresses were calculated from the hourly values. We used the scalar average of the monthly mean magnitudes during the peak spawning period (April–June) as our primary physical forcing to explore the hypothesis that the important factor was whether fish

© 1999 NRC Canada

Table 1. Summary of SS_G of year-classes 1968–1993: geographically based mean lengths at age 2 (SDs in parentheses) estimated separately from the SS and BoF, proportion of year-classes within the SS region, and number of individuals (N) estimated from research vessel surveys.

Year-class	SS mean length at age 2 (cm)	BoF mean length at age 2 (cm)	SS_G	N
1968	33.9 (2.7)	34.8 (1.8)	0.97	5 458 514
1969	29.2 (2.4)	31.8 (2.7)	0.98	13 211 318
1970	26.9 (2.9)		1	272 732
1971	29.9 (2.7)	31.5 (2.8)	0.84	26 797 262
1972	30.9 (2.5)	32.2 (2.1)	0.90	26 950 598
1973	31.5 (3.1)	37 (2)	0.83	4 032 985
1974	31 (3)	33.4 (3.4)	0.64	6 677 248
1975	34.7 (3.3)	38.2 (3.7)	0.89	47 201 832
1976	33 (3)	37.7 (3)	0.84	6 201 386
1977	29.6 (3)	34.6 (2.9)	0.52	16 254 005
1978	31.7 (3.2)	34.4 (2.8)	0.46	8 275 671
1979	29.7 (3.1)	33.2 (4.2)	0.14	32 529 585
1980	24.1 (3)	32 (3.3)	0.64	39 440 070
1981	25.5 (4.1)	33.2 (3.5)	0.54	7 572 376
1982	24.5 (3.5)	31.6 (3.7)	0.38	30 985 516
1983	28.7 (5.7)	35.4 (2.1)	0.74	13 172 362
1984	29.3 (2.8)	36.8 (2.5)	0.96	13 425 186
1985	29.6 (3.6)	38 (1.7)	0.73	2 168 612
1986	31.9 (2.4)	36.8 (3)	0.50	2 943 344
1987	30.8 (3.2)	35.3 (3.7)	0.73	13 828 229
1988	30.6 (1.9)	37 (3)	0.60	15 038 949
1989	34.5 (3.9)	43.9 (3.8)	0.64	2 027 616
1990	30.1 (2.5)	35 (2.4)	0.87	3 527 194
1991	31.6 (3.2)	38.2 (3.5)	0.84	1 500 713
1992	32.9 (3.1)	36.2 (3)	0.62	8 254 250
1993	30.3 (2.7)	35 (3.1)	0.85	20 495 074

during early life were retained in the SS region or not. This provides a crude measure of wind forcing during early life history and does not reflect some potentially important factors such as wind direction, stress variability, and the vertical structure in the wind-driven currents.

Potential drift patterns of larvae from Browns Bank were determined by tracking passive particles in three-dimensional model flow fields consisting of the climatological spring mean currents and the M2 tidal currents (C.G. Hannah, P.O. Box 1009, Department of Fisheries and Oceans, Dartmouth, NS B2Y 4A2, Canada, unpublished data). The flow fields were obtained from a circulation model (Lynch et al. 1992) initialized and forced by observational data on the tides, seasonal mean wind stress, and seasonal mean density fields (Han et al. 1997) and additional horizontal mixing (eddy diffusivity $K = 50\ m^2 \cdot s^{-1}$). The model fields agree well with observational current data from moored measurements and drifters in the Browns Bank region. The particle tracking was carried out using the methodology of Werner et al. (1993).

Results

Geographical index of retention/survival (SS_G)

The proportion of age 2 juveniles found in the SS region ranged from 0.14 to 1. The mean and median were 0.72 (SD = 0.21) and 0.74, respectively. In most instances, the distribution of juveniles would suggest that the majority of a year-class was retained in the SS region, with the exception of the 1978, 1979, and 1982 year-classes (Table 1).

Size-based index of retention/survival (SS_S)

Combining the data from the entire region (SS and BoF), parameters (proportions, means, and SDs) were initialized and (or) constrained for each year-class, prior to fitting the model. The most useful approach to fitting the model was to have some prior knowledge of parameter values as well as to examine visually the length frequency distributions. To gain a sense of year-class specific growth rate, we estimated mean length-at-age and SD for BoF and Browns Bank/SS separately (Table 1). The spatial distribution of age 2 haddock may not have remained constant since the egg/larval stage, which is one of the reasons that we wished to use a mixture analysis approach.

We judged the model fits using the goodness-of-fit criterion and the geographical mean lengths as a guideline to assess the model parameter estimates of mean length-at-age. When a bimodal model was the best fit, changing the starting values and rerunning the program checked the stability of the parameter estimates. Only those years that fit the goodness-of-fit criterion are presented (Table 2). Both bimodal and unimodal fits of year-classes 1971, 1972, 1979, 1981, and 1990 did not meet the goodness-of-fit criterion.

Mixtures of BoF- and SS-sized fish were found in several years, although irregular length frequency distributions in some years with very few data precluded an evaluation of the entire time series. That is, the length frequency distributions of the 1970, 1985, 1986, and 1989 year-classes were

© 1999 NRC Canada

Table 2. Summary of mixture analysis of year-classes 1968–1993.

Year-class	Mode 1 Mean	Mode 1 SD	Mode 2 Mean	Mode 2 SD	Mode 1 prop	Mode 2 prop	χ^2	p
1968	32.79	2.67			1.00		1.82	0.762
	(0.37)	(0.28)						
1969	28.28	2.44			1.00		2.85	0.723
	(0.22)	(0.16)						
1973	31.72	3.77			1.00		12.1	0.0596
	(0.19)	(0.14)						
1974	30.08	2.72	35.64	1.14	0.79	0.21	0.4808	0.7863
	(0.95)	(0.62)	(0.89)	(0.74)	(0.16)	(0.16)		
1975	34.64	3.89	39.2	2.06	0.89	0.11	12.41	0.134
	(0.65)	(0.24)	(1.16)	(1.27)	(0.14)	(0.14)		
1976	31.60	2.67	38.9	2.38	0.74	0.26	1.36	0.8518
	(0.84)	(0.57)	(1.8)	(1.1)	(0.15)	(0.15)		
1977	27.68	2.20	33.57	2.43	0.46	0.54	2.26	0.5195
	(0.98)	(0.55)	(1.1)	(0.54)	(0.17)	(0.17)		
1978	32.15	3.47			1.00		9.76	0.2025
	(0.12)	(0.09)						
1980	24.49	3.78	33.45	2.94	0.93	0.07	0.8849	0.9896
	(0.51)	(0.35)	(3.17)	(1.47)	(0.08)	(0.08)		
1982	23.54	2.98	31.45	2.83	0.62	0.38	8.53	0.288
	(0.66)	(0.4)	(0.95)	(0.53)	(0.1)	(0.1)		
1983	23.93	2.9	33.7	3.2	0.44	0.56	9.14	0.2425
	(0.81)	(0.56)	(0.75)	(0.52)	(0.08)	(0.08)		
1984	26.04	1.52	30.92	4.2	0.2	0.8	2.61	0.7603
	(0.64)	(0.71)	(0.71)	(0.34)	(0.11)	(0.11)		
1987	30.43	3.22	37.72	2	0.93	0.07	1.38	0.9265
	(0.63)	(0.43)	(2.78)	(1.54)	(0.1)	(0.1)		
1988	29.27	1.87	33.45	4.53	0.45	0.55	3.78	0.7064
	(0.45)	(0.5)	(1.11)	(0.48)	(0.15)	(0.15)		
1991	29.92	2.24	37.71	2.26	0.77	0.23	3.45	0.3277
	(0.31)	(0.25)	(0.8)	(0.62)	(0.06)	(0.06)		
1992	32.00	4.02			1.00		10.4	0.1089
	(0.44)	(0.33)						
1993	31.40	3.56			1.00		6.89	0.5488
	(0.2)	(0.15)						

Note: Mode 1 and Mode 2 refer to the model estimates that correspond to SS-sized and BoF-sized juveniles, respectively, and "prop" refers to the model estimates of the proportions of the length frequency distributions for each mode. The SEs of the model estimates are given in parentheses. χ^2 is the χ^2 approximation minimized in the optimization program, and p is the probability that the model fit the data.

too irregular to classify as either normal or bimodal. These year-classes were also associated with very low abundance, and so it is probable that the year-classes were not sampled well enough to conduct mixture analysis. The proportions of BoF- and SS-sized fish varied somewhat, but larger proportions were generally of SS-sized fish, suggesting that retention was the most common condition and (or) that retention favoured survival (Table 2; Figs. 4 and 5).

If SS_G and SS_S were reflecting the surviving proportion retained near their spawning grounds during early life history, then we would expect them to be correlated. However, the two indices were not significantly correlated ($r = 0.161$, $p = 0.563$, $n = 17$) (Table 3).

Is either SS_G or SS_S related to survival?

Both SS_G and SS_S are based on information about juveniles. Clearly, any retention index constructed from information about juveniles represents the proportion of a year-class retained *and* surviving. This raises the question of whether there is differential survival between the SS region and BoF during early life history. The Browns Bank partial gyre is hypothesized to retain eggs and larvae, and both SS_G and SS_S suggest that retention favours survival. We hypothesized that as wind stress increases, more larvae are advected away from the bank and lost to the population. We explored representations of the wind field including the vector-averaged wind stress, scalar-averaged wind stress, and scalar-averaged wind stress variance (which includes high-frequency components of the wind field) over the peak period of spawning (April–June). We then examined the relationship between survival to age 1 (ln(age 1 population numbers at time t/age 3 + biomass at time $t - 1$)) and representations of wind stress. The strongest correlation was between survival and wind stress magnitude ($r = -0.5$, $p = 0.011$, $n = 25$), suggesting that survival is lower as higher proportions of larvae are advected away from the spawning area (Table 3; Fig. 6*a*). It

© 1999 NRC Canada

Fig. 4. Selected examples of model fit from the mixture analysis optimization program showing unimodal model fits (top panels) and varying degrees of bimodality (middle and bottom panels). Parameter estimates of mean length at age 2 are given below the histograms, SD's are given in parentheses below the means, and parameter estimates of proportions are given within histograms. 69YC refers to the 1969 year-class, etc.

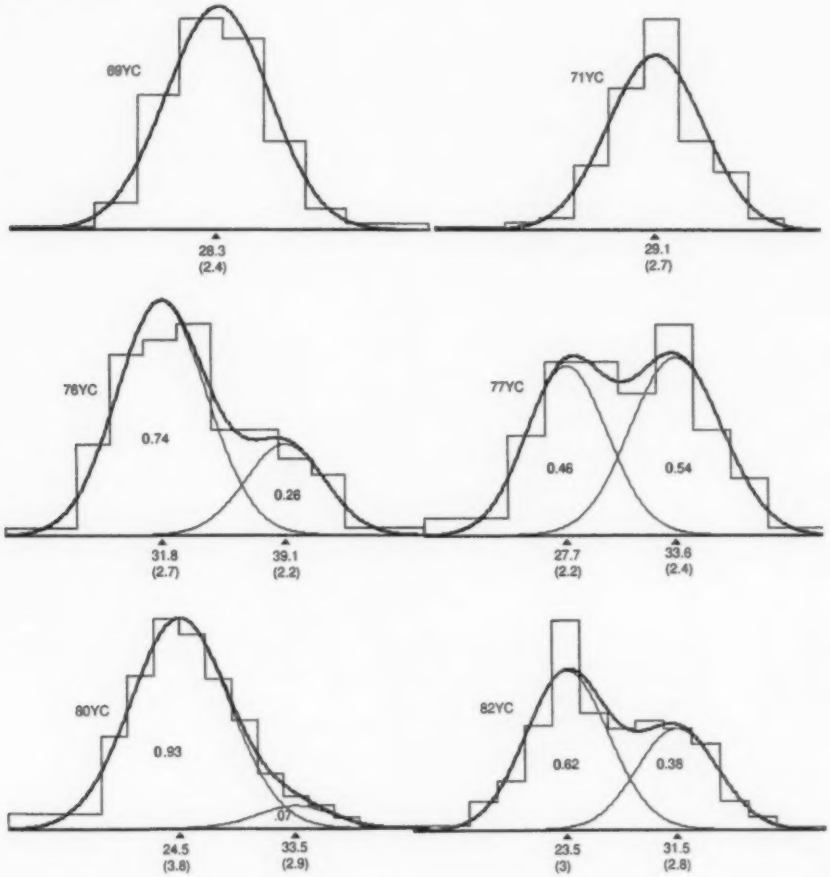

appears that in the complex circulation field in southwestern Nova Scotia, the magnitude of wind stress is more important than its direction. Moreover, it also implies that the longer time over which the monthly stresses act outweighs the stronger (by a factor of 3.4 on average) but shorter period high-frequency components.

Given that wind-based retention favours survival, we expected that either the SS_G or the SS_S would be positively related to survival and negatively related to wind stress. There was no relationship between SS_G and survival ($r = -0.11$, $p = 0.613$, $n = 24$) or wind stress ($r = -0.1$, $p = 0.632$, $n = 26$). However, SS_S is significantly related to survival ($r = 0.57$, $p = 0.027$, $n = 15$) (Fig. 6*b*) but not to wind stress ($r = -0.43$, $p = 0.084$, $n = 17$), although the sign of the correlation is in the expected direction (Table 3).

The relationship between SS_S and survival is heavily influenced by the 1984 year-class. If that datum is omitted from the analysis, the correlation between SS_S and survival is not significant. Due to low abundance (which reflects poor survival), we could not use the mixture analysis on the 1970, 1985, and 1986-year-classes. It is notable that these year-classes were associated with high wind stress. The expected relationship between SS_S, survival, and wind stress may be weakened when survival is low, simply because we cannot conduct mixture analysis.

SS_S has more potential as an index of retention/survival than does SS_G. First, there was evidence of bimodality within the SS region, suggesting that juveniles had migrated from the BoF, and second, SS_G shows no relationship with wind stress or survival. Third, the magnitude of the growth difference (BoF size – SS size) is related to survival ($r = -0.61$ $p = 0.002$, $n = 23$) (Fig. 6*c*). Given that survival is related to wind stress, then the relationship between low survival and greater growth differences may reflect an earlier divergence in growth rates and a higher mortality during early life due to increased advection off the bank. We have also observed that bimodality is easier to detect if the growth differences are larger. There was a negative relationship between SS_S and growth differences ($r = -0.6$, $p = 0.012$, $n = 17$) (Table 3). Although this might mean that small growth

© 1999 NRC Canada

Fig. 5. Time series of SS_S (size-based index of the surviving proportion of a haddock year-class retained in the SS region). The index ranges from 0 proportion of SS-sized juveniles surviving (little or no retention) to 1 (more retention) but no survival of BoF-sized juveniles. Open bars represent years in which length-at-age distributions were too irregular to conduct mixture analysis. Shaded bars represent poor model fits (and therefore, no index of retention/survival).

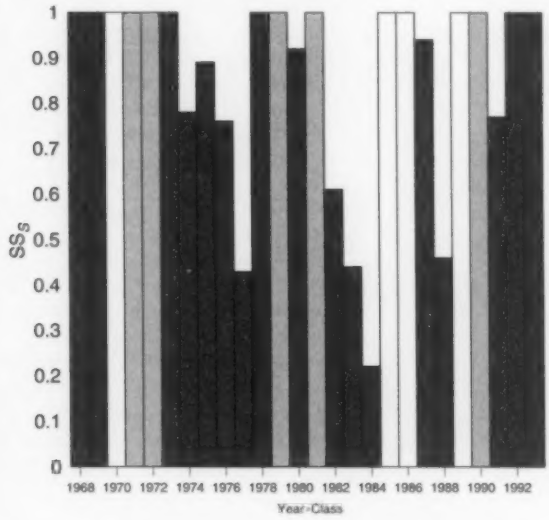

differences reflect similar environmental regimes in the BoF and SS, the relationship between the difference in growth rates and survival could also suggest that the degree of bimodality may have a biological basis and is not merely an issue of detection due to sample size or sensitivity of the mixture analysis.

Does the physical modelling suggest significant larval retention?

Particle tracking in the climatological spring flow field indicates that for a release depth of 10 m approximating the vertical position of haddock eggs and larvae, there is a bifurcation of the drift pathways. Some particles remain on Browns Bank but most drift towards the BoF (Fig. 7). This supports the underlying hypotheses of variability in a leaky gyre potentially affecting haddock growth and survival. However, various particle tracking experiments in this flow field indicate greater drift towards the BoF than implied by SS_G or SS_S. For example, for a release of particles at 10 m spread over the principal haddock spawning zone on Browns Bank (water depths <100 m west of 65°30′W), about 50% remain in the release area after 5–6 days, and about 30% remain after 10–12 days. This difference between model drift and biologically inferred drift may be because the physical measure of retention represents the fate of passive particles, while SS_S represents the *surviving* proportion of retained animals. The disparity is also expected to be partly due to the physical model's underestimation of the eastward flow on northern Browns Bank but may also reflect other physical factors such as interannual variability and turbulence influences and other biological factors such as a broader spawning distribution (e.g., Waiwood and Buzeta 1989) and biological behaviour (e.g., Suthers and Frank 1989).

Table 3. Pearson correlation matrix of SS_G, SS_S, survival, wind stress, and growth difference between the BoF and SS (BoF mean length at age 2 – SS mean length at age 2).

	SS_G	Survival	Wind stress	Growth difference
SS_S				
r	0.16	0.57*	–0.43	–0.6*
p	0.536	0.027	0.084	0.012
n	17	15	17	17
SS_G				
r		–0.11	–0.01	–0.2
p		0.613	0.632	0.349
n		24	26	25
Survival				
r			–0.5*	–0.61**
p			0.011	0.002
n			25	23
Wind stress				
r				0.21
p				0.312
n				25

Note: *Correlation significant at the 0.05 level (two-tailed); **correlation significant at the 0.01 level (two-tailed).

Discussion

We have presented geographical (SS_G) and size-based (SS_S) indices and evaluated their potential as indices for retention/survival during the early life history stage. SS_S has a greater potential, largely because it accounts for the non-stationarity of juvenile distributions and there is a suggestion that SS_S is related to survival. We thus have limited support for our hypothesis that variability in size-at-age may be due to variability in retention or dispersal during the early life history stage. SS_S may represent the surviving proportion of a year-class retained offshore in the Browns Bank region relative to the surviving proportion advected to the BoF during early life history.

Geographically induced differences in length-at-age have been used previously to document immigration/emigration of larvae and juvenile fish (Bjorke and Saetre 1994) as well as to estimate the proportion of a year-class of adult fish advected away from an area during early life history (Shepherd and Pope 1993).

The advantage of a retention/survival index based on juveniles rather than on egg/larval studies is that the latter can be biased by the timing of surveys relative to the timing of peak larval abundance. Such "aliasing" means that comparison of interannual distribution and abundance is difficult. Another advantage of a juvenile-based retention/survival index is that while the abundance of juveniles is related to the abundance of adults, there is no clear relationship between egg abundance, larval abundance, and subsequent recruitment.

The disadvantages of SS_S include that sufficient sample sizes are needed to estimate components of a length frequency distribution, which is not always possible during pe-

© 1999 NRC Canada

Fig. 6. (*a*) Relationship between survival (ln(age 1 population numbers at time *t*/age 3 + biomass at time $t - 1$)) and wind stress (average wind stress in pascals for April–June from Sable Island). (*b*). Relationship between survival (ln(age 1 numbers at time *t*/age 3 + biomass at time $t - 1$)) and SS_G. (*c*) Difference in geographically based mean length at age 2 in the BoF and SS as a function of survival.

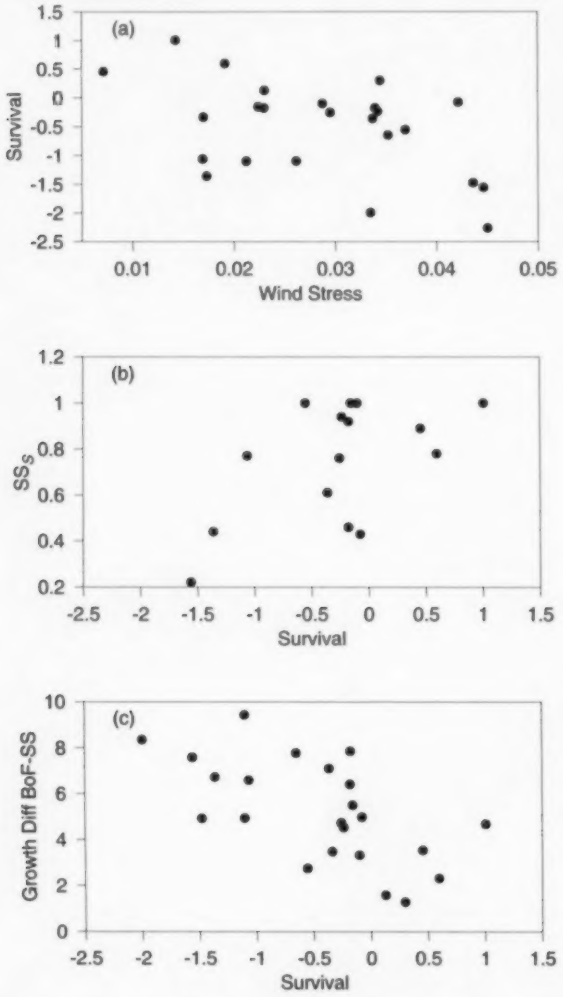

riods of very low abundance. The 1970, 1985, 1986, and 1989 year-classes were associated with very low abundance, which is associated with low survival, and were not sampled well enough to conduct mixture analysis. The fact that we were not able to obtain a value for SS_S in extremely low survival years may have contributed to the tenuous nature of the correlation between survival and SS_S. An additional disadvantage of the SS_s index is that the model failed to fit all years for which we had sufficient sample sizes, and this decreased our statistical power to assess the index in the context of wind stress and survival. In any event, the relationship between SS_S and survival lends support to the hypothesis that retention promotes higher survival.

Do growth differences at age 2 reflect growth differences during early life history?

The underlying assumption is that SS_S reflects the surviving proportion of a year-class retained in the SS region during early life history. There is evidence to support that assumption. In laboratory studies, growth differentials observed during the larval stage were maintained in the juvenile stages (Rosenberg and Haugen 1982; Chambers et al. 1988). There is also evidence that eggs and larvae advected away from Browns Bank survive. Suthers and Frank (1989) studied the spatial distribution of postlarval and pelagic juvenile Atlantic cod in the Brown Banks region. They found no age differences among inshore (towards the BoF) and offshore (Browns Bank), implying that the Browns Bank circulation influences dispersion at the egg stage and (or) the postlarval stage.

If growth differences are established early in life during the larval/early juvenile stage, it follows that small differences in length at age 2 reflect that a given cohort grew in a similar environmental regime, whereas larger differences in length at age 2 reflect that components of a given cohort grew up in dissimilar growth regimes. We observed that larger growth differences are associated with lower survival, implying a survival gradient between the BoF and SS regions. Although a survival gradient fits in with our conceptual model of dispersal during early life stages, we cannot rule out that small growth differences could reflect similar environmental regimes between SS and BoF concomitant with relatively higher survival in both areas.

Larval dispersal strategies and SS_S

In the past, larval dispersal strategies have included either drift or retention as a separate survival mechanism. More recently, there has been a greater appreciation of the diversity of survival mechanisms. Larval dispersal patterns can result in a variety of metapopulation structures (see Bailey 1997). Campana et al. (1989*a*) proposed that the spatial separation of a cohort due to the Browns Bank gyre may be part of a larval dispersal strategy that enhances survival of the southwestern Nova Scotian haddock population. If so, we would assume equal survivorship between the portion advected and that retained, over the longer term. That is, in some years, survival would be higher in the BoF region and in others it would be higher in the SS region.

Our results suggest that low survival is associated with a high wind stress, which would imply a higher probability of survival of those retained in the Browns Bank region. However, the growth rate of juveniles found in the BoF is higher than that of juveniles on Browns Bank and eastward. This is unusual, as higher growth rate is typically associated with an increased probability of survival. For example, the results of an individually based model showed that larger larvae stay large and have increased survival (Gallego and Heath 1997) and that, on a population level, mortality decreases with an increase in size (Houde 1997). Therefore, we might expect advection away from Browns Bank to enhance survival through enhanced growth rate

Further information to address whether survival differs between the Browns Bank and inshore (BoF) regions can be derived from the Fisheries Ecology Program studies. Stratification has been implied as a factor in concentrating larvae

© 1999 NRC Canada

Fig. 7. Springtime passive particle distributions after 30 days, released at 10 m from the Browns Bank region, within the 100-m isobath (light shading). Darker shading represents the 200-m isobath.

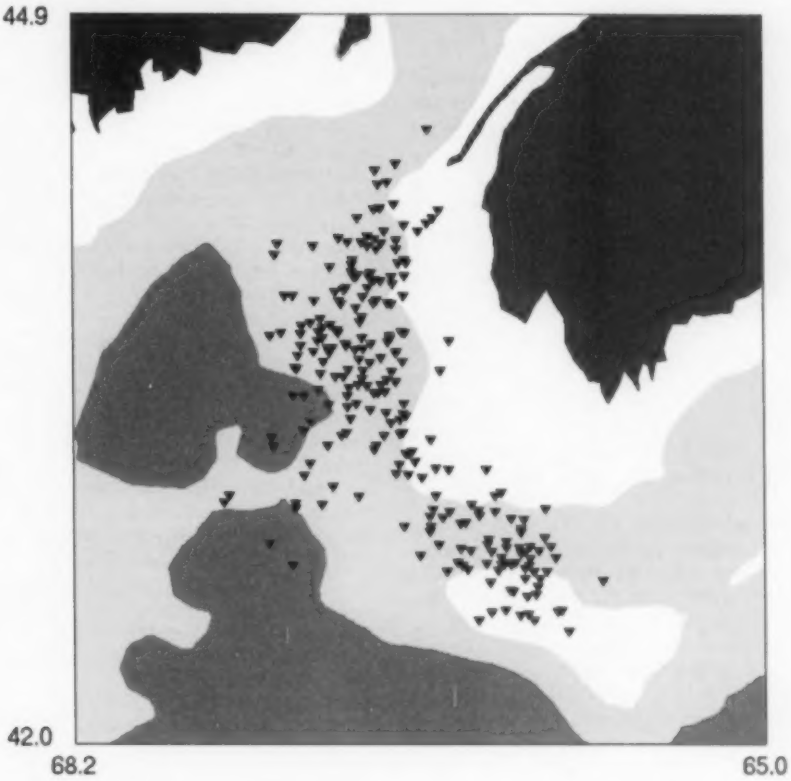

and their prey in the same area, thereby improving opportunities to feed and survive. The inshore region (towards BoF) is well mixed (Smith 1983, 1989) relative to areas further seaward. Frank et al. (1989) observed better larval condition in stratified waters than in well-mixed waters, suggesting that the inshore area would be less favourable for early larval growth and survival.

There is no information on the growth differences of haddock between BoF and Browns Bank during the postlarval stage. Suthers et al. (1989) observed that the growth of postlarval Atlantic cod advected from Browns Bank inshore was slower than their Browns Bank counterparts of similar age. Larval predators have been observed to be more abundant inshore than offshore and could have been responsible for the generation of such a gradient (Suthers and Frank 1990). Wildish et al. (1989) measured the benthic macrofaunal production of Browns Bank and reported that it was lower than that measured in the mixed fine sediments of the BoF. The implication is that newly settled juveniles would find themselves in a food-rich environment in the BoF. It is possible that the initial conditions for advected haddock are unfavourable (due to increased abundance of predators) but that those that do survive to adopt a demersal habitat are able to take advantage of an environment that enhances growth.

The indication in the physical modelling of a spatially structured circulation regime with both retention on Browns Bank and drift towards the BoF supports our conceptual model that variable drift (e.g., due to variable wind forcing) can lead to variable growth and survival. The difference between the extent of retention in the Browns Bank region in the physical model and that implied by SS_S is partly because the latter represents the surviving proportion of a year-class retained, while the physical model represents the fate of passive particles. We can use the difference between the extent of retention predicted by the physical particle-based model and SS_S to estimate the differential mortality between the SS and BoF regions (see Appendix). Assuming exponential mortality with a constant mortality rate, we estimate a differential mortality between BoF and SS of 0.06–0.09·day^{-1}. This difference is plausible given the range of larval mortality (0.08 –0.5·day^{-1}) estimated by Campana et al. (1989*b*).

Werner et al. (1996) developed a model to integrate the trophodynamics of individual Atlantic cod and haddock larvae and the advective processes on Georges Bank affecting the whole population. The authors concluded that the distinction between trophodynamic and advective processes was inappropriate due to their interactive effects on survival. That is, a better approach to understanding trophodynamic and advective processes would be to examine the interaction between processes. The model of Werner et al. (1996) showed that larvae grew more quickly in the areas of highest retention which were patterned by circulation. Further, the magnitude of the influences of trophodynamic and advective processes changed over time. In this context, our study can

© 1999 NRC Canada

be used as a guide in the development of models integrating both trophodynamic and advective processes.

Acknowledgements

We thank Jim Simon and Peter Comeau for their technical assistance and the many individuals who participated in the annual Department of Fisheries and Oceans research vessel surveys. We also thank Charles Hannah and John Loder for valuable discussion and Steve Campana for comments on a previous version of the manuscript. This is a contribution of the Global Ocean Ecosystems Dynamics (GLOBEC) program, funded by the Department of Fisheries and Oceans and the Natural Sciences and Engineering Research Council of Canada.

References

Bailey, K.M. 1997. Structural dynamics and ecology of flatfish populations. J. Sea Res. **37** : 269–280.

Bjorke, H., and Saetre, R. 1994. Transport of larvae and juvenile fish into central and northern Norwegian waters. Fish. Oceanogr. **3**: 106–119.

Campana, S.E., Smith, S.J., and Hurley, P.C.F. 1989*a*. A drift-retention dichotomy for larval haddock (*Melanogrammus aeglefinus*) spawned on Browns Bank. Can. J. Fish. Aquat. Sci. **46**(Suppl. 1): 93–102.

Campana, S.E., Frank, K.T., Hurley, P.C.F., Koeller, P.A., Page, F.H., and Smith, P.C. 1989*b*. Survival and abundance of young Atlantic cod (*Gadus morhua*) and haddock (*Melanogrammus aeglefinus*) as indicators of year-class strength. Can. J. Fish. Aquat. Sci. **46**(Suppl. 1): 171–182.

Chambers, R.C., Leggett, W.C., and Brown, J.A. 1988. Variation in and among early life history traits of laboratory-reared winter flounder *Pseudopleuronectes americanus*. Mar. Ecol. Prog. Ser. **47**: 1–15.

Clark, D.S., and Brown, L.L. 1996. Assessment of cod in Division 4X in 1996. DFO Atl. Fish. Res. Doc. 96/101.

Frank, K.T. 1988. Independent distributions of fish larvae and their prey: natural paradox or sampling artifact? Can. J. Fish. Aquat. Sci. **45**: 48–59.

Frank, K.T., Page, F.H., and McRuer, J.K. 1989. Hydrographic effects on the vertical distribution of haddock (*Melanogrammus aeglefinus*) eggs and larvae on the southwestern Scotian Shelf. Can. J. Fish. Aquat. Sci. **46**(Suppl. 1): 82–92.

Gallego, A., and Heath, M. 1997. The effect of growth-dependent mortality, external environment and internal dynamics on larval fish otolith growth: an individual based modelling approach. J. Fish Biol. **51**(Suppl. A): 121–134.

Halliday, R.G., and Koeller, P.A. 1981. A history of Canadian groundfish trawling surveys and data usage in ICNAF divisions 4TVWX. *In* Bottom trawl surveys. *Edited by* W.G. Doubleday and D. Rivard. Can. Spec. Publ. Fish. Aquat. Sci. No. 58. pp. 27–41

Han, G., Hannah, C.G., Loder, J.W., and Smith, P.C. 1999. Seasonal variation of the three-dimensional mean circulation over the Scotian Shelf. J. Geophys. Res. **102**: 1011–1025.

Houde, E.D. 1997. Patterns and trends in larval-stage growth and mortality of teleost fish. J. Fish Biol. **51**(Suppl. A): 52–83.

Hurley, P.C.F., and Campana, S.E. 1989. Distribution and abundance of haddock (*Melanogrammus aeglefinus*) and Atlantic cod (*Gadus morhua*) eggs and larvae in the waters off southwest Nova Scotia. Can. J. Fish. Aquat. Sci. **46**(Suppl. 1): 103–112.

Hurley, P.C.F., Black, G.A.P., Mohn, R.K., and Comeau, P. 1997. Assessment of 4X haddock in 1996 and the first half of 1997. DFO Can. Stock Assess. Secretariat Res. Doc. 97/108.

Krohn, M., and Kerr, S.R. 1997. Declining weight-at-age in northern cod and the potential importance of the early years and size-selective fishing mortality. NAFO Sci. Counc. Stud. **29**: 43–50.

Lynch, D.R., Werner, F.E., Greenberg, D.A., and Loder, J.W. 1992. Diagnostic model for the baroclinic, wind-driven and tidal circulation in shallow seas. Continental Shelf Res. **12**: 37–64.

MacDonald, P.D.M., and Pitcher, T.J. 1979. Age-groups from size–frequency data: a versatile and efficient method of analyzing distribution mixtures. J. Fish. Res. Board Can. **36**: 987–1001.

Marshall, C.T. 1995. Biological and geographical limits on the production dynamics of haddock (*Melanogrammus aeglefinus*) on the southwestern Scotian Shelf. Ph.D. thesis, Dalhousie University, Halifax, N.S.

O'Boyle, R.N., Sinclair, M., Conover, R.J., Mann, K.H., and Kohler, A.C. 1984. Temporal and spatial distribution of ichthyoplankton communities of the Scotian Shelf in relation to biological, hydrological, and physiological features. Rapp. P.-v. Réun. Cons. Int. Explor. Mer, **183**: 27–40.

Petrie, B., and Lively, R. 1979. Offshore meteorological measurements with a CODS discus buoy. Atmosphere, **17**: 169–176.

Rosenberg, A.A., and Haugen, A.S. 1982. Individual growth and size-selective mortality of larval turbot (*Scophthalmus maximus*) reared in enclosures. Mar. Biol. **72**: 73–77.

Sandstrom, H. 1980. On the wind-induced sea level changes on the Scotian Shelf. J. Geophys. Res. **85**: 461–468.

Shepherd, J.G., and Pope, J.G. 1993. Alternative methods for the estimation of immigration to the Icelandic cod stock. Fish. Oceanogr. **2**: 254–259.

Smith, P.C. 1983. The mean and seasonal circulation off southwest Nova Scotia. J. Phys. Oceanogr. **13**: 1034–1054.

Smith, P.C. 1989. Circulation and dispersion on Browns Bank. Can. J. Fish. Aquat. Sci. **46**: 539–559.

Smith, S., and Banke, E. 1975. Variation of the seasurface drag coefficient with wind speed. Q. J. R. Meteorol. Soc. **101**: 665–673.

Suthers, I.M., and Frank, K.T. 1989. Inter-annual distributions of larval and pelagic juvenile cod (*Gadus morhua*) in southwestern Nova Scotia determined with two different gear types. Can. J. Fish. Aquat. Sci. **46**: 591–602.

Suthers, I.M., and Frank, K.T. 1990. Zooplankton biomass gradient off south-western Nova Scotia: nearshore ctenophore predation or hydrographic separation? J. Plankton Res. **12**: 831–850.

Suthers, I.M., Frank, K.T., and Campana, S.E. 1989. Spatial comparison of recent growth in postlarval Atlantic cod (*Gadus morhua*) off southwestern Nova Scotia: inferior growth in a presumed nursery area. Can. J. Fish. Aquat. Sci. **46**(Suppl. 1): 113–124.

Waiwood, K.G., and Buzeta, M.-I. 1989. Reproductive biology of southwest Scotian Shelf haddock (*Melanogrammus aeglefinus*). Can. J. Fish. Aquat. Sci. **46**(Suppl. 1): 153–170.

Werner, F.E., Page, F.H., Lynch, D.R., Loder, J.W., Lough, R.G., Perry, R.I., Greenberg, D.A., and Sinclair, M.M. 1993. Influences of mean advection and simple behavior on the distribution of cod and haddock early stages on Georges Bank. Fish. Oceanogr. **2**: 43–64.

Werner, F.E., Perry, R.I., Lough, R.G. and Naimie, C.E. 1996. Trophodynamic and advective influences on Georges Bank larval cod and haddock. Deep-Sea Res. II, **43**: 1793–1822.

Wildish, D.J., Wilson, A.J., and Frost, B. 1989. Benthic macrofaunal production of Browns Bank, Northwest Atlantic. Can. J. Fish. Aquat. Sci. **46**: 584–590.

© 1999 NRC Canada

Appendix

The difference between the particle-based retention from the circulation model and the SS_S retention/survival index can be used to derive a rough estimate of the differential mortality between the BoF and SS that would be required to transform the circulation model retention to the SS_S proportion retained and surviving.

Let BoF_P and SS_P be the particle-based proportions in the BoF and SS, respectively; BoF_S and SS_S are the size at age 2 proportions. Assuming exponential mortality with constant mortality rates M_{BoF} and M_{SS}, we obtain

$$\left(\frac{\mathrm{BoF_P}}{\mathrm{SS_P}}\right)e^{-(M_{BoF}-M_{SS})t}=\left(\frac{\mathrm{BoF_S}}{\mathrm{SS_S}}\right)$$

or

$$\Delta M = -\ln(F)/t$$

where t is time (days), $\Delta M = M_{BoF} - M_{SS}$, and

$$F=\left(\frac{\mathrm{BoF_S}}{\mathrm{SS_S}}\right)\Big/\left(\frac{\mathrm{BoF_P}}{\mathrm{SS_P}}\right)$$

Assuming that this differential mortality occurs during the 40- to 60-day larval period, with (BoF_P, SS_P, BoF_S, SS_S) = (0.80, 0.20, 0.10, 0.90), we obtain a differential mortality between BoF and SS of 0.06–0.09·day^{-1}.

© 1999 NRC Canada

Ideal free distribution theory as a tool to examine juvenile coho salmon (*Oncorhynchus kisutch*) habitat choice under different conditions of food abundance and cover

Guillermo R. Giannico and Michael C. Healey

Abstract: We investigated the mechanisms affecting habitat choice by juvenile coho salmon (*Oncorhynchus kisutch*) in relation to the patchy distribution of food and cover. We tested the following hypotheses: (*i*) the distribution of juvenile coho, both between patches in a pool and between separate pools in a channel, corresponds numerically to the food input rate of those habitat patches as predicted by the "input-matching rule" of ideal free distribution (IFD) and (*ii*) the addition of instream cover, by increasing visual isolation among competitors, promotes input matching both within and between pools. We conducted our experimental work in artificial channels and we used two different types of cover, instream and overhead. In the absence of cover and with either no differences or relatively small differences in food abundance between patches, the spatial distribution of juvenile coho responded numerically to the input rate of food as predicted by the IFD. However, when differences in food abundance between patches were relatively large or cover was present, fish distributions consistently undermatched food input rate in the rich patch. Coho foraged in open patches away from cover within single pools but preferred pools with cover when choosing between separate pools. Several IFD models were used to examine the observed dispersion patterns.

Résumé : Nous avons étudié les mécanismes influant sur le choix de l'habitat de saumons cohos juvéniles (*Oncorhynchus kisutch*) dans le contexte d'une répartition inégale de la nourriture et du couvert. Nous avons testé les hypothèses suivantes : (*i*) la répartition des cohos juvéniles, tant entre les zones d'une fosse et entre des fosses distinctes d'un même chenal, correspond numériquement au taux d'entrée de la nourriture dans ces zones d'habitat tel que prédit par la règle « de correspondance des intrants » d'une distribution libre idéale (DLI) et (*ii*) l'ajout d'un couvert en cours d'eau, qui accroît l'isolement visuel des compétiteurs, favorise l'appariement aux intrants tant au sein d'une fosse qu'entre les fosses. Nous avons effectué nos travaux expérimentaux dans des chenaux artificiels et utilisé deux types de couvert, un en cours d'eau et l'autre au-dessus. En l'absence d'un couvert, et avec des écarts d'abondance de nourriture entre les zones nuls ou très faibles, la répartition spatiale des cohos juvéniles réagissait numériquement aux taux d'intrants de la nourriture, tels que prévu par la DLI. Par ailleurs, lorsque les écarts d'abondance de la nourriture entre les zones étaient relativement importants ou qu'il y avait présence d'un couvert, la répartition des poissons était constamment décalée par rapport aux taux d'intrants de la nourriture dans les zones riches. Les cohos recherchaient leur nourriture dans les zones dégagées loin du couvert quand ils étaient dans des fosses uniques, mais préféraient les fosses avec couvert lorsqu'ils pouvaient choisir entre deux fosses distinctes. Plusieurs modèles DLI ont été utilisés pour l'examen des régimes de dispersion observés.

[Traduit par la Rédaction]

Introduction

During their first year or more of life, juvenile coho salmon (*Oncorhynchus kisutch*) inhabit coastal streams and small tributaries of large rivers before migrating to sea as smolts (Sandercock 1991). Both overhead riparian cover and submerged structures have been considered indispensable components of coho salmon nursery habitat for a variety of reasons. Low-hanging overhead cover, such as undercut banks, renders fish less visible to potential predators (Helfman 1981; Shirvell 1990). Instream cover, in turn, provides refuge not only from predators but also from water current (Fausch 1993) and, simultaneously, can increase visual isolation among young coho, thus reducing aggressive interactions and increasing the density of competitors in food-rich habitats (Bugert et al. 1991; Fausch 1993).

Many researchers have examined the effects of cover on the density and spatial distribution of juvenile coho salmon. However, one cannot find clear consensus in the literature on whether the presence of cover makes stream reaches more or less suitable for the young fish. While some studies found positive correlation between coho salmon densities and instream cover abundance (Bisson et al. 1982, 1987; Dolloff 1986; Dolloff and Reeves 1990; Shirvell 1990), others reported that juvenile coho preferred open areas or lacked as-

Received February 16, 1999. Accepted August 20, 1999.
J15021

G.R. Giannico[1] and M.C. Healey. Institute for Resources and Environment, University of British Columbia, 2206 East Mall, Vancouver, BC V6T 1Z3, Canada.

[1]Author to whom all correspondence should be addressed.
e-mail: giannico@interchange.ubc.ca

© 1999 NRC Canada

sociation with cover (Bugert and Bjorn 1991; Bugert et al. 1991; Fausch 1993; Spalding et al. 1995). These contradictory results may have a double cause. First, there are important differences among these studies in terms of methodology, type of cover, and habitat scales being considered, as well as time of the year when the work was done. Second, the use of cover by animals is not constant; it varies over time and space in response to both ontogenetic development (body growth, increased motility and coordination, enhanced learning capacity, etc.) and changes in environmental factors (predation risk, temperature, water discharge, photoperiod, etc.).

Almost three decades ago, a number of authors (Orians 1969; Fretwell and Lucas 1970) began the development and elaboration of a conceptual framework relating the spatial distribution of animals to resource availability, competition, and predation risks. The models derived from this framework constitute the body of what is currently known as ideal free distribution (IFD) theory (see review by Kacelnik et al. 1992). The original models assumed, among other things, that animals always know the distribution of resources and competitors (hence, they are "ideal"), that all competitors have identical abilities (they are "equal") and there is no exclusion of some individuals by others (they are "free" to leave or enter any patch), and that travel time between patches is negligible (Fretwell and Lucas 1970; Milinski and Parker 1991; Kacelnik et al. 1992). Based on these assumptions, IFD theory predicts the equilibrium distribution of competitors to be the one at which the benefits to all competitors are equal across habitat patches and no individual can increase its payoff by switching patches. Although individual fitness was the payoff currency used by Fretwell and Lucas (1970), a second generation of models used food intake rate as a convenient (although not perfect) surrogate for fitness. As a result, the equilibrium distribution prediction became known as the "equal-intake prediction."

In continuous-input systems, patches have a constant input of resources and the quality of each patch is determined by both the resource input rate and the high interference ($m = 1$) among competitors scrambling to take the resources (Fretwell 1972). Under continuous-input conditions, the equal-intake prediction implies that all individuals will distribute across patches in direct proportion to the amount of resources available in those patches. This type of distribution has been termed "numerical response" (Fretwell and Lucas 1970), "input-matching rule" (Parker 1978) or "habitat-matching rule" (Pulliam and Caraco 1984). Although the verification of the input-matching rule is simple in principle, the fact that continuous-input foraging systems are relatively rare limits its applicability in natural situations.

Several researchers have confirmed input matching in continuous-input systems, even when the assumption of "equal" abilities among competitors was violated (see review in Parker and Sutherland 1986). Therefore, unequal intake among animals due to differences in their competitive abilities does not necessarily keep them from reaching an input-matching distribution. In fact, this is one of several possible equilibrium distributions predicted by Parker and Sutherland (1986) in their IFD model of unequal competitors (UC). Violation of other assumptions of the original IFD model makes the ensuing equilibrium distribution of competitors depart from input matching and frequently results in undermatching (i.e., when fewer competitors than predicted by input matching occupy the resource-rich patches, while poorer patches are overexploited). Two common explanations for undermatching include the ideal despotic distribution (IDD) model (see Fretwell and Lucas 1970; Fretwell 1972), in which competitors are not "free" to switch patches due to the territorial behaviour of dominant individuals, and the perceptual limit model (PLM) (see Abrahams 1986; Gray and Kennedy 1994), in which competitors are limited in their ability to perceive differences among patches.

Continuous-input foraging systems are characteristic of the habitat of stream-dwelling juvenile coho salmon. Therefore, the aim of this study is to use IFD theory and models as tools to better understand juvenile coho salmon spatial distribution and their microhabitat selection under different conditions of food abundance and cover in a stream environment. We compared the distribution of coho between patches that differed in food and cover availability and tested the following hypotheses: (*i*) the distribution of juvenile coho, both between patches in a pool and between separate pools in a channel, corresponds numerically to the food input rate of those habitat patches as predicted by the input-matching rule and (*ii*) the addition of instream cover, by increasing visual isolation among competitors, promotes input matching both within and between pools. Our first hypothesis assumes that coho are "ideal" samplers and that they are "free" to move between patches. Departures from the expected pattern are likely to occur either because of despotism (coho form dominance hierarchies) or perceptual constraints (due to sampling or information processing limitations by the fish). If input matching does not occur due to despotism, our second hypothesis predicts that increasing habitat complexity (i.e., addition of instream cover) will reduce aggressive interactions and allow more fish to move into the food-rich patch. By contrast, if input matching fails because of perceptual constraints, input matching will be further reduced in habitats with instream cover. We tested both hypotheses within individual pools and between pools. We expected fish to be able to compare and choose between adjacent patches in a single pool more easily than between separate pools.

Despite the potential value of IFD theory as a tool to examine the distribution of drift-feeding fish, only two other studies have applied it to juvenile salmonids. Grand (1997) recently tested the input-matching prediction of Parker and Sutherland's (1986) UC model using juvenile coho salmon, and subsequently, Grand and Dill (1997) applied that model to quantify the energetic value of overhanging cover for the young fish. Both the objectives and experimental conditions of those studies differed from ours.

Materials and methods

Our experiments were performed in two wooden stream channels at the Cultus Lake Research Laboratory (Department of Fisheries and Oceans), Cultus Lake, B.C. These channels were 0.9 m wide, 0.4 m deep, and 17.4 m long. They received Cultus Lake water pumped at a rate of about 120 $L \cdot min^{-1}$. Summer water temperature in the channels was maintained at 12–13°C by mixing lake hypolimnion water (6–8°C) with lake epilimnion water (13–19°C), which entered by independent pipelines.

© 1999 NRC Canada

We conducted four groups of experiments: (*a*) single pools without cover, (*b*) single pools with cover, (*c*) paired pools without cover, and (*d*) paired pools with cover. Experiment *a* tested whether age-0 coho distribute between adjacent patches within a single pool in response to their profitability as predicted by input-matching IFD. Experiment *b* tested whether the presence of either instream or overhead cover improved matching between fish distribution and food input within individual pools. These two types of single-pool experiments were not applied sequentially; instead, treatments within each group were randomly applied to 12 experimental pools between May 18 and July 28, 1992. Experiment *c* tested whether coho distribute between separate pools, in proportion to their food availability. Finally, experiment *d* tested whether the distribution of fish between pools was affected by cover. These double-pool experiments were also randomly applied (no sequential order) to six experimental pools between August 3 and October 2, 1992.

The age-0 coho salmon used in the experiments were of hatchery origin (Robertson Creek Hatchery, Vancouver Island) but not hatchery raised. They were transferred to an outdoor holding channel at an early fry stage. In that channel, they were fed by means of automatic feeders, raised with cover structures, and exposed to avian predators (although fine-mesh screens protected them from actual predation). The experimental subjects were randomly chosen from a larger preselected group of 300 fish of relatively similar size (May mean fork length = 51 ± 2 mm (SD), mean weight = 1.63 ± 0.11 g (SD)). Homogeneous size among individuals was important in reducing initial differences in competitive abilities.

Single-pool experiments

For single-pool experiments, each channel was divided into six 2.44-m-long pools (12 pools total) using 0.31-m-high wooden partitions (Fig. 1*a*). These partitions had screened openings to allow water flow. Water velocity was slow, varying from 3 to 7 $cm \cdot s^{-1}$ at 15 cm from the bottom at different points in each pool. Twelve fish were randomly assigned to each of 12 pools (N = 144 total). This number created a fish density (5.5 $fish \cdot m^{-2}$) within the range observed in productive coho streams during the summer (Ptolomy 1993). The same individuals were used through the whole series of single-pool experiments. Thus, each group of 12 fish received different treatments (different feeding ratios, both in the presence and in the absence of cover). Because all treatments were randomly assigned to pools, fish could anticipate neither patch profitability nor the type of cover, if any at all, that they were going to get. Such treatment randomization across pools was intended to maximize the independence among replicates and eliminate any carryover effects between trials.

Fish were fed and observed from behind two L-shaped portable blinds. Each blind had a horizontal 1 × 0.6 m plywood platform to stand on and a vertical 1 × 1.6 m sheet of plywood to hide behind. One of the blinds, which had two feeding slots and one aluminum slide sloping from each slot towards the water at a 45° angle, was always placed immediately upstream from the "trial" pool. The other blind, which had a small window (10 × 25 cm) covered with a plastic screen (25-mm mesh size), was placed immediately downstream from the trial pool. In this manner, each blind's platform temporarily covered a small part (0.6 m long) of the pools adjacent to the trial pool. Fish were fed and observed from behind each blind's vertical plywood sheet. The results of a series of pilot trials showed that after blind placement, a maximum of 8 min and 15 s was needed for fish to attain the same even distribution across patches that they had after 24 h of exposure to the blinds. Therefore, each time the blinds were relocated, we waited 10 min before beginning a trial.

Pieces of freeze-dried shrimp (*Euphausia pacifica*) were used as food before and during experiments. Shrimp pieces (approximate size = 1 × 0.4 mm, weight = 15 mg) were delivered as individual prey. Because they stayed afloat for a long time (over 20 min), they allowed the creation of habitat patches of different foraging quality within a pool. Shrimp pieces were dropped from the upstream blind down its slides into both the right half and the left half of each pool, simulating drifting prey as in natural streams. Differences in patch profitability were produced by different shrimp delivery rates between right and left sides of a pool and maintained by means of a floating polyurethane rope down the centre of each pool that prevented shrimp from drifting between patches. The adjacent patches created in this way were assumed to be equally accessible to fish. Four different patch profitability ratios were used: 1:1, 1:2, 1:5, and 1:11. A single piece of shrimp was delivered as prey into each patch every 10 s to create the 1:1 profitability ratio. To obtain the 1:2, 1:5, and 1:11 desired ratios, one piece of shrimp was delivered into the food-rich patch every 10 s and into the food-poor patch every 20, 50, or 110 s. This delivery regime simultaneously increased differences between patches and reduced total amount of available food.

The distribution of coho was recorded from behind the downstream blind every 30 s over a total period of 6 min for all treatments, including no-food control periods before trials (0:0 profitability ratio). Feeding experiments were 6 min long because in pilot trials, the earliest sign of satiation shown by any individual was observed after 9 min. Both the type of treatment and the poorer patch in each pool were randomly designated before each trial; this procedure reduced resource spatial predictability for the fish. Thirty replicates were run for each treatment. At night, pools were covered with plastic screens (25-mm mesh size) to keep predators out. These screens were removed 2 h before beginning the morning trials (i.e., 05:00).

In the second type of single-pool experiments, we tested the effect of two different factors, food and cover. The structures used to provide cover were randomly assigned to one of the two patches in each pool. The combination of food and instream cover resulted in eight different treatments that were randomly applied to each of the 12 pools. In two of those treatments, both patches in each pool only differed in instream cover availability (cover versus no cover); their foraging quality was equivalent (0:0 control trials and 1:1 feeding ratio). In the other six treatments, patches differed in both cover presence and food availability (under either 1:2, 1:5, or 1:11 feeding ratios; three with instream cover in the food-rich patch and three with cover in the food-poor patch). A comparable set of eight treatment combinations was conducted with overhead rather than instream cover.

Instream cover was provided by twelve rectangular plywood blinds (15 × 40 cm) placed in one patch as shown in Fig. 1*b*. These rectangular plywood sheets rested on their short side and were oriented parallel to the water flow, thereby reducing water deflection that could have potentially created "resting" areas for the fish. Structures were placed in the pools for 9 h overnight prior to morning trials and for 5 h during midday prior to afternoon trials. Fish had sufficient time to acclimatize to the presence of instream structures, as indicated by the results of pilot trials. These trials showed that after 90 min (t = −1.58, df = 5, p = 0.174) and 120 min (t = 0.67, df = 5, p = 0.530) of instream structure placement, fish distributions among patches did not differ from those observed prior to the installation of structures.

In the overhead cover treatments, a rectangular plywood sheet (220 × 45 cm) was supported 15 cm above the water surface, as an undercut bank, over one of the two pool patches. The height of the plywood sheet above the water surface helped to reduce differences in the amount of light between covered and uncovered pool patches. These structures were also placed for either 9 h (overnight) or 5 h (early afternoon) before beginning the trials.

Control experiments

To distinguish the effect of visual isolation on fish behaviour

© 1999 NRC Canada

Fig. 1. (*a*) Diagram of experimental channel section divided into series of individual pools by wooden partitions. Partitions had windows, covered with fine mesh, that allowed water flow through but prevented food and coho salmon from moving among pools. A floating polyurethane rope divided each pool into two patches: A and B. L, pool length; *W*, pool width; *H*, pool height; *D*, water column depth. (*b*) View of single experimental pool with instream cover in patch B. A floating rope (M) divided the pool into two halves.

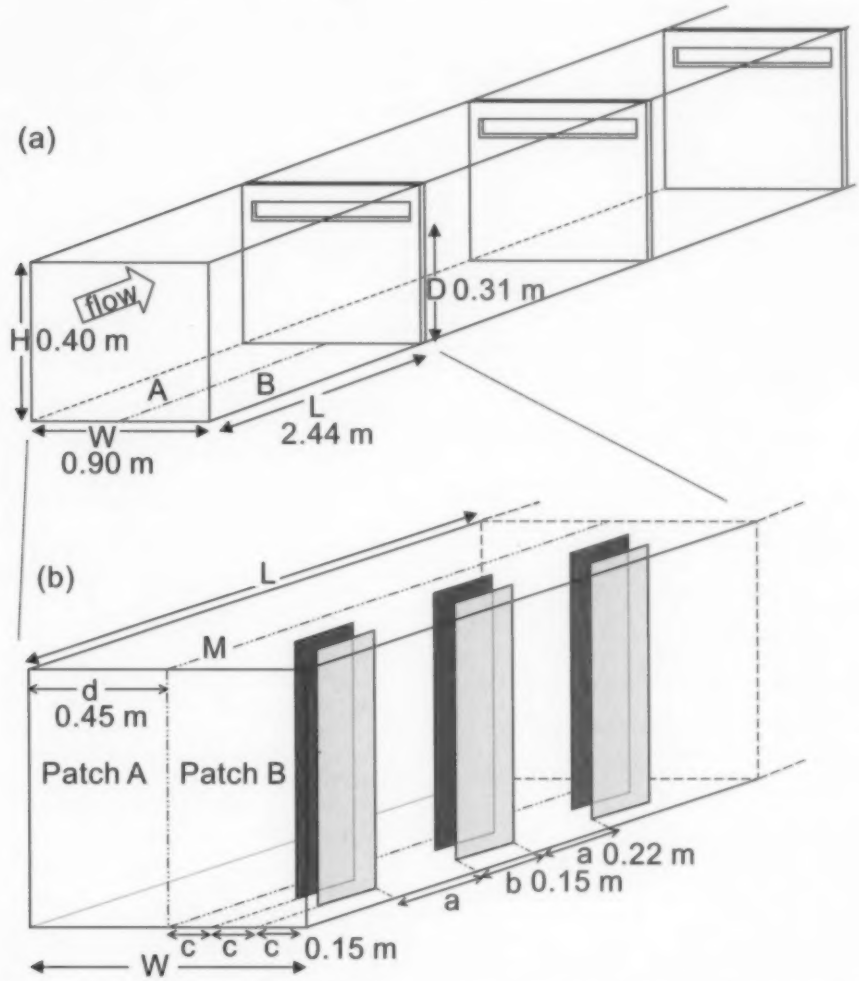

from any effect that the physical presence of the instream structures could have had, we conducted a comparable set of eight treatment combinations but using clear Plexiglas sheets rather than plywood. For each control treatment with Plexiglas sheets, 20 replicates were obtained.

Paired-pool experiments

For our third and fourth types of experiments, we divided each channel into three separate experimental units (488 cm long) consisting of two pools (each 194 cm long) interconnected by a gravel and cobble riffle (100 cm long). We used automatic feeders to deliver shrimp pieces at specified rates in each one of the pools. In these experiments, we tested fish pool choice in response to food only or to the combination of food and cover applying the following five treatments: 1:1 feeding ratio, 1:5 feeding ratio, 1:1 feeding ratio with cover in one pool, 1:5 feeding ratio with cover in the food-rich pool, and 1:5 feeding ratio with cover in the food-poor pool of each pair. Instream cover was provided by the same small plywood blinds described earlier. But in this case, they were evenly distributed throughout one entire pool, not just a patch half a pool in size. Food and cover were randomly assigned to the six experimental paired-pool units, and nine replicates of each of the five treatments were run.

To maintain the profitability ratios between pools, surface sieves (wooden-framed cheesecloth screens) were placed on the riffles to stop floating shrimp from washing downstream. Sieves were brushed twice a day.

During the paired-pool experiments, six "naive" coho were taken from the stock tanks, at the beginning of each week, and randomly assigned and released into each pair of pools ($N = 36$ total). The resulting density of juvenile coho salmon (3.1 fish·m^{-2}) was equivalent to that observed in many British Columbia streams during late summer (Ptolomy 1993). By the time that these groups of experiments had started (late summer), variation in size among fish in our stock tanks had increased notably from that of our earlier

© 1999 NRC Canada

Fig. 2. Mean proportion of coho salmon observed in the rich patch. Observations were made every 30 s during the final 4 min of 6-min-long trials for each of the five different profitability ratios. Means were calculated using data from 25 replicate tests. The vertical bars are ±2 SE. The broken line represents fish proportions predicted by the IFD input-matching rule.

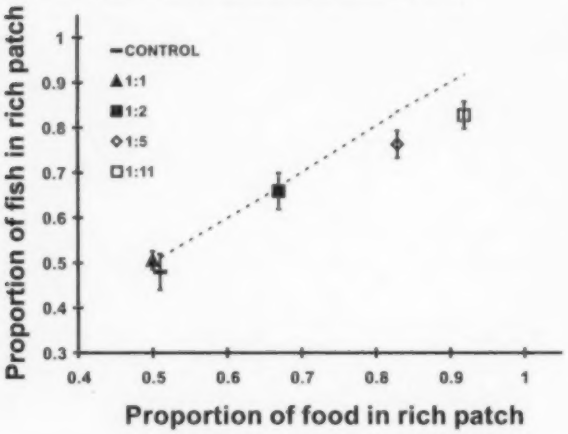

trials (August mean fork length = 77 ± 7 mm (SD), mean weight = 5.93 ± 0.49 g (SD); September mean length = 78 ± 7 mm (SD), weight = 6.26 ± 0.57 g (SD)). This variation in size could be considered evidence of differences in individual intake rates. Because bigger coho fry are generally dominant (Chapman 1962), we marked the fish individually to detect any correlation between patch quality and fish size. Individual coho weight and fork length were recorded, and they were individually marked in their fins with small dots of dye (Alcian blue) injected with a needleless high-pressure dental syringe (Pan-jet).

On the morning of the seventh day of each trial, all fish were removed from the pools using unbaited minnow traps, which had been placed the previous night. Those that did not enter the traps were subsequently removed by electrofishing.

Data analyses

All statistical analyses were conducted using SAS systems software (SAS Institute Inc. 1988). We used the Shapiro and Wilk statistic (W) (Zar 1984) to test departures from normality.

Before analyzing the effect on coho spatial distribution of the various treatments, we investigated possible behavioural differences among pools because the 12 groups of fish could have received different proportions of dominant and subordinate fish in spite of equal initial sizes. To test this, a one-way ANOVA was performed for each individual treatment (1:1, 1:2, 1:5, and 1:11 feeding ratios) as well as for the unfed control (0:0). Pool was the factor considered in the analysis, and each individual unit represented a different level of this factor. Differences between morning and afternoon results were examined using a paired t test across food treatments without cover.

During our single-pool experiments, the number of fish in the richer patch increased with relative patch profitability (Fig. 2). Fish continued to move into the richer patch as they gathered more information about its relative quality. This caused a smaller mean number of fish in the food-rich patch during the first 2 min of observation than during the remainder of the trial, particularly under high feeding ratios (1:5 and 1:11). Therefore, only the mean number of fish per patch during the last 4 min of each trial was used in our analyses. We used one-way ANOVA to determine the effects of different feeding ratios and t tests to compare the mean number of coho occupying the food-rich patch with that predicted by IFD's input-matching rule. Reported p values are two-tailed, unless stated otherwise, and power values are provided only for tests that failed to reject the null hypothesis. We also calculated the binomial probabilities of obtaining the observed fish proportions from a population of input-matching fish.

Two-way ANOVA was used to determine the effects of food availability, presence of cover, and their interaction on the spatial distribution of fish. Whenever interactions between factors were significant, we compared the means of one of the factors separately for each level of the other factor using Tukey's studentized range test, which controls for type I experimentwise error rate (Zar 1984).

Results

Our data were normally distributed. The only exception to this pattern was the distribution of the mean number of fish in the richer patch for the 30 trials under a 1:11 feeding ratio ($W = 0.8647$, $p = 0.001$). There were no differences in fish behaviour between morning and afternoon trials ($t = 0.718$, df = 124, $p = 0.452$).

Our null hypothesis of no difference in fish spatial distribution among pools was rejected only under unfed control (0:0) conditions ($F = 4.76$, df = 1, $p = 0.002$). The associated r^2 value indicated that "pool" accounted for 74% of the variation in the observed fish spatial distribution when they were not being fed. We did not find that fish spatial distributions were significantly different among those pools when feeding treatments were applied (1:1 profitability ratio: $F = 1.27$, df = 1, $p = 0.142$; 1:2 profitability ratio: $F = 0.93$, df = 1, $p = 0.524$; 1:5 profitability ratio: $F = 1.25$, df = 1, $p = 0.320$; 1:11 profitability ratio: $F = 0.30$, df = 1, $p = 0.971$). The exclusion of the first pool of each channel from subsequent analyses eliminated this a priori side-bias in fish distribution during no-food control trials ($F = 1.13$, df = 1, $p = 0.247$). Therefore, our results are based on data obtained from the remaining 10 pools, and the number of replicates was reduced from 30 to 25 for single-pool experiments without cover and from 20 to 16 for single-pool experiments with cover and control with Plexiglas.

Single-pool experiments

In our single-pool experiments without cover, the distribution of coho between pool patches responded to changes in food abundance (Fig. 2) (one-way ANOVA, $F = 131.43$, df = 4, error df = 120, $p < 0.001$). The proportion of fish in each patch did not differ significantly from the proportion of food, as predicted by the IFD input-matching rule, when differences in patch food abundance either did not exist or were relatively small (Table 1). When differences in food availability between patches were large (1:5 and 1:11 feeding ratios), fish distributions deviated significantly from those predicted by the input-matching rule (Table 1). Although the proportion of juvenile salmon in the rich patch increased as differences between patches augmented, they undermatched food proportions (Fig. 2).

If we assume that fish are "ideal" and achieve input matching, at the 1:5 feeding ratio the binomial probability of finding nine fish in the rich patch (instead of 10) and three fish in the poor patch (instead of two) is $p = 0.20$. In turn, under the 1:11 feeding ratio the probability of observing 10 fish (instead of 11) in the rich patch and two in the poor patch (instead of 1) is $p = 0.18$.

© 1999 NRC Canada

Table 1. Single-pool experiments comparing observed and input-matching predicted coho salmon proportions among patches under different cover treatments and feeding ratios.

Cover treatment	Feeding ratio	df	t	p (power of test)	Outcome
No cover	0:0	24	–1.074	0.293 (0.83)	Matching
	1:1	24	0.559	0.581 (0.75)	Matching
	1:2	24	–0.421	0.678 (0.71)	Matching
	1:5	24	–5.637	<0.001	Undermatching
	1:11	24	–5.569	<0.001	Undermatching
Instream cover	0:0	15	0.538	0.598 (0.74)	Matching
	1:1	15	5.483	<0.001	Overmatching*
Instream cover in rich patch	1:2	15	–5.669	<0.001	Undermatching
	1:5	15	–6365	<0.001	Undermatching
	1:11	15	–7.771	<0.001	Undermatching
Instream cover in poor patch	1:2	15	0.876	0.395 (0.78)	Matching
	1:5	15	–1.979	0.066 (0.88)	Matching
	1:11	15	–2.652	0.018	Undermatching
Overhead cover	0:0	15	–0.815	0.428 (0.79)	Matching
	1:1	15	4.807	<0.001	Overmatching*
Overhead cover in rich patch	1:2	15	–8.321	<0.001	Undermatching
	1:5	15	–11.235	<0.001	Undermatching
	1:11	15	–12.381	<0.001	Undermatching
Overhead cover in poor patch	1:2	15	1.480	0.159 (0.85)	Matching
	1:5	15	–4.486	<0.001	Undermatching
	1:11	15	–6.886	<0.001	Undermatching

Note: Fish proportion in food-rich patch is used when patches differ in food abundance.
*Overmatching observed in pool with no cover.

The addition of cover, either instream or overhead, altered coho's response to patch profitability (Figs. 3 and 4). This response was observed regardless of patch profitability, provided there was food. In general, the distributions deviated further from input matching when cover was added to the rich patch than in experiments without cover.

In experiments with instream cover, coho distributed evenly between patches during the no-food control periods (Table 1; Fig. 3). But when food was available and cover was present in the rich patch, the proportion of fish in it always undermatched the proportion of food (Fig. 3*a*). They underused the patch with instream wooden structures even under a 1:1 feeding ratio (Table 1). As patch differences grew larger, so did the proportion of fish choosing the rich patch, but it never matched the proportion of food available in it. Juvenile coho salmon consistently underused the rich patch with instream structures compared with both the predictions of the IFD input-matching rule (Table 1; Fig. 3*a*) and the distributions observed in our experiments without cover. However, if cover was placed in the poor patch, more fish used the rich patch and the majority of the resulting distributions approximated those observed in our experiments with no cover. Under a 1:1 feeding ratio, fish overestimated the abundance of food in the clear patch (Table 1; Fig. 3*b*). During trials with 1:2 and 1:5 feeding ratios, this preference for the clear patch may have contributed to the observed matching between fish and patch food proportions (Table 1). The proportion of fish that chose the rich and clear patch did not increase proportionately with differences in patch profitability between the 1:5 and 1:11 feeding ratios, and undermatching was observed at the 1:11 ratio (Table 1; Fig. 3*b*).

A two-way ANOVA indicated that coho patch choice in these experiments was independently affected by both food availability (F = 32.46, df = 4, error df = 150, $p < 0.001$) and instream cover (F = 60.45, df = 1, error df = 150, $p < 0.001$) and by the interaction between them (F = 3.11, df = 4, error df = 150, $p = 0.011$). Therefore, we compared the mean number of fish in the rich patch under each of the four feeding ratios (1:1, 1:2, 1:5, 1:11) for each level of the instream cover treatment (present versus absent) using Tukey's studentized range test. Groupings resulting from this test changed with instream cover position (rich versus poor patch), indicating that the interaction effects changed with different treatment combinations (the test's groupings are shown in Fig. 3).

Exchanging the wooden structures for similar ones made of clear Plexiglas, which became almost invisible when submerged, confirmed that visual interference and not changes to water flow was the main effect that opaque instream structures had on fish. In our experiment with transparent structures, fish response to the different feeding ratios was almost identical to that observed in the experiments without cover (Table 2). A two-way ANOVA including both feeding ratio and Plexiglas structures as the main factors indicated that only food had a significant effect on the distribution of juvenile coho salmon during this experiment and that neither the effects of clear structures nor their interaction with feeding treatments was significant (Table 2).

The effect of overhead cover on fish patch choice was qualitatively similar to that observed for opaque instream structures but was quantitatively more extreme (Fig. 4). At any of the four feeding ratios, fish proportions in the rich patch with overhead cover were the lowest of all our experiments and, hence, significantly smaller than those predicted

© 1999 NRC Canada

Fig. 3. Mean proportion of coho salmon observed in the rich patch (*a*) with instream cover in the rich patch and (*b*) with instream cover in the poor patch. Observations were made every 30 s during the final 4 min of 6-min-long trials for each of the five different profitability ratios. Means were calculated using data from 16 replicate tests. The vertical bars are ±2 SE. The broken lines represent fish proportions predicted by the IFD input-matching rule. Circles are Fig. 2 results. Treatments with same letter in parentheses were classified in the same group with Tukey's test ($\alpha = 0.05$).

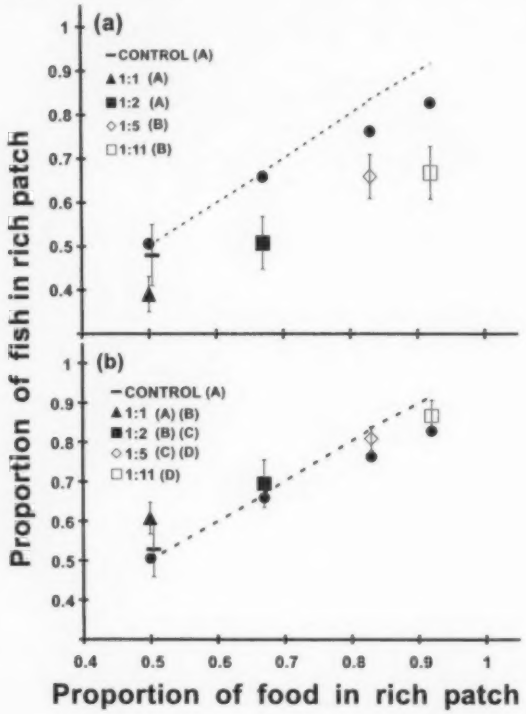

Fig. 4. Mean proportion of coho salmon observed in the rich patch (*a*) with overhead cover placed in the rich patch and (*b*) with overhead cover placed in the poor patch. Observations were made every 30 s during the final 4 min of 6-min-long trials for each of the five different profitability ratios. Means were calculated using data from 16 replicate tests. The vertical bars are ±2 SE. The broken lines represent fish proportions predicted by the IFD input-matching rule. Solid circles are Fig. 2 results and open circles are Fig. 3 results. Treatments with same letter in parentheses were classified in the same group with Tukey's test ($\alpha = 0.05$).

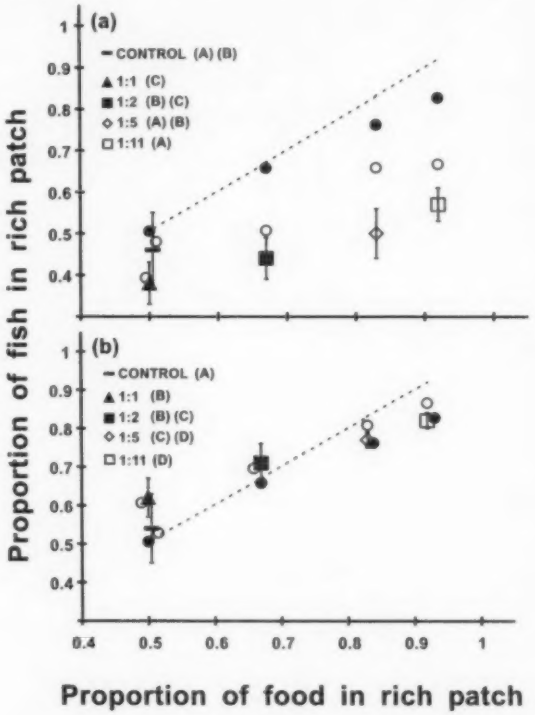

Table 2. Single-pool experiments comparing observed coho salmon proportions among patches in pools with no cover and in pools with Plexiglas structures in the rich patch under different feeding ratios.

Feeding ratio	df	*t*	*p* (power of test)
0:0	15	–0.108	0.914 (0.69)
1:1	15	–2.069	0.057 (0.89)
1:2	15	–1.628	0.111 (0.83)
1:5	15	–0.758	0.458 (0.77)
1:11	15	–0.986	0.332 (0.79)

Note: Fish proportion in food-rich pool is used when pools differ in food abundance.

by the input-matching rule of IFD (Table 1; Fig. 4*a*). The only exceptions were the no-food control trials, during which fish did not show preference for either patch (Table 1). In contrast, if overhead cover was on the poor patch, fish proportions in the rich and clear patch either coincided with or approached input-matching rule predictions (Fig. 4*b*). With overhead cover in the poor patch and under a 1:1 feeding ratio, overmatching was observed in the rich patch. Instead, fish distributions matched patch input rates of food during both no-food control and 1:2 feeding ratio trials (Table 1). At 1:5 and 1:11 feeding ratios, undermatching in the rich and clear patch was observed (Table 1; Fig. 4*b*).

A two-way ANOVA indicated that the effects of both treatments, patch food abundance ($F = 18.48$, df = 4, error df = 150, $p < 0.001$) and overhead cover ($F = 126.60$, df = 1, error df = 150, $p < 0.001$), were highly significant. The interaction between these treatments was also significant ($F = 8.34$, df = 4, error df = 150, $p < 0.001$), and therefore, Tukey's studentized range test for multiple comparisons among means was used. As was the case with instream cover, groupings resulting from this test changed depending on whether overhead cover was associated with the rich or poor patch (the test's groupings are shown in Fig. 4).

Paired-pool experiments

In paired-pool experiments without cover, the feeding ratio between pools was the only factor considered. When the

© 1999 NRC Canada

Table 3. Paired-pool experiments comparing observed and input-matching predicted coho salmon proportions among separate pools under different cover treatments and feeding ratios.

Cover treatment	Feeding ratio	df	t	p (power of test)	Outcome
No cover	1:1	8	–0.686	0.512 (0.69)	Matching
	1:5	8	–4.400	0.002	Undermatching
Cover in one pool	1:1	8	2.874	0.020	Overmatching*
Cover in rich pool	1:5	8	–0.359	0.728 (0.65)	Matching
Cover in poor pool	1:5	8	–4.910	<0.001	Undermatching

Note: Fish proportion in food-rich pool is used when pools differ in food abundance.
*Overmatching observed in pool with no cover.

Fig. 5. Distribution of coho salmon between two pools in response to food input equal in both pools, no cover present (1:1), food input equal in both pools, instream cover present in one of them (++1:1), food input in one of the pools five times higher than in the other one, no cover present (5:1), food input in one of the pools five times higher than in the other one, instream cover present in the food-poor pool (5:1++), and food input in one of the pools five times higher than in the other one, instream cover present in the food-rich pool (++5:1). The vertical bars are ±2 SE. Squares represent fish proportions predicted by the IFD input-matching rule, and circles represent mean fish proportions observed in the food-rich pool.

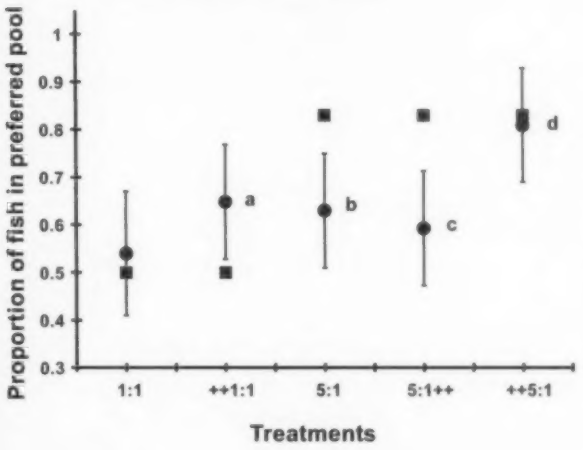

ratio was 1:1, juvenile coho salmon distributed quite evenly between pools, thus matching food input rate into the pools (Table 3; Fig. 5). Under a 1:5 ratio, more fish preferred the richer pool, but the proportion that occupied it by the end of the week-long trials was significantly lower than that predicted by input matching (Table 3; *b* in Fig. 5).

The presence of instream cover, in the double-pool manipulations, induced further variation in the final distribution of fish. Between two pools with equal abundance of food (1:1 ratio), one with instream structures and the other one without them, significantly more coho preferred the pool with cover (Table 3; *a* in Fig. 5). In experimental units receiving a 1:5 feeding ratio, if cover was in the poor pool, the rich pool attracted more fish than the poor one but a proportion significantly smaller than that predicted by the input-matching rule of IFD (Table 3; *c* in Fig. 5). However, if cover was placed in the rich pool, the combined effect of higher food abundance and instream cover increased fish proportions in that pool to levels that did not differ significantly from those predicted by the input-matching rule (Table 3; *d* in Fig. 5). Juvenile coho choice of pool in these double-pool experiments did not indicate a relationship between fish size and pool quality ($r^2 = 0.12$).

One-way ANOVA contrasts between treatments indicated that fish distributions were significantly different only when (*i*) the 1:1 feeding ratio without cover was compared with the 1:1 feeding ratio with cover ($F = 6.71$, df = 1, error df = 40, $p = 0.013$) and (*ii*) the 5:1 feeding ratio with cover in the poor pool was compared with the 5:1 feeding ratio with cover in the rich pool ($F = 9.66$, df = 1, error df = 40, $p = 0.004$).

Discussion

In structurally simple pool habitat with either no differences or relatively small differences in food abundance between patches, the spatial distribution of juvenile coho salmon responded numerically to the input rate of food as predicted by the input-matching rule of IFD. However, when differences in food abundance between patches were relatively large or habitat structural complexity was increased (e.g., with addition of either instream or overhead cover), the numerical distributions of fish consistently undermatched food input rate (Fig. 2). These results confirm our first hypothesis (input matching) only under very simple environmental conditions because juvenile coho seem to distribute in an "ideal" way as long as there are neither major differences in patch foraging quality nor cover structures (patch differences caused by a 1:2 feeding ratio can be considered relatively small by comparison with those created by 1:5 and 1:11 feeding ratios).

Such limited input matching, which increasingly turns into undermatching as differences between patches grow, would unlikely result from the random distribution of fish. The random selection of patches spreads competitors evenly between patches (Abrahams 1986; Kacelnik et al. 1992) and can frequently cause distributions like the ones in our no-food control and 1:1 feeding ratio trials. However, the input matching observed under the 1:2 feeding ratio or the level of undermatching that occurred at the 1:5 and 1:11 ratios has a very low probability of being the result of a random distribution of competitors. Grand (1997) found that the proportion of juvenile coho salmon undermatched the proportion of food in the rich patch of experimental glides, and towards the end of her trials, fish distributions were almost random. Her results showed significant correlation between the com-

© 1999 NRC Canada

petitive weight (or ability) of individuals (rather than their number) in the poor patch and the proportion of resources in it, providing quantitative support for Parker and Sutherland's (1986) "input-matching of competitive weights" prediction. In Grand's (1997) study, not all of the predictions of the UC model (Parker and Sutherland 1986; Sutherland and Parker 1992) were met, possibly due to the strong relationship found between fish competitive abilities and dominance rank. Although the competitive skills of fish changed between patches, the predicted segregation of competitor types across patches ("truncated" distribution, sensu Parker and Sutherland (1986), with the best competitors settling in the best patches and the poorer competitors in patches of lower quality) was not observed. Only a few of the most competitive (and dominant) individuals (15) spent 90% of their time in the rich patch monopolizing its resources, whereas the rest of the fish (115) scrambled for variable amounts of time in both patches (with an estimated average of 60% of the time in the rich patch). This could account for the lower than expected payoff per competitive weight that good competitors received (except for the 15 top fish, which did very well) and the proportionately higher than expected payoff for poor competitors that Grand (1997) reported.

Although the UC model (Parker and Sutherland 1986; Sutherland and Parker 1992) predicts undermatching as we observed in our single-pool experiments without cover, it does not anticipate the results that we obtained in the other experiments. In our single-pool experiments, we could not determine whether or not there was a truncated distribution of phenotypes across patches because we were not able to follow individuals. But in our double-pool trials, in which the final distribution of individually marked fish was recorded, the lack of relationship between fish size and quality of the pool that they occupied suggests that there was no segregation of phenotypes between patches. Fish size was used as a surrogate measure for competitive ability and dominance rank because competitive skills of juvenile coho are positively correlated with body size (Grand 1997) and larger individuals are dominant over smaller ones (Chapman 1962).

Given the dominance hierarchies that juvenile coho form in habitats with slow current (Chapman 1962), we anticipated undermatching and considered the IDD model (Fretwell and Lucas 1970) to be a suitable tool to explain our results. Other researches (Dolloff 1986; Bugert et al. 1991; Fausch 1993) found that juvenile coho salmon densities may increase in the presence of cover, which is supposed to reduce aggressive interactions by increasing visual isolation among competitors. Our second hypothesis predicts that the addition of instream structures reduces or eliminates undermatching in the rich patch by neutralizing the effects of juvenile coho's despotic behaviour and allowing subordinate individuals to forage in it. But this hypothesis was not confirmed by our experimental results. We observed that the presence of instream structures in the rich patch induces juvenile coho to forage in the clear and poor patch in numbers that are disproportionately high for the amount of food available in it. Contrary to what we anticipated, by increasing fish densities in the open patch, cover did not reduce but rather increased the probability of aggressive interactions among juvenile coho salmon. However, in the relatively crowded conditions of the open patch, our direct observations (combined with information from videotaped trials) indicated that despotic behaviour was infrequent during feeding trials. Aggressive displays were mainly observed during the no-food control trials and ceased almost entirely as soon as feeding began. It is possible that the nature of the scramble competition for food observed in our trials minimized any benefits of aggressive behaviours. Individual feeding success may have depended more on the early detection and fast appropriation of food than on its active defense. Other authors have reported that aggressive interactions among foraging fish are infrequent under conditions like ours, which render resource defense uneconomical (Abrahams 1989; Milinski and Parker 1991). However, dominant individuals do not need to display overt aggression all the time because the risk of being attacked may discourage subordinate individuals from trying to get the food items that arrive (Holmgren 1995).

The increased deviations from input matching caused by the addition of cover suggest that fish patch selection is affected by the physical complexity of the habitat (Figs. 3 and 5). Since salmonids are visual predators, it is likely that the presence of instream structures or the reduced amount of light under overhead cover hinders their ability to detect prey and accurately assess patch profitability. The fact that clear Plexiglas structures did not affect fish patch choice confirms that departures from the results of the no-cover experiments were caused by visual constraints (Fig. 4). Based on their limited perception, fish may be acting as "ideal" foragers trying to equalize their rates of prey capture across patches, but from the perspective of an outside observer, their distributions do not match the actual distribution of food resources.

In our single-pool experiments, two different factors acted independently or in a combined manner to affect fish distributions. One of the factors was the gradual reduction in the total amount of food delivered per trial as patch differences in food abundance increased with each feeding treatment (i.e., less food was delivered at the 1:5 than at the 1:2 ratio and so on), and the other factor was cover. With regard to food, its delivery protocol may have reduced its abundance to levels at which an increasing proportion of fish were unable to detect patch differences and ended up choosing patches at random as predicted by the PLM (Abrahams 1986; Gray and Kennedy 1994). This in itself could explain why, in the no-cover experiments under both 1:5 and 1:11 feeding ratios, we observed a tendency to equalize fish numbers between patches.

Juvenile coho salmon were indifferent to cover in the absence of food but avoided cover to different degrees depending on whether it was placed in the food-rich or food-poor patch. At a 1:1 feeding ratio, the interaction between food and cover altered the even distribution across patches that we had observed in trials without cover. When patches differed in foraging quality (1:2, 1:5, and 1:11 ratios), the addition of instream cover to the rich patch increased the number of fish that foraged in the poor patch (Fig. 3*a*). Likewise, cover in the poor patch increased the proportion of juvenile coho feeding in the rich patch (Fig. 3*b*). This led to either input matching (1:2 and 1:5 feeding ratios with instream cover and 1:2 ratio with overhead cover) or overmatching (1:1 ratio with instream or overhead cover). Unlike reduc-

© 1999 NRC Canada

tions in food abundance, which may increase the proportion of fish that have to choose foraging patches at random, cover makes juvenile coho overestimate food abundance in the open areas and distribute accordingly.

Overhead cover is believed to protect fish from predators (Helfman 1981; Shirvell 1990), and because it does not isolate competitors from each other or from their prey, we did not expect it to affect the distribution of juvenile coho the way that instream cover does. Several authors (Dolloff and Reeves 1990; Bugert et al. 1991; Fausch 1993) have reported that coho fry in natural streams are, in general, less responsive to overhead cover than to instream cover and wander to forage farther away from it than other juvenile salmonids do. In our no-food control trials, juvenile coho distributed evenly across patches regardless of the placement of overhead cover. It is possible that in the absence of predation risk, the value of overhead cover becomes so negligible that juvenile coho show little or no attraction to it (Grand and Dill 1997; Reinhardt and Healey 1997). In trials with food, however, fish distributions departed from input matching in similar or more extreme ways than those observed with instream structures (Fig. 5). It is possible that shading underneath overhead cover may have affected the ability of the fish to assess patch foraging quality despite the overhead structures being 15 cm above the water surface to allow relatively similar amounts of light into both patches.

Grand and Dill (1997) suggest that, under risk of predation, fish integrate the value of both overhead cover and food when selecting a foraging site. They observed that the presence of cover made their poor patches more attractive to juvenile coho salmon, a trend that was reversed only when they added extra food to the uncovered patch. Although their findings seem to contradict our results, this discrepancy may be explained by differences between our experimental subjects, setups, and methods of recording use of patch. Thus, while Grand and Dill (1997) used wild coho salmon for their experiments, we used fish of hatchery origin. However, although the origin of the fish could contribute to the abovementioned difference, it is unlikely to be the only cause (particularly since our fish were not raised the way that most hatchery fish are). Other factors responsible for the different outcomes could be the predation treatment that Grand and Dill's (1997) fish were exposed to and their overhead structures occupying only a small percentage of the "covered" patches. In our trials, fish may have been more prone to forage in the "open" patch because predation risk was very low or nonexistent. In addition, many fish that were not under cover were still recorded as using cover by Grand and Dill (1997) because they were occupying the covered patch (even when the average amount of time that they estimated that fish actually spent under cover was only 8%). In contrast, in our experiments, all individuals that were not directly below the overhead structures were in the uncovered patch and "recorded" accordingly.

In our double-pool experiments, juvenile coho responded positively, although not proportionately, to pool foraging quality. When pools received equal amounts of food, fish achieved input-matching distributions. When one of the pools was five times richer in food than the other, the young coho preferred the rich pool, but their proportions undermatched those of food. Due to the increased distance and isolation between patches (which translates into additional sampling costs), fish are expected to switch patches less often and therefore to gather less accurate information about patch quality, which leads to undermatching (Bernstein et al. 1991). The final distribution may represent the equilibrium between two opposing tendencies, one to increase undermatching as the result of fish lacking adequate information on patch quality and the other to reduce undermatching as a consequence of fish switching patches less often (Milinski 1994). Given the option, juvenile coho preferred pools with instream cover, even if these were food-poor pools. But the pools that attracted the highest fish proportions offered both instream cover and the largest proportion of food. The preference that juvenile coho salmon showed in these experiments for pools with instream cover agrees with what Lonzarich and Quinn (1995) observed at the stream reach level. However, it contrasts with what Reinhardt and Healey (1997) observed on a similar spatial scale and in the absence of predation.

Our seemingly contradictory results (juvenile coho favouring pools with woody instream structures but avoiding the patch with cover within a pool) and their differences with what other authors have recently found (Grand 1997; Grand and Dill 1997; Reinhardt and Healey 1997) help explain, to some extent, the lack of consensus that one finds in the literature with regard to habitat selection and cover use by juvenile coho. Our results and those of others indicate that juvenile coho salmon use cover in a flexible manner in response to a variety of factors, such as perception of food availability, predation risk, density of competitors, ontogenetic phase, size-specific needs, and distance between resource patches. The preference that we observed that juvenile coho salmon have for pools with cover and, within those pools, for open areas without cover indicates the need for a combination of accessible refuge and open foraging sites, where prey and perhaps also predators are easily detected. This may be a behavioural adaptation to a relatively brief freshwater phase before smolting, in which both fish winter survival and smolting rate are positively correlated with body size (Sandercock 1991). Therefore, any behaviour that maximizes food intake and growth is likely to be favoured in these populations, even at the expense of increased risks. Thus, although feeding in open areas may increase the threat of predation, a large number of small-size risk-taking individuals prefer to forage in such areas because they face less competition from the larger and risk-averse members of their cohort (Reinhardt and Healey 1997). The high densities reached by juvenile coho salmon in nursery habitat of coastal streams may indeed lower the individual risk of predation in open areas, as suggested by the greater number of fish foraging farther away from cover when densities are high than when individuals are tested in isolation (Dill and Fraser 1984).

It is evident that optimum salmonid nursery habitat is the result of the combination of many different factors, cover availability being just one of them. Thus, degraded habitat cannot be transformed into productive habitat by simple woody debris or boulder placement projects alone. Unfortunately, many habitat restoration initiatives in British Columbia seem to be based on this premise and suggest that isolated instream structure placement projects could be the answer to the problem of salmonid habitat degradation. Al-

© 1999 NRC Canada

though IFD theory could help increase the efficacy of some of these enhancement projects, as Grand and Dill (1997) suggested, the applicability of its various models will not always be possible or simple under natural, uncontrolled conditions. However, even if enhancement projects were effective at a local level, due to their mobility, juvenile salmonids could always respond to them with increased migration into the enhanced areas. Therefore, unless the larger scale problems that altered the system in the first place are controlled, salmonid production in the entire watershed is not likely to augment. The best approach to increasing the success of small-scale habitat restoration projects requires their integration with strategies aimed at preserving stream reach scale components (e.g., riparian forests) and plans designed to protect watershed-scale components (e.g., hydrologic regime, channel morphology, and water quality and quantity).

Acknowledgements

The experimental work was completed with the valuable assistance of Krzysztof (Chris) Bobinski. Special thanks to Jim Servizi and all the staff of the Cultus Lake Research Laboratory, Department of Fisheries and Oceans, for allowing us to use the experimental stream channels and their facilities. Wesley Hochachka provided invaluable statistical advice. Critical reviews from Scott Hinch, Jordan Rosenfeld, and Blair Holtby significantly improved the manuscript. The Corporation of the Township of Langley, British Columbia, provided generous collaborative support through Peter Scales. Financial support for this research was provided by a Natural Sciences and Engineering Research Council of Canada scholarship and a British Columbia Science Council GREAT award to G.R.G. and a Natural Sciences and Engineering Research Council of Canada operating grant to M.C.H.

References

Abrahams, M.V. 1986. Patch choice under perceptual constraints: a cause for departures from an ideal free distribution. Behav. Ecol. Sociobiol. **19**: 409–415.

Abrahams, M.V. 1989. Foraging guppies and the ideal free distribution: the influence of information on patch choice. Ethology, **82**:116–126.

Bernstein, C., Kacelnik, A., and Krebs, J.R. 1991. Individual decisions and the distribution of predators in a patchy environment. II. The influence of travel costs and structure of the environment. J. Anim. Ecol. **60**: 205–225.

Bisson, P.A., Nielsen, J.L., Palmason, R.A., and Grove, L.E. 1982. A system of naming habitat types in small streams, with examples of habitat utilization by salmonids during low streamflow. *In* Acquisition and utilization of aquatic habitat inventory information. *Edited by* N.B. Armantrout. American Fisheries Society, Bethesda, Md. pp. 62–73.

Bisson, P.A., Bilby, R.E., Bryant, M.D., Dolloff, C.A., Grette, G.B., House, R.A., Murphy, M.L., Koski, K.V., and Sedell, J.R. 1987. Large woody debris in forested streams in the Pacific Northwest: past, present, and future. *In* Streamside management: forestry and fishery interactions. *Edited by* E.O. Salo and T.W. Cundy. Institute of Forest Resources, University of Washington, Seattle, Wash. pp. 143–190.

Bugert, R.M., and Bjornn, T.C. 1991. Habitat use by steelhead and coho salmon and their responses to predators and cover in laboratory streams. Trans. Am. Fish. Soc. **120**: 486–493.

Bugert, R.M., Bjornn, T.C., and Meehan, W.R. 1991. Summer habitat use by young salmonids and their responses to cover and predators in a small southeast Alaska stream. Trans. Am. Fish. Soc. **120**: 474–485.

Chapman, D.W. 1962. Aggressive behaviour in juvenile coho salmon as a cause of emigration. J. Fish. Res. Board Can. **19**: 1047–1080.

Dill, L.M., and Fraser, A.H.G. 1984. Risk of predation and the feeding behavior of juvenile coho salmon (*Oncorhynchus kisutch*). Behav. Ecol. Sociobiol. **16**: 65–71.

Dolloff, C.A. 1986. Effects of stream cleaning on juvenile coho salmon and Dolly Varden in southeast Alaska. Trans. Am. Fish. Soc. **116**: 829–838.

Dolloff, C.A., and Reeves, G.H. 1990. Microhabitat partitioning among stream-dwelling juvenile coho salmon, *Oncorhynchus kisutch*, and Dolly Varden, *Salvelinus malma*. Can. J. Fish. Aquat. Sci. **47**: 2297–2306.

Fausch, K.D. 1993. Experimental analysis of microhabitat selection by juvenile steelhead (*Oncorhynchus mykiss*) and coho salmon (*Oncorhynchus kisutch*) in a British Columbia stream. Can. J. Fish. Aquat. Sci. **50**: 1198–1207.

Fretwell, S.D. 1972. Populations in a seasonal environment. Princeton University Press, Princeton, N.J.

Fretwell, S.D., and Lucas, H.L. 1970. On territorial behavior and other factors influencing habitat distribution in birds. I. Theoretical development. Acta Biotheor. **19**: 16–36.

Grand, T.C. 1997. Foraging site selection by juvenile coho salmon: ideal free distributions of unequal competitors. Anim. Behav. **53**: 185–196.

Grand, T.C., and Dill, L.M. 1997. The energetic equivalence of cover to juvenile coho salmon (*Oncorhynchus kisutch*): ideal free distribution theory applied. Behav. Ecol. **8**: 437–447.

Gray, R.D., and Kennedy, M. 1994. Perceptual constraints on optimal foraging: a reason for departures from the ideal free distribution? Anim. Behav. **47**: 469–471.

Helfman, G.S. 1981. The advantage to fish of hovering in shade. Copeia, **1981**: 392–400.

Holmgren, N. 1995. The ideal free distribution of unequal competitors: predictions from a behaviour-based functional response. J. Anim. Ecol. **64**: 197–212.

Kacelnik, A., Krebs, J.R., and Bernstein, C. 1992. The ideal free distribution and predator prey populations. Trends Ecol. Evol. **2**: 50–55.

Lonzarich, D.G., and Quinn, T.P. 1995. Experimental evidence for the effect of depth and structure on the distribution, growth, and survival of stream fishes. Can. J. Zool. **73**: 2223–2230.

Milinski, M. 1994. Ideal free theory predicts more than only input matching — a critique of Kennedy and Gray's review. Oikos, **71**: 163–166.

Milinski, M., and Parker, G.A. 1991. Competition for resources. *In* Behavioural ecology: an evolutionary approach. 3rd ed. *Edited by* J.R. Krebs and N.B. Davies. Blackwell Scientific Publications Ltd., Oxford, England. pp. 137–168.

Orians, G.H. 1969. On the evolution of mating systems in birds and mammals. Am. Nat. **103**: 589–603.

Parker, G.A. 1978. Searching for mates. *In* Behavioural ecology: an evolutionary approach. 1st ed. *Edited by* J.R. Krebs and N.B. Davies. Blackwell Scientific Publications Ltd., Oxford, England. pp. 214–244.

Parker, G.A., and Sutherland, W.J. 1986. Ideal free distributions when individuals differ in competitive ability: phenotype-limited ideal free models. Anim. Behav. **34**: 1222–1242.

© 1999 NRC Canada

Ptolomy, R.A. 1993. Maximum salmonid densities in fluvial habitats in British Columbia. *In* Proceedings of the Coho Workshop, May 26–28, 1992, Nanaimo, B.C. *Edited by* L. Berg and P.W. Delaney. Department of Fisheries and Oceans, Vancouver, B.C. pp. 223–250.

Pulliam, R.H., and Caraco, T. 1984. Living in groups, is there an optimal group size? *In* Behavioural ecology. 1st ed. *Edited by* J.R. Krebs and N.B. Davies. Blackwell Scientific Publications Ltd., Oxford, England. pp. 122–147.

Reinhardt, U.G., and Healey, M.C. 1997. Size-dependent foraging behaviour and use of cover in juvenile coho salmon under predation risk. Can. J. Zool. **75**: 1642–1651.

Sandercock, F.K. 1991. Life history of coho salmon. *In* Pacific salmon life histories. *Edited by* C. Groot and L. Margolis. University of British Columbia Press, Vancouver, B.C. pp. 395–445.

SAS Institute Inc. 1988. SAS/STAT user's guide. Release 6.03 edition. SAS Institute Inc., Cary, N.C.

Shirvell, C.S. 1990. Role of instream rootwads as juvenile coho salmon (*Oncorhynchus kisutch*) and steelhead trout (*O. mykiss*) cover habitat under varying streamflows. Can. J. Fish. Aquat. Sci. **47**: 852–861.

Spalding, S., Peterson, N.P., and Quinn, T.P. 1995. Summer distribution, survival and growth of juvenile coho salmon under varying experimental conditions of brushy instream cover. Trans. Am. Fish. Soc. **124**: 124–130.

Sutherland, W.J., and Parker, G.A. 1992. The relationships between continuous input and interference models of ideal free distributions with unequal competitors. Anim. Behav. **44**: 345–355.

Zar, J.H. 1984. Biostatistical analysis. 2nd ed. Prentice-Hall, Englewood Cliffs, N.J.

© 1999 NRC Canada

Multivariate regression relationships between ocean conditions and early marine survival of coho salmon (*Oncorhynchus kisutch*)

Kristen E. Ryding and John R. Skalski

Abstract: Washington State hatcheries have released coded wire tagged coho salmon (*Oncorhynchus kisutch*) since the early 1970s and have recorded data on the number and ages of adult returns. From these data, we isolated marine survival from release to age 2 using a multinomial model incorporating the multivariate structure of the age-at-return data. Only hatcheries on or near the coast were used in the analysis in order to isolate marine effects. Using models to explore linear and curvilinear relationships, early marine survival was regressed against environmental covariates of sea surface temperature (SST), coastal upwelling, and the date of spring transitions. With hatcheries serving as replicates, curvilinear relationships were found between survival and both June SST and the date of spring transition. Maximum survival occurred for a June SST of 13.45°C and for a spring transition date around April 2. The regression results support the idea of optimal environmental conditions for coho salmon survival and may help fisheries managers better understand the dynamics of early marine survival of salmonids.

Résumé : Les pisciculteures de l'État du Washington libèrent des saumons cohos (*Oncorhynchus kisutch*) marqués par fils codés depuis le début des années 1970 et elles ont recueilli des données sur le nombre et l'âge des adultes qui sont revenus aux installations. Nous avons déterminé, à partir de ces données, le taux de survie en mer, entre le moment de la mise à l'eau et l'âge 2, en utilisant un modèle multinomial tenant compte de la structure multivariée des données sur l'âge au moment du retour. L'analyse n'a porté que sur les pisciculteures situées sur la côte ou à proximité de celle-ci afin d'isoler les effets liés à la mer. Des modèles permettant d'examiner les relations linéaires et non linéaires ont été utilisés pour effectuer une régression de la survie en mer peu de temps après l'arrivée des poissons en fonction des covariables environnementales que sont la température de la surface de la mer (TSM), les remontées côtières et la date des transitions de printemps. En utilisant les pisciculteures comme témoins, des relations non linéaires ont été trouvées entre la survie et la TSM de juin et la date de transition de printemps. La survie maximale a été notée pour une TSM de juin de 13,45°C et pour une date de transition de printemps se situant aux environs du 2 avril. Les résultats de la régression appuient l'hypothèse de conditions environnementales optimales pour la survie du saumon coho et pourraient aider les gestionnaires des pêches à mieux comprendre la dynamique de la survie des salmonidés peu de temps après leur arrivée en mer.

[Traduit par la Rédaction]

Introduction

The success of salmon management practices is measured by the numbers of adult returns, and when adult returns are low, freshwater influences rather than marine influences often take much of the blame as the source for high mortality (Snake River Salmon Recovery Team 1993). But what if mortality in the marine environment is the major source for the variation in adult returns? For example, if survival in the ocean is on the order of 5%, a 1–2% change in survival will be reflected in a 20–40% change in adult returns. However, when in-river survival during smolt outmigration to the ocean is of the order of 50%, a 1–2% change in freshwater survival will produce only a 2–4% change in adult returns. This is why small changes in ocean survival can be important to the fisheries resources and industries that rely on adult returns. It is becoming increasingly clear that understanding the relationship between the marine environment and salmon survival is central to better management of our salmonid resources.

The purpose of this paper is to introduce a multivariate approach to analyzing coded wire tagged (CWT) age-at-return data in order to regress first-year ocean survival probabilities against coastal ocean conditions and climate covariates. Survival probabilities, regression coefficients, and associated variances of the parameter estimates will be derived using maximum likelihood theory (Casella and Berger 1990). The methods will be illustrated using regional data from 15 coho salmon (*Oncorhynchus kisutch*) hatchery stocks in Washington State from 1970 to 1991. Meta-analysis (Eddy et al. 1992) will be subsequently used to make broad regional inferences regarding the effect of climate conditions on the interannual variability of marine survival of coastal coho stocks. The analysis of coho hatchery

Received October 15, 1998. Accepted July 10, 1999.
J14831

K.E. Ryding.[1] Quantitative Ecology and Resource Management, Box 351720, University of Washington, Seattle, WA 98195-1270, U.S.A.
J.R. Skalski. School of Fisheries, Box 358218, University of Washington, Seattle, WA 98195-1270, U.S.A.

[1]Author to whom all correspondence should be addressed.
e-mail: kristen@cqs.washington.edu

© 1999 NRC Canada

data will illustrate the importance of basing inferences concerning ocean effects on regional tag return data and the need to examine nonlinear survival relationships when exploring climate conditions.

Numerous studies have found correlations between marine survival of Pacific Northwest salmon and other commercial fish and ocean conditions off the coast of Oregon, Washington, and the North Pacific. Positive correlations have been found between cumulative upwelling and salmon survival (Gunsolus 1978; Scarnecchia 1981; Nickelson and Lichatowich 1984; Nickelson 1986) and cumulative upwelling and salmon growth rates (Fisher and Pearcy 1988; Holtby et al. 1990). Fewer studies have pointed to a relationship between sea surface temperature (SST) and smolt survival. Negative correlations between coastal SST and smolt survival in the year of migration for both coho and chinook salmon (*Oncorhynchus tshawytscha*) have been reported (Nickelson 1986; Holtby and Scrivner 1989; Hyun 1996). Holtby and Scrivener (1989) also noted lower smolt survival during years of higher temperatures and low salinity and suggested that variability in smolt survival was associated with variations in SST during the first few months of ocean residence. Nickelson (1986) reported that in years of strong upwelling conditions, smolt survival was negatively correlation with June SST in the year of smolt outmigration. Additionally, McFarlane and Beamish (1992) found an increase in year-class abundance of sablefish (*Anoplopoma fimbria*) after extended periods of below-average SST off the coast of Vancouver Island.

Many studies of the past decade have also focused on the concepts of decadal-scale fluctuations in climate conditions in the North Pacific Ocean and the subsequent effect on marine ecosystems. Of particular relevance to the time period of this study is the abrupt shift in oceanic conditions that occurred in the winter of 1976–1977 (Beamish 1993; Beamish and Bouillon 1993; Francis and Hare 1994; Trenberth and Hurrell 1994). The "shift" was marked by a rise in SST along the North American coast and a deepening and eastward movement in the center of the Aleutian Low pressure system, affecting wind-driven currents. Ocean conditions occurring after 1977 are thought to unfavorable for the survival of Pacific Northwest salmon (Francis et al. 1998). Nevertheless, considerable variability in the return rates of salmonids appears to exist within these regimes. The purpose of this paper is to describe those factors that may be responsible for these short-term interannual changes in early coho survival.

The analysis in this paper differs from previous studies in two ways. First, the historical approaches to regression used in analyzing CWT data (Gunsolus 1978; Scarnecchia 1981; McCarl and Rettig 1983; Nickelson and Lichatowich 1984; Nickelson 1986) have been to collapse the multidimensional return data into one-dimensional estimates of total returns or recovery proportions. However, return data of adult salmonids are multivariate in nature, with one cohort having adult returns over several age-classes. Ignoring the multivariate nature of the data risks losing information. Second, the relationships between survival and ocean conditions have been generally assumed to be linear (Gunsolus 1978; Scarnecchia 1981; Nickelson and Lichatowich 1984; Nickelson 1986; Fisher and Pearcy 1988; Holtby et. al. 1990; Hyun 1996). In contrast, this paper will examine the multivariate structure of the age-at-return data using multivariate and quadratic regression techniques to more accurately describe the survival relationships.

Materials and methods

Study area

The study area (Fig. 1) incorporated 15 Washington State hatcheries located in the Juan de Fuca Strait, coastal Washington, and on the Columbia River below Bonneville Dam (river kilometre 234). Hatchery fish with outmigration routes free of dams were chosen for the analysis in order to minimize the confounding effects of hydroelectric production. Puget Sound hatcheries were left out of the analysis because fish from these hatcheries appear to have different migration patterns (Pearcy and Fisher 1988). The hatcheries were divided into three geographic regions determined by location of ocean entry. The Juan de Fuca Strait region included two hatcheries with outmigrants passing through the Strait. The coastal region included hatcheries located on rivers with outmigration routes leading directly to the ocean. Hatcheries located in the Lower Columbia River region had outmigration routes passing through the mouth of the Columbia River (Fig. 1; Table 1). Each hatchery served as a replicate in the analysis, and inferences were made both by region and across all hatcheries. The specific brood years from each hatchery used in the analysis are summarized in Table 1.

Data

Data used to calculate survival estimates were CWT release numbers and adult recovery numbers of coho salmon obtained from the Regional Mark Processing Center (1993), managed by the Pacific States Marine Fisheries Commission. The CWT data for hatchery fish were chosen for the analysis because more accurate recovery information was available from hatchery sources than from wild stocks. The specific CWT release data used in the analysis included the tag (batch) numbers, release numbers per batch, the hatchery where the releases occurred, date of release, and brood year of the fish. CWT recovery data include the year of recovery, the batch number, and the total number of expanded recoveries for a particular batch from the commercial fishery and hatcheries. The analysis encompassed the brood years from 1970 to 1991, although no one hatchery included all years (Table 1). The CWT release and return data for each hatchery are given in Ryding (1998) and are available upon request.

The ocean conditions that were used as covariates in the analysis included (*i*) SST, (*ii*) coastal upwelling conditions, and (*iii*) the date of spring transition (Table 2). The two measures of SST used in the analysis were the (*a*) average June SST and (*b*) the summer SST. Ryding (1998) also looked at the North Pacific index (NPI) (Trenberth and Hurrell 1994) and the Pacific Northwest index (Ebbesmeyer and Strickland 1995), but found no convincing relationships with early ocean survival of coho. The summer SST was calculated as the average of the monthly averages of SST from May to September. Measurements of SST were taken from observations made off the coast of Washington State. Upwelling conditions used in the analysis were monthly averages measured on the Bakun index, taken at 45°N latitude and 48°N latitude (both at 125°W longitude). The units in the Bakun index are in metric tons·s^{-1}. 100 mi of coastline^{-1} (Bakun 1973). The upwelling covariate was calculated as the total of the monthly averages from March through September. The spring transition was defined as the approximate calendar date when coastal upwelling replaces the downwelling conditions of winter. The specific date was calculated for the coastal waters near the mouth of the Columbia River from data on changes in wind patterns off the coast of Washington and Oregon (Ingraham and Miyihara 1988).

© 1999 NRC Canada

Fig. 1. Locations of hatcheries used in the CWT analysis and the regions in which they occur. The locations of upwelling and SST measurements are also shown. Numbers correspond to the hatchery names listed in Table 1.

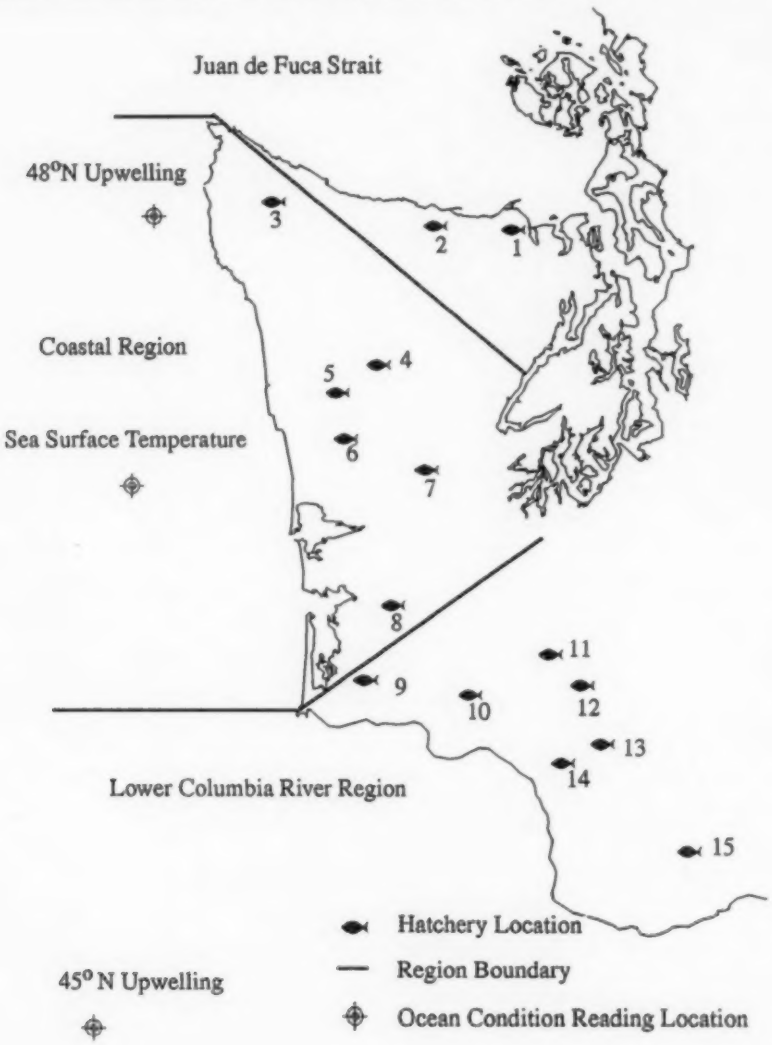

Statistical methods

A multinomial survival model incorporating marine survival probabilities to age-at-return was developed to take advantage of the multivariate age-at-return data of the CWT returns. The expected number of fish at any age recovered in the fishery or at the hatchery can be expressed as

$$(1) \qquad E(O_{ij}) = R_i P_{ij} \left(\prod_{n=2}^{j} S_{in} \right) M_{ij}$$

for fishery recoveries and

$$(2) \qquad E(H_{ij}) = R_i (1 - P_{ij}) \left(\prod_{n=2}^{j} S_{in} \right) M_{ij}$$

for hatchery returns, where R_i is the total number of CWT marked smolts released from a hatchery for the ith brood year (i = 1, 2,..., n), O_{ij} is the number of CWT-marked fish recovered in the fishery of the ith brood year (i = 1, 2,..., n) of the jth age-class (j = 2, 3, 4), H_{ij} is the number of CWT-marked fish recovered at the hatchery of the ith brood year (i = 1, 2,..., n) of the jth age-class (j = 2, 3, 4), S_{ij} is the probability of a fish from the ith brood year (i = 1, 2,..., n) surviving to the jth age-class given survival to age-class $j - 1$ (j = 2, 3, 4), P_{ij} is the probability of being caught in the fishery for the ith brood year (i = 1, 2,..., n) at the jth age-class (j = 2, 3, 4), M_{ij} is the probability of maturing at the jth age-class (j = 2, 3, 4) for the ith brood year (i = 1, 2,..., n), and $t_{ij} = H_{ij} + O_{ij}$ is the number of expanded recoveries of CWT-tagged fish from both the fishery and hatchery of the ith brood year (i = 1, 2,..., n) in the jth age-class (j = 2, 3, 4).

The expected number of j-year fish recovered from the fishery and hatchery (total recoveries) is then

© 1999 NRC Canada

Table 1. Location and available brood years of data for the 15 Washington State hatcheries used in the CWT analysis.

Region	Hatchery*	Brood years	Years of data
Juan de Fuca Strait	Dungeness Hatchery (1)	1970–1972, 1975–1980, 1983, 1986, 1989, 1991	13
	Lower Elwha Hatchery (2)	1978–1982, 1985–1989, 1991	11
Coastal	Soleduck Hatchery (3)	1971, 1972, 1974–1976, 1980–1988, 1990, 1991	16
	Quinault Lake Hatchery (4)	1977–1986, 1988–1991	14
	Quinault National Fish Hatchery (5)	1973–1991	19
	Humptulips Hatchery (6)	1980, 1982–1991	11
	Bingham Creek (Simpson) Hatchery (7)	1971–1975, 1980–1991	17
	Willapa Hatchery (8)	1971, 1974, 1980–1986	9
Lower Columbia	Grays River Hatchery (9)	1974–1985, 1988–1991	16
	Elochomin Hatchery (10)	1972, 1974, 1983–1985, 1988–1990	8
	Cowlitz Hatchery (11)	1972, 1980–1991	13
	Toutle Hatchery (12)	1972, 1977, 1978, 1986–1991	9
	Kalama Creek Hatchery (13)	1977, 1985–1989, 1991	7
	Kalama Falls Hatchery (14)	1983–1985, 1988–1991	7
	Washougal Hatchery (15)	1974, 1977–1982, 1988–1991	11

*Number corresponds to locations in Fig. 1.

$$(3)\quad E(H_{ij} + O_{ij}) = E(t_{ij}) = R_i P_{ij} \left(\prod_{n=2}^{j} S_{in} \right) M_{ij} + R_i (1 - P_{ij}) \left(\prod_{n=2}^{j} S_{in} \right) M_{ij}$$

$$E(t_{ij}) = R_i P_{ij} \left(\prod_{n=2}^{j} S_{in} \right) M_{ij} - R_i P_{ij} \left(\prod_{n=2}^{j} S_{in} \right) M_{ij} + R_i \left(\prod_{n=2}^{j} S_{in} \right) M_{ij}$$

$$E(t_{ij}) = R_i \left(\prod_{n=2}^{j} S_{in} \right) M_{ij}.$$

The parameter M_{ij} may also be thought of as the probability that the fish will be of a certain size or type (i.e., jack or adult) so as to be seen in either the fishery or the hatchery. The important aspect of eq. 3 is that by combining recoveries from both the fishery and hatchery, calculations of fishing effort become unnecessary.

The multinomial model uses the probabilities of recovery at 2, 3, and 4 years of age as the cell probabilities. The observations were the number of adults of each age-class estimated to have returned using tag recoveries from both the fishery and hatchery (i.e., t_{i2}, t_{i3}, and t_{i4}). The regression of survival from release to age 2 (i.e., about 1.5 years of age) for a cohort against covariate values of ocean conditions in the year of outmigration (early ocean residence) was based on a proportional hazards (PH) model (McCullagh and Nelder 1989), given by

$$(4)\quad S_2 = S_0^{e^{\underline{x}\cdot\underline{\beta}}}$$

where S_0 is the baseline survival, $\underline{x}$ is the vector of the covariates of interest, and $\underline{\beta}$ is the vector of regression coefficients.

The PH model was chosen because of its flexibility and the ease of parameter interpretation. Positive values of the regression coefficient β indicate a negative association of survival with the covariate, and negative coefficients indicate positive relationships between survival and the covariate. Substituting the PH model for survival to age 2 (i.e., eq. 4), θ_1 for the probability of surviving to and maturing at age 3 given survival to age 2 (i.e., $\theta_1 = S_3 M_3$), and θ_2 for the probability of surviving and maturing to age 4 given survival to age 2 (i.e., $\theta_2 = S_3 S_4 M_4$) yields the following likelihood model:

$$(5)\quad L(S_0, \beta, M_2, \theta_1, \theta_2 | R_i, t_{i2}, t_{i3}, t_{i4}, x_i) = \prod_{i=1}^{n} \left(\frac{R_i}{\prod_{j=2}^{4} t_{ij}} \right) (S_0^{e^{x_i \beta}} M_2)^{t_{i2}} (S_0^{e^{x_i \beta}} \theta_1)^{t_{i3}} \times (S_0^{e^{x_i \beta}} \theta_2)^{t_{i4}} (1 - S_0^{e^{x_i \beta}} (M_2 + \theta_1 + \theta_2))^{R_i - \sum_{j=2}^{4} t_{ij}}.$$

The model parameters S_0, β, θ_1, and θ_2 were estimated using maximum likelihood methods (Casella and Berger 1990, pp. 289–297). Numerical optimization, using FLETCH (Fletcher 1970), iteratively solved for the maximum likelihood estimates and provided asymptotic variance estimates.

The stochastic CWT model used several assumptions about the tag data that are standard to mark–recapture data analysis. The tag groups were assumed to be representative of the population of inference, and all tagged fish had an equal probability of surviving and migrating back to the hatchery in a particular year. In addition, release numbers of tagged smolts were assumed to be known without error, and recovered fish were correctly identified to batch, brood year, and age-at-recovery. Fish caught in the fishery were assumed to be a random sample of the fish migrating in that year (i.e., no bias toward tagged fish in the fishery). The fish inspected for tags in the fishery were also assumed to be representative of all fish in the fishery and the fraction of fish sampled was known without error. In addition, the model also assumed that the release groups were closed to emigration and immigration and the number of tagged hatchery fish straying to the spawning grounds, an area where tags are less likely to be detected, was negligible. Also, the parameter M_{ij} was assumed constant across all brood years (i.e., $M_{ij} = M_j \; \forall \; j$) for a stock from the same hatchery.

The four parameters (i.e., S_0, M_2, θ_1, and θ_2) plus one regression coefficient (β) for each of the covariates in the PH model were estimated independently for each of the 15 hatcheries. Each estima-

© 1999 NRC Canada

Table 2. Covariate values used in the regression analysis.

Observation year	Brood year	June SST (°C)	Summer average SST (°C)	45°N June upwelling (Bakun units)	48°N upwelling (Bakun units)	Spring transition date (calendar day)
1972	1970	13.13	12.716	55	51	103.103
1973	1971	12.72	13.768	27	122	74.192
1974	1972	12.67	13.590	80	76	102.707
1975	1973	11.84	12.964	98	156	73.967
1976	1974	12.66	13.414	56	25	84.664
1977	1975	12.63	13.190	71	125	71.799
1978	1976	14.84	13.704	34	83	85.182
1979	1977	12.78	14.296	86	173	74.417
1980	1978	12.90	13.720	32	197	109.416
1981	1979	13.86	14.162	8	94	94.603
1982	1980	11.98	13.284	59	213	83.305
1983	1981	14.51	14.596	19	67	95.214
1984	1982	12.20	13.550	37	88	107.567
1985	1983	12.84	13.702	52	197	70.756
1986	1984	14.22	13.966	25	132	94.796
1987	1985	12.99	13.922	43	133	101.224
1988	1986	13.78	13.808	14	119	88.555
1989	1987	13.44	14.372	43	93	99.036
1990	1988	13.40	14.654	15	113	83.043
1991	1989	12.87	13.754	59	112	71.920
1992	1990	14.57	14.420	61	152	69.205
1993	1991	14.89	14.280	24	11	130.761

ble parameter required one brood year's worth of data, or degree of freedom. For purposes of estimation, it was necessary to have more degrees of freedom than estimable parameters. A minimum of seven brood years of data were deemed necessary from a hatchery in order to estimate the parameters in a likelihood model with one covariate and have at least two degrees of freedom remaining. There were only 15 Washington State hatcheries out of 29 hatcheries releasing coho salmon from the Juan de Fuca Strait, coastal, and Lower Columbia River regions with an adequate amount of brood year data for an analysis with one covariate. Eight of the 15 hatcheries had 11 or fewer years of data, and most of these hatcheries were located in the Lower Columbia River region (Table 1). Models with more than two regression covariates would have excluded most of the hatcheries from the Lower Columbia River region. For this reason, no more than two covariates were modeled at a time.

Interannual variability in the CWT returns was high, so there was reason to believe that the variances derived from the multinomial likelihood model were underestimated. The variances obtained directly from the likelihood (eq. 5) were based only on multinomial sampling error and do not take into account the extra-likelihood variation resulting from changes in parameter values over time. Therefore, the estimated variances were multiplied by a scale parameter calculated from differences between the observed and expected CWT return numbers to account for some of the year-to-year variability not explained by the covariates. The scale parameter (SP) was calculated according to the expressions

$$\text{(6)}\qquad \text{SP} = \frac{\sum_{i=1}^{n}\left(\sum_{j=i}^{4}\frac{(\text{Observed}_{ij}-\text{Expected}_{ij})^2}{\text{Expected}_{ij}}\right)}{\text{df}}$$

$$\text{(7)}\qquad \text{df} = 3(n-p)$$

where j is a cell from the multinomial likelihood, n is the number of brood years, p is the number of parameters estimated in the model, and df is the degrees of freedom.

If a covariate has an effect on the marine survival of juvenile coho, then the effect should be seen across the replicate hatcheries within a region. Therefore, the weighted mean for a regression coefficient (i.e., $\hat{\beta}_i$) was estimated to test the hypothesis H_0: $\bar{\beta} = 0$ versus H_a: $\bar{\beta} \neq 0$ at a significance level of $\alpha = 0.10$. The weighted mean was calculated according to the formula (Neter et al.1996)

$$\text{(8)}\qquad \hat{\bar{\beta}} = (X'WX)^{-1}X'W\underset{\sim}{\hat{\beta}}$$

where X was a vector of ones of length equal to the number of regression coefficients, W was a diagonal matrix of weights equal to the inverse of the variances of the coefficients, and $\hat{\beta}$ was the vector of the estimated regression coefficients. The variance estimate of $\hat{\beta}$ was calculated according to the formula

$$\text{(9)}\qquad \hat{\text{Var}}(\hat{\bar{\beta}}) = \frac{\sum_{i=1}^{n}\frac{W_i(\hat{\beta}_i-\hat{\bar{\beta}})^2}{n-1}}{n\sum_{i=1}^{n}W_i}$$

where n was now the number of regression coefficients averaged over.

A weighted t test

$$\text{(10)}\qquad t_{\text{df}} = \frac{\hat{\bar{\beta}}-0}{\sqrt{\hat{\text{Var}}(\hat{\bar{\beta}})}}$$

was performed to test the null hypothesis (i.e., H_0: $\bar{\beta} = 0$), where df = $n - 1$ degrees of freedom. A significant t test result was interpreted to mean that the effect of a covariate was consistent across hatcheries and correlated with survival from release to age 2.

© 1999 NRC Canada

Table 3. Correlation matrix for ocean covariates used in the survival analysis.

Covariate	June SST	Summer SST	45°N June upwelling	48°N cumulative upwelling	Spring transition date
June SST	1.0				
Summer SST	0.6061*	1.0			
45°N June upwelling	–0.5761*	–0.4943*	1.0		
48°N cumulative upwelling	–0.4022*	–0.0640	0.2718	1.0	
Spring transition date	0.2819	0.1001	–0.4079*	–0.4982*	1.0

*Significant at the $\alpha = 0.10$ level.

Results

Our first step in examining survival relationships over time was to test whether coho survival differed before and after the 1976–1977 regime shift hypothesized (Beamish 1993; Francis and Hare 1994). Most of the cohorts used in the study were released after the 1976–1977 regime shift took place. However, for the four hatcheries with enough brood years of releases before 1977, we found no significant differences in coho marine survival for the releases before or after 1977 ($p = 0.238$). Subsequently, we explored whether oceanographic variables may account for the interannual variation in adult returns observed in the CWT data.

Four covariates associated with ocean conditions were found to have a significant linear relationship with coho survival to age 2, based on the results of the meta-analysis using the weighted t test. Summer average temperature had a significant positive relationship with survival ($p = 0.034$), while June upwelling strength at 45°N was negatively correlated with survival ($p = 0.088$). Cumulative upwelling had only a marginally positive correlation with survival ($p = 0.108$). The date of spring transition showed a negative association with survival to age ($p = 0.001$). Cumulative upwelling at 45°N, summer upwelling at 48°N, and summer upwelling at 45°N had no significant association with survival ($p > 0.10$).

Correlation between the environmental covariates, however, makes it difficult to determine which factors are driving the survival processes and which are spurious relationships (Table 3). Although the correlation between June SST and the date of spring transition was small ($r = 0.282$), there is nevertheless a functional relationship between these variables. An early spring transition would lead to lower June SST because there would be a longer period in which cooler water was brought to the surface layer than in years of a late spring transition. However, upwelling strength may be a more important factor in influencing SST than duration alone, as indicated by a strong negative correlation between June SST and both cumulative upwelling ($r = –0.402$) and June upwelling at 45°N ($r = –0.576$). Cumulative upwelling, which incorporates both upwelling strength and duration, also had a strong negative correlation with spring transition ($r = –0.499$).

The covariates were also analyzed using quadratic models based on the suggestion of Cury and Roy (1989) and Gargett (1997) that optimal ocean conditions for salmonid survival might exist. The four significant linear covariates and June SST were analyzed using a quadratic model for survival to age 2. The mean of the quadratic term for the June SST in the survival model was nonsignificant when all hatcheries were taken into account (Table 4). However, plots of the survival curves for each region strongly suggest a curvilinear relationship (Fig. 2). When the quadratic terms from each of the regions were analyzed separately, the quadratic regression coefficient for the Juan de Fuca Strait was significantly negative ($p = 0.006$), for the coast was significantly positive ($p = 0.059$), and for the Lower Columbia River was also positive but nonsignificant. The hatcheries in the Juan de Fuca Strait showed a different June SST – survival relationship than found in the other two regions and in part explains why the overall effect was nonsignificant. The hatcheries from the coastal and Lower Columbia River regions all showed similar convex relationships between survival and June SST and have maximum survival probabilities in a narrow band in the middle of the temperature range (Fig. 2). The average maximum from the survivorship curves for the coastal and Lower Columbia River hatcheries was 13.45°C, with a maximum survival occurring in a range from 13.07 to 13.71°C across hatcheries.

The quadratic relationship between spring transition and survivorship was highly significant ($p < 0.001$) (Table 5). This result is seen most clearly in the survivorship curves (Fig. 3). Only two hatcheries in the coastal region did not exhibit the same convex survivorship curves as the other hatcheries; however, they both did show a decrease in survivorship with an increase in spring transition date. The average maximum across all hatcheries was on day-of-the-year 91 (i.e., April 2). The coastal and Lower Columbia River hatcheries had the same average maximum on day-of-the-year 89 (i.e., March 31). Both June SST (Fig. 2) and spring transition (Fig. 3) had positive quadratic terms and as a result show similar convex survivorship curves.

The nonlinear relationship between cumulative upwelling at 48°N and survival to age 2 was also found to be significant ($p = 0.051$) (Table 6). Both the Juan de Fuca Strait and coastal regions had significant quadratic terms (Table 6), and the similarity between the regions is reflected in the survivorship curves (Fig. 4). However, the Lower Columbia River region shows less of a quadratic relationship overall (Fig. 4*c*) than the other two regions, and this is reflected in the nonsignificance of the quadratic term ($p = 0.295$).

Discussion

This analysis of ocean survival of coho salmon relies on three important aspects: a multivariate analysis of age-at-

© 1999 NRC Canada

Fig. 2. Fitted curves from the quadratic PH model for June SST versus survivorship for hatcheries in the (*a*) Juan de Fuca Strait, (*b*) coastal, and (*c*) Lower Columbia River regions. Each line represents a different hatchery used in the CWT analysis.

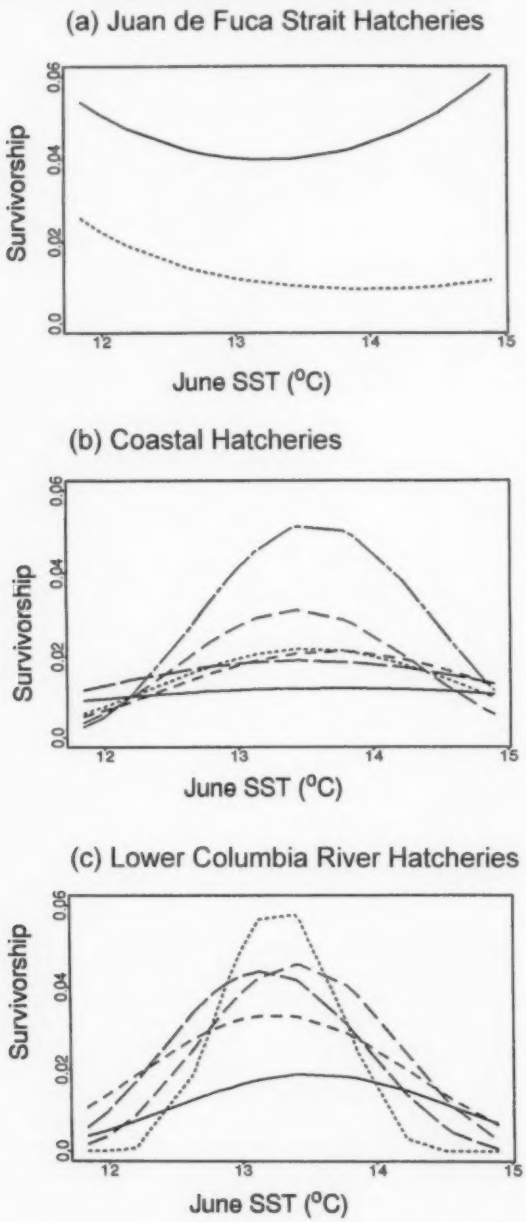

return data, examination of curvilinear relationships, and the use of replicate hatcheries in a meta-analysis of regional effects. The significance of each of these aspects is discussed below in detail, along with a discussion of the data and the assumptions of the statistical method.

Data quality and assumptions

As mentioned earlier, none of the hatcheries had CWT release and return data for all years between 1970 and 1991, leaving gaps in the time series. However, these data gaps should have had little effect on the analysis for two reasons. A time series analysis that is sensitive to missing observations was not performed. Instead, a regression analysis was performed between observations of first-year survival and predictor variables of ocean condition, where it is more important to cover the potential range of predictor values (Table 1) than it is to have consecutive observations. The focus was on the estimates of first-year survival that should be independent over time and not reliant upon consecutive years of cohort data.

Many of the assumptions in the analysis of mark–recapture data apply equally well to CWT data. Overestimation of tagged returns would over estimate survival estimates, and the underestimation of returns could underestimate survival estimates. Errors in sampling fractions, release numbers, and reporting rates could bias the survival estimates in either direction. Unfortunately, information to verify these numbers is generally unavailable. Tag loss rates for CWT data are not often estimated or are not estimated reliably. However, the numbers of observed recoveries are adjusted slightly upward to account for unreadable tags or tag loss during reading (Markey et al. 1991). The assumption that the population of CWT fish was closed to emigration seems reasonable because even if a fish did stray to another hatchery, it would be detected and recorded as a CWT return. The use of jacks as a metric of year-class success is consistent with the assumption that the parameter is constant across brood years.

Table 4. Average regression coefficients estimated from the CWT analysis of June SST for the linear and quadratic models for each region and overall.

Model	Linear nodel coefficient	Quadratic model	
		Linear term	Quadratic term
Juan de Fuca Strait hatcheries			
$\hat{\beta}$	–0.0191	0.0228	–0.0431
SE($\hat{\beta}$)	0.0900	0.0570	0.0004
p value	0.9560	0.7580	0.0060
Coastal hatcheries			
$\hat{\beta}$	–0.0180	–0.0488	0.0733
SE($\hat{\beta}$)	0.0062	0.0133	0.0300
p value	0.0770	0.0140	0.0590
Lower Columbia River hatcheries			
$\hat{\beta}$	0.1324	0.0189	0.1618
SE($\hat{\beta}$)	0.0599	0.0336	0.1178
p value	0.0690	0.6040	0.2420
Overall (across all hatcheries)			
$\hat{\beta}$	0.0982	–0.0003	0.1008*
SE($\hat{\beta}$)	0.0730	0.0226	0.0841
p value	0.2000	0.9910	0.2534*

*For June SST, the average of the quadratic terms across all hatcheries in the coastal and Lower Columbia River regions was significant.

© 1999 NRC Canada

Table 5. Average regression coefficients estimated from the CWT analysis of spring transition for the linear and quadratic models for each region and overall.

Model	Linear model coefficient	Quadratic model	
		Linear term	Quadratic term
Juan de Fuca Strait hatcheries			
$\hat{\beta}$	0.0008	–0.0243	0.0537
SE($\hat{\beta}$)	0.0018	0.0356	0.0010
p value	0.7540	0.6180	0.0120
Coastal hatcheries			
$\hat{\beta}$	0.0342	0.0053	0.0603
SE($\hat{\beta}$)	0.0091	0.0125	0.0122
p value	0.0130	0.6900	0.0040
Lower Columbia River hatcheries			
$\hat{\beta}$	0.0741	0.00228	0.0754
SE($\hat{\beta}$)	0.0133	0.0315	0.0054
p value	0.0010	0.7240	<0.001
Overall (across all hatcheries)			
$\hat{\beta}$	0.0464	0.0066	0.0653
SE($\hat{\beta}$)	0.0109	0.0120	0.0054
p value	<0.001	0.5920	<0.001

Fig. 3. Fitted curves from the quadratic PH model for spring transition data versus survivorship for hatcheries in the (*a*) Juan de Fuca Strait, (*b*) coastal, and (*c*) Lower Columbia River regions. Each line represents a different hatchery used in the CWT analysis.

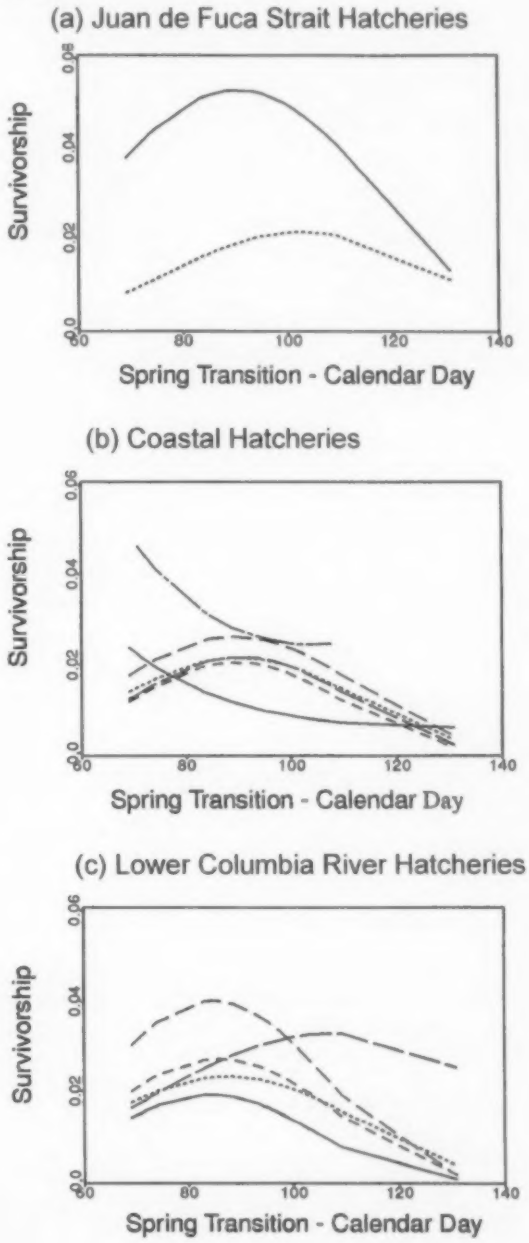

Multinomial survival model

The multivariate data analysis provides a means to estimate first-year ocean survival concurrently with investigating survival relationships. All model parameters were estimated from the CWT data alone, using likelihood equations (eq. 5) and maximum likelihood methods. Estimates of model parameters based on auxiliary data were unnecessary. Furthermore, estimates of fishing effort were unnecessary in order to differentiate the effects of ocean survival from the effects of the salmonid fisheries. By using total returns from both the fisheries and hatchery escapement, the variability induced by fluctuations in fishing effort and success can be minimized. The age-structure information from the CWT returns also retains the underlying error structure of the original data. Analyses based on the proper error structure and response model should have greater power to identify survival relationships.

Curvilinear survival relationships

The quadratic relationships between the environmental covariates and age-2 survival are important results for two reasons. First, the similarities in response across most of the hatcheries strongly support the conclusion that curvilinear survival relationships exist. Second, this is the first time that quadratic survival relationships have been seen for a salmonid species. Simply looking at linear relationships can obscure or preclude the possibility of detecting important survival relationships.

Our analysis found three significant curvilinear relationships between environmental covariates and survival. In the survivorship curves for all three covariates, maximum survival was similar for each hatchery. For example, in the June SST survivorship curves, the maxima for all hatcheries in the coastal and Lower Columbia River regions occur between 13.07 and 13.71°C with a mean of 13.45°C (SE = 0.20°C). Survivorship curves show a consistent maximum

© 1999 NRC Canada

Table 6. Average regression coefficients estimated from the CWT analysis of cumulative upwelling at 48°N for the linear and quadratic models for each region and overall.

Model	Linear model coefficient	Quadratic model	
		Linear term	Quadratic term
Juan de Fuca Strait hatcheries			
$\hat{\beta}$	–0.0450	–2.6230	0.7830
SE($\hat{\beta}$)	0.0146	0.0032	0.0016
p value	0.2000	<0.001	0.001
Coastal hatcheries			
$\hat{\beta}$	–0.0798	–2.3136	0.6124
SE($\hat{\beta}$)	0.1039	0.3957	0.0156
p value	0.4770	0.0020	0.0040
Lower Columbia River hatcheries			
$\hat{\beta}$	–0.3344	–1.3166	0.1557
SE($\hat{\beta}$)	0.0614	0.5035	0.1295
p value	0.0020	0.0590	0.2950
Overall (across all hatcheries)			
$\hat{\beta}$	–0.1318	–1.7053	0.2572
SE($\hat{\beta}$)	0.0768	0.3805	0.1186
p value	0.1080	<0.001	0.0510

for survival at all hatcheries with a spring transition date around April 2 (SE = 7.25 days). The survivorship curves based on cumulative upwelling were somewhat more variable yet consistent in their interpretation. In all cases, survival of coho salmon to age 2 ranged from a low of less than 1% to a high of 6% under optimal conditions.

The results of the June SST, date of spring transition, and 48°N cumulative upwelling quadratic models seem to agree with the hypothesis for the existence of optimal environmental conditions put forth by Cury and Roy (1989) and Gargett (1997). Dome-shaped response curves are commonly found in ecology and population biology but until recently have not been widely found in fisheries literature (Sharp 1995). The important management implication is that regardless of hatchery practices, returns of salmonid adults may be governed by a narrow set of oceanographic conditions.

Possible survival mechanism

Both Cury and Roy (1989) and Gargett (1997) have suggested that optimal ocean conditions may exist for the survival of marine fish. They stated that these optimal conditions for survival are related to the water column stability of the ocean. However, these authors have differing opinions as to what environmental factors are responsible for the stability and mixing in the water column.

Using a yearly average of upwelling indices, Cury and Roy (1989) showed a "dome shaped" relationship between Pacific sardine (*Sardinops sagax caerulea*) recruitment and upwelling off the California coast, with upwelling units between 100 and 120 ($m^3 \cdot s \cdot 100$ mi of coastline^{-1}) having the maximum recruitment. The reasoning behind the hypothesis has to do with the winds responsible for coastal upwelling. Upwelling indices are proportional to wind speed squared (Bakun 1973), with northerly alongshore winds inducing upwelling and bringing nutrients into the coastal upwelling region and enhancing primary production. However, when

Fig. 4. Fitted curves from the quadratic PH model for the cumulative upwelling at 48°N data versus survivorship for hatcheries in the (*a*) Juan de Fuca Strait, (*b*) coastal, and (*c*) Lower Columbia River regions. Each line represents a different hatchery used in the CWT analysis.

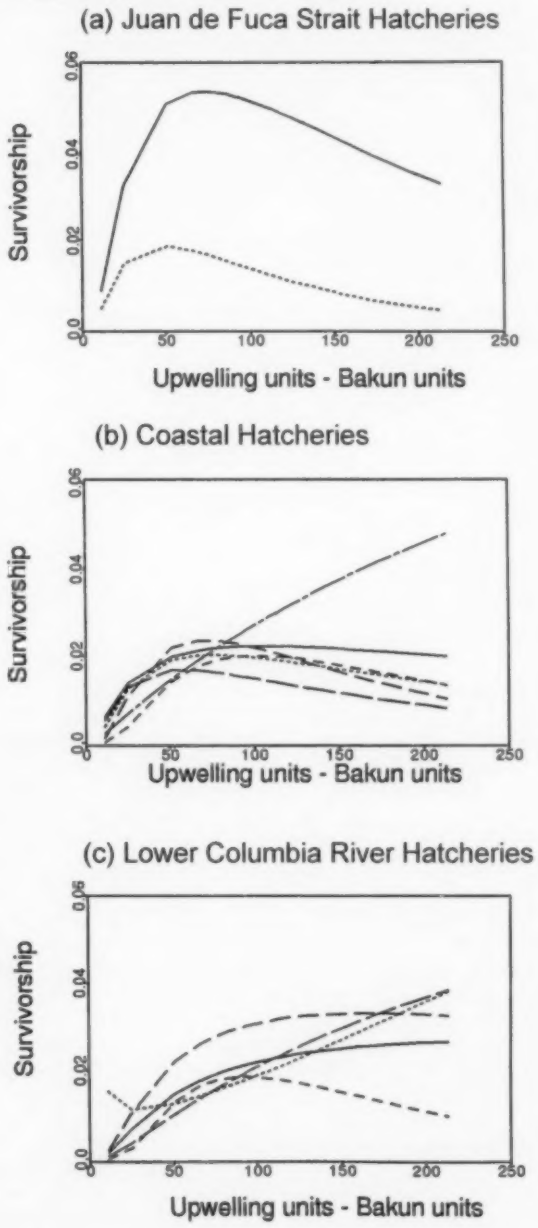

© 1999 NRC Canada

wind speed becomes too high, mixing in the upper surface water layer starts to take place and begins to break up patches of phytoplankton (Demers et al. 1987). Cury and Roy (1989) suggested that turbulence as a result of high winds could limit recruitment in upwelling areas.

The quadratic relationship between June SST and survival that we found lends support to the upwelling hypothesis of Cury and Roy (1989). Eleven hatcheries from two regions all showed a maximum coho marine survival rate at a June SST of about 13.45°C (SE = 0.20°C). However, SST is affected by upwelling that brings cooler water into the surface layer (Knauss 1978). Increased upwelling reduces the affect of seasonal water warming and, as such, is negatively correlated with SST (Schwing and Mendelssohn 1997). On the other hand, higher June SST is indicative of weaker upwelling conditions because seasonal warming has taken place. Weaker upwelling conditions have a detrimental effect on primary production and subsequent food availability for young coho.

An additional hypothesis relating the effects of local winds on primary production was proposed by Huntsman and Barber (1977). They showed that sustained winds may negatively affect primary production and suggested that a relaxation in winds could slow the transport of nutrients offshore, allowing phytoplankton blooms to take place. Sustained higher wind speeds would increase the monthly average upwelling index, while months with more relaxation periods would tend to lower the monthly index. Whether the curvilinear relationships between upwelling and survival were due to the plankton patchiness or lack of phytoplankton blooms, the exact mechanism cannot be deduced without additional empirical data.

Gargett (1997) presented the idea of coastal water column stability being influenced by the strength of the winter Aleutian Low. In conditions of high water column stability, vertical movement of water that introduces nutrients into the upper layers of the water column is restricted, although light conditions remain optimal for phytoplankton production. When water column stability is low, nutrients are abundant, but the vertical movement of nutrients reduces the light levels required for phytoplankton growth. Gargett (1997) proposed the existence of conditions where upwelling is sufficient for nutrient input to the coastal waters and yet having enough stability to maintain light levels. The argument of Gargett (1997) for the existence of optimal conditions was used primarily to explain the variation in production between northern (Alaskan) and southern (to northern California) stocks of salmon.

In the water column stability hypothesis proposed by Gargett (1997), water column stability was driven by the strength of the Aleutian Low pressure system. Using the NPI (Trenberth and Hurrell 1994) as a measure of the strength of the Aleutian Low, a regression analysis between the NPI and hatchery data showed no relationship between the strength of the Aleutian Low pressure system and coho marine survival (Ryding 1998). Alternatively, Chelton et al. (1982) suggested that upwelling may be governed by variations in the California Current.

The relationship between spring transition and coho survival should also be emphasized. The significance of the date of spring transition implies that the conditions at ocean entry dominate coho survival. In our analysis, optimum time for spring transition was calculated to be April 2 (SE = 7.25 days). This date would allow sufficient time for the establishment of smaller prey species to become abundant when smolts enter the ocean. The negative correlation between the other upwelling variables could indicate that spring transitions occurring earlier could be associated with stronger winds, which may hinder food production. Spring transitions occurring later in April may not allow enough time for the establishment of coho prey. Although water column stability is important, our data suggest that the timing of ocean entry by smolts relative to the date of spring transition may be a key factor affecting ocean survival.

Spatial replication

Replication and the ability to demonstrate reproducibility of effects is a cornerstone in statistical inference (Hurlbert 1984). In these analyses, hatcheries served as spatial replicates to assess reproducibility of observed survival relationships. Often, the analysis of CWT data from individual hatcheries resulted in statistically significant regression coefficients across brood years. However, when their relationships were assessed along with relationships estimated from other local hatcheries, no consistency could be found. The meta-analysis used in this study helped avoid spurious correlations that could have occurred from the analysis of return data from just one or a few hatcheries. The meta-analysis also helped identify regionally important factors that were consistently related to juvenile salmon survival. Demonstrating consistency of regression relationships across neighboring hatcheries is an important analytical technique in showing the reproducibility of results.

Acknowledgments

This study was funded by the Bonneville Power Administration, contract No. DE-BI79-87BP35885.

References

Bakun, A. 1973. Coastal upwelling indices, west coast North America, 1946–1971. NOAA Tech. Rep. NMFS SSRF-671.

Beamish, R.J. 1993. Climate and exceptional fish production off the west coast of North America. Can. J. Fish. Aquat. Sci. **50**: 2270–2291.

Beamish, R.J., and Bouillon, D.R. 1993. Pacific salmon production trends in relation to climate. Can. J. Fish. Aquat. Sci. **50**: 1002–1016.

Casella, G., and Berger, R.L. 1990. Statistical inference. Duxbury Press, Belmont, Calif.

Chelton, D.B., Bernal, P.A., and McGowan, J.A. 1982. Large-scale interannual physical and biological interaction in the California Current. J. Mar. Res. **40**: 1095–1125.

Cury, P., and Roy, C. 1989. Optimal environmental window and pelagic fish recruitment success in upwelling areas. Can. J. Fish. Aquat. Sci. **46**: 670–680.

Demers, S.J., Therriault, J.C., Bourget, E., and Bah, A. 1987. Resuspension in the shallow sublittoral zone of a macrotidal estuarine environment: wind influence. Limnol. Oceanogr. **32**: 327–339.

Ebbesmeyer, C.C., and Strickland, R.M. 1995. Oyster condition and climate: evidence from Willapa Bay. Publ. WSG-MR 95-02.

© 1999 NRC Canada

Washington Sea Grant Program, University of Washington, Seattle, Wash.

Eddy, D.M., Hasselbard, V., and Shachter, R. 1992. Meta-analysis by the confidence profile method. Academic Press, Inc., San Diego, Calif.

Fisher, J.P., and Pearcy, W.G. 1988. Growth of juvenile coho (*Oncorhynchus kisutch*) in the ocean off Oregon and Washington, USA, in years of differing coastal upwelling. Can. J. Fish. Aquat. Sci. **45**: 1036–1044.

Fletcher, R. 1970. A new approach to variable metric algorithms. Comput. J. **13**: 317–322.

Francis, R.C., and Hare, S.R. 1994. Decadal-scale regime shifts in the large marine ecosystems of the Northeast Pacific: a case for historical science. Fish. Oceanogr. **3**: 279–291.

Francis, R.C., Hare, S.R., Hollowed, A.B., and Wooster, W.S. 1998. Effects of interdecadal climate variability on the oceanic ecosystems of the NE Pacific. Fish. Oceanogr. **7**: 1–21.

Gargett, A.E. 1997. The optimal stability "window": a mechanism underlying decadal fluctuations in North Pacific salmon stocks? Fish. Oceanogr. **6**: 109–117.

Gunsolus, R.T. 1978. The status of Oregon coho and recommendations for managing the production, harvest and escapement of wild and hatchery-reared stocks. Oreg. Dep. Fish Wildl. Proc. Rep.

Holtby, L.B., and Scrivener, J.C. 1989. Observed and simulated effects of climatic variability, clear-cut logging and fishing on the numbers of chum salmon (*Oncorhynchus keta*) and coho salmon (*O. kisutch*) returning to Carnation Creek, British Columbia. *In* Proceedings of the National Workshop on Effects of Habitat Alteration on Salmonid Stocks. *Edited by* C.D. Leavings, L.B. Holtby, and M.A. Henderson. Can. Spec. Publ. Fish. Aquat. Sci. No. 105. pp. 62–81.

Holtby, L.B., Andersen, B.C., and Kadowaki, R.K. 1990. Importance of smolt size and early ocean growth to interannual variability in marine survival of coho *salmon (Oncorhynchus kisutch*). Can. J. Fish. Aquat. Sci. **47**: 2181–2194.

Huntsman, S.A., and Barber, R.T. 1977. Primary production off northwest Africa: the relationship to wind and nutrient condition. Deep-Sea Res. **24**: 25–33.

Hurlbert, S.H. 1984. Pseudoreplication and the design of ecological field experiments. Ecol. Monogr. **54**.

Hyun, S.Y. 1996. Ocean distributions of the Columbia River Hanford Reach and Snake River fall chinook salmon (*Oncorhynchus tshawytscha*) stocks in the effect of interannual ocean conditions on their survival. M.S. thesis, University of Washington, Seattle, Wash.

Ingraham, W.J., Jr., and Miyihara, R.K. 1988. Ocean surface current simulations in the North Pacific Ocean and Bering Sea (OSCURS-numerical model). NOAA Tech. Memo. NMFS F/NWC-130.

Knauss, J.A. 1978. Introduction to physical oceanography. Prentice-Hall, Inc., Englewood Cliffs, N.J.

Markey, S.L., McGowen, J.E., and Crumley, P. 1991. 1989 results from micro-tagged salmon experimental groups. State Wash. Dep. Fish. Prog. Rep. No. 294.

McCarl, B.A., and Rettig, R.B. 1983. Influence of hatchery smolt releases on adult salmon production and its variability. Can. J. Fish. Aquat. Sci. **40**: 1880–1886.

McCullagh, P., and Nelder, J.A. 1989. Generalized linear models. Chapman and Hall, London, U.K.

McFarlane, G.A., and Beamish, R.J. 1992. Climatic influence linking copepod production with strong year-classes in sablefish, *Anoplopoma fimbria*. Can. J. Fish. Aquat. Sci. **49**: 743–753.

Neter, J., Kutner, M.H., Nachtsheim, C.J., and Wasserman, W. 1996. Applied linear statistical models. 3rd ed. Richard D. Irwin, Chicago, Ill.

Nickelson, T.E. 1986. Influences of upwelling, ocean temperature and smolt abundance on marine survival of coho salmon (*Oncorhynchus kisutch*) in the Oregon production area. Can. J. Fish. Aquat. Sci. **43**: 527–535.

Nickelson, T.E., and Lichatowich, J.A. 1984. The influence of the marine environment in the interannual variation in coho salmon abundance: an overview. *In* The influence of ocean conditions on the production of salmonids in the North Pacific. *Edited by* W.G. Pearcy. Oregon Sea Grant Program, Corvallis, Oreg.

Pearcy, W.G., and Fisher, J.P. 1988. Migrations of coho salmon, *Oncorhynchus kisutch*, during their first summer in the ocean. Fish. Bull. U.S. **86**: 173–195.

Regional Mark Processing Center. 1993. Regional Mark Information System (RMIS) user manual. Version 1.0. Pacific States Marine Fisheries Commission, Portland, Oreg.

Ryding, K.E. 1998. Analyzing adult returns to assess ocean effects and salmon survival relationships. M.S. thesis, University of Washington, Seattle, Wash.

Scarnecchia, D.L. 1981. Effects of stream flow and upwelling on yield of wild coho (*Oncorhynchus kisutch*). Can. J. Fish. Aquat. Sci. **38**: 471–475.

Schwing, F.B., and Mendelssohn, R. 1997. Increased coastal upwelling in the California current system. J. Geophys. Res. **102**(C2): 3421–3438.

Sharp, G.D. 1995. It's about time: new beginning and old good ideas in fisheries science. Fish. Oceanogr. **4**: 324–341.

Snake River Salmon Recovery Team. 1993. Snake River salmon recovery plan. National Marine Fisheries Service, Seattle, Wash.

Trenberth, K.E., and Hurrell, J.W. 1994. Decadal atmospheric–ocean variations in the Pacific Ocean. Clim. Dyn. **9**: 303–319.

© 1999 NRC Canada

A neural network model for forecasting fish stock recruitment

D.G. Chen and D.M. Ware

Abstract: A neural network model is developed to forecast the recruiting biomass of fish. The west coast of Vancouver Island, British Columbia, Pacific herring (*Clupea pallasi*) stock is selected as an example application based on data compiled from long-term ecosystem research and stock assessment programs. A fuzzy logic decision procedure was used to evaluate all possible neural networks. The output from the two "optimal" networks was compared with the output from a multiple regression analysis and a standard Ricker climate stock–recruitment model. The performance of the neural network models in reproducing a 41-year time series was far superior (R^2 between the fitted and observed recruitment is about 60–70%) to the multiple linear regression model (R^2 = 0.29) and the Ricker climate stock–recruitment model (R^2 = 42%). This pilot study demonstrates how artificial neural networks can be used to improve the accuracy of fishery stock forecasts and hence the management of the fishery resources by making the actual harvest rate (catch/stock biomass) closer to the target harvest rate (desired catch/stock biomass).

Résumé : Les auteurs ont élaboré un modèle neuronal afin de modéliser et de prévoir la biomasse de poisson recrutée. Ils ont choisi le stock de hareng (*Clupea pallasi*) de la côte ouest de l'île de Vancouver (Colombie-Britannique) comme exemple d'application fondée sur les données compilées à partir des travaux de recherche à long terme sur les écosystèmes et des programmes d'évaluation des stocks. Une méthode de décision logique floue a été utilisée pour évaluer tous les réseaux neuronaux possibles. Les résultats des deux réseaux « optimaux » ont été comparés aux résultats d'une analyse de régression multiple et d'un modèle stock–recrutement standard de Ricker en fonction du climat. La performance des modèles neuronaux pour la reproduction d'une série chronologique portant sur une période de 41 ans était nettement supérieure (R^2 entre le recrutement ajusté et le recrutement observé = 60 % à 70 % environ) au modèle de régression linéaire multiple (R^2 = 0,29), et au modèle de Ricker (R^2 = 42 %). La présente étude pilote montre de quelle manière les modèles neuronaux artificiels peuvent être utilisés pour rendre plus précises les prévisions des stocks de poisson, et de ce fait la gestion des ressources halieutiques, en rapprochant le taux de capture réel (rapport des captures sur la biomasse du stock) du taux de capture désiré (rapport des captures désirées sur la biomasse du stock).

[Traduit par la Rédaction]

Introduction

To set accurate preseason fishing quotas, it is important to be able to forecast the biomass of young fish (recruits) that will join the fishable stock for the first time before the fishing season opens. Experience has proven that the level of recruitment is difficult to forecast for most fish stocks because the survival of juvenile fish is affected by a number of variables. For example, the biomass of 3-year-old recruits to the west coast of Vancouver Island (WCVI), British Columbia, Pacific herring (*Clupea pallasi*) stock over the last 60 years has fluctuated over a 350-fold range in response to interannual and decadal time scale variations in the spawning biomass (of parents) and in the state of the environment, which in turn affects the Pacific herring food supply and mortality rate (Ware 1991; Robinson and Ware 1994; Ware and McFarlane 1995). A long-term ecosystem research program has identified that the key variables determining Pacific herring recruitment are the lagged biomass of adult spawners, the summer biomass of Pacific hake (*Merluccius productus*), which is a significant predator, and two lagged environmental factors (annual sea surface temperature (SST) and salinity). The annual SST is believed to be a general indicator of mortality and the state of the food supply (Tanasichuk et al. 1991; Ware 1991; Ware and McFarlane 1995). In many cases, it is difficult to clarify and model the mechanism controlling recruitment by using conventional mathematical and statistical methods because the survival process is nonlinearly related to several factors. Recognizing the complexity of the problem and the ability of neural network models to approximate nonlinear relationships, we developed an artificial neural network model for forecasting Pacific herring recruitment to the WCVI stock. This study complements and extends recent applications of neural network analysis to fisheries forecasting problems (e.g., Jarre-Teichmann et al. 1995; Lek et al. 1995; Aoki and Komatsu 1997; Guegan et al. 1998).

Artificial neural networks are computer algorithms that simulate the activity of neurons and information processing in the human brain. In general, a neural network is an interconnected network of simple processing layers where typically the first layer (input layer) makes independent computations and passes the results to a hidden layer. This

Received January 22, 1999. Accepted August 27, 1999.
J14985

D.G. Chen[1] and D.M. Ware. Department of Fisheries and Oceans, Pacific Biological Station, Nanaimo, BC V9R 5K6, Canada.

[1]Author to whom all correspondence should be addressed.
e-mail: chend@pac.dfo-mpo.gc.ca

© 1999 NRC Canada

Fig. 1. Topology of the three-layer feed-forward neural network.

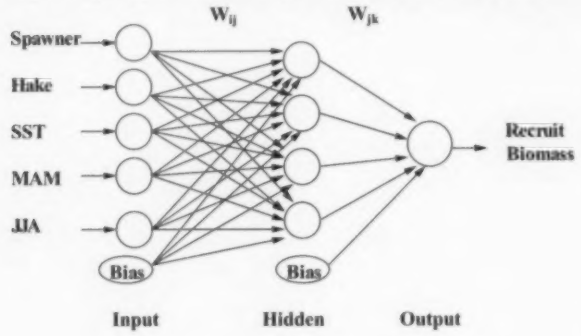

layer may in turn make an independent computation and pass the results to another hidden layer. This signal process may continue to produce more hidden layers depending on the complexities of the problem. Finally, the last layer (output layer) determines the output from the network. Each processing layer makes the computation based on the weighted sum of its inputs. This signal processing between layers enables neural networks to model complex linear and nonlinear systems (Chen et al. 1990; Weigend et al. 1992). Unlike the more commonly used regression models, neural networks do not require a particular functional relationship or distribution assumptions about the data. This makes neural network modeling a powerful tool for exploring complex, nonlinear biological problems like recruitment forecasting.

Neural network model

Feed-forward neural network

There are many different types of neural networks, which differ from one another in architecture and training algorithms. The multilayer feed-forward neural network with back-propagation learning algorithm is one of the most successful networks in application and will be used in this paper (Ripley 1994*a*; Venables and Ripley 1994). Funahashi (1989) has shown that neural networks with at least one hidden layer can approximate a variety of conditions. Therefore, we choose one hidden layer for our model network and denote the structure of this type of neural network as $n_{\text{input}} - n_{\text{hidden}} - n_{\text{output}}$, where n_{input}, n_{hidden}, and n_{output} represent the numbers of neurons in the input, hidden, and output layers, respectively. This class of neural networks typically consists of three neural layers: an input layer, a hidden layer, and an output layer. For our forecasting application, the input layer consists of five input neurons (i.e., spawning biomass of Pacific herring, biomass of predatory Pacific hake, mean annual SST, spring (March, April, and May average) (MAM) salinity, and summer (June, July, and August average) (JJA) salinity) and one output neuron (biomass of Pacific herring recruits) in the output layer. All the neurons in one layer are connected with all the neurons in the next layer (Fig. 1).

The topology of a 5–4–1 feed-forward neural network with a bias neuron is illustrated in Fig. 1. In this type of network, the input layer is determined by the incoming signals. This upper layer distributes the input signals to neurons in the hidden layer. Each hidden neuron sums all its input signals by a dot product between its input vector and its weight and then adds a "bias" input. The final result is then transformed by an "activation function" (in neural network terminology) to produce an input signal to the output layer. The output layer processes its input signals in the same fashion. The entire process can be written mathematically as

$$(1) \qquad y_k = \phi_o\left\{\beta_k + \sum_j w_{jk}\,\phi_h\left(\beta_j + \sum_i w_{ij}x_i\right)\right\}$$

where x_i are the input signals (these are the "independent" variables in regression terminology), y_k are the output signals (these are the "dependent" variables in regression terminology), w_{ij} are the weights between input neuron i to hidden neuron j, and w_{jk} are the weights between hidden neuron j and output neuron k. The β_j and β_k are the biases for the hidden and output layers, which behave like the intercept in a regression, and ϕ_h and ϕ_o are activation functions for the hidden and output layers; ϕ_h and ϕ_o can be any monotonic smooth function. However, the logistic function defined as

$$f(x) = \frac{1}{1 + \exp(-x)}$$

is the most commonly used.

It follows that a multiple linear regression is really a special type of neural network where there is no hidden layer and ϕ_h and ϕ_o are linear functions. By allowing ϕ_h or ϕ_o to be monotonic smooth functions, the neural network can approximate the relationship between the input and output signals in a nonlinear way. In a neural network model, the weights between neurons are the links between the inputs and the outputs, in effect the links between the problem and its solution. The weights contain all the information about the network. Therefore, the objective is to train the network to find a series of weights that yield an output signal that has a small error relative to the observed output. The most commonly used error criterion is the least squares error function

$$E = \sum_p \left\| t^p - y^p \right\|^2$$

where t^p is the observed target value and y^p the modeled output for the pth pattern. Other error functions can also be used such as the likelihood error function (e.g., White 1989; Spackman 1992).

Back-propagation training

We use a back-propagation training procedure. The objective of back-propagation learning is to adjust the weights in order to minimize the error function. These weight adjustments occur backwards, layer by layer in a looping pattern, starting with the output layer and ending with the input layer. Weight adaptations are produced by the steepest decent algorithm (also called gradient descent). The iteration step can be summarized by

$$w_{st}^{\text{new}} = w_{st}^{\text{old}} + \Delta w_{st} = w_{st}^{\text{old}} + \eta \frac{\partial E}{\partial w_{st}}$$

© 1999 NRC Canada

where Δw_{st} is the weight change between neuron s to neuron t in the next layer and η is the learning rate. The learning rate is chosen to balance the speed and the convergence of the iteration process. Specifically, the smaller η is, the more training iterations will occur and the minimization process will tend to converge. In contrast, with a large η, divergence could occur, particularly in the case of a small input sample and a large number of weights.

The minimization procedure outlined above experienced some difficulties due to local minima. Consequently, we evaluated the solutions for different initial values of the weights by training the networks with different starting values. The results indicated that different runs produced different convergences. There were also signs of network overtraining. To solve these problems, we make use of Ripley (1994*a*)'s regularization in which the error function E is changed to $E + \lambda C(f)$ with the penalty C being the second derivatives of f such as

$$\sum_{i,o} \frac{\partial^2 y_o}{\partial x_i^2} \, dx \approx \frac{1}{P} \sum_{i,o,p} \frac{\partial^2 y_o}{\partial x_i^2}$$

where f is defined in eq. 1, $\Sigma_{i,o,p}$ is the summation for all input, output, and patterns and P is the total number of patterns. This technique is called a weight decay and is specific to neural networks that use a least squares error penalty for the weights. The weight decay technique improves the optimization process and also avoids overfitting. Based on Bayesian theory, Ripley (1993, 1994*b*) suggested that $\lambda \approx 10^{-4}$ to 10^{-2}.

Performance evaluation: a fuzzy logic decision-making procedure

To assess the performance of different neural networks, four criteria were used to evaluate the training and testing procedures: (*i*) the correlation coefficient (R^2) between the observed biomass of Pacific herring recruits R_i and the predicted $\hat{R}_i$ (neural net fit to the training data set), (*ii*) mean prediction error (MPE) between the observed and predicted recruit biomass, defined as

$$\text{MPE} = \frac{1}{n} \sum_{i=1}^{n} \text{PE}_i$$

where $\text{PE}_i = R_i - \hat{R}_i$ is the prediction error and n is the number of observations in the training or testing data sets, (*iii*) variance (VAR) of the prediction errors, defined as

$$\text{VAR} = \frac{1}{n-1} \sum_{i=1}^{n} (\text{PE}_i - \text{MPE})^2$$

and (*iv*) mean absolute percent error (MAPE) between the observed and predicted recruit biomass, defined as

$$\text{MAPE} = \frac{1}{n} \sum_{i} \frac{\left| R_i - \hat{R}_i \right|}{R_i}.$$

Using these four criteria, it is possible to rank the performance of each neural network. The "optimal" networks should have larger R^2 and smaller MPE, VAR, and MAPE. For each neural network, eight performance measurements were calculated (four for the training data set and four for the test data set). Although it is relatively simple to rank each network by each criterion, it is not trivial to rank the networks across the eight criteria. To do this, we used a decision procedure based on fuzzy logic concepts. To the best of our knowledge, this is one of the first applications of a fuzzy logic decision procedure for finding the optimal neural network. A fuzzy logic decision procedure evaluates each network by weighting each criterion by its relative importance. The importance weight is assigned by the analyst who decides how important each criterion is to the forecasting task. Details are given in the Appendix.

Analysis

Data description

The desired output of the forecasting model is the biomass of 3-year-old Pacific herring recruits (in year t). The input data consist of five variables: biomass of spawners (i.e., parents) in the year in which the recruits were born ($t - 3$ years), biomass of Pacific hake (an important predator) in year $t - 3$, annual mean SST in year $t - 3$, and two proxy indices of lower trophic level productivity, the average MAM and JJA salinities, both in year $t - 3$. Estimates of Pacific herring recruit biomass and Pacific herring spawning biomass were derived from age-structured model output by Schweigert et al. (1997). Estimates of Pacific hake biomass for the period 1935–1984 were obtained from Francis et al. (1984) and, later, for the period 1985–1996 from Canadian offshore trawl and hydroacoustic surveys. The annual mean SST data in the year of birth came from the lighthouse at Amphitrite Point, which is located on the lower WCVI. The mean SST for 1939 was missing and was therefore estimated from the cross-correlation between the Amphitrite Point time series and the nearby Kains Island time series. Monthly mean sea surface salinity data were available from Amphitrite Point for the period 1935 to the present with the exception of 1939, which contained some missing data. The missing salinity data for March, April, and May 1939 were estimated from the significant cross-correlation regressions with Kains Island. The missing data for June were estimated from the July data at Amphitrite Point. We also used two measures of salinity: average MAM and JJA. We used these two variables because it is generally believed that the relative size of a Pacific herring year-class when it recruits to the spawning stock is determined sometime during the first growing season. The Pacific herring studied in this project are born in March, and their first growing season ends in September–October. Hence, the average salinity in the spring is believed to be a proxy indicator of feeding conditions that Pacific herring experience during their first 3 months of life, while summer salinity is believed to reflect feeding conditions during the last half of the growing season. Since Pacific herring recruitment could be determined during either or both of these periods, we tested the prediction capability of both variables. In addition, correlation analysis indicated that the average MAM and JJA salinities are poorly correlated ($R^2 = 0.18$), which justifies the use of both time series as independent input variables.

The biomass of Pacific herring recruits (lagged back to the year of birth for the period 1935–1992) and the associated

© 1999 NRC Canada

Fig. 2. Time series plots for the output variable Pacific herring recruit biomass (kt) and the five input variables Pacific herring spawner biomass (kt), annual SST (°C), Pacific hake biomass (kt), and spring and summer salinities (‰). The circles indicate observed values and the line is the supersmoothed trend.

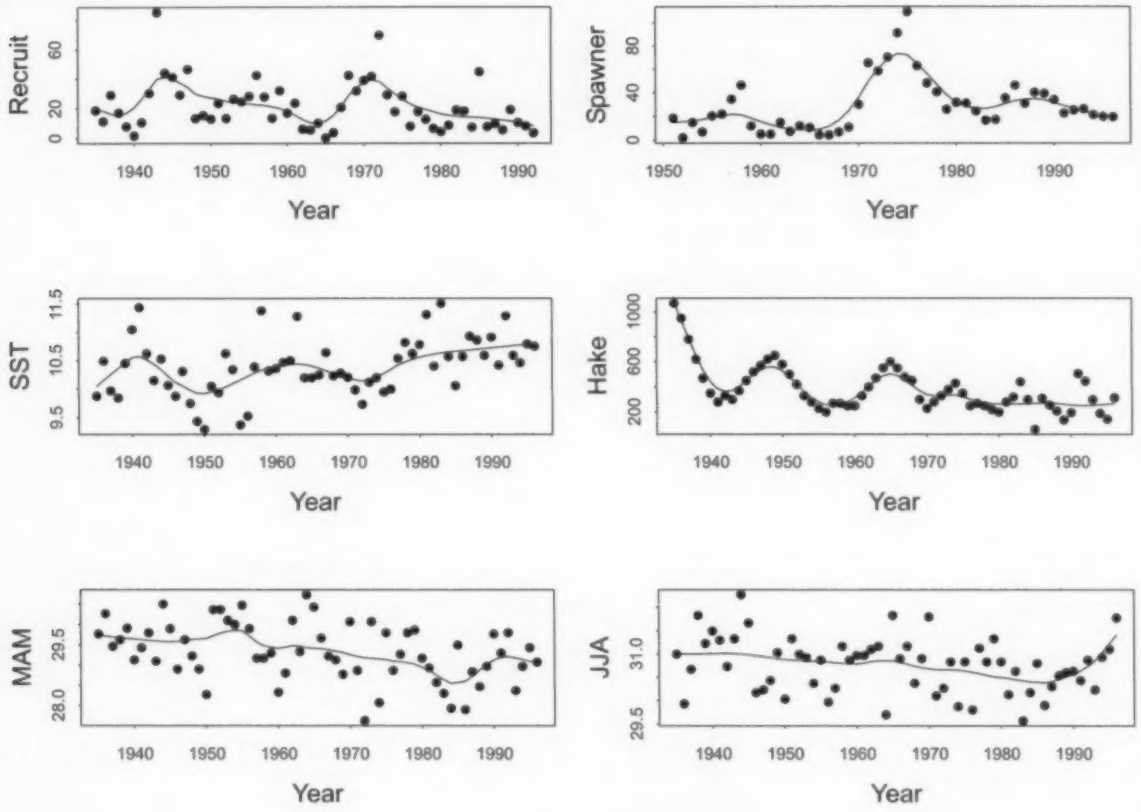

five input time series (also in the year of birth) are plotted in Fig. 2. Note that spawner biomass data are only available for the period 1951–1996. The line in each plot is the supersmoothed trend, which is an extension of locally weighted regression smoothing (LOWESS) with local cross-validation to choose the LOWESS span parameter (MathSoft Inc. 1995, pp. 7–45). The Pacific herring recruit biomass time series indicates that recruitment increased from 1935 to 1943 and then declined until 1965. The fishery was closed in 1967 and for the next 4 years to conserve the spawning stock. The biomass of recruits that were born during this period increased sharply but has recently declined during a protracted period of generally unfavorable environmental conditions (Ware and McFarlane 1995).

A key objective for assessing and managing many fish populations is to be able to forecast, from existing information, the biomass of recruits that will be available to the fishery the next year. Figure 3 shows the relationship between Pacific herring recruitment and each of the input variables. As expected from biological considerations, in harvested populations, there is a tendency for recruitment to increase at low and moderate spawner biomasses. Conversely, recruitment is negatively correlated with the annual SST and Pacific hake biomass. While there is a tendency for recruitment to increase with summer salinity, there is no obvious relationship between recruitment and spring salinity.

Evaluation of the possible neural networks

The available time series were used to generate training, testing, and prediction data sets. The training data set included all the input and recruitment data for the complete time series with 5 years of data excluded for testing. Four test data sets were generated: one where five points were randomly selected and excluded and three test data sets where five high-biomass, five middle-biomass, and five low-biomass points were selected based on the average recruitment (see Figs. 4 and 5). This random selection process was repeated several times with similar outcome. This led us to consider three extreme cases to evaluate the models: high, middle, and low biomass. Early indications of the strength of the 1993–1996 year-classes were also available and were used to create a prediction data set. Although these data are not well determined at this stage, they give a preliminary indication of the biomass of recruits in the 1993–1996 year-classes and were therefore included in the analysis.

Since there is no information on the biomass of spawners from 1935 to 1950, this constrained us to consider two types of neural networks to maximize the use of the available data.

© 1999 NRC Canada

Fig. 3. Relationship between Pacific herring recruitment biomass (kt) and the five input variables. Circles indicate observed values and the line shows the supersmoothed trend.

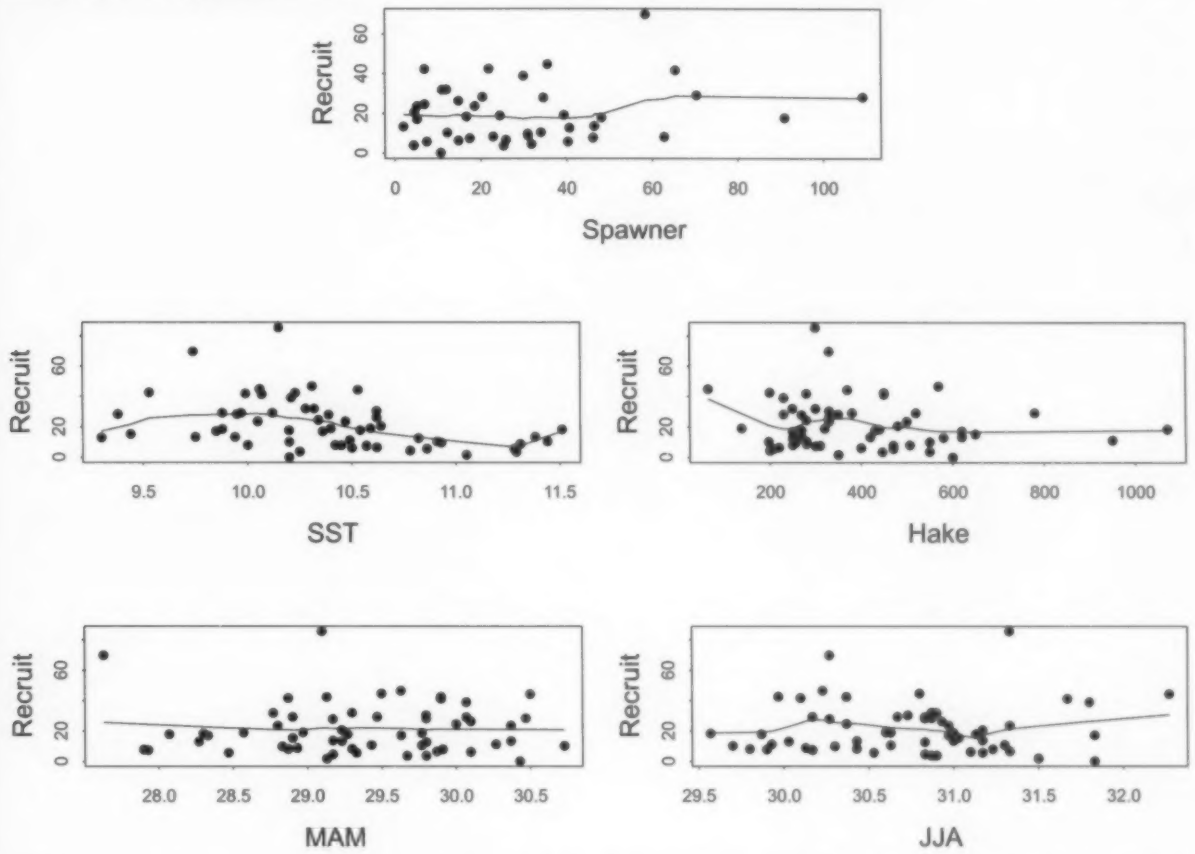

The first type, a 5-to-1 network, uses all five variables as inputs but is restricted to the period 1951–1992. The second type, a 4-to-1 network, excludes the spawner biomass and only uses the time series for the four remaining input variables, which begin in 1935.

The performance of a neural network depends on the number of neurons in the hidden layer. Generally speaking, the more neurons there are in the hidden layer, the better the network performs during training. However, the more neurons there are increases the risk of overtraining, which leads to poorer predictions. We used a fuzzy logic procedure (described in the Appendix) to evaluate the performance of networks with one to five neurons in the hidden layer for the 5-to-1 neural network and one to four hidden neurons for the 4-to-1 network (see Table 1).

Eight criteria (four for training and four for testing) were evaluated for each network. The importance weights (used by the fuzzy logic procedure) for these eight criteria are shown at the top of Table 1. The value of the weights reflects our opinion about the importance of the prediction in each case. For both the training and test results, we wanted lower mean residual errors and higher R^2 and put less emphasis on the residual variance and MAPE. We required good performances for both the training and testing phases, since poor training undermines the model prediction. To balance both considerations, we have given much higher fuzzy importance to the testing results than to the training results based on our preferences. Table 1 shows the results for the 5-to-1 networks. The columns headed "rank" indicate the rank order of each network for each criterion. For example, for the R^2 criterion, the 5-3-1 network had the highest rank (5) and the 5-1-1 network the lowest rank (1). In contrast, for the mean residual error, residual variance, and MAPE, the networks with the lowest values received the highest rank. The total rank for each neural network is the sum of the product of the rank and the related importance index. For both the training and testing processes, the total ranks for the four cases (random, high, middle, and low recruit biomass) were summed to determine the final rank for each neural network. For both the 5-to-1 and 4-to-1 networks, the highest total rank was obtained by the neural networks with two hidden neurons. Hence, the 5-2-1 and 4-2-1 networks were selected as the "best" forecasting models for further evaluation.

Results and discussion

Model fitting

Figures 4 and 5 show the resulting forecasts for the 5-2-1

© 1999 NRC Canada

Fig. 4. Results for the 5-2-1 neural network. The left panels show the relationship between the observed recruit biomass and the corresponding trained recruit biomass for each neural network model and the 1:1 line. The right panels show the Pacific herring recruit biomass time series, where the circles indicate the observed biomass and the line the corresponding trained output for each neural network model. Nine asterisks are also shown for each case: the first five represent the test data and the last four the forecast values from the neural network.

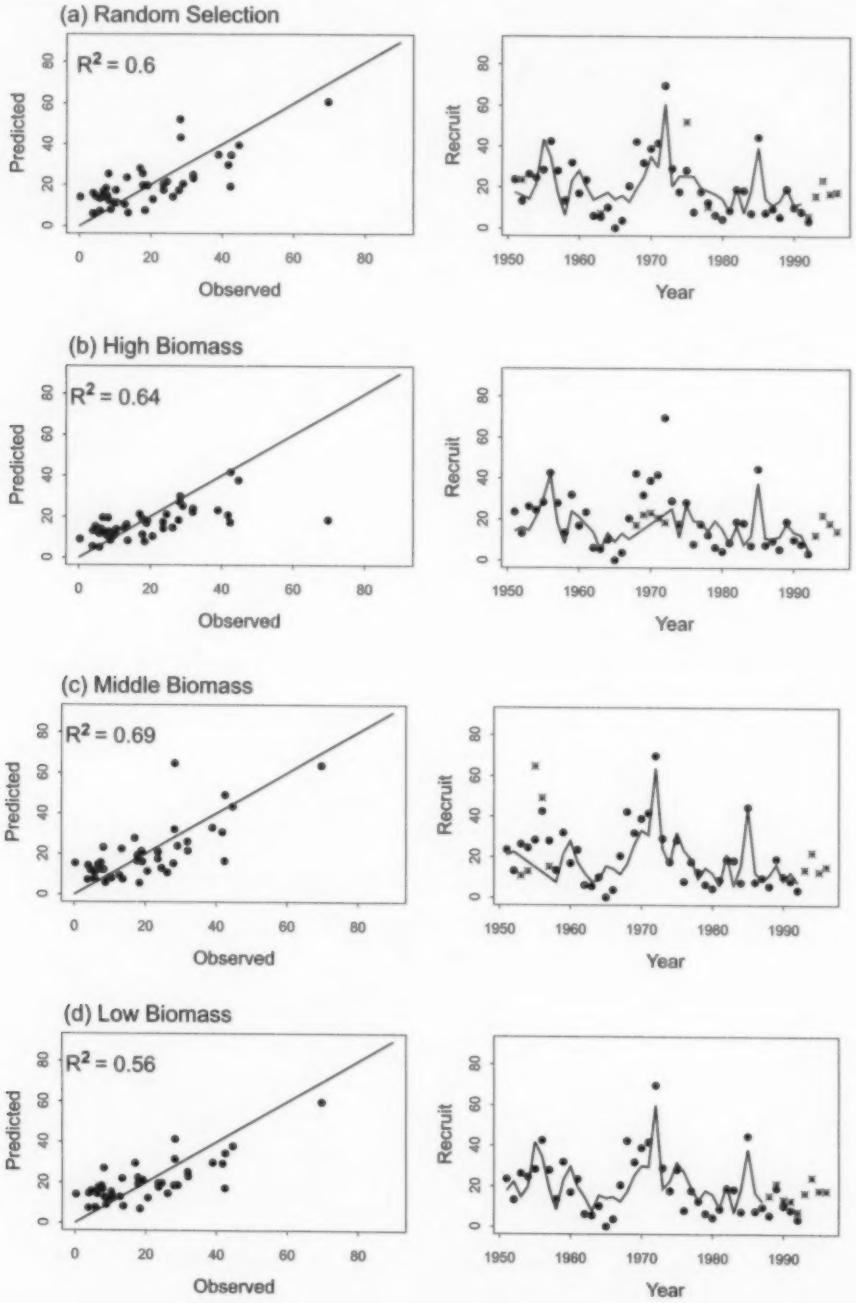

and 4-2-1 networks, respectively. In both figures, four test cases were generated from the test data: a random selection of five recruitments and the five highest, five middle, and five lowest recruitments. These data were omitted from the training procedure. Figures 4 and 5 indicate that the training process successfully reproduced the time series patterns in

© 1999 NRC Canada

Fig. 5. Results for the 4-2-1 neural network. The left panels show the relationship between the observed recruit biomass and the corresponding trained recruit biomass for each neural network model and the 1:1 line. The right panels show the Pacific herring recruit biomass time series, where the circles indicate the observed biomass and the line the corresponding trained output for each neural network model. Nine asterisks are also shown for each case: the first five represent the test data and the last four the forecast values from the neural network.

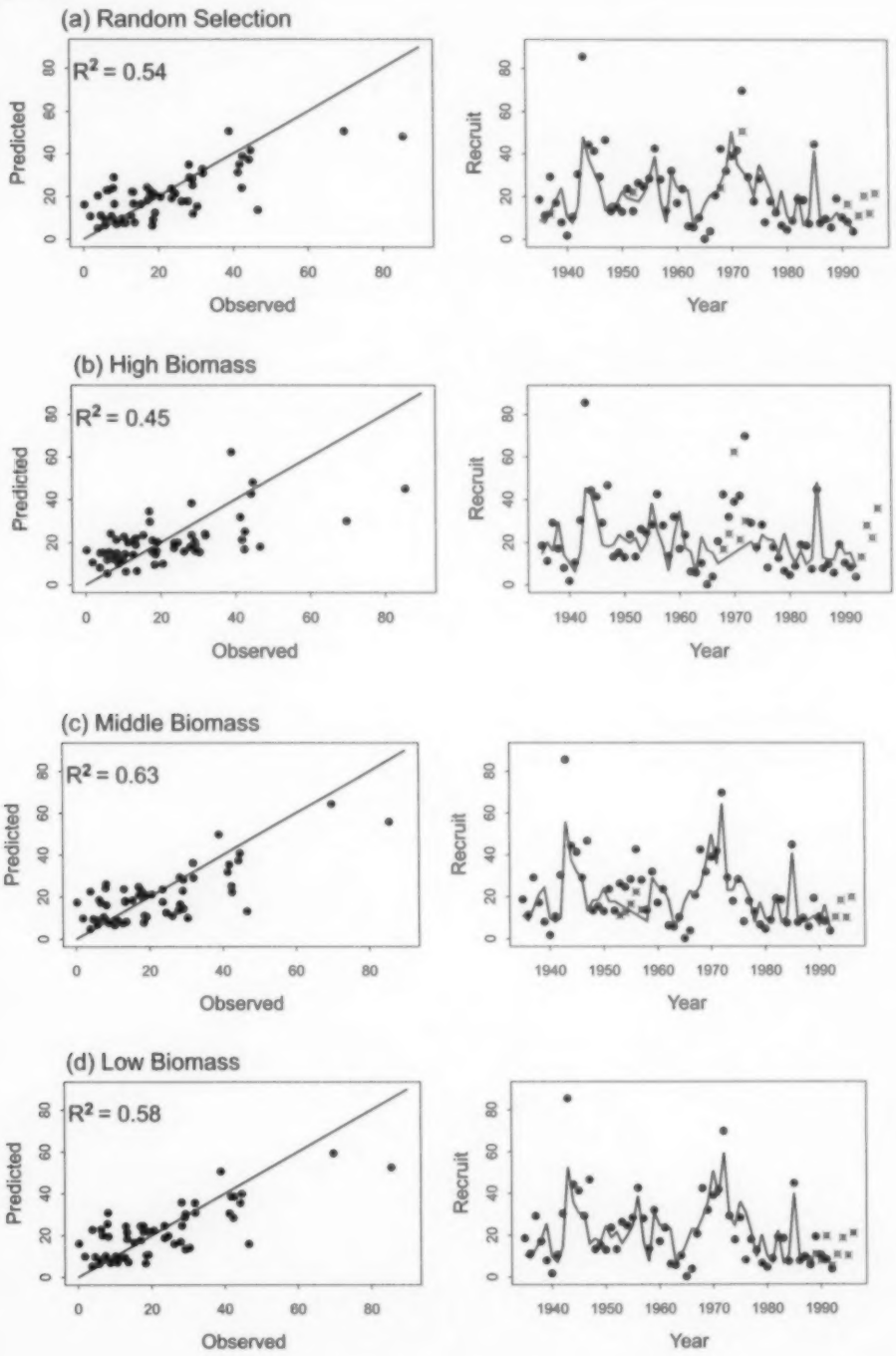

© 1999 NRC Canada

Table 1. Evaluation of neural network models.

		Training								Testing										
	Importance:	0.2		0.5		0.15		0.1		0.7		0.9		0.4		0.3		Test	Neural	Grand
Case	Network	R^2	Rank	MPE	Rank	VAR	Rank	MAPE	Rank	R^2	Rank	MPE	Rank	VAR	Rank	MAPE	Rank	total	total	total
Random	5-5-1	0.8	3	0.2	2	55.7	3	1.4	5	0.9	2	−7.6	2	215.8	2	0.5	3	4.9	7.5	32.2
	5-4-1	0.8	4	0.1	4	54.1	4	1.5	4	0.9	3	−4.4	5	106.2	4	0.3	5	9.7	13.5	39.6
	5-3-1	0.8	5	0.2	1	53.6	5	1.5	3	0.9	1	−10.0	1	285.5	1	0.8	1	2.3	4.9	38.1
	5-2-1	0.6	2	0.0	5	88.9	2	2.1	2	0.9	4	−7.2	3	107.9	3	0.5	4	7.9	11.3	43.9
	5-1-1	0.5	1	−0.1	3	108.8	1	2.4	1	0.9	5	−4.5	4	6.4	5	0.6	2	9.7	11.7	41.3
High	5-5-1	0.6	2	0.1	1	43.4	2	1.5	2	0.2	2	24.6	1	249.6	4	0.5	2	4.5	5.9	
	5-4-1	0.6	4	0.1	2	43.2	5	1.5	5	0.3	4	24.5	2	255.3	3	0.5	3	6.7	9.8	
	5-3-1	0.6	5	0.1	3	43.3	4	1.5	4	0.3	3	24.5	4	255.4	2	0.5	4	7.7	11.2	
	5-2-1	0.6	3	0.1	4	43.3	3	1.5	3	0.3	5	24.5	3	256.1	1	0.5	5	8.1	11.5	
	5-1-1	0.5	1	0.1	5	62.1	1	1.9	1	0.1	1	24.5	5	197.3	5	0.5	1	7.5	10.5	
Middle	5-5-1	0.6	1	−0.1	1	77.4	1	2.3	1	0.3	5	1.0	1	417.1	5	0.6	3	7.3	8.3	
	5-4-1	0.7	4	0.0	5	74.7	5	2.1	5	0.3	1	0.5	5	431.6	1	0.6	1	5.9	10.5	
	5-3-1	0.7	5	0.0	4	74.8	4	2.1	4	0.3	2	0.6	4	429.8	2	0.6	2	6.4	10.4	
	5-2-1	0.7	2	0.0	2	75.2	2	2.1	2	0.3	4	0.7	2	425.5	4	0.6	4	7.4	9.3	
	5-1-1	0.7	3	0.0	3	75.0	3	2.1	3	0.3	3	0.3	3	427.3	3	0.6	5	7.5	10.4	
Low	5-5-1	0.8	5	0.1	4	47.1	5	1.4	5	0.1	2	−3.9	4	69.5	1	0.8	3	6.3	10.6	
	5-4-1	0.8	4	0.2	1	49.1	4	1.4	4	0.0	1	−5.0	2	59.3	2	1.0	1	3.6	5.9	
	5-3-1	0.7	3	−0.1	2	61.1	3	1.5	3	0.1	3	−2.2	5	42.4	3	0.6	5	9.3	11.7	
	5-2-1	0.6	2	−0.1	3	96.4	2	2.1	2	0.8	5	−4.7	3	8.7	5	0.7	4	9.4	11.8	
	5-1-1	0.5	1	0.0	5	105.5	1	2.3	1	0.6	4	−5.6	1	14.5	4	1.0	2	5.9	8.9	
Random	4-4-1	0.6	4	−0.3	2	85.6	4	1.3	4	0.5	2	7.6	2	325.7	2	0.8	1	4.3	7.1	32.8
	4-3-1	0.6	3	−0.4	1	103.7	3	1.5	3	0.6	3	7.6	3	258.3	3	0.7	2	6.6	8.5	33.4
	4-2-1	0.5	2	−0.3	3	110.5	2	1.8	2	0.7	4	7.5	4	214.8	4	0.6	4	9.2	11.6	37.0
	4-1-1	0.3	1	0.0	4	158.9	1	2.2	1	0.2	1	13.6	1	495.6	1	0.7	3	2.9	5.4	26.8
High	4-4-1	0.7	4	−0.1	2	77.3	4	1.5	4	0.1	4	7.0	4	318.2	4	0.3	4	9.2	12.0	
	4-3-1	0.5	3	−0.6	1	103.2	3	1.5	3	0.0	3	7.3	3	381.3	2	0.4	3	6.5	8.4	
	4-2-1	0.5	2	−0.1	3	123.1	2	1.9	2	0.0	2	13.6	2	608.0	1	0.5	1	3.9	6.3	
	4-1-1	0.3	1	−0.1	4	148.5	1	2.2	1	0.0	1	17.9	1	345.8	3	0.4	2	3.4	5.9	
Middle	4-4-1	0.7	4	−0.1	4	90.7	4	1.6	4	0.5	2	16.2	1	32.7	2	0.5	1	3.4	7.2	
	4-3-1	0.7	3	−0.2	2	101.4	3	1.8	3	0.9	4	15.5	2	11.0	4	0.5	2	6.8	9.2	
	4-2-1	0.6	2	−0.4	1	107.4	2	1.9	2	0.9	3	14.9	3	11.6	3	0.5	4	7.2	8.6	
	4-1-1	0.4	1	−0.1	3	174.4	1	2.0	1	0.1	1	3.2	4	305.0	1	0.5	3	5.6	7.6	
Low	4-4-1	0.7	4	−0.6	1	91.5	4	1.2	4	0.0	2	−4.1	2	227.4	1	1.3	2	4.2	6.5	
	4-3-1	0.6	3	−0.6	2	112.8	3	1.6	3	0.0	1	−1.9	3	96.9	2	0.8	3	5.1	7.5	
	4-2-1	0.6	2	−0.4	3	118.2	2	1.8	2	0.1	3	−1.0	4	50.1	3	0.6	4	8.1	10.5	
	4-1-1	0.3	1	−0.1	4	188.1	1	2.2	1	0.6	4	−8.9	1	13.8	4	1.4	1	5.6	8.1	

Note: The "Case" column corresponds to the random, high, middle, and low recruit biomass testing data sets. The "Network" column lists the neural networks evaluated for each case. The R^2, MPE, VAR, and MAPE columns for the "Training" and "Testing" processes indicate the neural network model results, followed by their ranks for each evaluation criterion. The "Test total" column shows the total rank for the testing process, calculated by summing the product of the ranks and the associated importance. The "Neural total" column shows the total rank for the combined training and testing evaluations and was calculated by summing the product of the ranks and the associated importance. The "Grand total" column indicates the total rank for each neural network model for all four cases, calculated by summing the "Neural total" for all cases. The optimal neural network model should have the highest grand total score.

© 1999 NRC Canada

Table 2. Weight structures for the neural networks. The last row indicates the total weight connecting the hidden layer to the output layer. The rest of the data show the weights between the input layer and the hidden layer.

	Net 5-2-1		Net 4-2-1	
	Σw_{ij}	$\Sigma \lvert w_{ij} \rvert$	Σw_{ij}	$\Sigma \lvert w_{ij} \rvert$
Spawner	–5.12	13.60	na	na
Pacific hake	8.56	20.40	–14.46	40.52
SST	5.65	12.69	15.51	35.95
MAM	–0.22	12.28	12.61	21.95
JJA	–5.02	15.46	–9.50	17.96
Hidden to output	–9.49		–2.17	

Table 3. Neural network model recruitment prediction for the years 1993–1996.

	Random	High	Middle	Low	Average
Net 5-2-1					
1993	15.908	12.653	13.912	16.689	14.791
1994	23.527	22.314	22.197	24.395	23.108
1995	16.992	18.402	12.883	17.996	16.568
1996	17.702	14.536	15.229	17.724	16.298
Net 4-2-1					
1993	11.235	13.233	10.281	10.702	11.363
1994	20.394	28.002	18.187	18.639	21.306
1995	12.286	22.243	10.019	10.385	13.733
1996	21.553	35.896	19.753	20.963	24.541

each case with an R^2 of about 60%. The test was most accurate for the random and low recruit biomass cases, based on the analysis of testing ranks in Table 1.

Analysis of weights

Weights between layers indicate the strength of the connections in the neural network. The training algorithm finds the combination of weights that optimizes the performance of the network model. These connecting weights can then be used to determine the most important inputs once the optimal network is found. Aoki and Komatsu (1997) used this approach for an analysis of the weight structure for the application of neural network mode to sardine prediction.

The connecting weights with the highest absolute values indicate the most important factors. The positive or negative signs associated with the weights indicate a corresponding positive or negative relationship between the input variable and the output variable (recruit biomass). Table 2 summarizes the weight structures among the input, hidden, and output layers. These results show that Pacific hake biomass and SST are consistently the most important factors in both trained neural networks.

The relationship between the inputs and outputs can be revealed by a two-step weight analysis, since they are connected first from the input layer to the hidden layer and second from the hidden layer to the output layer. A positive relationship between the input layer and output layer occurs only when the relationships between the input to the hidden layer and the hidden to the output layer are all positive or negative. Table 2 shows that the hidden layer to the output layer is negatively related based on the strong negative weight structure (total weights are –9.49 and –2.17 for net 5-2-1 and 4-2-1, respectively). Therefore, a strong negative weight structure for the input spawner (total = –5.12 in Table 2) indicates a positive relationship between spawner and recruitment biomass. In contrast, negative relationships between the output (recruit biomass) and Pacific hake biomass and SST can be seen from the strong positive weight structures (total weights being 8.56 and 5.65 in Table 2 for net 5-2-1). This finding is consistent with previous work (Tanasichuk et al. 1991; Ware 1991; Ware and McFarlane 1995). The negative total weight for Pacific hake biomass in net 4-2-1 (total = –14.52) is an unexpected result, which probably indicates that the biomass of spawners, which was not available as an input in net 4-2-1, has an important influence on the weight structure and therefore should be included in a recruitment forecasting model.

Table 4. ANOVA table for the multiple regression.

Coefficient	Value	SE	t	$P(>\lvert t \rvert)$
Intercept	73.362	30.606	2.397	0.022
Spawner	–0.04	0.169	–0.238	0.813
SST	–8.215	3.146	–2.611	0.013
Pacific hake	–0.708	0.359	–1.973	0.056
MAM	–4.983	6.217	–0.801	0.428
JJA	–8.892	9.329	–0.953	0.347

Table 5. ANOVA table for the Ricker climate stock–recruitment model.

Coefficient	Value	SE	t	$P(>\lvert t \rvert)$
Intercept	22.8584	10.7882	2.1188	0.0411
Spawner	–0.0327	0.0071	–4.5848	0.0001
SST	–1.0667	0.3477	–3.068	0.0041
Pacific hake	–0.0012	0.0014	–0.9083	0.3698
MAM	–0.2165	0.2478	–0.874	0.3879
JJA	–0.1427	0.3424	–0.4168	0.6793

Independent predictions

Table 3 summarizes the recruitment predictions for the 1993–1996 year-classes from the 5-2-1 and 4-2-1 neural networks for the four cases. The last column represents the average value produced by the four test cases. Some preliminary information on the biomass of Pacific herring recruits is available for the 1993, 1994, and 1995 year-classes (these year-classes recruited to the fishery in 1996, 1997, and 1998, respectively). The early signs are that the 1993 year-class is about 4000 t, the 1994 year-class is about 28 000 t, and the 1995 year-class is about 7000 t (Schweigert et al. 1997). Both models forecast that the 1994 year-class should be much larger than the 1993 and 1995 year-classes, which appears to be the case.

Comparison with other forecasting models

Multiple regression

A multiple regression analysis was done to compare the accuracy of the predictions with the neural network model predictions because a multiple regression is just a special type of neural network. The multiple regression contained five lagged, independent variables, Pacific herring spawner

© 1999 NRC Canada

biomass, SST, Pacific hake biomass, MAM salinity, and JJA salinity, and one dependent variable, Pacific herring recruit biomass. All variables were log transformed to comply with the assumptions of homogeneity and normality required by regression analysis.

The F statistic of 2.979 with degrees of freedom of 5 and 36 corresponds to a p value of 0.024, which indicates that the regression is highly significant. Table 4 shows the resulting ANOVA table. This table also indicates that the SST and Pacific hake biomass input variables tend to be more important than spawner biomass and salinity (MAM and JJA) based on the p value for the t test. Comparison with Fig. 4 indicates that the multiple regression ($R^2 = 0.29$) performed poorly compared with the neural network model ($R^2 = 0.60$). The failure of the multiple regression model is further highlighted by its inferior forecasts of the biomass of the 1993, 1994, and 1995 year-classes (16.9, 19.1, and 15.9 kt, respectively).

Ricker climate stock–recruitment model

The Ricker curve is a well-known model for analyzing fish stock–recruitment relationships (Ricker 1975). This model can be expressed as

$$R_t = \alpha S_t \exp(-\beta S_t)$$

where R_t is the recruit biomass and S_t is the spawner biomass. This model can be extended to incorporate environmental effects in the following fashion:

$$(2) \qquad R_t = \alpha S_t \exp(-\beta S_t + \gamma X_t)$$

where X_t is a vector of environmental variables; in this case, X_t = (Pacific hake biomass, SST, MAM, JJA). Schweigert and Noakes (1990) have evaluated this approach for Pacific herring stock assessment forecasts.

The model in eq. 2 is log transformed as

$$(3) \qquad Y = \log(R_t/S_t) = \log(\alpha) - \beta S_t + \gamma X_t$$

so that the parameters can be estimated by multiple linear regression.

For comparison with the neural network model, we fit the same data to the linearized Ricker environmental model (eq. 3). The model fit is highly significant with a p value of 0.0009. The resulting parameter estimates and the associated statistics are summarized in Table 5. This ANOVA table indicates that SST and Pacific hake biomass are more important than salinities (MAM and JJA) based on the p value for the t test. It can be seen that the Ricker climate stock–recruitment model ($R^2 = 0.42$) performs better than the multiple regression model but not as well as the neural network model. This poorer performance is also apparent from the forecasts of the biomass of the 1993, 1994, and 1995 year-classes (23.1, 14.9, and 12.2 kt, respectively).

Conclusions

This study demonstrates that neural network models can perform reasonably well in predicting the biomass of fish that will recruit to the fishery, given prior information on the state of several key factors during the first year of life of the year-class. Specifically, information on the biomass of their parents (i.e., spawners), the biomass of a key predator species (i.e., Pacific hake), and some important environmental variables that are believed to be proxy indicators of other predators and general feeding conditions is required. Comparison with a multiple regression and modified Ricker model demonstrated the superior ability of the neural network model to fit the underlying complex relationships between recruitment and the independent variables.

Similar to a multiple regression and Ricker model, the influence of each independent variable can be assessed from the values of the weights in the neural network. The weight structure indicates that biomass of Pacific hake is the most important factor determining the strength of the recruiting year-class of Pacific herring, with annual SST an important secondary factor. At times, water salinity and biomass of parents can also be important. These conclusions are consistent with our current understanding of the ecology of the WCVI Pacific herring (Ware and McFarlane 1995). The negative correlation between annual SST and biomass of Pacific herring recruits to the WCVI stock has been a consistent feature of the recruitment time series since Tester (1948) first discovered it about 50 years ago. The importance of Pacific herring spawners (i.e., the parents) in determining year-class size is apparent in Table 2. However, recent work indicated that the parent–recruit relationship is masked by the temperature effect (Ware 1996). The weight structure for the other two environmental indices examined, spring salinity and summer salinity, which are suspected to be proxy indicators of general feeding conditions (or different components of the food supply) for juvenile and adult Pacific herring, appeared to be important factors in some years. In general, more recruits tend to be produced when the spring and summer salinities are higher (in the 5-2-1 network), which implies more favorable feeding conditions for Pacific herring (Ware 1991).

This study illustrates how artificial neural networks can be applied to improve the accuracy of fishery stock forecasts and management. The most efficient neural networks that we examined (the 5-2-1 and 4-2-1 networks) explained about 60–70% of the variances in Pacific herring recruitment over the last 41 years. These forecasts appear to improve on the accuracy of previous approaches that have been examined (Schweigert and Noakes 1990; Ware 1991; Stocker and Noakes 1998). For British Columbia stocks of Pacific herring, the target harvest rate is 0.2 and is defined as the ratio of the annual catch to the fishable adult stock biomass. For a short-lived species like Pacific herring, where recruits can make up 30–50% of the fishable biomass, an accurate recruitment forecast can significantly improve the management of the fishery by enabling the actual harvest rate to be closer, on average, to the target 20% harvest rate. In many cases, the stock assessment analyst and the fisheries manager would also like to know something about the uncertainty in the recruitment forecast. We are exploring how to implement this feature by incorporating a bootstrapping procedure.

Acknowledgements

We thank Dr. Brent Hargreaves for suggesting that we apply a neural network model to the recruitment forecasting problem and Dr. Tim Mulligan for the useful suggestions on the draft manuscript.

© 1999 NRC Canada

References

Aoki, I., and Komatsu, T. 1997. Analysis and prediction of the fluctuation of sardine abundance using a neural network. Oceanol. Acta, **20**: 81–88.

Chen, S., Billings, S.A., and Grant, P.M. 1990. Nonlinear system identification using neural networks. Int. J. Control, **51**: 1191–1214.

Francis, R.C., McFarlane, G.A., Hollowed, A.B., Swartzman, G.L., and Getz, W.M. 1984. Status and management of the Pacific hake resource and fishery off the west coast of the United States and Canada. Northwest Atl. Fish. Cent. Processed Rep. 84-18.

Funahashi, K. 1989. On the approximate realization of continuous mapping by neural networks. Neural Networks, **2**: 183–332.

Guegan, J., Lek, S., and Oberdorff, T. 1998. Energy availability and habitat heterogeneity predict global rivine fish divisity. Nature (Lond.), **391**: 382–384.

Jarre-Teichmann, A., Brey, T., and Haltof H. 1995. Exploring the use of neural networks for biomass forecasts in the Peruvian upwelling ecosystem. Naga. ICLARM Q. Rep. **18**: 38–40.

Lek, S., Belaud, A., Dimopoulos, I., Lauga, J., and Moreau. J. 1995. Improved estimation, using neural networks, of the food consumption of fish populations. Mar. Freshwater Res. **46**: 1229–1236.

MathSoft Inc. 1995. S-PLUS manual. S-PLUS guide to statistical and mathematical analysis. Version 3.3. MathSoft Inc., StatSci Division, Seattle, Wash.

Ricker, W.E. 1975. Computation and interpretation of biological statistics of fish populations. Bull. Fish. Res. Board Can. No. 191.

Ripley, B.D. 1993. Statistical aspects of neural networks. *In* Networks and chaos-statistical and probabilistic aspects. *Edited by* O.E. Barndroff-Nielsen, J.L. Jensen, and W.S. Kendall. Chapman and Hall, London, U.K. pp. 40–123.

Ripley, B.D. 1994*a*. Neural network and related methods for classification. J. R. Stat. Soc. Ser. B. (Methodol.), **56**: 409–456.

Ripley, B.D. 1994*b*. Neural networks and flexible regression and discrimination. Adv. Appl. Stat. **2**: 39–57.

Robinson, C.L.K., and Ware, D.M. 1994. Modelling pelagic fish and plankton trophodynamics off southwestern Vancouver Island, British Columbia. Can. J. Fish. Aquat. Sci. **51**: 1737–1751.

Schweigert, J.F., and Noakes, D. J. 1990. Forecasting Pacific herring (*Clupea harengus pallasi*) recruitment from spawner abundance and environmental information. Proceedings of the International Herring Symposium, October 1990, Anchorage, Alaska. Alaska Sea Grant College Program, Alaska. pp. 373–387.

Schweigert, J.F., Fort, C., and Hamer, L. 1997. Stock assessment for British Columbia herring in 1996 and forecasts of the potential catch in 1997. Can. Tech. Rep. Fish. Aquat. Sci. No. 2173.

Spackman, K.A. 1992. Maximum likelihood training of connectionist models: comparison with least-squares back propagation and logistic regression. Proc. 15th Annu. Symp. Comput. Appl. Med. Care, Nov. 1991. Institute of Electrical and Electronics Engineers, New York. pp. 285–289.

Stocker, M., and Noakes, D.J. 1988. Evaluating forecasting procedures for predicting Pacific herring (*Clupea harengus pallasi*) recruitment in British Columbia. Can. J. Fish. Aquat. Sci. **45**: 928–935.

Tanasichuk, R.W., Ware, D.M., Shaw, W., and McFarlane, G.A. 1991. Variations in the diet, daily ration and feeding periodicity of Pacific hake (*Merluccius productus*) and spiny dogfish (*Squalus acanthias*) off the lower west coast of Vancouver Island. Can. J. Fish. Aquat. Sci. **48**: 2118–2128.

Tester, A.L. 1948. The efficacy of catch limitations in regulating the British Columbia herring fishery. Trans. R. Soc. Can. **62**: 135–163.

Venables, W.N., and Ripley. B.D. 1994. Modern applied statistics with S-Plus. Springer-Verlag, New York.

Ware, D.M. 1991. Climate, predator and prey: behavior of a linked oscillating system. Long-term variability of pelagic fish populations and their environment. *Edited by* T. Kawasaki et al. Pergamon Press, Tokyo. pp. 279–291.

Ware, D.M. 1996. Herring carrying capacity and sustainable harvest rates in different climate regimes. Pac. Stock Assess. Rev. Comm. Working Pap. H96-3.

Ware, D.M., and McFarlane, G.A. 1995. Climate-induced changes in Pacific hake (*Merluccius productus*) abundance and pelagic community interactions in the Vancouver Island upwelling system. *In* Climate change and northern fish populations. *Edited by* R.J. Beamish. Can. Spec. Publ. Fish. Aquat. Sci. No. 121. pp. 509–521.

Weigend, A.S., Huberman, B.A., and Rumelhart, D.E. 1992. Predicting sunspots and exchange rates with a connectionist network. *In* Nonlinear modeling and forecasting. *Edited by* M. Casdagli and S. Eubank. Proceedings Vol. 12. SFI studies in the sciences of complexity. Addison-Wesley, Reading, Mass. pp. 395–432.

White, H. 1989. Some asymptotic results for learning in single hidden-layer feed-forward network models. J. Am. Stat. Assoc. **84**(408): 1003–1013.

Appendix. Fuzzy logic based decision-making procedure

Suppose that K evaluation criteria (or indicators) are selected ($K = 8$ in this paper), denoted by C_k, $k = 1,..., K$, and L neural networks are to be evaluated, denoted by Net_l, $l = 1,..., L$. Each of these criteria can be assigned a certain importance for evaluating the performance of a specific neural network. Note that key feature here is that it is the analyst's (or some other expert's) opinion of the importance of the criterion that is used to evaluate a network. This relative importance defines the membership (in a fuzzy logic sense) of that criterion.

Some clarification is needed here for what is meant by "membership." To understand this, we need to introduce some set theory concepts. The traditional set is defined by a collection of some elements. For example, if we have a set

$$A = \{\text{Pacific herring, Pacific hake}\}$$

then we can precisely classify any fish caught, anywhere, as to whether it belongs to set A or not. If the fish belongs to set A, then we can say it has a 100% possibility (or membership) of belonging to set A; otherwise, the possibility (or membership) is zero. We can never find a fish that is halfway between these two possibilities.

However, classifying the evaluation criteria C_k into an importance set is not as simple as the traditional "yes or no" solution, but rather requires something in between. For example, how well a neural network model performed in the testing phase was more important from our perspective than how it performed in the training phase because we would like to use the model forecasts for future planning and management of the Pacific herring fishery. Consequently, we choose memberships of 0.8 and 0.3 for the R^2 criteria in the testing and training evaluations. The membership and its corresponding element constitutes a fuzzy set, denoted by

$$F_C = \left\{C_1/m_{C_1},...,C_K/m_{C_K}\right\}$$

© 1999 NRC Canada

where m_{C_k} is the membership for C_k, $k = 1,..., K$. The same definition can be made for the Net_l, $l = 1,..., L$ as

$$F_{\text{Net}} = \left\{\text{Net}_1/m_{\text{Net}_1}, \ldots, \text{Net}_L/m_{\text{Net}_L}\right\}.$$

McNeill and Freiberger (1993) provided a good introduction to the concept and development of fuzzy logic theory, and Welstead (1994) covered all the computational aspects with a realization in C/C++. A comprehensive implementation of fuzzy logic can be found in Fuller (1995). The basic operations for fuzzy sets include intersection, union, complement, and implication.

The procedure for deciding which neural network is the best requires evaluating each network for each criterion and then weighting each network by the relative importance of that criterion. We then use the logic implication operation $A \rightarrow B$, which means that given A, what is B? Here, the importance membership for a particular criterion is A, and each neural network's ranking for that criterion is B. If Larsen implication is used, then the calculation of $A \rightarrow B$ is $A \rightarrow B = AB$, which means that given a particular criterion's (A) importance, does that imply a good neural network's (B) ranking for that criterion? This procedure assigns higher weights to neural networks with higher importance membership values. The final score for each neural network is the sum of all the results from the implication operation for that network. The "optimal" neural network is chosen by determining which network had the highest final score. The procedure is summarized in the following table:

	$C_1 \ldots C_K$	Final score
Net_1	$\vdots$	$\vdots$
$\vdots$	$m_{C_k} m_{\text{Net}_l}$	$\sum_{k=1}^{K} m_{C_k} m_{\text{Net}_l}$
Net_L	$\vdots$	$\vdots$

References

Fuller, R. 1995. Neural fuzzy systems. Abo Akademis Trykeri, Abo.

McNeill, D., and Freiberger, P. 1993. Fuzzy logic. Simon and Schuster, New York.

Welstead, S.T. 1994. Neural network and fuzzy logic applications in C/C++. John Wiley & Sons, Inc., New York.

© 1999 NRC Canada

Effect of time of day, time of year, and life history strategy on time budgeting in juvenile Atlantic salmon, *Salmo salar*

Sveinn K. Valdimarsson and Neil B. Metcalfe

Abstract: Traditionally, behavioural studies on juvenile Atlantic salmon, *Salmo salar*, have been conducted during the day in summer. It is known that Atlantic salmon become nocturnal in winter, but very little is known about their behaviour at that time. Therefore, observations in a seminatural stream were carried out during the day and night, from February to June, comparing diel and seasonal differences in behaviour between fish adopting alternative life history strategies. The results showed a general trend for more activity in spring than in winter, and the fish were found to be foraging at surprisingly low light levels. There were differences in relative feeding rate between the life history strategies; the early migrant fish foraged mostly during the day whereas the delayed migrant fish did more foraging at night. There is some evidence that the early migrant fish made fewer feeding attempts over the winter, which is surprising, since they grow faster over that period. This suggests differences in foraging efficiency, which could contribute to the separation into these two life history strategies.

Résumé : Les études du comportement des juvéniles du saumon de l'Atlantique, *Salmo salar*, ont traditionnellement été réalisées en été et pendant le jour. On sait que le saumon devient nocturne en hiver mais on connaît très mal son comportement pendant cette période. Nous avons procédé à des observations en cours d'eau semi-naturel pendant le jour et la nuit, de février à juin, afin de comparer les écarts nycthéméraux et saisonniers du comportement chez les poissons adoptant d'autres stratégies de cycle vital. Il a été noté une tendance générale à une plus grande activité au printemps qu'en hiver et les poissons recherchaient leur nourriture à des niveaux d'éclairement très faibles. Le taux d'alimentation relatif variait en fonction des stratégies de cycle vital : les poissons de migration hâtive se nourrissaient surtout le jour tandis que ceux à migration retardée se nourrissaient surtout la nuit. Il semble que les poissons à migration hâtive recherchaient moins de nourriture en hiver, ce qui est surprenant étant donné que leur croissance est plus rapide pendant cette période. Cela porte à croire à l'existence de différences touchant l'efficacité de la recherche de nourriture qui pourraient contribuer à l'adoption de l'une ou de l'autre de ces stratégies de cycle vital.

[Traduit par la Rédaction]

Introduction

Salmonids show diverse life history strategies both between and within species (e.g., Skúlason et al. 1989). The Atlantic salmon, *Salmo salar*, is no exception, with variable life history patterns in both the freshwater and marine stages of the life cycle (Metcalfe and Thorpe 1990). In the first autumn (1 year from fertilisation), life history variation produces changes in the size distribution of the fish: instead of the former normal curve, it becomes bimodal, with an upper modal group and a lower modal group. This bimodality is connected to the life history decision concerning age at seaward migration. The upper modal group ("early migrant") fish grow slowly over the winter, smolt, and migrate to the sea in the following spring, whereas the lower modal group ("delayed migrant") fish almost or completely cease growing over winter and spend at least another year in the river. This kind of pattern has been observed both in controlled hatchery conditions (Thorpe 1977; Higgins and Talbot 1985) and in the wild (Heggenes and Metcalfe 1991; Nicieza et al. 1991).

This bimodality is of special interest because it is uncommon for sibling animals to express such variation in life history, suggesting that it is an environmentally induced phenomenon. Furthermore, this gross variation in morphology and life history is associated with fine-tuned changes in behaviour. Several studies have shown differences in feeding behaviour between the two modal groups. As the modal groups diverge (during autumn), lower modal group fish show a significantly greater loss of appetite than upper modal group fish (Higgins and Talbot 1985; Metcalfe et al. 1986). Feeding in winter is reduced for all fish (Higgins and Talbot 1985), possibly due to their having a reduced metabolic rate at low temperatures (although rainbow trout, *Oncorhynchus mykiss*, have been observed to forage at temperatures as low as 0°C (Needham and Jones 1959)), but that does not explain why there should be a difference between the modal groups.

When water temperatures start to fall in autumn, juvenile salmonids begin to hide in cavities amongst stones in the substrate (Chapman and Bjornn 1969; Rimmer et al. 1983).

Received February 25, 1999. Accepted August 20. 1999. J15035

S.K. Valdimarsson[1] and N.B. Metcalfe. Fish Biology Group, Graham Kerr Building, Institute of Biomedical and Life Sciences, University of Glasgow, Glasgow G12 8QQ, U.K.

[1]Author to whom all correspondence should be addressed. e-mail: 933442va@udcf.gla.ac.uk

© 1999 NRC Canada

At night, however, the fish emerge from the streambed and become more active (Fraser et al. 1993; Griffith and Smith 1993; Heggenes et al. 1993). This change in daytime activity has been shown to be controlled by temperature (Fraser et al. 1995) and light intensity and time of year (Valdimarsson et al. 1997). However, very little is known about the behaviour of the fish at night, possibly because of difficulties in observing fish in the dark. Heggenes et al. (1993) observed juvenile brown trout, *Salmo trutta*, feeding at night, and it is reasonable to assume that the greatest investment in foraging takes place during twilight hours or at night because most of the day is spent in shelter. However, it has been pointed out that the feeding efficiency of Atlantic salmon is much lower at nighttime light levels than during the day (Fraser and Metcalfe 1997). Thus, foraging rates during brief daytime feeding bouts might be higher than those during the extended feeding periods at night.

To investigate this, we conducted an experiment to look at the behaviour of wintering juvenile Atlantic salmon when out of their streambed shelters. We particularly wanted to find out how foraging rates differed between day and night and especially how the life history strategies of the fish (upper versus lower modal group) affected their winter foraging behaviour.

Materials and methods

On 18 December 1994, 15 lower modal group (fork length (mean ± SE) 57.3 ± 0.88 mm, weight 1.68 ± 0.08 g) and 15 upper modal group (fork length 79.0 ± 1.10 mm, weight 4.60 ± 0.21 g) underyearling Atlantic salmon were anaesthetised and individually marked with small subcutaneous injections of Alcian blue dye. The fish were offspring of wild sea-run Atlantic salmon caught in the River Almond and had been reared in hatchery conditions prior to the experiment. They were then placed in an outdoor artificial stream at the University Field Station, Rowardennan, Scotland. The stream was in the form of a continuous, approximately oval-shaped loop with straight sides. The channel (depth 60 cm, width 60 cm) had an inside wall made from glass panels and an opaque outside wall made from meshed fibreglass. This arrangement allowed a clear side view of the stream from a darkened observation area inside the oval. In part of one of the straight sections was a variable-speed impeller that pumped the water in one direction; mesh screens isolated this section, thus creating distinct "upstream" and "downstream" ends and giving a total usable stream length of about 14 m. The surface velocity in the stream was 0.12–0.16 m/s depending on the depth. There was a constant turnover of freshwater pumped from Loch Lomond into the channel, keeping water quality high and temperatures at ambient. The roof of the channel was covered by metal mesh to prevent the fish from jumping out and predators from entering. The channel was landscaped with gravel into an alternating sequence of pool and riffle areas; water depth ranged from 10 to 55 cm. The gravel used for the streambed was rather fine (5–20 mm in diameter) to deter fish from hiding in streambed cavities. We embedded 42 shelters (made of 1-L plastic bottles cut lengthways in half to make a cavity measuring 17 × 8.5 × 4.25 cm) into the gravel so that their open side was against the glass observation walls. This allowed us to see and identify any fish inside them. These were provided in excess and were regularly spaced around the channel.

The inflowing water from Loch Lomond already contained zooplankton, but this was supplemented with a small amount of food (Fulmar pelleted salmon food, BOCM Pauls Ltd., Renfrew, U.K.), the amount of which was continually adjusted so as to be just sufficient to provide an excess of food, yet avoid the accumulation of waste. This was dispensed by an electronic feeder every 30 min throughout the 24 h into a hopper and was then carried by a flow of water along separate tubes to four evenly spaced locations in the tank so as to produce as even a distribution of food as possible. This appeared to have worked well, since all parts of the tank were within 3 m of a food source and there was no indication of the fish positioning themselves in relation to the feeding tubes. The tank was cleaned only when algae or fungi had built up to the point that our visibility was impaired; the fish were not touched during cleaning, nor was the water level altered. Individual fish were briefly removed from the stream tank and remarked and returned if their marks became faint. One lower modal group fish died in April and six upper modal group fish died in May–June, mostly due to fungal infections.

In April (when most of the upper modal group fish had begun to show external signs of smolting, i.e., silver coloration, darkened edges to fins), we put a trap at the downstream end of the stream so that they could "migrate" and leave the system if they chose to do so. The trap was checked every day. We set the criterion that on the first occasion that a fish was trapped, it was placed back in the main part of the stream tank, but on the second occasion, it was deemed to have migrated and so was removed. All upper modal group fish were trapped at least once and eight were trapped twice and therefore removed. The first fish was removed on 19 April 1995, and subsequent "migrants" were removed intermittently until the termination of the observations on 2 June 1995.

Observations on the activity patterns of the fish were made between 16 February and 2 June. Data were collected on 28 separate days, and observation sessions covered both day and night periods. Focal animal observations were carried out by locating fish that were outside the refuges. A minimum period of 2 h elapsed between successive observations of the same individual fish, and wherever possible, data from both upper modal group and lower modal group fish were collected during the same observational period. During each 5-min observation of a single fish, we recorded onto audiocassette tape the occurrence and duration of mutually exclusive behaviours: attempted feeding, resting on the bottom, holding station in the water column (i.e., swimming against the current), and moving (i.e., swimming around). Attempted feeding was defined as when the fish swam directly towards something in the water column and apparently ate it (it was not usually possible to identify food items or their fate). Aggressive behaviour was never seen during observations.

Observations at night were carried out using an image intensifier (Modulux image intensifier, Davon Optical Ltd., with a Canon 28-mm lens) with infrared lights (470 nm) providing additional light. This allowed us to watch the fish even though the visible light level was below 0.01 lx (Atlantic salmon are unable to see light in the infrared part of the spectrum (Ali 1961)), but it was not possible to recognise the individual dye marks on the fish. Therefore, after each observation, a small torch (emitting visible light) was used to identify the marks of each fish. The fish were very sensitive to all visible light in the observational area, with their immediate reaction being to go straight onto the bottom and lie still and in some cases to enter the shelters. Therefore, a blanket was placed over the observer's head and the image intensifier to prevent light from the viewing screen from reflecting off their face, and no observations were made for at least 30 min after each use of the torch (a time that we assumed sufficient for the fish to resume normal behaviour).

We measured both the water temperature and natural light intensity at the time of each focal observation. Temperature was measured with a digital thermometer permanently placed in the stream. Preliminary records showed no variation in water temperature between eight different places in the stream, and so only a single reading was taken thereafter. Atlantic salmon have a spectral sensitivity very similar to that of humans (Ali 1961), and light intensity

© 1999 NRC Canada

Table 1. Breakdown of 5-min focal observations of juvenile Atlantic salmon out of their shelters by date, season, and time of day for upper (UMG) and lower modal group (LMG) fish.

Date	Season	Time of day	Total number of observations	Number of observations	
				UMG	LMG
16 February	Winter	Night	4	2	2
		Day	1	0	1
17		Night	1	0	1
		Day	2	2	0
23		Night	3	2	1
24		Night	1	1	0
1 March		Night	2	1	1
6		Day	3	2	1
14		Night	7	3	4
15		Night	4	3	1
19		Day	2	1	1
30		Night	2	0	2
31		Night	10	4	6
4 April		Day	1	0	1
5		Night	1	0	1
21		Night	2	1	1
1 May	Spring	Day	1	0	1
2		Night	5	3	2
		Day	3	2	1
4		Day	4	2	2
5		Night	5	2	3
11		Day	5	3	2
12		Night	4	2	2
		Day	4	2	2
16		Night	6	3	3
17		Day	4	2	2
23		Day	5	3	2
26		Night	6	4	2
		Day	5	2	3
30		Night	4	2	2
		Day	1	1	0
31		Day	3	1	2
1 June		Day	1	0	1
2		Day	1	1	0

was measured using a Skye Instruments SKL 300 photometer (luxmeter), range 0.01–2000 lx. The light intensity was measured on the substrate close to the location of fish. In order to compare the activity of the fish during the day and the night, observations were classified as being during the day if the light intensity exceeded 100 lx and during the night if the light intensity was below 0.1 lx. Similarly, winter was defined as from the start of the observations on 16 February until 30 April (water temperatures (mean ± SE) 4.6 ± 0.16°C) whereas spring was from 1 May to the end of the experiment on 2 June (water temperatures increasing from 6 to 13°C). A 9-day interval between the last winter and first spring observations (Table 1) helped to define this break. The rate of feeding was quantified as the number of feeding attempts per minute whereas the other activities were measured as a percentage (arcsine transformed) of the total observation period (5 min). The data were analysed by using three-way ANOVAs looking at the effect of time of year (winter or spring), time of day (night or day), and life history pattern (upper modal group or lower modal group) on each type of behaviour. The significant patterns indicated by the three-way ANOVAs were then explored further by separate two-way ANOVAs looking at the effects of time of year and time of day within each modal group. These are only described when they offer new insights.

A total number of 113 observations were made (57 on upper modal group fish and 56 on lower modal group fish) (Table 1). Individual fish were observed between one and seven times, giving an average number of 3.7 observations per fish.

Results

The overall relative feeding rate (number of feeding attempts per minute) did not differ between winter and spring (Table 2; Fig. 1*a*), nor did it differ overall between the modal groups (Table 2; Fig. 1*a*). The fish did, however, make more feeding attempts during the day than at night (Table 2; Fig. 1*a*); this is more pronounced in the upper modal fish whereas the lower modal fish made as many feeding attempts during the day as during the night (two-way ANOVA, effect of time of day; lower modal group only: $F_{(1,53)} = 0.76$, $P = 0.76$; upper modal group only: $F_{(1,53)} = 20.61$, $P < 0.001$). There was no difference between the modal groups in the overall seasonal variation in feeding attempts (Table 2; Fig. 1*a*), with fish in both modal groups making as many feeding attempts in winter as in spring. However, there was a significant difference between them in the time of day at which most feeding activity took place (Table 2; Fig. 1*a*): the lower modal group fish fed as actively by night as by day whereas the upper modal group fish fed more actively during the day than during the night (Fig. 1*a*). The relative daytime and nighttime feeding rates differed between winter and spring (Table 2; Fig. 1*a*) such that in winter, feeding rates were overall higher by night whereas in spring, they were higher by day. This is mostly due to the lower modal group fish making far more feeding attempts during the night in winter whereas in spring, they foraged more during the day (Table 2; Fig. 1*a*). The interaction between the life history strategy, season, and time of day was not significant (Table 2; Fig. 1*a*).

A similar analysis was carried out on the extent to which fish spent their time resting on the bottom. The arcsine-transformed percentage (used in all analyses but not in the figures) of time spent on the bottom by fish out of shelter was only significantly affected by time of year (Table 2; Fig. 1*d*). Thus, in the winter the fish spent more time on the bottom than in spring; indeed, fish were not seen resting on the bottom at temperatures above 7°C (Fig. 1*d*). There was no difference between the life history strategies (Table 2; Fig. 1*d*), nor were there differences between night and day (Table 2; Fig. 1*d*). There were no significant interactions (Table 2; Fig. 1*d*).

The (arcsine-transformed) proportion of time that the fish spent moving was affected by season, with the fish being more likely to be found swimming around in spring than in winter (Table 2; Fig. 1*c*). Overall the fish were also more likely to be found swimming around during the day than during the night (Table 2; Fig. 1*c*); however, this was only significant for the upper modal group (two-way ANOVA, effect of time of day; upper modal group fish only: $F_{(1,53)} = 16.05$, $P < 0.001$; lower modal group fish only: $F_{(1,53)} = 0.33$, $P = 0.57$). The upper modal group fish spent more time moving than did the lower modal group fish (Table 2; Fig. 1*c*).

© 1999 NRC Canada

Table 2. Three-way ANOVA examing the effect of time of year (TY, winter or spring), time of day (TD, night or day), and life history pattern (MG, upper modal group or lower modal group) on three types of behaviour.

Behaviour and source	df	MS	*F*	*P*
Number of feeding attempts per minute				
Error	105	0.759		
MG	1	0.233	0.306	0.581
TY	1	0.011	0.014	0.905
TD	1	4.325	5.698	0.019
MG × TY	1	0.013	0.017	0.896
MG × TD	1	6.364	8.383	0.005
TY × TD	1	5.429	7.151	0.009
MG × TY × TD	1	2.355	3.102	0.081
Percentage of time spent lying on the bottom				
Error	105	646.544		
MG	1	43.510	0.067	0.796
TY	1	13793.04	21.333	<0.001
TD	1	0.8	0.001	0.972
MG × TY	1	43.510	0.067	0.796
MG × TD	1	26.01	0.04	0.841
TY × TD	1	0.8	0.001	0.972
MG × TY × TD	1	26.01	0.04	0.841
Percentage of time spent moving				
Error	105	109.542		
MG	1	602.416	5.499	0.021
TY	1	4445.063	40.579	<0.001
TD	1	1100.450	10.046	0.002
MG × TY	1	51.759	0.473	0.493
MG × TD	1	598.945	5.468	0.021
TY × TD	1	2.723	0.025	0.875
MG × TY × TD	1	26.052	0.238	0.627

Note: All percentages are arcsine transformed.

Moreover, whereas the lower modal group fish moved as much as the upper modal group fish during the night, they swam around less during the day (Table 2; Fig. 1*c*). There was no difference between the modal groups in how their movement rates varied seasonally (Table 2; Fig. 1*c*), as both groups changed from being largely stationary in the winter to being more mobile in the spring. There was also no seasonal difference in the diel variation in movement rates (Table 2; Fig. 1*c*), nor was the three-way interaction significant (Table 2; Fig. 1*c*).

The proportion of time spent holding station over the bottom was not subjected to statistical analysis, since it was clearly not independent of the other main activities. However, there was a clear tendency for fish to hold station more in spring than in winter and more at night than by day (Fig. 1*b*).

Discussion

Very few studies have attempted to look at Atlantic salmon behaviour at night. Presumably this is due to technical difficulties, since the immediate response of juvenile salmon when approached by an observer is to hide (Chapman and Bjornn 1969; Grant and Noakes 1987). During daylight, observers can try to conceal themselves from the fish, but at night, this becomes more difficult, since the observers need light to see. Even the smallest amount of light makes the fish change their behaviour (personal observations), and infrared light is quickly absorbed by water, making observations in all but very shallow water impossible. In this study, an image intensifier was used with additional strong infrared lights. There were no apparent changes in the behaviour of the fish when the infrared lights were switched on, and the extra light made observations easier. However, it was impossible to quantify successful feeding attempts and to recognise individuals without using a torch projecting visible light.

Atlantic salmon were found to feed at surprisingly low light levels both in winter and in spring. Their feeding efficiency is naturally not as good at low light levels, as is to be expected from a visual forager (Fraser and Metcalfe 1997), but fish were observed to forage at light levels below 0.01 lx (the lower limit of the meter used to measure light intensity). The reduced feeding efficiency at low light intensities is further exemplified by the choice of microhabitat in relation to light intensity (Metcalfe et al. 1997). By moving into slacker water at low light intensities, the fish are not getting the same amount of food as they would if they could feed in more profitable faster flowing water at higher light intensities, since the amount of drift food passing them is proportional to water velocity. Fraser and Metcalfe (1997) observed no feeding at all in complete darkness. However, complete darkness is probably very rare in the natural world, and on most nights, there is some light provided by several sources such as the moon, stars, aurora borealis, or anthropogenic lights reflected off clouds. If seen from underneath, an insect drifting in the current will be silhouetted against this small amount of light (and may also create a faint shadow) and will therefore be easier to see. In complete darkness, a drifting prey item will not make any shadow or contrast with the background and will therefore be invisible. The usual summer foraging position of juvenile Atlantic salmon is to hold position just a few millimetres off the bottom and dart forwards and upwards to intercept prey items being carried past in the current (Kalleberg 1958; Wankowski 1981). During this study the fish were often seen taking this position during the night, invariably feeding on items passing above them. Only once (and then during a very bright night with a full moon) was an Atlantic salmon seen to take a prey item off the bottom. This method of feeding on overhead items could explain why Atlantic salmon can forage at very low light levels.

There was a general trend for the fish to become more active in spring than in winter. They stopped resting on the bottom and started to move around more instead of being stationary. This increase in activity was probably linked to temperature, which is, of course, not surprising, since the metabolic rate of the fish increases with temperature and they therefore need more energy or food. In turn, this results in them moving off the substrate, since drift food density is proportional to current velocity (Elliott 1967; Chapman and Bjornn 1969), which increases with distance off the bottom of the stream. However, there was no increase in the overall number of feeding attempts per minute as the temperatures rose, but the pattern of feeding changed, with the fish starting to feed more during the day when it is easier to locate prey (Fraser and Metcalfe 1997).

© 1999 NRC Canada

Because of the longer nights in winter and since most of the daytime at that time of year is spent sheltering, the lower modal fish seem to make more feeding attempts per 24 h than the upper modal fish. This is then reversed in the spring when nighttime feeding becomes less important (fewer feeding attempts and shorter nights) and upper modal fish appear to forage more actively than those in the lower modal group. However, it is important to note that our sample size for the daytime behaviour in winter is very small (Table 1), and therefore, an alternative explanation is that individual variation rather than life history strategy may in part be responsible for the pattern observed. However, the difference between the modes in their winter feeding rates when emerged during the daytime is probably not of great importance, since both groups of fish spend most of the winter daytime sheltering.

Although the upper modal group fish appear to make fewer feeding attempts per 24 h over the winter than the lower modal group fish, they normally grow faster during that period (i.e., Higgins and Talbot 1985). It is possible that by using the day to feed, they are more successful in locating and catching prey items. It has been shown that winter feeding efficiency in Atlantic salmon decreases in relation to light intensity, and even under the best conditions (full moon and clear sky), their feeding efficiency at night is only about 35% of their daytime efficiency (Fraser and Metcalfe 1997). Therefore, by feeding predominantly during the day, the upper modal group fish could receive an equivalent or greater amount of food by making fewer but more successful feeding attempts than the lower modal group fish. Metcalfe et al. (1999) have shown that short daytime foraging bouts have a major impact on the growth rates of wintering salmon. Therefore, even though the upper modal group fish are hiding for most of the day and are active for most of the night in winter, they may not really be nocturnal foragers in terms of the relative amount of their daily intake that is obtained by night versus by day. This is further indicated by the study of Metcalfe et al. (1998), who found that the degree to which upper modal group fish were nocturnal depended on their body size, with the smallest premigrants being most diurnal, presumably because they had the greatest need to feed efficiently.

Another possible cause of the differences in diel activity schedules of upper and lower modal group fish is that the preferred feeding time of juvenile salmonids is actually at dawn and dusk (as suggested by Eriksson 1973). Since this study did not test this possibility directly, it cannot be ruled out. However, both groups were observed foraging both at night and by day (albeit at different rates), and during scan sample observations on sheltering (Valdimarsson et al. 1997), there were no indications that the fish were foraging especially actively at dawn and dusk or that they were aggressively defending territories.

There is some inconsistency in the literature about whether Atlantic salmon are mainly crepuscular or nocturnal foragers in winter. Some early papers reported that Atlantic salmon are crepuscular (Hoar 1942; Kalleberg 1958) whereas more recent studies showed that they switch to being almost exclusively nocturnal (Fraser et al. 1993; Heggenes et al. 1993). It has been shown in Arctic char, *Salvelinus alpinus*, and rainbow trout that under a given set of conditions, some individuals are predominantly nocturnal foragers whereas others forage more diurnally (Alanärä and Brännäs 1997; Brännäs and Alanärä 1997). The same has also been found in sea bass, *Dicentrarchus labrax*, an unrelated marine fish (Sanchez-Vazquez et al. 1994, 1995), but this "dualism" has only been reported for general movement (rather than foraging) patterns in Atlantic salmon (Richardson and McCleave 1974). The dualism in foraging activity that is revealed by this experiment and that of Metcalfe et al. (1998) suggests that during the summer, the fish that are biased towards diurnal

Fig. 1. Activity outside shelters during winter and spring of juvenile Atlantic salmon adopting alternative life history pathways (upper modal group or early migrants (UMG) and lower modal group or delayed migrants (LMG)). All values are means ± SE; see text for definitions of winter and spring. (*a*) Number of feeding attempts per minute; (*b*) percentage of time spent holding station by swimming against the current; (*c*) percentage of time spent moving; (*d*) percentage of time spent lying on the bottom of the stream.

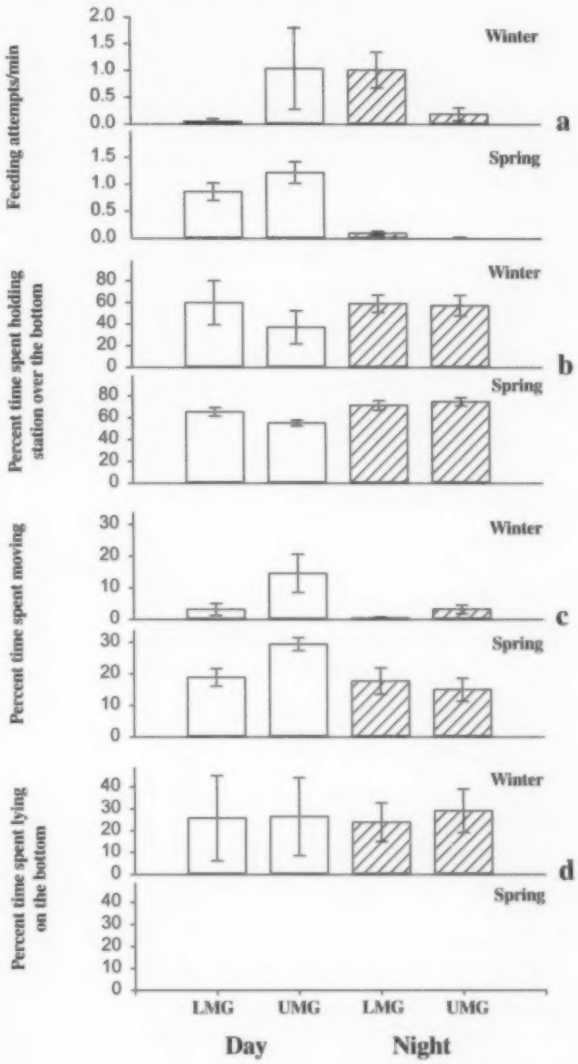

© 1999 NRC Canada

activity will grow faster than the more nocturnal fish, due to a greater feeding efficiency by day and longer daylight hours. It is therefore tempting to suggest that one of the proximate causes of the divergence in growth rates and consequent bimodality in the size distribution of Atlantic salmon might be the existence of both predominantly diurnal and nocturnal foragers within the population. This would suggest a genetic basis for the separation. Whereas some authors have demonstrated a genetic component to the bimodal separation (Bailey et al. 1980; Thorpe et al. 1983), others have shown a more environmental basis (Adams and Thorpe 1989; Metcalfe and Thorpe 1990). However, an important point from the studies of Alanärä and Brännäs (1997) and Brännäs and Alanärä (1997) is that the fish were often very marginal in their diel activity preference, being only slightly more diurnal than nocturnal or vice versa. The growth of these individuals will itself be intermediate between the extremes of a totally diurnal or totally nocturnal fish. This could generate a complete spectrum of growth rates, themselves subject to environmental conditions. This would produce environmentally controlled life history strategies even if the alternative activity patterns were entirely genetically determined. While this is speculation at this stage, it may warrant further investigation by looking at the feeding rates of individual fish at different times of the day in the spring and early summer of the first year of life, before the separation into the modal groups commences.

Acknowledgments

We thank John Armstrong, Victoria Braithwaite, Colin Bull, Vivien Cameron, Chris Cutts, Neil Fraser, Rab McMath, Valerie Maier, Frances Neat, Alfredo Nicieza, and Elaine Thorpe for their great assistance in various stages of this experiment, J.S. Griffith and an anonymous referee for helpful comments on the manuscript, and BOCM Pauls for provision of fish feed.

References

Adams, C.E., and Thorpe, J.E. 1989. Photoperiod and temperature influences on growth in juvenile Atlantic salmon, *Salmo salar* L. *In* Aquaculture — a biotechnology in progress. *Edited by* N. Depauw, E. Jaspers, H. Ackefors, and N. Wilkins. European Aquaculture Society, Bredene, Belgium. pp. 797–799.

Alanärä, A., and Brännäs, E. 1997. Diurnal and nocturnal feeding activity in Arctic char (*Salvelinus alpinus*) and rainbow trout (*Oncorhynchus mykiss*). Can. J. Fish. Aquat. Sci. **54**: 2894–2900.

Ali, M.A. 1961. Histophysiological studies on the juvenile Atlantic salmon (*Salmo salar*) retina. II. Responses to light intensities, wavelengths, temperatures and continuous light or dark. Can. J. Zool. **39**: 511–526.

Bailey, J.K., Saunders, R.L., and Buseta, M.I. 1980. Influence of parental smolt age and sea age on growth and smolting of hatchery-reared Atlantic salmon (*Salmo salar*). Can. J. Fish. Aquat. Sci. **37**: 1379–1386.

Brännäs, E., and Alanärä, A. 1997. Is diel dualism in feeding activity influenced by competition between individuals? Can. J. Zool. **75**: 661–669.

Chapman, D.W., and Bjornn, T.C. 1969. Distribution of salmonids in streams, with special reference to food and feeding. *In* Proceedings of a Symposium on Salmon and Trout in Streams. *Edited by* T.G. Northcote. H.R. MacMillan Lectures in Fisheries. University of British Columbia, Vancouver, B.C. pp. 153–176.

Elliott, J.M. 1967. Invertebrate drift in a Dartmoor stream. Arch. Hydrobiol. **63**: 202–237.

Eriksson, L.O. 1973. Spring inversion of the diel rhythm of locomotor activity in young sea going brown trout, *Salmo trutta* L., and Atlantic salmon, *Salmo salar* L. Aquilo Ser Zool. **14**: 68–79.

Fraser, N.H.C., and Metcalfe, N.B. 1997. The cost of being nocturnal: feeding efficiency in relation to light intensity in juvenile Atlantic salmon. Funct. Ecol. **11**: 385–391.

Fraser, N.H.C., Metcalfe, N.B., and Thorpe, J.E. 1993. Temperature-dependent switch between diurnal and nocturnal foraging in salmon. Proc. R. Soc. Lond. Ser. B, Biol. Sci. **252**: 135–139.

Fraser, N.H.C., Heggenes, J., Metcalfe, N.B., and Thorpe, J.E. 1995. Low summer temperatures cause juvenile Atlantic salmon to become nocturnal. Can. J. Zool. **73**: 446–451.

Grant, J.W.A., and Noakes, D.L.G. 1987. Escape behaviour and use of cover by young of the year brook trout, *Salvelinus fontinalis*. Can. J. Fish. Aquat. Sci. **44**: 1390–1396.

Griffith, J.S., and Smith, R.W. 1993. Use of winter concealment cover by juvenile cutthroat and brown trout in the South Fork of the Snake River, Idaho. N. Am. J. Fish. Manage. **13**: 823–830.

Heggenes, J., and Metcalfe, N.B. 1991. Bimodal size distribution in wild juvenile Atlantic salmon populations and their relationship with age at smolt migration. J. Fish Biol. **39**: 905–907.

Heggenes, J., Krog, O.M.W., Lindas, O.R., Dokk, J.G., and Bremnes, T. 1993. Homeostatic behavioural responses in a changing environment: brown trout (*Salmo trutta*) become nocturnal during winter. J. Anim. Ecol. **62**: 295–308.

Higgins, P.J., and Talbot, C. 1985. Growth and feeding in juvenile Atlantic salmon. *In* Nutrition and feeding in fish. *Edited by* C.B. Cowey, A.M. Mackie, and J.G. Bell. Academic Press, London, U.K. pp. 243–263.

Hoar, W.S. 1942. Diurnal variations in feeding activity of young salmon and trout. J. Fish. Res. Board Can. **6**: 90–101.

Kalleberg, H. 1958. Observations in a stream tank of territoriality and competition in juvenile salmon and trout (*Salmo salar* L. and *Salmo trutta* L.). Inst. Freshwater Res. Drottningholm Rep. **39**: 55–98.

Metcalfe, N.B., and Thorpe, J.E. 1990. Determinants of geographical variation in the age of seaward-migrating salmon, *Salmo salar*. J. Anim. Ecol. **59**: 135–145.

Metcalfe, N.B., Huntingford, F.A., and Thorpe, J.E. 1986. Seasonal changes in feeding motivation of juvenile Atlantic salmon (*Salmo salar*). Can. J. Zool. **64**: 2439–2446.

Metcalfe, N.B., Valdimarsson, S.K., and Fraser, N.H.C. 1997. Habitat profitability and choice in a sit-and-wait predator: juvenile salmon prefer slower currents on darker nights. J. Anim. Ecol. **66**: 866–875.

Metcalfe, N.B., Fraser, N.H.C., and Burns, M.D. 1998. State-dependent shifts between nocturnal and diurnal activity in salmon. Proc. R. Soc. Lond. Ser. B, Biol. Sci. **265**: 1503–1507.

Metcalfe, N.B., Fraser, N.H.C., and Burns, M.D. 1999. Food availability and the nocturnal vs diurnal foraging trade-off in juvenile salmon. J. Anim. Ecol. **68**: 371–381.

Needham, P.R., and Jones, A.C. 1959. Flow temperaure, solar radiation, and ice in relation to activity of fishes in Sagehen Creek, California. Ecology, **40**: 465–474.

Nicieza, A.G., Braña, F., and Toledo, M.M. 1991. Development of length-bimodality and smolting in wild stocks of Atlantic salmon, *Salmo salar* L., under different growth contitions. J. Fish Biol. **38**: 509–523.

Richardson, N.E., and McCleave, J.D. 1974. Locomotor activity

© 1999 NRC Canada

rhythms of juvenile Atlantic salmon (*Salmo salar*) in various light conditions. Biol. Bull. **147**: 422–432.

Rimmer, D.M., Paim, U., and Saunders, R.L. 1983. Autumnal habitat shift of juvenile Atlantic salmon (*Salmo salar*) in a small river. Can. J. Fish. Aquat. Sci. **40**: 671–680.

Sanchez-Vazquez, F.J., Martinez, M., Zamora, S., and Madrid, J.A. 1994. Design and performance of an accurate demand feeder for study of feeding behaviour in sea bass, *Dicentrarchus labrax* L. Physiol. Behav. **56**: 789–794.

Sanchez-Vazquez, F.J., Madrid, J.A., and Zamora, S. 1995. Circadian rhythms of feeding activity in sea bass, *Dicentrarchus labrax* L.: dual phasing capacity of diel demand-feeding pattern. J. Biol. Rhythms, **10**: 256–266.

Skúlason, S., Snorrason, S.S., Noakes, D.L.G., Ferguson, M.M., and Malmquist, H.J. 1989. Segregation in spawning and early life history among polymorphic Arctic charr, *Salvelinus alpinus*, in Thingvallavatn, Iceland. J. Fish Biol. **35**(Suppl. A): 225–232.

Thorpe, J.E. 1977. Bimodal distribution of length of juvenile Atlantic salmon (*Salmo salar*) under artificial rearing conditions. J. Fish Biol. **11**: 175–184.

Thorpe, J.E., Morgan, R.I.G., Talbot, C., and Miles, M.S. 1983. Inheritance of developmental rates in Atlantic salmon (*Salmo salar*). Aquaculture, **33**: 119–128.

Valdimarsson, S.K., Metcalfe, N.B., Thorpe, J.E., and Huntingford, F.A. 1997. Seasonal changes in sheltering: effect of light and temperature on diel activity in juvenile salmon. Anim. Behav. **54**: 1405–1412.

Wankowski, J.W.J. 1981. Behavioural aspects of predation by juvenile Atlantic salmon (*Salmon salar* L.) on particulate drifting prey. Anim. Behav. **29**: 557–571.

© 1999 NRC Canada

Maximum reproductive rate of fish at low population sizes

Ransom A. Myers, Keith G. Bowen, and Nicholas J. Barrowman

Abstract: We examine a database of over 700 spawner–recruitment series to search for parameters that are constant, or nearly so, at the level of a species or above. We find that the number of spawners produced per spawner each year at low populations, i.e., the maximum annual reproductive rate, is relatively constant within species and that there is relatively little variation among species. This quantity can be interpreted as a standardized slope at the origin of a spawner–recruitment function. We employ variance components models that assume that the log of the standardized slope at the origin is a normal random variable. This approach allows improved estimates of spawner–recruitment parameters, estimation of empirical prior distributions for Bayesian analysis, estimation of the biological limits of fishing, calculation of the maximum sustainable yield, and impact assessment of dams and pollution.

Résumé : Nous étudions une base de données comptant plus de 700 séries géniteur-recrutement à la recherche de paramètres qui sont constants, ou presque, au niveau de l'espèce ou à un niveau hiérarchique supérieur. Nous avons trouvé que le nombre de géniteurs produits par géniteur chaque année dans des populations peu abondantes, c'est-à-dire le taux de reproduction annuel maximal, est relativement constant dans une espèce, et qu'il y a peu de variation d'une espèce à l'autre. Cette valeur peut être interprétée comme une pente normalisée à l'origine d'une fonction géniteur-recrutement. Nous avons recours à des modèles de composantes de la variance selon lesquels le log de la pente normalisée à l'origine est une variable aléatoire normale. Cette approche permet d'obtenir de meilleures estimations des paramètres du rapport géniteur-recrutement, une estimation des données empiriques avant les répartitions pour l'analyse bayesienne, une estimation des limites biologiques de la pêche, un calcul de la production maximale équilibrée, et une évaluation des impacts des barrages et de la pollution.

[Traduit par la Rédaction]

Introduction

Perhaps the most fundamental parameter in population biology is the reproductive rate at low population size. We will analyze this parameter in terms of the maximum reproductive rate, which we define as the average rate at which replacement spawners are produced per spawner at low abundance in the absence of anthropogenic mortality (after a time delay for the age at maturity). The maximum reproductive rate is central to the following: the population growth rate r (Cole 1954; Pimm 1991; Myers et al. 1997*b*), limits to overfishing (Mace 1994; Cook et al. 1997; Myers and Mertz 1998), estimation of the dynamic behaviour of the population, i.e., whether the population has oscillatory or chaotic behaviour, extinction models and population viability analysis (Lande et al. 1997), establishment of biological reference points for management, e.g., most of the commonly used reference points for recruitment overfishing require estimates of the maximum lifetime reproductive rate (Myers et al. 1994), and estimation of the long-term consequence of mortality caused by pollution, dams, or entrainment by powerplants (Barnthouse et al. 1988).

The purposes of this paper are (*i*) to provide a comprehensive analysis of the maximum reproductive rate in terms of a relatively simple statistical model, (*ii*) to attempt to determine under what conditions this parameter is invariant, i.e., constant for a species or group of species, and (*iii*) to provide empirical Bayesian priors for the estimates (Hilborn and Liermann 1998; Millar and Meyer 2000). We use the extensive database of stock and recruitment data compiled in Myers et al. (1995) and Myers and Barrowman (1996).

Received June 1, 1999. Accepted September 24, 1999.
J15156

R.A. Myers.[1] Killam Memorial Chair in Ocean Studies, Department of Biology, Dalhousie University, Halifax, NS B3H 4J1, Canada.
K.G. Bowen and N.J. Barrowman. Department of Mathematics and Statistics, Dalhousie University, Halifax, NS B3H 4J1, Canada.

[1]Author to whom all correspondence should be addressed.
email: ransom.myers@dal.ca

Formulation

Estimating reproductive rate

Semelparous species, whose members conveniently die after reproduction, immensely simplify the lives of students of their population biology. For example, in many insects and in pink salmon (*Oncorhynchus gorbuscha*), one generation follows the next in easy units, e.g., the number of spawning females. The relationship between the numbers in year t, N_t, and the numbers in year t plus the age at maturity, a_{mat}, is typically given in the form

$$(1) \qquad N_{t+a_{mat}} = \alpha N_t e^{-f(N_t)}$$

where the density-dependent mortality, $f(N_t)$, is a non-negative function such that $f(N_t) \to 0$ as $N_t \to 0$.

© 1999 NRC Canada

The dynamics of iteroparous species are more complicated. Typically, the number of recruits belonging to year-class t, R_t, is a function of the egg production or a proxy such as weight of spawners at time t, S_t, as in the form

$$(2) \qquad R_t = \alpha S_t e^{-f(S_t)}$$

where $f(S_t)$ is the density-dependent mortality as before.

The Ricker model has the form

$$(3) \qquad R_t = \alpha S_t e^{-\beta S_t}$$

where α is the slope at the origin (measured perhaps in recruits per kilogram of spawners). Density-dependent mortality is assumed to be the product of β and the spawner biomass. Dividing by S_t and taking logarithms gives

$$(4) \qquad \log \frac{R_t}{S_t} = \log \alpha - \beta S_t$$

i.e., a linear model for log survival.

For the forthcoming calculations, the slope at the origin, α, must be standardized. First consider

$$\hat{\alpha} = \alpha \cdot \mathrm{SPR}_{F=0}$$

where $\mathrm{SPR}_{F=0}$ is the spawning biomass resulting from each recruit (perhaps in units of kilograms of spawners per recruit) in the limit of no fishing mortality ($F = 0$). This quantity, $\hat{\alpha}$, represents the number of spawners produced by each spawner over its lifetime at very low spawner abundance, i.e., assuming absolutely no density dependence. The quantity $\tilde{\alpha}$ required for our calculations is the number of spawners produced by each spawner per year (after a lag of a years, where a is the age at maturity). If adult survival (the proportion surviving each year, which in the absence of fishing is e^{-M}) is p_s, then $\hat{\alpha} = \sum_{i=0}^{\infty} p_s^i \tilde{\alpha}$, or summing the geometric series:

$$(5) \qquad \tilde{\alpha} = \hat{\alpha}(1 - p_s) = \alpha \cdot \mathrm{SPR}_{F=0}(1 - p_s).$$

This quantity $\tilde{\alpha}$ is the maximum annual reproductive rate and will be the main focus of this study.

A word of warning is needed in the interpretation of the maximum annual reproductive rate. The above formulation is for the deterministic case. However, if stochastic variations in survival are included, then the quantity $\tilde{\alpha}$ would be interpreted as the maximum of the average annual reproductive rate. In other words, the reproductive rate may be higher or lower for any given year.

We also provide estimates of "steepness", denoted by z and first defined by Mace and Doonan (1988), because this is the parameter actually used in many assessments (Hilborn and Walters 1992). The steepness parameter z for the Beverton–Holt model is defined to be the proportion of recruitment, relative to the recruitment at the equilibrium with no fishing, when the spawner abundance or biomass is reduced to 20% of the virgin level. This is related to the maximum lifetime reproductive rate $\hat{\alpha}$ by

$$z = \frac{\hat{\alpha}}{4 + \hat{\alpha}}$$

where $0.2 < z < 1$.

Note that at the limit of small population size, the Ricker and Beverton–Holt models coincide, i.e., the slope at the origin, α, is the same. In this context, z can be estimated from either model; however, it can only be applied directly to the dynamics of the Beverton–Holt model. Our estimate of steepness should be viewed as conservative (see Appendix 2).

To summarize, we have introduced notations for the three most common ways that the maximum reproductive rate is used in the analysis of fish population dynamics. First, we have defined $\hat{\alpha}$ to be the maximum lifetime reproductive rate (the adjective "lifetime" would not usually be used but is important here). This quantity is used in many calculations to determine maximum sustainable yield (MSY) and the limits of fishing mortality. The second is the quantity of steepness, z, which is a simple transformation of $\hat{\alpha}$. The third quantity, $\tilde{\alpha}$, is used in calculations where an annual recruitment rate is needed, e.g., for estimating the maximum population growth rate (Myers et al. 1997*b*).

The Ricker model provides a reasonable model for estimating the slope at the origin

The simplest form of density-dependent mortality is linear, i.e., $f(S) = \beta S$, in eq. 1. We will show that under reasonable conditions, this is perhaps the best first approximation. A simple generalization of the Ricker model is

$$(6) \qquad f(S) = \beta S^{\gamma}$$

where γ controls the degree of nonlinearity in the functional form of density dependence (Bellows 1981). For most of the data sets that we examine, there are not sufficient data to estimate γ; however, our purpose is only to ensure that estimates of α are robust to our assumptions about γ. We will examine data for Atlantic cod (*Gadus morhua*) because there are excellent data for these populations and all have been reduced to low levels, which will enhance our ability to estimate α. We held γ fixed at values of 0.5, 0.75, 1, 1.25, and 1.5 (Figs. 1 and 2) and estimated $\tilde{\alpha}$ and β.

The functional fits are displayed in terms of survival ($\log(R/S)$) versus S, where R has been multiplied by $\mathrm{SPR}_{F=0}(1 - p_s)$.

If $\gamma < 1$, then survival is a convex function of spawner biomass, and the limit of survival is infinity as $S \to 0$. Thus, this model is unrealistic for this case. Furthermore, an examination of the survival versus spawner curve reveals that it does not become appreciably convex until below the lowest observed spawner abundance (Fig. 1). For $\gamma > 1$, survival is a concave function, and the derivative of survival as $S \to 0$ will always be zero.

In practice, the Ricker model is a reasonably cautious estimate of the limit for management purposes. If $\gamma < 1$ is assumed, then a greater α is estimated, while the assumption of $\gamma > 1$ results in only a slight decrease in the estimate of α (Figs. 1 and 2). If we examine the four cod populations with the largest range in observed spawner biomass, the estimate of the slope at the origin appears reasonable in all cases for the Ricker model, while the estimate for $\gamma = 0.5$ is inflated commensurately with the gap between the origin and the lowest observation of spawner abundance.

© 1999 NRC Canada

Fig. 1. Survival, $\log(R/S)$, versus spawner abundance for six cod stocks. The modeled density-dependent mortality of the form $f(S) = \beta S^{\gamma}$ is shown for $\gamma = 1.5$ (dashed line), $\gamma = 1$ (Ricker case, dotted line), and $\gamma = 0.5$ (solid line). We have standardized recruitment by multiplying by $SPR_{F=0}(1 - p_s)$, which allows survival to be interpreted as the annual replacement of spawners per spawner. Thus, the extrapolation of the fitted curves to zero spawner abundance provides an estimate of $\log \tilde{\alpha}$, i.e., the logarithm of the maximum annual reproductive rate.

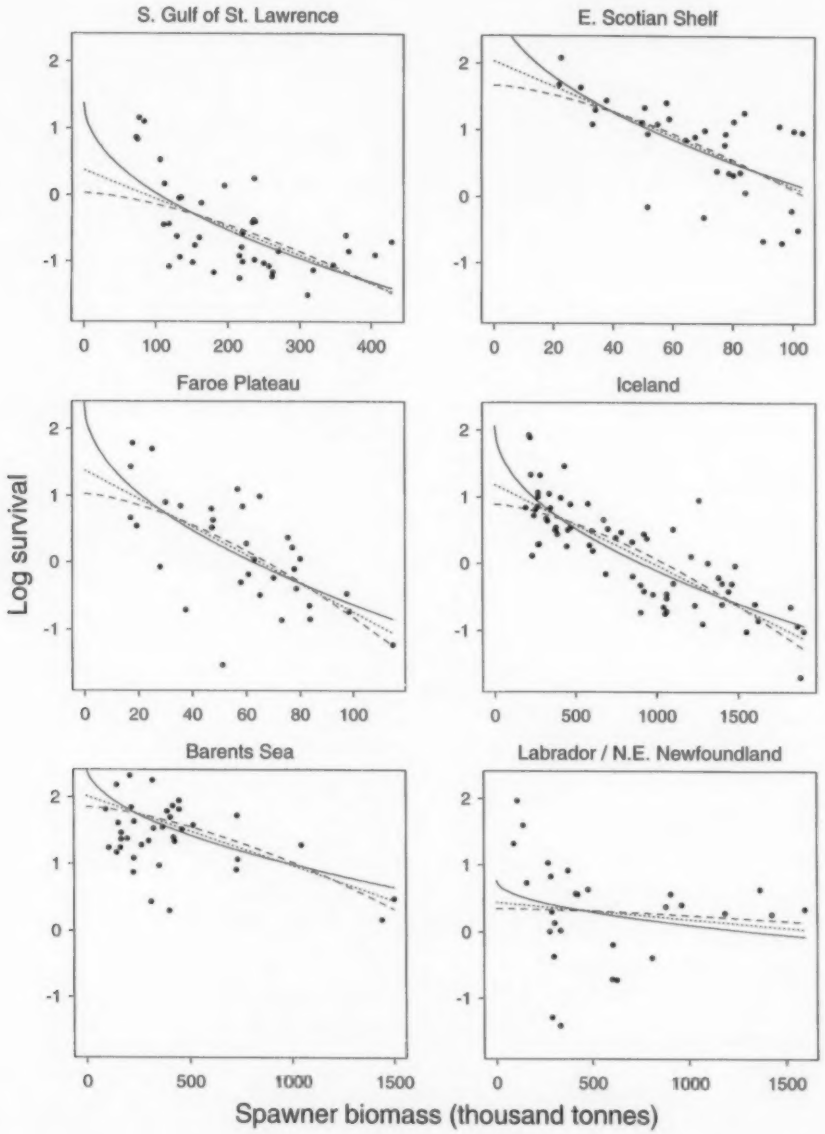

We also considered another common three-parameter model, the "Shepherd function," i.e.:

$$(7) \qquad R = \frac{\alpha S}{1 + (S/K)^{\delta}}.$$

This model was first proposed by Maynard Smith and Slatkin (1973) and was discussed by Bellows (1981). The parameter K has dimensions of biomass and may be interpreted as the "threshold biomass" for the model. For values of biomass S greater than the threshold K, density-dependent effects dominate. The parameter δ may be called the "degree of compensation" of the model, since it controls the degree to which the (density-independent) numerator is compensated for by the (density-dependent) denominator. If $\delta = 1$, then the Beverton–Holt model is recovered. However, for $\delta < 1$, survival is infinity as $S \to 0$; again, in this case the model cannot be considered as a reliable method for extrapolation to low population sizes. For $\delta > 1$, the derivative of survival as $S \to 0$ will always be zero. However, even in the

© 1999 NRC Canada

Fig. 2. Box plots of the logarithm of the scaled slope at the origin, log $\tilde{\alpha}$, for the 20 major cod stocks in the North Atlantic as a function of the form of density-dependent mortality $f(S) = \beta S^{\gamma}$. For each box plot, the median is marked with a white line and the gray area shows the 95% confidence interval for the median location. When $\gamma = 1$, the Ricker model is recovered.

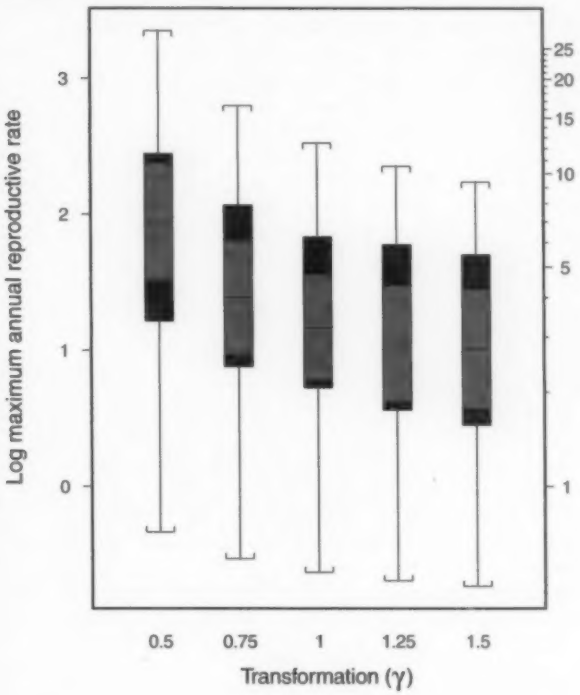

Beverton–Holt case ($\delta = 1$), many estimates of the slope at the origin will be infinity. That is, if $K \to 0$, then $\alpha \to \infty$ is a perfectly feasible solution.

The Deriso–Schnute model (Hilborn and Walters 1992), an alternative three-parameter model, has the Ricker and the Beverton–Holt as special cases. However, it suffers from the same problems that we described above: survival is not constrained to be finite except when the model is a Ricker model, or it has the derivative of survival as $S \to 0$ constrained to be zero.

Any estimation of the slope at the origin is necessarily an extrapolation, since there cannot be observations arbitrarily close to zero spawner abundance. The simplest extrapolation is a linear one (in the relationship between log survival and spawner abundance), while alternative assumptions will often produce unreasonable estimates.

One situation in which a Ricker model would not give a reliable estimate would be if mortality increased at low spawner abundances, known as depensation or the Allee effect. Myers et al. (1995) carried out a metaanalysis and could find no convincing evidence that depensation occurred for exploited fish populations. However, Liermann and Hilborn (1997), using a Bayesian approach, demonstrated that the data were consistent with moderate levels of depensation for several taxa. We conclude that the estimate of the α from the Ricker model will usually provide a reasonable estimate for both ecological and management needs, e.g., when F_{τ} (sometimes called $F_{\text{extinction}}$), the smallest fishing mortality associated with extinction, is needed.

In this section, we have argued that the Ricker model is often a reasonable model for the estimation of the $\tilde{\alpha}$ (some alternative approaches are discussed below). For the cod populations in the North Atlantic, we have seen that the estimates are only slightly modified if survival is a concave function of spawner biomass. The alternative assumption, that log survival is a convex function, which usually results in the assumption that survival greatly increases at low spawner biomass (Fig. 1), is not strongly supported by the data and may be very dangerous for management decisions in extrapolations to low abundance.

Estimation method

Mixed effects models

Our contention is that focusing on one population at a time can be misleading. In this section, we shall demonstrate how this can be avoided by incorporating the estimation of the Ricker model into a standard linear mixed model. Parameter estimation is easy using widely available software, e.g. SAS or S-PLUS.

We will change the notation slightly to put the results in the standard notation of variance components and mixed models. We consider p populations, subscripted by i, for each of which we want to estimate the parameters of a Ricker model (eq. 4) of the form

$$(8) \qquad \log \frac{R_{i,t}}{S_{i,t}} = \log \tilde{\alpha}_i + \beta_i S_{i,t} + \varepsilon_{it}$$

where $R_{i,t}$ is recruitment to year-class t in population i, $S_{i,t}$ is spawner abundance in year t in population i, $\tilde{\alpha}_i$ and β_i are the Ricker model parameters for population i, and ε_{it} is estimation error, assumed normal. We assume that $\log \tilde{\alpha}_i$ is a normal random variable and define $\mu + a_i = \log \tilde{\alpha}_i$, where μ is the mean of the log-transformed maximum annual reproductive rates and a_i is the random effect for population i. (Note that we will repeat the above calculations using the lifetime reproductive rate instead of the annual reproductive rate.)

We consider the log survival, $\log(R/S)$, of a year-class from a given population as an element of a vector $\mathbf{y}$. If there are n_i observations for population i, then the first n_1 elements of the vector $\mathbf{y}$ will be the n_1 log survivals for the first population, followed by the n_2 log survivals for the second population, and so on.

We consider the fixed effects of the model first. The parameters that we estimate are the overall mean, μ, and p regression parameters, β_i. We consider the spawner abundances, $S_{i,t}$, as known and estimate the density-dependent regression parameter β_i for each population. The standard mixed model notation for the vector of fixed effects parameters is $\boldsymbol{\beta}$. The unknown vector $\boldsymbol{\beta}$ consists of the overall mean μ and the $p\beta_i$s. The vector $\boldsymbol{\beta}$ is related to $\mathbf{y}$ by the known model matrix $\mathbf{X}$, whose elements are 0, 1, and $S_{i,t}$; the form of this matrix is given below.

For the vector of random effects composed of the a_i, we shall use the standard mixed model notation $\mathbf{u}$. The vector $\mathbf{u}$

© 1999 NRC Canada

is related to $\mathbf{y}$ by a known model matrix $\mathbf{Z}$ whose form is given below.

In standard mixed model notation, we have

$$\mathbf{y} = \mathbf{X}\beta + \mathbf{Z}\mathbf{u} + \varepsilon. \tag{9}$$

Here, ε is an unknown random error vector. For example, consider the simple case of two populations, each of which is observed for 3 years with the first year denoted by 1. The above equation can then be written as

$$\mathbf{y} = \begin{bmatrix} y_{11} \\ y_{12} \\ y_{13} \\ y_{21} \\ y_{22} \\ y_{23} \end{bmatrix} = \begin{bmatrix} 1 & S_{11} & \cdot \\ 1 & S_{12} & \cdot \\ 1 & S_{13} & \cdot \\ 1 & \cdot & S_{21} \\ 1 & \cdot & S_{22} \\ 1 & \cdot & S_{23} \end{bmatrix} \begin{bmatrix} \mu \\ \beta_1 \\ \beta_2 \end{bmatrix} + \begin{bmatrix} 1 & \cdot \\ 1 & \cdot \\ 1 & \cdot \\ \cdot & 1 \\ \cdot & 1 \\ \cdot & 1 \end{bmatrix} \begin{bmatrix} a_1 \\ a_2 \end{bmatrix} + \begin{bmatrix} \varepsilon_{11} \\ \varepsilon_{12} \\ \varepsilon_{13} \\ \varepsilon_{21} \\ \varepsilon_{22} \\ \varepsilon_{23} \end{bmatrix} \tag{10}$$

where $y_{i,t} = \log(R_{i,t}/S_{i,t})$. The generalization provided by the mixed model enables one not only to model the mean of $\mathbf{y}$ (as in the standard linear model), but to model the variance of $\mathbf{y}$ as well. We assume that $\mathbf{u}$ and ε are uncorrelated and have multivariate normal distributions with expectations $\mathbf{0}$ and variances $\mathbf{D}$ and $\mathbf{R}$, respectively. The variance of $\mathbf{y}$ is thus

$$\mathbf{V} = \mathbf{Z}\mathbf{D}\mathbf{Z}' + \mathbf{R}. \tag{11}$$

One can model the variance of the data, $\mathbf{y}$, by specifying the structure of $\mathbf{D}$ and $\mathbf{R}$. We assume that $\mathbf{D} = \sigma_a^2\mathbf{I}$ (where $\mathbf{I}$ is the identity matrix), i.e., that the variability among populations of $\log \tilde{\alpha}_i$ is normally distributed with variance σ_a^2. In the simplest case, one might assume that the error variance is the same for all populations, i.e., $\mathbf{R} = \sigma^2\mathbf{I}$. (Note that when $\mathbf{R} = \sigma^2\mathbf{I}$ and $\mathbf{Z} = \mathbf{0}$, the mixed model reduces to the standard linear model.) However, we estimate a separate estimation error variance, σ_i^2, for each population. We also test whether the residuals are autocorrelated. If they are, we can estimate a separate autocorrelation parameter, ρ_i, for each population. This results in a block diagonal structure for $\mathbf{R}$, with blocks

$$\sigma_i^2 \begin{bmatrix} 1 & \rho_i & \rho_i^2 & \cdots \\ \rho_i & 1 & \rho_i & \cdots \\ \rho_i^2 & \rho_i & 1 & \cdots \\ \vdots & \vdots & \vdots & \ddots \end{bmatrix}. \tag{12}$$

Estimation of variance components

Now that we have transformed the problem into this form, estimation is trivial because high-quality software exists for this problem (Appendix 1). The likelihood function for the data vector $\mathbf{y} \sim N_N(\mathbf{X}\beta, \mathbf{V})$ is

$$L = L(\beta, \mathbf{V}|\mathbf{y}) = \frac{e^{-\frac{1}{2}(\mathbf{y}-\mathbf{X}\beta)'\mathbf{V}^{-1}(\mathbf{y}-\mathbf{X}\beta)}}{(2\pi)^{\frac{N}{2}}|\mathbf{V}|^{\frac{1}{2}}} \tag{13}$$

where N is the number of fixed effects estimated, i.e., $N = 1 + p$. There are two common approaches to the estimation of variance components based on this function: maximum likelihood (ML) and restricted maximum likelihood (REML) (Searle et al. 1992). REML differs from ML for this model in that it takes into account the degrees of freedom used for estimating the fixed effects, whereas ML does not. Furthermore, in the case of balanced data, REML solutions are identical to ANOVA estimators, which have known optimality properties. For these reasons, we will use REML but will consider ML to check sensitivity. Denote the resulting estimates of $\mathbf{D}$ and $\mathbf{R}$ by $\hat{\mathbf{D}}$ and $\hat{\mathbf{R}}$, respectively.

It is possible for the estimate of the variance among populations, $\hat{\sigma}_a^2$, to be zero. This often occurs when only a few populations are available for analysis and should not be interpreted as implying that there is no variability among populations in the maximum annual reproductive rate.

Estimation of individual population parameters

The use of mixed models allows us to obtain improved estimates of parameters for any one population. In general, we wish not only to estimate the fixed model parameters, but also to predict the random variables for each population. In our case, we wish to estimate the density-dependent parameter β and predict the slope at the origin for each population, which is assumed to be a random variable. The terminological distinction between estimation of fixed effects and prediction of random effects is awkward and unnecessary (Robinson 1991); we will "estimate" both fixed and random effects, with the understanding that for random effects, we are in fact obtaining estimates of their realized values.

The best linear unbiased estimators (BLUEs) $\tilde{\beta}$ of the fixed effects β and the best linear unbiased predictors (BLUPs) $\tilde{\mathbf{u}}$ of the random effects $\mathbf{u}$ may be obtained from the mixed model equations

$$\begin{bmatrix} \mathbf{X}'\mathbf{R}^{-1}\mathbf{X} & \mathbf{X}'\mathbf{R}^{-1}\mathbf{Z} \\ \mathbf{Z}'\mathbf{R}^{-1}\mathbf{X} & \mathbf{Z}'\mathbf{R}^{-1}\mathbf{Z} + \mathbf{D}^{-1} \end{bmatrix} \begin{bmatrix} \tilde{\beta} \\ \tilde{\mathbf{u}} \end{bmatrix} = \begin{bmatrix} \mathbf{X}'\mathbf{R}^{-1}\mathbf{y} \\ \mathbf{Z}'\mathbf{R}^{-1}\mathbf{y} \end{bmatrix}. \tag{14}$$

Without the $\mathbf{D}^{-1}$ in the lower right-hand submatrix of the matrix on the left, eq. 14 would be the ML equations for the model treated as if $\mathbf{u}$ represented fixed effects, rather than random effects. Although the above equation has been discussed in terms of classical methods, the same result is arrived at using a formal Bayes analysis of incorporating prior information into the analysis of data (Searle et al. 1992).

Since we do not know the variance–covariance matrices $\mathbf{D}$ and $\mathbf{R}$, we substitute $\hat{\mathbf{D}}$ and $\hat{\mathbf{R}}$ into eq. 14 to obtain empirical BLUEs and BLUPs.

The variance–covariance matrix for $[\tilde{\beta}\ \tilde{\mathbf{u}}]'$ is

$$\mathbf{C} = \begin{bmatrix} \mathbf{X}'\mathbf{R}^{-1}\mathbf{X} & \mathbf{X}'\mathbf{R}^{-1}\mathbf{Z} \\ \mathbf{Z}'\mathbf{R}^{-1}\mathbf{X} & \mathbf{Z}'\mathbf{R}^{-1}\mathbf{Z} + \mathbf{D}^{-1} \end{bmatrix}^{-} \tag{15}$$

where the superscript minus on the above matrix represents a generalized inverse. An approximate variance–covariance matrix $\hat{\mathbf{C}}$ may be obtained by substituting $\hat{\mathbf{D}}$ and $\hat{\mathbf{R}}$ into eq. 15. The approximate standard error for any linear combination $\mathbf{L}$ of the vector $[\tilde{\beta}\ \tilde{\mathbf{u}}]'$ may be obtained from

© 1999 NRC Canada

(16) $\sqrt{\mathbf{L}'\hat{\mathbf{C}}\mathbf{L}}$.

Note that these standard errors will tend to be underestimates of the standard errors of the empirical BLUPs and BLUEs (Searle et al. 1992).

Our estimation methods above provide estimates of μ for each species and (the realized values of) the a_i. As long as the log-transformed values are considered, the interpretation is simple; however, the interpretation of the values on an untransformed scale is more complex. For a species, the median $\tilde{\alpha}$ is $\exp(\mu)$, and the expectation is $\exp(\mu + 0.5\,\sigma_a^2)$, where the expectation and median are taken with respect to the distribution of the random effects. This estimate is complicated by the estimation error of the μ and the σ_a^2, which we will ignore here. To keep things simple, we will discuss our results in terms of the log-transformed values and the medians of $\tilde{a}$ for a species, except where noted.

Data sources and treatment

The data that we used are estimates obtained from assessments compiled by Myers et al. (1995). The database is available from the first author. For marine populations, population numbers and fishing mortality were usually estimated using sequential population analysis (SPA) of commercial and (or) recreational catch at age data for most marine populations. SPA techniques include virtual population analysis (VPA), cohort analysis, and related methods that reconstruct population size from catch at age data (see Hilborn and Walters (1992, chaps. 10 and 11) for a description of the methods used to reconstruct the population history). Briefly, the catch at age is combined with estimates from research surveys and (or) commercial catch rates to estimate the numbers at age in the final year and to reconstruct previous numbers at age under the assumption that catch at age is known without error and that natural mortality at age is known and constant.

For salmon stocks, spawner abundance is the estimate of the number of fish reaching the spawning grounds, and recruitment is estimated by combining catch and the number of upstream migrants.

SPA techniques were used for the freshwater species except for brook trout (*Salvelinus fontinalis*). The brook trout populations were from introduced populations in California mountain lakes (DeGisi 1994); these populations were estimated using research gill nets and ML depletion estimation.

Time series of less than 10 paired spawner–recruit observations are not included in this analysis. The $SPR_{F=0}$ was calculated using estimates of natural mortality, weight at age, and maturity at age. Maturity and weight at age were usually estimated from research surveys carried out for each population.

A major source of uncertainty in the SPA estimates of recruitment and spawning stock biomass (SSB) is that they usually assume that catches are known without error. This is particularly important when estimates of discarding and misreporting are not included in the catch at age data used in the SPA. These errors are clearly important for some periods of time for some of the cod stocks (Myers et al. 1997*a*), and these errors will affect our estimates of the number of replacements that each spawner can produce at low population densities ($\tilde{\alpha}$).

The data for this analysis are available at R.A. Myers' web site (http://fish.dal.ca/welcome.html).

Results

We first used ML for a standard Ricker model to obtain single-population estimates of $\log \tilde{\alpha}$ for each population (Fig. 3). Then, for each species in our database, we applied the mixed model to the data from all of the populations belonging to that species, obtaining estimates and predictions as follows. We used REML to estimate σ_a^2, the true variability among populations in the log-transformed maximum annual reproductive rate, and for each population, σ_i^2, the estimation error variance. These estimated variance components were then used to obtain the empirical BLUE of the mean log-transformed maximum annual reproductive rate, μ, for the species and the empirical BLUP of $\log \tilde{\alpha}$ for each population (Table 1). For completeness, we have given the mixed model estimates for the mean and variability at the family level; however, they should be used with great caution because they may not be representative of any given species. More detailed results (which include stock-level estimates) are available at R.A. Myers' web site.

Note that there is less variance among the BLUP estimates than among the single-population estimates (Fig. 4).

The estimates for populations with large estimation error variances (e.g., due to relatively few data points) and that are far from the mean for the species, e.g. Gulf of Maine cod (MLE:$\log \tilde{\alpha}$ = 2.85, BLUP:$\log \tilde{\alpha}$ = 1.84), are pulled towards the mean more than those for populations with lower estimation error variance and that are close to the species mean, e.g. Iceland cod (MLE:$\log \tilde{\alpha}$ = 1.19, BLUP: $\log \tilde{\alpha}$ = 1.19).

As expected, the estimate of the true variability in the maximum annual reproductive rate is much less than the sample variability because individual estimates contain estimation error. For example, for pink salmon, if $\tilde{\alpha}$ is estimated separately for each stock, then there is an order of magnitude range of the estimates. However, if $\tilde{\alpha}$ is assumed to be a random variable, then the mixed model estimates suggest that the true range is very small, with all the true values being very close to 3 (Fig. 3). Cod show a similar picture. The median number of replacement spawners per spawner per year for cod at low abundance is between 3 and 4, resulting in a maximum net reproductive rate (if there is no fishing mortality) of between 15 and 20. The maximum annual reproductive rate for Atlantic herring (*Clupea harengus*) appears to be slightly less, and for hakes of the genus *Merluccius*, e.g., silver hake (*Merluccius bilinearis*) and Pacific hake (*Merluccius productus*), it is around 1. Some anadromous species, e.g., sockeye salmon (*Oncorhynchus nerka*), appear to have a maximum annual reproductive rate of around 4 or 5, while others, e.g., pink salmon, have a much lower rate.

The most remarkable aspect of the results is the relative constancy of the estimates of the maximum annual reproductive rate. For species for which we have more than one population in our analysis, the median of the estimated maximum reproductive rate is almost always between 1 and 7 (Fig. 5*a*).

For the species with multiple populations, only Pacific ocean perch (*Sebastes alutus*) and silver hake have an esti-

© 1999 NRC Canada

Fig. 3. Histograms by species of the individual ML estimates of the log of the maximum annual reproductive rate, log $\tilde{\alpha}$, compared with probability densities based on REML estimates of the true variability in log $\tilde{\alpha}$ from our mixed model analysis (dotted line). Note that the top axis of each plot shows the untransformed annual reproductive rate. The number of populations (n) for each histogram is also given.

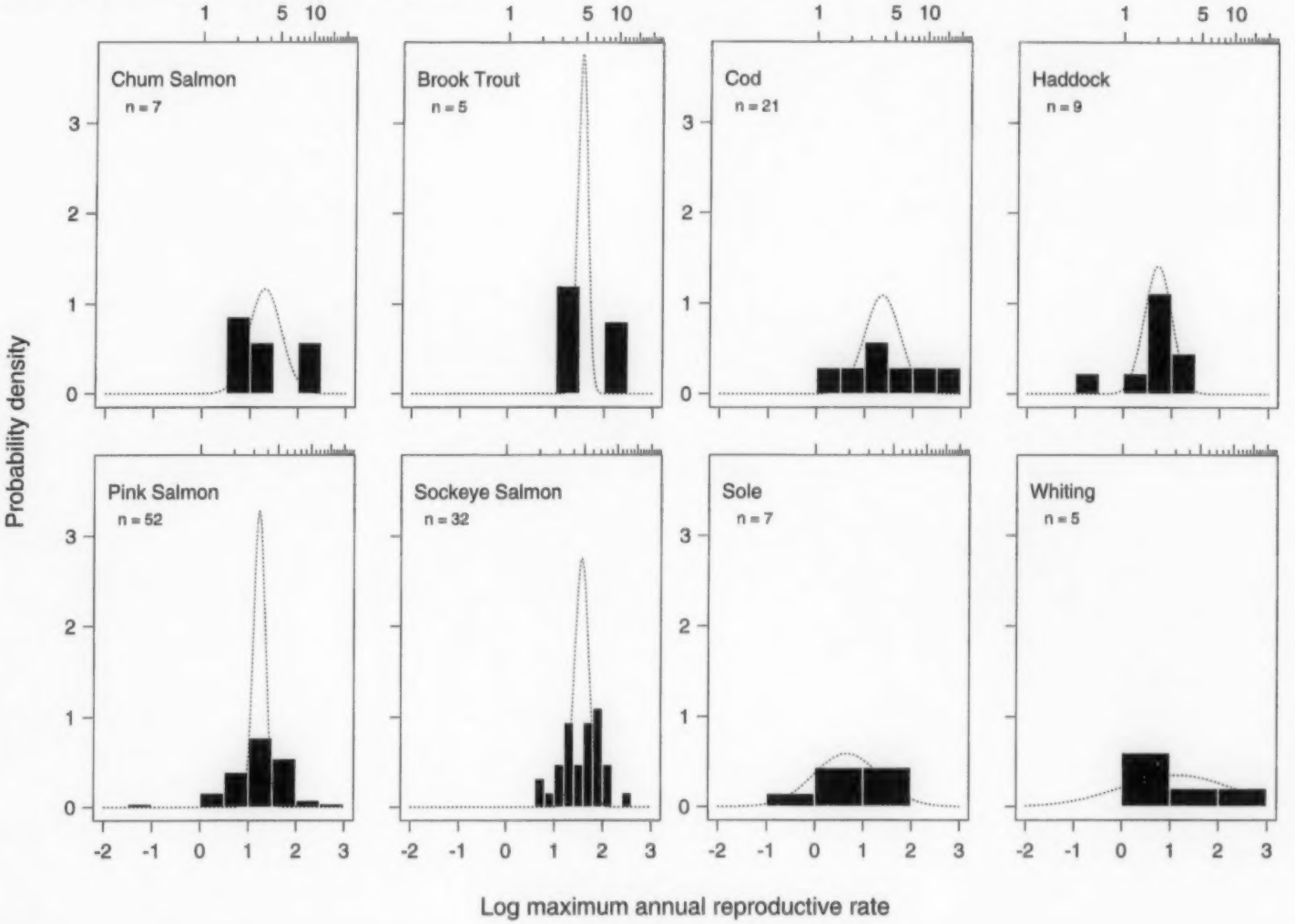

© 1999 NRC Canada

mated maximum annual reproductive rate of less than 1. The low estimate for Pacific ocean perch results in a very low estimate for the expected maximum lifetime reproductive rate, i.e., it is about 3 (Table 1; Fig. 6*a*). Relatively low estimates of the maximum lifetime annual reproductive rate and steepness were estimated for the other *Sebastes* species (Table 1). We do not know whether these low estimates are real, e.g., are somehow related to their low natural mortality and oviviparous reproduction, or an artifact. The age-based assessments of the *Sebastes* species are unusually uncertain because of aging difficulties. It is also possible that the environmental conditions in recent years, when the low estimates of spawning biomass and recruitment were made, have been unusual and have resulted in lower than average estimates. In any case, it is crucial to determine if the assessments are correct and exploit these species more cautiously than other species.

The estimates of the maximum annual reproductive rate for species for which we have only one population are much more variable than for the species with many populations (Figs. 5*b* and 6*b*). The greater variability in these estimates is at least partially caused by estimation error. However, several species have maximum reproductive rates that suggest that they cannot sustain intense fisheries. In some cases, this is certainly true. The southern bluefin tuna (*Thunnus maccoyii*) in the Southern Ocean has been greatly reduced by overfishing. In other cases, there may be serious problems with the assessments.

Despite the large variation in the individual estimates, our general conclusion about the relative constancy of the maximum annual reproductive rate stands; the estimates are usually around 3. There are exceptions for individual stocks, but these usually have large standard errors.

Note that herring has a smaller maximum reproductive rate than many species. The lower mean is due to a few stocks in the northern North Atlantic that have been reduced to very low levels (the Iceland stocks, the Norway stock (often called the "Arcto-Norwegian" stock), and the Georges Bank stocks).

We also considered a model that allowed the residuals to be autocorrelated (see Appendix 1 for the computer code used in the estimation). This approach is probably preferable if autocorrelation is substantial in the model residuals, but may pull the individual estimates too far towards the population mean.

We repeated the above analysis for the lifetime maximum reproductive rate and display the results in terms of the expected lifetime maximum reproductive rate and the steepness. Among taxonomic groups, the lifetime reproductive rate appears to be more variable than the annual rate; however, for species with similar natural mortalities after reproduction, the results are again relatively constant.

The results for the steepness are displayed as the median, the 20th percentiles, and the 80th percentiles (Table 1). These can be be used to approximate priors for Bayesian analyses that commonly use steepness (Punt and Hilborn 1997).

It is useful to compare the median for a species of the maximum annual reproductive rate (the uncorrected value) with the expectation, where the median and expectation are taken with respect to the distribution of the random effects (Fig. 7). The corrected estimates are higher by a factor of $\exp(0.5\sigma_a^2)$. This effect is usually small except for species where the estimate of the variability among populations is unusually large, e.g., for blueback herring (*Alosa aestivalis*).

A generalization

The unexpected generalization that comes from our analysis is that the annual reproductive rate within a species often shows relatively little variation and that the variation in annual reproductive rate among species is surprisingly small, usually ranging from 1 to 7 for species for which we have several populations represented in our analysis.

This is a broad generalization that may have great implications for the management and conservation of fish populations. Although the generalization appears to be firmly established for many well-studied species, these are primarily temperate-zone species.

Possible exceptions

In this section, we will discuss several populations that appear to have anomalously high or low annual reproductive rates. It is unclear whether these rates are real or due to limitations in the assessments.

The blueback herring appears to have a relatively high maximum annual reproductive rate. This relatively high number is consistent with the fast growth rate experienced by this species and other *Alosa* species when they recolonize former habitat (Crecco and Gibson 1990). However, it is possible that these high rates of population growth are caused by movement of fish upstream over obstructions and not population growth per se. This hypothesis needs to be evaluated.

Chinook salmon (*Oncorhynchus tshawytscha*) also appears to have relatively high maximum annual reproductive rates. These appear to be real and are probably conservative. The values that are in the figures for chinook salmon are from the northern limit of the range. The values for the Columbia River appear to be much higher, but it is impossible to estimate the "natural" rates because of dam-induced mortality.

The ayu (*Plecoglossus altivelis*, Plecoglossidae, Salmoniformes) from Lake Biwa, Japan, is the only univoltine species in the database, and it appears to have a very high annual reproductive rate (Table 1) (Suzuki and Kitahara 1996). The analysis appears to be sound and is backed up by fishery-independent survey data, but it is possible that the application of VPA for this species may have led to biases.

Among the lowest estimates of the maximum reproductive rates are those for several species on the west coast of North America: Pacific ocean perch, sablefish (*Anoplopoma fimbria*), and chilipepper rockfish (*Sebastes goodei*). These stocks all are assessed in a similar manner. The assessments on these stocks do not have reliable fishery-independent estimates of abundance, do not have a large amount of aging data, and often assume that the population is at the unfished equilibrium at the beginning of the fishery. It is critical for the management of these stocks to determine whether their actual maximum reproductive rate is as low as it appears to be, or if the assessments are reliable.

These cases represent anomalies, which may represent fundamental inconsistencies with our broad generalization about the reproductive rate, or may well be explained by

© 1999 NRC Canada

Table 1. Mixed model estimates at the species and family levels and corresponding estimates of the percentiles of z (the steepness parameter).

Species	n	$\widehat{\log \tilde{\alpha}}$	SE	$\hat{\sigma}_a^2$	$\hat{\tilde{\alpha}}$	z_{20}	z_{med}	z_{80}
Aulopiformes								
Synodontidae	**1**	**0.31**	**0.07**		2		**0.34**	
Bombay duck (*Harpodon nehereus*)	1	0.31	0.07		2		0.34	
Clupeiformes								
Clupeidae	**34**	**1.06**	**0.19**	**1.16**	**17.1**	**0.49**	**0.71**	**0.86**
Anadromous alewife (*Alosa pseudoharengus*)	4	1.29	0.09	0	5.7		0.59	
Anadromous American shad (*Alosa sapidissima*)	1	1.65	0.3		18.5		0.82	
Atlantic menhaden (*Brevoortia tyrannus*)	1	2.2	0.12		24.8		0.86	
Blueback herring (*Alosa aestivalis*)	3	2.6	0.55	0.81	31.9	0.71	0.84	0.92
Gulf menhaden (*Brevoortia patronus*)	1	1.25	0.16		5.3		0.57	
Atlantic herring (*Clupea harengus*)	18	0.73	0.28	1.31	22.1	0.52	0.74	0.88
Pacific sardine (*Sardinops sagax*)	2	0.66	0.89	1.56	12.7	0.34	0.59	0.81
Spanish sardine (*Sardina pilchardus*)	1	–0.56	0.75		2.1		0.34	
Sprat (*Sprattus sprattus*)	3	0.87	0.55	0.71	10.7	0.48	0.65	0.79
Engraulidae	**4**	**1.28**	**0.57**	**1.14**	**11.5**	**0.4**	**0.62**	**0.8**
Anchovy (*Engraulis encrasicolus*)	2	0.7	0.13	0	3.6		0.47	
Gold-spotted grenadier anchovy (*Coilia dussumieri*)	1	2.73	0.19		17.6		0.81	
Northern anchovy (*Engraulis mordax*)	1	0.33	0.41		3.1		0.43	
Gadiformes								
Gadidae	**49**	**1.01**	**0.12**	**0.51**	**19.6**	**0.67**	**0.79**	**0.87**
Blue whiting (*Micromesistius poutassou*)	2	0.59	0.33	0	10		0.71	
Atlantic cod (*Gadus morhua*)	21	1.37	0.15	0.37	26	0.76	0.84	0.9
Haddock (*Melanogrammus aeglefinus*)	9	0.72	0.21	0.28	13	0.64	0.74	0.82
Hake (*Merluccius hubbsi*)	1	1.18	0.45		18		0.82	
Pacific hake (*Merluccius productus*)	1	–0.95	0.83		1.9		0.32	
Pollock or saithe (*Pollachius virens*)	5	1.16	0.14	0.05	18	0.78	0.81	0.84
Silver hake (*Merluccius bilinearis*)	3	–0.18	0.29	0.16	2.7	0.31	0.39	0.47
Walleye pollock (*Theragra chalcogramma*)	2	0.28	0.24	0.01	5	0.53	0.55	0.58
Whiting (*Merlangius merlangus*)	5	1.14	0.51	1.16	30.8	0.64	0.81	0.91
Lophiiformes								
Lophiidae	**1**	**–0.07**	**0.32**		**6.7**		**0.64**	
Black anglerfish (*Lophius budegassa*)	1	–0.07	0.32		6.7		0.63	
Perciformes								
Carangidae	**3**	**0.27**	**0.21**	**0**	**4**		**0.5**	
Horse mackerel (*Trachurus trachurus*)	2	0.52	0.8	0	12.1		0.75	
Mediterranean horse mackerel (*Trachurus mediterraneus*)	1	0.25	0.22		3.5		0.47	
Lutjanidae	**1**	**1.9**	**0.9**		**47.8**		**0.95**	
Red snapper (*Lutjanus campechanus*)	1	1.9	0.9		47.8		0.92	
Percichthyidae	**1**	**0.95**	**0.16**		**18.6**		**0.82**	
Striped bass (*Morone saxatilis*)	1	0.95	0.16		18.6		0.82	
Percidae	**2**	**0.91**	**0.57**	**0.28**	**9.5**	**0.57**	**0.67**	**0.76**
Walleye (*Stizostedion vitreum*)	2	0.91	0.57	0.28	9.5	0.57	0.67	0.76
Scianidae	**1**	**1.88**	**0.28**		**26.1**		**0.87**	
White croaker (*Argyrosomus argentatus*)	1	1.88	0.28		26.1		0.87	
Scombridae	**8**	**0.34**	**0.39**	**1.12**	**7.5**	**0.3**	**0.52**	**0.72**
Atlantic bluefin tuna (*Thunnus thynnus*)	1	–0.4	0.23		5.2		0.56	
Bigeye tuna (*Thunnus obesus*)	2	0.73	0.08	0	5.3		0.57	
Chub mackerel (*Scomber japonicus*)	1	–0.05	0.33		2.4		0.38	
Atlantic mackerel (*Scomber scombrus*)	2	1.11	0.91	1.29	31.8	0.62	0.81	0.92
Southern bluefin tuna (*Thunnus maccoyii*)	1	–1.5	0.09		2.9		0.42	
Yellowfin tuna (*Thunnus albacares*)	1	1.43	0.21		9.3		0.7	
Sparidae	**3**	**2.48**	**0.41**	**0**	**65.9**		**0.95**	
New Zealand snapper (*Pagrus auratus*)	2	1.34	1.31	0	65.6		0.94	
Scup (*Stenotomus chrysops*)	1	2.6	0.38		74.6		0.95	

© 1999 NRC Canada

Table 1 (*concluded*).

Species	n	$\widehat{\log \tilde{\alpha}}$	SE	$\hat{\sigma}_a^2$	$\hat{\tilde{\alpha}}$	z_{20}	z_{med}	z_{80}
Xiphiidae	**1**	**1.7**	**0.05**		**30.1**		**0.88**	
Swordfish (*Xiphias gladius*)	1	1.7	0.05		30.1		0.88	
Pleuronectiformes								
Pleuronectidae	**14**	**0.79**	**0.18**	**0.34**	**18.8**	**0.71**	**0.8**	**0.87**
European flounder (*Platichthys flesus*)	1	–0.03	0.42		5.3		0.57	
Greenland halibut (*Reinhardtius hippoglossoides*)	3	0.75	0.68	1.32	29.3	0.59	0.79	0.91
Plaice (*Pleuronectes platessa*)	8	0.92	0.17	0.08	25.1	0.83	0.86	0.88
Yellowtail flounder (*Pleuronectes ferrugineus*)	2	0.79	0.34	0.14	13	0.69	0.75	0.81
Soleidae	**7**	**0.66**	**0.35**	**0.68**	**28.7**	**0.72**	**0.84**	**0.91**
Sole (*Solea vulgaris*)	7	0.66	0.35	0.68	28.7	0.72	0.84	0.91
Salmoniformes								
Esocidae	**2**	**0.51**	**0.19**	**0.03**	**6.1**	**0.57**	**0.6**	**0.64**
Northern pike (*Esox lucius*)	2	0.51	0.19	0.03	6.1	0.57	0.6	0.64
Plecoglossidae	**1**	**4.73**	**0.16**		**123.5**		**0.97**	
Ayu (*Plecoglossus altivelis*)	1	4.73	0.16		123.5		0.97	
Salmonidae	**106**	**1.43**	**0.05**	**0.18**	**25.1**	**0.8**	**0.85**	**0.89**
Atlantic salmon (*Salmo salar*)	3	1.46	0.25	0.16	5.1	0.46	0.54	0.62
Chinook salmon (*Oncorhynchus tshawytscha*)	6	1.99	0.13	0	7.3		0.65	
Chum salmon (*Oncorhynchus keta*)	7	1.31	0.24	0.34	4.4	0.36	0.48	0.6
Freshwater brook trout (*Salvelinus fontinalis*)	5	1.55	0.24	0.11	27.4	0.83	0.87	0.89
Lake trout (*Salvelinus namaycush*)	1	0.92	0.08		24.1		0.86	
Pink salmon (*Oncorhynchus gorbuscha*)	52	1.22	0.07	0.12	3.6	0.39	0.46	0.53
Sockeye salmon (*Oncorhynchus nerka*)	32	1.57	0.08	0.15	5.2	0.47	0.55	0.62
Scorpaeniformes								
Anoplopomatidae	**1**	**–2.35**	**0.47**		**1.4**		**0.28**	
Sablefish (*Anoplopoma fimbria*)	1	–2.35	0.47		1.4		0.26	
Hexagrammidae	**1**	**1.13**	**0.49**		**12**		**0.77**	
Atka mackerel (*Pleurogrammus monopterygius*)	1	1.13	0.49		12		0.75	
Scorpaenidae	**5**	**–1.57**	**0.24**	**0.17**	**2.8**	**0.31**	**0.39**	**0.48**
Chilipepper (*Sebastes goodei*)	1	–0.85	0.57		2.1		0.35	
Pacific ocean perch (*Sebastes alutus*)	3	–1.93	0.18	0	3		0.43	
Deepwater redfish (*Sebastes mentella*)	1	–1.08	0.18		3.6		0.47	

Note: Listed are the empirical BLUE of the mean value of the log-transformed maximum annual reproductive rate ($\widehat{\log \tilde{\alpha}}$), its standard error, the estimated variance among populations ($\hat{\sigma}_a^2$) (where possible), the estimated expected maximum lifetime reproductive rate for a species, where the expectation is taken over the distribution of the random effects ($\tilde{\alpha}$), the 20th percentile of z (z_{20}) (where possible), the median of z (z_{med}), and the 80th percentile of z (z_{80}) (where possible). The mixed model estimates are given at the species and family levels, but the family-level estimates (shown in boldface) should be used with caution.

other factors, e.g., assessment problems or the possibility that the data for these species come from only a relatively short time period, which may not be representative of the average reproductive rate.

Limitations and alternative approaches

Our approach to estimating the standardized slope at the origin of spawner–recruit functions is based on well-studied statistical methods and has intuitive appeal and appears to be a promising method for categorizing species in terms of their vulnerability to overfishing. However, researchers should be aware of its limitations and of alternative approaches.

The first limitation is the functional form assumed for density-dependent mortality. The Ricker model and the non-linear Ricker model (eq. 6) are not appropriate for some species. This is a serious limitation of the methods described here. For example, we did not consider coho salmon (*Oncorhynchus kisutch*) in this analysis because the shape of the spawner–recruitment curve was clearly asymptotic, simi-

Fig. 4. Comparison of the maximum annual reproductive rate, $\log \tilde{\alpha}$, obtained from individual regressions on each cod population in the North Atlantic with the empirical BLUPs obtained from a mixed model analysis. Notice that the mixed model estimates have lower variance than the individual estimates.

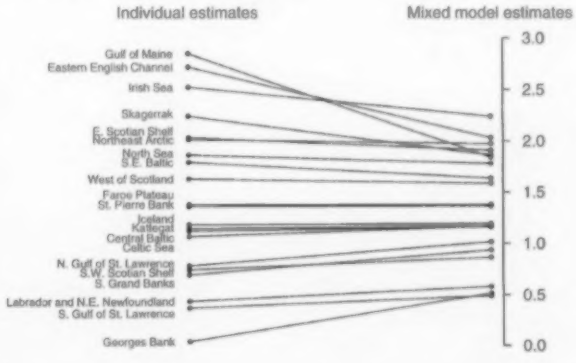

© 1999 NRC Canada

Fig. 5. Estimates of the log of the maximum annual reproductive rate for (*a*) species with multiple populations in the database, where the error bars represent the estimated standard deviation of the log of the maximum annual reproductive rate (this estimate is sometimes zero if only two or three populations are used in the analysis), and (*b*) species with only one population in the database, where the error bars represent the standard error of the estimate.

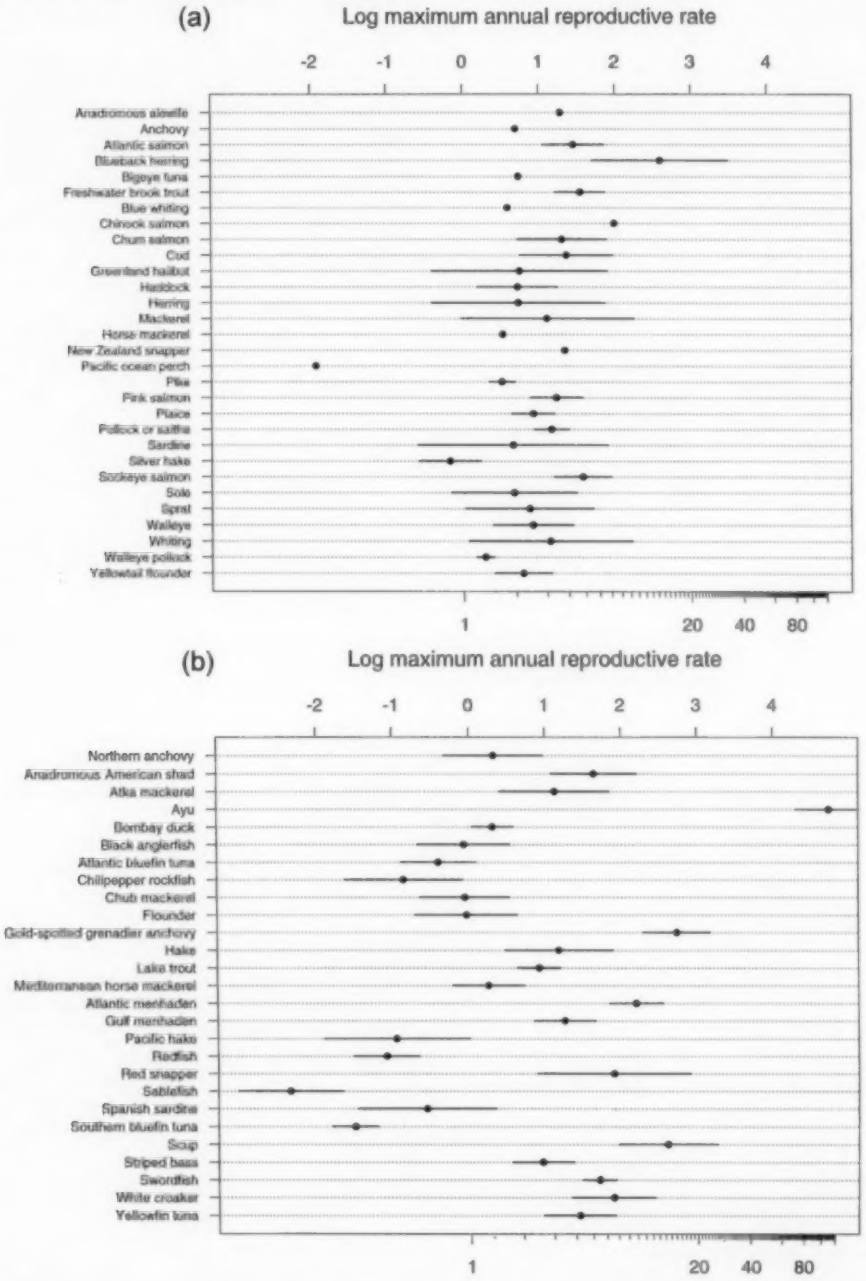

lar to a Beverton–Holt function. For such functions, nonlinear mixed models are required and will be considered in a future paper using the methods of Lindstrom and Bates (1990).

The second limitation is that we have assumed that the distribution of $\tilde{\alpha}$ is approximately lognormal. This appears to be a reasonable approximation in most cases considered here, but violations of the assumption may cause biases (Verbeke and Lesaffre 1996).

A third limitation is the assumption that the recruitment distribution for given spawner abundance is lognormal. This

© 1999 NRC Canada

Fig. 6. Estimates of the log of the maximum lifetime reproductive rate for (*a*) species with multiple populations in the database, where the error bars represent the estimated standard deviation of the log of the maximum lifetime reproductive rate, and (*b*) species with only one population in the database, where the error bars represent the standard error of the estimate.

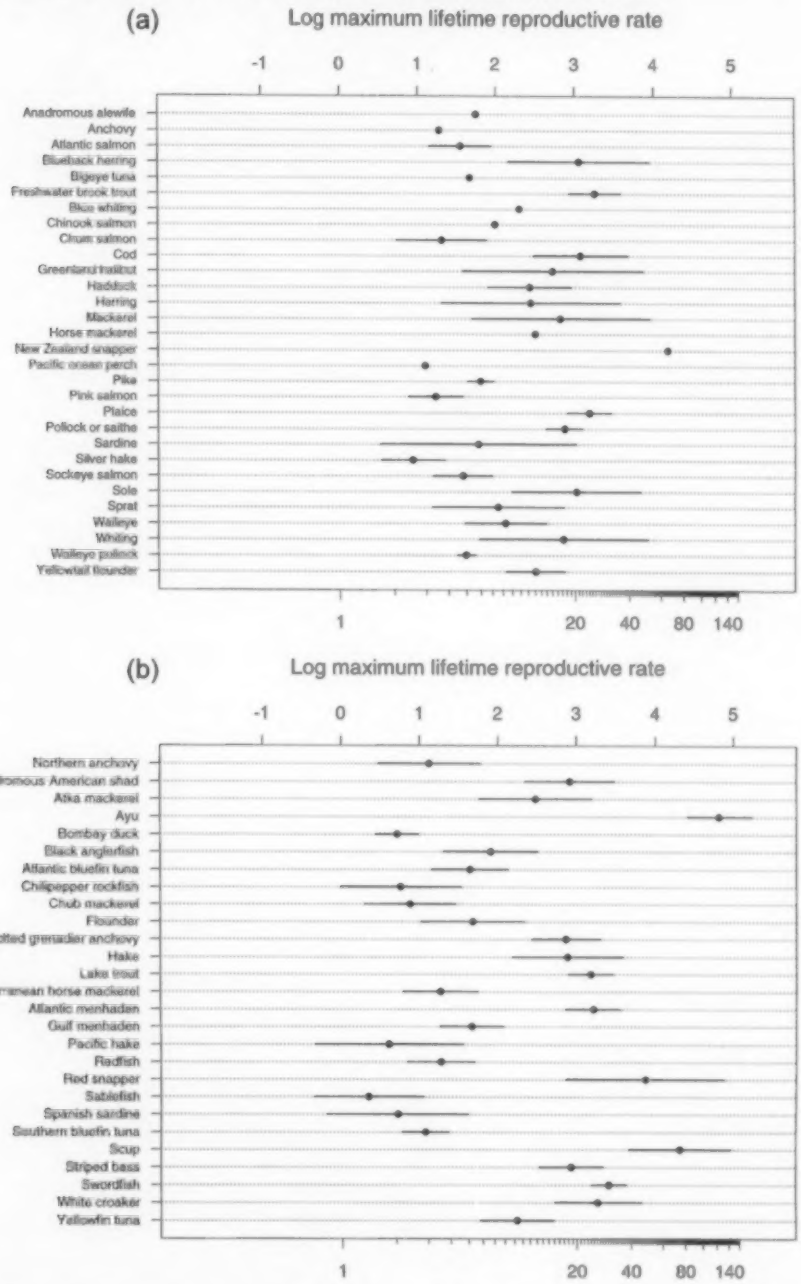

is by far the most common assumption used in fitting spawner–recruitment models (Hilborn and Walters 1992); however, it may not always be the most appropriate assumption. The gamma distribution appears to give more reasonable fits to some stock–recruitment data (Myers et al. 1995; R.A. Myers, K.G. Bowen, and I.A. Zouros, unpublished data).

A fourth limitation is the assumption that all populations within a taxon are comparable, i.e., the maximum reproductive rate for populations within a species (or higher taxon) is described by a lognormal distribution. It is possible that this parameter may vary in a systematic way among populations, e.g., populations in colder conditions may have a lower max-

© 1999 NRC Canada

Fig. 7. Comparison of the uncorrected (simple exponential transform) and corrected (lognormal) values for the maximum annual reproductive rate. Notice that without the lognormal correction, the maximum annual reproductive rate will be underestimated.

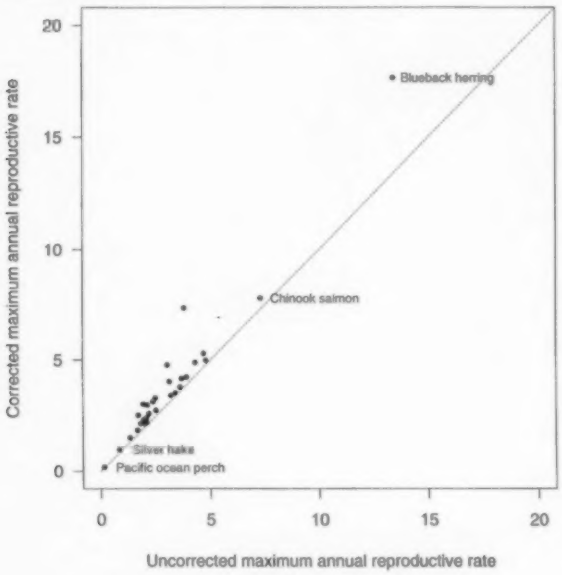

imum reproductive rate. Such hypotheses can be investigated by letting the maximum reproductive rate be a random variable whose mean is a function of a covariate such as temperature or latitude.

If any of the above four assumptions appears to be violated seriously, then an alternative approach is needed. Perhaps the most convenient alternative framework for this type of model is either a Bayes or empirical Bayes hierarchical approach (Efron 1996). Punt and Hilborn (1997) have recently reviewed these approaches in fisheries management. McAllister (1994) implemented an empirical Bayes approach to estimating a parameter functionally related to the slope at the origin, viz. the steepness parameter, using an earlier version of the database used here.

The ML estimators that we have used to estimate the underlying distribution of annual reproductive rates may result in estimates that are less "heavy tailed" than they should be (Searle et al. 1992; Efron 1996).

It should be remembered that this analysis does not circumvent known biases, e.g., estimation error in spawner abundance and time series bias in the treatment of spawner–recruitment relationships (for a review, see Hilborn and Walters 1992).

Discussion

The analysis presented in this paper suggests a new and unsuspected finding: the maximum annual reproductive rate for any of the species examined is typically between 1 and 7. This number may be less for some species and more for others, but the relative constancy of the annual reproductive rate is an unanticipated, and very important, finding. This analysis is consistent with our preliminary analysis (Myers et al. 1996).

The common belief that there is no relationship between spawner biomass and recruitment is founded on the notion that the maximum reproductive rate for fish is essentially infinite, a belief based on the observation that fecundity of fish is often large and cursory examination of spawner–recruitment plots that often show no strong reduction of recruitment at low spawner abundances over the range of the observations. This erroneous belief is caused by the lack of attention paid to the information content of different data sets (Myers and Barrowman 1996; Myers 1997).

Hypotheses

This broad generalization demands an explanation. First, consider the lower limit of the annual reproductive rate at low abundance. This represents the "average" value that should occur at low abundance. Clearly, if this value is much less than 1, then the population may very well go extinct because the value would probably be below 1 for considerable lengths of time because of variation in the environment.

Why, then, would the annual reproductive rate be bounded at the upper end? A reasonable, but speculative, answer is that a very high value of the reproductive rate would imply an excess of resources that are not exploited. In this case, other competitors would be expected to evolve to exploit these resources.

Reducing uncertainty

The uncertainty of the biological processes underlying the population dynamics of exploited species can be greatly reduced by combining data from many studies. The relative constancy of the maximum reproductive rate allows for simple, broad conclusions to be reached on the management of fish stocks. That the maximum reproductive rate is typically around 1–7 replacement spawners per spawner per year is a powerful tool for the management of fish stocks. It allows the maximum exploitation rate to be estimated quickly (Mace 1994; Myers and Mertz 1998) and the recovery rates of exploited fish populations to be calculated (Myers et al. 1997*b*).

Many of the crucial parameters needed for fisheries management can be estimated using the maximum reproductive rate analyzed here together with simple approximations (Myers et al. 1997*b*; Myers and Mertz 1998). For example, the steepness parameter that we compiled is now commonly used in assessments, and our analysis provides reasonable ML estimates that can be used in empirical Bayes assessment procedures. All that is required to use these approximations are data on natural mortality, age at maturity, and the maximum reproductive rate. These approximate formulas will require testing and verification, but this approach should allow progress to be made on critical issues. Thus, even if the maximum reproductive rate is not known for a species, the estimates compiled in this paper allow it to be approximated, or our estimates can be used in forming priors for a Bayesian analysis.

Acknowledgments

We wish to thank the Killam Foundation, the Canadian Foun-

© 1999 NRC Canada

dation for Innovation, and the Natural Sciences and Engineering Research Council of Canada for financial support. We thank Stacey Fowlow for programming assistance. We thank the hundreds of assessment biologists whose hard work made this meta-analysis possible. Special thanks to Pamela Mace whose input was key to developing these ideas. This paper is dedicated to the memory of my (R.A.M.) great friend, Gordon Mertz.

References

Barnthouse, L.W., Klauda, R.J., Vaughan, D.S., and Kendall, R.L. 1988. Science, law, and the Hudson River power plants: a case study in envioronmental assessment. Am. Fish. Soc. Monogr. **4**.

Bellows, T.S. 1981. The descriptive properties of some models for density dependence. J. Anim. Ecol. **50**: 139–156.

Cole, L.C. 1954. The population consequences of life history phenomena. Q. Rev. Biol. **29**: 103–137.

Cook, R.M., Sinclair, A., and Stefansson, G. 1997. Potential collapse of North Sea cod stocks. Nature (Lond.), **358**: 521–522.

Crecco, V.A., and Gibson, M. 1990. Stock assessment of river herring from selected Atlantic coast rivers. Spec. Rep. 19. Atlantic States Marine Fisheries Commission, Washington, D.C.

DeGisi, J.S. 1994. Year class strength and catchability of mountain lake brook trout. Master's thesis, University of British Columbia, Vancouver, B.C.

Efron, B. 1996. Empirical Bayes methods for combining likelihoods. J. Am. Stat. Assoc. **91**: 538–565.

Hilborn, R., and Liermann, M. 1998. Standing on the shoulders of giants: learning from experience in fisheries. Rev. Fish Biol. Fish. **8**: 1–11.

Hilborn, R., and Walters, C.J. 1992. Quantitative fisheries stock assessment: choice, dynamics and uncertainty. Chapman and Hall, New York.

Lande, R., Engen, S., and Saether, B.E. 1997. Optimal harvesting, exonomic discounting and extinction risk in fluctuating populations. Nature (Lond.), **372**: 88–90.

Liermann, M., and Hilborn, R. 1997. Depensation in fish stocks: a hierarchic Bayesian metaanalysis. Can. J. Fish. Aquat. Sci. **54**: 1976–1985.

Lindstrom, M.J., and Bates, D.M. 1990. Nonlinear mixed effects models for repeated measures data. Biometrics, **46**: 673–687.

Mace, P.M. 1994. Relationships between common biological reference points used as threshold and targets of fisheries management strategies. Can. J. Fish. Aquat. Sci. **51**: 110–122.

Mace, P.M., and Doonan, I.J. 1988. A generalized bioeconomic simulation model for fish population dynamics. N.Z. Fish. Assess. Res. Doc. 88/4.

Maynard Smith, J., and Slatkin, M. 1973. The stability of predator–prey systems. Ecology, **54**: 384–384.

McAllister, M.K., Pikitch, E.K., Punt, A.E., and Hilborn, R. 1994. A Bayesian approach to stock assessment and harvest decisions using the sampling/importance resampling algorithm. Can. J. Fish. Aquat. Sci. **51**: 2673–2688.

Millar, R.B., and Meyer, R. 2000. Nonlinear state space modelling of fisheries biomass dynamics by using Metropolis–Hastings within Gibbs sampling. Appl. Stat. In press.

Myers, R.A. 1997. Comment and reanalysis: paradigms for recruitment studies. Can. J. Fish. Aquat. Sci. **54**: 978–981.

Myers, R.A., and Barrowman, N.J. 1996. Is fish recruitment related to spawner abundance? Fish. Bull. U.S. **94**: 707–724.

Myers, R.A., and Mertz, G. 1998. The limits of exploitation: a precautionary approach. Ecol. Appl. **8**(Suppl. 1): s165–s169.

Myers, R.A., Rosenberg, A.A., Mace, P.M., Barrowman, N.J., and Restrepo, V.R. 1994. In search of thresholds for recruitment overfishing. ICES J. Mar. Sci. **51**: 191–205.

Myers, R.A., Bridson, J., and Barrowman, N.J. 1995. Summary of worldwide stock and recruitment data. Can. Tech. Rep. Fish. Aquat. Sci. No. 2024.

Myers, R.A., Mertz, G., and Barrowman, N.J. 1996. Invariants of spawner–recruitment relationships for marine, anadromous, and freshwater species. ICES C.M. 1996/D:11.

Myers, R.A., Hutchings, J.A., and Barrowman, N.J. 1997*a*. Why do fish stocks collapse? The example of cod in eastern Canada. Ecol. Appl. **7**: 91–106.

Myers, R.A., Mertz, G., and Fowlow, S. 1997*b*. Maximum population growth rates and recovery times of Atlantic cod, *Gadus morhua*. Fish. Bull. U.S. **95**: 762–772.

Pimm, S.L. 1991. The balance of nature. University of Chicago Press, Chicago, Ill.

Punt, A., and Hilborn, R. 1997. Fisheries stock assessment and decision analysis: the Bayesian approach. Rev. Fish Biol. Fish. **7**: 35–65.

Robinson, G.K. 1991. That BLUP is a good thing: the estimation of random effects. Stat. Sci. **6**: 15–51. With comments and a rejoinder by the author.

Searle, S.R., Casella, G., and McCulloch, C.E. 1992. Variance components. John Wiley & Sons, New York.

Suzuki, N., and Kitahara, T. 1996. Relation of recruitment to the number of caught juveniles in the ayu population of Lake Biwa. Fish. Sci. **62**: 15–20.

Verbeke, G., and Lesaffre, E. 1996. A linear mixed-effects model with heterogeneity in the random-effects population. J. Am. Stat. Assoc. **91**: 217–221.

Appendix 1. Estimation in SAS

This appendix demonstrates how to fit the proposed model to data for a single species. In the SAS data step, a data set is created with three variables per observation: the name of the stock (i.e., population), `stock`, the number or biomass of spawners, `s`, and the survival, `surv`, respectively. The survival is $\log(R/S)$, where recruitment, R, has been multiplied by $\mathrm{SPR}_{F=0}(1-p_s)$, so we will obtain estimates of $\tilde{\alpha}$ in the appropriate units.

The SAS code for fitting the model with autocorrelated recruitment is

```
proc mixed method=reml;
  class stock;
  model surv= s*stock/solution;
  random int /subject=stock;
  repeated /subject=stock group=stock type=AR(1);
```

This model assumes autocorrelated errors and fits a separate first-order autocorrelation parameter and error variance for each stock. The method of estimation is REML.

© 1999 NRC Canada

Appendix 2. Robustness simulations

In order to test the robustness of the estimates from our model, we used simulations based on real data. The approach was to mimic the data for the 20 cod populations in the North Atlantic as closely as possible. In all cases, we used the observed spawner abundances, the estimated density-dependent parameters ($\hat{\beta}_i$), the estimated residual variance for each population, and the estimated mean (1.37) and variance (0.37) of the log $\tilde{\alpha}$ parameters. For each simulation, we randomly generated values for log $\tilde{\alpha}$. Then, using the observed spawner abundances, the $\hat{\beta}_i$s and the residual error variance that we produced simulated recruitment values that would closely match the actual data. We generated 1000 "realizations" of the 20 populations, randomly generating new log $\tilde{\alpha}$ values and then simulating recruitment in each case.

Fig. A1. Histograms of estimates of $\log\alpha$ and σ_a^2 from simulations described in Appendix 2. The vertical dotted lines indicate the true estimates obtained using the data on 20 cod populations. Results from three different simulations are shown: (*a*) data simulated to match the model exactly, i.e., residuals and slope at the origin simulated from a lognormal distribution and expected recruitment given by a Ricker model, (*b*) residuals and slope at the origin simulated from a gamma distribution and expected recruitment given by a Ricker model, and (*c*) residuals and slope at the origin simulated from a lognormal distribution and expected recruitment given by a Beverton–Holt model.

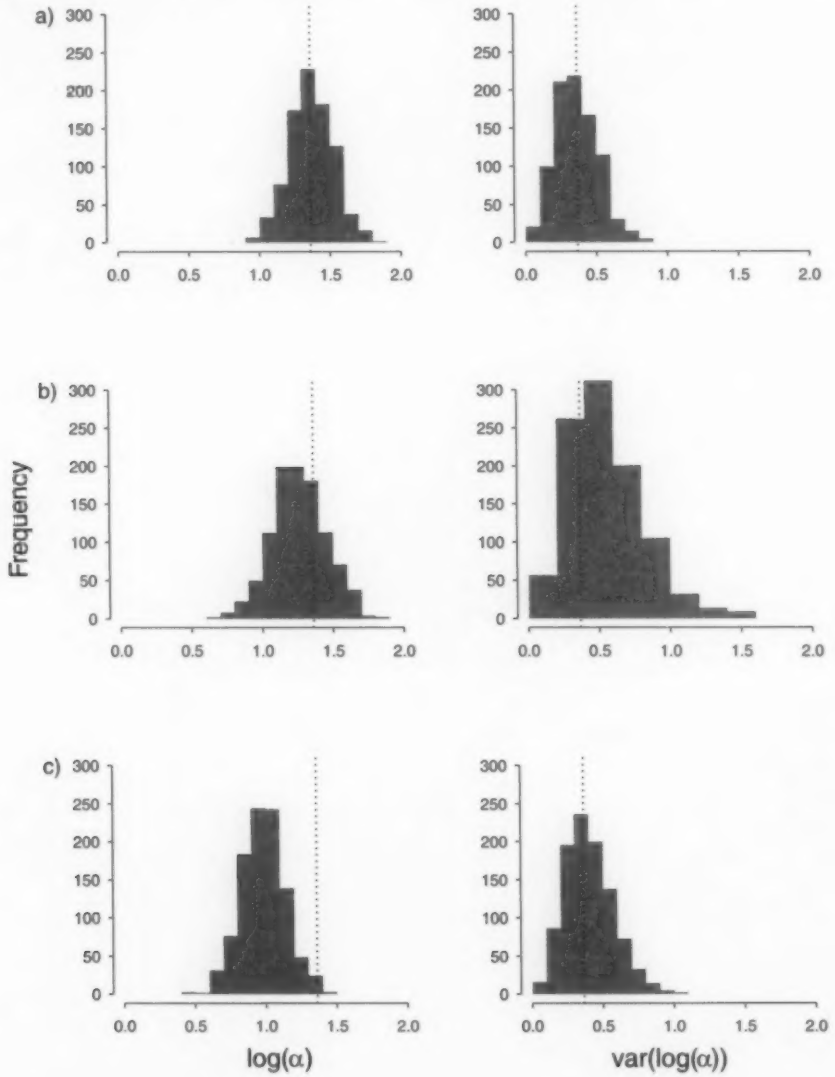

© 1999 NRC Canada

We conducted three simulations. In each case, the model that we fit was a Ricker with lognormal distributions for both the error and the slope at the origin. In the first simulation, we generated data that matched this model exactly, i.e., a parametric bootstrap. In the second simulation, we generated data that was from a Ricker but had gamma (instead of lognormal) distributed residuals and slope at the origin. This was done to test the robustness of our inferences to misspecification of the probability distributions. In the last simulation, we generated data from a Beverton–Holt model with lognormal errors and slope at the origin. This was done to test the robustness of our inferences to misspecification of the spawner–recruitment model. From the histograms of the estimated log $\tilde{\alpha}$ values, we can see that when our model was matched exactly by the data, the estimates were unbiased (Fig. A1*a*). When the distributional assumptions were violated, the value for log $\tilde{\alpha}$ was underestimated, while the variance was overestimated (Fig. A1*b*). When the form of the model was incorrect, log $\tilde{\alpha}$ was underestimated and the variance was relatively unbiased (Fig. A1*c*).

© 1999 NRC Canada

A biophysical model of the interaction between vertical migration of crustacean zooplankton and circulation in the Lower St. Lawrence Estuary

Bruno A. Zakardjian, Jeffrey A. Runge, Stephane Plourde, and Yves Gratton

Abstract: As an essential step in modeling the influence of circulation on the population dynamics of marine planktonic copepods, we define a simple formulation of swimming behavior that can be used in both Eulerian and Lagrangian models. This formulation forces aggregation of the population toward a preferential depth and can be stage specific and time varying, thus allowing description of either diurnal or seasonal vertical migration. We use the formulation to examine the interaction between the circulation and vertical distribution in controlling horizontal distribution of the common planktonic copepod *Calanus finmarchicus* in the Lower St. Lawrence Estuary, Canada. We first introduce diel migration into a simple one-dimensional model and then into a model of residual two-dimensional circulation patterns representative of conditions encountered in the Lower St. Lawrence Estuary. Results from the latter indicate that interactions between circulation and stage-specific swimming behaviors are the main mechanisms for aggregation of planktonic crustaceans at the head of the Laurentian Channel and highlight the implications of flushing of the surface-dwelling young stages for the population dynamics of *C. finmarchicus* in the Lower St. Lawrence Estuary.

Résumé : À titre d'étape essentielle dans la modélisation de l'influence de la circulation sur la dynamique des populations de copépodes planctoniques marins, nous établissons une formulation simple du comportement natatoire qui peut être utilisée dans des modèles tant eulériens que lagrangiens. Cette formulation postule qu'il y a regroupement de la population vers une profondeur préférée et peut tenir compte des différents stades de développement et varier dans le temps, permettant ainsi une description de la migration verticale diurne ou saisonnière. Nous utilisons cette formulation pour examiner l'interaction entre la circulation et la distribution verticale en rapport avec la distribution horizontale du copépode planctonique commun *Calanus finmarchicus* dans l'estuaire maritime du Saint-Laurent, au Canada. Nous avons d'abord introduit la migration nycthémérale dans un modèle simple unidimensionnel, puis dans un modèle de profils de circulation résiduelle bidimensionnel représentatif des conditions observées dans l'estuaire maritime du Saint-Laurent. Les résultats du dernier modèle indiquent que les interactions entre la circulation et les comportements natatoires des différents stades de développement constituent les principaux mécanismes de regroupement des crustacés planctoniques à la tête du chenal Laurentien, et mettent en évidence les implications du lessivage des jeunes stades qui se tiennent dans les eaux superficielles pour la dynamique des populations de *C. finmarchicus* dans l'estuaire maritime du Saint-Laurent.

[Traduit par la Rédaction]

Introduction

Global Ocean Ecosystem Dynamics (GLOBEC) is an international program developed for the purpose of understanding the influence of physical processes on the abundance and distribution of key zooplankton and fish populations through the use of coupled biological–physical models (e.g., Eckman 1994; Wiebe et al. 1996). The planktonic copepod *Calanus finmarchicus* is predominant in zooplankton communities of northern subarctic waters and has been targeted for study in North Atlantic GLOBEC-related programs. As a species that undergoes diel (e.g., Durbin et al. 1995) and seasonal (e.g., Kaartvedt 1996; Hirche 1996) vertical migrations, *C. finmarchicus* represents one of the challenges to the investigation of biological–physical interactions in zooplankton: how to model actively swimming organisms in flow fields.

The swimming ability of copepods can be estimated as at least 1 body length (BL)·s^{-1} (e.g., Paffenhöfer et al. 1996), which for adult *C. finmarchicus* yields swimming velocities of more than 10 m·h^{-1}. Such swimming velocities are one order of magnitude higher than typical vertical velocities in the ocean and one order less than typical horizontal velocities. In response to vertical gradients at several time and

Received December 23, 1998. Accepted April 20, 1999.
J14951

B.A. Zakardjian[1] **and Y. Gratton.** INRS-Océanologie, Rimouski, QC G5L 3A1, Canada.
J.A. Runge. Department of Fisheries and Oceans, Maurice Lamontagne Institute, Division of Ocean Sciences, Mont-Joli, QC G5H 3Z4, Canada.
S. Plourde. Département de biologie, Université Laval, Pavillon Vachon, Ste-Foy, QC G1K 7P4, Canada.

[1]Author to whom all correspondence should be addressed.
e-mail: bruno_zakardjian@uqar.uquebec.ca

© 1999 NRC Canada

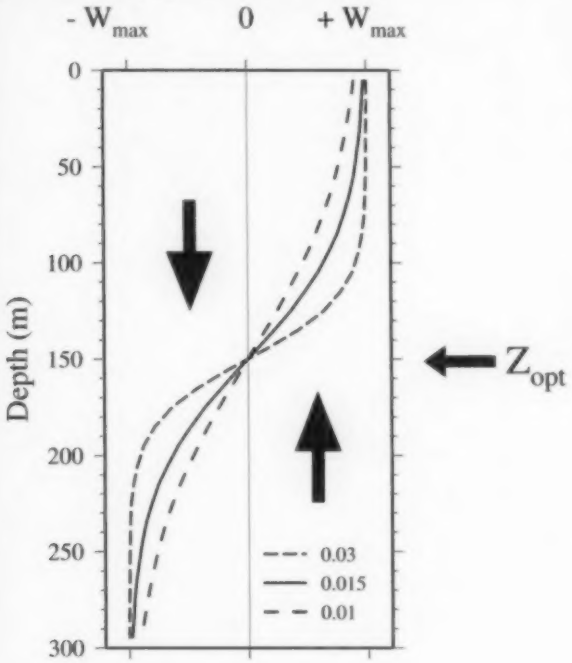

Fig. 1. Depth variations of vertical migration velocity W_{mig} calculated for optimal depth Z_{opt} = 150 m and with the scaling parameter α varying between 0.01 and 0.03.

space scales, copepods may vertically migrate. This behavior must be incorporated into biophysical models in order to properly understand the dynamics of copepod populations (e.g., Slagstad and Tande 1996; Hannah et al. 1998; Steele and Henderson 1998).

In this study, we present a general formulation of copepod vertical swimming behavior and vertical distribution that accomodates both seasonal ontogenetic and diel vertical migration patterns in Eulerian grid models. Its applicability is tested with the help of two concurrent modeling approaches, one Eulerian (computing the time evolution of copepod abundance) and the other pseudo-Lagrangian (computing particle trajectories), by application in a strong hydrodynamic forcing regime in the Lower St. Lawrence Estuary (LSLE), Canada. We discuss processes that can lead to aggregations of zooplankton in the Laurentian Channel at the head of the LSLE and conditions for differential advective export of copepod life history stages from the LSLE.

Materials and methods

Model formulation

The model is a process model in which we consider a simple population of swimming zooplankton neglecting growth and mortality rates. The model is based on the classical advection–diffusion equation to which a swimming term is added:

$$(1) \qquad \frac{\partial C}{\partial t} + \nabla \vec{U} C = \nabla [K \nabla C] + \frac{\partial W_{mig} C}{\partial z}$$

where C is the concentration of copepods, $\vec{U}$ is the current vector, K is the diffusion tensor, and W_{mig} is the swimming velocity. The swimming velocity W_{mig} is formulated with a maximum velocity W_{max} and an optimal depth Z_{opt}:

$$(2) \qquad W_{mig}(z) = W_{max} \tanh[\alpha(z - Z_{opt})]$$

where tanh is the hyperbolic tangent function and α is a scaling parameter (Fig. 1). This resembles the equation in Franks (1992) except that we consider time-varying $Z_{opt} = f(t)$ on diurnal time scales. The optimal or preferential depth, Z_{opt}, may be a specific isolume, isotherm, depth of maximum food concentration, or simply the mode in abundance from direct field observations of vertical distribution. This formulation implies that the organisms are swimming downward from the surface and upward from the bottom toward their optimal or preferential depth. Direct observations of swimming behavior from ADCP data confirm this approach (Heywood 1996). The further away from Z_{opt}, the closer the swimming velocity to W_{max} (Fig. 1).

The model is two-dimensional and extends vertically to 300 m depth (30 equal layers of Δz = 10 m) and horizontally to 100 km (10 equal rows of Δx = 10 km). The time increment is 0.1 h. For all simulations, the initial conditions are a homogeneously distributed population of 10 individuals·m^{-3}, i.e., a depth-integrated abundance of 3000 individuals·m^{-2}. Boundary conditions are no fluxes at the sea surface, bottom, or upstream boundary (Neuman condition with spatial derivatives set to zero for all variables). The downstream boundary is open (Dirichlet condition) with zooplankton abundance set to zero at all depths, i.e., no import of organisms from the downstream surrounding area.

Except the swimming term, eq. 1 is discretized using a semi-implicit Crank–Nicolson scheme derived from the control volume approach (see Roach 1972). The discrete scheme for the swimming term is defined independently of the control volume approach and considers the swimming behavior in each layer rather than at their boundaries. In this scheme, it is assumed that for a layer n with swimming velocity $W_{mig}(n)$ and concentration $C(n)$, an amount $|W_{mig}(n)| \times C(n)$ leaves the layer (independently of the sign of $W_{mig}(n)$), while other organisms enter the layer from the surrounding depths in the proportions $|W_{mig}(n + 1)| \times C(n + 1)$ for $W_{mig}(n + 1) < 0$ *(upward swimming) and* $|W_{mig}(n - 1)| \times C(n - 1)$ when $W_{mig}(n - 1) > 0$ (downward swimming). There is no swimming import from the $n - 1$ and $n + 1$ layers for the surface and bottom layer, respectively. A similar scheme was used by Andersen and Nival (1991). The scheme is conservative in the sense that the vertical sum of all the terms is zero whatever the position of Z_{opt} in the water column. It is nearly a backward scheme for an advective term, but it allows aggregations of organisms at depth Z_{opt}. We solved the complete equation with the Choleski double-scanning method (also called the Thomas algorithm in Roach 1972) in alternate directions.

To further examine the interaction between vertical migration and circulation, we computed particle trajectories under the same swimming and hydrodynamic conditions. These trajectories are calculated using the following simple set of discrete equations:

$$(3) \begin{cases} z(t) = z(t-1) + \Delta t \times w[z(t-1), x(t-1)] + \Delta t \times W_{mig}[z(t-1)] \\ x(t) = x(t-1) + \Delta t \times u[z(t-1), x(t-1)] \end{cases}$$

with a set of 25 $[z(0), x(0)]$ regularly dispatched in the model domain.

Simple test of the model: one-dimensional modeling of diel vertical migration

As a simple illustration of the model, Fig. 2 shows the result of a one-dimensional simulation of diel vertical migration over an initial 2-day period. For this simulation, the diurnal variation in Z_{opt} is

© 1999 NRC Canada

Fig. 2. Two-day simulation of the depth abundance of a diel-migrating simple population (left panels) and corresponding night and day vertical distribution (right panels) for maximum velocity W_{max} varying from 50 to 100 m·h^{-1}.

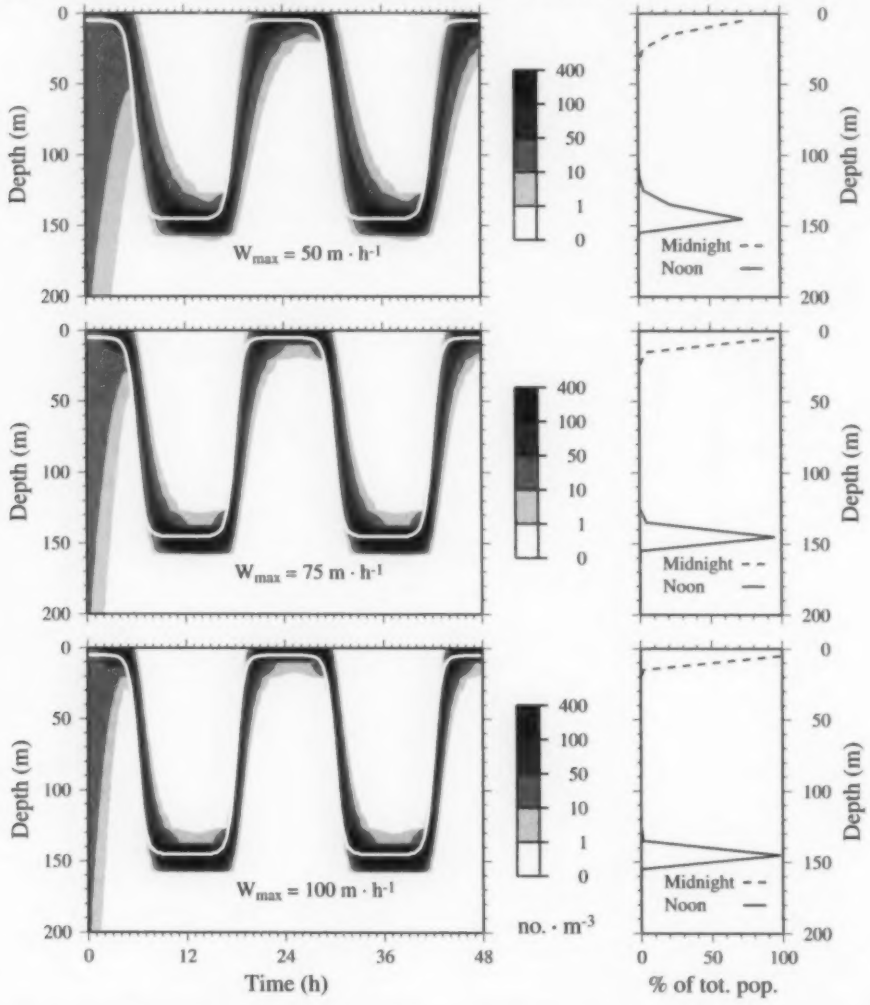

described by a function coupling hyperbolic tangent and sinusoidal variations around a mean depth $\bar{Z}$ with amplitude ΔZ and period T = 24 h:

$$(4) \qquad Z_{opt} = \bar{Z} + \Delta Z \tanh\left[4\cos\left(\frac{2\pi t}{T}\right)\right].$$

Here, $\bar{Z}$ and ΔZ have been defined as $\bar{Z} = \Delta Z = Z_{max}/2$, where Z_{max} = 150 m is the depth of observed daytime maximal abundance of *C. finmarchicus* females in the Gulf of St. Lawrence in autumn (described afterward). The cos function drives the periodicity and the tanh function generates a constant 8-h day and night Z_{opt}. The numeral 4 applied to the tanh function argument drives the duration of transition from the night to day Z_{opt} (here, <4 h). Durbin et al. (1995) described *C. finmarchicus* diel migration between 0 and 150 m in the Gulf of Maine, with ascent and descent taking no more than 3 h. From such observations, we can estimate the maximum steady swimming velocity W_{max} to be at least 50 m·h^{-1} for the bulk of the population, i.e., 5 BL·s^{-1} or more. For the first simulations, the α parameter was set at 0.015, the vertical turbulent diffusivity was set at 10 m^2·day^{-1}, and W_{max} ranged from 50 to 100 m·h^{-1}.

With W_{max} = 50 m·h^{-1}, the initially homogeneous population aggregates around Z_{opt} in less than 6 h and thereafter follows the time variation of Z_{opt} (Fig. 2). Note that the time needed for an organism to swim the entire depth domain (300 m) is 6 h at W_{max}. The vertical distribution at noon and at night (right panels) resembles the observed vertical distribution of adult *C. finmarchicus* in the Gulf of St. Lawrence in autumn (described afterward); however, the descent and ascent of the population take more than 4 h. Hence, a swimming velocity of 50 m·h^{-1} achieves complete diel migration but with a time lag of about 2 h with reference to the time variation in Z_{opt}. A higher W_{max} results in closer coupling between Z_{opt} and the maximal abundance depth, but this can lead to unrealistic aggregation in very narrow layers.

Two parameters may be used to broaden distribution about the optimal depth. First, the α parameter in the swimming speed formulation (eq. 2) drives the decrease of W_{mig} near Z_{opt} (see Fig. 1). Increasing α tightens the high values of W_{mig} near Z_{opt} and consequently augments the aggregations of individuals in a narrow layer (Fig. 3), while decreasing α has the opposite effect; it also in-

© 1999 NRC Canada

Fig. 3. Sensitivity of the night and day vertical distributions of a diel-migrating simple population to the α parameter (top panels) and biological diffusivity K_{mig} (bottom panels).

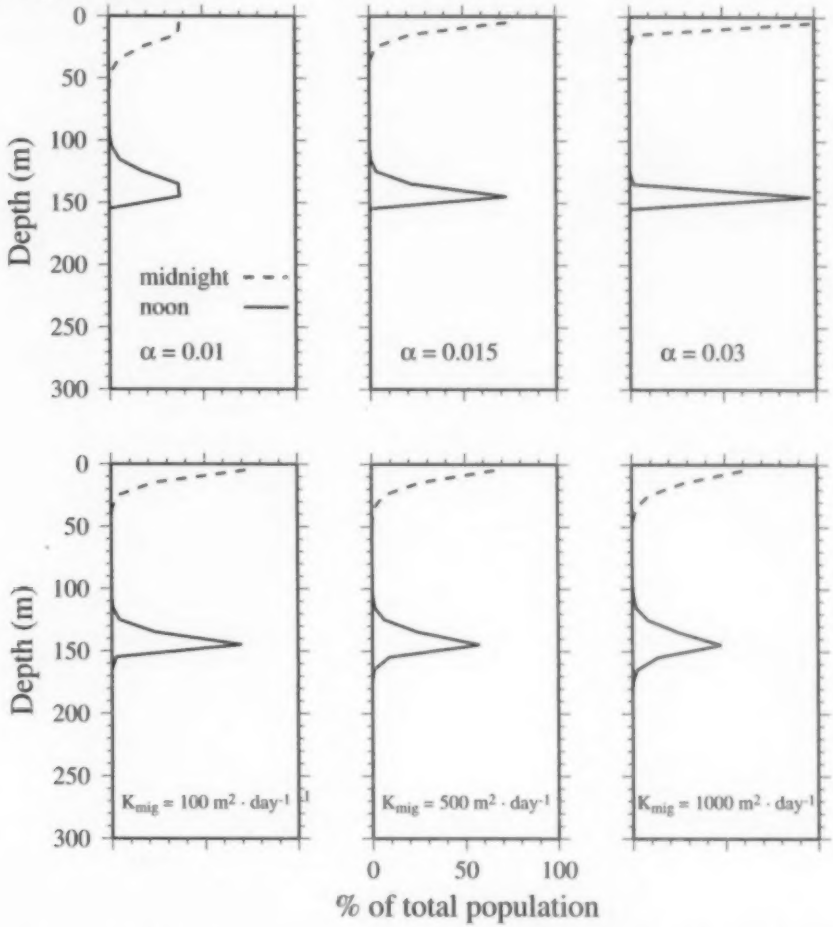

creases the time lag between Z_{opt} and the depth of maximal abundance and can prolong duration of ascent and descent to >4 h. Due to the asymptotic form of the tanh function, a very low value for α has the same effect as decreasing W_{max} and limits aggregation of the population.

Second, the distribution about Z_{opt} may also be controlled through adjustment of the turbulent motion. The swimming ability of marine planktonic copepods is typically higher than turbulent velocity fluctuations; hence, copepod movement is, in general, independent of oceanic turbulent activity in the upper ocean (Yamazaki and Squires 1996). However, the swimming behavior of marine zooplankton is not portrayed in its complexity by the model. Copepod movement is often nonlinear and multidirectional (e.g., Paffenhöfer et al. 1996) in response to external and internal factors such as food availability, gut fullness, and presence of predators. These factors would act on individuals as dispersion functions, through short-term fluctuations of W_{mig} around a mean steady swimming velocity ($W_{mig} = \overline{W}_{mig} + W'_{mig}$), but are not explicitly considered in models. Similar to the parameterization of turbulent diffusivity from turbulent velocity fluctuations, these individual dispersion processes may be introduced as a biological diffusivity. This approach was implicitly used by Wroblewski (1982) in his modeling study of *Calanus marshallae* in the Oregon upwelling zone. He used a 10-fold higher diffusivity coefficient (86.4 $m^2 \cdot day^{-1}$ instead of 8.64 $m^2 \cdot day^{-1}$) for swimming copepodite stages in order to avoid unrealistic aggregation. We investigated the influence of biological diffusivity, K_{mig}, on the patterns of vertical distribution using higher values of turbulent diffusivity in eq. 1. Very high values, on the order of 500 $m^2 \cdot day^{-1}$ or more, are required to significantly broaden distribution about Z_{opt} (Fig. 3). An advantage of this approach is the absence of a time lag between Z_{opt} and depth of the maximal abundance. However, high biological diffusivities may not be justified on the basis of observations or theory.

At the present time, we cannot recommend one approach over another. For the analysis that follows, we have adopted the standard values of α = 0.015, W_{max} = 75 $m \cdot h^{-1}$, and K_{mig} = 100 $m^2 \cdot day^{-1}$, which is a moderate biological diffusivity close to the value used by Wroblewski (1982). These parameters permitted simulation of diurnal swimming behavior with reasonably good agreement with observations.

Results

Mean hydrodynamic conditions in the LSLE

In regions of strong hydrodynamic forcing, such as the LSLE, the swimming ability and behavior of marine plank-

© 1999 NRC Canada

Fig. 4. Geographical location and details of the LSLE. The 50-, 200-, and 300-m isobaths show the location of the Laurentian Channel and the bathymetric peculiarities at the head of the Channel and near the north coast.

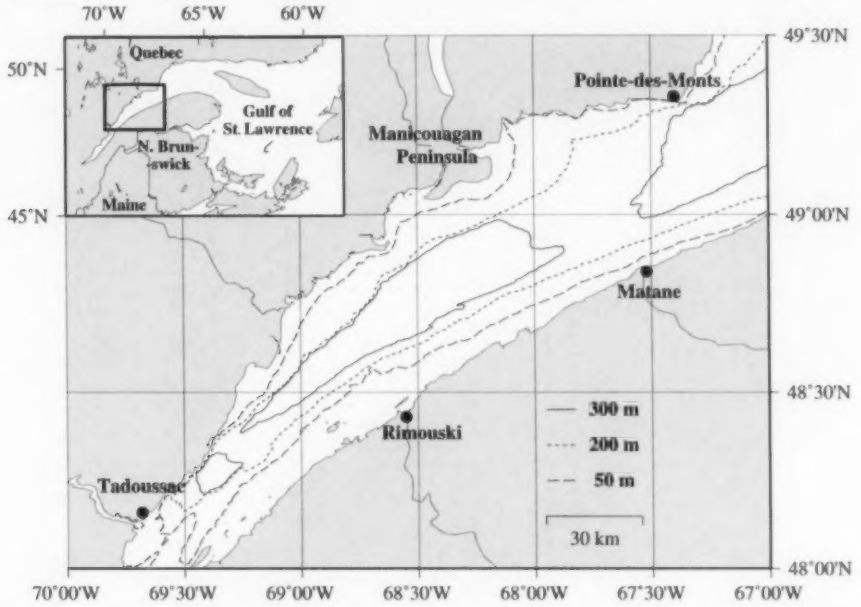

tonic copepods can lead to complex spatiotemporal distributions, making it difficult to separate the role of biological processes from the impact of advective transport. The mean hydrodynamic conditions in the LSLE are characterized by the freshwater runoff from the St. Lawrence, the Saguenay River, and the Manicouagan, Bersimis, and aux Outardes rivers, the topographic particularities and dimensions of the Estuary, and a strong tidal forcing (see Koutitonsky and Bugden 1991). Physical conditions are also strongly dependent on atmospheric events at synoptic or seasonal time scales (Koutitonsky and Bugden 1991; Mertz et al. 1992).

Two characteristics of the LSLE are of particular relevance to the modeling of the distribution of small, swimming organisms. The bathymetric feature at the head of the Laurentian Channel, where the bottom shoals abruptly from 300 to 50 m depth in less than 20 km (Fig. 4), interacts with tidal forcing from the Atlantic Ocean, inducing strong vertical motion near the head of the Channel and leading to the creation of a marked internal tide that affects the first half of the LSLE (Forrester 1974; Therriault and Lacroix 1976; Gratton et al. 1988; Koutitonsky and Bugden 1991). Marked vertical motion is also frequently observed near the north coast of the LSLE, due to wind conditions and similar bathymetry associated with the northern wall of the Laurentian Channel (e.g., Simard et al. 1986). The other major characteristic is the marked downstream residual flow in the southern part of the LSLE that results from the discharge of the St. Lawrence and Saguenay river systems. This flushing, which affects the upper 50 m of the water column, is a major factor determining the timing of the spring phytoplankton bloom in the LSLE (Therriault and Levasseur 1985, 1986; B.A. Zakardjian et al., unpublished results).

The mean circulation pattern in the LSLE was portrayed with an idealized stream function (Fig. 5, top panel). The stream function was calculated by numerically solving a simple elliptic equation whose parameters were adjusted to give realistic horizontal and vertical velocities. One half of this calculated elliptic stream function was used to model the mean vertical motion at the head of the Laurentian Channel. A constant stream function for the rest of the model domain gave surface and deep baroclinic currents similar to observed ADCP profiles in the LSLE in spring (Fig. 5, bottom panel), i.e., high seaward surface velocity (0.5 $m \cdot s^{-1}$) and surface baroclinicity (0.5 $m \cdot s^{-1}$ over 50 m). Below 50 m, the current reverses and flows slowly upstream. Analogous to the classical estuarine pattern, the two-layer circulation in the Laurentian Channel is typical of the LSLE (e.g., El-Sabh 1979; Koutitonsky and Bugden 1991). In this flow field, the vertical motions (Fig. 5, middle panel) result from the continuity between the deep upstream current and the surface downstream current and reach maximal values of about 35 $m \cdot day^{-1}$. The upwelled waters come mainly from the 70- to 150-m layer, which is within the depth range of the cold intermediate water, as generally observed in the upward motion zone at the head of the Laurentian Channel. While this is a simple representation that neglects a large part of the complex hydrodynamics of the area, it is nevertheless representative of the mean residual circulation prevailing in the first half of the LSLE in spring and summer.

Figure 6 (top panel) shows 10-day calculated trajectories based on an individual particle model representing non-swimming organisms in the prescribed flow field. The particles originally in the surface layer are rapidly flushed out the western half of the LSLE. Deeper particles have a longer residence time, but they are finally upwelled into the surface layer and then rapidly flushed. Results of the corresponding Eulerian simulation (Fig. 6, bottom panel) show that the concentration of organisms in the surface layer dramatically

© 1999 NRC Canada

Fig. 5. Stream function Ψ (top panel), vertical velocities *W* (middle panel), and horizontal velocities *U* (bottom panels) with the detail of the *U* baroclinicity (bottom-right panel) used in the simulations. The calculated baroclinic current *U* that prevails in the second half of the simulated area is compared with measured residual currents (crosses in the bottom-right panel) from the COUPPB90 experiment (station 023, leg G2).

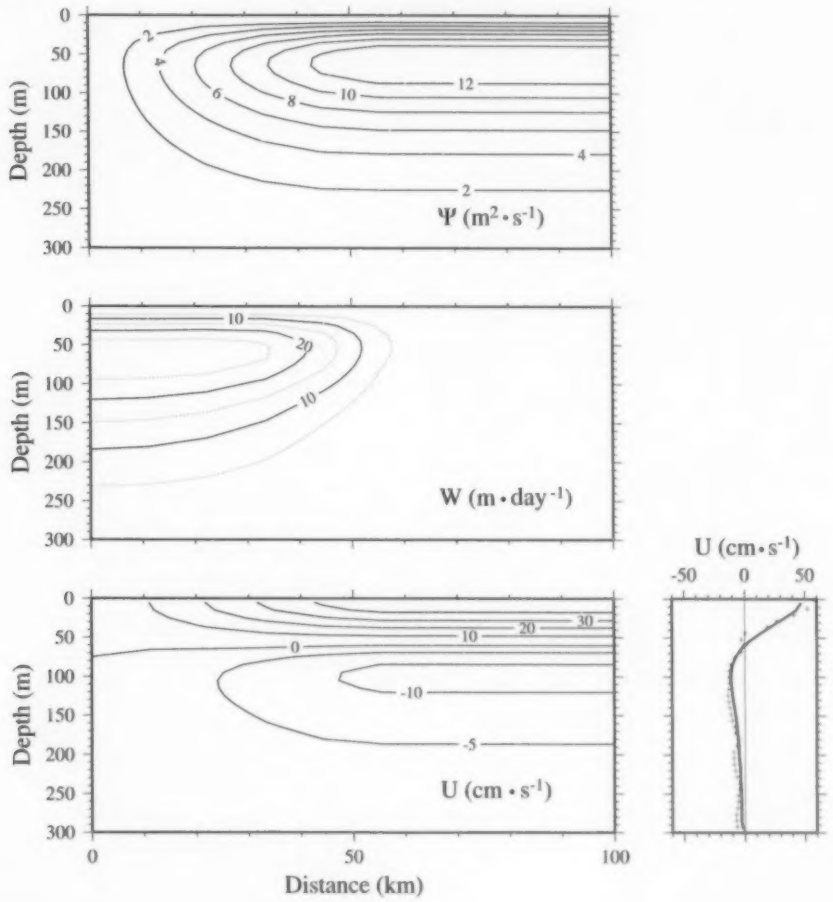

decreases over the initial 20 days due to flushing of the upper layer. Deeper-dwelling organisms are conserved for a longer period but are eventually flushed over a 2- to 4-week period due to the draining of the deeper layers.

Clearly, without some import of organisms at depth from the downstream boundary, a population of nonswimming copepods cannot maintain itself in this flow field. These simulations do not take into account in situ production, which would contribute to population maintenance; the specific production rates of marine copepods are about 0.04–0.07·day^{-1} (generation times of 15–30 days). These rates are insufficient to maintain populations in the flow field, as the residence time in the surface layer is 3–4 days and would be less than 30 days for deeper organisms (i.e., taking into account the upstream currents and the upwelling in the surface layer). Note that reduction of flushing rates in the surface layer to 0.15 m·s^{-1} increases plankton residence time in the area, but by no more than 10 days, implying that the residence time of the organisms would be always close to or less than a generation time.

Vertical migration scenarios

Calanus finmarchicus exhibits several vertical migration patterns according to life stage or time of the year (e.g., Fig. 7). For example, young copepodite stages (CI–CIII) move at most 25–50 m in the water column and are generally confined to the upper 100 m. Preferential depth for the stage CIV–CV population is relatively shallow (75 m) and temporally invariant in May but deepens to 175 m in autumn. Only a part of the stage CIV–CV population exhibits diurnal vertical migrations in September, probably because the remainder of the population is in diapause. Adult females undertake an extensive vertical migration in autumn, but not in spring, where they are distributed in the surface 100 m both day and night.

Based on these observations, we examine two scenarios for the interaction between the circulation and the vertical distribution of *C. finmarchicus* in the LSLE. The first and simplest assumes time-constant preferential depth (Z_{opt}): the diapause depth for stage CV (175 m), the cold intermediate layer (75 m) in May for stages CIV–CVI and part of stages

© 1999 NRC Canada

Fig. 6. Nonswimming scenario. Top panel: 10-day calculated trajectories for nonswimming organisms (free-floating particles); bottom panel: depth-integrated abundance after 5, 10, 20, and 40 days of simulation. The trajectories are from 25 initially homogeneously distributed particles; crosses and circles are for the initial and final positions, respectively.

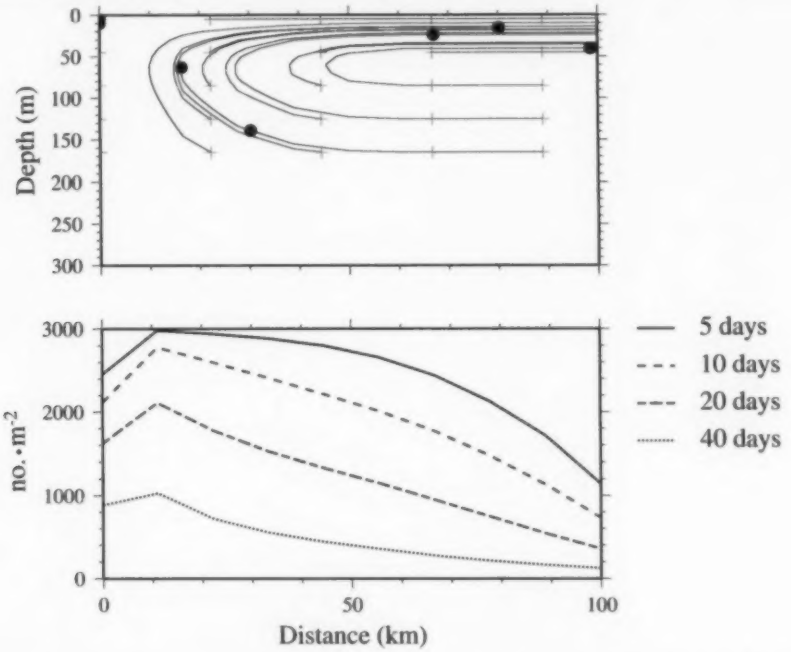

CI–CIII, and the upper surface layer (25 m) for stages CI–CIII (as in autumn). In the 10-day particle trajectories for these cases (Fig. 8, left panels), there is rapid migration of copepods toward the imposed optimal depth, even in the region of strong vertical motion. This clearly demonstrates how the swimming ability of *C. finmarchicus* life stages dominates over the vertical advection, which is as high as 35 m·day^{-1} in the model simulation. Once copepodites have attained their optimal depth, they are subject to the prevailing horizontal advection. Copepods constrained to the surface layer (Z_{opt} = 25 m) are rapidly flushed, whereas when Z_{opt} = 75 m the organisms aggregate upstream. A similar but less rapid (because the horizontal velocity is lower) upstream aggregation occurs when Z_{opt} = 175 m.

The analogous Eulerian grid simulations illustrate the time evolution of the entire population. When Z_{opt} = 25 m, a downstream patch of higher abundance within the first 10 days results from the outward movement of the population (Fig. 9, left panels); after 10 days, most of the initial population has been flushed out. The upstream patch that persists for up to 10–15 days indicates that a small part of the population may be temporarily retained upstream where the vertical component of the stream flow dominates. The simulations when Z_{opt} = 75 and 175 m indicate that copepods would congregate in dense patches upstream in a very localized area. In these two latter simulations, no organisms are lost from the area, as they are not exposed to the flushing of the upper mixed layer.

A second scenario assumes diel vertical migration based on observations in September (see Fig. 7) of *C. finmarchicus* females (migrating between 0 and 150 m), stages CI–CIII (migrating between 0 and 50 m), and for a deep-dwelling hypothetical population (migrating between 150 and 300 m). Ten-day particle trajectories for these three cases (Fig. 8, right panels) show horizontal distortion of the vertical trajectory resulting from transport by horizontal currents. In the case of copepodites migrating only in the upper layer, the distortion is mainly downstream, implying a net downstream transport. In the case of deep migrating organisms, the distortion is upstream and will lead to congregation upstream. The intermediate case, i.e., copepods migrating between 0 and 150 m, shows both upstream and downstream distortion as individuals spend half of their time in the upper flushed layer and the other half in the underlying intermediate water where upstream transport dominates. Because of the higher downstream velocity in the upper layer, the trajectory exhibits a net downstream transport. The corresponding Eulerian simulations (Fig. 9, right panels) confirm these results. A population migrating only in the surface layer would be flushed out in less than 20 days. The deep migrating population would aggregate upstream. For the intermediate case, the pattern is more complex during the first 15 days (i.e., localized maxima of abundance in the second half of the area), but the long-term net outward transport is clearly evident.

Discussion

Quantitative description of zooplankton vertical distribution and migration behavior is essential for accurate biophysical modeling of zooplankton abundance and distribution in relation to physical processes. Several different formulations of vertical migration have been put forward in numerical studies of planktonic crustaceans, including vertical distribution as a function of food availability and

© 1999 NRC Canada

Fig. 7. Observed night (shaded) and day (open) vertical distributions for *C. finmarchicus* stages CI–CIII, CIV–CV, and female CVI (CVIf) in May and September in the Gulf of St. Lawrence. Data represent means of oblique vertical tows taken with a BIONESS multinet sampler between 10:00 and 15:00 (day) and between 22:00 and 02:00 (night) at two adjacent stations in the northwest Gulf (J.A. Runge et al., unpublished).

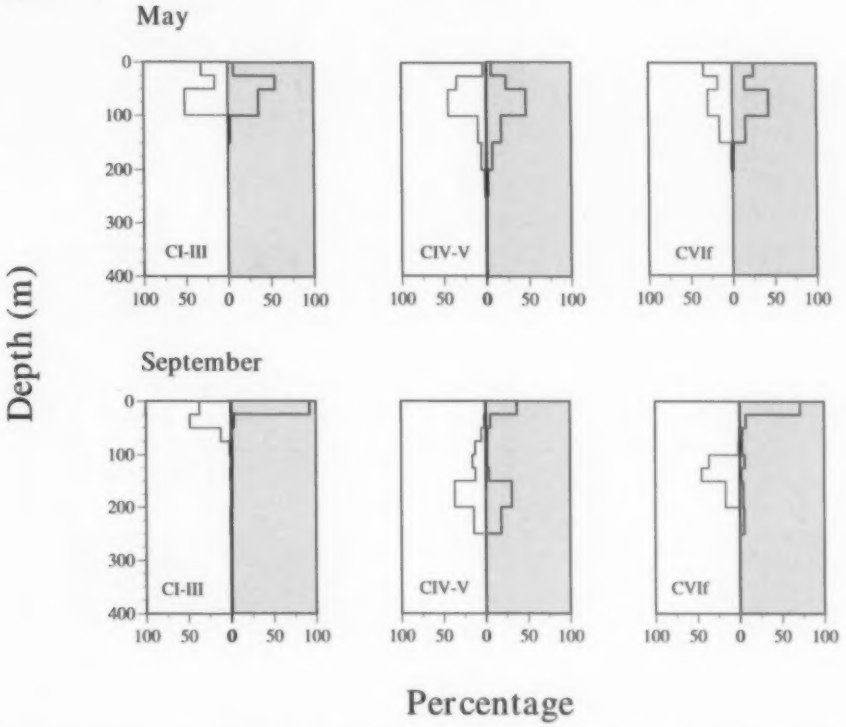

light (e.g., Andersen and Nival 1991), simple depth-constant but time-varying migration velocity (e.g., Wroblewski 1982), imposed preferential depths in particle trajectory studies (Hannah et al. 1998) or depth selection in Eulerian grids (Lynch et al. 1998), and trophic-based models (Moloney and Gibbons 1996). The formulation presented here is easy to use in both Lagrangian and Eulerian models and permits any continuous function for the time-varying Z_{opt}, facilitating comparison of various vertical distribution scenarios. We successfully tested the model with subdaily variations of Z_{opt} (diel migrations) representing relatively high-frequency vertical movement. Any lower-frequency swimming behavior (e.g., seasonal) can also be reproduced by the model.

Swimming speeds of planktonic copepods during migration are not well-documented and must be inferred from laboratory observations or diel time series of vertical distribution. Adult *C. finmarchicus* migrating daily between 0 and 150 m must sustain swimming velocities of at least 50 $m \cdot h^{-1}$ or 5 $BL \cdot s^{-1}$. The threshold value of W_{max} depends on the depth domain exploited by the organisms during a daily cycle (i.e., copepods migrating daily over more extended depth intervals may require higher swimming velocities in order to achieve perfect timing and depth regulation). A similar range of diel vertical migration was observed by Durbin et al. (1995) in the Gulf of Maine. Wishner and Allison (1986) observed diel vertical migration of *C. finmarchicus* over a depth range of 300–400 m, implying swimming speeds of 100 $m \cdot h^{-1}$ (10 $BL \cdot s^{-1}$). Baliño and Asknes (1993) described dawn ascent and dusk descent of zooplankton scattering layers with migration velocities up to 60–90 $m \cdot h^{-1}$ in a Norway fjord, and Heywood (1996) measured vertical swimming velocities for zooplankton up to 70–200 $m \cdot h^{-1}$. Similar high values may be deduced from field studies of other larger-sized copepod species, such as *Metridia pacifica* (Enright 1977) and *Pleuromamma* sp. (Enright 1977; Wishner and Allison 1986). Smaller species may also exhibit high relative swimming speeds, in terms of body lengths per second (e.g., *Acartia tranteri* at 10 $BL \cdot s^{-1}$; see Kimmerer and McKinnon 1987). Comparably relative swimming velocities, on the order of several body lengths per second, have been measured for other marine copepods or freshwater small crustaceans, but these refer to jump or burst velocities (e.g., Saiz and Alcaraz 1992; Gorski and Dodson 1996; Paffenhöfer et al. 1996). These estimates represent short-term laboratory observations under various conditions of food supply, light, and turbulence but, as previously noted by Enright (1977), without incentive for sustained movement. This may explain the frequent discrepancy between laboratory estimates of swimming speed and the somewhat higher velocities inferred from field studies.

Although maximum steady swimming velocity in terms of body lengths per second is not precisely known, we can infer, based on the above-mentioned researches, that it is more than 5 $BL \cdot s^{-1}$ in *C. finmarchicus* for the adult and late copepodite stages. It is generally assumed that younger stages do

© 1999 NRC Canada

Fig. 8. Ten-day calculated trajectories for the different scenarios of swimming behaviors. Left panels: swimming organisms with fixed optimal depth Z_{opt} = 25 m (top panel), Z_{opt} = 75 m (middle panel), and Z_{opt} = 175 m (bottom panel); right panels: diel-migrating organisms with night and day migration between 0 and 50 m (top panel), between 0 and 150 m (middle panel), and between 150 and 300 m (bottom panel). The trajectories are from 25 initially homogeneously distributed particles, crosses and circles are for the initial and final positions, respectively, and the heavy line in each right panel details one particle trajectory.

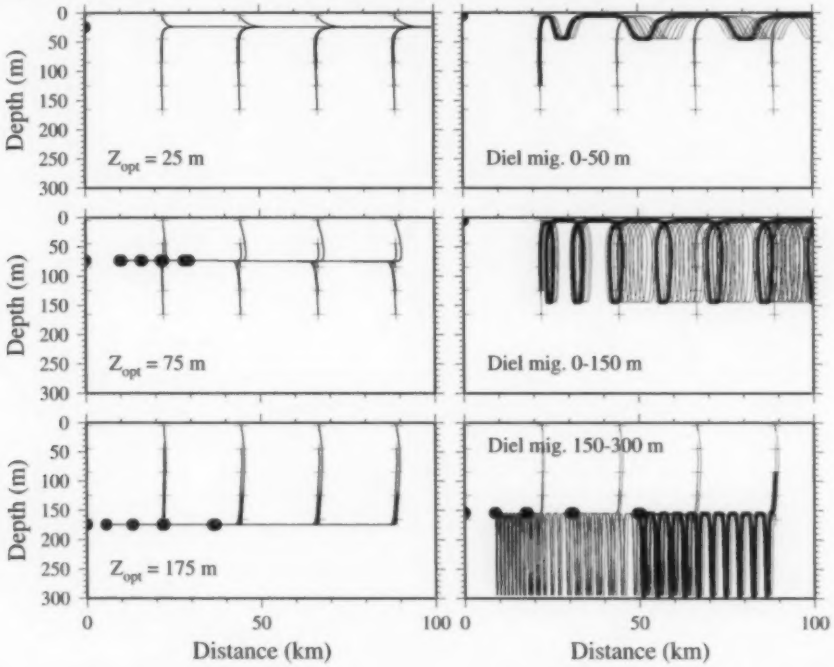

not have sufficient swimming ability to undertake significant diurnal or seasonal vertical migration. However, limited vertical migration in the upper layer may simply be difficult to detect. For example, Huntley and Brooks (1982) described diurnal vertical migration behaviors for all the feeding stages of *Calanus pacificus* with a progressive increase in migration amplitude with age. Definition of swimming ability in terms of body length would be consistent with this finding. Assuming a maximum value of 7 BL·s^{-1} and an ascent and descent duration of 3 h (as generally observed; see Andersen and Nival 1991; Durbin et al. 1995), the maximum swimming velocities calculated in Table 1 allow determination of the maximum vertical range for diel migration for each life history stage. Considering that vertical migrations of less than 25–50 m are not well detected by classical observational methods, only copepodite stages at or older than CII may exhibit consistently observable vertical migration. Our data (e.g., Fig. 7) show small but nevertheless distinct differences in night and day vertical profiles of abundance of younger *C. finmarchicus* copepodite stages and more marked patterns for stages CIV–CVI in autumn. In the Gulf of Maine, Durbin et al. (1995) noted that all copepodites stages can exhibit diurnal vertical migration, even though migration was less extensive in stages CI and CII (i.e., <150 m) than in the older stages.

We investigated the body length approach by comparison of the field observations with the simulations (Fig. 10). In these simulations, Z_{opt} varies between 0 and 150 m, as previously defined, while W_{max} was set to values for stage NIV to CII in Table 1. The simulation starts at midnight with an initial population aggregated in the surface layer. From these simulations, it appears that naupliar stages are unable to undertake diel migration that can be detectable with the usual methods; the differences between night and day depth of maximal abundance are 20-m spaced and the population is unable to aggregate. Stage CI is able to perform detectable vertical migration but does not display strong aggregation. Stage CII would exhibit behaviors similar, although less extensive, to those of adults. These results agree with the previously described observations. Note that our body length assumptions imply that the relationship W_{mig}/body length is the same for each stage despite morphological differences between nauplii and copepodites as well as between the first and last copepodite stages. Indeed, nauplii stages may have W_{max} much less than 7 BL·s^{-1} due to their limited locomotory appendices. As the organism develops, its ability for sustained swimming tends to the adult one (7 BL·s^{-1}). Considering stage-varying W_{max}/body length ratios can be a future refinement of the model.

One artificial characteristic of our model is the asymmetry of the daytime vertical distribution, where all of the population is aggregated at or above Z_{opt} but not below. This is due to the structure of the model, which forces the copepods to swim downward during the descent phase until they reach Z_{opt}, at which point, their swimming velocity is zero and they are prevented from deeper descent. With our W_{mig} for-

© 1999 NRC Canada

Fig. 9. Depth-integrated abundance along the simulated area after 5, 10, 20, and 30 days for the six scenarios of swimming behaviors. Left panels: swimming organisms with fixed optimal depth Z_{opt} = 25 m (upper panel), Z_{opt} = 75 m (middle panel), and Z_{opt} = 175 m (bottom panel); right panels: diel-migrating organisms with night and day migration between 0 and 50 m (top panel), between 0 and 150 m (middle panel), and between 150 and 300 m (lower panel).

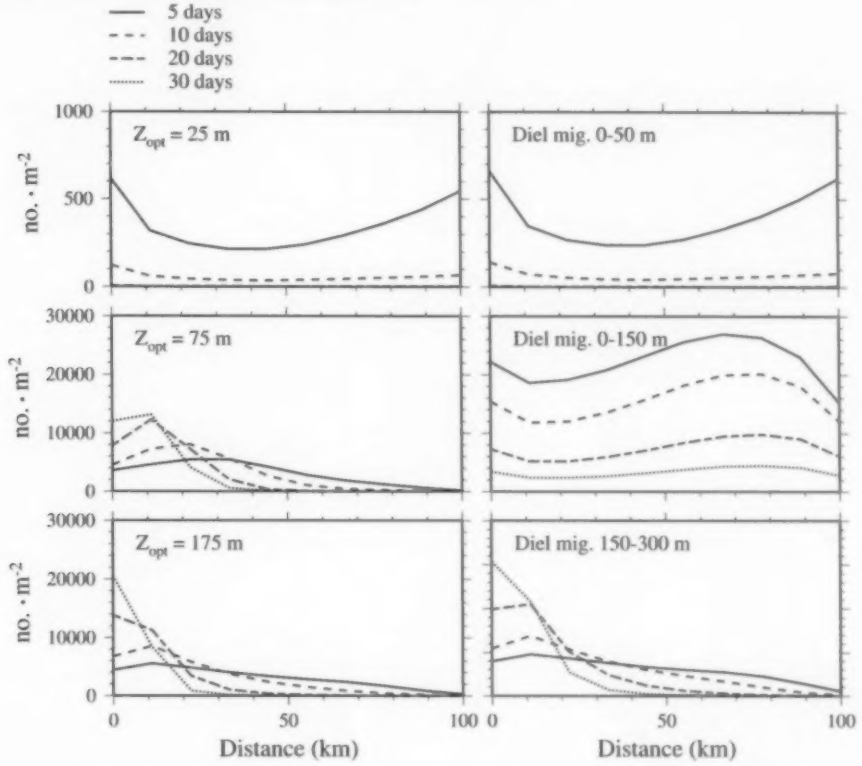

Table 1. Estimation of the maximum range (Δz) of diel vertical migration for life stages of *C. finmarchicus*, assuming a maximum swimming speed (W_{mig}) of 7 BL·s^{-1} and a maximum duration of 3 h for daily ascent or descent.

Stage	Mean BL (μm)	W_{mig} as 7 BL·s^{-1} (m·h^{-1})	Δz
NI	150	3.8	11.4
NII	200	5.0	15.0
NIII	300	7.6	22.7
NIV	450	11.3	33.9
NV	600	15.1	45.3
NVI	750	18.9	56.7
CI	900	22.7	68.1
CII	1300	32.9	98.7
CIII	1700	42.8	128.5
CIV	2100	52.92	158.8
CV	2600	65.5	196.6
CVI	3000	75.6	226.8

mulation, the only way for organisms to be distributed deeper than daytime Z_{opt} is to use high biological diffusivity (see. Fig. 3). Inclusion of sinking behavior, which is currently neglected in our model, would also distribute organisms deeper into the water column during the day. However, we consider that these aspects would not strongly alter the results of our two-dimensional simulations.

Earlier investigation of the role of swimming behavior and circulation in determining the distribution of planktonic crustaceans in the LSLE was conducted by Simard et al. (1986), who observed a long (100 km) and narrow (10 km) euphausiid patch upstream and along the northern coast of the estuary. The patch followed bathymetry (50-m isoline), and concurrent thermohaline measurements revealed conditions of upwelling all along the north coast. They argued that negative phototaxis and the strong swimming ability of euphausids kept them out of the upper layer while the deep upwelling circulation transported them toward the head of the Laurentian Channel. The simulations we describe here quantify similar aggregation processes in the LSLE. Runge and Simard (1990) hypothesized that such processes may occur for other deep-dwelling planktonic crustaceans. In addition to adult and overwintering stages of *C. finmarchicus*, these include the planktonic copepods *Calanus hyperboreus* and *Calanus glacialis* and pelagic amphipods.

The dynamics of patch formation and surface layer circulation in the LSLE are, of course, more complex than our simple two-dimensional approach. The flow fields that we

© 1999 NRC Canada

Fig. 10. Two-day simulation of the depth abundance of a diel-migrating simple population (left panels) and corresponding night and day vertical distribution (right panels) for maximum velocity W_{max} varying from 10 to 30 m·h^{-1}, i.e., for stage NIV to CII.

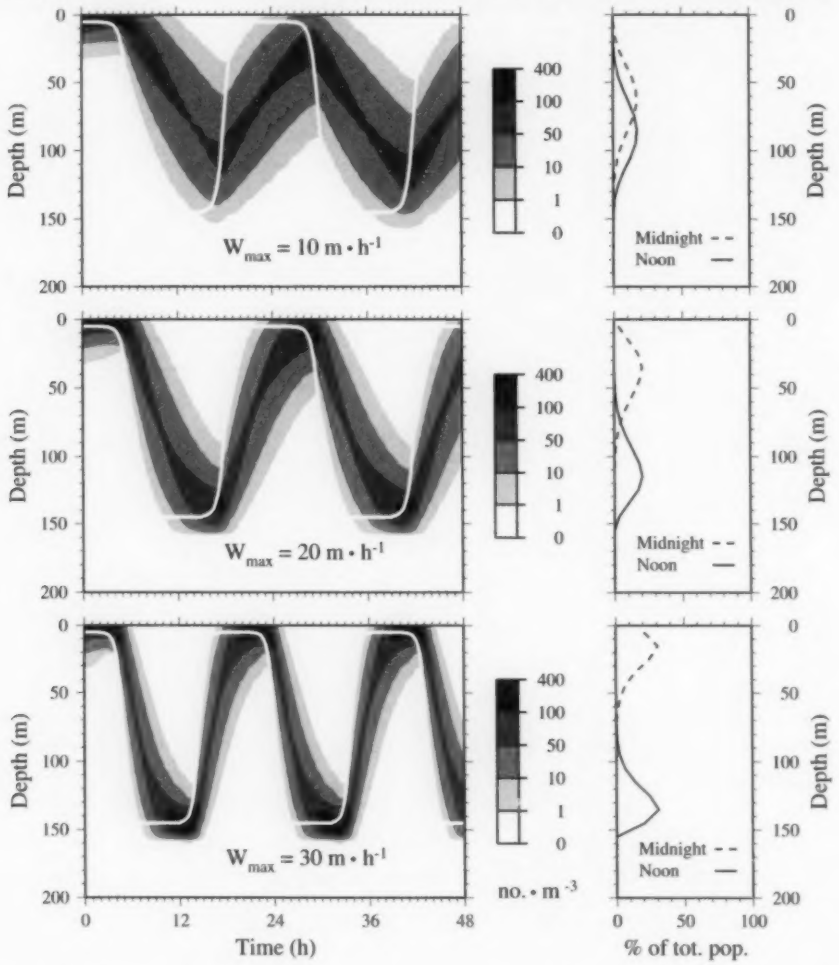

used are representative of the mean large-scale circulation in the upstream half of the LSLE: a deep and slow upstream transport of the cold intermediate water, which is tidally upwelled at the head of the Laurentian Channel, and flushing of the upper layer by the runoff-driven jet, as described by Koutitonsky and Bugden (1991) and by Gratton et al. (1988) from satellite observations of temperature. The tidally induced vertical motions at the head of the Laurentian Channel can be stronger than those used in our model. Vertical velocities up to 20–35 m·h^{-1} are inferred (Gratton et al. 1988; Chassé 1994), but such high velocities would operate intermittently, i.e., at midflow. The maximum upward velocities in our model are 1.5 m·h^{-1} (36 m·day^{-1}) and result from the continuity of the deep upstream and surface downstream flows. Although this is one order of magnitude less than the tidally induced upward velocity that can occur at the head of the Laurentian Channel, we assumed that these lower velocities are realistic mean long-term values. The maximum tidally induced vertical velocities are lower than the estimated sustained swimming speeds of *C. finmarchicus* (≈75 m·h^{-1}) and much lower than the swimming speeds of euphausiids (1–5 cm·s^{-1}; see references in Simard et al. 1986). Hence, a much higher vertical velocity that may occur intermittently at midflow would not impede the depth regulation of these organisms.

The width scale of the zooplankton patches in the simulations that we present here depends directly on the width of the upwelling zone, which is 50 km in our flow field (Fig. 5). Surface circulation patterns in the active mixing zone at the head of the Laurentian Channel involve strong transverse currents carrying water to the runoff-driven jet flow along the southern coast. However, the flushing of the surface layer in our model is not unrealistic. Surface velocities in the southern jet can be as high as 30–40 cm·s^{-1}, whereas transverse currents are generally lower, about 20–30 cm·s^{-1} (El Sabh 1979; Koutitonsky 1979). Transverse currents should be included in more refined versions, but consideration of transverse currents should not greatly alter

© 1999 NRC Canada

either the large-scale pattern of net outward transport at the surface or the aggregation processes described here.

One new result of the analysis here, with reference to the earlier hypothesis of Simard et al. (1986), is that diel-migrating organisms inhabiting the surface layer at night may not be able to congregate upstream or even to maintain themselves in the estuary. Due to the large prevailing vertical current shear (30 $cm \cdot s^{-1}$ over 50 m and more than 40 $cm \cdot s^{-1}$ over 100 m) in the LSLE, even a short stay in the surface layer can lead to large horizontal displacements and eventual flushing. On average, a vertical migrator must reside in the deeper layers four times longer in order to compensate for the surface flushing. However, because diel migration is in general nearly symmetric, the time spent at depth is never four times the time spent at the surface, even in mid-June when daylength is maximum. Therefore, only organisms that avoid the upper flushed layer may be able to congregate at the head of the Laurentian Channel.

This conclusion would not be affected by inclusion of the barotropic tidal flow, which our model has excluded. Except in the vicinity of the head of the Laurentian Channel where it can lead to complex circulation processes, tidal forcing only drives reverse upstream and downstream excursions of the order of 10 km (Savenkoff et al. 1997). In order for there to be long-term unidirectional transport, there must be an exact matching between tidal and migration periods (Hill 1991); hence, there would be no net directional transport in the case of diel migration.

Runge and Simard (1990) hypothesized that upstream advection of deep-dwelling individuals and seaward flushing of plankton at the surface have a major effect on both the zooplankton community composition and the specie populations dynamics in the LSLE. Despite the simplicity of the physical forcing in our model, the numerical tools presented here permit investigation of this hypothesis and its implications. Clearly, surface-living copepods, and even diel-migrating species in some cases, do not stay sufficiently long in the LSLE to achieve a complete reproduction cycle. In contrast, deep-living organisms would accumulate upstream with increasing abundance if there were a constant downstream import from the Gulf of St. Lawrence.

Calanus finmarchicus has time-varying and stage-specific swimming behaviors so that the effect of the interaction of swimming and circulation on the population dynamics is complex. As an example, Plourde and Runge (1993) showed that the timing of the annual reproduction event of *C. finmarchicus* in the LSLE is closely coupled with the onset of the late phytoplankton bloom. B.A. Zakardjian et al. (unpublished results) suggested that the onset of the phytoplankton bloom in the LSLE is mainly driven by the seasonal evolution of the buoyancy-driven circulation in the LSLE, the main factor being the decrease in surface layer flushing in late spring – early summer. The main argument is that the time scale of the phytoplankton bloom (5–15 days) closely matches the residence time of the surface layer. Exit from the diapausing CV stage implies a spring migration of *C. finmarchicus* females toward the surface where they mature and spawn with time scales of about 7 days for both gonad maturation and onset of spawning (e.g., Plourde and Runge 1993). Here again, the time scales of the biological processes match the residence time in the surface layer so that the onset of the reproduction event may be also driven by hydrodynamic processes. Later in the season, the different preferential depth of the naupliar and copepodite stages will imply stage-specific input–output from the adjacent northern Gulf area, which may give peculiar patterns in the mean annual life cycle of *C. finmarchicus* in the LSLE. The next step will be to embed the vertical migration model into a more detailed life cycle model of *C. finmarchicus* in order to study the effect of different scenarios of stage-specific swimming behaviors on the population dynamics of this species.

Acknowledgments

This work is a contribution to the GLOBEC-Canada program and was supported by grants from the Natural Sciences and Engineering Research Council of Canada and the Canadian Department of Fisheries and Oceans. The technical contribution of P. Joly, M. Boulé, and numerous other Department of Fisheries and Oceans personnel to the collection of BIONESS data is gratefully acknowledged.

References

Andersen, V., and Nival., P. 1991. A model of the diel vertical migration of zooplankton based on euphausiids. J. Mar. Res. **49**: 153–175.

Baliño, B.M., and Aksnes, D.L. 1993. Winter distribution and migration of the sound scattering layers, zooplankton and micronekton in Masfjorden, Western Norway. Mar. Ecol. Prog. Ser. **102**: 35–50.

Chassé, J. 1994. Modélisation tridimensionnelle de la circulation dans l'Estuaire du Saint-Laurent. Ph.D. thesis, Université du Québec à Rimouski, Rimouski, Qué.

Durbin, E.G., Gilman, S.L., Campbell, R.G., and Durbin, A.G. 1995. Abundance, biomass, vertical migration and estimated development rate of the copepod *Calanus finmarchicus* in the southern Gulf of Maine during late spring. Continental Shelf Res. **15**: 571–591.

Eckman, J.E. 1994. Modelling the physical–biological coupling in the ocean: the U.S. GLOBEC program. Deep-Sea Res. II, **41**: 1–5.

El-Sabh, M.I. 1979. The lower St. Lawrence estuary as a physical oceanographic system. Nat. Can. **106**: 55–73.

Enright, J.T. 1977. Copepods in a hurry: sustained high-speed upward migration. Limnol. Oceanogr. **22**: 118–125.

Forrester, W.D. 1974. Internal tides in the St. Lawrence estuary. J. Mar. Res. **32**: 55–66.

Franks, P.J.S. 1992. Sink or swim: accumulation of biomass at fronts. Mar. Ecol. Prog. Ser. **82**: 1–12.

Gorski, P.R., and Dodson, S.I. 1996. Free-swimming *Daphnia pulex* can avoid following Stokes' law. Limnol. Oceanogr. **41**: 1815–1821.

Gratton, Y., Mertz, G., and Gagné, J.A. 1988. Satellite observations of tidal upwelling and mixing in the St. Lawrence estuary. J. Geophys. Res. **93**(C6): 6947–6954.

Hannah, C.G., Naimie, C.E., Loder, J.W., and Werner, F.E. 1998. Upper-ocean transport mechanisms from the Gulf of Maine to Georges Bank, with implications for *Calanus* supply. Continental Shelf Res. **15**: 1887–1912.

Heywood, K.J. 1996. Diel vertical migration of zooplankton in the Northeast Atlantic. J. Plankton Res. **18**: 163–184.

Hill, A.E. 1991. Vertical migration in tidal currents. Mar. Ecol. Prog. Ser. **75**: 39–54.

© 1999 NRC Canada

Hirche, H.J. 1996. Diapause in the marine copepod *Calanus finmarchicus* — a review. Ophelia, **44**: 129–143.

Huntley, M., and Brooks, E.R. 1982. Effects of age and food availability on diel vertical migration of *Calanus pacificus*. Mar. Biol. **71**: 23–31.

Kaartvedt, S. 1996. Habitat preference during overwintering and timing of seasonal vertical migration of *Calanus finmarchicus*. Ophelia, **44**: 145–156.

Kimmerer, W.J., and McKinnon, A.D. 1987. Zooplankton in a marine bay. 2. Vertical migration to maintain horizontal distributions. Mar. Ecol. Prog. Ser. **41**: 53–60.

Koutitonsky, V.G. 1979. Transport de masses d'eau à l'embouchure du Saint-Laurent. Nat. Can. **106**: 75–88.

Koutitonsky, V.G., and Bugden, G.L. 1991. The physical oceanography of the gulf of St. Lawrence: a review with emphasis on the synoptic variability of the motion. *In* The Gulf of St. Lawrence: small ocean or big estuary? *Edited by* J.-C. Therriault. Can. Spec. Publ. Fish. Aquat. Sci. No. 113. pp. 57–90.

Lynch, D.R., Gentleman, W.C., McGillicuddy, D.J., Jr., and Davis, C.S. 1998. Biological/physical simulations of *Calanus finmarchicus* population dynamics in the Gulf of Maine. Mar. Ecol. Prog. Ser. **169**: 189–210.

Mertz, G., Koutitonsky, V.G., Gratton, Y., and El-Sabh, M.I. 1992. Wind-induced eddy motion in the Lower St. Lawrence estuary. Estuarine Coastal Shelf Sci. **34**: 543–556.

Moloney, C.L., and Gibbons, M.J. 1996. Sampling and analysis of gut contents in relation to environmental variability and diel vertical migration by herbivorous zooplankton. J. Plankton Res. **18**: 1535–1556.

Paffenhöfer, G.-A., Strickler, J.R., Lewis, K.D., and Richman, S. 1996. Motion behavior of nauplii and early copepodid stages of marine planktonik copepods. J. Plankton Res. **18**: 1699–1715.

Plourde, S., and Runge, J.A. 1993. Reproduction of the planktonic copepod *Calanus finmarchicus* in the Lower St. Lawrence Estuary: relation to the cycle of phytoplankton production and evidence for a *Calanus* pump. Mar. Ecol. Prog. Ser. **102**: 217–227.

Roach, P.J. 1972. Computational fluid dynamics. Hermosa Publishers, Albuquerque, N.Mex.

Runge, J.A., and Simard, Y. 1990. Zooplankton in the St. Lawrence Estuary: the imprint of physical processes on its composition and distribution. *In* Oceanography of a large-scale estuarine system, the St. Lawrence. *Edited by* M.I. El-Sabh and N. Silverberg. Coastal Estuarine Stud. No. 39. Springer-Verlag, New York. pp. 296–320.

Saiz, E., and Alcaraz, M. 1992. Free-swimming behavior of *Acartia clausi* (Copepoda: Calanoida) under turbulent water movement. Mar. Ecol. Prog. Ser. **80**: 229–236.

Savenkoff, C., Vézina, A.F., and Gratton, Y. 1997. Effect of freshwater pulse on mesoscale circulation and phytoplankton distribution in the lower St. Lawrence estuary. J. Mar. Res. **55**: 353–381.

Simard, Y., deLafontaine, R., and Therriault, J.-C. 1986. Aggregation of euphausiids along a coastal shelf in an upwelling environment. Mar. Ecol. Prog. Ser. **32**: 203–215.

Slagstad, D., and Tande, K.S. 1996. The importance of seasonal vertical migration in across shelf transport of *Calanus finmarchicus*. Ophelia, **44**: 189–205.

Steele, J.H., and Henderson, E.W. 1998. Vertical migration of copepods. J. Plankton Res. **20**: 787–799.

Therriault, J.-C., and Lacroix, G. 1976. Nutrients, chlorophyll, and internal tides in the St. Lawrence Estuary. J. Fish. Res. Board Can. **33**: 2747–2757.

Therriault, J.-C., and Levasseur, M. 1985. Control of phytoplankton production in the lower St. Lawrence estuary: light and freshwater runoff. Nat. Can. **112**: 77–96.

Therriault, J.-C., and Levasseur, M. 1986. Freshwater runoff control of the spatio-temporal distribution of phytoplankton in the Lower St. Lawrence Estuary (Canada). *In* The role of freshwater outflow in coastal marine ecosystems. *Edited by* S. Skreslet. NATO ASI Ser. Vol. G7. Springer-Verlag, Berlin and Heidelberg. pp. 251–260.

Wiebe, P.H., Beardsley, R.C., Mountain, D.G., and Bucklin, A. 1996. Global Ocean Ecosystem Dynamics — initial program in Northwest Atlantic. Sea Technol. **37**: 67–76.

Wishner, K.F., and Allison, S.K. 1986. The distribution and abundance of copepods in relation to the physical structure of the Gulf Stream. Deep-Sea Res. **33**: 705–731.

Wroblewski, J.S. 1982. Interactions of currents and vertical migrations in maintaining *Calanus marshallae* in the Oregon upwelling zone. Deep-Sea Res. **29**: 665–686.

Yamazaki, H., and Squires, K.D. 1996. Comparison of oceanic turbulence and copepod swimming. Mar. Ecol. Prog. Ser. **144**: 299–301.

© 1999 NRC Canada

Simulated and observed response of the southwest Vancouver Island pelagic ecosystem to oceanic conditions in the 1990s

Clifford L.K. Robinson and Daniel M. Ware

Abstract: In this paper, we discuss changes in the ocean climate around La Perouse Bank off southwestern Vancouver Island, British Columbia, and its influence on the functioning of the pelagic ecosystem. We compare results of a one-dimensional simulation model of plankton and fish production and biomass dynamics with empirical data collected in the 1990s. Comparisons of simulation results with empirical data indicate that the La Perouse model can account for relative interannual changes in copepod biomass, euphausiid biomass and production, the consumption of Pacific herring (*Clupea pallasi*) by Pacific hake (*Merluccius productus*), and the growth condition factor of Pacific hake. The model is less successful at capturing changes in spring diatom biomass, the proportion of euphausiids in the Pacific hake diet, and interannual variability in the Pacific herring condition factor. A measure of overall model performance suggests that the La Perouse ecosystem model performs equally well in both strong and weak upwelling periods. The La Perouse ecosystem model has been used to generate an annual index of net phytoplankton and macrozooplankton production for the coastal upwelling region off southwestern Vancouver Island from 1967 to 1998.

Résumé : Dans le présent article, nous traitons des changements dans le climat océanique de la région du banc La Perouse au large du sud-ouest de l'île de Vancouver, en Colombie-Britannique, et de l'impact du climat océanique sur le fonctionnement de l'écosystème pélagique. Nous comparons les résultats d'un modèle de simulation unidimensionnel de la production de plancton et de poissons et de la dynamique de la biomasse avec des données empiriques recueillies dans les années 90. Les comparaisons des résultats de la simulation avec les données empiriques indiquent que le modèle conçu pour le banc La Perouse peut rendre compte des changements interannuels relatifs de la biomasse de copépodes, de la biomasse et de la production d'euphausiacés, de la consommation de hareng du Pacifique (*Clupea pallasi*) par le merlu du Pacifique (*Merluccius productus*) et du coefficient de condition lié à la croissance du merlu du Pacifique. Le modèle rend moins bien compte des changements dans la biomasse printanière de diatomées, de la proportion d'euphausiacés dans le régime alimentaire du merlu du Pacifique et de la variabilité interannuelle du coefficient de condition du hareng du Pacifique. La mesure de la performance globale du modèle appliqué à l'écosystème du banc La Perouse montre que ce modèle est aussi efficace pour les périodes de fortes remontées d'eau que de faibles remontées d'eau. Le modèle de l'écosystème du banc La Perouse a été utilisé pour produire un indice annuel de la production nette de phytoplancton et de macrozooplancton pour la zone côtière de remontée d'eau du sud-ouest de l'île de Vancouver de 1967 à 1998.

[Traduit par la Rédaction]

Introduction

Ocean climate events during the 1990s have resulted in two of the six largest annual sea surface temperature (SST) anomalies (1992 and 1997 El Niños) measured at Amphitrite Point lighthouse on southwestern Vancouver Island, British Columbia, since 1935. There are well-documented linkages between water temperatures at Amphitrite Point and other environmental factors such as coastal upwelling and between temperatures and the structure and functioning of the La Perouse Bank pelagic ecosystem (Fig. 1) (Robinson 1994; Ware and McFarlane 1995). Major changes in this productive coastal upwelling system can therefore be expected from the highly positive SST anomalies measured during the 1990s.

Coupled with changes in the physical environment off southwestern Vancouver Island are changes in the La Perouse pelagic fish community. Recent observations indicate that there have been increased biomasses of migratory chub mackerel (*Scomber japonicus*), a reappearance of the Pacific sardine (*Sardinops sagax*) (Hargreaves et al. 1994), and more abundant, smaller migratory Pacific hake (*Merluccius productus*) (Ware and McFarlane 1995). It is also apparent that the La Perouse ecosystem has undergone significant changes in its production dynamics. Pacific herring (*Clupea pallasi*) stocks have experienced poorer growth in the 1990s, which is suspected to be linked to a decline in the availability of a key zooplanktonic prey, the euphausiids (Tanasichuk 1997). Tanasichuk (1998) provided further support for this hypothesis by showing an 80% reduction in the biomass of

Received July 16, 1998. Accepted February 19, 1999.
J14695

C.L.K. Robinson.[1] Northwest Ecosystems Institute, Box 513, Lantzville, BC V0R 2H0, Canada.
D.M. Ware. Department of Fisheries and Oceans, Pacific Biological Station, Nanaimo, BC V9R 5K6, Canada.

[1]Author to whom all correspondence should be addressed.
e-mail: clkrnei@island.net

© 1999 NRC Canada

Fig. 1. Location of the La Perouse ecosystem off southwestern Vancouver Island, British Columbia, Canada.

the euphausiids *Euphausia pacifica* and *Thysanoessa spinifera* during the 1991–1997 upwelling seasons. Together, the observed changes in the fish community and in lower trophic levels in the La Perouse Bank region warrant further investigation because of the importance of this area in supporting major commercial fisheries (Ware and McFarlane 1995).

One tool that has been developed to explore the linkages between ocean climate variability and zooplankton and pelagic fish production in this coastal upwelling system is the La Perouse Bank ecosystem model (Robinson 1994; Robinson and Ware 1994). This one-dimensional simulation model of dominant pelagic fish and plankton species calculates the daily biomass and production of species pools and is forced by weekly observations in SST, solar radiation, and upwelling conditions and by seasonal changes in fish biomass. The model was initially developed using data collected by Canadian Department of Fisheries and Oceans (DFO) surveys during 1985–1990. See Robinson (1994) and Robinson and Ware (1994) for further discussion of the La Perouse simulation model and Ware and McFarlane (1995) and McFarlane et al. (1997) for a detailed discussion about the La Perouse Bank surveys and upwelling ecosystem.

The main objectives of this paper are to (*i*) use updated environmental and fish time series in the La Perouse ecosystem model to generate simulated estimates of plankton biomass and production, (*ii*) test the predictive capability of the model by comparing model results with independently derived estimates of plankton biomass and fish consumption and body condition during the 1990s, and (*iii*) outline the future expansion of the La Perouse model to include the northern Vancouver Island continental shelf as part of the Canadian GLOBEC WestSea modelling program.

© 1999 NRC Canada

Fig. 2. Overview of major feeding interactions and environmental forcing functions included in the La Perouse ecosystem model. Refer to Robinson and Ware (1994) for a detailed discussion of the model.

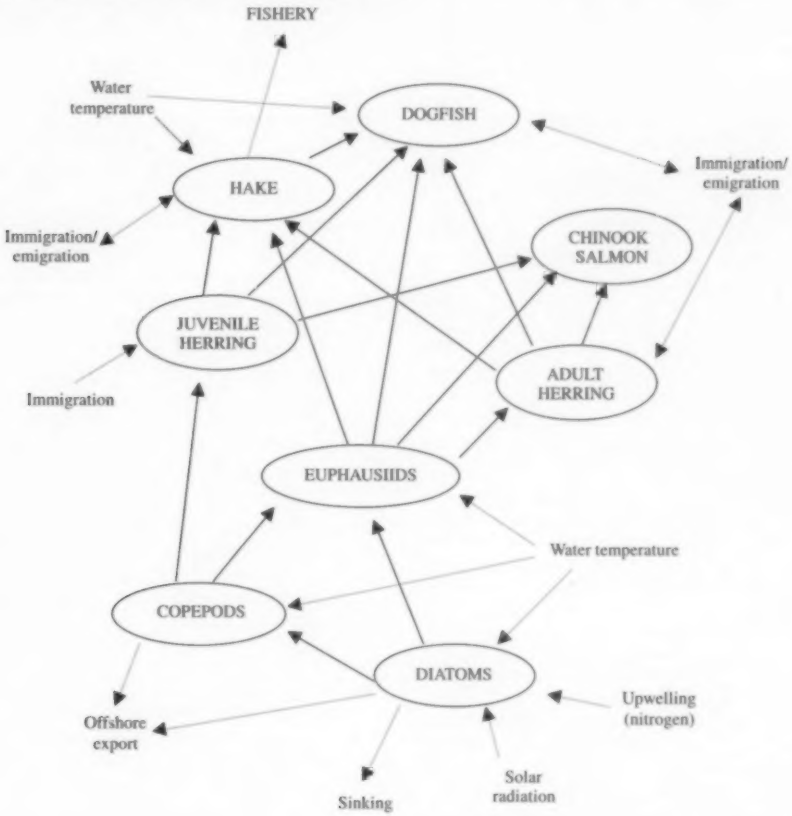

Methods

The La Perouse Bank ecosystem model was developed to estimate daily plankton and fish production in relation to interannual variability in ocean climate (Robinson and Ware 1994). Model simulations were conducted from 1972 to 1990 (Robinson 1994) and are extended here to 1997. The model was run for each year independently from January 1 to December 31. Simulation results indicate that plankton model parameter values from one year have little impact on production dynamics simulated the next year (Robinson 1994), and so the same initial (January 1) plankton biomasses and ingestion parameters were used each year from 1972 to 1997. The model units of grams carbon per square metre were converted to tonnes wet weight per square kilometre assuming that 6.75% of wet weight is carbon and that 1 t wet weight·km^{-2} = 1 g wet weight·m^{-2}.

The trophodynamical interactions of eight species pools included in the La Perouse Bank model are shown in Fig. 2. The fish–fish and fish–zooplankton feeding interactions have been well described by field studies (Tanasichuk et al. 1991; Ware and McFarlane 1995). The plankton–plankton feeding interactions are not well known in the La Perouse region but have been inferred from studies conducted in other coastal upwelling regions that have similar pelagic community structure (e.g., southern Benguela Current). Copepods (e.g., *Calanus* spp.) and euphausiids (*Euphausia* spp.) in coastal upwelling systems are known to feed primarily on phytoplankton, such as the diatoms (Parsons et al. 1984). Euphausiids are also known to feed on smaller stages of copepods (e.g., nauplii), especially when diatoms are not as abundant (Pillar et al. 1992). In the La Perouse model, euphausiids feed on an arbitrary maximum proportion (40%) of copepods. This proportion in the diet is fully realized when the copepod biomass is high relative to diatom biomass.

The trophodynamical interactions are forced by three environmental factors: SST, solar radiation, and wind-forced upwelling. Daily SSTs for Amphitrite Point lighthouse were obtained from H. Freeland, DFO, Institute of Ocean Science, Sydney, B.C. Weekly averages were calculated from daily values, starting January 1 for each year from 1972 to 1997. Daily values of bright sunshine from Tofino airport were obtained from Environment Canada, Climate Data Services, Vancouver, B.C. Weekly averages were calculated from the daily values, starting January 1 for each year from 1972 to 1997. Hours of bright sunshine were converted to surface radiation using the following equation: radiation (g cal·m^{-2}) = 31.3 + 5.06 × SS, where SS is a tenth of an hour of bright sunshine (r^2 = 0.90; Robinson 1994). The relative magnitude of upwelling and offshore Ekman transport used in the La Perouse model was estimated from the Bakun upwelling index (BUI). Daily BUI values (cubic metres per second per 100 m of coastline) were obtained for a station at 48°N, 125°W from the U.S. Navy Fleet Numerical Meteorological and Oceanographic Center, Monterey, Calif. Weekly averages were calculated from the daily values, starting January 1 for each year from 1972 to 1997.

The La Perouse Bank ecosystem model also requires seasonal and interannual estimates of Pacific hake and Pacific herring biomass. Robinson and Ware (1994) assumed that adult herring forag-

© 1999 NRC Canada

ing in the La Perouse region originate primarily from the southwestern coast of Vancouver Island (Barkley Sound) and secondarily from the southern Strait of Georgia. Stock biomass (spawners and catch) for each region from 1972 to 1997 was taken from Schweigert et al. (1998). A herring production simulation model (D.M. Ware, unpublished data) was used to estimate that juvenile herring biomass (ages 0+ and 1+) is, on average, 63% of the biomass of adult herring (ages 2+ to 9+). Note that the annual estimates of juvenile and adult herring biomass presented here for 1972–1990 differ slightly from the values used in Robinson and Ware (1994). However, sensitivity analyses indicated that the revised 1972–1990 herring biomass pattern had relatively little impact on interannual plankton production trends. The correlation between the revised and original model output for diatoms is r = 0.86, for copepods is r = 0.93, and for euphausiids is r = 0.94. Hake biomass in the La Perouse region was estimated using an empirical relationship derived by Ware and McFarlane (1995): initial biomass of migratory hake (kilotonnes) = June–July average SST × 196.4 – 2231.8. It was assumed that if the June–July average SST was <11.9°C, then hake biomass was 100 kt. Foreign, domestic, and joint venture hake catches for the west coast of Vancouver Island were taken from Rutherford (1996).

Recent biological sampling

Spatially averaged estimates of chlorophyll *a* concentrations for the La Perouse region were obtained from the Japanese National Space Development Agency's Ocean Color and Temperature Scanner (OCTS) located onboard the Advanced Earth Observing Satellite. The data were processed and analyzed by Ecosat Geobotanical Surveys Inc., Richmond, B.C. OCTS chlorophyll *a* concentration anomalies were compared with simulated diatom biomass anomalies from early March to mid-May (11 weeks) in 1997.

The longest available time series of copepod biomass data for the La Perouse region has been assembled by Mackas (1995 and unpublished data), who calculated a shelf copepod biomass anomaly (deviations from the long-term seasonal average) for the period 1985–1995. In this study, we used the copepod biomass anomalies that Mackas calculated from zooplankton samples collected from June to September (the majority of sampling was conducted in August).

Tanasichuk (1998) measured the biomass and production of the euphausiid *T. spinifera* during the upwelling season (June–October) in Barkley Sound, near the La Perouse region. He conducted bongo net sampling several times per month during the upwelling season from 1991 to 1997 to estimate adult euphausiid (>10 mm) biomass. Tanasichuk measured biomass and production as the sum of growth and molting. We converted Tanasichuk's euphausiid biomass estimates from milligrams dry weight per square metre to grams carbon per square metre, assuming that carbon is 40% of dry mass.

Studies have shown that the major primary and secondary prey of hake, by mass, are euphausiids and herring, respectively (Tanasichuk et al. 1991; Ware and McFarlane 1995). DFO has collected stomach contents data for hake in the La Perouse region during August annually since 1985. Stomach contents data have been used to calculate the tonnes of euphausiids and herring consumed per tonne of hake during August. August consumption (C_A) was calculated using the Elliot–Persson equation in Tanasichuk et al. (1991): C_A = 24h × 31d × MSFI × R × B_h, where h is hours, d is days, R is hourly hake ration (0.02% body weight·h^{-1}), B_h is hake biomass in August (tonnes), and MSFI is the mean stomach fullness index expressed as a percentage of hake body mass. The MSFI is weighted by the relative abundance of hake in the area where samples were collected.

Results and discussion

In the sections below, we compare model predictions with recent observations for the following components: (*i*) diatom biomass, (*ii*) copepod biomass, (*iii*) euphausiid biomass and production, (*iv*) Pacific hake biomass, (*v*) consumption of euphausiids and Pacific herring by Pacific hake, and (*vi*) Pacific hake and Pacific herring condition factors.

Diatom biomass

The model predicts a higher and longer lasting spring bloom than indicated by the OCTS peak around day 96 (Fig. 3*a*). The OCTS data also indicate two small phytoplankton blooms between days 103 and 138, while the simulated diatom biomass was flatter during this period. The model captures most of the timing and duration of the first major diatom bloom caused by upwelling when the OCTS data were compared with model output for the start of the upwelling period (days 138–166; Fig 3*a*). When the OCTS data are compared with weekly averages of environmental data, there is a significant positive correlation with sunshine (r = 0.75; Fig 3*b*). There is also a positive correspondence between the temporal pattern in OCTS chlorophyll *a* concentrations and the weekly averaged BUI (r = 0.47, p = 0.15) but no relationship between water temperature and OCTS data. At present, the simplified assumptions used in the model concerning available light are likely not fully capturing the observed phytoplankton dynamics. Unfortunately, few data are currently available to rectify this weakness in the model.

Copepod biomass

There is a significant correlation (r = 0.97, p < 0.01) between the average simulated August copepod biomass and the Mackas shelf copepod biomass anomaly between 1985 and 1993. However, the correlation degrades to r = 0.42 (p = 0.19) when data from 1994 and 1995 are included (Fig. 4). The discrepancy between the simulated and observed results in 1994 and 1995 is due to very high simulated August copepod biomass and a very low observed biomass. The high simulated copepod biomass can be directly related to a substantial reduction in upwelling observed in August 1994 and 1995; upwelling in August 1994 was the second lowest and in 1995 the fourth lowest recorded in the 31-year BUI record. In the La Perouse region (and in the model), copepod biomass is transported offshore as a positive function of upwelling (Mackas 1992; Robinson 1994). Thus, when upwelling is low, copepod biomass should accumulate in the La Perouse region.

A reduction in offshore transport, however, does not explain the low field estimates of copepod biomass observed in 1994 and 1995 (Fig. 4). The field estimates of copepod biomass are derived for relatively large (meso)zooplankton species such *as Calanus marshallae*, *Pseudocalanus* spp., and *Acartia longiremis* (Mackas 1995). The field data suggest that the biomass of mesozooplankton in the La Perouse region is lower with reduced upwelling. It is well known that zooplankton community structure is tightly coupled with upwelling dynamics (Parsons et al. 1984; and below). However, because zooplankton in the La Perouse region have usually been sampled with relatively large-meshed nets (e.g., 0.22 mm), a lack of data precludes testing for an expected increase in microzooplankton biomass with reduced upwelling. Overall, it is likely that the model fails to predict changes in

© 1999 NRC Canada

Fig. 3. Comparison of simulated diatom biomass with OCTS-derived chlorophyll *a* concentrations for the spring (March–May) of 1997. The bottom panel shows the relationship between OCTS chlorophyll *a* concentrations and weekly averaged hours of bright sunshine ($r = 0.75$, $p < 0.01$).

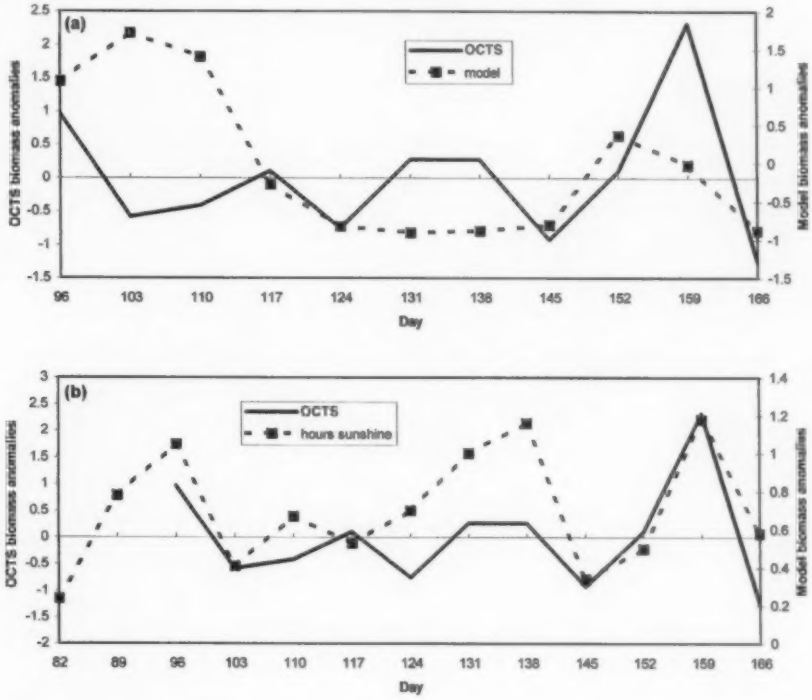

copepod biomass in 1994 and 1995 because of potential changes in the size structure of the zooplankton community in response to substantial reductions in upwelling. The microbial loop community may be more prominent when upwelling is low (Painting et al. 1993).

Euphausiid biomass and production

There are significant positive correlations between simulated and field estimates of *T. spinifera* biomass and production ($r = 0.81$, $p < 0.01$ and $r = 0.87$, $p < 0.01$, respectively). Thus, the simplified assumptions used in the La Perouse model seem to capture the relative interannual variability in coastal euphausiid production and biomass (Fig. 5). The La Perouse model, however, simulates on average a five times higher absolute euphausiid biomass and a three times higher production than Tanasichuk (1998) measured in the field. We would expect a priori that field estimates of adult euphausiid biomass sampled using bongo nets would have high coefficients of variability (Shaw and Robinson 1998), and so the apparent differences between simulated and field estimates are not unreasonable.

The discrepancy between simulated and field estimates of euphausiid production is likely due to the methods used. Tanasichuk (1998) calculated adult euphausiid production from field data as the sum of growth and molting. This approach assumes that instantaneous growth rates can be determined from measures of population size structure over time. However, the assumption of sampling the same euphausiid population over time is dubious given their patchiness and the limitations of bongo net sampling (Shaw and Robinson 1998). Robinson and Ware (1994) used a different method for estimating euphausiid production. It is well known that production can be estimated by summing losses due to mortality over a specified interval (Parsons et al. 1984). Thus, $P = (B_t - B_0) + E$, where P is production, B_t is biomass at time t, B_0 is biomass at the start, and E is the biomass loss through mortality. In model simulations, euphausiid biomass on December 31 is within 5% of euphausiid biomass on January 1; hence, a summation of euphausiid mortality during the year yields an estimate of production. We assumed that the majority of euphausiid mortality is due to predation from resident and migratory fish, based on sampling more than 30 000 stomachs since 1985 (Ware and McFarlane 1995). We conclude that the different methods used for calculating production are responsible for the discrepancy between the simulated and field estimates of euphausiid production and that estimates based on fish consumption may be more realistic.

A recent study by Iguchi and Ikeda (1995) found that the net growth efficiency of the euphausiid *E. pacifica* is about 35% at temperatures between 10 and 15°C. This result is important because it indicates that production estimates of euphausiids may be higher than we previously assumed (Robinson and Ware 1994). In the La Perouse Bank model, euphausiid production was calculated as a function of the ingestion rate and gross growth efficiency (GGE). Note that GGE is roughly 90% of net growth efficiency (Parsons et al. 1984). The highest estimate of GGE used in simulations when the model was developed was 25%. At this GGE, the

© 1999 NRC Canada

Fig. 4. Relationship between simulated August copepod biomass and shelf annual copepod biomass anomaly (Mackas 1995 and unpublished data).

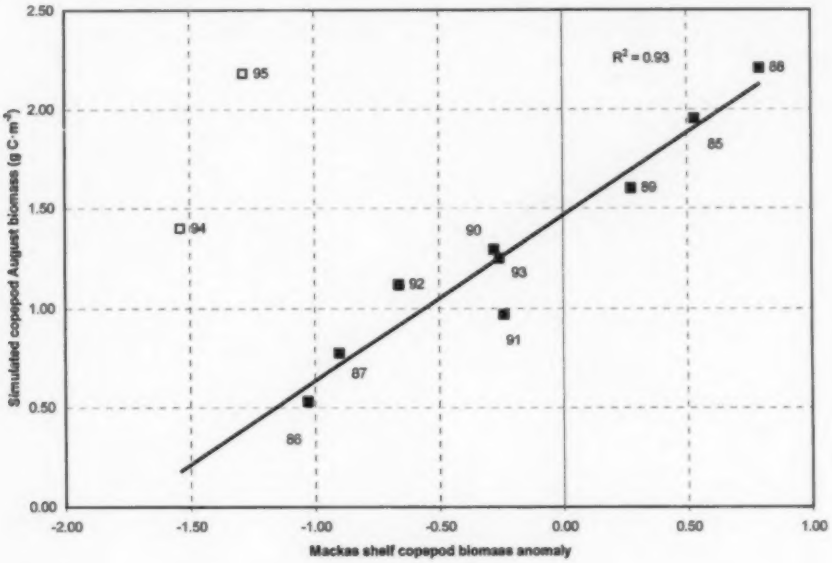

Fig. 5. Comparison of the simulated versus observed trend in euphausiid biomass from 1991 to 1997. Observed data from Tanasichuk (1998).

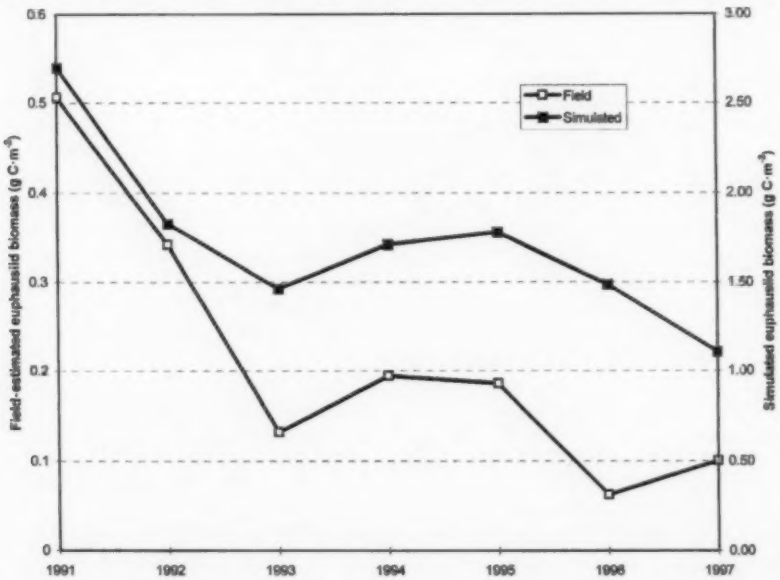

euphausiid pool required additional biomass to offset predation pressure from pelagic fish predators. Robinson and Ware (1994) hypothesized a regional mechanism of importation and accumulation of euphausiids in the La Perouse region to offset the high mortality caused by fish predation. If a higher euphausiid GGE of 32% (Iguchi and Ikeda 1995) is used in model simulations, then there is no requirement for additional import of euphausiids from surrounding regions to balance the mortality rate. The demand for euphausiids by pelagic fish predators in the La Perouse region can be met by the newly obtained and higher estimates of euphausiid growth.

Pacific hake biomass

The validity of the SST function used to estimate hake biomass was tested by comparing values with estimates made from DFO hydroacoustic surveys in the La Perouse region from 1983 to 1994. There is a significant positive correlation

© 1999 NRC Canada

Fig. 6. Relationship between simulated tonnes of Pacific herring eaten per tonne of Pacific hake per day versus the observed proportion of herring in hake stomachs (MSFIH) collected in the La Perouse region in August of each year since 1985.

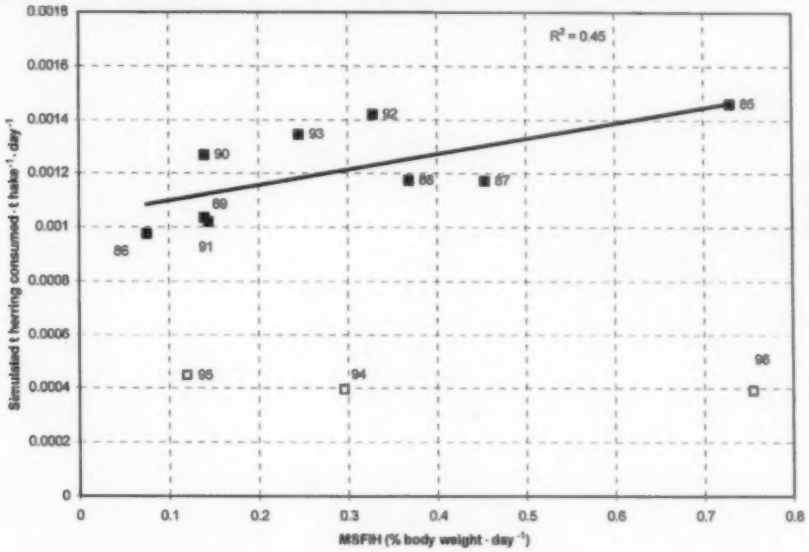

between SST-derived hake biomass and hydroacoustically derived hake biomass estimates ($r = 0.79$, $p < 0.05$, $n = 11$). To understand the potential influence of different hake biomass estimates on model results, we compared plankton and fish production simulated using hake biomass estimates from the SST function and from hydroacoustic data. Simulation results indicate that very similar interannual patterns in plankton and fish production are generated (diatoms, $r = 0.93$; copepods, $r = 0.96$; euphausiids, $r = 0.89$; juvenile herring, $r = 0.94$; adult herring, $r = 0.84$; hake, $r = 0.98$). We conclude that the hake biomass – SST relationship provides a reasonable estimate of hake biomass in the La Perouse region in summer. The utility of this relationship is that it can be used to hindcast hake biomass for periods when hydroacoustic and trawl surveys were not conducted (pre-1983).

Consumption of prey by Pacific hake

There is a significant positive correlation between field estimates of the hake MSFI for herring and the simulated tonnes of herring consumed per tonne of hake from 1985 to 1993. ($R^2 = 0.46$, $p < 0.05$). However, this correlation degrades to an $R^2 = 0.01$ when data from 1994–96 are included (Fig. 6). The correlation breaks down because the model consistently underestimates the consumption of herring in 1994, 1995, and 1996, while field observations indicate a wide and higher range of consumption of herring by hake. The ingestion of herring by model hake is a function of the relationship between hake and euphausiids (Robinson and Ware 1994). The more euphausiids consumed by hake, the fewer herring are consumed and vice versa. Additionally, the biomass of hake in the La Perouse region is inversely related to euphausiid biomass. When euphausiid biomass is low, hake migrate from the La Perouse region to richer feeding areas along the shelf break (Ware and McFarlane 1995), so the consumption of herring should decrease. Because simulated estimates of euphausiid biomass agree with observed estimates (see Fig. 5), the underestimated consumption of herring by model hake is most likely due to simplified assumptions used regarding the across- and along-shelf movements of hake in the La Perouse region.

Model estimates of euphausiids consumed by hake do not agree well with the observed hake MSFI for euphausiids. The discrepancy may be due to the fact that the model assumes a constant size-averaged hake population, while recent data indicate that the proportion of the hake stock consisting of hake <50 cm can range from 35 to 82%. Smaller hake feed primarily on euphausiids, and thus, large temporal changes in the proportion of small hake biomass will have substantial influences on the observed MSFI euphausiid values. The relationship between MSFI for herring in hake versus August SST was discussed by Ware and McFarlane (1995) for the period 1983–1991. We have updated this time series to 1996 and note that the dome-shaped relationship previously identified still exists. The ingestion of herring by hake is related to water temperature, and it peaks at between 13.6 and 14°C. At temperatures above 14.2°C the percentage of herring in the hake diet decreases. This may be due to the increased presence of a higher number of smaller (<50 cm) euphausiid-feeding hake in the La Perouse region during warmer summers ($r = 0.58$, $p < 0.05$) and to changes in hake distribution in warm summers (Ware and McFarlane 1995).

Pacific hake and Pacific herring condition factor

Hake condition factor (K) was calculated from the average mass and length of hake caught by DFO in the La Perouse region in August using the following relationship: $K = W/L^3$, where W is mass (grams) and L is length (centimetres). High values of K imply that hake have experienced good growing conditions. There is a significant positive correlation between the observed hake condition factor and simulated hake production during the upwelling season ($r = 0.68$, $p < 0.01$) for the period 1983–1996 (Fig. 7). The two variables are

© 1999 NRC Canada

Fig. 7. Relationship between the observed offshore Pacific hake condition factor and simulated hake production.

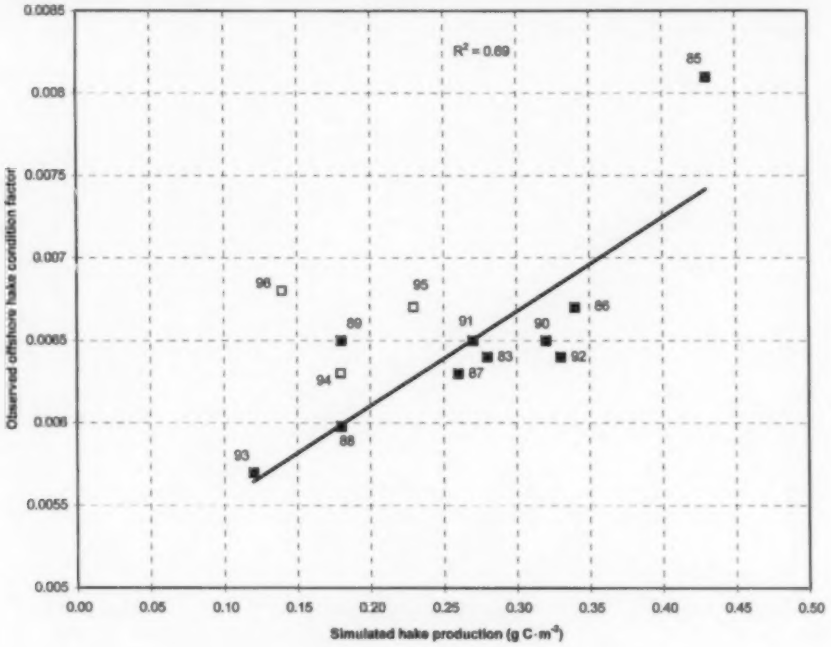

even more strongly correlated when data from the anomalous years 1994, 1995, and 1996 are excluded ($r = 0.84$). The observed hake condition factor is most strongly related to the August biomass model of euphausiids.

The condition factor of > age 2+ herring was also calculated from mass and length data collected by DFO in the La Perouse region in August 1985–1996. In this case, there was no relationship between the observed herring condition factor and simulated herring production. The strongest correlation was found in July ($r = 0.42$, $p = 0.21$). Observed herring condition factor was also not correlated with any zooplankton output from the model.

An evaluation of observed fish condition factors with the environmental time series indicates that herring condition is significantly, positively correlated with the August–September average SST ($r = 0.87$, $p < 0.01$; Fig. 8), while hake condition is negatively correlated with June SST ($r = -0.58$, $p < 0.05$). We expected a strong correlation between herring condition and the state of the environment during the August–September herring growing season (August–September; Tanasichuk 1997). The negative correlation between hake condition and June SST may be a density effect. Recall that a 1° increase in water temperature in early summer roughly corresponds to a 170-kt increase in hake biomass (Ware and McFarlane 1995). Thus, all else being equal, a warmer June would correspond to more hake in the La Perouse region and subsequently a lower condition of each hake.

Summary of model results versus observations

Several strengths and weaknesses of the La Perouse ecosystem model in representing the real world are apparent when simulated output is compared with empirical data. The three main weaknesses of the model that need addressing are the (*i*) important influence of light conditions and mixed layer depth on spring bloom dynamics of diatoms, (*ii*) proportion of euphausiids in the hake diet, and (*iii*) interannual variability in herring condition factor. The major strengths of the La Perouse model have been demonstrated by its ability to account for relative changes in several key biological properties. The model adequately describes (*i*) interannual variability in copepod biomass, (*ii*) interannual variability in euphausiid biomass and production, (*iii*) relative consumption of herring by hake, and (*iv*) hake condition factor.

A major finding is that the interannual variability in copepod biomass was well described by the model from the mid-1980s to 1993 (Fig. 4) but not in 1994 and 1995 when there was a substantial decrease in upwelling intensity in August. This result suggests that model structure (and performance) may be more suited to periods exhibiting stronger upwelling. We tested for this by developing a measure of model performance and by comparing the measure with monthly upwelling intensity. The model performance measure was calculated for each year as the sum of residual errors from four relationships: (*i*) the Mackas copepod anomaly versus simulated August copepod biomass (Fig. 4), (*ii*) the observed versus simulated euphausiid biomass (Fig. 5), (*iii*) the hake MSFIH versus the simulated tonnes of herring consumed per tonne of hake per day (Fig. 6), and (*iv*) the simulated hake versus observed hake condition factor (Fig. 7). Figure 9 shows a nonsignificant negative correlation between the measure of model performance and the strength of upwelling. The model performs equally well in years of low upwelling compared with years of stronger upwelling.

The overall model performance is not substantially affected by the intensity of upwelling, but the performance in

© 1999 NRC Canada

Fig. 8. Relationship between the observed Pacific herring condition factor and the average August–September SST at Amphitrite Point lighthouse.

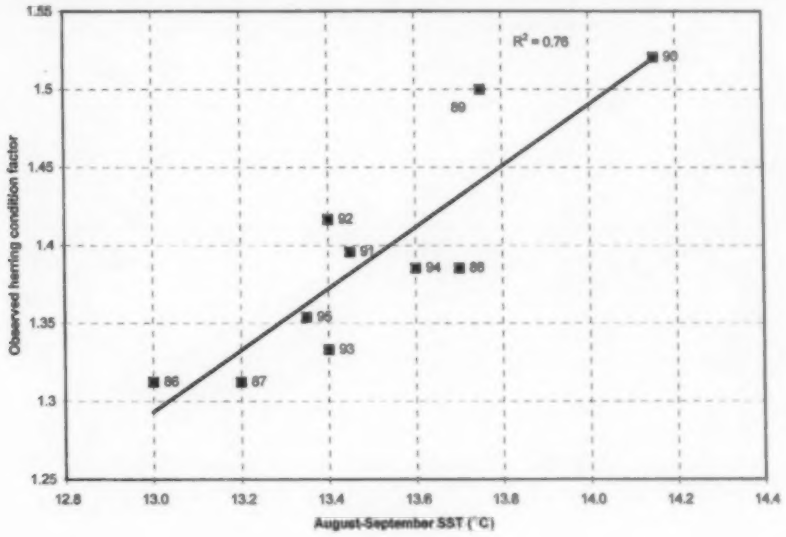

Fig. 9. Relative measure of the overall performance of the La Perouse ecosystem model plotted against the averaged June–October BUI for 1985–1996. The correlation coefficient $r = -0.09$ is not significant.

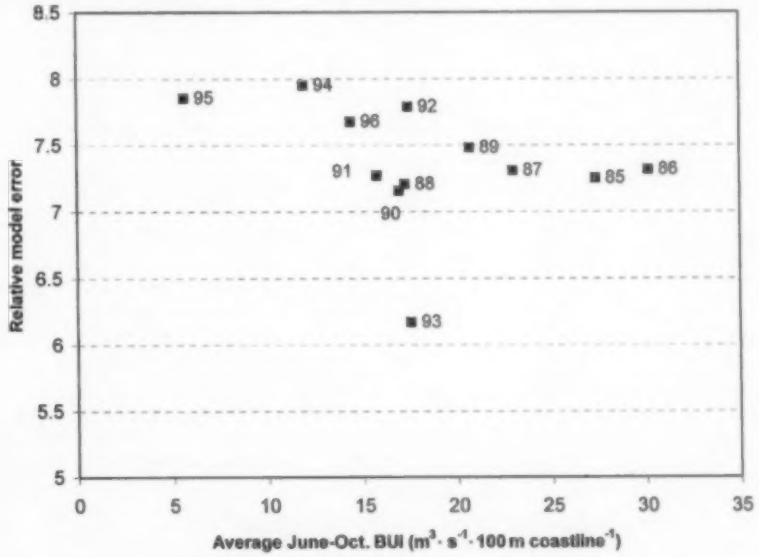

predicting copepod biomass is significantly affected by the intensity of upwelling. As alluded to above, we suspect that there could be a substantial change in mesoplankton biomass with changes in upwelling. In the southern Benguela coastal upwelling region, the biomass of mesozooplankton is inversely correlated with gross primary production as determined by upwelling (Verheye et al. 1992). The change in mesozooplankton biomass in relation to upwelling is likely a reflection of additional changes in plankton food web structure. During periods of upwelling, netphytoplankton (e.g., diatoms), mesozooplankton, and macrozooplankton dominate plankton communities, while nanophytoplankton (e.g., microflagellates) and microzooplankton dominate during quiescent periods. Brodeur and Pearcy (1992) have also suggested that there are major changes in the taxonomic composition of the diet of many pelagic fishes in coastal upwelling areas off Washington and Oregon in relation to upwelling intensity. During strong upwelling, pelagic fishes are highly dependant on euphausiids, but they have higher trophic diversity in years of reduced upwelling. This agrees with model estimates of reduced euphausiid biomass in years of reduced upwelling (Fig. 5).

© 1999 NRC Canada

Fig. 10. Index of annual diatom and euphausiid production for the La Perouse region from 1968 to 1998. Updated from Robinson (1994).

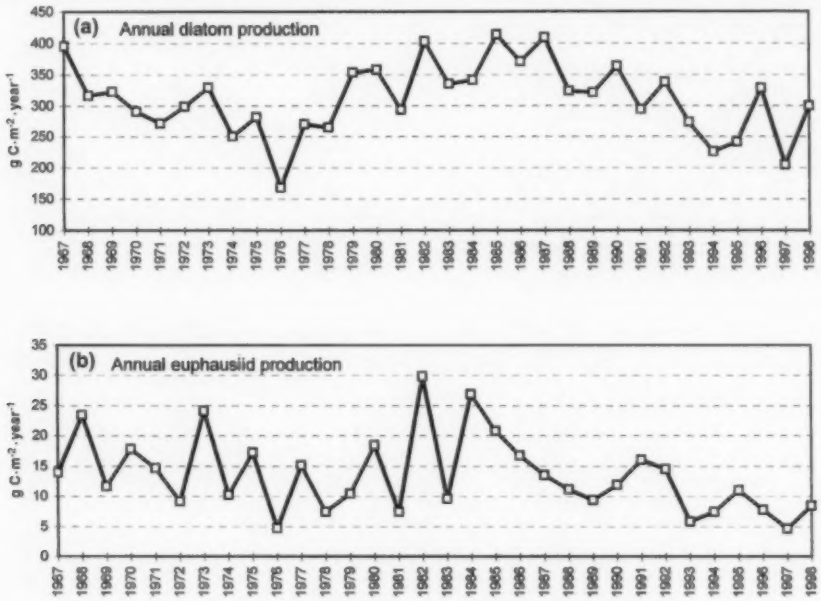

We conclude that the species pools and feeding interactions presently included in the La Perouse ecosystem model are capable of describing changes in netphytoplankton, macrozooplankton, and pelagic fish biomass or production over a wide range of upwelling conditions. However, the model is less capable of predicting changes in mesozooplankton over a wide range of upwelling conditions. This model deficiency may be related to changes in plankton community structure and can only be assessed by a field program designed to sample nanophytoplankton, microzooplankton, and other components of the microbial food web.

An index of plankton production

It is frequently hypothesized that temporal changes in ocean climate affect zooplankton biomass or production, which in turn impacts fish populations (see articles in Beamish 1995). However, very few long-term plankton time series exist to test this hypothesis. In this paper, we have provided evidence that the La Perouse ecosystem model reasonably captures the production dynamics of netphytoplankton and macrozooplankton observed off southwestern Vancouver Island. Below, we discuss the utility of using the La Perouse model to generate an index of annual diatom and euphausiid production for southwestern Vancouver Island. We have obtained environmental and fishery data required to force the model (see Methods) for the period 1967–1998. The intent of the index is to provide researchers with an independent source of plankton data for testing hypotheses about marine fish production variability.

The simulated response of the La Perouse ecosystem to observed changes in ocean climate over the period 1967–1998 is shown in Fig. 10. The La Perouse model indicates that diatom production dropped from about 400 g $C \cdot m^{-2} \cdot year^{-1}$ in 1967 to a low of about 160 g $C \cdot m^{-2} \cdot year^{-1}$ in 1976, while peaking again 9 years later in 1985 at 410 g $C \cdot m^{-2} \cdot year^{-1}$ (Fig. 10). After that, diatom production declined by half to a low of about 200 g $C \cdot m^{-2} \cdot year^{-1}$ in 1997. Annual euphausiid production is more variable than diatom production (coefficient of variation of 47 versus 18%, respectively) and exhibited a sixfold decline from its peak in annual production in 1982 to a low in annual production in 1997.

The simulated time series of plankton production indicates two important trends. First, there has been a substantial and relatively steady decline in diatom and euphausiid production since the early to mid-1980s. The decline is primarily a result of a major reduction in upwelling intensity, as measured by the BUI (Fig. 9). In general, average coastal upwelling peaked during the June–October upwelling seasons of 1985 and 1986 at 27 and 30 $m^{-3} \cdot s^{-1}$ per 100 m of coastline, respectively. After 1986, there was a steady decline in coastal upwelling to a 32-year low (and only negative) BUI value in 1997 of –7.8 $m^{-3} \cdot s^{-1}$ per 100 m of coastline. Second, simulated annual diatom and euphausiid production estimates of the La Perouse ecosystem in 1997 were the second lowest and the lowest, respectively, in the 32-year production time series. We anticipate that the extremely unproductive state of the La Perouse pelagic ecosystem during the extreme 1997 El Niño event may have significant negative impacts on future returns of resident and migratory fish such as Pacific herring and Pacific salmon, respectively.

Future research

Given the observed dramatic decline in euphausiid biomass and production, and the simulated current low productivity state of the pelagic ecosystem, there is an urgent need to further investigate the impacts of short- and long-term variability in ocean climate on the recruitment and production forecasts of commercially important west coast pelagic

© 1999 NRC Canada

fish stocks (e.g., hake, herring, and salmon) and to improve our understanding of the plankton production processes. The La Perouse Bank ecosystem model provides a template upon which to build a more realistic fishery management tool. Under the Canadian GLOBEC WestSea research program, the La Perouse Bank ecosystem model will be coupled with a fully nonlinear, three-dimensional, prognostic finite-element physical oceanographic model (QUODDY; Lynch et al. 1996). The QUODDY model will be capable of simulating the transition between upwelling and downwelling regimes, variability in upwelling magnitude, horizontal transport, mixed layer depth, and water temperatures. The physical model domain will span the latitudinal range of 47–52° and extend about 100 km beyond the continental slope. Output from QUODDY will be used to force the West Coast Vancouver Island ecosystem model.

The WestSea modelling program will result in several important advancements in our understanding of the functioning of the West Coast Vancouver Island shelf and shelf break production systems. The program has several components, including (*i*) particle tracking studies of nutrient inputs and zooplankton accumulations (see Smith et al. 1999), (*ii*) temporal and spatial evaluations of phytoplankton biomass and production, (*iii*) development of a new algorithm for calculating mixed layer depth, (*iv*) assembly and synthesis of existing fishery and zooplankton data for northern Vancouver Island, (*v*) enhancement of the La Perouse Bank ecosystem model, (*vi*) linking of inner and outer, northern and southern shelf ecosystem models, and (*vii*) incorporation of other biological components like juvenile salmon. The coupled biophysical model will be used prognostically to forecast ecosystem production trends based on physical forcing of the lower trophic levels and natural and anthropogenic forcing of the higher trophic levels given a highly variable coastal ocean climate.

Acknowledgments

Funding for this study was provided by the Natural Sciences and Engineering Research Council of Canada and DFO funded Canada GLOBEC WestSea research program. We wish to thank H. Freeland for providing SST anomaly data for Amphitrite Point and R. Tanasichuk for providing euphausiid biomass data. Dr. R. Brodeur and an anonymous reviewer provided suggestions for improving the manuscript.

References

Beamish, R.J. (*Editor*).1995. Climate changes and northern fish populations. Can. Spec. Publ. Fish. Aquat. Sci. No. 121.

Brodeur, R.D., and Pearcy, W.G. 1992. Effects of environmental variability on trophic interactions and food web structure in a pelagic upwelling ecosystem. Mar. Ecol. Prog. Ser. **84**: 101–119.

Hargreaves, N.B., Ware, D.M., and McFarlane, G.A. 1994. Return of the Pacific sardine (*Sardinops sagax*) to the British Columbia coast in 1992. Can. J. Fish. Aquat. Sci. **51**: 460–463.

Iguchi, N., and Ikeda, T. 1995. Growth, metabolism and growth efficiency of a euphausiid crustacean *Euphausia pacifica* in the southern Japan Sea, as influenced by temperature. J. Plankton Res. **17**: 1757–1769.

Lynch, D.R., Ip, J.T.C., Naimie, C.E., and Werner, F.E. 1996. Comprehensive coastal circulation model with application to the Gulf of Maine. Continental Shelf Res. **16**: 875–906.

Mackas, D.L. 1992. The seasonal cycle of zooplankton off southwestern British Columbia: 1979–89. Can. J. Fish. Aquat. Sci. **49**: 903–921.

Mackas, D.L. 1995. Interannual variability of the zooplankton community off southern Vancouver Island. *In* Climate change and northern fish populations. *Edited by* R.J. Beamish. Can. Spec. Publ. Fish. Aquat. Sci. No. 121. pp. 603–615.

McFarlane, G.A., Ware, D.M., Thomson, R.E., Mackas, D.L., and Robinson, C.L.K. 1997. Physical, biological and fisheries oceanography of a large ecosystem (west coast of Vancouver Island) and implications for management. Oceanol. Acta, **20**: 191–200.

Painting, S.J., Moloney, C.L., Probyn, T.A., and Tibbles, B. 1993. Microheterotrophic pathways in the southern Benguela upwelling system. S. Afr. J. Mar. Sci. **12**: 527–543.

Parsons, T.R., Takahashi, M., and Hargrave, B. 1984. Biological oceanographic processes. Pergamon Press, New York.

Pillar, S.C., Stuart, V., Barange, M., and Gibbons, M.J. 1992. Community structure and trophic ecology of euphausiids in the Benguela ecosystem. S. Afr. J. Mar. Sci. **12**: 393–409.

Robinson, C.L.K. 1994. The influence of ocean climate on coastal plankton and fish production. Fish. Oceanogr. **3**:159–171.

Robinson, C.L.K., and Ware, D.M. 1994. Modelling pelagic fish and plankton trophodynamics off south-western Vancouver Island, British Columbia. Can. J. Fish. Aquat. Sci. **51**: 1737–1751.

Rutherford, K.L. 1996. Catch and effort statistics of the Canadian groundfish fishery of the Pacific coast in 1993. Can. Tech. Rep. Fish. Aquat. Sci. No. 2097.

Schweigert, J.F., Fort, C., and Tanasichuk, R. 1998. Stock assessment for British Columbia herring in 1997 and forecasts of the potential catch in 1998. Can. Tech. Rep. Fish. Aquat. Sci. No. 2217.

Shaw, W., and Robinson, C.L.K. 1998. Night versus day abundance estimates of zooplankton in the British Columbia coastal marine. Mar. Ecol. Prog. Ser. **173**: 1–11.

Smith, C.L., Hill, A.E., Foreman, M.G.G., and Pena, M.A. 1999. A numerical investigation of horizontal transport resulting from interactions between diel vertical migration and tidal currents off the west coast of Vancouver Island. Can. J. Fish. Aquat. Sci. **56**. In press.

Tanasichuk, R.W. 1997. Influence of biomass and ocean climate on the growth of Pacific herring (*Clupea pallasi*) from the southwest coast of Vancouver Island. Can. J. Fish. Aquat. Sci. **54**: 2782–2788.

Tanasichuk, R.W. 1998. Interannual variations in the population biology and productivity of the euphausiid *Thysanoessa spinifera* in Barkley Sound, Canada, with special reference to the 1992 and 1993 warm ocean years. Mar. Ecol. Prog. Ser. **173**: 181–195.

Tanasichuk, R.W., Ware, D.M., Shaw, W., and McFarlane, G.A. 1991. Variations in diet, daily ration, and feeding periodicity of Pacific hake (*Merluccius productus*) and spiny dogfish (*Squalus acanthias*) off the lower west coast of Vancouver Island. Can. J. Fish. Aquat. Sci. **48**: 2118–2128.

Verheye, H.M., Hutchings, L., Hugget, J.A., and Painting, S.J. 1992. Mesozooplankton dynamics in the Benguela ecosystem with emphasis on the herbivorous copepods. S. Afr. J. Mar. Sci. **12**: 561–584.

Ware, D.M., and McFarlane, G.A. 1995. Climate induced changes in Pacific hake (*Merluccius productus*) abundance and pelagic community interactions in the Vancouver Island upwelling system. *In* Climate change and northern fish populations. *Edited by* R.J. Beamish. Can. Spec. Publ. Fish. Aquat. Sci. No. 121. pp. 509–521.

© 1999 NRC Canada

Utility of storage lipid volumes in inferring recent trophic history of copepods

C.S. Reiss, I.A. McLaren, and P.A. Avendaño

Abstract: We were able to estimate lipid oil-sac volumes of *Pseudocalanus* spp. copepodids c3 to c5 on and around Western Bank, Scotian Shelf, during three cruises (October and November 1997 and January 1998) at stations on (<60 m depth) and off (>60 m depth) the bank. We test the hypothesis that storage lipid volume was not significantly different between locations during these three months. *Pseudocalanus* spp. are an important prey for Atlantic cod (*Gadus morhua*) larvae that are spawned and persist on the bank. However, in contrast with the greater concentration of *Pseudocalanus* spp. on relative to off the bank, size-adjusted oil-sac volumes were on average larger and less variable at off-bank stations. We conclude that the greater copepod concentration on the bank does not result from enhanced and uniform nutrition on the bank. Lipid volumes averaged larger in winter than in the autumn, indicating that nutritional condition of *Pseudocalanus* spp. copepodids does not decline subsequent to the autumn bloom. Although biochemical techniques are available to quantify the level of storage lipids in individual copepods, simple measurements of oil sacs and body sizes permit a rapid real-time assessment of their recent trophic history in relation to oceanographic structure.

Résumé : Nous avons pu évaluer le volume de la vésicule lipidique chez des copépodites des stades c3 à c5 de *Pseudocalanus* spp., sur le banc Western de la plate-forme Néo-Écossaise et au voisinage, lors de trois campagnes (octobre et novembre 1997 et janvier 1998) à des stations situées sur le banc (<60 m de profondeur) et au large du banc (>60 m de profondeur). Nous avons vérifié l'hypothèse selon laquelle le volume des réserves lipidiques ne présentait pas de différence significative d'un lieu à l'autre pendant ces trois mois. Les copépodes du genre *Pseudocalanus* spp. sont une proie importante des larves de morue qui naissent et demeurent sur le banc Western. Toutefois, alors que la concentration de *Pseudocalanus* spp. était plus importante sur le banc que dans les eaux du large, les volumes de la vésicule lipidique ajustés en fonction de la taille étaient en moyenne plus grands et moins variables dans les stations au large du banc. Nous concluons que la concentration plus élevée de copépodes sur le banc ne résulte pas d'une alimentation meilleure et plus constante à cet endroit. Le volume de lipides était en moyenne plus élevé en hiver qu'à l'automne, ce qui indique que les conditions d'alimentation des copépodites ne diminuent pas après la poussée automnale. Nous disposons de techniques biochimiques pour quantifier les réserves de lipides chez les copépodes, mais des mesures simples des vésicules lipidiques et de la taille corporelle permettent une évaluation rapide en temps réel de leurs données trophiques récentes par rapport à la structure océanographique.

[Traduit par la Rédaction]

Introduction

The factors that regulate copepod growth and survival may link variation in secondary production to survival of fish larvae, as hypothesized by Hjort (1914), Shelbourne (1957), and Ellertsen et al. (1989). Cushing (1990) summarized suggestions that year-class strength of temperate marine fish depend on the timing of seasonal phytoplankton blooms that nourish sufficient concentrations of prey of suitable size and quality for fish larvae. On the Scotian Shelf, however, a succession of fish species spawn over marine banks throughout the year. This suggests that for some species, seasonal (spring bloom) production cycles are not the only factors controlling larval fish survival (O'Boyle et al. 1984; Brander and Hurley 1992). Increased local production or retention of zooplankton and ichthyoplankton over shallow banks that are separated from surrounding shelf waters by fronts may provide an explanation (O'Boyle et al. 1984; Brander and Hurley 1992; Taggart et al. 1996).

The distribution of Atlantic cod (*Gadus morhua*) larvae in relation to prey has previously been examined at two scales on Western Bank, Scotian Shelf, to determine the general overlap of predator and prey during autumn (McLaren and Avendaño 1995; McLaren et al. 1997). Both studies found that autumn-spawned Atlantic cod larvae selectively fed on *Pseudocalanus* spp. and that concentrations of both predator and prey were substantially greater over the shoal of the bank (<60–70 m depth) relative to locations in deeper water surrounding the bank. They hypothesized that physical mechanisms were responsible for the persistent differences

Received July 28, 1998. Accepted May 6, 1999.
J14718

C.S. Reiss.[1] Departments of Oceanography and Biology, Dalhousie University, Halifax, NS B3H 4J1, Canada.
I.A. McLaren and P.A. Avendaño. Department of Biology, Dalhousie University, Halifax, NS B3H 4J1, Canada.

[1]Author to whom all correspondence should be addressed. e-mail: reiss@phys.ocean.dal.ca

© 1999 NRC Canada

Fig. 1. Chart of Western Bank, Scotian Shelf, showing locations of samples collected in October (circles), November (triangles), and January (squares) of 1997–1998. Off-bank stations are defined by the 60-m isobath

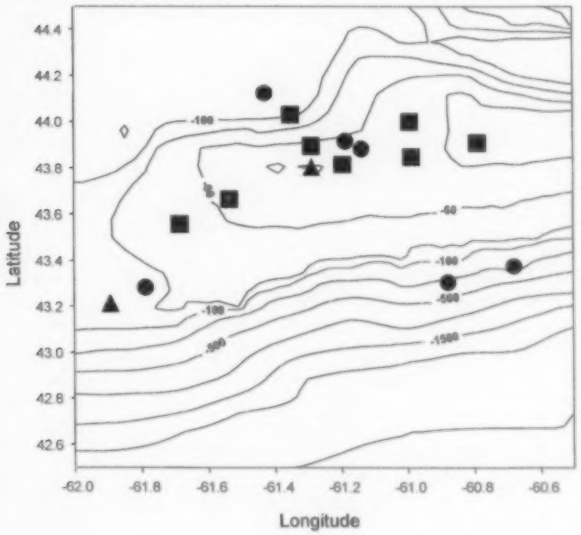

in copepod abundances on and off the bank because the analysis of stage–frequency distributions of *Pseudocalanus* spp. among stations did not reveal differences in development rate, as might be expected if there were spatial (oceanographic) differences in copepod growth and development related to food availability or temperature.

Food availability for zooplankton is generally thought to be greater on rather than off marine banks (O'Boyle et al. 1984), suggesting that food limitation may occur in areas removed from such banks. On the Scotian Shelf, however, Dauchez et al. (1996) found no evidence of nitrogen limitation in two size fractions of phytoplankton from Western Bank or Emerald Basin. Further, depth-integrated concentrations of total chlorophyll *a* exhibited the same seasonal patterns at both locations and averaged 18.5 ± 7.3 $mg \cdot m^{-2}$ on and off the bank with no significant differences between locations (summarized from table 2 in Dauchez et al. 1996). Some have argued that food limitation for copepods is less important, since their growth rates are generally temperature dependent in nature (Huntley and Lopez 1992). Nevertheless, variation in the nutritional condition of copepods at several spatial and temporal scales suggests that food limitation may occur at certain times or in certain locations (Hakanson 1984; Peterson et al. 1991; Tiselius et al. 1991). Even if rates of development and growth of structural body mass are unaffected above threshold food levels, differences in food concentration may produce considerable variation in the amounts of storage lipid accumulated by copepods (Escribano and McLaren 1992; Miller et al. 1998). Areas with strong horizontal gradients in water properties (frontal zones) or bathymetrically related stratification (on and off shoals of banks) represent appropriate locations to examine whether these variations in food availability and quality exist.

It is generally believed that the amount of lipid stored by organisms reflects their nutritional status and (or) recent trophic history (Hakanson 1984; Gallagher et al. 1986). For example, starvation experiments have shown that in several different copepod genera, lipid oil-sac volumes decreased rapidly over a period of several days (indicating a depletion of lipid reserves) when food was limited (Arts and Evans 1991; Carman et al. 1991). These results indicate a rapid response between recent water column feeding conditions and observed lipid concentrations (Kuosa and Gyllenberg 1989; Norrbin et al. 1990; Carman et al. 1991). In a recent review, Ferron and Leggett (1994) determined that lipid reserves were the appropriate measure for determining recent trophic history on the time scale of days to weeks. Furthermore, Corkett and McLaren (1969) showed that lipid volumes in adult *Pseudocalanus* continued to increase at experimental food levels above that permitting maximal rate of egg production. Nutritional condition and the feeding ecology of copepods have been examined using biochemical techniques to identify and quantify lipids (e.g., Hakanson 1984) and optical measurements to quantify relative amounts of lipids (Arts and Evans 1991; Carman et al. 1991; Miller et al. 1998). Estimates of the lipid store determined through optical measurements of the oil sac are strongly correlated with storage lipids quantified by biochemical methods in non-reproducing stages (Arts and Evans 1991; Carman et al. 1991; Miller et al. 1998). This relationship between biochemical and visual estimates of lipid quantity indicates that quantity of total storage lipids can be used to assess the relative nutritional condition and recent (days to weeks) trophic history of copepodids without quantifying the lipid type or the actual feeding regime experienced by the animal. Therefore, for species and stages that are actively developing during a sampling period (neither in diapause nor reproducing), simple inexpensive and rapid indices derived from oil-sac volumes between or among locations should be sufficient to compare the apparent recent trophic histories of copepods.

In this study, we use oil-sac volumes as a simple, rapid field method to assess apparent trophic histories (on the time scale of days to weeks) of *Pseudocalanus* spp. copepodids from different locations around Western Bank. If copepods of the same species in two samples have significantly different oil-sac volumes, after correction for differences among developmental stages and body sizes, then these animals have presumably had different recent trophic histories. In particular, we compare lipid stores in animals from the shoal of Western Bank (<60 m depth) and from surrounding waters (>60 m depth). We also examine the hypothesis that nutritional condition, as measured by oil-sac volume adjusted for body size, decreases through time following the presumed autumn bloom in primary production.

Materials and methods

Late-stage copepodids of *Pseudocalanus* spp. (probably almost all *Pseudocalanus newmani*) were collected at stations on and around Western Bank during autumn and winter of 1997 and 1998 (Fig. 1). Microzooplankton samples were collected using small (25 cm) ring nets equipped with 64-μm mesh that were attached to 60-cm BONGO frames. BONGO nets were towed in a double oblique manner to within 5 m of the bottom. We tried to use 50 individuals from each depth-integrated tow in our analyses. At stations where fewer than 50 animals are reported, the entire sample

© 1999 NRC Canada

Table 1. Hydrographic and biological data collected during 1997–1998 during cruises to Western Bank, Scotian Shelf.

Month, cruise, and ship	No. samples	Location	Mean depth (range) (m)	Salinity (SD) (psu)	Temperature (SD) (°C)	Bulk stratification (SD)	Biomass (SD) ($g \cdot 100\ m^{-3}$)
Oct. 1997, 97063,	2	On bank	55 (55–56)	30.71 (0.31)	11.13 (0.07)	0.0030 (0.003)	
Hudson	4	Off bank	113 (87–135)	30.89 (0.51)	10.05 (0.73)	0.0220 (0.014)	21.9 (6.0)
Nov.–Dec. 1997,	1	On bank	58 (54)	30.98 (0.05)	8.42 (0.00)	0.0052 (0.00)	29.7 (2.7)
97070, *Needler*	1	Off bank	90 (87)	31.45 (0.20)	7.43 (0.84)	0.0083 (0.84)	5.3 (2.0)
Jan. 1998, 98084,	4	On bank	54 (45–59)		1.93 (0.35)		7.9 (10.9)
Parizeau	3	Off bank	78 (58–110)		2.37 (0.06)		4.5 (2.7)

Note: Mean depth is the average depth of the water column, salinity is the average salinity of the upper 40 m of the water column, temperature is the average temperature of the upper 40 m of the water column, bulk stratification is the average bulk stratification at sampling stations, and biomass is the average biomass of sample wet weights from 333-μm-mesh nets at locations where samples were taken.

Table 2. Summary of lipid oil-sac volumes (mm^3) of stage c3 to c5 *Pseudocalanus* spp. copepodids collected during 3 months on and off Western Bank.

Location	Stage	Number	Mean	SD	Range
		October			
On bank	c3	18	0.0023	0.0015	0.0058
	c4	23	0.0022	0.0012	0.0044
	c5	57	0.0039	0.0022	0.0103
Off bank	c3	31	0.0027	0.0018	0.0071
	c4	48	0.0044	0.0038	0.0166
	c5	78	0.0068	0.0057	0.0319
		November			
On bank	c3	14	0.0014	0.0012	0.004
	c4	11	0.0028	0.0024	0.0067
	c5	25	0.0028	0.0018	0.0064
Off bank	c3	40	0.0013	0.0008	0.0029
	c4	8	0.0030	0.0014	0.0036
	c5	6	0.0051	0.0030	0.007
		January			
On bank	c3	94	0.0045	0.0020	0.0107
	c4	25	0.0056	0.0034	0.0169
	c5	37	0.0085	0.0036	0.0132
Off bank	c3	118	0.0051	0.0016	0.0081
	c4	13	0.0068	0.0034	0.0102
	c5	14	0.0087	0.0057	0.0192

Table 3. Results of ANCOVA for oil-sac volumes of stage c3, c4, and c5 *Pseudocalanus* spp. copepodids in relation to body size at stations nominally on and off Western Bank.

Source	df	Mean square	*F* ratio	*P* value
		October		
Location	1	0.34	0.79	0.38
$\log_e$ length	1	21.60	49.68	<0.001
Location × $\log_e$ length	1	0.16	0.37	0.54
Error	251	0.43		
		November		
Location	1	3.60	9.51	<0.001
$\log_e$ length	1	27.45	72.54	<0.001
Location × $\log_e$ length	1	3.50	9.24	<0.001
Error	100	0.38		
		January		
Location	1	0.32	1.86	0.17
$\log_e$ length	1	23.64	139.81	<0.001
Location × $\log_e$ length	1	0.04	0.26	0.61
Error	297	0.17		

Note: The ANCOVA includes the interaction of body size with location for each of three cruises during autumn and winter 1997–1998.

was sorted for individuals. The number of samples, water column depth, and other pertinent data are presented in Table 1. Stratification of the water column was determined by calculating the bulk stratification as (density at 40 m – density at 5 m)/(40 m – 5 m).

Copepod prosome and oil-sac lengths and widths in side view were measured by microscope with an optical micrometer aboard ship or within 4 days of the cruise when there was no evident "leakage" of lipids. Intact oil sacs were well defined, whereas leakage or oil-sac rupture was evident as numerous small oil globules within the body cavity. Only copepodid stages c3, c4, and c5 were used because younger stages store little lipid and are hard to measure, and the lipid in adults depends on their reproductive cycles. If the oil sac appeared to have a "thicker part" with a "thinner extension," the two parts were measured separately and total volume was calculated. Relative oil-sac volumes were then calculated assuming that they were simple cylinders (length × π × (0.5 × width)^2). Prosome length rather than body volume (as estimated from lengths and widths) was used as a measure of body size because of the reduced error associated with a single linear measurement. Body lengths and oil-sac volumes were $\log_e$ transformed, as the relationship between the two variables should be allometric. Effects of developmental stage (c3, c4, c5) were considered to be subsumed in size effects.

Differences in oil-sac volumes between locations (on or off the bank) and among months were examined using analysis of covariance (ANCOVA) with $\log_e$ prosome length as a covariate. We then compared oil-sac volumes among months using a two-way analysis of variance (ANOVA), with both month and location as fixed factors and $\log_e$ length as a covariate. The $\log_e$ oil-sac volumes were tested for normality for each combination of month, stage, and location using the Martinez–Igliewicz test (NCSS, Kaysville, Utah).

Results

In general, the means and the variances of oil-sac volumes increased with developmental stage and were not consistent among months. However, $\log_e$ transformation resulted in normality for each combination of month, location, and stage. Variation in estimated mean oil-sac size was readily discernable between locations and among months and developmental stages using the simple volume measurement (Table 2).

Oil-sac volume ($\log_e$, mm^3), when adjusted for body size, varied between locations and among months (cruises) during autumn and winter 1997–1998. During October, there was no significant length × location interaction (Table 3), and ad-

© 1999 NRC Canada

Fig. 2. Relationship between oil-sac volumes and body lengths of *Pseudocalanus* at stations on (circles) and off (>60 m depth, triangles) the crest of Western Bank during the three cruises in (A) October, (B) November, and (C) January of 1997–1998.

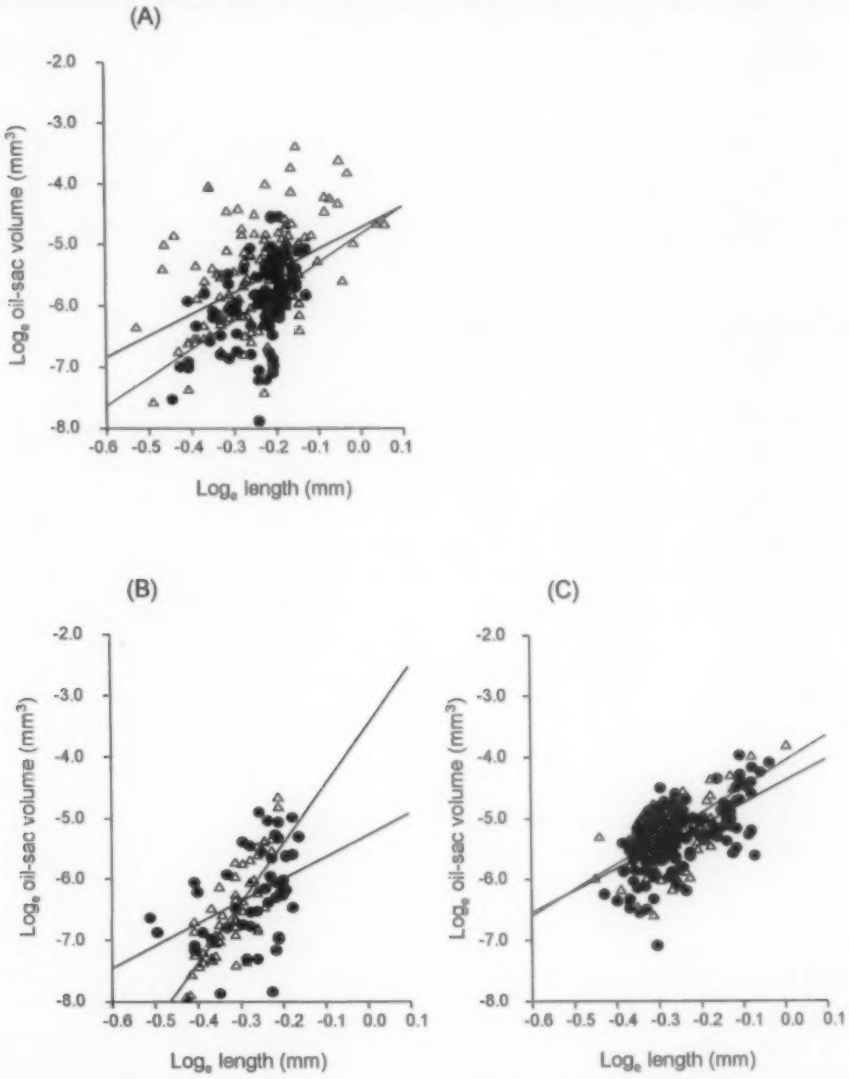

Table 4. Results of ANCOVA for oil-sac volumes of *Pseudocalanus* spp. copepodids during 2 months in relation to body sizes at combined stations on and off Western Bank without the interaction of body size and location.

Source	df	Mean square	*F* ratio	*P* value
		October		
Location	1	9.59	22.11	<0.001
log$_e$ length (mm)	1	28.04	64.63	<0.001
Error	252	0.43		
		January		
Location	1	2.13	12.6	<0.001
log$_e$ length (mm)	1	27.01	160.2	<0.001
Error	298	0.17		

justed oil-sac volumes without the interaction term were significantly larger off the bank (Table 4; see Fig. 3). Oil-sac volumes off the bank, however, were more variable than on the bank (Bartlett's test of residuals, χ^2 statistic = 55.67, $P < 0.001$) (Fig. 2A). In contrast, the marginal differences exhibited in November were confounded by a significant length × location interaction (Table 3). There was more variability in the animals collected on the bank than off the bank during this cruise (Bartlett's test of residuals, χ^2 statistic = 14.50, $P < 0.0001$) (Fig. 2B). In January, there was no significant interaction between length and location (Table 3) and little difference in variability between the two locations (Bartlett's test of residuals, χ^2 statistic = 10.00, $P > 0.99$) (Fig. 2C). Without the interaction term, adjusted oil-sac volumes were significantly larger in off-bank samples (Table 4; Fig. 3), al-

© 1999 NRC Canada

Table 5. Results of a two-way ANOVA of copepodid lipid oil-sac volume ($\log_e$, mm^3) with location (on or off Western Bank) and month (October, November, or January) as fixed factors and $\log_e$ length as a covariate.

Source	df	Sum of squares	Mean square	*F* ratio	*P* value
Covariate ($\log_e$ length)	1	75.84	75.84	242.68	<0.0001
Location	1	4.45	4.45	14.25	<0.0005
Month	2	101.24	50.62	161.98	<0.0001
Location × month	2	3.51	1.75	5.60	<0.001
Error	653	204.07	0.31		
Total (adjusted)	659	389.11			
Total	660				

though the absolute differences were very small and are probably not biologically meaningful.

Considerably more variation in oil-sac volume was expressed among than within months (cruises) (Fig. 3). Results of a two-way ANOVA, with month and location as fixed factors and $\log_e$ length as a covariate, revealed that body size adjusted mean oil-sac volumes both on and off the bank were lowest in November and highest in January (Table 5). These highest oil-sac volumes in January are of considerable interest, since the water temperatures were lowest, the water column was mixed (Table 1), and the sampling followed the presumed autumn primary production bloom. The significant interaction between location and month, however, precludes any further statistical inference.

Discussion

We were able to rapidly estimate lipid oil-sac volumes of *Pseudocalanus* spp. copepodids on and around Western Bank. Oil-sac volumes, adjusted for individual lengths, exhibited considerable spatiotemporal variability, suggesting that this technique is useful as an assay of recent trophic history of copepodids on the time scale of days to weeks (i.e., time scale of developmental stage durations) within and among shelf water masses.

The null hypothesis that lipid volumes of *Pseudocalanus* spp. copepodids on and off the shoal (<60 m depth) of Western Bank would not differ when adjusted for body size is rejected. In contrast with the logical alternative hypothesis that conditions for copepod nutrition would be better on the shoal of the bank (O'Boyle et al. 1984), there was a consistent, although not always significant, trend of larger oil-sac volumes and sometimes lower variability at off-bank stations. Although statistically detectable differences were found, they were small, and since all copepodids had measurable oil sacs, there is little evidence to suggest that food availability was below the levels required to support maximal reproductive rates of the copepods (Corkett and McLaren 1969) at all sampled locations and throughout the autumn. Furthermore, it has been suggested for *Pseudocalanus* (Corkett and McLaren 1978, pp. 131–132) and demonstrated for *Calanus* spp. (McLaren and Leonard 1995) that maximal growth rate of late copepodids is equivalent to maximal rate of production of egg matter. Thus, presence of a measurable lipid store probably indicates adequate nutrition for full growth and reproduction.

Fig. 3. Average oil-sac volumes for *Pseudocalanus* spp. adjusted for body size at locations on and off Western Bank during the three cruises in 1997–1998. Error bars are ±1 SE.

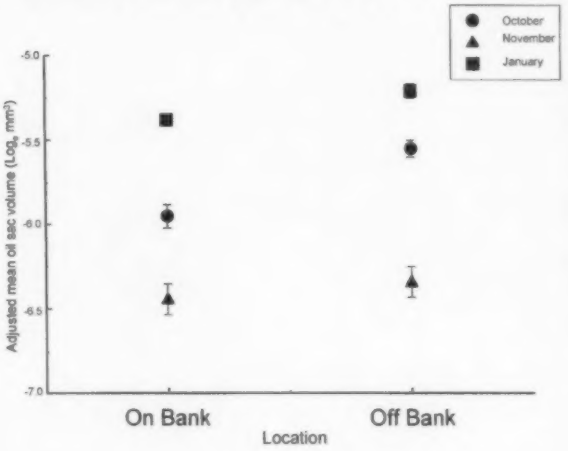

Recent studies have documented the presence of a gyre-like feature on the crest of Western Bank that may concentrate both ichthyoplankton and their zooplankton prey (Sanderson 1995; Taggart et al. 1996). McLaren and Avendaño (1995) and McLaren et al. (1997) found that Atlantic cod larvae fed preferentially on *Pseudocalanus* spp., with which they were concentrated on the bank. McLaren and Avendaño (1995) also tested the hypothesis that *Pseudocalanus* spp. copepodids on the bank benefitted from enhanced feeding conditions, as expressed in accelerated development, but found no clear differences in stage–frequency distributions on or off the bank. The present results indicate further that the greater concentration of *Pseudocalanus* spp. on Western Bank is not a consequence of enhanced nutrition, which might produce higher populations through increased survival or reproduction of the copepods. Rather, the increased concentrations of zooplankton seem attributable to physical processes of concentration and retention on the bank.

In this study, average plankton biomass (64-μm mesh) was higher on than off the bank for the two cruises where sufficient data were available (Table 1), and this is consistent with other studies of zooplankton biomass in the vicinity of the bank (McLaren and Avendaño 1995). The fact that oil-sac volumes were on average lower on the bank might suggest that the increased zooplankton biomass had a direct impact on the available food supply on the bank. However, evidence for such a compensatory response is, at this time, weak, especially given the absence of large differences in chlorophyll *a* biomass historically found on and off the bank (Dauchez et al. 1996).

Oil-sac volumes did not show a seasonal decline that might have been expected after an autumn bloom of phytoplankton. In fact, oil-sac volumes were highest in January and lowest in November. The high oil-sac volumes in January may have been a response to better feeding conditions or possibly an effect of reduced temperature (Table 1)

© 1999 NRC Canada

on metabolism (Huntley and Boyd 1984), permitting an increase in lipid storage.

This study demonstrates that apparent differences in recent trophic history of copepodids in space and time are detectable using simple oil-sac measurements. While biochemical techniques are now available to quantify storage lipids in individual copepods (Hakanson 1984; Miller et al. 1998), direct oil-sac measurements have an important advantage. The simplicity of the technique permits rapid assessment of large-scale patterns in near-real time, e.g., on cruises investigating the processes of secondary production related to physical oceanographic regimes.

Acknowledgements

We thank the captains and crews of the ships CCGS *Parizeau*, CCGS *Hudson*, and CCGS *Needler* for their skillful navigation. We also thank Dr. Rob Stephenson (Department of Fisheries and Oceans, St. Andrews, N.B.) for the opportunity to collaborate during the November 1997 cruise. Doug Sameoto and Alex Herman also allowed us to collect samples during October 1997. Thanks also to C.T. Taggart for his considerable input into this manuscript and to the two anonymous reviewers who strengthened some of the arguments presented here. This research was supported under the Canadian GLOBEC program by grants from the Natural Sciences and Engineering Research Council of Canada to I.A.M and C.T. Taggart.

References

Arts, M.T., and Evans, M.S. 1991. Optical–digital measurements of energy reserves in calanoid copepods: intersegmental distribution and seasonal patterns. Limnol. Oceanog. **36**: 289–298.

Brander, K., and Hurley, P. 1992. Distribution of early stage Atlantic cod (*Gadus morhua*), haddock (*Melanogrammus aeglefinus*), and witch flounder (*Glyptocephalus synogiossus*) eggs on the Scotian Shelf: a reappraisal of evidence on the coupling of cod spawning and plankton production. Can. J. Fish. Aquat. Sci. **49**: 238–251.

Carman, K.R., Thistle, D., Ertmen, S.C., and Foy, M. 1991. Nile red as a probe for lipid-storage products in benthic copepods. Mar. Ecol. Prog. Ser. **74**: 307–311.

Corkett, C.J., and McLaren, I.A. 1969. Egg production and oil storage by the copepod *Pseudocalanus* in the laboratory. J. Exp. Mar. Biol. Ecol. **3**: 90–105.

Corkett, C.J., and McLaren, I.A. 1978. The biology of *Pseudocalanus*. Adv. Mar. Biol. **15**: 1–231.

Cushing, D.H. 1990. Plankton production and year-class strength in fish populations: an update of the match/mis-match hypothesis. Adv. Mar. Biol. **26**: 249–293.

Dauchez, S., Legendre, L., Fortier, L., and Levasseur, M. 1996. Nitrate uptake by size-fractionated phytoplankton on the Scotian Shelf (Northwest Atlantic): spatial and temporal variability. J. Plankton Res. **18**: 577–595.

Ellertsen, B., Fossum, P., Solemdal, P., and Sundby, S. 1989. Relation between temperature and survival of eggs and first feeding larvae of northeast Atlantic cod (*Gadus morhua* L.). Rapp. P.-v. Réun. Cons. Int. Explor. Mer, **191**: 209–219.

Escribano, R., and McLaren, I.A. 1992. Influence of food and temperature on lengths and weights of two marine copepods. J. Exp. Mar. Biol. Ecol. **159**: 77–88.

Ferron, A., and Leggett, W.C. 1994. An appraisal of condition measures for marine fish larvae. Adv. Mar. Biol. **30**: 217–303.

Gallagher, S.M., Mann, R., and Sasaki, R.C. 1986. Lipid as an index of growth and viability in three species of bivalve larvae. Aquaculture, **56**: 81–103.

Hakanson, J.L. 1984. The long and short term feeding condition in field-caught *Calanus pacificus*, as determined from the lipid content. Limnol. Oceanogr. **29**: 794–804.

Hjort, J. 1914. Fluctuations in the great fisheries of northern Europe viewed in the light of biological research. Rapp. P.-v. Réun. Cons. Int. Explor. Mer, **20**: 1–288.

Huntley, M., and Boyd, C. 1984. Food-limiting growth of marine zooplankton. Am. Nat. **124**(4): 455–478.

Huntley, M., and Lopez, M.D.G. 1992. Temperature dependent production in marine copepods: a global synthesis. Am. Nat. **140**: 201–240.

Kuosa, H., and Gyllenberg, G. 1989. Lipid content and utilization of lipids in planktonic copepods in Lake Pääjärvi, southern Finland. Hydrobiologia, **171**: 215–222.

McLaren, I.A., and Avendaño, P. 1995. Prey field and diet of larval cod on Western Bank, Scotian Shelf. Can. J. Fish. Aquat. Sci. **52**: 448–463.

McLaren, I.A., and Leonard, A. 1995. Assessing the equivalence of growth and egg production. ICES J. Mar. Sci. **52**: 397–408.

McLaren, I.A., Avendaño, P., Taggart, C.T., and Lochmann, S.E. 1997. Feeding by larval cod in different water masses on Western Bank, Scotian Shelf. Fish. Oceanogr. **6**: 250–265.

Miller, C.B., Morgan, C.A., Prahl, F.G., and Sparrow, M.A. 1998. Storage lipids of the copepod *Calanus finmarchicus* from Georges Bank and the Gulf of Maine. Limnol. Oceanogr. **43**: 488–497.

Norrbin, M.F., Olsen, R.E., and Tande, K.S. 1990. Seasonal variation in lipid class and fatty acid composition of two small copepods in Balsfjorden, northern Norway. Mar. Biol. **105**: 205–211.

O'Boyle, R.N., Sinclair, M., Conover, R.J., Mann, K.H., and Kohler, A.C. 1984. Temporal and spatial distribution of ichthyoplankton communities on the Scotian Shelf in relation to biological, hydrological, and physiographic features. Rapp. P.-v. Réun. Cons. Int. Explor. Mer, **183**: 27–40.

Peterson, W.T., Tiselius, P., and Kiorboe, T. 1991. Copepod egg production, moulting and growth rates, and secondary production, in the Skagerak in August 1988. J. Plankton Res. **13**: 131–154.

Sanderson, B.G. 1995. On the structure of an eddy measured by drifters. J. Geophys. Res. **100**: 6767–6776.

Shelbourne, J.E. 1957. The feeding and condition of plaice larvae in good and bad plankton patches. J. Mar. Biol. Assoc. U. K. **36**: 539–552.

Taggart, C.T., Thompson, K.R., Maillet, G.R., Lochmann, S.E., and Griffin, D.E. 1996. Abundance and distribution of larval cod (*Gadus morhua*) and zooplankton in a gyre-like water mass on the Scotian Shelf. *In* Proceedings of the International Workshop on Survival Strategies in Early Life Stages of Marine Resources. *Edited by* Y.Y. Watanabe and Y. Oozecki. A.A. Balkema Publishers, Rotterdam, The Netherlands. pp. 155–173.

Tiselius, P., Nielsen, T.G., Breuel, G., Jaanus, A., Koshenko, A., and Witek, Z. 1991. Copepod egg production in the Skagerrak during SKAGEX, May–June 1990. Mar. Biol. **111**: 445–453.

© 1999 NRC Canada

A modelling study of the 1976 climate regime shift in the North Pacific Ocean

Julia Qiuying Wu and William W. Hsieh

Abstract: Around 1976, the North Pacific Ocean underwent a climate regime shift, with significant biological consequences. To model the changes in the ocean, an ocean general circulation model was forced by the wind stress and sea surface temperature monthly climatology of the 1952–1975 period in one numerical experiment and the 1976–1988 period in another. Changes in the ocean model between the two experiments revealed how the ocean might have changed under the 1976 climate regime shift. In winter, the intensified post-1976 Aleutian Low spun up the subarctic gyre and the subtropical gyre, except in the Gulf of Alaska, where the circulation weakened. Upwelling was generally enhanced in the subarctic and downwelling enhanced in the subtropical region, with temperature changes down to 600 m. In the post-1976 period, the meridional heat transports were also enhanced: poleward in the low latitudes, equatorward in the midlatitudes, and poleward in the high latitudes.

Résumé : Vers 1976, il s'est produit dans l'océan Pacifique Nord un changement de régime climatique qui a eu des conséquences biologiques importantes. Pour modéliser les changements de l'océan, un modèle de circulation générale de l'océan a été forcé par la climatologie mensuelle de la tension du vent et de la température superficielle de la mer pour la période de 1952 à 1975 dans une expérience numérique, et pour la période de 1976 à 1988 dans une autre expérience. Les modifications du modèle de l'océan entre les deux expériences a montré de quelle manière le changement de régime climatique de 1976 a pu modifier l'océan. En hiver, l'intensification de la dépression des Aléoutiennes après 1976 a activé le gyre subarctique et le gyre subtropical, sauf dans le golfe de l'Alaska, où on a observé un ralentissement de la circulation. La remontée des eaux froides était généralement accrue dans la circulation subarctique, et l'enfoncement des eaux plus prononcé dans la région subtropicale, avec des variations de température jusqu'à une profondeur de 600 m. À partir de 1976, on a également noté une augmentation des transports méridiens de chaleur — vers le pôle aux basses latitudes, vers l'équateur aux latitudes moyennes et vers le pôle aux hautes latitudes.

[Traduit par la Rédaction]

Introduction

The climate system can fluctuate about a mean state for many years, until the mean state itself abruptly shifts, resulting in a climate regime shift. A major climate regime shift occurred in the North Pacific Ocean around 1976, as reported by Nitta and Yamada (1989), Trenberth (1990), Tabata (1991), and Trenberth and Hurrell (1994). This large-scale atmospheric and oceanic climate change, lasting from about 1976 until 1988, is characterized by the intensification and southward shift of the Aleutian low pressure system in the winter half of the year. It is this system that transported warmer air northward along the west coast of North America and into Alaska and cold air over the central North Pacific. The air temperature and sea surface temperature (SST) increased along the west coast of North America and Alaska, but the SST decreased over the central North Pacific.

Changes in biological productivity have been reported as well. Mysak (1986) noted that the migration patterns of fish were altered due to changes in the ocean currents and temperatures. Venrick et al. (1987) found an increasing concentration of chlorophyll *a* in the central North Pacific between the late 1960s – early 1970s and the early 1980s. McFarlane and Beamish (1992) found that stronger sablefish (*Anoplopoma fimbria*) year-classes tends to occur during years of more intensive Aleutian lows and higher copepod abundance. Beamish and Bouillon (1993) found that there is a significant relationship between the Aleutian low pressure index and the annual North Pacific ocean salmon production.

Alexander (1992) pointed out that observed changes in the North Pacific Ocean SSTs can be largely accounted for by the atmospheric changes through the surface fluxes and mixing in the upper layers of the ocean. Trenberth and Hurrell (1994) indicated that the dominant atmosphere–ocean relationship in the North Pacific is one where atmospheric changes lead the SSTs by 1–2 months. Graham (1994) and Miller et al. (1994) used numeric models forced by observed wind and heat fluxes to investigate numerically the mechanism of the interdecadal variability of the Pacific Ocean. Their studies supported the idea that the 1976 oceanic climate shift was primarily driven by atmospheric dynamics. Lagerloef (1995) investigated the interdecadal variation in the Alaska gyre and suggested that the upper ocean climatic variability in this region is primarily wind forced.

These papers have only studied the changes in the surface waters; our paper aims to understand more completely the oceanic response, including that of the subsurface waters, to

Received August 28, 1998. Accepted August 27, 1999.
J14770

J.Q. Wu and W.W. Hsieh.[1] Oceanography/EOS, University of British Columbia, Vancouver, BC V6T 1Z4, Canada.

[1]Author to whom all correspondence should be addressed.
e-mail: william@ocgy.ubc.ca

© 1999 NRC Canada

Fig. 1. (*a*) Winter (DJF) wind stress climatology field of 1976–1988 (post-1976) minus that of 1952–1975 (pre-1976). (*b*) Zonally averaged zonal stress as a function of latitude. The broken line indicates post-1976 climatology and the solid line the pre-1976 climatology. The unit value is 0.1 N·m^{-2}.

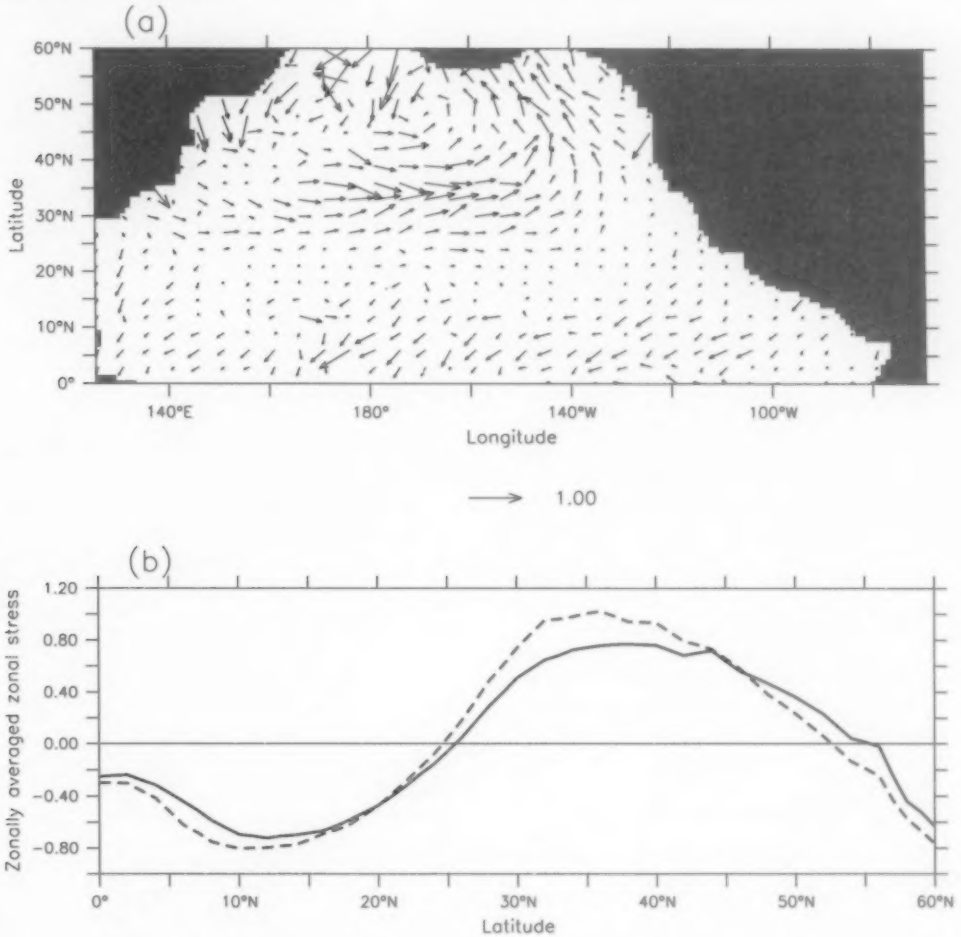

the atmospheric forcing change associated with the 1976 climate regime shift, by using the modular ocean model, developed originally at the Geophysical Fluid Dynamics Laboratory at Princeton University, Princeton, N.J. The interdecadal variations in major oceanic variables, such as transport stream function, currents, subsurface temperature, upwelling–downwelling velocities, meridional circulation, and heat transport, computed from the ocean model, provide a much more comprehensive picture of the climate regime shift than what can be learned from the SST and wind data alone.

Model

The domain of the model ocean covers the equatorial and North Pacific from 125°E to 70°W and from 20°S to 60°N, with a slightly idealized coastline. The horizontal resolution of the model ocean is 1° latitude × 1° longitude over the entire model domain. Some simplifications were introduced into the topography, e.g., the closure of the Sea of Okhotsk, Japan Sea, and other island seas and the elimination of the Hawaiian Islands and other small islands. In particular, the shallow area of the Bering Sea along the southwest coast of Alaska was masked out, since the large depth change between the Pacific and the shallow Bering Sea allows the propagation of fast topographic waves (Lee et al. 1992), which can greatly restrict the size of the integration time step. The model has 15 levels in the vertical, with seven of them in the upper 600 m, and a time step of 1800 s. The temperature and salinity in the top level are relaxed to the monthly climatological SST and salinity fields with a restoring time scale of 1 month (Bryan and Lewis 1979).

The lateral boundaries on the eastern, western, and northern walls of the basin are set to be nonslip, insulating, and impermeable. Along the southern nonslip boundary of the model ocean at 20°S, a Newtonian relaxation of the tracer variables (temperature and salinity) to the observed annual mean climatological values (World Ocean Atlas 1994) is ap-

© 1999 NRC Canada

Fig. 2. Winter (DJF) SST from the post-1976 climatology minus the pre-1976 climatology. The contour interval is 0.4°C. Negative anomalies are indicated by broken contours.

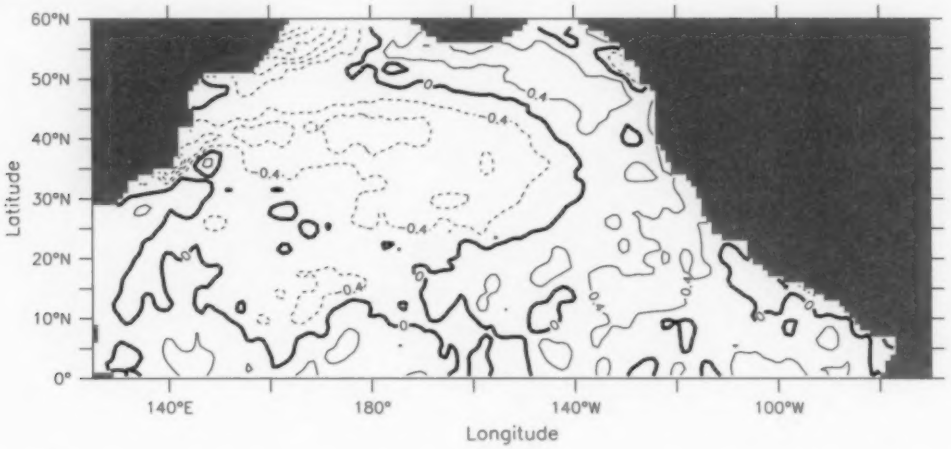

plied from the surface down to the bottom with a relaxation time scale of 1 year, which can reduce the artificial effect of walling off the exchange of tracers at the latitude of 20°S.

The horizontal eddy viscosity was 2.5×10^4 $m^2 \cdot s^{-1}$, while the horizontal diffusion coefficient was 2.5×10^3 $m^2 \cdot s^{-1}$. Richardson number-dependent vertical-mixing coefficients (Pacanowski and Philander 1981) were used for the vertical eddy viscosity and the vertical diffusion coefficient.

Forced by the surface wind stress, the ocean model computes the horizontal and vertical velocity components, temperature, and salinity at each grid point. Also computed are the depth-integrated transport stream function, mass transport, and heat transport.

Surface forcing fields and model runs

The monthly wind stress fields from 1952 to 1992 were calculated from the comprehensive ocean–atmosphere data set (COADS) (Woodruff et al. 1987), with the drag coefficients from Large and Pond (1981). Similarly, monthly SST fields were obtained from COADS. The monthly climatological wind stress and SST for different periods (1952–1992, 1952–1975, and 1976–1988) would be used for different experiments in this study.

The deepening of the Aleutian Low would imply an increase in the surface wind stress. The vector difference between the surface wind stress fields in the winter season for the pre-1976 case and the post-1976 case was calculated by subtracting the pre-1976 climatology (1952–1975) from the post-1976 climatology (1976–1988). A cyclonic circulation was present over the North Pacific north of 25°N (Fig. 1*a*), i.e., the cyclonic (anticlockwise) circulation in the Aleutian Low after 1976 was stronger than before 1976, in agreement with the observed lower sea level pressure after 1976 (Trenberth and Hurrell 1994). Figure 1*b* is the zonally averaged zonal stress for both the pre-1976 and post-1976 climatologies. In the Aleutian Low area, the zonally averaged zonal stress increased during 1976–1988, with a maximum increase of 30% at 35°N. In the tropics, the easterly trade winds for the post-1976 case also increased, although the increase was not as large as that for the midlatitude westerlies (Fig. 1*a*).

The SST over the North Pacific Ocean has been found to undergo significant changes between the pre- and post-1976 periods. The difference in wintertime SSTs between the two periods (Fig. 2) shows notable regional SST anomalies for 1976–1988, where warming occurred along the west coast of North America, up to Alaska (except for the British Columbian coast), while cooling occurred in the central and western North Pacific during the post-1976 period. Miller et al. (1994) derived the wintertime (December. January, February (DJF)) SST difference field between the 6 years after regime shift and the 6 years before the shift, yielding patterns very similar to Fig. 2. Royer (1989) indicated that there was a warming trend observed lasting from the late 1970s until the late 1980s near the Seward station in the Gulf of Alaska and in the Northeast Pacific north of 50°N.

For the negative SST anomalies along the British Columbia coast (Fig. 2), S. McKinnell (personal communication) found a similar result with the COADS data. However, from the lighthouse observations at Langara Island (54°15′N, 133°4′W), he found positive winter SST anomalies after 1976, in contrast with the COADS data; thus, the quality of the COADS data maybe poor in this area.

As we did not have sufficient salinity data to determine the monthly mean climatology over the different periods, the monthly climatology of sea surface salinity (SSS) from the World Ocean Atlas (1994) was used as the surface salinity restoring field for all our experiments.

The model was spun up from the rest state, with the surface boundary forced by the monthly climatological (1952–1992) wind stress field, and relaxed to the monthly climatological (1952–1992) SST field and the monthly climatological SSS field. After 21 years of spin-up, the model ocean was considered to be in a quasi-equilibrium state, with reasonable seasonal variations in the average kinetic energy density, but without significant interannual variations. This is the climatology run and is referred to as experiment A or the basic run.

© 1999 NRC Canada

To investigate the changes in the ocean from the regime shift of 1976 in the atmospheric forcing, two additional numerical experiments were performed. These experiments were initialized by the equilibrium state of the basic run (i.e., runs continued from the end of experiment A), but with the surface wind stress and SST forcing fields replaced by the COADS monthly climatological values computed from 1952 to 1975 in experiment B (pre-1976) and from 1976 to 1988 in experiment C (post-1976). Six-year runs were carried out for both the pre-1976 climatology and post-1976 climatology cases from the end of the basic run.

The average kinetic energy densities for the pre-1976 and post-1976 cases showed no significant interannual variations for the last 2 years of the 6-year runs. Between year 5 and year 6, the maximum change in the vertical velocity was less than 1.5%. For the temperature field, there are several sparsely distributed points in the merging area of Kuroshio and Oyashio, where the SST changed by a maximum value of 0.2°C. In all other areas, the SST changed by less than 0.05°C. At all other depths, the change in temperature was less than 0.1°C. So the model was considered to be in a quasi-steady state after 6 years of time integration, similar to the time required in Semtner and Chervin (1988). The average kinetic energy densities for the two cases showed the magnitude in the pre-1976 case to be smaller than in the post-1976 case, mainly from the weaker surface wind stress forcing in the former case. The variations of various oceanic variables are analysed based on the simulated data for the sixth year of experiments B and C.

Changes in the transport stream function

The vertically integrated transport stream functions for experiment B (pre-1976) and experiment C (post-1976) in January of year 6 and the difference between them are shown in Fig. 3. The subarctic gyre extended further south in the post-1976 case than in the pre-1976 case, with the southern boundary shifting from 36 to 33°N, due to the southward extension of the westerlies from the southward shift of the Aleutian Low after 1976. The Kuroshio and Oyashio transports reached 50 and 20 Sv (10^6 $m^3 \cdot s^{-1}$), respectively, in the post-1976 case, while they were only 40 and 11 Sv in the pre-1976 case.

In the subarctic area, the difference between the two cases (Fig. 3*c*) shows a cyclonic circulation, indicating that the subarctic gyre in the post-1976 case is stronger than before. This is expected, as the intensification of the Aleution Low system for the 1976–1988 period resulted in an increase in the wind stress curl in that area, which spun up the gyral circulation.

Another noticeable feature on Fig. 3*c* is the decrease in the transport stream function in the eastern and northern part of the Gulf of Alaska, which seems inconsistent with the conventional view that the strengthening Aleutian Low would intensify the gyre circulation. Lagerloef (1995) conducted an empirical orthogonal function analysis of the SST and dynamic height in the Gulf of Alaska for the period of 1968–1990 and pointed out that the intensified Aleutian Low did not spin up the Alaskan Gyre. In the northern and eastern part of the Gulf of Alaska, the wind stress difference between the post-1976 and pre-1976 periods was anticyclonic (Fig. 1*a*), i.e., negative curl, hence the weakening of the gyral circulation in that area.

The intensified westerlies at midlatitudes and slightly increased easterlies in the tropics imply an increased anticylonic wind stress curl in the subtropics, resulting in the strengthening of the subtropical gyre circulation (Fig. 3*c*). The enhanced subtropical gyre also intruded further south.

Changes in velocity and associated changes in temperature

Changes in horizontal velocity

The difference in the January surface currents (at 15 m depth) between the post-1976 case and pre-1976 case (Fig. 4*a*) and the currents in the pre-1976 case (Fig. 4*b*) reflect the dominant Ekman dynamics in the surface layer. In the Gulf of Alaska, the anomalous surface current flows northeastward (Fig. 4*a*), induced by the anomalous southeasterly wind stress (Fig. 1*a*). This anomalous northeastward Ekman drift transports the warm surface water from the south to the northern coastal area, leading to the convergence of surface water and the increase in SST. In contrast, in the pre-1976 case (Fig. 4*b*) the surface flows in the southern part of the Gulf of Alaska are southeastward, due to the westerly wind stress there (not shown), bringing the cold water from the Gulf of Alaska to the south, thereby maintaining the cold SST distribution.

In the central North Pacific between 25 and 45°N, there is a broad, enhanced surface Ekman drift flowing southward (Fig. 4*a*), induced by the increased westerly in the Aleutian Low system after the 1976 climate shift. With the large north–south temperature gradient field between mid-latitudes and high latitudes, the drift would advect the colder water from high latitudes to mid latitudes, producing large-scale negative temperature changes near the surface. In the Bering Sea, increased southwest flows transport very cold water from the northern part of the Bering Sea to the south, helping to create the negative temperature anomaly in the central North Pacific. In the midlatitude eastern Pacific, i.e., near the west coast of North America, the increased eastward flows may bring slightly warmer water from the central Pacific to the coast, causing the warming along the coast.

At low latitudes, even though the changes in wind stress are weaker than at higher latitudes, the small Coriolis parameter leads to large changes in the surface Ekman drift currents (Fig. 4*a*). Despite considerable fluctuations, the flows are generally directed northwestward north of the equator and are weak along the equator, especially on the western side. The increased northwestward flows in the North Equatorial Current system advect the slightly warmer water from low latitudes (about 10°N) to the tropics (about 20°N), especially on the eastern side where the temperature gradients are larger than those on the western side.

The simulated SST changes (Fig. 5) are very similar to those derived from the two climatologies of the post-1976 and pre-1976 periods (Fig. 2). This is expected because the model SST is relaxed to the SST climatology. Closer examination of Figs. 2 and 5 reveals that the simulated negative temperature change in the central North Pacific is slightly

© 1999 NRC Canada

Fig. 3. Vertically integrated transport stream function in January at the sixth year of (*a*) experiment B (pre-1976) and (*b*) experiment C (post-1976), with negative (broken) contours denoting cyclonic circulation. (*c*) Difference post-1976 minus pre-1976. The contour values are ±1, ±2, ±3, ±5, ±7, ±9, ±11, ±13, ±15, ±20, ±25, ±30, ±35, ±40, ±45, and ±50 Sv (10^6 $m^3 \cdot s^{-1}$).

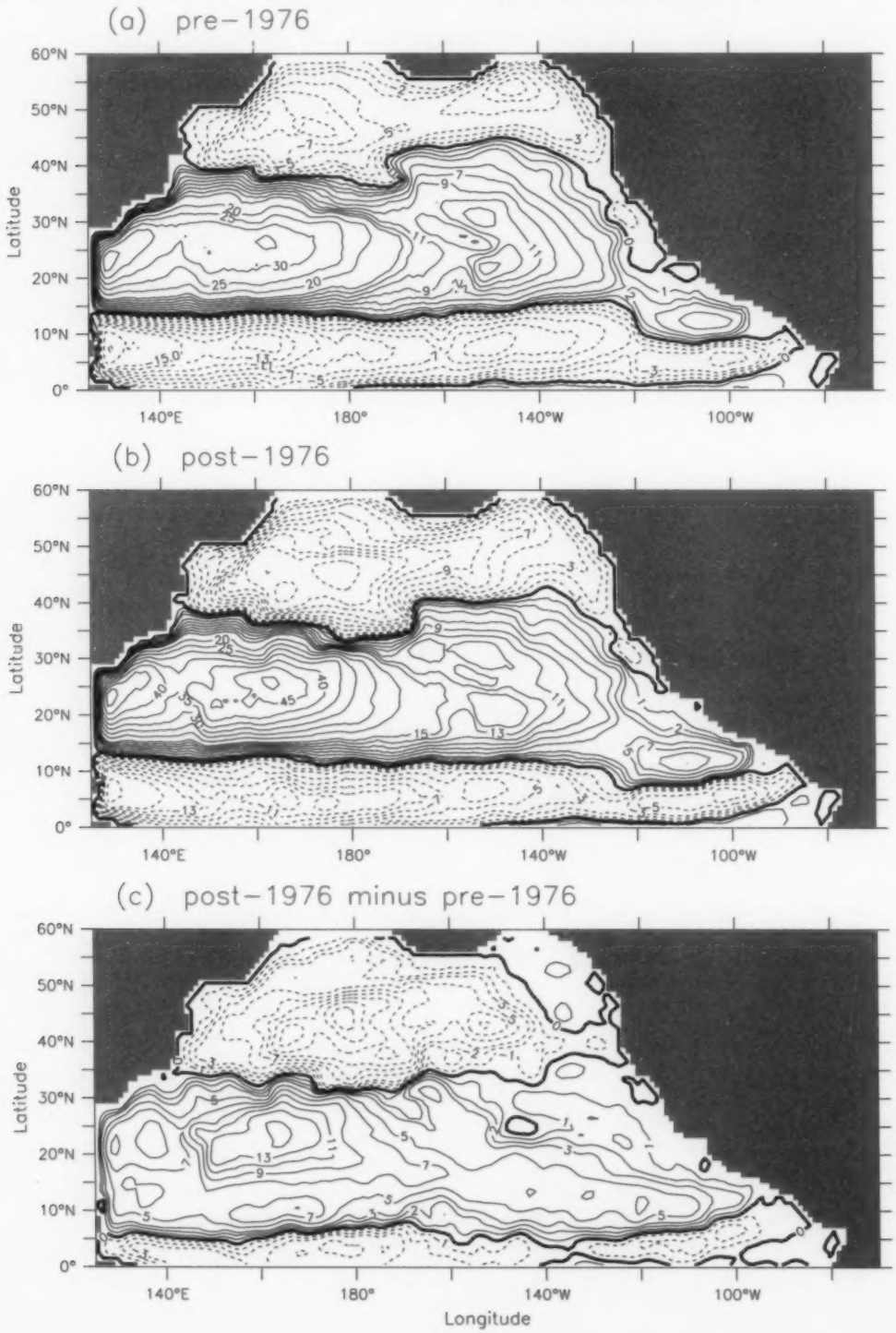

© 1999 NRC Canada

Fig. 4. (*a*) Difference in surface current (15 m depth) between the post-1976 case and the pre-1976 case in January at the sixth year (10^{-2} m·s^{-1}). (*b*) Surface current velocity at 15 m depth for the pre-1976 case in January at the sixth year.

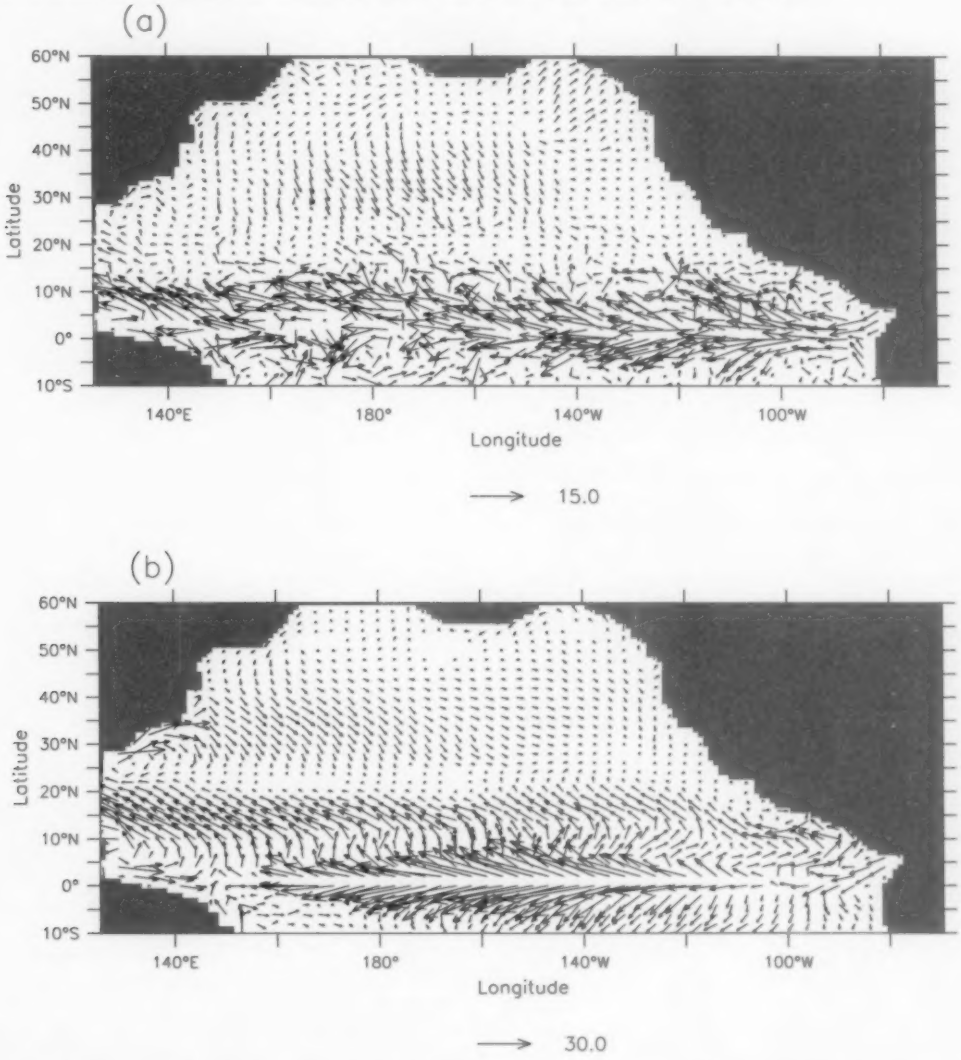

more intense than that derived from the two observed climatologies of the post-1976 and pre-1976 periods. This suggests that the surface wind stress forcing produces larger SST changes between the post-1976 case and the pre-1976 case than those specified in the surface relaxation boundary condition from the two reference SST climatologies. The intensified wind stress applied to the surface boundary in the model generates a stronger cooling in the central North Pacific, with the model relaxation surface boundary condition for SST trying to damp the excessive cooling. Eventually, the two boundary effects reach a balanced state, with the simulated temperature changes slightly stronger than those prescribed by the boundary conditions for SST. In other areas, the simulated SST changes appear to be similar to those prescribed, which indicate that the SST variations created by the changed wind stress are similar to the prescribed variations, so that the relaxation surface boundary condition did not have to introduce large heat flux adjustments.

Changes in vertical velocity

The change in the surface wind stress associated with the 1976 climate shift leads to the change in the surface currents, with increased divergence in the subarctic region, moderately increased convergence in the subtropic, and divergence in the equatorial region (Fig. 4*a*), leading to changes in upwelling and downwelling. Figure 6*a* is the difference in the vertical velocity pattern at 60 m depth during winter between the post-1976 case and the pre-1976 case. The upwelling along the equator increased from the western equatorial Pacific to the eastern equatorial Pacific. In the subarctic region, the pattern of anomalous vertical velocity is quite noisy, but generally the upwelling increased. Off the

© 1999 NRC Canada

Fig. 5. Simulated change in winter (DJF) SST between the post-1976 case and the pre-1976 case at the sixth year. The contour interval is 0.4°C.

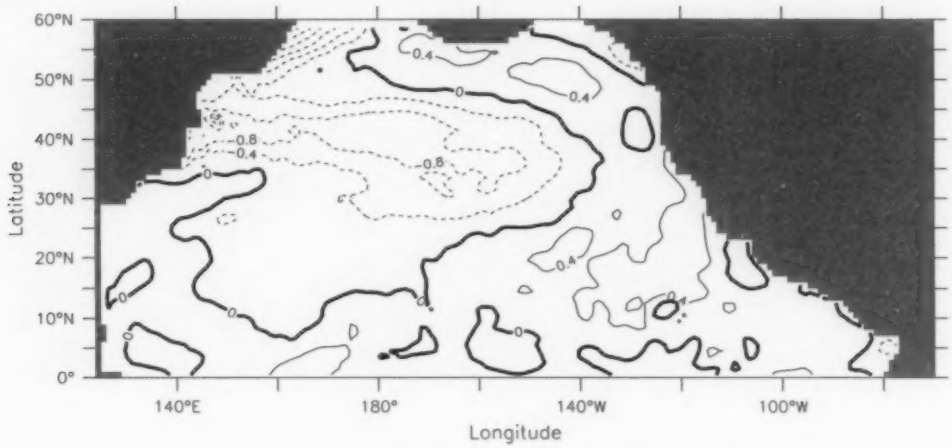

west coast of North America, there is generally anomalous downwelling from the northern boundary of the model domain to 40°N, as expected from the changes in surface currents. The enhanced northeastward surface currents flow onshore, inducing anomalous downwelling along the coast.

Zonally averaged vertical velocity (Fig. 6*b*) shows that in the subarctic area (south of 52°N), the upwelling strengthened in the post-1976 case. The value in the post-1976 case at 38°N is almost twice that in the pre-1976 case. In the subtropical area, the increased downwelling from the enhanced convergence of surface waters is also seen in Fig. 6*b*. The upwelling along the equator increased, but by a lesser percentage than the change in the subarctic region.

The meridional section of the vertical velocity difference between the two cases along 155°W (Fig. 7) shows that in the subarctic area, there are large regions of anomalous upwelling, and in the subtropical area, anomalous downwelling is interrupted by narrow upwelling bands. The change in the equatorial region is generally dominated by the increased upwelling, in a narrow zonal band in the upper layer, broadening with depth. Generally the largest changes are confined above 400 m depth. There are a few centers of large change in the broad downwelling area. The strongest one is located at 5°N and 100 m depth, and there is a second center around 15°N and 100 m depth. Two other weaker centers are found at 22 and 30°N. In the subarctic area, the increased upwelling is generally moderate; however, upwelling in the subarctic area has been enhanced by a larger percentage than in any other area (Fig. 6*b*). In the equatorial region, a decreased upwelling center is situated right at the equator, at 50 m depth, with two increased upwelling centers located on its two sides. Right under the decreased upwelling center, there is an increased upwelling center at 100 m depth. At 280 m depth, there are two enhanced upwelling centers on either side of the equator at 4°N and 4°S.

For the meridional section along 155°W, the temperature changes are largely confined to above 400 m depth (Fig. 8*a*), with the temperature change in the subsurface area mainly determined by the product of the vertical velocity change (Fig. 7) and the vertical temperature gradient (Fig. 8*b*).

At low latitudes, there is a positive temperature anomaly centered at 5°N and 120 m depth. Compared with the change in vertical velocity (Fig. 7), the positive temperature change matches the strongest downwelling anomaly center, with the former located slightly lower than the latter. The vertical temperature distribution (Fig. 8*b*) shows that the vertical temperature gradient at 5°N and 100 m depth is very large. Thus, the enhanced downwelling brings warmer water down to increase the water temperature in the layer below and form the temperature anomaly centered below the enhanced downwelling center. The same mechanism can be applied to explain the other two positive temperature anomalies centered at 16°N and 4°S. Similarly, the two anomalous upwelling centers located at a depth of 280 m on either side of the equator are responsible for the two weaker negative temperature anomalies centered at 320 m depth.

In the equatorial region, the upwelling changes in the upper waters do not appear to have much effect on the local temperature, since the upwelling changes are located above 80 m depth (Fig. 7) where the vertical temperature gradient is almost zero (Fig. 8*b*). However, between 100 and 300 m depth, temperature changes are positive despite the increased upwelling. The meridional velocity (not shown) reveals strong equatorward flow at such depth, thereby advecting the anormalously warm water on both sides of the equator (due to the enhanced downwelling) to converge towards the equator. Figure 7 also shows two narrow positive vertical velocity anomalous bands located at 18 and 25°N, with no corresponding cooling in Fig. 8*a*. These two vertical velocity anomalous bands are rather local to the 155°W section, as Fig. 6*a* illustrates the noisy nature of the upwelling anomalies. The overall zonal vertical velocity change in Fig. 6*b* shows enhanced downwelling at these latitudes.

At mid-latitudes and high latitudes, the temperature changes are negative and the pattern of the negative change is quite broad, with a maximum of −1.0°C at 80 m depth and 32°N. Increased upwelling in the subarctic area only extends southward to 33°N (Fig. 7), but the negative temperature change extends to 25°N in the upper water (Fig. 8*a*), due to the increased southward surface Ekman drift from the intensified westerlies.

The depth range to which the subsurface temperature vari-

© 1999 NRC Canada

Fig. 6. (*a*) Difference in the vertical velocity at 60 m depth in winter (DJF) between the post-1976 case and the pre-1976 case. Solid curves indicate a positive anomaly (i.e., either upwelling has increased or downwelling has decreased), and broken curves indicate a negative anomaly. The contour values are ±5, ±10, ±20, ±50, ±100, and ±200 cm·day^{-1} (1.157 × 10^{-7} m·s^{-1}). Laplacian smoothing was used as in Xie and Hsieh (1995). (*b*) Zonally averaged vertical velocity (cm·day^{-1}) at 60 m depth in DJF for the pre-1976 case (broken line) and the post-1976 case (solid line). The values between 10 and 60°N are multiplied by 5 for better visualization.

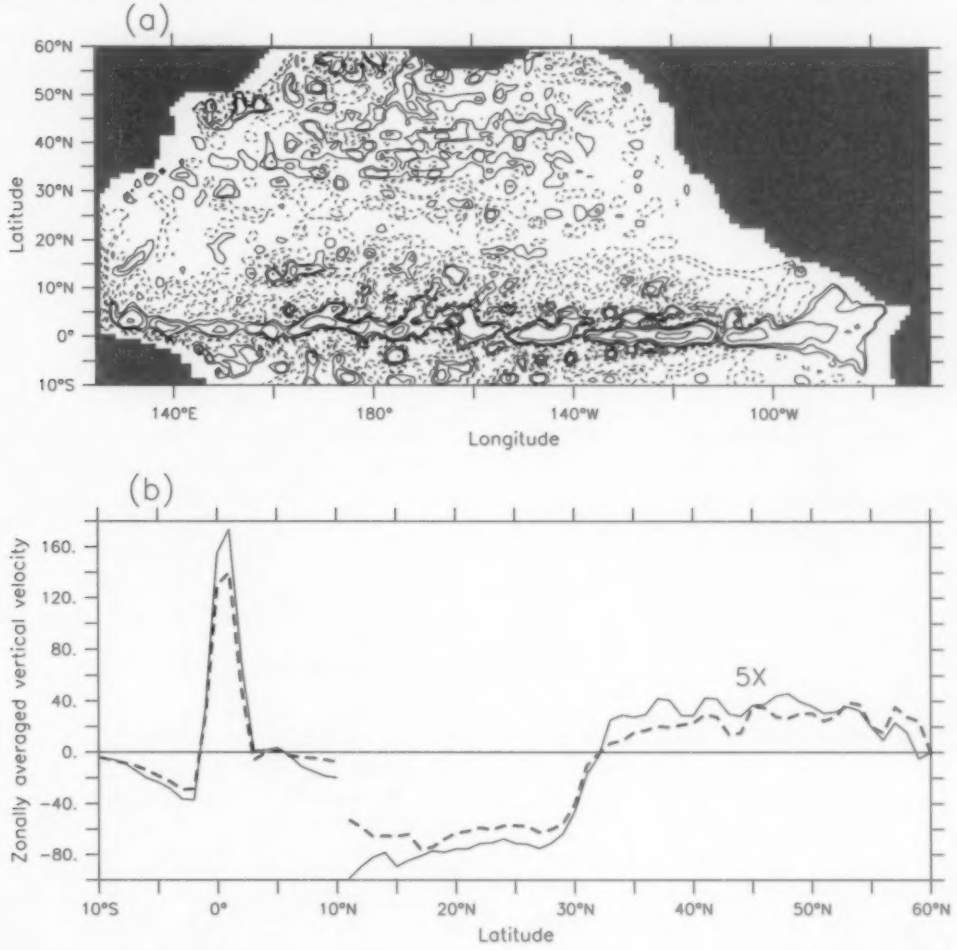

ations extend is slightly different for different longitude sections. Along the date line (not shown), the temperature variation penetrates down to 650 m depth, deeper than that along 155°W. A depth of 650 m is the typical range to which the subsurface temperature change penetrates in the western Pacific. The cooling of the subsurface waters between 25 and 55°N in our experiments agrees in magnitude and depth with the general cooling trend found in the oceanographic data from 1957 to 1981 (Antonov 1993), where the cooling trend continued to 500–600 m depth. So the 1976 climate regime shift may have contributed significantly to the cooling trend found by Antonov (1993).

Changes in meridional mass and heat transports

Figure 9 shows the change in the meridional mass transport between the post-1976 case and the pre-1976 case in January. The changes in both the surface boundary conditions, i.e., the surface wind stress and the SST, can contribute to the change in the meridional mass transport. One would speculate that the change in SST (Fig. 2), with cooling in the central North Pacific and warming along the equator, eastern tropical Pacific, and the coastal area off North America, would change the density structure of the surface water via the surface relaxation boundary condition, generating downward movement in the cooling area and upward movement in the warming area. The resulting change in thermohaline circulation is expected to be a clockwise meridional mass loop. However, the simulated change in meridional mass transport (Fig. 9) shows a strong clockwise cell only at low latitudes, with an anticlockwise cell at mid-latitudes. The increased Ekman suction along the equator strengthens the clockwise meridional cell just north of the equator, whereas the intensified westerlies of the Aleutian Low system increase the equatorward surface Ekman drift at

© 1999 NRC Canada

Fig. 7. Meridional section of vertical velocity change in winter (DJF) along 155°W between the post-1976 case and the pre-1976 case. Solid lines represent a positive vertical velocity change (either increase in upwelling or decrease in downwelling), and broken lines represent a negative change. The contour values are ±2, ±4, ±6, ±8, ±10, ±20, ±30, ±40, and ±50 cm·day^{-1} (1.157 × 10^{-7} m·s^{-1}).

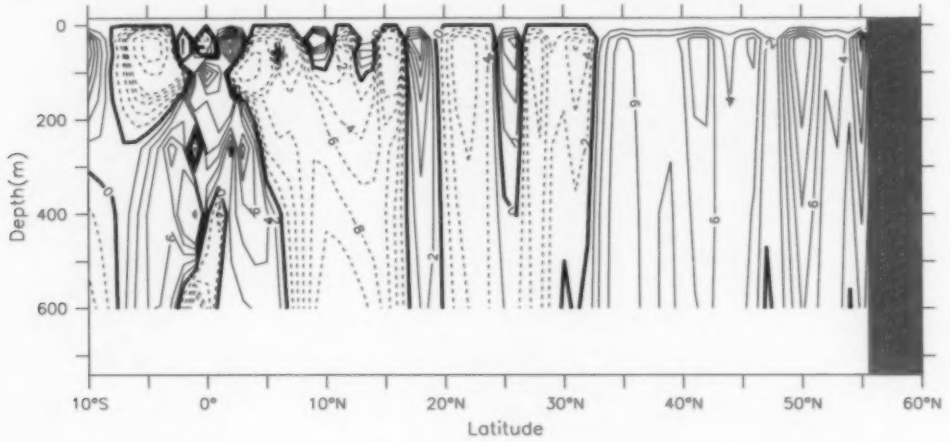

the midlatitudes, leading to the enhanced anticlockwise meridional cell. As the Ekman mass transport is inversely related to the Coriolis parameter f, the change in the mass transport is stronger in the equatorial region than at the midlatitudes, even though the change in the westerlies is stronger than in the equatorial winds.

According to Bryan and Lewis (1979), the meridional heat transport {HT} can be divided into three parts, the overturning component, the gyre component, and the diffusion component, as defined, respectively, by the three terms on the right-hand side of eq. 1:

$$(1) \qquad \{HT\} = \rho C_p \{[v][\theta] + [v'\theta'] + A_{HH} a^{-1} \partial_\phi [\theta]\}$$

where

$$\{\ \} = \int_{-H}^{0}\int_{\lambda_1}^{\lambda_2}(\ )a\cos\phi\, d\lambda dz$$

$$[\ ] = \frac{1}{\lambda_2 - \lambda_1}\int_{\lambda_1}^{\lambda_2}(\ )d\lambda$$

where λ is the longitude, ϕ is the latitude, θ is the potential temperature, v is the northward velocity component, A_{HH} is the horizontal diffusion coefficient, a is the earth's radius, ρ is the density, and C_p is the specific heat. The prime denotes the deviation of a variable from its zonal mean [ ]; { } integrates over a given latitudinal section. The first term, the overturning component, is the component of transport contributed by the correlations of zonally averaged currents and zonally averaged temperatures that are associated with overturning in the meridional plane. Physically, it can be thought of as the heat transport owing to the poleward flow of warm surface waters and the return flow of deep cold water. The second term, the gyre component, is the transport component due to the correlations of velocity and temperature in the horizontal plane. It can be counted as a net transport of heat by warm western boundary current moving poleward compensated by a return flow of colder water on the eastern side of the ocean. The last term is a horizontal diffusion term.

The total meridional heat transport (Fig. 10*a*) showed a maximum value at low latitudes for both the post-1976 case and the pre-1976 case. A comparison between Figs. 10*a* and 10*b* showed that the total meridional heat transport is mainly determined by the overturning component at low latitudes. There, the equatorial Ekman suction generates meridional cells, transporting heat poleward efficiently by carrying the warm surface waters poleward in the upper branch with a compensating equatorward flow of cold waters below. At midlatitudes, the westerly wind zone produces equatorward Ekman transport, causing the equatorward net heat transport. At high latitudes, winds are weak and mostly easterlies. Therefore, a weaker poleward Ekman transport combined with weaker temperature gradients yields smaller heat transport. The thermohaline forcing is working in the same direction as the wind forcing at low and high latitudes but in the opposite direction at midlatitudes, although the thermohaline effect is generally weak in the North Pacific.

Compared with the study of Bryan and Lewis (1979), the January poleward heat transport of this study is much larger. However, they pointed out that their simulated maximum heat transport is only 25% of that given by Oort and Vonder Haar (1976), who calculated the ocean heat transport as a residual term by combining heat storage data from the oceans with atmospheric heat balance estimates. Bryan (1982) also indicated that the heat transport at 24°N of Bryan and Lewis (1979) is only 50% of that estimated by Roemmich (1980) and Hall and Bryden (1982).

The discrepancy between the maximum value of heat transport of this study and that of Bryan and Lewis (1979) probably arises from the difference in model resolution and model parameters (e.g., horizontal viscosity and horizontal diffusivity). Bryan and Lewis (1979) performed an experiment in which the horizontal resolution was increased by a factor of 4 while the horizontal viscosity was decreased by a factor of 8 and the horizontal diffusivity by a factor of 2 and found that the heat flux at 24°N increased from 0.6 to 0.9 PW. The model resolution in this study is almost six times higher than that used in their study, and the horizontal vis-

© 1999 NRC Canada

Fig. 8. (*a*) Meridional section of temperature change in winter (DJF) along 155°W between the post-1976 case and the pre-1976 case. The contour interval is 0.2°C. (*b*) Meridional section of temperature distribution in DJF along 155°W for the pre-1976 case. The contour interval is 1°C.

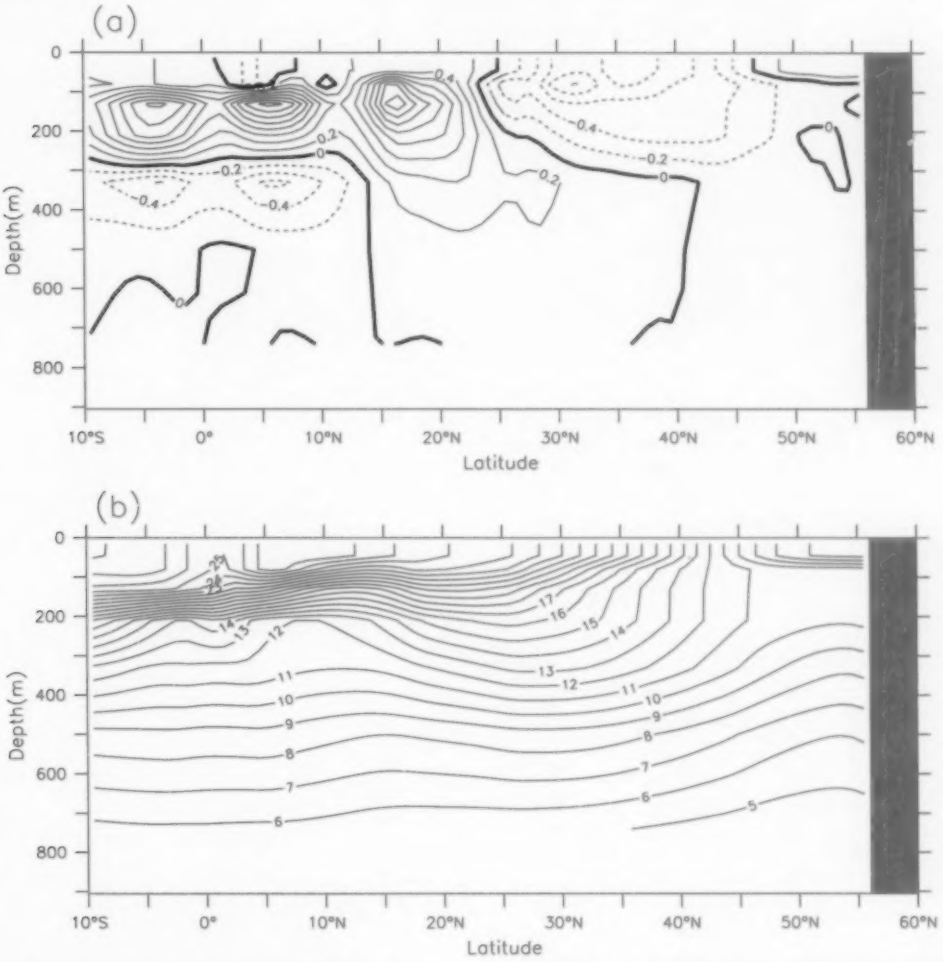

cosity is four times less; hence, the heat transport discrepancy is expected.

The change in the surface wind stress as a result of the 1976 climate shift will produce changes in the meridional heat transport. By comparing Fig. 10*a* with Fig. 10*b*, it is seen that at low latitudes the change in the heat transport due to the overturning component is the major effect changing the total heat transport. The largest variation of 1.5 PW on both Figs. 10*a* and 10*b* occurs at 7°N where the peak heat transport lies. The significant change in the meridional circulation at low latitudes (Fig. 9) is responsible for the large change in heat transport.

At midlatitudes, the contribution from the change in the overturning component is still the most important in determining the change in total heat transport. However, contributions from the gyre and diffusion components are not negligible. The equatorward heat transport by the overturning component is increased by a maximum of about 0.3 PW at 28°N, while the increased poleward heat transport by the gyre component has a maximum of 0.06 PW at 27°N and 0.04 PW by the diffusion component at 32°N. Thus, the change contributed by the overturning component is partly offset by the diffusion and gyre components.

The increase in the equatorward heat transport at midlatitudes by the overturning component mainly results from the increased meridional circulation at these latitudes (Fig. 9), which is largely due to the intensification of the westerlies in the Aleutian Low system. The gyre component at midlatitudes tends to transport heat poleward by having a warm northward western boundary current compensated by a cold return flow on the eastern boundary. Thus, the intensified subtropical gyre (Fig. 3*c*), resulting from the 1976 climatic shift, causes the increase in poleward heat transport by the gyre component in this latitude band. The diffusion component is determined by the meridional temperature gradient. From the simulated temperature change at the surface (Fig. 5) and subsurface (Fig. 8*a*), it is seen that the meridional temperature gradients are enhanced between 20 and 50°N, hence the increased heat transport by the diffusion term.

At high latitudes (north of 45°N), the very small total me-

© 1999 NRC Canada

Fig. 9. Difference in meridional mass transport between the post-1976 case and the pre-1976 case in January. The contour interval is 5×10^9 kg·s^{-1}. Anticlockwise circulation is indicated by broken contours.

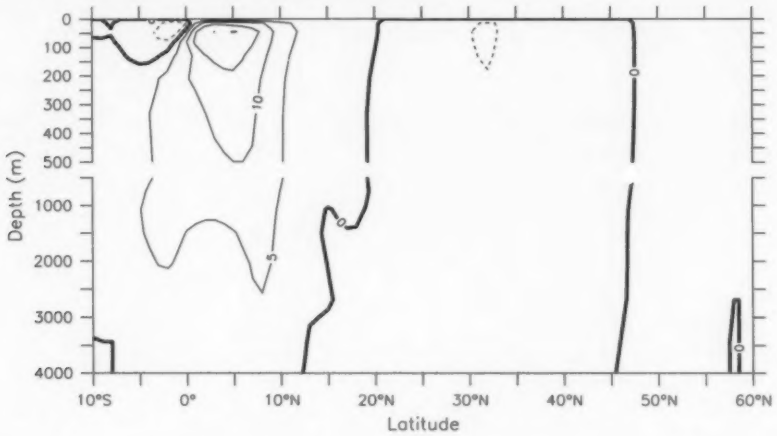

Fig. 10. (*a*) Total meridional heat transport, (*b*) meridional heat transport contributed by the overturning component, (*c*) gyre component of the meridional heat transport, and (*d*) diffusion component of the meridional heat transport. The solid line represents the pre-1976 case and the broken line the post-1976 case. The values between 40 and 60°N in Figs. 10*a* and 10*b* are multiplied by 5 for better visualization. Units are petawatts.

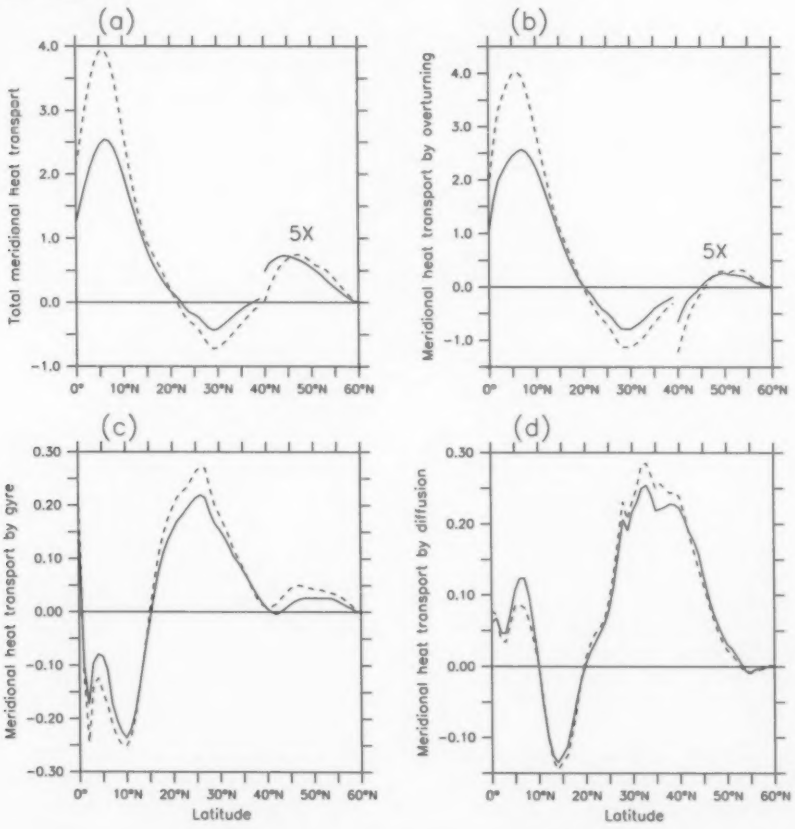

ridional heat transport is poleward. All three fractional components are poleward, except for the diffusion component north of 53°N. Generally the poleward overturning and gyre components in this latitudal band are enhanced by the 1976 climate shift, while the poleward diffusion component is decreased. The total change in the poleward heat transport at

© 1999 NRC Canada

high latitudes is about a 30% increase from the heat transport in the pre-1976 case.

Discussion

Associated with the climate regime shift are changes in the wind stress, surface heat flux, and freshwater flux, all of which affect the ocean. In our numerical experiments, only the wind stress has good enough data to allow us to implement the change in the wind stress forcing. The surface heat flux changes can only be implemented indirectly by the surface relaxation boundary condition. The change in the surface freshwater flux has not been modelled at all, since we lack adequate surface salinity data. In all our experiments, a monthly climatology of the SSS field from the World Ocean Atlas (1994) has been employed, as there were insufficient data to construct monthly salinity climatology for the pre-1976 and post-1976 periods. For data at station P (145°W, 50°N), Freeland and Whitney (1997) found an SST trend of +1.96°C per century and an SSS trend of –0.43 per century. Since the center of the climatology period 1952–1975 (pre-1976) and that of 1976–1988 (post-1976) are separated by 19 years, the SSS change from the trend of Freeland and Whitney (1997) would be –0.0817. We performed an additional numerical experiment where we assumed a uniform change in SSS between the two climatological periods for the region north of 40°N. Hence, the value 0.0817 was subtracted from the monthly climatology SSS data for each month at each grid point in the area north of 40°N, with a linear taper decreasing the value of the change from 0.0817 at 40°N to 0 at 35°N. At the lower latitudes, the SSS changes will be ignored, as the density is mainly determined by the temperature. Together with the wind stress and SST surface forcing field in the post-1976 period, the model was run again for 6 years (experiment S) from the end of the basic run. The difference in vertical velocity pattern at 60 m depth during DJF between experiment S (post-1976 with salinity modified) and experiment C (post-1976) showed that the change in vertical velocity at each individual grid point was less than 0.5% except for those in the merging area of the Kuroshio and Oyahio, which can reach 2%. The zonal averaged vertical velocity curves for both experiments S and C overlapped, and similarly for the total meridional heat transport. Hence, the uniform decrease in the SSS by an amount of 0.0817 at subpolar latitudes does not have significant impacts on the major results shown in this paper. While a uniform decrease in SSS is a simplistic assumption, this experiment does show that a uniform decrease in SSS does not have an impact anywhere near that of the shift in the wind stress.

Summary and conclusion

A numerical investigation into the oceanic changes associated with the 1976 climate regime shift has been carried out with the Geophysical Fluid Dynamics Laboratory ocean general circulation model. First, the model was spun up from the rest state with the surface boundary forced by the wind stress monthly climatology and relaxed to the SST and SSS monthly climatology. Two additional experiments were performed, one with the surface forcing replaced by the pre-1976 (1952–1975) monthly climatological wind stress and SST fields and the other by the post-1976 (1976–1988) monthly climatological values. During these experiments, the same SSS monthly climatology was used.

The simulated ocean circulations exhibited significant changes in response to the changes in the atmospheric forcing between the pre-1976 and post-1976 periods. The intensification of the post-1976 Aleutian Low system in winter spun up the subarctic gyre and the subtropical gyre, except in the northern and eastern part of the Gulf of Alaska, where the Alaskan gyral circulation weakened.

The deepening of the Aleutian Low generated stronger surface divergence in the subarctic area and stronger convergence in the subtropic. Hence, the upwelling was strengthened in the subarctic region and the downwelling enhanced in the subtropical area. Off the west coast of North America, north of 40°N, there was mainly anomalous downwelling, induced by the anomalous surface currents.

The meridional sections of the changes in the vertical velocity showed that significant changes in the vertical velocity were confined above depths of a few hundred metres. The increased upwelling in the subarctic, together with the vertical temperature gradients, produced large-scale cooling in the subsurface, and similarly for the increased downwelling in the subtropic, generating large-scale warming there. The significant changes in the subsurface thermal structure, mainly determined by the product of the vertical velocity change and the vertical temperature gradients, were generally limited to above 650 m depth.

The change in the large-scale circulation in the ocean certainly led to changes in the meridional circulation and heat transport. At low latitudes, the poleward heat transport was increased mainly from the strengthening of the meridional circulation there. At midlatitudes, the equatorward heat transport was enhanced mainly by the meridional component, although partly offset by the gyre and diffusion components. At high latitudes, the small poleward heat transport was slightly enhanced.

Acknowledgments

We are grateful to the Pacific Marine Environmental Laboratory staff for the Ferret plotting package and Ken Denman, Susan Haigh, Warren Lee, Skip McKinnell, Benyang Tang, and Susan Allen for helpful discussion. This research was supported by the the Canadian GLOBEC project funded by the Natural Sciences and Engineering Research Council of Canada and the Department of Fisheries and Oceans.

References

Alexander, M. 1992. Midlatitude atmosphere–ocean interaction during El Niño. I. The North Pacific Ocean. J. Clim. **5**: 944–958.

Antonov, J. 1993. Linear trends of temperature at intermediate and deep layers of the North Atlantic Ocean and the North Pacific Ocean. J. Clim. **6**: 1928–1942.

Beamish, R.J., and Bouillon, D.R. 1993. Pacific salmon production trends in relation to climate. Can. J. Fish. Aquat. Sci. **50**: 1002–1016.

Bryan, K. 1982. Seasonal variation in meridional overturning and poleward heat transport in the Atlantic and Pacific oceans: a model study. J. Mar. Res. **40**(Suppl.): 38–53.

© 1999 NRC Canada

Bryan, K., and Lewis, L.J. 1979. A water mass model of the world ocean. J. Geophys. Res. **84**(C5): 2503–2517.

Freeland, H.J., and Whitney, F.A. 1997. Evidence of secular change in the Northeast Pacific Ocean. WOCE International Project Office, Southampton, U.K. Int. WOCE Newsl. No. 26. pp. 34–36.

Graham, N.E. 1994. Decadal scale climate variability in the tropical and North Pacific during the 1970's and 1980's: observations and model results. Clim. Dyn. **10**: 135–162.

Hall, M., and Bryden, J. 1982. Direct estimates and mechanism of ocean heat transport. Deep-Sea Res. **29**: 339–359.

Lagerloef, G.S.E. 1995. Interdecadal variations in the Alaska gyre. J. Phys. Oceanogr. **25**: 2242–2258.

Large, W.G., and Pond, S. 1981. Open ocean momentum ux measurements in moderate to strong winds. J. Phys. Oceanogr. **11**: 324–326.

Lee, W.G., Holloway, G., and Hsieh, W.W. 1992. Importance of bottom topography in the seasonal cycle of the North Pacific subarctic gyre. Atmos.–Ocean, **30**: 140–145.

McFarlane, G.A., and Beamish, R.J. 1992. Climatic influence linking copepod production with strong year-classes in sablefish, *Anoplopoma fimbria*. Can. J. Fish. Aquat. Sci. **49**: 743–753.

Miller, A.J., Cayan, D.R., Barnett, T.P., Graham, N.E., and Oberhuber, J.M. 1994. Inter-decadal variability of the Pacific Ocean: model response to observed heat flux and wind stress anomalies. Clim. Dyn. **9**: 287–302.

Mysak, L.A. 1986. El Niño, interannual variability and fisheries in the northeast Pacific Ocean. Can. J. Fish. Aquat. Sci. **43**: 464–497.

Nitta, T., and Yamada, S. 1989. Recent warming of tropical sea surface temperature and its relationship to the northern hemisphere circulation. J. Meteorol. Soc. Jpn. **67**: 375–383.

Oort, A.H., and Vonder Haar, T.H. 1976. On the observed annual cycle in the ocean–atmosphere heat balance over the northern hemisphere. J. Phys. Oceanogr. **6**: 781–800.

Pacanowski, R.C., and Philander, S.G.H. 1981. Parameterization of vertical mixing in numerical models of tropical oceans. J. Phys. Oceanogr. **11**: 1443–1451.

Roemmich, D. 1980. Estimation of meridional heat flux in the North Atlantic by inverse methods. J. Phys. Oceanogr. **10**: 1972–1983.

Royer, T.C. 1989. Upper ocean temperature variability in the northeast Pacific Ocean: is it an indicator of global warming? J. Geophys. Res. **94**: 18 175 – 18 183.

Semtner, A.J., and Chervin, R.M. 1988. A simulation of the global ocean circulation with resolved eddies. J. Geophys. Res. **93**: 15 502 – 15 522.

Tabata, S. 1991. Annual and interannual variability of baroclinic transports across Line P in the northeast Pacific Ocean. Deep-Sea Res. **38**(Suppl. 1): S221–S245.

Trenberth, K.E. 1990. Recent observed interdecadal climate changes in the northern hemisphere. Bull. Am. Meteorol. Soc. **71**: 988–993.

Trenberth, K.E., and Hurrell, J.W. 1994. Decadal atmosphere–ocean variations in the Pacific. Clim. Dyn. **9**: 303–319.

Venrick, E.L., McGowan, J.A., Cayan, D.R., and Hayward, T.L. 1987. Climate and chlorophyll *a*: long-term trends in the central North Pacific Ocean. Science (Washington, D.C.), **238**: 70–72.

Woodruff, S.D., Slutz, R.J., Jenne, R.L., and Steurer, P.M. 1987. The comprehensive ocean–atmosphere data set. Bull. Am. Meteorol. Soc. **68**: 1239–1250.

World Ocean Atlas. 1994. CD-ROM data set documentation. Tech. Rep., National Oceanography Data Center, Ocean Climate Laboratory, U.S. Department of Commerce, NOAA, National Enviromental Satellite Data and Information Service, Washington, D.C.

Xie, L., and Hsieh, W.W. 1995. The global distribution of wind-induced upwelling. Fish. Oceanogr. **4**: 52–67.

© 1999 NRC Canada

Distribution of *Calanus* spp. on and around the Nova Scotia Shelf in April: evidence for an offshore source of *Calanus finmarchicus* to the central and western regions

Erica J.H. Head, Leslie R. Harris, and Brian Petrie

Abstract: Observations of hydrography and *Calanus* spp. abundance were made at stations on lines across the central and eastern Scotian Shelf (SS) in April 1995 and 1997 and on additional lines on the western SS and across Cabot Strait (CS) and the Laurentian Channel (LC) in 1997. *Calanus finmarchicus* was more abundant on the central and western SS than in the east, and *Calanus hyperboreus* was concentrated in the east and in areas influenced by the Nova Scotia Current. *Calanus* spp. on the eastern SS probably originated mainly from populations overwintering in the Gulf of St. Lawrence. High abundances of *C. finmarchicus* occurred at or beyond the shelf break when warm slope water was present, suggesting that they derived from a population overwintering in the deep water south of the SS. In both years, slope water was present in the near-surface layers at shelf stations of the Halifax Line (HL), but in 1997 the degree of intrusion was greater. *Calanus finmarchicus* abundances were also substantially higher at shelf stations of the HL in 1997, implying contribution from the offshore population to the populations in central and western SS regions. Consistent with the suggested difference in their origins, *C. finmarchicus* on the western SS belonged primarily to the new year's generation, whereas those on the eastern SS belonged mainly to that of the previous year.

Résumé : Des observations de paramètres hydrographiques et de l'abondance des *Calanus* spp. ont été faites à des stations réparties sur des transects traversant le milieu et la partie est de la plate-forme Scotian, en avril 1995 et 1997, et sur d'autres transects dans la partie est de la plate-forme où traversant le détroit de Cabot et le chenal Laurentien, en 1997. *Calanus finmarchicus* était plus abondant dans le centre et l'ouest de la plate-forme que dans l'est et *Calanus hyperboreus* était concentré dans l'est et dans les zones subissant l'influence du courant de la Nouvelle-Écosse. Les *Calanus* spp. de l'est de la plate-forme avaient sans doute pour origine principale des populations hivernant dans le golfe du Saint-Laurent. Les *C. finmarchicus* étaient très abondants à la bordure ou en deçà de la bordure de la plate-forme quand de l'eau plus chaude de la pente était présente, ce qui porte à croire qu'ils provenaient d'une population hivernant en eau profonde au sud de la plate-forme. Au cours des deux années, de l'eau de la pente était présente dans les couches à proximité de la surface aux stations de la plate-forme du transect d'Halifax, mais en 1997 l'intrusion était plus importante. Les *C. finmarchicus* étaient aussi passablement plus abondants aux stations de la plate-forme du transect d'Halifax en 1997, ce qui suppose un apport d'une population hauturière aux populations du centre et de l'ouest de la plate-forme. En accord avec la différence proposée pour leur origine, les *C. finmarchicus* de la partie ouest de la plate-forme appartenaient surtout à la génération de dernière année tandis que ceux de la partie est appartenaient surtout à celle de l'année précédente.

[Traduit par la Rédaction]

Introduction

Calanus finmarchicus, *Calanus glacialis*, and *Calanus hyperboreus* are all commonly found in the near-surface layers of the Scotian Shelf (SS) during spring and early summer and at depth in the shelf basins during fall (Sameoto and Herman 1990, 1992). *Calanus finmarchicus* is the dominant species over the southwestern SS, and *C. glacialis* and *C. hyperboreus* are more important in the northeast (Sameoto and Herman 1992). All three species may be regarded as expatriates on the SS. *Calanus finmarchicus* is a North Atlantic species distributed from the New England Shelf (40°N) in the southwest to the Greenland Sea and Barents Sea (80°N) in the northeast, and it shows maximal abundances in the western North Atlantic, the northern North Sea, and the Norwegian Sea (Planque et al. 1997). *Calanus glacialis* and *C. hyperboreus* are Arctic species, with the former mainly found over shelves (Conover 1988; Hirche 1991) and the latter generally associated with deep water (Conover 1988). All three species share the ability to overwinter at depth in a state of arrested development, or diapause. The timing of descent and ascent and the stage or stages that diapause vary between species. Sameoto and Herman (1992) discussed the likely springtime sources of

Received May 13, 1999. Accepted August 12, 1999.
J15139

E.J.H. Head,[1] L.R. Harris, and B. Petrie. Department of Fisheries and Oceans, Ocean Sciences Division, Bedford Institute of Oceanography, P.O. Box 1006, Dartmouth, NS B2Y 4A2, Canada.

[1]Author to whom all correspondence should be addressed.
e-mail: heade@mar.dfo-mpo.gc.ca

© 1999 NRC Canada

the *Calanus* spp. for the SS, on the basis of distributional data and current knowledge of the circulation. They concluded that *C. glacialis* and *C. hyperboreus* originated from populations overwintering in the Gulf of St. Lawrence (GSL), as did *C. finmarchicus* on the eastern SS. *Calanus finmarchicus* over the central and western regions, they suggested, derived from populations overwintering in the deep shelf basins.

In recent years, our understanding of the hydrography and circulation on the SS has been modified. This has been achieved in part by the systematic consolidation of hydrographic data from the Northwest Atlantic into a comprehensive database at the Bedford Institute, accompanied by the development of climatological mean temperature, salinity, and density fields for the SS and the Gulf of Maine (Petrie et al. 1996). In these data, the mean spring (May 15) surface temperature contours show the influence of outflow of cooler water from the GSL and the shoreward penetration of warmer water, depicted by the 5°C isotherm, from the northeast to the southwest, occurring mainly to the west of Sable Island (Fig. 1A). A similar pattern is seen in the mean wintertime (February 15) temperatures for the 2 and 3°C contours (Petrie et al. 1996). Thus, the warmer offshore waters have a greater influence in the central SS region than on the eastern SS.

The main features of the mean circulation (Fig. 1B) are based on the modelling work of Sheng and Thompson (1996) and Han et al. (1997). The former presented a diagnostic model of the mean surface winter (December–March) circulation, while the latter presented the average 5- to 25-m circulation for spring (April–May). The models feature a generally southwestward flow, the Nova Scotia Current (NSC), over the inner half of the shelf that originates predominantly from the GSL. The current splits roughly at Halifax into an inshore component that enters the Gulf of Maine and a branch that moves offshore toward the shelf edge in the vicinity of the Scotian Gulf. To the northeast, at the shelf edge, the current from the Newfoundland Shelf also splits into two components: the first moves towards the GSL where it augments outflow from the Gulf in the Laurentian Channel (LC); the second moves across the mouth of the LC where it is joined by the Gulf outflow. An important new feature that appears in the modelled surface wintertime currents is the strong onshore flow from the shelf break area that occurs in the vicinity of Western Bank (Sheng and Thompson, 1996). The 5- to 25-m average spring circulation of Han et al. (1997) shows the same feature but with less strength and also indicates a strong onshore component in the area of the Gully. These patterns represent the mean circulation, but they are subject to interannual, seasonal, and higher frequency variability.

In this paper, we present hydrographic data and observations of *Calanus* spp. distributions collected at stations on and around the SS in April 1995 and 1997. These observations, together with our current understanding of the circulation, have lead us to modify the conclusions of Sameoto and Herman (1992) regarding the springtime sources of *C. finmarchicus* to the central and western regions of the SS, such that it now appears that the *C. finmarchicus* population that overwinters in the deep ocean beyond the shelf break probably provides input to the central and western SS in spring on an annual basis.

Sampling procedures

Stations were sampled along the Halifax (HL) and Louisbourg lines (LL) between April 19 and 25, 1995, and along these and five additional lines (Browns Bank (BBL), Roseway (RL), Gully (GUL), Laurentian Channel (LCL), and Cabot Strait lines (CSL)) between April 18 and 28, 1997 (Fig. 1A). Hydrographic data were collected using a Seabird (model SBE 19) CTD system mounted on the frame of an optical plankton counter, deployed in vertical drops (April 1995), or a Seabird (model SBE 25) CTD system mounted on a CTD rosette (April 1997). Zooplankton were collected in vertical net hauls between 100 and 0 m, or between the near-bottom and 0 m if the bottom depth was <100 m. *Calanus* spp. on the SS do not migrate vertically to depths of >100 m on a diel basis in spring (Sameoto and Herman 1990), so that this depth range included all of the active population for day and night samples. A 0.75-m-diameter ring net fitted with a 200-μm-mesh was used for the net tows. The cod-end was attached to the weight on the bottom of the hydro wire and the towing bridle to a crossbow mounted on the wire at a height above the weight such that the net was held vertically. In this configuration, zooplankton were only collected as the net was towed upwards. The towing speed was about 0.5 $m \cdot s^{-1}$, and the volume of water sampled was assumed to be the volume of the cylinder filtered by the net. Over the entire 1997 sampling grid, only seven stations had bottom depths of <100 m and only three had bottom depths of <80 m (BBL 1, 65 m; LL6, 70 m; LCL7, 60 m). Thus, the volume of water filtered was similar at most sations. Samples were preserved in 2% formalin. Prosome lengths of the youngest stages of *C. glacialis* and *C. finmarchicus* varied regionally, and length–frequency distributions overlapped between stations. Thus, length–frequency distributions were determined for each stage for each station, which allowed differentiation between the species.

Results

Distribution of *Calanus* spp. in April 1995

In April 1995, *C. finmarchicus* was more abundant at stations beyond or at the shelf break than at stations on the shelf itself for both the HL and the LL (Fig. 2; Table 1), especially on the LL, where concentrations seaward of the 200-m contour were more than 10 times higher than those on the shelf. *Calanus glacialis* and *C. hyperboreus* tended to be more abundant at stations of the LL than at those of the HL (except at HL stations 1 and 2 (HL1 and HL2)) and more abundant at stations on the shelf than at those at or beyond the shelf break (by factors of roughly 2.5 and 4.3 for the HL and the LL, respectively).

The percent abundance by species of total *Calanus* varied from northeast to southwest (Table 1). *Calanus glacialis* and *C. hyperboreus* together accounted for >80% at LL1–LL6 and for >90% at HL1 and >70% at HL2. At shelf stations seaward HL2, however, *C. finmarchicus* accounted for >75%

© 1999 NRC Canada

Fig. 1. (A) Location of sampling stations (circles) and climatological springtime surface temperature contours (May 15; from Petrie et al. 1996). (B) Surface circulation of the main currents and location of various features on the SS (SG, Scotian Gulf; EB, Emerald Basin; WB, Western Bank; SI, Sable Island; BB, Banquereau Bank; St.P.B., St. Pierre Bank). The 200-m contour is shown in both panels.

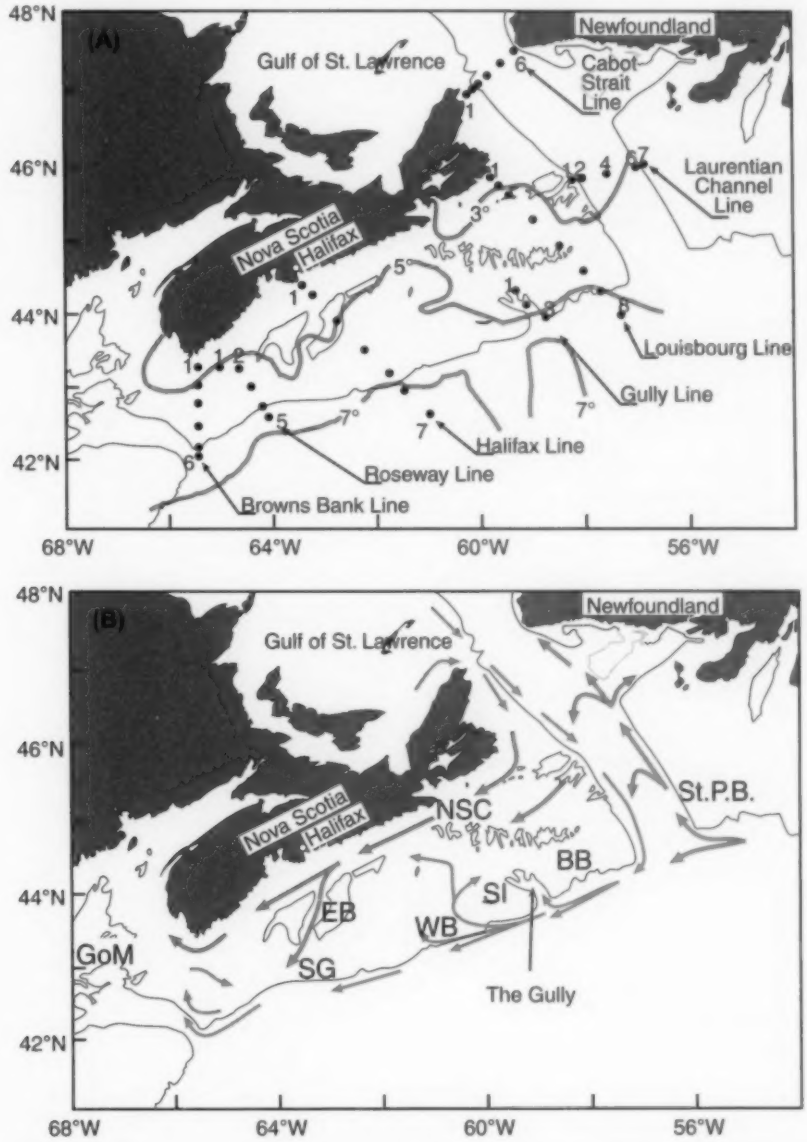

of total *Calanus*, and for both lines at stations beyond or at the shelf break, *C. finmarchicus* accounted for >90%.

Distribution of *Calanus* spp. in April 1997

In April 1997, *C. finmarchicus* abundances were relatively uniform at stations of the HL, regardless of whether they were on the shelf or beyond the shelf break (Fig. 3; Table 2). The same was true for the LL, where abundances were generally lower than at stations of the HL. At stations west of the HL and in the Gully, *C. finmarchicus* abundances were similar to those seen on the HL, while in the northeast (CSL and LCL), they were similar to those seen on the LL. *Calanus glacialis* had its highest abundances at stations on the southwestern SS, whereas *C. hyperboreus* was more concentrated in the east, at the inshore stations of the HL (HL1 and HL2) and at shelf break station of the RL (RL4).

The percent abundance of total *Calanus* by species varied from northeast to southwest, as in 1995. *Calanus glacialis* and *C. hyperboreus* together accounted for (on average) 74 and 73% of the total *Calanus* on the CSL and the LL, respectively, and they were particularly dominant on the western side of the CSL and the inshore half of the LL. *Calanus*

© 1999 NRC Canada

Fig. 2. Abundance of *Calanus* spp. on the SS in April 1995. The areas of the circles are proportional to the number of animals·m^{-2}.

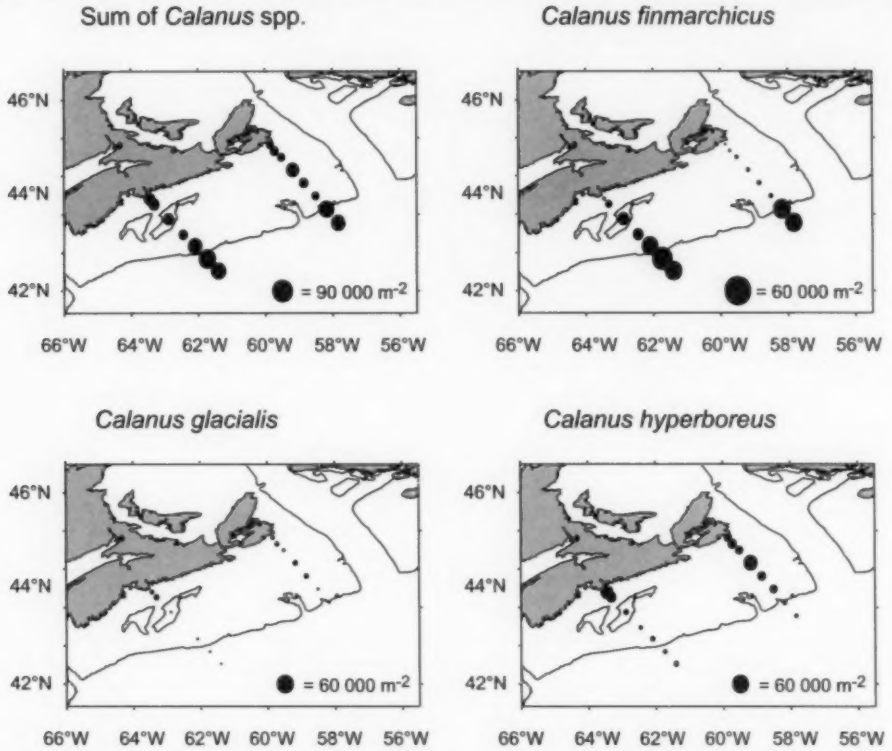

Table 1. Abundances (individuals·m^{-2}) of *Calanus* spp. at stations on the SS in April 1995.

	C. finmarchicus	*C. glacialis*	*C. hyperboreus*	Total *Calanus*
Halifax Line				
HL1	2 014	2909	22 722	27 644
HL2	6 875	4552	13 390	24 817
HL3	19 459	1019	4 262	24 740
HL4	15 463	0	2 497	17 960
HL5	39 121	1017	3 831	43 968
HL6	59 348	904	2 983	63 235
HL7	42 834	687	4 145	47 666
Louisbourg Line				
LL1	725	2674	9 248	12 647
LL2	1 428	3401	11 628	16 457
LL3	2 262	1840	9 155	13 257
LL4	2 529	4007	28 153	34 689
LL5	3 132	3539	10 647	17 318
LL6	2 827	1252	8 527	12 606
LL7	43 851	1279	3 835	48 965
LL8	40 863	0	2 477	43 340

finmarchicus accounted for 65% of the total *Calanus* at the single station south of St. Pierre Bank, however, and for an average of 48% at stations of the LCL. In 1997, as in 1995, *C. glacialis* and *C. hyperboreus* together accounted for >90% at HL1, but in 1997, in contrast with 1995, *C. finmarchicus* was more important at HL2 (about 70%). In the Gully and farther to the southwest, *C. finmarchicus* was dominant, accounting for on average 88% (GUL), 84% (HL, excluding HL1), 73% (RL), and 77% (BBL) of the total *Calanus*.

Distribution of stage compositions in *C. finmarchicus* populations

Stage compositions of *C. finmarchicus* populations were compared by dividing the population into four groups. The

© 1999 NRC Canada

Fig. 3. Abundance of *Calanus* spp. on the SS in April 1997. The areas of the circles are proportional to the number of animals·m^{-2}.

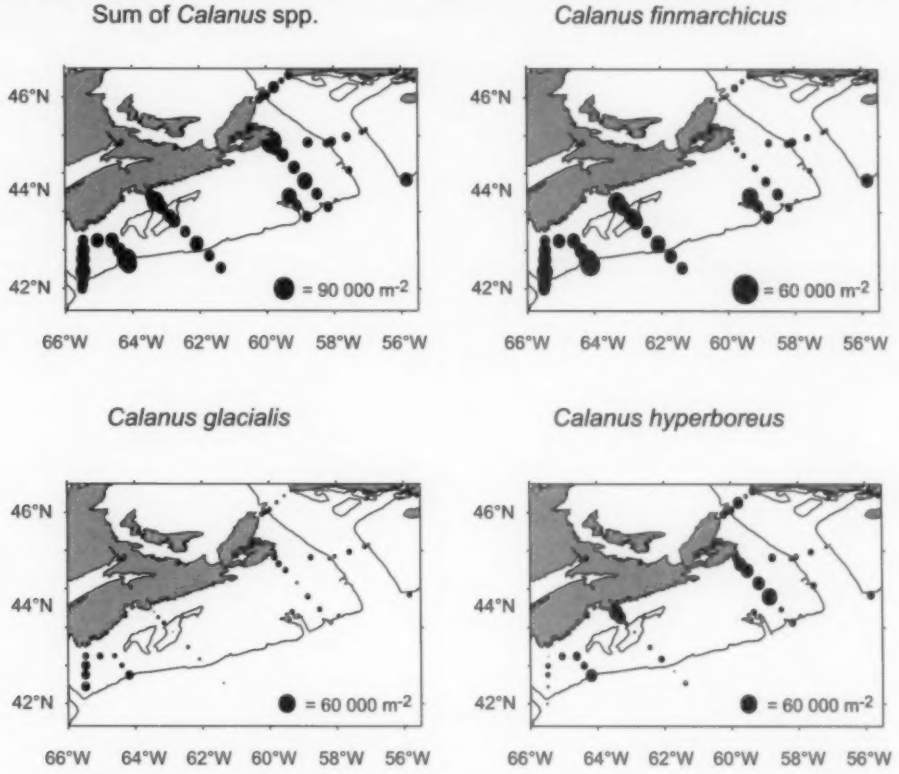

group including the youngest stages (CI–CIII) undoubtedly belonged to the new year's generation (G1), whereas the other groups (CIV, CV, and adults) might have belonged to either the G1 or the previous year's (G0) generation. In both 1995 and 1997, *C. finmarchicus* populations on the northeast SS (LL1–LL4) and in the NSC at HL1 were dominated by overwintered G0 adults, CV, and CIV (Figs. 4 and 5), with the exception of HL1 in 1995 and LL3 in 1997, where the G0 late stages were still relatively abundant. Similar stage compositions occurred in CS and on the western half of the LCL in 1997. Elsewhere, populations were generally dominated by G1, most often as CI–CIII and CIV. The latter are thought to belong mainly to G1 in these populations because they were quite abundant in the near-surface layers, whereas they are not abundant in overwintering populations (Sameoto and Herman 1990). Exceptions to this general pattern were on St. Pierre Bank (LCL7), Banquereau Bank, and at GUL1, where adults were completely absent, and HL6 in 1997, where CI–CIII were absent.

Surface temperature distribution as depicted by satellite imagery

An AVHRR image of sea surface temperature of the SS taken on April 27, 1997 (Fig. 6A), shows the coldest temperatures (about −1°C) in the GSL, CS, and LC and over the northeastern tip of the SS. There was relatively cold water over the entire eastern SS and in the NSC (Fig. 1B). Warmer water appears to move onshore through the Gully, with an arm extending east northeast over Banquereau Bank and onto the midshelf region, where the surface water was relatively warm (about 3.5°C), with temperatures similar to those of offshore waters. Over the southwestern SS, cold water derived from the NSC appears to flow towards the shelf break in the vicinity of the RL and to mix with warm offshore water during its passage over the shelf.

An AVHRR image of sea surface temperature taken on April 22, 1997 (Fig. 6B), shows regions to the southeast of the SS that are not visible in the April 27 image. In this image, it appears that a cyclonic eddy was forming seaward of the shelf break in the vicinity of the LL. The outside edge of this eddy was marked by relatively cold water that surrounded a core of relatively warm water. A second less distinct eddy was located to the northeast, at the mouth of the LC, and a third, farther east, near the shelf break of the Newfoundland Shelf.

Temperature and salinity distributions as measured in CTD profiles

There was more relatively warm, salty water in the upper 100 m at stations on the HL in 1997 as compared with April 1995, particularly at HL3–HL7 (Fig. 7). In Fig. 8, temperature–salinity plots for water at 10-m intervals in the 0–50 m depth range are compared with April climatological data taken from atlases in the BIO database (Petrie et al. 1996, 1999) for three water masses that might influence stations of the HL: Scotian Slope (SSL) water (characteristic of

© 1999 NRC Canada

Table 2. Abundances (individuals·m^{-2}) of *Calanus* spp. at stations on and near the SS in April 1997.

	C. finmarchicus	*C. glacialis*	*C. hyperboreus*	Total *Calanus*
Browns Bank Line				
BB1	14 932	5 860	296	21 088
BB2	21 513	10 889	3 946	36 348
BB3	25 782	10 294	3 745	39 821
BB4	36 809	10 780	1 302	48 891
BB5	24 923	149	511	25 583
BB6	19 761	120	902	20 783
Roseway Line				
RL1	21 814	5 562	6 662	34 038
RL2	25 009	3 293	8 934	37 236
RL3	24 731	3 571	7 035	35 337
RL4	51 117	9 917	18 487	79 520
RL5	55 275	0	1 153	56 428
Halifax Line				
HL1	108	414	27 305	27 827
HL2	44 475	2 011	18 125	64 611
HL3	28 598	321	1 175	30 094
HL4	15 617	2 149	3 413	21 178
HL5	31 721	1 302	5 367	38 391
HL6	21 951	0	497	22 449
HL7	17 404	551	3 363	21 319
Gully Line				
GUL1	38 058	3 232	5008	46 298
GUL2	16 419	75	1835	18 329
GUL3	19 569	192	1268	21 029
Louisbourg Line				
LL1	1 869	5 847	10 143	17 859
LL2	4 073	5 221	21 176	30 469
LL3	3 632	4 407	23 368	31 407
LL4	5 810	1 451	21 569	28 831
LL5	11 054	4 226	33 859	49 139
LL6	16 374	3 618	4 063	24 055
LL7	8 109	2 495	7 381	17 985
Laurentian Channel Line				
LC1	6 543	2 102	3 562	12 206
LC2	8 396	2 396	3 948	14 740
LC4	5 980	4 231	4 954	15 165
LC6	2 353	2 888	1 412	6 653
LC7	2 084	1 234	368	3 686
Cabot Strait Line				
CS1	1 168	3 616	7 969	12 753
CS2	2 685	3 917	4 251	10 853
CS3	1 959	3 270	7 171	12 401
CS4	6 723	2 061	15 436	24 220
CS5	3 234	1 193	2 710	7 137
CS6	4 572	1 446	8 622	14 640
Off St. Pierre Bank				
SPB1	22 207	3 785	8 141	34 133

the mid-Scotian Slope region), Newfoundland Slope (NFS) water, and NSC water (characteristic of an area off Canso, on the northeastern SS). In both 1995 and 1997 at HL7, the temperature–salinity values lay between those of SSL and NFS water, indicating that mixture of these water masses contributed to the observed temperature–salinity characteristics. At HL6, temperature–salinity properties were more characteristic of SSL water. In both years, at HL4 and HL3, the temperature–salinity characteristics lay on a line joining SSL and NSC waters. The simplest interpretation of this observation is that the waters in both years are composed of a mixture of SSL and NSC water, although the contribution of SSL water was greater in 1997 than in 1995, since the temperature–salinity values in 1997 are closer to the values typical of SSL water. There is an indication of SSL water as far inshore as HL2 in the 0–50 m range in 1997, although in

© 1999 NRC Canada

Fig. 4. Stage composition (% of total) of *C. finmarchicus* at stations of the HL and LL in April 1995. The areas hatched left to right descending represent the percentage of CI–CIII copepodites, the areas hatched left to right ascending represent the percentage of CIV, the white areas represent the percentage of CV, and the black areas represent the percentage of adults.

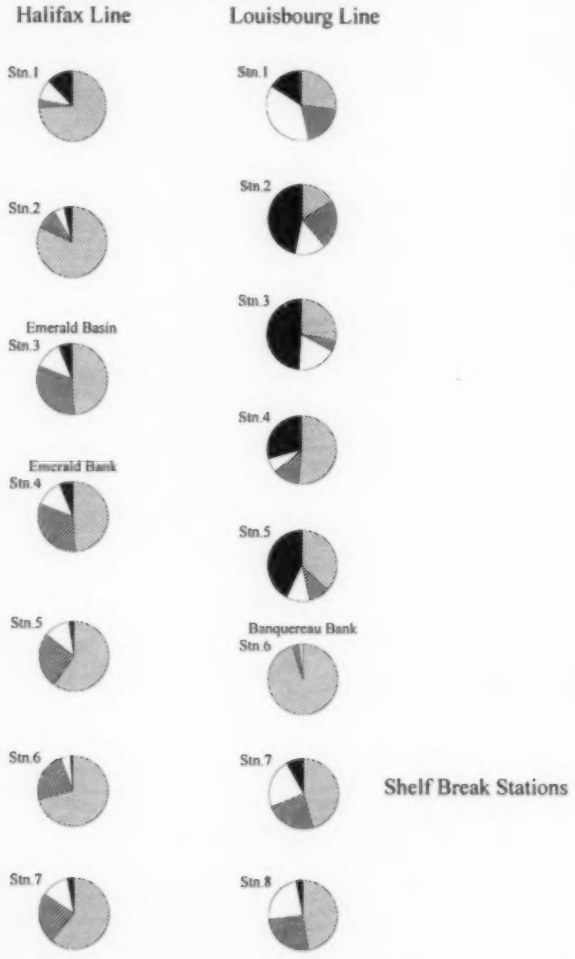

both years, NSC water was prevelant. In both years, the temperature–salinity properties at HL1 were characteristic of NSC water.

Temperature and salinity profiles (to 100 m or bottom) at shelf stations on the LL (LL1–LL6) were very similar in April 1995 and 1997 (data not shown). There was little stratification at any of the stations in terms of either temperature or salinity. Temperatures ranged between a minimum of about –1°C at inshore stations (LL1 and LL2) to maximum of about 2°C on Banquereau Bank (LL6). Salinities ranged between about 30.5 and about 32.5‰, with lowest values occurring inshore, near the surface, and the highest values occurring at the midshelf stations at depth (LL3 and LL5). Temperature and salinity profiles to 100 m at the shelf break (LL7) were very different in 1995 and 1997 (Fig. 9). In 1995, there was a shallow, relatively cold fresh layer overlying increasingly warmer, saltier water. In 1997, there was no stratification and the water was colder and a little less saline than even the surface waters in 1995. The temperature–salinity properties of water taken at 10-m intervals throughout the 0–50 m depth range indicated that SSL water was present and dominated in 1995. It may have been mixed with NFS water in the surface layers. In 1997, however, the temperature–salinity properties at LL7 were close to those typical of NFS water.

Discussion

Temperature distribution versus climatological circulation

Circulation patterns on the SS, derived from hydrographic and current measurements and circulation models (Fig. 1B), contain features that are consistent with the satellite image of sea surface temperature of April 27, 1997 (Fig. 6A): the influence of the outflow from the GSL over the eastern SS and in the NSC (e.g., see Sutcliffe et al. 1976), the pathway of the NSC over the western shelf, and the emergence of the latter in the region of the RL (Sheng and Thompson 1996; Han et al. 1997).

The atlas of monthly and seasonal mean hydrographic properties indicates that isotherms intrude from the offshore on the central shelf during the winter and spring months (Fig. 1A) (Petrie et al. 1996), and as seen in profiles taken along the HL in April 1995 and 1997 (Figs. 7 and 8), the historical data show that the degree to which intrusion occurs may vary from year to year (also see Petrie and Drinkwater 1993). Wintertime subsurface intrusion of offshore water, via the Scotian Gulf, was noted in the early 1950s (Hachey 1953), and the role of such subsurface intrusions in stimulating primary productivity in the region of the HL was examined in the 1970s (Fournier et al. 1977, 1979; Houghton et al. 1978). These Scotian Gulf intrusions occur mostly at depths of >50 m (Petrie and Drinkwater 1993), however, and the more recent models (Fig. 1B), which suggest an influx of water from beyond the shelf break in the near-surface layers around the southwestern flank of Western Bank and perhaps through the Gully, are more consistent with the April 1997 satellite observations of sea surface temperature.

Distribution of *C. hyperboreus* and *C. glacialis* versus circulation and inferred sources

The distributions of *C. hyperboreus* and *C. glacialis* on the SS in both 1995 and 1997 (Figs. 2 and 3) were somewhat similar to those in previous reports. For example, the prevelance of *C. hyperboreus* and *C. glacialis* over the eastern SS (LL1–LL6) and their association with the NSC (e.g., HL1 and HL2, RL1–RL4) were noted by Tremblay and Roff (1983), Herman et al. (1991), and Sameoto and Herman (1992). Both species were considered to originate from populations that overwinter in the GSL, which is consistent with their distributions in 1995 and 1997 and the circulation scheme in Fig. 1B. In apparent contradiction to this view, however, in April 1997, *C. glacialis* abundances were higher at stations on the BBL (BBL2–BBL4) than either on the eastern SS (LL1–LL6) or in CS (CSL1–CSL6), while abundances in the NSC off Halifax (HL1 and HL2) were quite low. This may indicate another more local source to the

© 1999 NRC Canada

Fig. 5. Stage composition (% of total) of *C. finmarchicus* at stations on lines on the SS and in CS and the LC in April 1997. The areas hatched left ro right descending represent the percentage of CI–CIII copepodites, the areas hatched left to right ascending represent the percentage of CIV, the white areas represent the percentage of CV, and the black areas represent the percentage of adults.

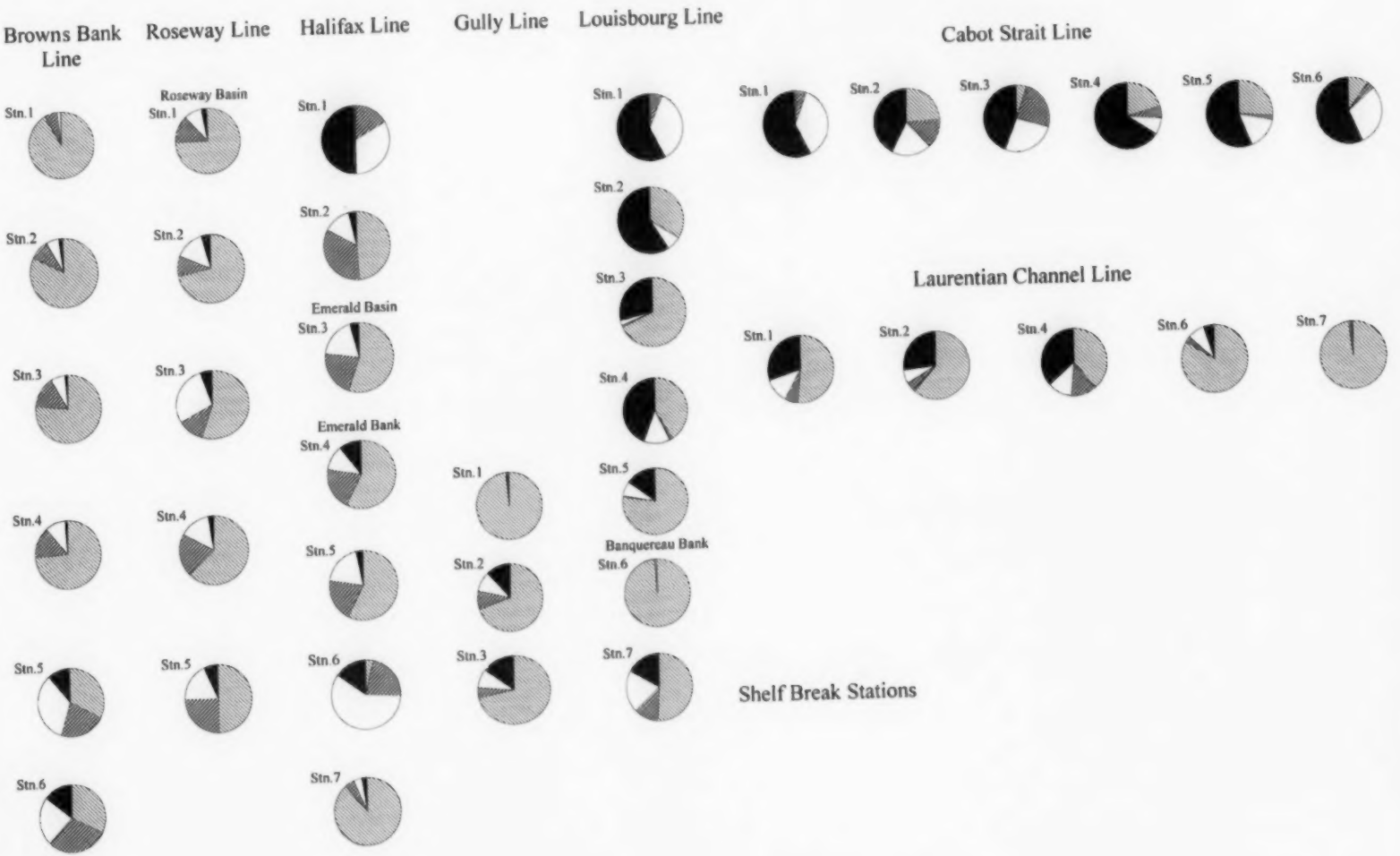

© 1999 NRC Canada

Fig. 6. AVHRR (advanced very high resolution radiometer) images of sea surface temperature captured on (A) April 27 and (B) April 22, 1997. Black areas are land or cloud covered.

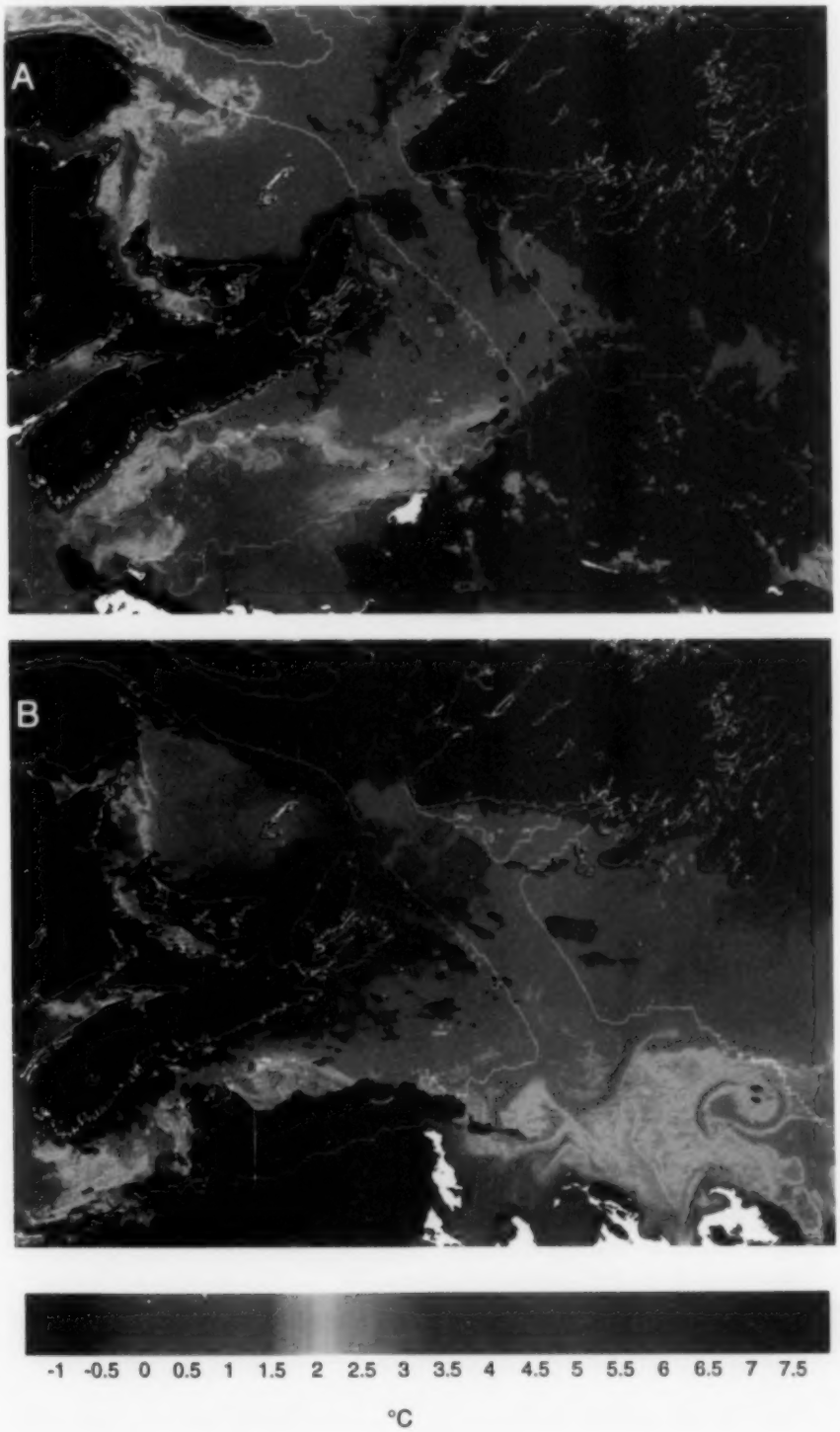

© 1999 NRC Canada

Fig. 7. Temperature (solid line) and salinity (broken line) profiles to 100 m (or bottom) at stations along the HL in April 1995 (upper panels) and April 1997 (lower panels).

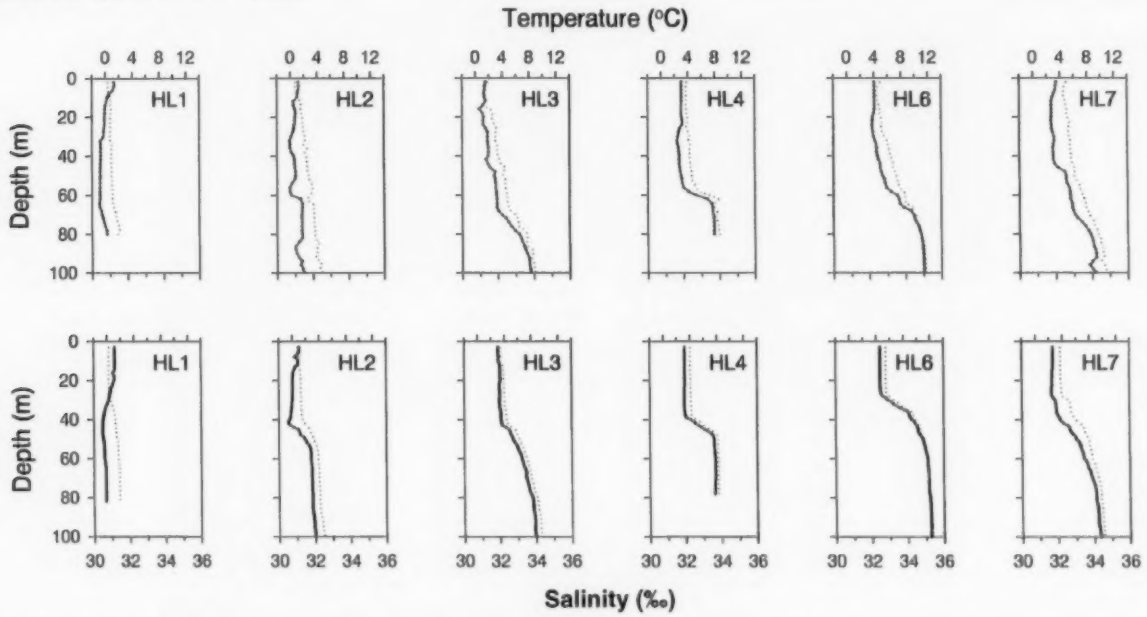

southwestern SS or temporal variability in supply from the upstream source (e.g., the NSC). Also, in April 1997, abundances of *C. hyperboreus* were higher on the eastern SS than in CS, which might suggest additional input to the near-surface layers from populations overwintering in the eastern SS basins (Sameoto and Herman 1992).

Distribution of abundance and stage composition of *C. finmarchicus* populations versus circulation and inferred sources

Calanus finmarchicus abundances were generally higher over the middle and southwestern regions of the SS than in the northeast in April 1995 and 1997 (Figs. 2 and 3). Sameoto and Herman (1992) suggested that *C. finmarchicus* on the eastern SS was derived from populations overwintering in the GSL and local deep shelf basins. The fact that the abundance of *C. finmarchicus* over the eastern SS (1995 and 1997) and its suggested CS source (1997) (Figs. 2 and 3) were similar and low is consistent with this view, assuming that the eastern SS basins provided little input. In addition, the stage compositions of *C. finmarchicus* populations at stations on the northeast SS (LL1–LL4), in CS (CSL1–CSL4), and in the NSC (HL1) were similar, with a relatively high proportion of overwintered (G0) adults and CV (Figs. 4 and 5). These stage compositions were in distinct contrast with those at stations at or beyond the shelf break of the LL and in the Gully and farther southwest, where the G1 young-of-the-year CI–CIII and CIV were generally dominant, but consistent with observations in the lower St. Lawrence Estuary that overwintered *C. finmarchicus* do not start reproducing until after the start of the spring bloom, which occurs there in June (Runge and Plourde 1996). On the eastern SS and in CS, the spring bloom was underway in April 1995 and 1997, with surface chlorophyll concentrations of up to about 9 $\mu g \cdot L^{-1}$ (unpublished data), so that reproduction was probably just starting in these areas.

Sameoto and Herman (1992) suggested that *C. finmarchicus* on the central and southwestern regions of the SS is derived from populations overwintering in the deep basins (e.g., Emerald Basin), and they concluded that the slope is not an important source. The observations presented here suggest another interpretation. In April 1995, *C. finmarchicus* abundances were higher at stations at and beyond the shelf break than on the shelf for both HL and LL (HL6, HL7, LL7, and LL8) (Fig. 2). In April 1997, abundances at and beyond the shelf break of HL (HL6 and HL7) were again quite high, but at the shelf break station of LL (LL7), *C. finmarchicus* abundance was low (Fig. 3). Temperature and salinity profiles at these stations show that when *C. finmarchicus* abundances were high (HL6 and HL7, 1995 and 1997; LL7, 1995), there were significant contributions of warm SSL water in the near-surface layers (Figs. 7–9), whereas when *C. finmarchicus* abundance was low (LL7, 1997), the water column (0–100 m) comprised cooler NFS water. The coincidence of high abundances of *C. finmarchicus* with warm slope water along the shelf break suggests that the *C. finmarchicus* found here originated from the population that overwinters in the deep ocean beyond the shelf break.

Slope water made a greater contribution in the near-surface layers (<50 m) at shelf stations of the HL (HL2–HL4) in April 1997 than in 1995, and abundances of *C. finmarchicus* at these stations were substantially higher in 1997. Thus, it appears that the intrusion of slope water from the shelf break brought *C. finmarchicus* from the offshore population onto the shelf. Furthermore, from the circulation scheme, it seems likely that this influx of offshore zooplank-

© 1999 NRC Canada

Fig. 8. Temperature–salinity plots of water from 10-m intervals in the 0–50 m depth range at stations along the HL in April 1995 and 1997, together with climatological data for SSL water, NFS water, and NSC water, taken from the Bedford Institute hydrographic database.

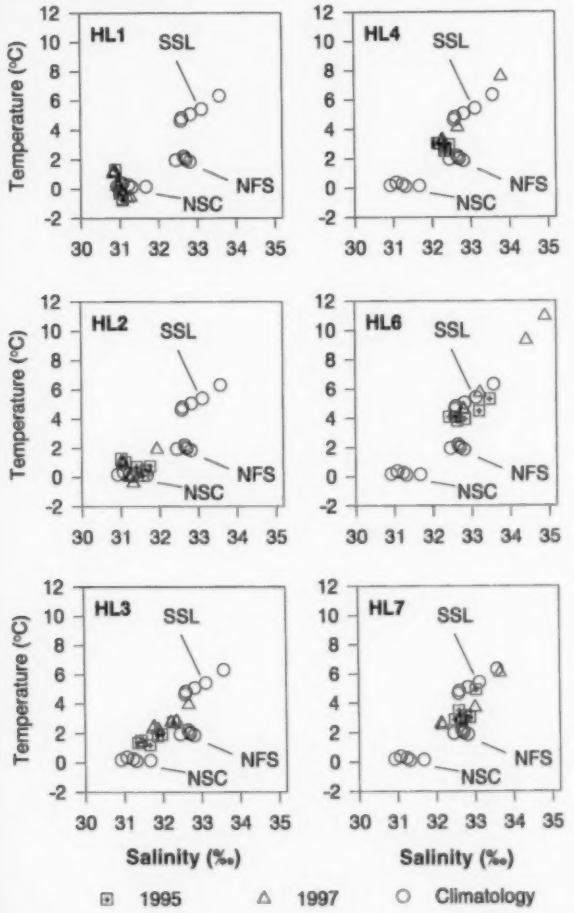

ton was being advected to the west, after mixing with the NSC in the vicinity of HL2 (Figs. 1B and 6A). It should be noted that while it is clear that the larger volumes of slope water seen on the shelf in 1997 were associated with higher abundances of *C. finmarchicus*, no direct correlation is to be expected, since most of the population in April was G1, whose abundances were determined by a combination of environmental factors as well as the abundance of their G0 parents. Another area where offshore water might intrude is the Gully. Models suggest that there is influx from beyond the shelf break through the Gully (Fig. 1B) (Han et al. 1997), and in 1997, *Calanus* species compositions at stations in the Gully were similar to those of the warmer SSL water to the west rather than to those on the eastern shelf or at the shelf break of the LL (Fig. 3; Table 2).

On-shelf transport of *C. finmarchicus*, as described above, would be expected to vary from year to year, since the degree of intrusion of offshore water varies annually and the size and distribution of the offshore population probably do as well. From this 2-year data set, it is unclear whether the influx of *C. finmarchicus* was particularly high in 1997 or particularly low in 1995, although since these intrusions are regular annual events in the vicinity of the HL, some on-shelf transport probably occurs every year. It is possible that *C. finmarchicus* populations overwintering in the region's shelf basins add to the overall population on the central and western SS in spring, but their contribution may be low, especially in years when on-shelf transport is high. In a previous study, it was concluded that the basins were the major source (Sameoto and Herman 1990), but it now seems that this view was based on anomolous data. In 1985 and 1986, during the study period of Sameoto and Herman (1990), concentrations of *C. finmarchicus* at depths >250 m in Emerald Basin in the fall were 5–10 times higher than those found during the present (mid-1990s) study period (Sameoto et al. 1998). Thus, in the mid-1980s, for two years, the contribution of the basins was much more important. In all the other years between 1984 and 1997, however, concentrations of *C. finmarchicus* in Emerald Basin were close to those of the mid-1990s, so that conclusions based on data from those two years may not be generally applicable.

In both 1995 and 1997, the stage compositions of *C. finmarchicus* populations everywhere at or beyond the shelf break, in the Gully and farther west, were somewhat similar and generally dominated by young-of-the-year (G1) CI–CIII or CIV. Unusual stage compositions occurred on Banquereau Bank (LL6) and St. Pierre Bank (LCL7), where the shallow depths (about 60 m) probably precluded the occurrence of late stages, and at HL6, where the absence of young stages might be attributable to the presence of unusually high concentrations of an invertebrate predator (*Euchaeta* spp.) (unpublished data). Overall, however, the stage composition of the G1 individuals at a particular station depends on a combination of factors including the timing of reproduction in the G0 parental generation and the duration of the reproductive period, vertical distribution and physical processes, predation, and ambient and previously experienced conditions of temperature and food concentration. Thus, it is not possible to account for all of the differences seen between stations or between years (Figs. 4 and 5), although some comments can be made regarding potential sources of the G0 parental generation.

At an ambient temperature of 3.5°C (surface temperature on the mid-SS in 1997), the development time from egg to stage CIII is about 6 weeks and for egg to stage CIV is about 7 weeks (Corkett et al. 1986). Thus, for the populations found along the shelf break and on the central and western SS, reproduction probably started in early to mid-February. For the populations at and beyond the shelf break, if *C. finmarchicus* overwintering offshore in the vicinity of the SS start to emerge at the same time as those overwintering in the deep water south of Newfoundland (January; Planque et al. 1997), then mature females should be present in the surface layers by February. For the central and western SS populations, mature females have been observed on the central SS in February (McLaren et al. 1989; Sameoto and Herman 1990), which might derive either from the offshore (by intrusion) or from Emerald Basin. Recent

© 1999 NRC Canada

Fig. 9. Temperature (solid line) and salinity (broken line) profiles of 100 m at the shelf break station of the LL (LL7) collected in April 1995 (upper left panel) and April 1997 (upper right panel) and temperature–salinity plots of water from 10-m intervals in the 0–50 m depth range, together with climatological data for the SSL, NFS, and GSL outflow, taken from the Bedford Institute hydrographic database.

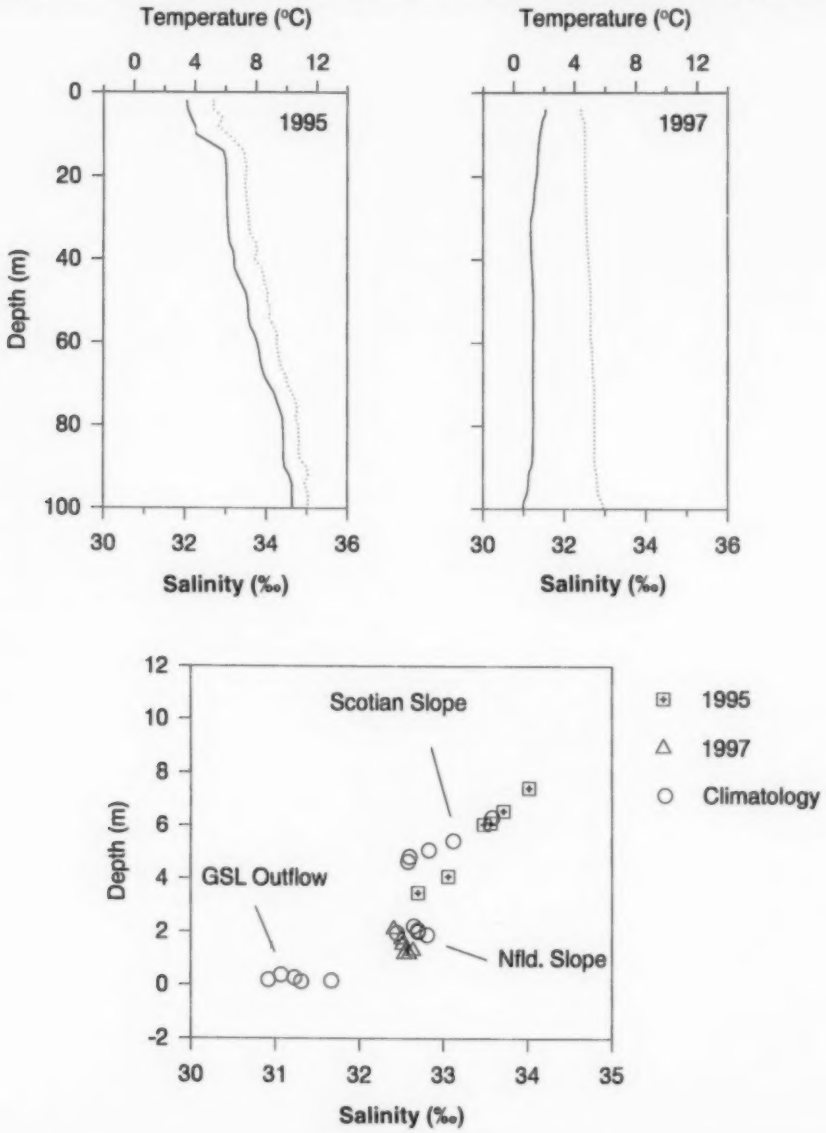

observations in Emerald Basin, made with a moored optical plankton counter, showed a continuous decrease in the concentration of *C. finmarchicus* at overwintering depths over the December–April period (1992–1993), with no abrupt decrease that could be attributed to a synchronized vertical migration event (D.D. Sameoto, personal communication). Thus, although predation at depth may have accounted in part for this observation (euphausiids and silver hake (*Merluccius bilinearis*) are abundant year-round predators in Emerald Basin), it is also possible that mature females derived from the Emerald Basin overwintering population might be appearing in the surface layers by February.

The deep ocean as source of *C. finmarchicus* to continental shelves elsewhere and inferences for the SS system

An annual springtime invasion of the shallow northern North Sea by *C. finmarchicus* from the adjacent slope region has been recognized for some time (reviewed in Franz et al. 1991). Stephens et al. (1998) have shown that the annual mean abundance of *C. finmarchicus* in the northern North Sea is related to the volume of water transported on to the shelf from the north at the end of winter, and Backhaus et al. (1994) have proposed a model, which incorporates information on hydrodynamics and the seasonal vertical migration behaviour of *C. finmarchicus*, that provides a mechanism by

© 1999 NRC Canada

which copepods at depth along the continental slope can invade the shelf from the north in spring and return there in late summer. In addition, a recent particle-tracking study has shown how overwintering copepods might be contained within a local gyre (in the Faröe-Shetland Channel) or within a more extended gyre system, which encompasses the Northeast Atlantic and Norwegian Sea (Bryant et al. 1998). In order for the *C. finmarchicus* population to reappear each year at the shelf break of the SS, either a similar retention area or a sustained advective source would be required, or perhaps a combination of both. For the deep ocean adjacent to the SS, it seems plausible that overwintering copepods might be retained within a cyclonic gyre bordered to the north by the continental slope and to the south by the north wall of the Gulf Stream and stretching from near Cape Hatteras (in the Gulf Stream – Deep Water Boundary Current crossover region) in the west to the tail of the Grand Bank in the east (Csanady and Hamilton 1988). On the other hand, it is also possible that the current along the shelf break (Fig. 1B) may provide an advective source for *C. finmarchicus*, which ultimately derives from the abundant population in the Labrador Sea (Head et al. 1999). At this stage, these suggestions are largely speculative, but they could perhaps be investigated by systematic sampling in the deep waters beyond the shelf break of the SS.

Climatological circulation versus hydrographic and biological observations at the shelf break of the LL

One of the notable features of the circulation scheme presented in Fig. 1B is that it shows apparently continuous flow from northeast to southwest along the shelf break. In April 1997, however, temperature and salinity properties were quite different at HL6 and LL7, indicating a disruption of this flow. This disruption is also apparent in images of sea surface temperature (Fig. 6). The image from April 22 (Fig. 6B) indicates that the discontinuity may have arisen because a mesoscale eddy was forming near the shelf break in the area of the LL and transporting the cold water away towards the northeast. Another feature of the circulation scheme is that it shows outflow from the GSL joining the shelf break current as it emerges from the LC. In neither 1995 nor 1997 did there appear to be important contributions of western CS water (GSL outflow, mean temperature from –0.2 to 0.5°C, salinity from 31.4 to 31.8‰) at LL7 in the 0–50 m depth range (Fig. 9). In April 1997, when the temperature–salinity properties at LL7 were close to those characteristic of NFS water, it would appear that most of the flow was from the northeast across the mouth of the LC. Despite this, the *Calanus* spp. abundances (Fig. 3) and *C. finmarchicus* stage composition at LL7 resembled those found at LCL1 and LCL2 more closely than they did those at a station off St. Pierre Bank, where the abundance of *C. finmarchicus* was nearly three times higher and where the stage composition of *C. finmarchicus* (data not shown) was very similar to that found at LCL6. Temperature–salinity properties at LCL2 suggested mixing of GSL outflow and NFS waters in the 0–50 m depth range, as suggested by the circulation scheme (Fig. 1B). Thus, from both the hydrographic and biological observations, it appears that water arriving at LL7 from the northeast across the mouth of the LC was mixing with the outflow from it, but that this outflow contained only a limited contribution of GSL water.

Summary and identification of areas for future study

The distribution patterns of *Calanus* spp. abundance on the SS in April 1995 and 1997 were similar to those presented in previous studies. Also, as in previous studies, it is surmised here that the springtime source of *Calanus* spp. on the eastern SS and in the NSC is the populations overwintering in the GSL, which arrive via CS. In contrast with previous studies, however, for the central and western SS regions, our recent observations suggest that there is a previously unrecognized source of *C. finmarchicus*, namely a population that overwinters in the deep ocean beyond the shelf break. *Calanus finmarchicus* is transported onto the SS from the slope region by intrusion of warm offshore water in the midregion of the SS in late winter – early spring. The degree of warm water intrusion and level of influx of copepods vary from year to year, although the two may not be closely correlated, since concentrations of *C. finmarchicus* in the offshore population probably vary from year to year. At this stage, on the basis of only two years of data, our understanding of the contribution of the offshore population to the shelf in a climatological sense and of the on-shelf transport mechanism remains rudimentary. In the future, however, sampling that includes more stations beyond the shelf break and modelling studies that include particle tracking could help to answer these questions.

Another question that remains unanswered relates to the potential contribution of *C. finmarchicus* populations overwintering in the shelf basins to the shelf populations in the central and western regions. This question could, in theory, be answered by frequent hydrographic and biological sampling during the late winter – early spring period, but since the contribution of the shelf basins probably varies from year to year, any conclusions based on detailed sampling in just one year would not be appropriate and the problem may not be as tractable as it appears.

Two more questions that arise concern the source of the shelf break population and the subsequent fate of the on-shelf population. For the shelf break source, does it derive from a population that overwinters in a local gyre-like system south of the SS, or does it result from a continuous advective stream arriving from outside the local area? For the fate, do large numbers return from the shelf to the deep ocean, and if so, are they retained within the proposed gyre, or are they advected out of the area? It is unfortunate that answers to these questions are unlikely to be attainable in the near future, since they require extensive sampling and circulation modelling over large previously undersampled areas.

Acknowledgements

The authors would like to thank Heidi Bishop and Linda Payzant for processing AVHRR satellite imagery (received at the Bedford Institute), Liam Petrie for help with graphics, Doug Sameoto and Ken Drinkwater for comments on an earlier version of the the manuscript, and the captains and ships' crews and scientific staff of the CCGS *Parizeau* (1995) and CCGS *Hudson* (1997).

© 1999 NRC Canada

References

Backhaus, J.O., Harms, I.H., Krause, M., and Heath, M.R. 1994. An hypothesis concerning the space–time succession of *Calanus finmarchicus* in the northern North Sea. ICES J. Mar. Sci. **51**: 169–180.

Bryant, A.D., Hainbucher, D., and Heath, M.R. 1998. Basin-scale advection and population persistence of *Calanus finmarchicus*. Fish. Oceanogr. **7**: 235–244.

Conover, R.J. 1988. Comparative life histories in the genera *Calanus* and *Neocalanus* in high latitudes of the Northern Hemisphere. Hydrobiologia, **167/168**: 127–142.

Corkett, C.J., McLaren, I.A., and Sevigny, J.-M. 1986. The rearing of the marine calanoid copepods *Calanus finmarchicus* (Gunnerus), *C. glacialis* Jashnov and *C. hyperboreus* Kroyer with comment on the equiproportional rule. Proceedings of the Second International Conference on Copepods. Syllogeus, **58**: 539–546.

Csanady, G.T., and Hamilton, P. 1988. Circulation of slope water. Continental Shelf Res. **8**: 565–624.

Fournier, R.O., Marra, J., Bohrer, R., and Van Det, M. 1977. Plankton dynamics and nutrient enrichment of the Scotian Shelf. J. Fish. Res. Board Can. **34**: 1004–1018.

Fournier, R.O., Van Det, M., Wilson, J.S., and Hargraves, N.B. 1979. Influence of the shelf-break front off Nova Scotia on phytoplankton standing stock in winter. J. Fish. Res. Board Can. **36**: 1228–1237.

Franz, H.G., Colebrook, J.M., Gamble, J.C., and Krause, M. 1991. The zooplankton of the North Sea. Neth. J. Sea Res. **28**: 1–52.

Hachey, H.B. 1953. A winter incursion of slope water on the Scotian Shelf. J. Fish. Res. Board Can. **10**: 148–153.

Han, G., Hannah, C., Loder, J., and Smith, P. 1997. Seasonal variation of the three-dimensional mean circulation over the Scotian Shelf. J. Geophys. Res. **102**: 1011–1025.

Head, E.J.H., Harris, L.R., and Campbell, R.W. 1999. Investigations on the ecology of *Calanus* spp. in the Labrador Sea. I. Relationship between the phytoplankton bloom and reproduction and development of *Calanus finmarchicus* in spring. Mar. Ecol. Prog. Ser. In press.

Herman, A.W., Sameoto, D.D., Shunnian, C., Mitchell, M.R., Petrie, B., and Cochrane, N. 1991. Sources of zooplankton on the Nova Scotian Shelf and their aggregations within deep-shelf basins. Continental Shelf Res. **11**: 211–238.

Hirche, H.-J. 1991. Distribution of dominant calanoid copepod species in the Greenland Sea during late fall. Polar Biol. **11**: 351–361.

Houghton, R.W., Smith, P.C., and Fournier, R.O. 1978. A simple model for cross-shelf mixing on the Scotian Shelf. J. Fish. Res. Board Can. **35**: 414–421.

McLaren, I.A., Tremblay, M.J., Corkett, C.J., and Roff, J.C. 1989. Copepod production on the Scotian Shelf based on life-history analyses and laboratory rearings. Can. J. Fish. Aquat. Sci. **46**: 560–583.

Petrie, B., and Drinkwater, K. 1993. Temperature and salinity variability on the Scotian Shelf and in the Gulf of Maine 1945–1990. J. Geophys. Res. **98**: 20 079 – 20 089.

Petrie, B., Drinkwater, K., Gregory, D., Pettipas, R., and Sandström, A. 1996. Temperature and salinity atlas for the Scotian Shelf and the Gulf of Maine. Can. Tech. Rep. Hydrogr. Ocean Sci. No. 171.

Petrie, B., Drinkwater, K., Gregory, D., and Pettipas, R. 1999. Temperature and salinity atlas for the Newfoundland and Labrador shelves. Can. Tech. Rep. Hydrogr. Ocean Sci. (www.mar.Dfo-mpo.gc.ca/science/ocean/welcome.html).

Planque, B., Hays, G.C., Ibanez, F., and Gamble, J.C. 1997. Large scale spatial variations in the seasonal abundance of *Calanus finmarchicus*. Deep-Sea Res. I, **44**: 315–326.

Runge, J.A., and Plourde, S. 1996. Fecundity characteristics of *Calanus finmarchicus* in coastal waters of eastern Canada. Ophelia, **44**: 171–187.

Sameoto, D.D., and Herman, A.W. 1990. Life cycle and distribution of *Calanus finmarchicus* in deep basins on the Nova Scotia shelf and seasonal changes in *Calanus* spp. Mar. Ecol. Prog. Ser. **66**: 225–237.

Sameoto, D.D., and Herman, A.W. 1992. Effect of the outflow from the Gulf of St. Lawrence on Nova Scotian shelf zooplankton. Can. J. Fish. Aquat. Sci. **49**: 857–869.

Sameoto, D., Kennedy, M.K., and Cochrane, N. 1998. Zooplankton changes along the Halifax and Louisbourg transects in 1996. DFO Can. Stock Assess. Secretariat. Res. Doc. 97/82.

Sheng, J., and Thompson, K. 1996. A robust method for diagnosing regional shelf circulation from scattered density profiles. J. Geophys. Res. **101**: 25 647 – 25 659.

Stephens, J.A., Jordan, M.B., Taylor, A.H., and Proctor, R. 1998. The effects of fluctuations in North Sea flows on zooplankton abundance. J. Plankton Res. **20**: 943–956.

Sutcliffe, W.H., Jr., Loucks, R.H., and Drinkwater, K.F. 1976. Coastal circulation and physical oceanography of the Scotian Shelf and the Gulf of Maine. J. Fish. Res. Board Can. **33**: 98–115.

Tremblay, M.J., and Roff, J.C. 1983. Community gradients in the Scotian Shelf zooplankton. Can. J. Fish. Aquat. Sci. **40**: 598–611.

© 1999 NRC Canada

Stable carbon isotopes as pelagic food web tracers in adjacent shelf and slope regions off British Columbia, Canada

R. Ian Perry, Peter A. Thompson, David L. Mackas, Paul J. Harrison, and Douglas R. Yelland

Abstract: Surveys were conducted in spring 1992 to examine the use of $^{13}C/^{12}C$ ratios to differentiate pelagic food webs and to trace food web interactions between adjacent continental shelf and slope/deep ocean environments off southwestern British Columbia, Canada. Salinity was used to define shelf or slope/deep ocean water masses and their productivity conditions because eddies and meanders at the shelf break were observed to draw water off the shelf. The $^{13}C/^{12}C$ ratio of plankton was related to the mean upper layer (0–50 m) salinity. ^{13}C abundance was enriched (relative to ^{12}C) in the shelf water mass compared with the slope water mass. This enrichment persisted up the food web from particulate organic matter through three size-classes of zooplankton to larval fish. The cross-shelf spatial scale separating these food webs, as determined from spatial semivariograms of $^{13}C/^{12}C$ and the upper layer mean salinity, was 40–45 km, similar to the Rossby radius for eddies at this location (50 km). Larval fish may provide a means to monitor exchanges of plankton between geographically adjacent food webs if time scales for incorporation of new isotope signatures from diets into tissues are determined.

Résumé : Des relevés ont été effectués au printemps de 1992 afin d'étudier la possibilité d'utiliser les rapports $^{13}C/^{12}C$ pour différencier les réseaux trophiques pélagiques et suivre les interactions des réseaux trophiques entre des environnements océaniques voisins du plateau continental et du talus et du fond au large du sud-ouest de la Colombie-Britannique (Canada). La salinité a été utilisée pour définir les masses d'eau du plateau continental et celles du talus et du fond de l'océan de même que les conditions de productivité car des tourbillons et des méandres au niveau de la rupture de pente ont pour effet de retirer de l'eau du plateau. Le rapport $^{13}C/^{12}C$ du plancton présentait une relation avec la salinité de la couche moyenne supérieure (0–50 m). Il y avait enrichissement en ^{13}C (par rapport au ^{12}C) dans la masse d'eau du plateau comparativement à celle de la pente. Cet enrichissement persistait dans le réseau trophique : de la matière organique particulaire aux trois classes de taille du zooplancton et aux larves de poisson. La distance, au-dessus du plateau, qui séparait ces réseaux trophiques, tel que déterminé à partir de semi-variogrammes spatiaux du $^{13}C/^{12}C$ et de la salinité de la couche moyenne supérieure, était de 40 à 45 km, valeur semblable au rayon Rossby des tourbillons à cet endroit (50 km). Les larves de poisson peuvent servir à contrôler les échanges de plancton entre des réseaux trophiques voisins si l'on détermine le moment d'apparition des nouvelles signatures isotopiques des proies vers les tissus.

[Traduit par la Rédaction]

Introduction

Naturally occurring stable isotopes of carbon are both good indicators of the habitat source of carbon and good tracers of food web interactions in marine environments (Fry and Sherr 1984; Pond et al. 1997). Ratios of $^{13}C/^{12}C$ of marine plankton have been shown to have large-scale latitudinal gradients (Rau et al. 1989), to vary along gradients of 300 km between Arctic seas (Dunton et al. 1989; Saupe et al. 1989), and to vary between coastal and offshore marine systems, in which they have been used to determine the contribution of terrestrial-derived carbon to marine food webs (e.g., Thayer et al. 1983).

Prerequisites for the use of carbon isotopes as tracers of coastal and deep ocean food web exchanges are detectable and consistent differences in $^{13}C/^{12}C$ ratios between these two environments. In the Northeast Pacific, Kline (1997) used $^{13}C/^{12}C$ ratios of zooplankton to differentiate carbon derived from the Gulf of Alaska from carbon produced in Prince William Sound. He further determined which forage fishes in Prince William Sound were likely to depend on the (uncertain) supply of carbon from the offshore Gulf of Alaska. It is not clear, however, whether such an approach can be applied to open ocean ecosystems, in particular across the relatively short distances that separate continental

Received August 6, 1998. Accepted August 20, 1999.
J14730

R.I. Perry.[1] Department of Fisheries and Oceans, Pacific Biological Station, Nanaimo, BC V9R 5K6, Canada.
P.A. Thompson. Department of Aquaculture, University of Tasmania, Launceston, Tasmania 7250, Australia.
D.L. Mackas and D.R. Yelland. Department of Fisheries and Oceans, Institute of Ocean Sciences, Sidney, BC V8L 4B2, Canada.
P.J. Harrison. Department of Earth and Ocean Sciences, University of British Columbia, Vancouver, BC V6T 1Z4, Canada.

[1]Author to whom all correspondence should be addressed.
e-mail: perryi@pac.dfo-mpo.gc.ca

© 1999 NRC Canada

Fig. 1. Map of the study area off the southwest coast of Vancouver Island (inset) and the detailed sampling locations for conductivity–temperature–depth profiles and transects and POM, zooplankton, and larval fish isotope analyses.

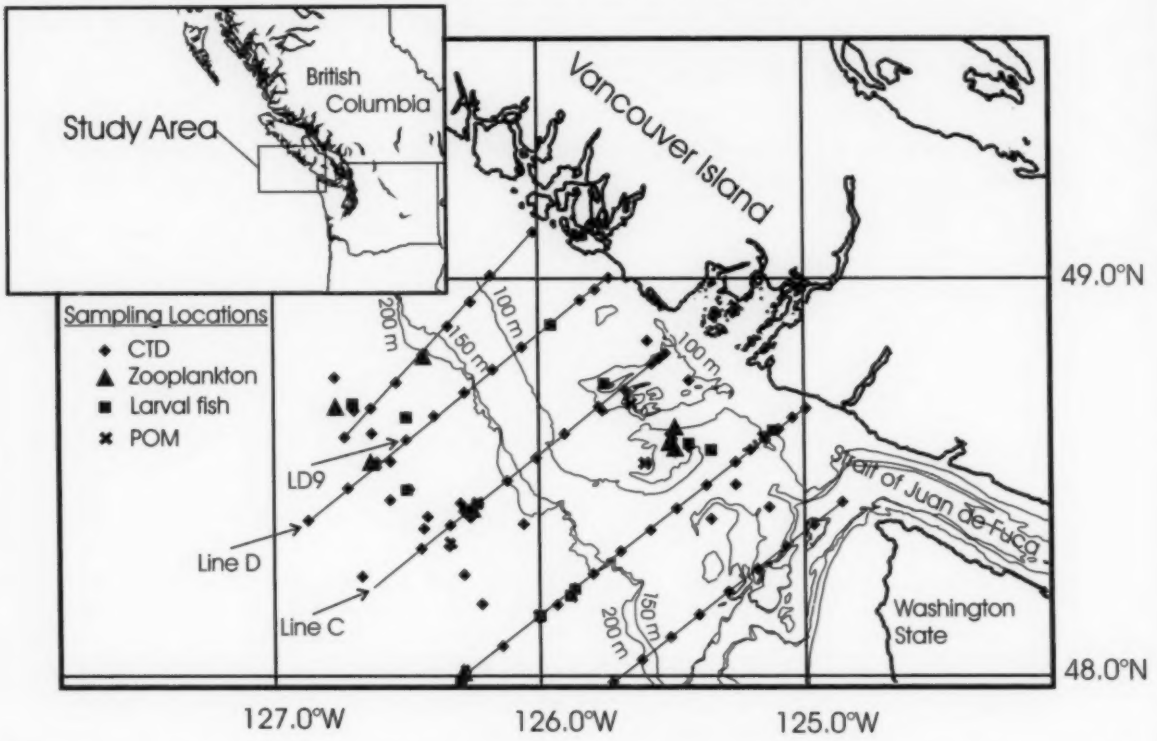

shelf environments from deep ocean environments. Exchanges between continental shelf and adjacent deep ocean regions are important for understanding the processes controlling plankton and fish production in shelf ecosystems. Such exchanges can occur through several processes, including instabilities in along-slope currents (such as jets and meanders), eddies, internal tides, and upwelling (Huthnance 1995). Cross-shelf exchanges may increase shelf production by supplying nutrients and plankton to the shelf and may decrease shelf production by removing zooplankton and fish larvae from the shelf (e.g., Parrish et al. 1981).

The isotope studies noted above, combined with cross-shelf interactions, suggest that $^{13}C/^{12}C$ ratios may be useful for estimating the spatial scales separating different marine pelagic food webs and for identifying exchanges of carbon among these food webs. These ratios may also be relevant to the study of variability in commercial fish populations, since, if there are interannual differences in food web structure and exchanges of carbon between regions, these ratios may identify which is the appropriate food web (shelf or deep ocean) to monitor for comparisons with fish population variability. The objectives of this study were to determine (*i*) the ability of stable carbon isotope ratios ($^{13}C/^{12}C$) to distinguish plankton ecosystems in adjacent shelf and slope/deep ocean regions off the British Columbia coast during spring, (*ii*) the persistence of the differences of these $^{13}C/^{12}C$ ratios through the trophic web from particulate organic material (POM) (phytoplankton) to larval fishes, and (*iii*) the spatial scale of the gradient between these distinct shelf and slope pelagic food webs.

Methods

Samples were collected from the continental shelf and adjacent slope off the southwest coast of Vancouver Island, British Columbia, during two simultaneous surveys. One survey (WR9204), conducted from 7 to 16 April 1992, was a broad-scale survey of larval fish off Vancouver Island, with a particular focus on sablefish (*Anoplopoma fimbria*). The second survey (OE9202) was conducted from 5 to 16 April 1992 to collect water property information and detailed plankton samples on and off the southern Vancouver Island continental shelf. Sampling locations for both surveys with information relevant to the present study are shown in Fig. 1.

Water samples were collected on survey OE9202 using General Oceanics Go-Flo bottles on a rosette sampler. Subsamples (50-mL aliquots) for chlorophyll *a* were filtered onto Whatman glass fibre filters (GF), frozen, and analysed in the laboratory using standard methods (Parsons et al. 1984). Subsamples for nutrient analyses were stored in glass and plastic test tubes, quick-frozen at –40°C, and analysed after thawing using standard methods (Macdonald and McLaughlin 1982) on a Technicon Autoanalyzer II. Vertical profiles of temperature and salinity were sampled using a Guildline CTD (model 8755), and in vivo fluorescence was measured during the same profiles using a Seatech fluorometer.

POM for carbon isotope analysis was collected from four locations on the continental shelf and three locations along the slope (Fig. 1). Water samples were collected from the surface mixed

© 1999 NRC Canada

Table 1. Weekly mean coastal upwelling indices for the first half of 1992 for location 48°N, 125°W.

Week beginning (1992):	Weekly mean upwelling index
5 January	–87
12 January	–69
19 January	–163
26 January	–217
2 February	–99
9 February	–120
16 February	–120
23 February	–73
1 March	–17
8 March	–2
15 March	3
22 March	23
29 March	–6
5 April*	–8
12 April*	–50
19 April	–54
26 April	10
3 May	59
10 May	32
17 May	29
24 May	19
31 May	53
7 June	11
14 June	40
21 June	38

Note: The surveys described in this study took place from 5 to 16 April 1992 and are marked with asterisks. Mean values are $m^3 \cdot s^{-1}$ per 100 m of shoreline, with negative values indicating downwelling. Data are from NOAA/NMFS Pacific Fisheries Environmental Group, Monterey, Calif.

layer using the Go-Flo bottles. For example, where the mixed layer depth was 50 m, 3-L samples were collected at each of 50, 40, 30, 25, 20, 15, 10, and 0 m depths. These samples were mixed into a large carboy and siphoned onto 116- and 28-μm Nitex netting. Organisms passing through the netting were filtered onto glass fibre filters. Organisms collected on the netting were washed with filtered seawater and recollected on glass fibre filters, which were stored at –20°C. Phytoplankton samples for enumeration were collected from replicate casts and from floating sediment traps deployed in the same area for another project and preserved in acid Lugols solution.

On survey WR9204, larval fish were collected at night from the surface using a neuston sampler with 500-μm-mesh netting (Mason and Phillips 1986). Tow duration was typically 15 min at a speed of 154 $cm \cdot s^{-1}$ (3 kn). See Shaw et al. (1988) for further details on these methods. On survey OE9202, plankton and larval fish were collected using a variety of techniques. Typically, two net tows were made at each location. The first was either a bongo plankton net or a BIONESS multiple opening and closing sampler (Sameoto et al. 1980) towed obliquely from 50 m to the surface; each sampler had a mouth opening of 0.25 m^2 and a mesh size of 236 μm. The second tow was a 0.25-m^2 ring net with 100-μm mesh, towed vertically from 50 m to the surface. All zooplankton samples were screened through 425- then 236-μm-mesh netting and frozen as three size fractions: >425, 237–425, and 100–236 μm. On both surveys, larval fish were removed from the samples and frozen separately. In total, nine locations in each of the shelf and slope regions were sampled for isotopic composition of zooplankton and larval fish, seven of which coincided with the locations sampled for POM (Fig. 1).

Samples were thawed in the laboratory and processed for carbon and nitrogen composition and bulk $^{13}C/^{12}C$ ratios of whole plankton samples or individual zooplankters and larval fish. Samples for isotope analyses were dried at 60°C for 24 h and then ground to a fine powder. Subsamples of zooplankton were also processed for taxonomic composition. In addition, a number of samples were kept frozen and processed for isotope ratios without thawing. Mean values of $^{13}C/^{12}C$ between the whole samples that had remained frozen and individual zooplankters that had been thawed and sorted were not significantly different (t test, $p = 0.19$) when examined within a region (e.g. slope region). Analyses of $^{13}C/^{12}C$ ratios for POM and animal samples followed standard techniques (e.g., Peterson and Fry 1987) using PeeDee Belemnite (PDB) limestone as the reference:

$$(1) \qquad \delta^{13}C\ (‰) = \left[\frac{(^{13}C/^{12}C)_{sample}}{(^{13}C/^{12}C)_{PDB}} - 1\right] \times 1000.$$

Reproducibility of results was ±0.1‰. Carbon and nitrogen elemental composition was determined by combustion in a Carbo Erba model 1106 elemental analyser (Howarth 1977), which was coupled to a VG PRISM mass spectrometer for the carbon isotope analyses (Cifuentes et al. 1988). Isotope ratios are expressed using the conventional delta (δ) notation.

Samples were not treated to remove lipids prior to isotope analyses. A regression of $\delta^{13}C$ versus the carbon to nitrogen ratio showed a significant but very weak relationship (least-squares regression, $R^2 = 0.12$, $p \leq 0.001$), which did not justify correcting the data for lipids, for example, by using the empirical relationship of McConnaughey and McRoy (1979).

The characteristic spatial autocorrelation structure of $\delta^{13}C$ ($\gamma_{(h,\varphi)}$) oriented across the shelf and slope region was calculated from empirical directional semivariograms (Kaluzny et al. 1996):

$$(2) \qquad \gamma_{(h,\varphi)} = \frac{1}{2|N_{(h,\varphi)}|} \sum_{N_{(h,\varphi)}} (Z_i - Z_j)^2$$

in which h represents the separation distance, φ the direction (defined here as the cross-shelf direction 225 ± 22.5°T), $N_{(h,\varphi)}$ the set of all pairwise geographic distances $i - j = h$ in the direction φ, $|N_{(h,\varphi)}|$ the number of distinct pairs in $N_{(h,\varphi)}$, and Z_i and Z_j the data values at locations i and j, respectively. Directional semivariograms were also calculated for the vertical (0–50 m) mean salinity values (see next section) for comparison with the $\delta^{13}C$ spatial scales. All statistical calculations were performed using S-Plus (Statistical Sciences, Inc. 1995).

Results

The normal winter circulation along the outer coast of southwestern British Columbia is wind driven to the north across both the shelf and slope regions; the normal summer circulation is a northward-flowing, buoyancy-driven coastal current and a southward-flowing current at the shelf break driven by the wind, with sporadic episodes of upwelling (Freeland et al. 1984). The change between these seasonal patterns is a transition period when the flow is predominantly barotropic and dominated by eddies (Thomson and Ware 1996). Based on analyses of current meter data from 1989 to 1995, Thomson and Ware (1996) defined a mean du-

© 1999 NRC Canada

Fig. 2. Vertical profiles of water property conditions in the slope/deep ocean environment and on the adjacent continental shelf. FL, fluorescence.

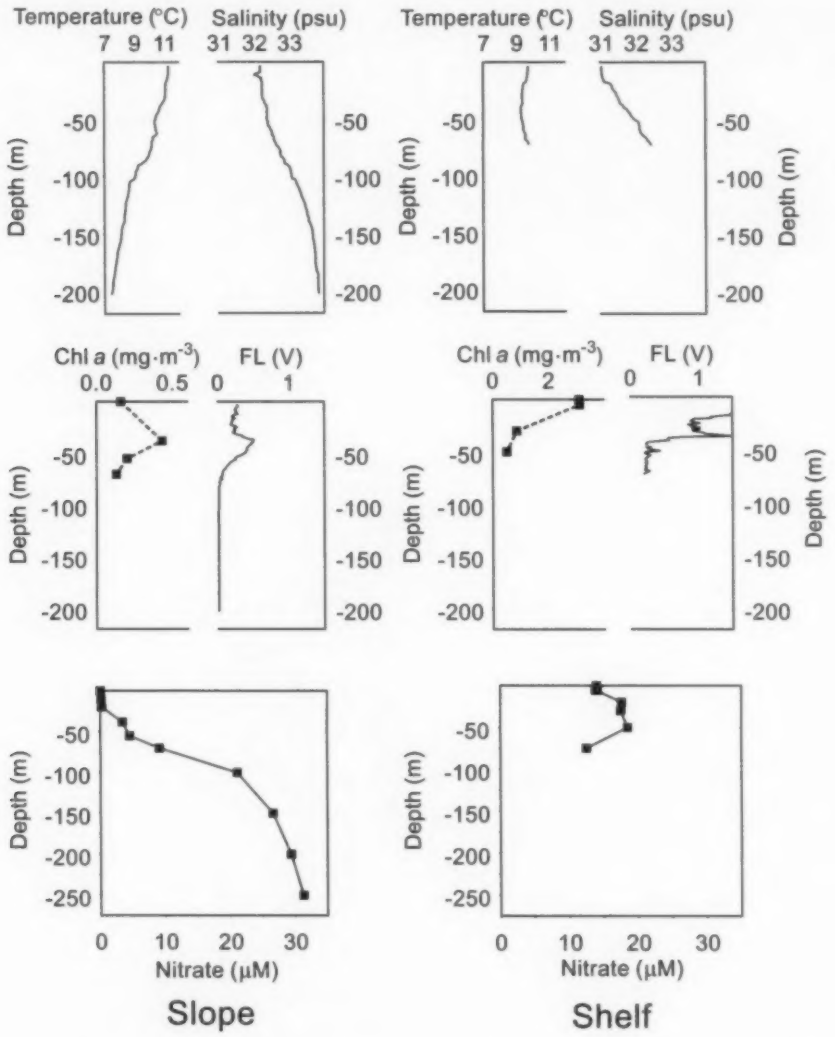

ration of 79 ± 39 days for the spring transition off the southern British Columbia coast, with a mean start date of 20 February. The timing of the spring transition coincides with the spring plankton bloom and with the spawning period for most open water marine fish species in British Columbia (e.g., Matarese et al. 1989).

The surveys of the present study took place during the spring transition, i.e., between the downwelling-favourable winds of winter and the upwelling-favourable winds of summer (Table 1). Conditions on the continental shelf were cooler and fresher, with higher nutrient and chlorophyll concentrations, compared with adjacent continental slope locations (Fig. 2). The species composition of phytoplankton and larval fishes also differed between shelf and slope locations (Table 2). Diatoms dominated in shelf waters, and larval fish composition showed the expected differences between shelf and deepwater species (e.g., Doyle 1992). Differences in zooplankton composition were less clear, with somewhat more benthic invertebrate larvae in shelf waters (Table 2).

Temperature–salinity (TS) plots help to define the characteristic shelf and slope water masses (Fig. 3). TS properties at station D4 on the shelf and at station D11 off the shelf along line D (Fig. 1) illustrate that the different water masses could be distinguished by salinities greater than (off shelf) or less than (on shelf) 32.0–32.2 psu. These water masses were not strictly related to bathymetry, however, i.e., with "shelf" defined as bottom depths less than 200 m and "slope" defined as bottom depths greater than 200 m. For example, salinity profiles on two adjacent sections across this area (lines C and D, Fig. 1) indicated that shelf water (salinity <32 psu) occurred close to the shelf break (200-m isobath) on line C but occurred offshore of the shelf break by 28.5 km on line D (Fig. 4). This is consistent with an offshore flow and mesoscale eddies at the shelf break identified

© 1999 NRC Canada

Table 2. Typical dominant taxa at slope and shelf locations sampled off the west coast of Vancouver Island during April 1992 (% of total abundance at that location).

	Slope		Shelf	
Phytoplankton	*Coscinodiscus* sp.	14	*Thalassiosira decipiens*	95
	Chaetoceros sp.	43		
	Stephanopyxis nipponica	14		
	Dinophysis tripos	14		
	Protoperidinium sp.	14		
Zooplankton (100–236 μm)	*Oithona* sp.	36	Copepod nauplii	39
	Microstella rosea	8	Copepod eggs	5
	Copepod nauplii	33	*Limacina* sp.	19
	Limacina sp.	20	Bivalve veliger	12
Zooplankton (237–425 μm)	*Oithona* sp.	46	Copepod nauplii	21
	Pseudocalanus sp.	3	Calanoid copepodites	12
	Calanoid copepodites	6	*Oithona* sp.	14
	Copepod nauplii	9	*Pseudocalanus* sp.	8
	Limacina sp.	3	Euphausiid nauplii	11
			Ophiuroid larvae	5
			Limacina sp.	3
Larval fish	Sablefish (*Anoplopoma fimbria*)	80	Kelp greenling (*Hexagrammos decagrammus*)	58
	Brown Irish lord (*Hemilepidotus spinosus*)	5	Cabezon (*Scorpaenichthys marmoratus*)	30

Fig. 3. TS plot from three stations along transect line D off the west coast of Vancouver Island (see Fig. 1) showing the characteristic shelf (LD04) and deep ocean (LD11) water masses and their mixing at LD09. Open symbols indicate properties for depths <50 m and solid symbols for depths >50 m. Station LD04 (squares) is on the middle of the continental shelf, LD09 (inverted triangles) is at the shelf break but in water coming from the continental shelf (see Figs. 1, 4, and 5), and LD11 (circles) is in the deep ocean at the end of line D.

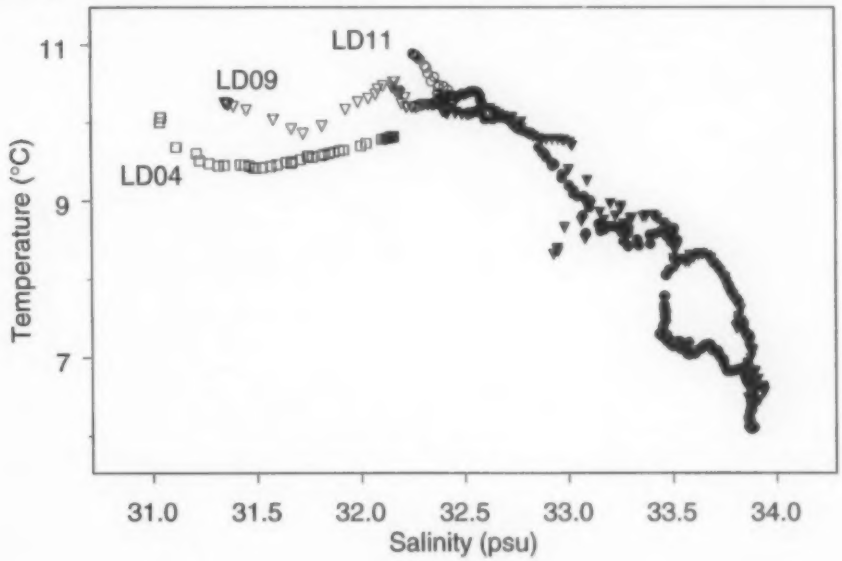

from geostrophic current analyses based on the TS profiles (Fig. 5). The TS profile for station D9 (48.6°N, 126.5°W, Fig. 3) demonstrates that mixing of the upper layers (<50 m) of slope and shelf water masses did occur within this off-shelf flow. To recognize this lack of a strict association of water masses with the bathymetry, we calculated the mean water column salinity from 0 to 50 m (which includes most or all of the vertical distribution of the POM, small zooplankton, and larval fishes that we investigated; Table 2) and defined the slope water mass as having 0–50 m mean salinities ≥32 psu and the shelf water mass as having mean salinities <32 psu.

There was a relationship between $\delta^{13}C$ and the 0–50 m mean salinity (Fig. 6), with lighter $\delta^{13}C$ ($\delta^{13}C < -19‰$) associated with the higher mean salinities typical of slope waters and heavier $\delta^{13}C$ ($\delta^{13}C \geq -19‰$) associated with the lower mean salinities typical of shelf waters off southern Vancouver Island. A contingency table analysis with the quadrants shown in Fig. 6 was significant (Fisher's exact test, $p = 0.03$), indicating characteristic associations of lighter

© 1999 NRC Canada

Fig. 4. Section profiles of salinity (psu) along hydrographic lines D and C. The solid line with diagonal hatching represents the bottom; the thick broken line indicates the 32-psu isohaline, which is used in this study to identify the front separating continental shelf from slope/deep ocean water masses. Transect locations are shown in Fig. 1. The triangle at 126.5°W in the top panel indicates the location of station LD09.

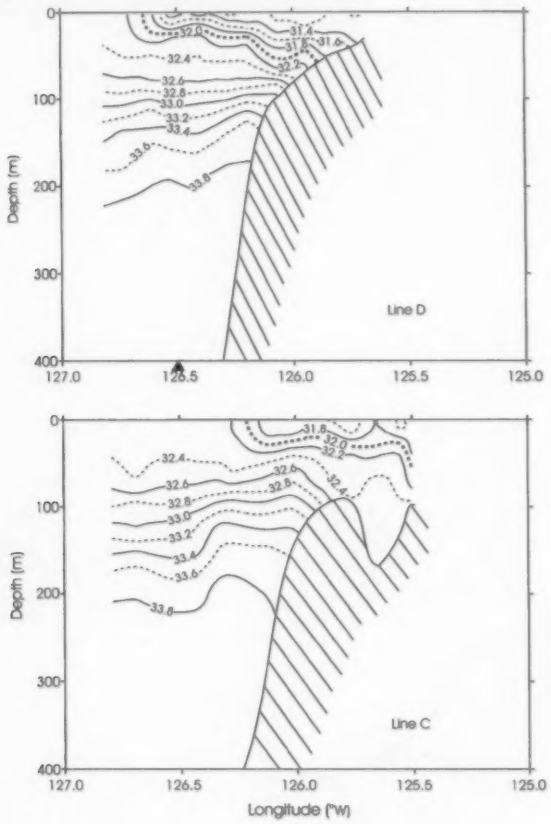

(heavier) $\delta^{13}C$ with slope (shelf) water masses. The two extreme values near $\delta^{13}C = -14‰$ were samples exclusively of the shelled marine mollusc *Limacina* sp. The shell of these molluscs contains calcium carbonate, which is enriched in $\delta^{13}C$ because it reflects the carbon isotope ratio of bicarbonate in seawater ($\delta^{13}C$ near 0‰; Fry and Sherr 1984).

Semivariograms calculated for the cross-shelf direction (Fig. 7) showed a marked increase in dissimilarity at separation distances greater than 40–45 km for both $\delta^{13}C$ and the upper layer mean salinity. This cross-shelf separation scale is similar to the internal deformation radius (Rossby radius) of about 50 km calculated at the continental slope off southwest Vancouver Island (Thomson and Ware 1996), which represents the typical scale of eddies at this location.

When examined by trophic level, there are clear differences in $\delta^{13}C$ between samples collected in slope and shelf water masses (defined using the 32-psu mean salinity criterion). Samples in the slope water were more negative (Fig. 8), i.e., the food web in the slope region was depleted in $^{13}C/^{12}C$ relative to the food web in the shelf region. These

Fig. 5. Geostrophic currents (arrows) and isopleths of geopotential height ($m^2 \cdot s^{-2}$) at 15 m calculated from the TS profiles sampled off the west coast of Vancouver Island during April 1992 (locations shown in Fig. 1). The specified level of no motion was 300 m. The two straight lines perpendicular to the coast indicate transect lines D (northern line) and C (southern line).

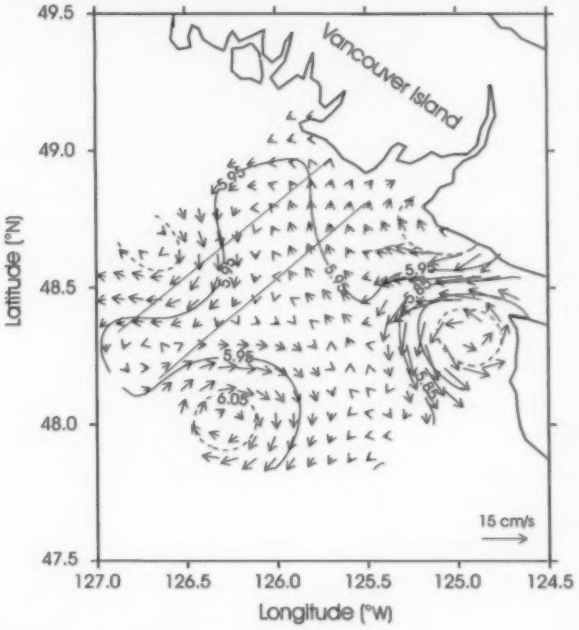

Fig. 6. Relationship of stable carbon isotope ratios for zooplankton and larval fish with vertical (0–50 m) mean salinity. Samples ≥32 psu are defined as the slope water mass; those <32 psu are the shelf water mass. The horizontal line at $\delta^{13}C = -19‰$ serves to separate shelf ($\delta^{13}C \geq -19‰$) and slope ($\delta^{13}C < -19‰$) for the contingency table analysis to test the relationship of $\delta^{13}C$ with mean salinity (see text for details).

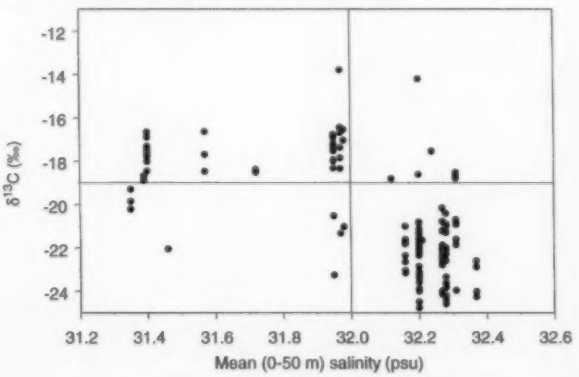

differences in $\delta^{13}C$ between slope and shelf waters were significant for all three trophic levels (POM, zooplankton, larval fish), even when separated into size-classes within the zooplankton group (Table 3). The only exception was the >116 µm POM fraction, which may not have been signifi-

© 1999 NRC Canada

Fig. 7. Directional semivariograms ($\gamma_{(h,\varphi)}$ with $\varphi = 225 \pm 22.5°$T, i.e., the cross-shelf direction) for $\delta^{13}C$ and upper layer (0–50 m) mean salinity as functions of the separation distances. The line represents a smoothing spline applied to the data to illustrate the trends.

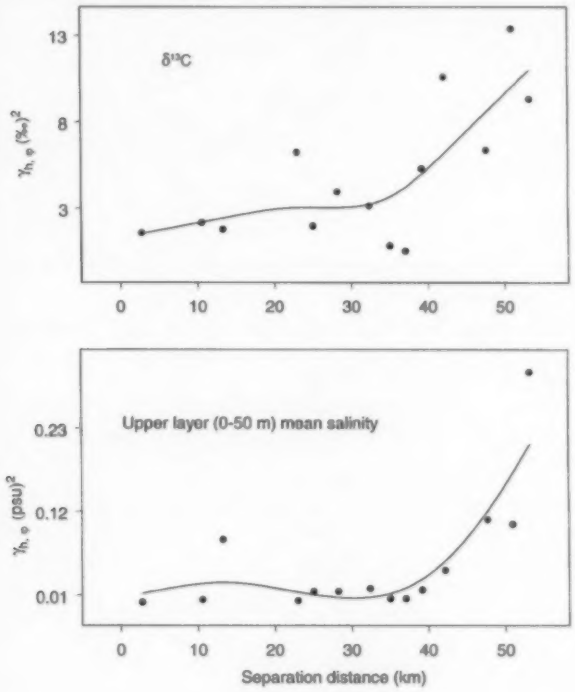

Fig. 8. Box and whisker plots of stable carbon isotope ratios in slope and shelf waters, with slope defined as 0–50 m mean salinities ≥32 psu and shelf as 0–50 m mean salinities <32 psu. The white line within a box is the median, the upper (lower) box edges define the 75th (25th) percentiles (interquartile distance), the whiskers represent values that fall within 1.5 times the interquartile distance, and asterisks are outliers. For all trophic levels, mean $\delta^{13}C$ values are significantly different between the slope and shelf regions (ANOVA, $p < 0.05$; Table 3).

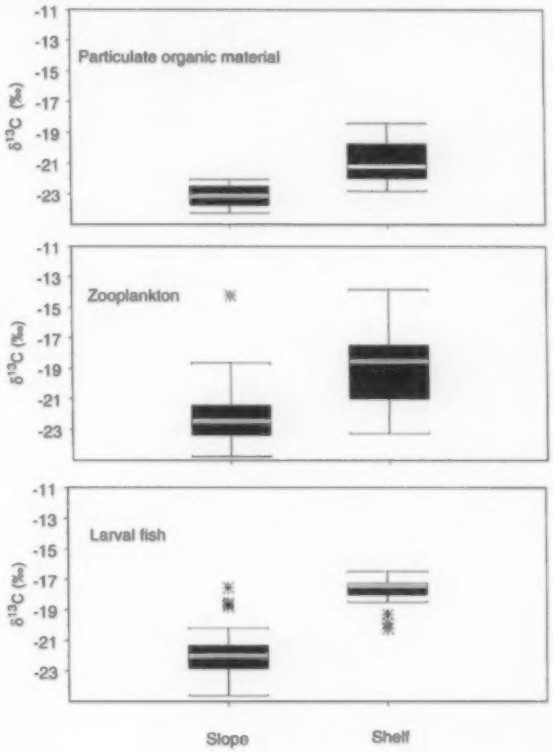

cantly different due to a very small amount of material collected. Five fish larvae (three sablefish, one snailfish (Liparidinae), and one myctophid (Myctophidae)) with lengths ranging from 4 to 26 mm were examined for the species composition and carbon isotope ratios of their gut contents. In all cases, identifiable gut contents were predominantly copepod and euphausiid nauplii and copepodites. The gut contents were always more negative than the original fish larva; the mean (± 1 SE) difference of $\delta^{13}C$ between gut contents and larvae was 1.7 ± 0.5‰. This is within the range of increases of 0–2‰ per trophic level as observed for $\delta^{13}C$ in other studies (DeNiro and Epstein 1978; Peterson and Fry 1987).

The plankton samples collected at station D9 (Fig. 1) provide an example of $\delta^{13}C$ as a tracer of the exchange of biota among food webs in different systems. This station was located in water of 1000 m depth, yet its 0–50 m mean salinity was 31.97 psu (station D9 was located at 126.5°W, Fig. 4), which was characteristic of the shelf water mass, and its TS profile demonstrated that the upper layers were composed of shelf water mixed with some slope water (Fig. 3). In contrast, the mean salinity at the adjacent station to the south on line C was 32.28 psu, characteristic of the slope water mass. Calculation of the geostrophic currents (Fig. 5) clearly indicates this off shelf flowing meander along line D, with upper layer velocities approaching 4.5 cm·s^{-1}. A return meander can also be seen approaching the shelf between lines C and B. A zooplankton sample at station D9 had a bulk $\delta^{13}C$ of −17.9‰, also characteristic of the shelf water mass. Four fish larvae were collected at station D9, ranging in length from 8 to 14 mm: one sablefish (12 mm in length), one lingcod (*Ophiodon elongatus*), and two cabezon (*Scorpaenichthys marmoratus*). The $\delta^{13}C$ of all larvae were greater than −18.4‰ (with $\delta^{13}C$ for the three nonsablefish larvae greater than −17.4‰). Doyle (1992) identified both lingcod and cabezon as typical shelf species that spawn in shallow water but that may experience advection off the shelf. The high (less negative) carbon isotope ratios of these larvae are consistent with their origin and feeding on the shelf. A simple two-end-point mixing model (e.g., Loneragan et al. 1997) can be used to determine the contributions of slope (and shelf) carbon to these larvae:

$$(3) \qquad f_{slope}(\%) = \left\{1 - \frac{[(\delta^{13}C_{slope} + \eta) - \delta^{13}C_{sample}]}{[(\delta^{13}C_{slope} + \eta) - (\delta^{13}C_{shelf} + \eta)]}\right\} \times 100$$

with f_{slope} representing the percentage of slope carbon in the sample, $\delta^{13}C_{slope}$ and $\delta^{13}C_{shelf}$ the carbon isotope ratio for the zooplankton of the slope and shelf regions (Table 3), respec-

© 1999 NRC Canada

Table 3. Statistical comparison of $\delta^{13}C$ between adjacent slope and shelf environments off the west coast of Vancouver Island during April 1992 for the various trophic levels and their size-classes.

		Slope $\delta^{13}C$ (‰)		Shelf $\delta^{13}C$ (‰)		Comparison between slope and shelf	
		Mean	SD	Mean	SD	Difference (shelf – slope)	Significantly different? (ANOVA)
POM[a]	<28 μm	–23.6	0.57	–22.1	0.56	1.5	Yes ($p < 0.05$)
	28–116 μm	–23.0	1.07	–19.5	0.83	3.5	Yes ($p < 0.05$)
	>116 μm	–22.2	0.44	–21.7	0.98	0.5	No ($p > 0.05$)
	Overall	–23.0	0.60	–20.9	1.00	2.1	Yes ($p = 0.001$)
Zooplankton	100–236 μm	–22.0	1.64	–18.3	0.37	3.7	Yes ($p = 0.014$)
	237–425 μm	–21.9	1.35	–18.8	2.65	3.1	Yes ($p < 0.001$)
	Overall	–22.2	1.98	–18.9	2.41	3.3	Yes ($p < 0.001$)
Larval fish	Overall	–22.0	1.50	–17.7	0.98	4.3	Yes ($p < 0.001$)

[a]POM is particulate organic material.

tively, and η the enrichment between gut contents and larval fish as observed in this study. In order to incorporate the variability in isotope ratios within each source region (Table 3), the mean ± 1 SE was used for the zooplankton in each region ($\delta^{13}C_{slope} = -22.2 \pm 0.3‰$, $\delta^{13}C_{shelf} = -18.9 \pm 0.6‰$) and for the trophic enrichment factor η (1.7 ± 0.5‰). Using the extreme values of these ranges in eq. 3 provides estimates of the percentage of slope carbon in the four fish larvae as follows: sablefish, 2–53%; cabezon, 0–31%; cabezon, 0–14%; lingcod, 0–9%. These results suggest a higher proportion of slope carbon in the sablefish larva, reflecting its origin in the slope region and implying that it had not been a feeding member of the shelf food web for as long as the other three larvae. Sablefish is a commercially important species that spawns along the shelf break in spring but frequently is transported onto the shelf in the near-surface waters (McFarlane et al. 1997). The values used in this calculation reflect conditions over the southern continental shelf of Vancouver Island in spring 1992 and are not likely to reflect values at other times of the year because of seasonal variations in the factors causing fractionation of ^{13}C by phytoplankton (see next section).

Discussion

We have demonstrated that there were distinct differences in the stable carbon isotope ratios of the pelagic food web between the continental shelf and adjacent slope/deep ocean off the southwest coast of Vancouver Island in spring 1992. The range of the difference in the mean $^{13}C/^{12}C$ ratios was 0.5–3.5‰ for POM, 3.1–3.7‰ for zooplankton, and 4.3‰ for fish larvae, with the slope food web depleted in $^{13}C/^{12}C$ relative to the food web on the shelf (Table 3). These differences are of similar magnitude and in the same direction as the differences between stable carbon isotope ratios in zooplankton between the Gulf of Alaska and Prince William Sound (about 4‰; Kline 1997) and between the Gulf of Alaska and the Bering Sea at the Aleutian Passes (about 2.5‰; Schell 1996). This range may reflect the general scale of $\delta^{13}C$ differences between the zooplankton of the deep ocean ecosystem of the Northeast Pacific/Gulf of Alaska and the surrounding ecosystems of its continental margins. It is also consistent with the hypothesis of Schell et al. (1998) that zooplankton growing in regions of high primary productivity, which tend to be the shallow continental margins, should be enriched in $\delta^{13}C$ compared with less productive areas such as the deep ocean.

Such geographic variability in isotope ratios over short distances have lead Schell et al. (1998) to advise caution if isotope ratios are used to infer trophic status and habitat usage for long-lived marine animals such as mammals and birds. Off southwest Vancouver Island, we have identified a characteristic cross-shelf spatial scale of 40–45 km, beyond which the differences of $\delta^{13}C$ increase markedly. The similarity of this spatial autocorrelation scale for $\delta^{13}C$ with that of the upper layer mean salinity suggests that this length scale is likely determined by physical processes. The similarity of these length scales with the internal Rossby radius at this location (about 50 km) further suggests that it is the size of eddies and meanders at the shelf break that separates these food webs. This is consistent with the observation that eddies dominate the prevailing flow pattern at the shelf break during spring, until upwelling-favourable winds begin to establish the summer flow conditions (Thomson and Ware 1996).

We do not mean to imply, however, that salinity is the sole cause of the differences in $\delta^{13}C$; rather, we have used salinity as an index for shelf and slope water masses and their productivity and species compositions. An important question concerns the reasons for the initial differences in $\delta^{13}C$ of the POM between shelf and slope environments. Studies of phytoplankton suggest that carbon fractionation depends on a number of factors relating to growth rates, nutrient (including CO_2) supply and uptake mechanisms, and species composition (and therefore cell size). Carbon isotope fractionation can be affected by factors such as temperature (Rau et al. 1997), salinity (somewhat more negative when grown at 32 psu compared with 35 psu; Leboulanger et al. 1995), and photoperiod (less negative $\delta^{13}C$ under conditions of increasing frequency of light–dark alternations; Leboulanger et al. 1995). The $\delta^{13}C$ of phytoplankton is negatively related to aqueous CO_2 concentration but positively related to temperature (Rau et al. 1997) and positively related to growth rate and nutrient supply (Laws et al. 1995; Bidigare et al. 1997). Fry and Wainwright (1991) found enriched $\delta^{13}C$ values (in the range of –15 to –19‰) in fast-growing spring diatom populations on Georges Bank compared with ^{13}C-depleted values of –21 to –25‰ for other

© 1999 NRC Canada

(less fast growing) phytoplankton in the area. Zooplankton that were feeding on these fast-growing diatoms were also enriched in $\delta^{13}C$. Similar results of increased $\delta^{13}C$ during a bloom of (predominantly) diatoms were simulated in a controlled ecosystem experiment by Nakatsuka et al. (1992).

Off southwestern British Columbia during our surveys, temperature and salinity were similar between adjacent shelf and slope locations, with conditions on the shelf only slightly cooler (1–2°C) and fresher (1 psu, from 0–50 m means, although this was sufficient to distinguish different water masses) than over the slope region. Phytoplankton species composition on the shelf was dominated by diatoms, and nutrient concentrations were substantially higher on the shelf. Unfortunately, aqueous CO_2 concentrations were not measured in either region on these surveys. Measurements made across the shelf break in this region during spring in other years, however, have found P_{CO_2} on the shelf to be less than 20% different (lower) than P_{CO_2} over the slope and deep ocean (F. Whitney, Department of Fisheries and Oceans, Institute of Ocean Sciences, Sidney, B.C., personal communication). We do not expect the $\delta^{13}C$ of this aqueous CO_2 to be different between shelf and slope environments (C.S. Wong, Department of Fisheries and Oceans, Institute of Ocean Sciences, Sidney, B.C., personal communication). Taken together, the observed conditions are consistent with a higher degree of carbon isotope fractionation and less negative $\delta^{13}C$ in phytoplankton on the continental shelf at the time of the surveys, which then persisted up the trophic web to distinguish the zooplankton and larval fish feeding within each region.

These persistent differences in $\delta^{13}C$ across space and trophic levels suggest that they may be used to identify the spatial "boundaries" between marine food webs and to trace exchanges of plankton among these food webs. To trace such exchanges, however, information needs to be available on a number of aspects of the isotope ecology of marine animals, including differences in the allocation and isotopic fractionation of the diet to different tissues (Gannes et al. 1997) and the time scales for incorporation of new isotopic signatures into the tissues. Hesslein et al. (1993) suggested that isotopic differences in fast-growing fish exposed to diets with different isotopic composition should reflect the relative growth rates of the fish. Larval fish should be preferred organisms for such studies of exchanges among food webs, as they are fast growing, their location of origin (e.g., shelf or slope/deep ocean region) can often be better determined than other zooplankton, and they have less independent movement than adult fish.

Some of the uncertainties involved in fractionation and the allocation of nutrients to different animal tissues may be resolved by the use of fatty acids such as eicosapentaenoic (20:5*n*–3) and docosahexaenoic (22:6*n*–3) acids. These are essential for animal growth, in particular for the successful transition from endogenous to exogenous food in sablefish larvae (Whyte et al. 1994), but which the animals are unable to synthesize themselves. As part of the Canadian Global Ocean Ecosystems Dynamics (GLOBEC) project, we are now using compound-specific isotope analyses (e.g., Abrajano et al. 1994) to determine the role of these essential fatty acids as tracers of the source of carbon and food web exchanges of larval and juvenile fishes and invertebrates off the coast of British Columbia. The use of other stable isotopes, such as nitrogen and sulfur, would provide further details of food web structure and the interactions of animals at various trophic levels.

In summary, this study has concluded that there were distinct differences in $^{13}C/^{12}C$ ratios between continental shelf and slope/deep ocean food webs across southwestern Vancouver Island in spring 1992, likely resulting from different species composition and better growth conditions for phytoplankton in the continental shelf environment at that time. These characteristic differences persisted up through the food web from POM to zooplankton and to larval fishes. The spatial scale separating these food webs (defined by their different $\delta^{13}C$ values) was about 40–45 km, which is consistent with the scale separating the upper layer mean salinities (as an index of productivity conditions) and with the scale for eddies and meanders in this region. Studies are currently underway to examine $^{13}C/^{12}C$ ratios of essential fatty acids as detailed tracers of carbon sources and food web interactions and tracers of plankton and fish movements off the coast of British Columbia.

Acknowledgements

We thank Brenda Waddell for her help with sampling at sea and in the laboratory, Bill Andrews for sampling at sea on survey WR9204, Sharon Foord for laboratory analyses, Bente Nielsen and Tom Pedersen for the stable isotope analyses, Moira Galbraith for species identifications of the plankton samples, Frank Whitney and C.S. Wong for discussion on cross-shelf CO_2 conditions, and Rick Thomson for discussions of eddies at the shelf break. We also thank Nathalie Waser, Doug Hay, Yongwen Gao, and two anonymous reviewers for their comments on the manuscript. This study would not have been possible without the excellent cooperation of the officers and crews of the CCGS *John P. Yully* and the CCGS *W.E. Ricker*. This is a contribution of the Canada GLOBEC program, supported by the Department of Fisheries and Oceans and the Natural Sciences and Engineering Research Council of Canada.

References

Abrajano, T.A., Jr., Murphy, D.E., Fang, J., Comet, P., and Brooks, J.M. 1994. $^{13}C/^{12}C$ ratios in individual fatty acids of marine mytilids with and without bacterial symbionts. Org. Geochem. **21**: 611–617.

Bidigare, R.R., Fluegge, A., Freeman, K.H., Hanson, K.L., Hayes, J.M., Hollander, D., Jaspar, J.P., King, L.L., Laws, E.A., Milder, J., Millero, F.J., Pancost, R., Popp, B.N., Steinberg, P.A., and Wakeham, S.G. 1997. Consistent fractionation of ^{13}C in nature and in the laboratory: growth-rate effects in some haptophyte alage. Geochim. Cosmochim. Acta, **11**: 279–292.

Cifuentes, L.A., Sharp, J.H., and Fagel, M.W. 1988. Stable carbon and nitrogen isotope biogeochemistry in the Delaware estuary. Limnol. Oceanogr. **33**: 1102–1115.

DeNiro, M.J., and Epstein, S. 1978. Influence of diet on the distribution of carbon isotopes in animals. Geochim. Cosmochim. Acta, **42**: 495–506.

Doyle, M.J. 1992. Patterns in distribution and abundance of ichthyoplankton off Washington, Oregon, and northern Califor-

© 1999 NRC Canada

nia (1980 to 1987). AFSC Processed Rep. 92-14. Alaska Fisheries Science Center, NMFS/NOAA, Seattle, Wash.

Dunton, K.H, Saupe, S.M., Golikov, A.N., Schell, D.M., and Schonberg, S.V. 1989. Trophic relationships and isotopic gradients among arctic and subarctic marine fauna. Mar. Ecol. Prog. Ser. **56**: 89–97.

Freeland, H.J., Crawford, W.R., and Thomson, R.E. 1984. Currents along the Pacific coast of Canada. Atmos.-Ocean, **22**: 151–172.

Fry, B., and Sherr, E.B. 1984. $\delta^{13}C$ measurments as indicators of carbon flow in marine and freshwater ecosystems. Contrib. Mar. Sci. **27**: 15–47.

Fry, B., and Wainwright, S.C. 1991. Diatom sources of ^{13}C-rich carbon in marine food webs. Mar. Ecol. Prog. Ser. **76**: 149–157.

Gannes, L.Z., O'Brien, D.M., and Del Rio, C.M. 1997. Stable isotopes in animal ecology: assumptions, caveats, and a call for more laboratory experiments. Ecology, **78**: 1271–1276.

Hesslein, R.H., Hallard, K.A., and Ramlal, P. 1993. Replacement of sulfur, carbon, and nitrogen in tissue of growing broad whitefish (*Coregonus nasus*) in response to a change in diet traced by $\delta^{34}S$, $\delta^{13}C$, and $\delta^{15}N$. Can. J. Fish. Aquat. Sci. **50**: 2071–2076.

Howarth, C.D. 1977. The Carbo Erba analyser; carbon, hydrogen, nitrogen and oxygen. *In* Instrumental organic elemental analyses. *Edited by* R. Bechar. Academic Press, New York. pp. 75–111.

Huthnance, J.M. 1995. Circulation, exchange and water masses at the ocean margin: the role of physical processes at the shelf edge. Prog. Oceanog. **35**: 353–431.

Kaluzny, S.P., Vega, S.C., Cardoso, T.P., and Shelly, A.A. 1996. S+SPATIALSTATS user's manual, version 1.0. Mathsoft, Seattle, Wash.

Kline, T.C, Jr. 1997. Confirming forage fish food web dependencies in Prince William Sound using natural stable isotope tracers. *In* Proceedings, Forage Fishes in Marine Ecosystems. AK-SG-97-01. Alaska Sea Grant College Program, Fairbanks, Alaska. pp. 257–269.

Laws, E.A., Popp, B.N., Bidigare, R.R., Kennicutt, M.C., and Macko, S.A. 1995. Dependence of phytoplankton carbon isotopic composition on growth rate and $[CO_{2aq}]$: theoretical considerations and experimental results. Geochim. Cosmochim. Acta, **59**: 1131–1138.

Leboulanger, C., Descolas-Gros, C., Fontugne, M.R., Bentaleb, I., and Jupin, H. 1995. Interspecific variability and environmental influence on particulate organic carbon $\delta^{13}C$ in cultured marine phytoplankton. J. Plankton Res. **17**: 2079–2091.

Loneragan, N.R., Bunn, S.E., and Kellaway, D.M. 1997. Are mangroves and seagrasses sources of organic carbon for penaeid prawns in a tropical Australian estuary? A multiple stable-isotope study. Mar. Biol. **130**: 289–300.

Macdonald, R.W., and McLaughlin, F.A. 1982. The effect of storage by freezing on dissolved inorganic phosphate, nitrate and reactive silicate for samples from coastal and estuarine waters. Water Res. **16**: 95–104.

Mason, J., and Phillips, A. 1986. An improved otter surface sampler. Fish. Bull. U.S. **84**: 480–484.

Matarese, A.C., Kendall, A.W., Jr., Blood, D.M., and Vinter, B.M. 1989. Laboratory guide to early life stages of Northeast Pacific fishes. NOAA Tech. Rep. NMFS 80.

McConnaughey, T., and McRoy, C.P. 1979. Food-web structure and the fractionation of carbon isotopes in the Bering Sea. Mar. Biol. **53**: 257–262.

McFarlane, G.A., Saunders, M.A., Thomson, R.E., and Perry, R.I. 1997. Distribution and abundance of larval sablefish, *Anoplopoma fimbria*, off the west coast of Vancouver Island, and linkages to physical oceanography. *Edited by* M.E. Wilkins and M.W. Saunders. NOAA Tech. Rep. NMFS 130. pp. 27–38.

Nakatsuka, T., Handa, N., Wada, E., and Wong, C.S. 1992. The dynamic changes of stable isotopic ratios of carbon and nitrogen in suspended and sedimented particulate organic matter during a phytoplankton bloom. J. Mar. Res. **50**: 267–296.

Parrish, R.H., Nelson, C.S., and Bakun, A. 1981. Transport mechanisms and reproductive success of fishes in the California Current. Biol. Oceanogr. **1**: 175–203.

Parsons, T.R., Maita, Y., and Lalli, C.M. 1984. A manual of chemical and biological methods for seawater analysis. Pergamon Press, Oxford, U.K.

Peterson, B.J., and Fry, B. 1987. Stable isotopes in ecosystem studies. Annu. Rev. Ecol. Syst. **18**: 293–320.

Pond, D.W., Segonzac, M., Bell, M.V., Dixon, D.R., Fallick, A.E., and Sargent, J.R. 1997. Lipid and lipid carbon stable isotope composition of the hydrothermal vent shrimp *Mirocaris fortunata*: evidence for nutritional dependence on photosynthetically fixed carbon. Mar. Ecol. Prog. Ser. **157**: 221–231.

Rau, G.H., Takahashi, T., and Des Marais, D.J. 1989. Latitudinal variations in plankton $\delta^{13}C$: implications for CO_2 and productivity in past oceans. Nature (Lond.), **341**: 516–518.

Rau, G.H., Riebesell, U., and Wolf-Gladrow, D. 1997. CO_{2aq}-dependent photosynthetic ^{13}C fractionation in the ocean: a model versus measurements. Global Biogeochem. Cycles, **11**: 267–278.

Sameoto, D.D., Jarozynski, L.O., and Fraser, W.B. 1980. BIONESS, a new design in multiple net zooplankton samplers. Can. J. Fish. Aquat. Sci. **37**: 722–724.

Saupe, S.M., Schell, D.M., and Griffiths, W.B. 1989. Carbon-isotope ratio gradients in western arctic zooplankton. Mar. Biol. **103**: 427–432.

Schell, D.M. 1996. Testing conceptual models of marine mammal trophic dynamics using carbon and nitrogen stable isotope ratios. OCS Stud. MMS 95-0057. U.S. Department of the Interior. pp. 86–96.

Schell, D.M., Barnett, B.A., and Vinette, K.A. 1998. Carbon and nitrogen isotope ratios in zooplankton of the Bering, Chukchi and Beaufort seas. Mar. Ecol. Prog. Ser. **162**: 11–23.

Shaw, W., McFarlane, G.A., and Davenport, D. 1988. Distribution and abundance of larval sablefish (*Anoplopoma fimbria*) off the west coast of Vancouver Island, April 2–18, and May 10–18, 1986. Can. MS Rep. Fish. Aquat. Sci. No. 1970.

Statistical Sciences, Inc. 1995. S-Plus user's manual, version 3.3 for Windows. Statistical Sciences, Inc., Seattle, Wash.

Thayer, G.W., Govoni, J.J., and Connally, D.W. 1983. Stable carbon isotope ratios of the planktonic food web in the northern Gulf of Mexico. Bull. Mar. Sci. **33**: 247–256.

Thomson, R.E., and Ware, D.M. 1996. A current velocity index of ocean variability. J. Geophys. Res. **101**(C6): 14 297 – 14 310.

Whyte, J.N.C, Clarke, W.C., Ginther, N.G., Jensen, J.O.T., and Townsend, L.D. 1994. Influence of composition of *Brachionus plicatilis* and *Artemia* on growth of larval sablefish (*Anoplopoma fimbria* Pallas). Aquaculture, **119**: 47–61.

© 1999 NRC Canada

PERSPECTIVES

Predator-induced life history shifts in *Daphnia*: a synthesis of studies using meta-analysis

Howard P. Riessen

Abstract: *Daphnia* respond to kairomones from a variety of predators by altering their morphology, behavior, and life history. I use the statistical technique of meta-analysis to quantitatively evaluate the results of 27 independent studies that examine various life history responses of *Daphnia* to kairomones released from three common predators: *Chaoborus*, *Notonecta*, and planktivorous fish. *Daphnia* exhibit a fundamentally different set of life history responses to *Chaoborus* (delayed reproduction, decreased size of first clutch, slight tendency toward increased size at maturity) than they do to *Notonecta* and fish (earlier reproduction, increased clutch size, smaller size at maturity). These opposite responses appear to be related to different patterns of prey selection exhibited by the predators. Food level does not affect the life history responses of *Daphnia* to *Chaoborus* kairomones; however, the length of exposure to these kairomones does influence the degree of delay in reproduction. In addition, changes in size at maturity in response to predator kairomones are positively correlated with changes in both age at maturity and size of the first clutch. While the life history shifts exhibited by *Daphnia* in the presence of *Notonecta* and fish appear to be clearly adaptive, the fitness consequences of *Chaoborus*-induced responses are unclear.

Résumé : Les *Daphnia* réagissent aux kairomones de divers prédateurs en modifiant leur morphologie, leur comportement et leur cycle vital. J'ai appliqué la technique statistique de la méta-analyse à l'évaluation quantitative des résultats de 27 études indépendantes portant sur diverses réactions du cycle vital des *Daphnia* à des kairomones libérées par trois prédateurs communs : *Chaoborus*, *Notonecta* et un poisson planctivore. Les *Daphnia* présentent un ensemble de réponses du cycle de vie fondamentalement différentes à *Chaoborus* (reproduction retardée, diminution de taille de la première ponte et légère tendance à une augmentation de la taille à maturité) comparativement à la réaction à *Notonecta* et au poisson (reproduction plus hâtive, augmentation de la taille de la ponte et plus petite taille à maturité). Ces réactions contraires semblent liées à des modes différents de choix de la proie de la part des prédateurs. La quantité de nourriture ne modifie pas les réactions du cycle vital des *Daphnia* aux kairomones de *Chaoborus*, mais la durée de l'exposition à ces kairomones influe sur le retard de la reproduction. En outre, la modification de la taille à maturité en réaction aux kairomones du prédateur présente une corrélation positive avec les variations de l'âge à maturité et de la taille de la première ponte. Bien que les variations du cycle vital présentées par les *Daphnia* en présence d'un *Notonecta* et du poisson semblent clairement adaptatives, la valeur adaptative des réactions provoquées par *Chaoborus* est mal définie.

[Traduit par la Rédaction]

Introduction

Species often confront predators whose densities, and therefore impacts, vary considerably in time (seasonally and interannually) and space (among habitats). They also face the prospect that defenses needed to reduce this predation pressure can incur significant costs. One possible solution to this problem is for organisms to use reliable cues to elaborate defenses only in the presence of the predator and thus avoid the cost of defenses except when necessary (Dodson 1989; Stearns 1989; Harvell 1990). These induced antipredator defenses are common among aquatic organisms, which produce a variety of such responses in the presence of predator-released chemical cues (kairomones) (Havel 1987; Dodson 1989; Adler and Harvell 1990; Larsson and Dodson 1993). This is an especially common defensive tactic in *Daphnia* (Crustacea: Cladocera) and other freshwater zooplankton, where it involves modifications in prey morphology, behavior, and life history in response to a variety of fish and invertebrate predators. The best studied of these defenses in *Daphnia* involves production of "neck spines" in juvenile *Daphnia pulex* in response to kairomones released from predatory *Chaoborus* (phantom midge) larvae (Krueger and Dodson 1981; Havel 1985; Dodson 1989). These induced structures function to inhibit predation by *Chaoborus* (Krueger and Dodson 1981; Havel and Dodson 1984; Tollrian 1995*a*). Other *Daphnia* species develop elongated or expanded "helmets" in response to kairomones from

Received February 11, 1999. Accepted August 6, 1999. J15018

H.P. Riessen. Department of Biology, SUNY College at Buffalo, 1300 Elmwood Avenue, Buffalo, NY 14222-1095, U.S.A. e-mail: riessehp@buffalostate.edu

© 1999 NRC Canada

Chaoborus, notonectids (backswimmers), or planktivorous fish (Grant and Bayly 1981; Hebert and Grewe 1985; Dodson 1988*a*; Tollrian 1990, 1994; Hanazato 1991). Induced behavioral responses of *Daphnia* to kairomones from these same predators involve altering patterns of vertical migration in the water column (Dodson 1988*b*; Ramcharan et al. 1992; De Meester 1993; Loose and Dawidowicz 1994; Nesbitt et al. 1996). These changes reduce spatial overlap between *Daphnia* and the various predators, which decreases encounter probability between predator and prey and thus predation risk (Nesbitt et al. 1996).

Changes in a variety of *Daphnia* life history traits (e.g., age at maturity, size at maturity, clutch size) are also induced by predator kairomones. Many studies have detected induced life history changes (see below); however, the adaptive significance of these changes (i.e., whether they are the cost of induced morphological changes or independent antipredator adaptations) is not entirely clear (see Black 1993; Tollrian 1995*b*). In addition, these studies often report results that are not consistent with the results of other similar studies, or even with other results in the same study (e.g., see table 8 in Tollrian 1995*b*). This inconsistency in the nature of predator-induced life history changes in *Daphnia* may be partly explained by the specific experimental design employed in a study, which includes the type of predator kairomone to which *Daphnia* is exposed, the methods and degree of exposure to that kairomone, the quantity of food available to *Daphnia*, and the particular *Daphnia* species examined. Clonal variation in life history response within a *Daphnia* species, however, is also an important factor in this phenomenon (Spitze 1992; Boersma et al. 1998).

Given the diverse array of results in these studies, what general conclusions can be drawn concerning the nature of predator-induced life history shifts in *Daphnia*? In this paper, I use the statistical technique of meta-analysis to combine these various results quantitatively to produce a set of general conclusions for this phenomenon. I specifically analyze the responses of three important *Daphnia* life history traits (age at maturity, size at maturity, size of first clutch) to kairomones from three common predators: *Chaoborus*, *Notonecta*, and fish. I also analyze the influence of both food level and degree of exposure to kairomones on these life history changes and the relationship between changes in size at maturity and changes in the other life history traits. This synthesis produces a clearer picture of the evolution of these induced traits as a response to different types of predators.

Methods

Meta-analysis is a statistical technique that quantitatively evaluates the results of several independent studies, each investigating the same phenomenon, in order to examine their consistency with one another and the magnitude and significance of the overall effect that they display (Gurevitch et al. 1992; Gurevitch and Hedges 1993, 1999; Arnqvist and Wooster 1995). The outcome of each experiment in a study is represented by an "effect size," an index that reflects differences between experimental and control groups. In the present analysis, experimental groups are those with *Daphnia* that have been exposed to predator kairomones during their development, while control groups are those with animals that have not been exposed to these chemicals. As a measure of effect size, I use the standardized difference between the means of the experimental and control groups, d:

$$(1) \qquad d = \frac{\bar{X}_E - \bar{X}_C}{s} J$$

where $\bar{X}_C$ is the mean of the control group, $\bar{X}_E$ is mean of the experimental group, s is the pooled standard deviation of the control and experimental groups, and J is a correction term for bias due to small sample size (for details, see Gurevitch et al. 1992; Gurevitch and Hedges 1993; Rosenberg et al. 1997). This statistic measures the difference in standard deviation units between experimental and control groups and requires values for the mean, standard deviation, and sample size of each group in each experiment evaluated (Gurevitch and Hedges 1993). The overall cumulated effect size across studies within a class (e.g., for all studies examining a specific response to a particular predator), d_+, is calculated as a weighted average of the individual effect sizes for the studies in that class (Gurevitch et al. 1992; Gurevitch and Hedges 1993; Rosenberg et al. 1997). Studies with larger sample sizes are weighted more heavily, since they are assumed to yield more precise results. Calculation of the variance of d_+, its 95% CI, and other meta-analysis statistics is documented in detail in Gurevitch et al. (1992), Gurevitch and Hedges (1993), and Rosenberg et al. (1997).

I used the software program MetaWin (Rosenberg et al. 1997) to perform all analyses in this study, including calculation of the magnitude and significance of the overall effect size within a class of studies and the significance of differences in effect size among various classes of studies (e.g., comparing responses to kairomones from different predators). The magnitude of the overall effect size is generally interpreted as "small" if $d_+ = 0.2$, "medium" if $d_+ = 0.5$, "large" if $d_+ = 0.8$, and "very large" for values of $d_+ > 1.0$ (Gurevitch et al. 1992; Gurevitch and Hedges 1993). These effects are significant (i.e., significant differences exist between experimental and control groups) if the 95% CI around d_+ does not overlap zero (Gurevitch et al. 1992; Gurevitch and Hedges 1993). Significant differences between classes of studies within a meta-analysis are determined by calculation of Q_B, between-class heterogeneity, a measure of variation between classes in mean effect size, which is distributed as χ^2 with $m - 1$ degrees of freedom (where m is the number of classes) (Gurevitch et al. 1992; Gurevitch and Hedges 1993; Rosenberg et al. 1997). All meta-analyses in this study were performed using a mixed-effects model, which assumes random variation among studies within a class, making it more realistic than (and preferable to) the conventional parametric fixed-effects model (Gurevitch and Hedges 1993; Rosenberg et al. 1997).

I analyzed 27 independent studies that examined the effect of predator kairomones on life history traits in *Daphnia* and focused on three of the most important of these traits: age at maturity, size at maturity, and number of eggs in the first clutch (Table 1). All studies published before 1 July 1998 that examined these predator-induced life history shifts in *Daphnia* were included in the analysis, except for those few that either (*i*) failed to report standard deviations (or some measure that could be used to calculate standard deviations) for experimental and control groups (required for the calculation of d) or (*ii*) contained experimental and control groups with very small sample sizes ($n < 5$) (see Rosenberg et al. 1997). The included studies examined responses to kairomones from three different predators (Table 1): *Chaoborus* spp. (18 studies), *Notonecta* spp. (six studies), and various species of planktivorous fishes (10 studies). Several *Daphnia* species were investigated in these various experiments, although *D. pulex* was the most frequently used, especially in experiments with *Chaoborus* kairomones (Table 1). This pattern of using *D. pulex* in experiments testing the effect of *Chaoborus* kairomones was so strong (16 of

© 1999 NRC Canada

Table 1. Studies examined in the meta-analysis for age at maturity (Age), size at maturity (Size), and number of eggs in first clutch (Clutch).

Study	Predator[a]	*Daphnia*[b]	Age	Size	Clutch
Black 1993	Ch (a), N (u)	pul	●	●	●
Black and Dodson 1990	Ch (a)	pul	●	●	●
Dodson and Havel 1988	N (u)	pul	●	●	●
Hanazato 1995	F (m)	gal, amb	●	●	●
Hanazato and Dodson 1992	Ch (a)	pul	●	●	●
Havel and Dodson 1987	Ch (a)	pul	●	●	●
Ketola and Vuorinen 1989	Ch (x)	pul, mag	●	●	●
Lüning 1992	Ch (f), N (g)	pul			●
Lüning 1994	Ch (f)	pul	●	●	●
Lüning 1995	Ch (f)	pul	●	●	●
Macháček 1993	F (r)	gal, obt	●	●	●
Macháček 1995	F (r)	gal	●	●	●
Reede 1995	F (p)	gal × hya	●	●	●
Reede 1997	F (p)	gal × hya	●	●	●
Reede and Ringelberg 1995	F (p)	gal × hya	●	●	
Repka et al. 1994	Ch (o), N (x)	pul	●	●	●
Repka and Pihlajamaa 1996	Ch (o)	pul	●	●	
Riessen and Sprules 1990	Ch (a)	pul	●	●	●
Scheiner and Berrigan 1998	Ch (a)	pul	●	●	●
Stibor 1992	F (i)	hya		●	●
Stibor and Lüning 1994	Ch (f), N (g), F (i)	hya		●	
Tollrian 1995*b*	Ch (f)	pul	●	●	●
Vuorinen et al. 1989	Ch (c)	pul		●	
Walls et al. 1991	Ch (c)	pul	●		●
Walls et al. 1997	Ch (x)	pul	●	●	●
Weber and Declerck 1997	Ch (a), F (p)	gal	●	●	●
Weider and Pijanowska 1993	N (g), F (d)	mag	●	●	●

Note: ● = means, standard deviations, and sample sizes of experimental and control groups reported for this trait.

[a]Predator kairomones examined (species identified in parentheses): Ch, *Chaoborus* (a, *C. americanus*; c, *C. crystallinus*; f, *C. flavicans*; o, *C. obscuripes*; x, unidentified *Chaoborus* species); N, *Notonecta* (g, *N. glauca*; u, *N. undulata*; x, unidentified *Notonecta* species); F, fish (d, *Leucaspius delineatus* (7 cm); i, *Leuciscus idus* (5 cm); m, *Lepomis macrochirus* (7 cm); p, *Perca fluviatilis* (3–4 cm); r, *Rutilus rutilus* (6–7 cm)).

[b]*Daphnia* species examined: pul, *D. pulex*; gal, *D. galeata*; amb, *D. ambigua*; mag, *D. magna*; obt, *D. obtusa*; hya, *D. hyalina*.

the 18 *Chaoborus* studies) that I limited the meta-analysis for the response to *Chaoborus* to this single *Daphnia* species. Experiments with *Notonecta* and fish kairomones, however, examined several *Daphnia* species (Table 1), and the results for all of these species were therefore pooled for the meta-analysis of these two predators.

Three sets of criteria were used to select the experiments within each study that would be included in the primary meta-analysis (that examining general overall effects of predator kairomones) for each of the three life history traits. First, in studies containing multiple experiments that used the same *Daphnia* clone, I selected only those one or two experiments that represented the "typical" response of that clone. This process eliminated bias in the analysis that would otherwise favor the responses of clones that were used in multiple experiments and provided a fair evaluation of the overall response of a diverse array of clones from different studies. Second, in situations where more than one concentration of predator kairomones was evaluated in a study (e.g., Reede 1995; Reede and Ringelberg 1995), only the experimental group with the highest kairomone concentration was included in the meta-analysis. Third, in studies where the period of *Daphnia*'s exposure to kairomones during its development was varied (see below), those experiments with longer periods of exposure were selected over those with shorter exposure times for inclusion in the meta-analysis. The numbers of experiments included in the meta-analysis using these criteria (for age at maturity, size at maturity, and size of first clutch, respectively) were 18, 17, and 16 for responses to *Chaoborus* kairomones, five, eight, and seven for responses to *Notonecta* kairomones, and 11, 12, and 11 for responses to fish kairomones.

Two separate meta-analyses were performed on specific subsets of studies to examine the influences of (*i*) algal food concentration and (*ii*) the degree of exposure to kairomones on the life history responses of *Daphnia* to these predator chemicals. The studies selected in these two subsets were each explicitly designed to test for the effects of food concentration or kairomone exposure. Five such studies (Black and Dodson 1990; Walls et al. 1991; Repka et al. 1994; Tollrian 1995*b*; Walls et al. 1997), each with one set of experiments, examined the effect of high (≈1.0–1.4 mg C·L^{-1}) versus low (≈ 0.1–0.2 mg C·L^{-1}) algal food concentration on the response of *D. pulex* to *Chaoborus* kairomones. Three studies (Lüning 1994; Tollrian 1995*b*; Repka and Pihlajamaa 1996), each with one to four sets of experiments, examined the effect of early (embryo to instar 1) versus complete (entire period of development) exposure to *Chaoborus* kairomones in *D. pulex*. These analyses provided an examination of the effect of these two factors (food level, degree of kairomone exposure) on the life history response of *D. pulex* to *Chaoborus*.

Body size is an especially important life history trait for *Daphnia* and other cladocerans and greatly influences other life history traits (Lynch 1980). I analyzed the relationship between body size and the other life history traits examined by correlating values of *d* for size at maturity with those for age at maturity and size of the first clutch. Twenty-three of the 27 studies analyzed in the meta-

© 1999 NRC Canada

Fig. 1. Overall effect sizes for life history responses of *Daphnia* to predator kairomones (Ch, *Chaoborus*; N, *Notonecta*; F, fish). Age, age at maturity (positive value indicates delayed reproduction); size, size at maturity (positive value indicates larger body size); clutch, number of eggs in the first clutch (positive value indicates larger clutch size). Error bars represent 95% CI.

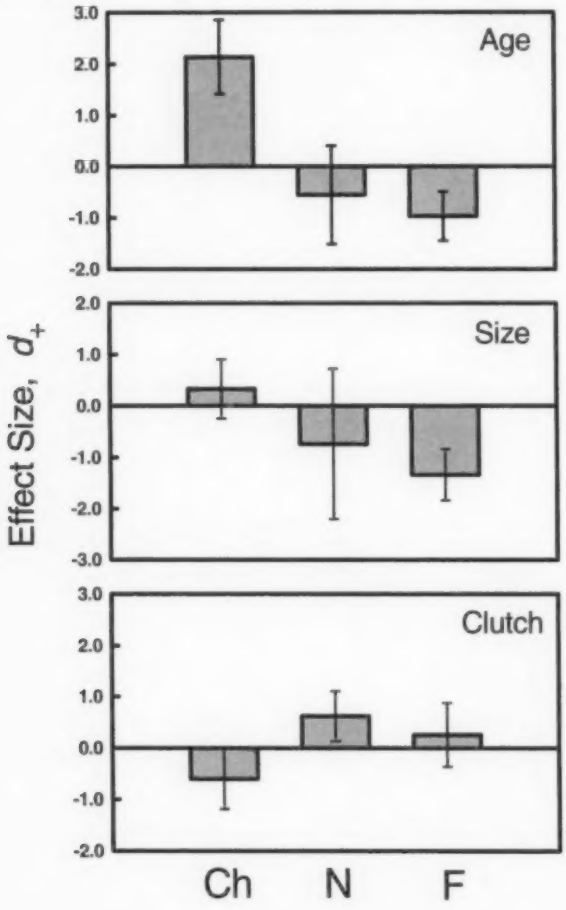

analysis provided one or more experiments each in which the response of *Daphnia* size at maturity to predator kairomones could be directly compared in the same experiment with the response of age at maturity and (or) size of the first clutch (Table 1). Thus, regardless of the specific methodologies of the individual studies or the type of predator kairomone involved, I was able to determine if an increase or decrease in size at maturity was associated with increases or decreases in values for the other two life history traits.

Results

Daphnia exhibit fundamentally different life history responses to *Chaoborus* than they do to *Notonecta* and fish, with the latter two predators eliciting responses that are similar to each other (Fig. 1). The reaction to *Chaoborus* kairomones by *D. pulex* involves delayed reproduction and reduced clutch size, with the increase in age at maturity representing an especially large (d_+ = 2.13) and significant effect. There is also a slight tendency for *D. pulex* to increase body size (size at maturity), but this effect is relatively small (d_+ = 0.32) and not significant. Kairomones from *Notonecta* and fish produce an opposite response in *Daphnia*: earlier reproduction, smaller size at maturity, and increased clutch size, with the decreases in both age and size at maturity in response to fish constituting very large effects. Although the reactions of age and size at maturity to *Notonecta* and of first clutch size to fish are not significantly different from zero, the overall pattern of response to both of these predators is the same. The direction of change in each of the three life history traits is the same for *Notonecta* and fish, and there are no significant differences between the responses to these predators ($Q_B \leq 1.60$, 1 df, $P > 0.20$ for each trait). Combining experiments with *Notonecta* and fish into a single class yields overall responses that are significant or near significant for each of the traits: $d_+ = -0.85 \pm 0.42$ for age at maturity, $d_+ = -1.13 \pm 0.51$ for size at maturity, and $d_+ = 0.40 \pm 0.42$ for size of the first clutch. Each of the life history responses to *Chaoborus*, however, is significantly different from the respective response to *Notonecta* and fish kairomones ($Q_B = 45.71$, 1 df, $P << 0.001$ for age at maturity; $Q_B = 14.96$, 1 df, $P < 0.001$ for size at maturity; $Q_B = 7.18$, 1 df, $P = 0.007$ for size of the first clutch), indicating a distinct dichotomy in the life history response of *Daphnia* to *Chaoborus* on the one hand and *Notonecta* and fish on the other.

Fig. 2. Effect of algal food concentration on response of *D. pulex* to *Chaoborus* kairomones. Open bars, low food concentration (≈0.1–0.2 mg C·L^{-1}); stippled bars, high food concentration (≈1.0–1.4 mg C·L^{-1}). Error bars represent 95% CI. The number of experiments analyzed (high versus low food) is indicated in parentheses for each trait. Abbreviations as in Fig. 1.

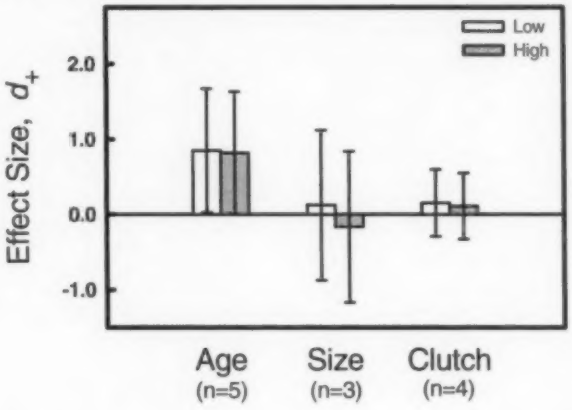

Food level did not affect the response of *D. pulex* to *Chaoborus* kairomones for any of the life history traits analyzed (Fig. 2). In the subset of studies that examined the influence of food, *Daphnia* exhibited similar increases in age at maturity (Q_B = 0.003, 1 df, P = 0.96) and similar nonsignificant responses in size at maturity (Q_B = 0.160, 1 df, P = 0.69) and size of the first clutch (Q_B = 0.016, 1 df, P = 0.90) regardless of the quantity of food provided in the treatments.

The effect of the degree of exposure to *Chaoborus* kairomones on the life history responses of *D. pulex* is more com-

© 1999 NRC Canada

Fig. 3. Effect of degree of exposure to *Chaoborus* kairomones on response of *D. pulex*. Open bars, early exposure only (embryo to instar 1); stippled bars, complete exposure (entire period of development). Error bars represent 95% CI. The number of experiments analyzed (early versus complete exposure) is indicated in parentheses for each trait. Abbreviations as in Fig. 1.

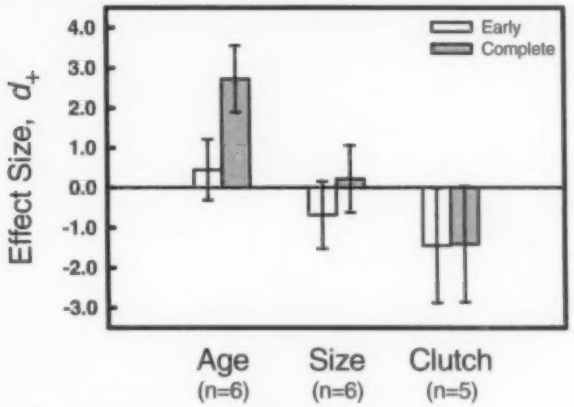

plex than the effect of food (Fig. 3). While it would seem logical to predict that animals exposed to kairomones for longer periods of time should exhibit stronger responses, this was only observed for the increase in age at maturity (Q_B = 15.70, 1 df, $P < 0.001$). *Daphnia pulex* exposed to *Chaoborus* kairomones for their entire life displayed an extremely large (d_+ = 2.72) and significant delay in reproduction, while those exposed only early in their development exhibited a much smaller (d_+ = 0.45) and nonsignificant response. The decrease in size of the first clutch and the nonsignificant responses in size at maturity, however, were not influenced by the length of exposure to *Chaoborus* kairomones (Q_B = 0.001, 1 df, P = 0.97 and Q_B = 2.24, 1 df, P = 0.13, respectively). Thus the length of exposure to kairomones influenced the degree of delay in reproduction but not the other two life history traits.

Changes in size at maturity in response to predator kairomones are positively correlated with changes in both age at maturity (r = 0.404, P = 0.002) (Fig. 4A) and size of the first clutch (r = 0.334, P = 0.022) (Fig. 4B). *Daphnia* that increase their body size (most of these are responses to *Chaoborus*) tend to exhibit delayed reproduction, while those that reduce body size (responses to fish and *Notonecta* as well as some *Chaoborus*) tend to reproduce earlier (Fig. 4A). There is also a tendency for *Daphnia* that increase size at maturity to increase egg production in the first clutch, while a reduction in mature body size is associated with decreased egg production (Fig. 4B). This latter correlation is even stronger if the responses to *Chaoborus* (n = 30, r = 0.567, P = 0.001) (Fig. 4B, solid circles) are considered separately from the responses to *Notonecta* and fish (n = 17, r = 0.532, P = 0.028) (Fig. 4B, open symbols).

Discussion

The life history shift exhibited by *Daphnia* in response to the presence of *Chaoborus* (delayed reproduction, decreased clutch size, and a slight tendency toward increased size at

Fig. 4. Correlations between effect sizes (d) of life history traits. (A) Correlation between size at maturity (size) and age at maturity (age) (r = 0.404, P = 0.002); (B) correlation between size at maturity (size) and number of eggs in first clutch (clutch) (r = 0.334, P = 0.022). Each point represents results from a single experiment in which the responses of the two traits to predator kairomones (●, *Chaoborus*; ▽, *Notonecta*; □, fish) are reported. Values of $d > 0$ for a trait indicate an increase in this trait in response to predator kairomones, with higher values indicating a greater increase. The opposite is true for values of $d < 0$.

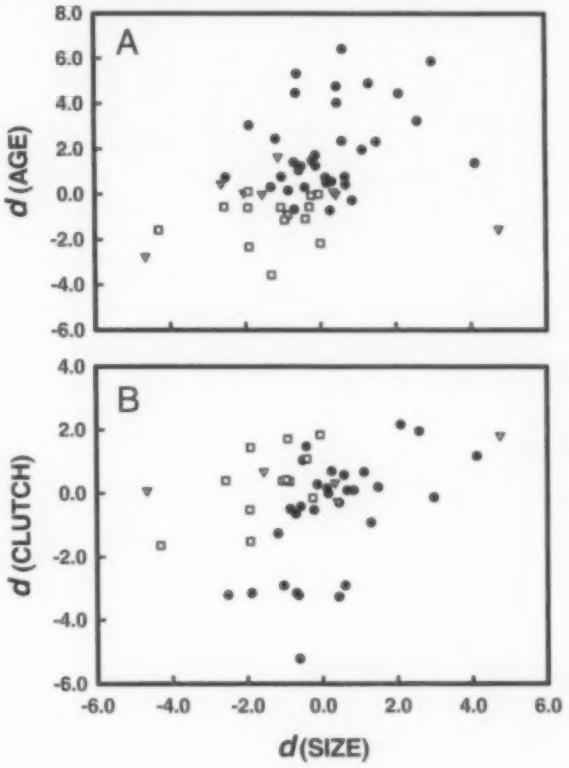

maturity) is fundamentally different from the changes that result from exposure to *Notonecta* and fish predators (earlier reproduction, increased clutch size, and smaller size at maturity) (Fig. 1). The form of the response is thus predator specific, with *Daphnia* clearly able to distinguish between kairomones released by different predators and to then respond with different suites of life history traits. These responses, however, are not influenced by the quantity of food available to *Daphnia* (at least for *D. pulex* responses to *Chaoborus* kairomones) (Fig. 2) and are only somewhat affected by the degree of exposure to the chemical cue released by the predator. While the length of exposure to *Chaoborus* kairomones during development does influence the degree of delay in reproduction in *D. pulex*, it does not result in differences in either size at maturity or size of the first clutch (Fig. 3). This result indicates that developmental changes in response to kairomones that produce alterations in the body size and clutch size of the primiparous instar (usually instar 5 in *D. pulex*) are completed by the end of the

© 1999 NRC Canada

first instar. Further exposure to kairomones during juvenile development does not result in greater changes. For the response in age at maturity, however, a maximum change requires continual exposure to kairomones during development. Exposure that is limited to the developing embryo and first instar results in only a relatively small delay in reproduction in *Daphnia*. Thus the underlying regulatory mechanisms that produce the life history changes (e.g., relative allocation of energy to growth and reproduction) are influenced in different ways by the predator kairomones.

The correlations between changes in size at maturity and changes in the other two life history traits (Fig. 4) are the result of either (*i*) a direct effect of changes in one trait on values in another or (*ii*) independent adaptive responses to the predators. Although the second explanation cannot be ruled out, the first appears more likely in this situation and may result in trade-offs between traits, in which the benefit of altering one compensates for the cost of changing another. For example, the benefits of increased body size may exceed the costs of the associated effect of delayed maturity under certain circumstances (H.P. Riessen, unpublished data). The positive correlation between size and age at maturity (Fig. 4A) is probably a direct consequence of an energy trade-off between somatic growth and reproduction (see Lynch 1980; Threlkeld 1987). *Daphnia* that increase their body size do so at the expense of reproduction, resulting in a delay in maturity. The positive correlation between size at maturity and size of the first clutch (Fig. 4B) is probably a similar direct consequence of larger *Daphnia* being able to produce more eggs (Green 1956; Lynch 1980; Threlkeld 1987).

Differences in the patterns of prey selection exhibited by the three predators produce different selection pressures on *Daphnia* that appear to be responsible for the observed responses in size at maturity. Third- and fourth-instar *Chaoborus* larvae are gape-limited predators that are unable to ingest large *Daphnia* (Swift and Fedorenko 1975; Swift 1992) and therefore select moderately small to medium-sized individuals (1.0–1.5 mm body length) as prey (Dodson 1970; Pastorok 1981; Riessen 1992; Tollrian 1995*a*). *Notonecta* and planktivorous fish, on the other hand, are not gape limited and preferentially select the largest *Daphnia* available (O'Brien 1979; Greene 1983; Scott and Murdoch 1983). *Daphnia*, therefore, would be able to reduce their predation risk by increasing their body size in the presence of *Chaoborus* and decreasing it in the presence of *Notonecta* and fish.

The fitness consequences of each integrated suite of life history changes produced by *Daphnia* in response to a predator are linked to the form of prey selection exhibited by that predator but are also dependent on the precise physiological and evolutionary trade-offs that occur between the various traits. The distinct decrease in size at maturity exhibited by *Daphnia* when in the presence of *Notonecta* and fish clearly appears to be an adaptive response to reduce vulnerability to predators that select large prey. The other associated life history changes in response to these predators (earlier reproduction and increased clutch size) also appear to be adaptive (i.e., increase fitness) in that they both enhance reproductive ability. Earlier reproduction, which is an especially prevalent response to fish (Fig. 1), may be a consequence of smaller size at maturity as a result of a trade-off in the allocation of energy between somatic growth and reproduction (Fig. 4A). Increased clutch size, which is an especially prevalent response to *Notonecta* (Fig. 1), may be associated with smaller neonates as a result of an energetic trade-off between number of eggs and egg size. Smaller neonates would result in smaller adults that are less vulnerable to *Notonecta* and fish, but they may also result in lower juvenile survivorship in poor food environments (Tessier and Consolatti 1989).

The adaptive nature of the life history shifts displayed by *Daphnia* in the presence of *Chaoborus* is far less clear. *Daphnia pulex* exhibit a relatively modest average increase in body size (Fig. 1), which may result in reduced vulnerability to *Chaoborus* for most clones; however, increases in body size do not necessarily always produce reductions in vulnerability to this predator (H.P. Riessen, unpublished data). In addition, it is difficult to understand the adaptive benefit for those *D. pulex* clones that decrease their size at maturity in response to *Chaoborus*. The other life history responses (delayed reproduction, reduced clutch size) are even more problematic in that they actually decrease fitness by diminishing reproductive output. It is possible that they constitute a cost that is paid as part of a trade-off for one or more morphological or behavioral responses that reduce mortality from *Chaoborus* predation, such as neck spine induction, altered vertical migration behavior, or possibly the production of larger neonates.

The meta-analyses performed in this study describe the "typical" life history responses of *Daphnia* to three common predators (Fig. 1). As such, they represent average values for either a variety of *Daphnia* species (responses to *Notonecta* and fish) or a variety of clones of one species, *D. pulex* (responses to *Chaoborus*). Understanding these trends is an important step in the process of deciphering the nature of these induced life history shifts in *Daphnia* as well as its life history evolution in general. It does not, however, provide a complete picture of the phenomenon. Hidden in the "typical" responses to the different predators is a considerable amount of variation both among *Daphnia* species and (most interestingly) among clones of individual species (see Spitze 1992; Boersma et al. 1998). Such variation is probably the result of the selection of different integrated suites of traits (morphological, behavioral, life history) in individual clones that function to adapt particular clones to specific environmental conditions (e.g., different types and densities of predators). The ultimate challenge in understanding the ecological and evolutionary nature of these induced life history shifts thus lies in understanding the variation that exists among species and clones and the fitness consequences of the individual responses.

Acknowledgements

I thank Michael Brett for his advice on performing and interpreting meta-analysis procedures and Randal Snyder for discussions on and technical assistance with this study. Funding was provided by grants from SUNY College at Buffalo and the State of New York/UUP Professional Development and Quality of Working Life Committee.

© 1999 NRC Canada

References

Adler, F.R., and Harvell, C.D. 1990. Inducible defenses, phenotypic variability and biotic environments. Trends Ecol. Evol. **5**: 407–410.

Arnqvist, G., and Wooster, D. 1995. Meta-analysis: synthesizing research findings in ecology and evolution. Trends Ecol. Evol. **10**: 236–240.

Black, A.R. 1993. Predator-induced phenotypic plasticity in *Daphnia pulex*: life history and morphological responses to *Notonecta* and *Chaoborus*. Limnol. Oceanogr. **38**: 986–996.

Black, A.R., and Dodson, S.I. 1990. Demographic costs of *Chaoborus*-induced phenotypic plasticity in *Daphnia pulex*. Oecologia (Berl.), **83**: 117–122.

Boersma, M., Spaak, P., and De Meester, L. 1998. Predator-mediated plasticity in morphology, life history, and behavior of *Daphnia*: the uncoupling of responses. Am. Nat. **152**: 237–248.

De Meester, L. 1993. Genotype, fish-mediated chemicals, and phototactic behavior in *Daphnia magna*. Ecology, **74**: 1467–1474.

Dodson, S.I. 1970. Complementary feeding niches sustained by size-selective predation. Limnol. Oceanogr. **15**: 131–137.

Dodson, S.I. 1988*a*. Cyclomorphosis in *Daphnia galeata mendotae* Birge and *D. retrocurva* Forbes as a predator-induced response. Freshwater Biol. **19**: 109–114.

Dodson, S. 1988*b*. The ecological role of chemical stimuli for the zooplankton: predator-avoidance behavior in *Daphnia*. Limnol. Oceanogr. **33**: 1431–1439.

Dodson, S. 1989. Predator-induced reaction norms. BioScience, **39**: 447–452.

Dodson, S.I., and Havel, J.E. 1988. Indirect prey effects: some morphological and life history responses of *Daphnia pulex* exposed to *Notonecta undulata*. Limnol. Oceanogr. **33**: 1274–1285.

Grant, J.W.G., and Bayly, I.A.E. 1981. Predator induction of crests in morphs of the *Daphnia carinata* King complex. Limnol. Oceanogr. **26**: 201–218.

Green, J. 1956. Growth, size and reproduction in *Daphnia* (Crustacea: Cladocera). Proc. Zool. Soc. Lond. **126**: 173–204.

Greene, C.H. 1983. Selective predation in freshwater zooplankton communities. Int. Rev. Gesamten Hydrobiol. **68**: 297–315.

Gurevitch, J., and Hedges, L.V. 1993. Meta-analysis: combining the results of independent experiments. *In* Design and analysis of ecological experiments. *Edited by* S.M. Scheiner and J. Gurevitch. Chapman and Hall, New York. pp. 378–398.

Gurevitch, J., and Hedges, L.V. 1999. Statistical issues in ecological meta-analyses. Ecology, **80**: 1142–1149.

Gurevitch, J., Morrow, L.L., Wallace, A., and Walsh, J.S. 1992. A meta-analysis of competition in field experiments. Am. Nat. **140**: 539–572.

Hanazato, T. 1991. Induction of development of high helmets by a *Chaoborus*-released chemical in *Daphnia galeata*. Arch. Hydrobiol. **122**: 167–175.

Hanazato, T. 1995. Life history responses of two *Daphnia* species of different sizes against a fish kairomone. Jpn. J. Limnol. **56**: 27–32.

Hanazato, T., and Dodson, S.I. 1992. Complex effects of a kairomone of *Chaoborus* and an insecticide on *Daphnia pulex*. J. Plankton Res. **14**: 1743–1755.

Harvell, C.D. 1990. The ecology and evolution of inducible defenses. Q. Rev. Biol. **65**: 323–340.

Havel, J.E. 1985. Cyclomorphosis of *Daphnia pulex* spined morphs. Limnol. Oceanogr. **30**: 853–861.

Havel, J.E. 1987. Predator-induced defenses: a review. *In* Predation: direct and indirect impacts on aquatic communities. *Edited by* W.C. Kerfoot and A. Sih. University Press of New England, Hanover, N.H. pp. 263–278.

Havel, J.E., and Dodson, S.I. 1984. *Chaoborus* predation on typical and spined morphs of *Daphnia pulex*: behavioral observations. Limnol. Oceanogr. **29**: 487–494.

Havel, J.E., and Dodson, S.I. 1987. Reproductive costs of *Chaoborus*-induced polymorphism in *Daphnia pulex*. Hydrobiologia, **150**: 273–281.

Hebert, P.D.N., and Grewe, P.M. 1985. *Chaoborus*-induced shifts in the morphology of *Daphnia ambigua*. Limnol. Oceanogr. **30**: 1291–1297.

Ketola, M., and Vuorinen, I. 1989. Modification of life-history parameters of *Daphnia pulex* Leydig and *D. magna* Straus by the presence of *Chaoborus* sp. Hydrobiologia, **179**: 149–155.

Krueger, D.A., and Dodson, S.I. 1981. Embryological induction and predation ecology in *Daphnia pulex*. Limnol. Oceanogr. **26**: 219–223.

Larsson, P., and Dodson, S. 1993. Chemical communication in planktonic animals. Arch. Hydrobiol. **129**: 129–155.

Loose, C.J., and Dawidowicz, P. 1994. Trade-offs in diel vertical migration by zooplankton: the costs of predator avoidance. Ecology, **75**: 2255–2263.

Lüning, J. 1992. Phenotypic plasticity of *Daphnia pulex* in the presence of invertebrate predators: morphological and life history responses. Oecologia (Berl.), **92**: 383–390.

Lüning, J. 1994. Anti-predator defenses in *Daphnia* — are life-history changes always linked to induced neck spines? Oikos, **69**: 427–436.

Lüning, J. 1995. Life-history responses to *Chaoborus* of spined and unspined *Daphnia pulex*. J. Plankton Res. **17**: 71–84.

Lynch, M. 1980. The evolution of cladoceran life histories. Q. Rev. Biol. **55**: 23–42.

Macháček, J. 1993. Comparison of the response of *Daphnia galeata* and *Daphnia obtusa* to fish-produced chemical substance. Limnol. Oceanogr. **38**: 1544–1550.

Macháček, J. 1995. Inducibility of life history changes by fish kairomone in various developmental stages of *Daphnia*. J. Plankton Res. **17**: 1513–1520.

Nesbitt, L.M., Riessen, H.P., and Ramcharan, C.W. 1996. Opposing predation pressures and induced vertical migration responses in *Daphnia*. Limnol. Oceanogr. **41**: 1306–1311.

O'Brien, W.J. 1979. The predator–prey interaction of planktivorous fish and zooplankton. Am. Sci. **67**: 572–581.

Pastorok, R.A. 1981. Prey vulnerability and size selection by *Chaoborus larvae*. Ecology, **62**: 1311–1324.

Ramcharan, C.W., Dodson, S.I., and Lee, J. 1992. Predation risk, prey behavior, and feeding rate in *Daphnia pulex*. Can. J. Fish. Aquat. Sci. **49**: 159–165.

Reede, T. 1995. Life history shifts in response to different levels of fish kairomones in *Daphnia*. J. Plankton Res. **17**: 1661–1667.

Reede, T. 1997. Effects of neonate size and food concentration on the life history responses of a clone of the hybrid *Daphnia hyalina* × *galeata* to fish kairomones. Freshwater Biol. **37**: 389–396.

Reede, T., and Ringelberg, J. 1995. The influence of a fish exudate on two clones of the hybrid *Daphnia galeata* × *hyalina*. Hydrobiologia, **307**: 207–212.

Repka, S., and Pihlajamaa, K. 1996. Predator-induced phenotypic plasticity in *Daphnia pulex*: uncoupling morphological defenses and life history shifts. Hydrobiologia, **339**: 67–71.

Repka, S., Ketola, M., and Walls, M. 1994. Specificity of predator-induced neck spine and alteration in life history traits in *Daphnia pulex*. Hydrobiologia, **294**: 129–140.

Riessen, H.P. 1992. Cost–benefit model for the induction of an antipredator defense. Am. Nat. **140**: 349–362.

Riessen, H.P., and Sprules, W.G. 1990. Demographic costs of antipredator defenses in *Daphnia pulex*. Ecology, **71**: 1536–1546.

© 1999 NRC Canada

Rosenberg, M.S., Adams, D.C., and Gurevitch, J. 1997. MetaWin: statistical software for meta-analysis with resampling tests. Version 1.0. Sinauer Associates, Sunderland, Mass.

Scheiner, S.M., and Berrigan, D. 1998. The genetics of phenotypic plasticity. VIII. The cost of plasticity in *Daphnia pulex*. Evolution, **52**: 368–378.

Scott, M.A., and Murdoch, W.W. 1983. Selective predation by the backswimmer, *Notonecta*. Limnol. Oceanogr. **28**: 352–366.

Spitze, K. 1992. Predator-mediated plasticity of prey life history and morphology: *Chaoborus americanus* predation on *Daphnia pulex*. Am. Nat. **139**: 229–247.

Stearns, S.C. 1989. The evolutionary significance of phenotypic plasticity. BioScience, **39**: 436–445.

Stibor, H. 1992. Predator induced life-history shifts in a freshwater cladoceran. Oecologia (Berl.), **92**: 162–165.

Stibor, H., and Lüning, J. 1994. Predator-induced phenotypic variation in the pattern of growth and reproduction in *Daphnia hyalina* (Crustacea: Cladocera). Funct. Ecol. **8**: 97–101.

Swift, M.C. 1992. Prey capture by the four larval instars of *Chaoborus crystallinus*. Limnol. Oceanogr. **37**: 14–24.

Swift, M.C., and Fedorenko, A.Y. 1975. Some aspects of prey capture by *Chaoborus* larvae. Limnol. Oceanogr. **20**: 418–425.

Tessier, A.J., and Consolatti, N.L. 1989. Variation in offspring size in *Daphnia* and consequences for individual fitness. Oikos, **56**: 269–276.

Threlkeld, S.T. 1987. *Daphnia* life history strategies and resource allocation patterns. *In Daphnia. Edited by* R.H. Peters and R. de Bernardi. Mem. Ist. Ital. Idrobiol. **45**: 353–366.

Tollrian, R. 1990. Predator-induced helmet formation in *Daphnia cucullata* (Sars). Arch. Hydrobiol. **119**: 191–196.

Tollrian, R. 1994. Fish-kairomone induced morphological changes in *Daphnia lumholtzi* (Sars). Arch. Hydrobiol. **130**: 69–75.

Tollrian, R. 1995*a*. *Chaoborus crystallinus* predation on *Daphnia pulex*: can induced morphological changes balance effects of body size on vulnerability? Oecologia (Berl.), **101**: 151–155.

Tollrian, R. 1995*b*. Predator-induced morphological defenses: costs, life history shifts, and maternal effects in *Daphnia pulex*. Ecology, **76**: 1691–1705.

Vuorinen, I., Ketola, M., and Walls, M. 1989. Defensive spine formation in *Daphnia pulex* Leydig and induction by *Chaoborus crystallinus* De Geer. Limnol. Oceanogr. **34**: 245–248.

Walls, M., Caswell, H., and Ketola, M. 1991. Demographic costs of *Chaoborus*-induced defences in *Daphnia pulex*: a sensitivity analysis. Oecologia (Berl.), **87**: 43–50.

Walls, M., Laurén-Määttä, C., Ketola, M., Ohra-Aho, P., Reinikainen, M., and Repka, S. 1997. Phenotypic plasticity of *Daphnia* life history traits: the roles of predation, food level and toxic cyanobacteria. Freshwater Biol. **38**: 353–364.

Weber, A., and Declerck, S. 1997. Phenotypic plasticity of *Daphnia* life history traits in response to predator kairomones: genetic variability and evolutionary potential. Hydrobiologia, **360**: 89–99.

Weider, L.J., and Pijanowska, J. 1993. Plasticity of *Daphnia* life histories in response to chemical cues from predators. Oikos, **67**: 385–392.

© 1999 NRC Canada

The first marine biological station in Canada: 100 years of scientific research at St. Andrews

Edward A. Trippel

Abstract: The first marine biological station in Canada was established in St. Andrews, New Brunswick, in July 1899. The original station was a portable laboratory and was moved between various summer research sites in Atlantic Canada before a permanent station was established in St. Andrews in 1908. Early research included practical problems in the fisheries and descriptive work of coastal fauna and was performed by university researchers. *Contributions to Canadian Biology*, a journal founded to report the findings of the early station's researchers, in time evolved into the *Canadian Journal of Fisheries and Aquatic Sciences*. For the first 75 years, the station was managed as part of the Fisheries Research Board of Canada and its predecessors, and since 1979 by the Department of Fisheries and Oceans (from 1972 to 1978, two other government departments held this responsibility). Research on fisheries, the environment, oceanography, and aquaculture has dominated the station's history. July 1999 marked the 100th anniversary of marine research in St. Andrews. We celebrate and remember with pride our accomplishments and look forward to the future of conserving Canada's aquatic environment and the livelihood of Atlantic Canadians.

Résumé : Au Canada, la première station de biologie marine a été établie à St. Andrews (Nouveau-Brunswick) en juillet 1899. À l'origine, il ne s'agissait que d'un laboratoire mobile qui était transporté en été d'un site de recherche à l'autre dans le Canada atlantique. La station permanente a été établie à St. Andrews en 1908. Les premiers travaux de recherche, effectués par des chercheurs universitaires, ont porté sur des problèmes pratiques dans le secteur des pêches et sur des descriptions de la faune côtière. *Contributions to Canadian Biology*, revue fondée pour communiquer les résultats des travaux des premiers chercheurs, est devenue par la suite le *Journal canadien des sciences halieutiques et aquatiques*. Pendant 75 ans, la station a été gérée dans le cadre de l'Office des recherches sur les pêcheries du Canada et ses prédécesseurs, et depuis 1979, par Pêches et Océans Canada (de 1972 à 1978, deux autres ministères en ont assumé la gestion). La recherche sur les pêches, l'environnement, l'océanographie et l'aquaculture a dominé l'histoire de la station. En juillet 1999, la station de St. Andrews a fêté cent ans de recherches marines. C'est avec fierté que nous célébrons et que nous nous rappelons nos réalisations. Nous comptons poursuivre notre tâche et continuer à conserver l'environnement aquatique du Canada et le mode de vie des habitants du Canada atlantique.

[Traduit par la Rédaction]

> ...And the biologists at that time were inclined to think that to really get a good knowledge of biology, you had to be at the seashore. For as a Biological Station that was very important, because life had been presumed to have originated in the shallow water at the shore and you had a great variety of animals and the sea which you needed to know about, and that was important.
>
> A.G. Huntsman, 1973 (University of Toronto Archives)

Portable and permanent biological stations, 1899–1932

For centuries, the oceans have provided a source of living for many coastal nations, but it was only in the latter part of the nineteenth century that great curiosity and fascination in marine scientific research gained momentum. Scientists eager to pursue marine studies lobbied hard for the establishment of coastal laboratories, and several of the world's first marine biological stations were founded. Prof. E.E. Prince, Commissioner and General Inspector of Fisheries for Canada, recognized the need for a Canadian marine biological station and in 1893 noted that

> ...the necessity is now perceived for an institution devoted to the accurate investigation of fishery problems, the elucidation and final settlement of perplexing questions which have baffled practical men, the collection of exact observations on the food, habits, and life-history of fishes, and the accumulation in this way of useful scientific knowledge in order to promote the prosperity of our coast and inland fisheries.

Passamaquoddy Bay (Bay of Fundy) and the Gulf of St. Lawrence were considered by E.E. Prince as candidate sites for the operation of a marine biological station on Canada's Atlantic coast, and in July 1899 the construction of a portable "floating" station was completed (Fig. 1).

A "Board of Management of the Marine Biological Station" was established to oversee the operations of the station, with E.E. Prince as the Board's chairman. The first Board members included some of Canada's most distinguished scientists of the time representing eight eastern Canadian universities. Although the first site of operation was proposed to be the Gulf of St. Lawrence, the Marine Biological Station was operated at St. Andrews during the summers

Received June 9, 1999. Accepted September 1, 1999.
J15180

E.A. Trippel. Department of Fisheries and Oceans, St. Andrews Biological Station, 531 Brandy Cove Road, St. Andrews, NB E5B 2L9, Canada.
e-mail: trippele@mar.dfo-mpo.gc.ca

© 1999 NRC Canada

Fig. 1. Marine Biological Station at Indian Point, St. Andrews, N.B., in 1899. E.E. Prince described the station as "a neat one-story structure of wood, well lighted from the roof and sides, and somewhat resembling a Pullman car...Its total length is 50 feet (15 m), the principal room, or main laboratory, occupying the central part of the structure...."

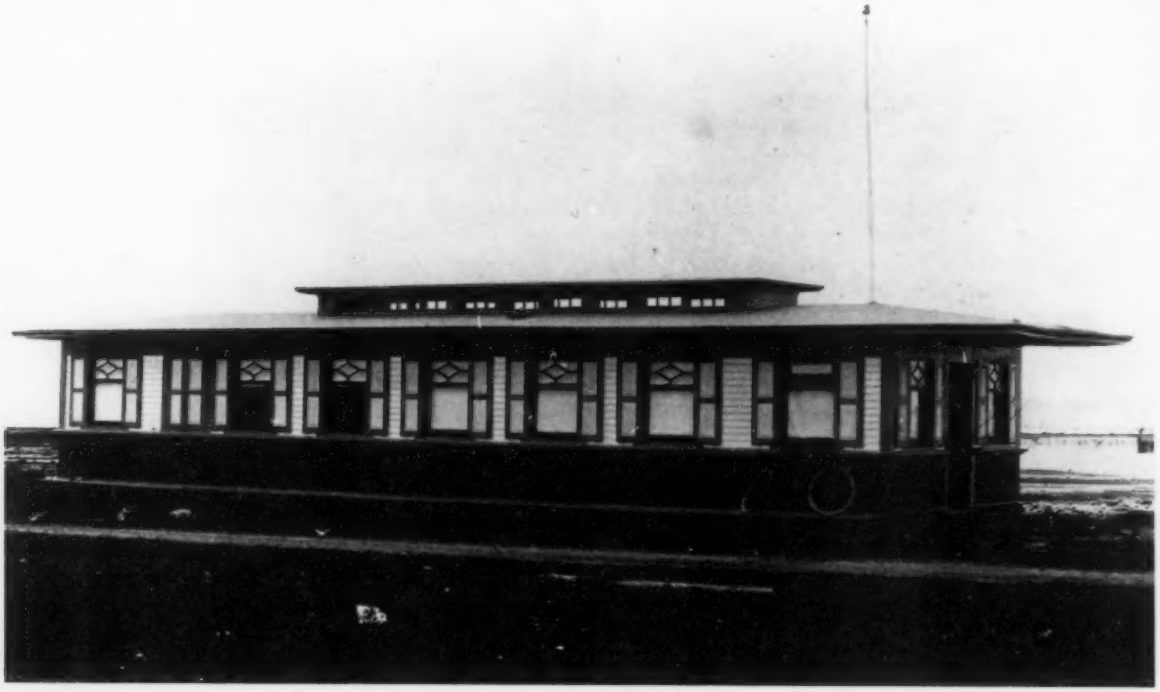

Fig. 2. The Marine Biological Station was operated at St. Andrews from 1899 to 1901. In 1901, the portable station was placed on a scow and moved to and operated at Canso, N.S. (1901–1902), Malpeque, P.E.I. (1903–1904), and Gaspé, Que. (1905–1906).

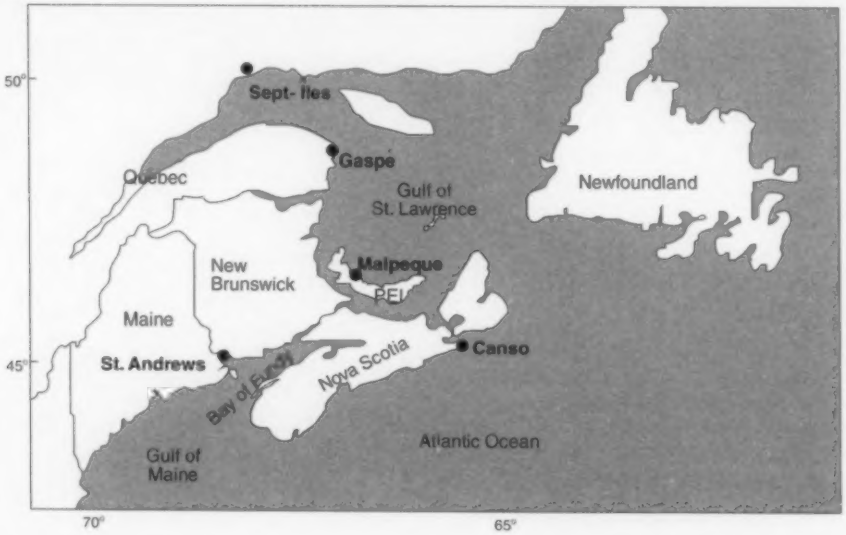

of 1899 and 1900. In 1901 the station was placed on a scow and moved to Canso, Nova Scotia, where it operated for 2 years and then was subsequently moved to Malpeque, Prince Edward Island (1903–1904), and Gaspé, Quebec (1905–1906) (Fig. 2). The station was damaged while being towed from Gaspé to Sept- Îles in 1907 and was abandoned at Grand Vallée, Quebec. Alternate facilities were found that allowed a scientific program to be conducted at Sept-Îles in 1907 (Fig. 2).

The scientific work at the portable station was performed

© 1999 NRC Canada

Table 1. Station directors, number of full-time staff, and responsible authorities for the management of the Biological Station.

	Station directors	Number of full-time staff	Station management history
Marine Biological Station of Canada scientists-in-charge, 1899–1907			
1899–1900	E.E. Prince (St. Andrews)		Board of Management of the Marine Biological Station (1899–1912)[a]
1901–1904	R.R. Wright (Canso, Malpeque)		
1905–1907	J. Stafford (Gaspé, Sept-Îles)		
St. Andrews Biological Station[b] directors since 1908			
1908–1909	D.P. Penhallow (resident director)		
1910–1911	L.W. Bailey, A.B. Macallum, R.R. Wright (directors-in-charge)		
1910–1920	A.G. Huntsman (curator-in-charge), except J.W. Mavor in 1914		Biological Board of Canada (1912–1937)[a]
192i–1934	A.G. Huntsman	2 (1924), 6 (1930), 11 (1933)	
1934–1940	A.H. Leim		Fisheries Research Board of Canada (1937–1973)[a]
1941–1954	A.W.H. Needler	10 (1945)	
1954–1967	J.L. Hart	25 (1955), 134 (1966)	
1967–1972	J.M. Anderson		
1972–1975	R.O. Brinkhurst		Department of the Environment, Fisheries and Marine Service (1973–1976)
1975–1976	D.J. Scarratt, E.J. Sandeman, P.J.G. Carrothers (acting directors)		Department of Fisheries and the Environment, Fisheries and Marine Service (1976–1979)
1977–1992	R.H. Cook	84 (1989)	Department of Fisheries and Oceans (1979–present)
1992–1997	W.M. Watson-Wright		
1997–present	T.W. Sephton	64 (1999)	

[a]From 1899–1973, the three boards reported to Marine and Fisheries, Fisheries Branch (1899–1914), Naval Services, Fisheries Branch (1914–1920), Marine and Fisheries, Fisheries Branch (1920–1930), Department of Fisheries (1930–1969), Department of Fisheries and Forestry (1969–1971), and Department of the Environment, Fisheries and Marine Services (1971–1973).
[b]Referred to as the Atlantic Biological Station until about 1955.

by experienced investigators from the various universities. As virtually everything was unstudied, it was not surprising that their research was primarily descriptive and involved coastal fauna, although a substantial amount of applied research was conducted. Fifty-eight published papers and reports by 20 different investigators were generated. Their research encompassed surveys of local marine fishes, invertebrates, and plants, including plankton, research on the diet of commercial fishes, studies on the fisheries and life history of herring, lobsters, oysters, and clams, the physiology of marine animals, the effects of polluted waters on fish life, and the chemistry of animals and seawater. A sampling of their efforts and that of subsequent investigators is provided in the References section, which lists a selection of 100 key contributions published by station scientists in the twentieth century.

Of great significance was the initiation by E.E. Prince of a scientific journal called *Contributions to Canadian Biology* (1902–1925) that provided a venue for publication of the novel findings of the station's summer investigators. This journal would in time evolve into one of the world's leading fisheries scientific journals, having consecutive titles of *Contributions to Canadian Biology and Fisheries* (1926–1934), *Journal of the Biological Board of Canada* (1934–1937), *Journal of the Fisheries Research Board of Canada* (1938–1979), and *Canadian Journal of Fisheries and Aquatic Sciences* (1980–present).

The number of scientists desiring to conduct aquatic research soon outgrew the humble facilities of the portable station. After careful consideration, St. Andrews was chosen as the site for a permanent Atlantic Biological Station, beginning operations in 1908. St. Andrews offered excellent access to coastal fisheries and marine fauna and direct railway access overnight from Montreal. This permitted convenient travel arrangements for its main users, the university community of eastern Canada. In the same year, the Pacific Biological Station was also constructed in Nanaimo, British Columbia, providing Canada a marine research site on each of its coastlines with economically important fisheries. The station directors, number of full-time staff, and the boards and government departments responsible for the management of the Biological Station throughout its history are provided in Table 1.

Prof. D.P. Penhallow, the first director of the permanent station in St. Andrews, described the facilities of the Biological Station (Fig. 3) in his annual report for 1908:

> ...a laboratory building 79 × 31 feet; capable of accommodating nine junior and three senior investigators, together with necessary store rooms; a dwelling house...; and an aquarium in which should be kept for scientific and other purposes, such forms of marine life as would be brought back from the various expeditions in which the staff would engage.

The sheltered bays and rich feeding grounds in the area were ideal settings for research. The town of St. Andrews was also a well-established summer resort with many social amenities:

© 1999 NRC Canada

Fig. 3. Atlantic Biological Station, St. Andrews, N.B., in 1909. The central building is the main laboratory with the residence building behind it and a tank tower to the left to provide running salt water.

Fig. 4. The *Sea Gull* (10.7 m) was one of the station's first research vessels operating from 1908 to 1915. In total, 18 vessels have been in service at St. Andrews.

> While scientists...are not expected to engage largely in social diversions...their best work cannot be expected in the complete absence of all opportunities for pleasant mental and physical relaxation and recreation. These opportunities are afforded in admirable manner by the social life of St. Andrews, and favourable opportunities for summer amusements, and it is believed that these factors add very materially to the successful working of the station.
>
> D.P. Penhallow, 1906

Researchers primarily came to the station during the summer months to work on their own particular problems, which ranged from fishes to invertebrates to seaweed. Much of the research was done by Board members, who remained practising scientists. Researchers were supplied on-site accommodation and meals and had travel costs reimbursed. Research vessels were small and primarily accessed nearshore areas (Fig. 4). The important nearby herring fishery in the Bay of Fundy was among the first to prompt investigations that had some direct commercial importance, and this relevance to industry is reflected in the Board's mandate, and hence the station's activities. The Biological Board Act of 1912 and subsequent revisions state in part, "The Board...has the conduct and control of investigations of practical and economic problems connected with marine and freshwater fisheries, flora, and fauna, and such work as may be assigned to it by the Minister." Work was carried out that was of very considerable scientific value and, at the same time, provided essential background for subsequent research

© 1999 NRC Canada

aimed more directly at the solution of fisheries problems. The first recorded interest in salmon was in 1913 when Chairman of the Board E.E. Prince led in the experimental development of a new type of fish pass for carrying salmon over the falls in the Magaguadavic River. Research on the use of fish as a potential source of insulin was also conducted by Nobel Laureate J.R.R. Macleod.

While most of the scientists who worked at the station came from Canadian universities, some came from the United States and Europe. Many researchers were eminent in their fields. From 1914 to 1915, the Canadian Fisheries Expedition was launched with Dr. Johan Hjort of Bergen, Norway, cooperating with the Board in hydrographic sampling and examination of herring stocks throughout the Gulf of St. Lawrence, Nova Scotian Shelf, Bay of Fundy, and the Gulf of Maine. This expedition served as a benchmark of the region's marine knowledge for some time. A summary of some important events occurring during the 100-year history of the station is provided in Table 2.

New station, post-Second World War expansion, and the International Commission for the Northwest Atlantic Fisheries (ICNAF), 1932–1959

In 1932, during the Great Depression, a fire completely destroyed the wooden main laboratory of the station and, with it, the valued library holdings. Dr. A.G. Huntsman (Fig. 5), director from 1921 to 1934, immediately began construction of a brick laboratory on the same foundation as the original one. In order to raise funds, he redirected operating funds and salaries. Given the country's poor economic state, he was concerned that the Board might not approve the rebuilding of the laboratory. In 1935, Dr. A.H. Leim became director of the Biological Station and held this post to 1940 (Dr. Huntsman's decision to reconstruct the station without formal approval may have contributed in part to his removal from the directorship in 1934).

In the 10 years following 1931, a large effort was made on the important groundfish fisheries. The general life histories of cod and haddock were explored including growth, distribution, migrations, temperature preferences, spawning, and egg distribution and the fisheries and their statistics. Every year, some advancement in shellfish biology was made, as the station was the chief source of scientific advice in support of lobsters and scallops, the former eventually becoming the single most economically important species in Atlantic Canada. Overall, the invertebrate fisheries of the region generated either a comparable or a higher landed value than the finfish fisheries. By 1936, scallop studies covered food for adults, maturity, spawning, the physical requirements for egg development, drift of larvae, varying successes of the year-classes, and the possible effects of the increasing commercial fishery. The feasibility of oyster culture was examined intensively with several experimental farms set up in Atlantic Canada that acted as useful demonstration centres.

In oceanography, from 1931 to 1939, a series of research cruises studied the conditions off the Scotian Shelf including the origin of the coldwater layer and the significance of temporary migrations of Gulf Stream water on the Atlantic seaboard. The most powerful tides in the world occur in the Bay of Fundy, and these were studied intensively (difference between low and high tide being 7.6 m at St. Andrews).

The Biological Station's postwar expansion was fueled by increased modernization and technology developed during the war period. The advent of stern trawlers resulted in large commercial landings and focused new research activities on the offshore. Additional research vessels were on loan from Newfoundland after 1949, the year that it joined Confederation. With Canada now having both the St. John's and St. Andrews laboratories conducting east coast research, the Atlantic Biological Station name was no longer appropriate and shortly thereafter was referred to as the Biological Station (by the 1990s the St. Andrews Biological Station was the more commonly used name). The station was also substantially enlarged with the opening in 1959 of a new wing complete with expanded wet and dry laboratory facilities.

Until 1977, St. Andrews was responsible for providing scientific advice in support of the exploitation of Atlantic marine fishery resources for all but Newfoundland waters. In accordance with this enormous responsibility, the station developed a reputation for excellence in marine sciences. In 1949, the ICNAF was developed and comprised 10 member nations. It recommended to member countries regulations to protect the fisheries resources in the Northwest Atlantic. This organization had its second meeting in St. Andrews and its offices were located there for some time. The beginning of ICNAF and the associated responsibilities for Canada, the Board, and the station initiated a new age of science activities. Scientific advice on catch sampling (age structure), mesh size, and recruitment signals was sought from St. Andrews, and these demands increased steadily during the 1950s. Initial emphasis was placed on developing improved fishery statistics for haddock and cod, with redfish also demanding attention. The countries involved in ICNAF and the necessary meetings and working groups were a novel, yet necessary, approach to the multinational fishing efforts taking place in the region.

Clams and mussels in the Bay of Fundy are sometimes quite dangerous to eat due to the toxin-laden microalgae that they consume. A shellfish monitoring program initiated in 1943 led to the discovery in 1947 of the dinoflagellate that carries the paralytic shellfish poison, and the investigators assisted in establishing measures to protect the public. Toxic algae research continues at the station to this day, providing one of the world's longest term databases on this natural aquatic problem.

Fishery exploitation, end of the Fisheries Research Board, and the beginning of the Department of Fisheries and Oceans (DFO), 1960–1979

During the 1960s, as a result of growing ICNAF commitments, station scientific staff continued to take on greater roles in connection with marine fisheries exploitation (in 1964, Canadian jurisdiction extended to 12 mi (19 km)). Scientific activities were primarily on fishery research applied to estimating resource size and furthering the understanding

© 1999 NRC Canada

Table 2. Some important events in the history of the St. Andrews Biological Station.

1899–1907	
1899	Operations begin on the portable "floating" marine biological station
1902	First volume of *Contributions to Canadian Biology* published
1908–1932	
1908	Shore-based research started with construction of permanent biological station
1913	Experimental development of fish pass for carrying salmon over falls in the Magaguadavic River
1914/15	Canadian Fisheries Expedition
1920/24	Research on use of fish as a potential source of insulin
1921	North American Council on Fishery Investigations established
1925	Atlantic Fisheries Experimental Station was constructed in Halifax, and research on fish processing transferred there
1928	Year-round scientific work began
1929	Substation established for oyster investigations, Ellerslie, P.E.I.
1930	Hudson Bay Fisheries Expedition
1932–1945	
1932	Main building destroyed by fire and rebuilt
1933	North American Council on Fishery Investigations met at St. Andrews
1934	Full-time staff had effectively displaced students/volunteer scientists
1937	Fisheries Research Board Act passed
1940/45	Oceanographers assisted Navy with techniques in submarine detection
1943	Research vessel *J.J. Cowie* began operations
1944	Atlantic Herring Investigation Committee established
1945–1959	
1946	Atlantic Oceanographic Group established Field station, brook trout investigations, Ellerslie, P.E.I., established.
1949	International Commission for the Northwest Atlantic Fisheries (ICNAF) created
1950	Miramichi salmon unit established
1952	Meeting of ICNAF at St. Andrews
1956	International Passamaquoddy Fisheries Board established to evaluate potential impacts on marine life of constructing a dam to harness tidal power
1957	Research vessel *Harengus* began operations
1959	Opening of new wing complete with expanded wet and dry laboratory facilities
1960–1969	
1961	Atlantic Oceanographic Group moved to Halifax
1963	Bedford Institute of Oceanography (BIO) established in Dartmouth
1964	Canadian jurisdiction extended from 3 to 12 mi (5–19 km) First computer at the Biological Station was installed (storage capacity 3 kilobytes)
1966	Research vessel *E.E. Prince* began operations
1967	Human-made lobster reef developed in the Gulf of St. Lawrence
1968	First use of underwater manned submersibles for marine science in Atlantic Canada Oyster program at Ellerslie, P.E.I., transferred to Marine Ecology Laboratory in Dartmouth, N.S.
1969	Huntsman Marine Laboratory (HML) established in neighbouring Brandy Cove
1970–1979	
1970s	Environmental problems researched involving heavy metals such as mercury and cadmium, petroleum hydrocarbons, and pulp mill solutions
1970	Beginning of annual groundfish random stratified surveys conducted from Gulf of St. Lawrence to Gulf of Maine

© 1999 NRC Canada

Table 2 (*concluded*).

1972	Atlantic Herring Management Board established
	Final year of the Fisheries Research Board as a research arm of the Canadian Fisheries Service
1976	Station integrated into the regional structure of the Department of the Environment, Fisheries and Marine Services
1977	World's first integrated lobster culture facility operated
	Extension of coastal fisheries jurisdiction to 200 mi (320 km)
	Newly formed peer review body named the Canadian Atlantic Fishery Scientific Advisory Council (CAFSAC)
1978	Pilot Atlantic salmon sea cage culture project initiated at Deer Island, Passamaquoddy Bay
1979	Northwest Atlantic Fisheries Organisation (NAFO) superseded ICNAF
	Department of Fisheries and Oceans (DFO) created
1980–1989	
1981	Acid Rain Program began
	Gulf Fisheries Centre was established (Moncton, N.B.); assumed responsibility for the management and science activities of the Gulf of St. Lawrence
1984	International Court of Justice provided a ruling that divided Georges Bank into U.S. and Canadian sections
	Atlantic Reference Centre (ARC), an arm of the HML, occupied offices at the station
1985	Atlantic Salmon Demonstration and Development Farm in Lime Kiln Bay, southwest N.B., established
1986	New annual spring bottom trawl survey initiated on Georges Bank
1987/89	Rebuilding of invertebrate and large pelagic fisheries programs with significant involvement in the International Commission for the Conservation of Atlantic Tunas (ICCAT)
1990–1999	
1990s	Tagging of bluefin tuna and Atlantic salmon to monitor movement patterns in the Northwest Atlantic
	Fisheries Oceanography Group increased in importance
	Extensive research on the interactions of aquaculture and the environment
1992/93	Most of Atlantic Canada's groundfish fisheries were closed; the southern stocks that St. Andrews was mandated to provide advice for, however, continued to sustain fisheries
1993	Fisheries Resource Conservation Council (FRCC) created
	Station staff produced the first cultured halibut and haddock reared to juvenile stages in Atlantic Canada
1996	Station named DFO's Centre of Excellence for Finfish Aquaculture in Atlantic Canada
	Oceans Act passed
1997	Pelagic Research Group formed (herring resource assessments became more integrated with industry)

© 1999 NRC Canada

Fig. 5. Five station directors in 1973 (with active years in parentheses): J.M. Anderson (1967–1972), A.W.H. Needler (1941–1954), A.G. Huntsman (1921–1934), J.L. Hart (1954–1967), and R.O. Brinkhurst (1972–1975).

Fig. 6. Four station directors in 1999 (with active years in parentheses): J.M. Anderson (1967–1972), R.H. Cook (1977–1992), W.M. Watson-Wright (1992–1997), and T.W. Sephton (1997–present).

of stock structure, biology, and energetics. Apart from vital population statistics, research on groundfish focused on diurnal vertical migrations, swimming performance, daily ration levels at different temperatures, age determination, use of parasites for stock discrimination, tagging and movements, and fish community associations. During this period, St. Andrews scientists became particularly well known for their use of small underwater manned submersibles, which, for example, were used in the examination of a human-made reef to supplement lobster production in the Gulf of St. Lawrence and to observe herring spawning grounds on Georges Bank.

With the spruce budworm crisis in New Brunswick and its destruction of valuable timber, logging companies began the spraying of large forested areas with DDT. Consequently, within the station's pollution program, a large focus was placed on studying the effects of DDT spraying on Atlantic salmon survival, with experimental work conducted primarily on the Miramichi River. Station scientists clearly showed the negative effects on parr survival and the reduced ability of fish to return to natal rivers to spawn, resulting in changes to spraying compounds. The negative effect of the Greenland salmon gillnet fishery on recreational salmon fishing in the Maritimes was also discovered.

Several scientists at the station perceived marine aquaculture of Atlantic salmon to hold some promise. However, at the time, the station was not supposed to be involved in fish culture, and work using photoperiod manipulation to influence postsmolt growth reported in 1967 was downplayed and referred to as "controlled production of salmon to make biological gains." In the next decade, this early covert approach to aquaculture was to change considerably. Within a 20-year period, aquaculture research evolved to substantially complement the station's historic role in the harvest fisheries.

The station's director, Dr. J.M. Anderson (1967–1972) (Fig. 5), led the founding of the Huntsman Marine Laboratory (HML) and helped arrange a 50-year renewable land lease adjacent to the station on neighbouring Brandy Cove for its establishment. HML was developed with a consortium of eastern Canadian universities to serve as a research and teaching platform for marine biology. In time, industry and private organizations also showed an interest in the marine sciences and supported HML.

The final year of the Board as the research arm of the Canadian Fisheries Service came in 1972. The following year, staff of the station became employees of the Department of the Environment, and thereafter the Board lost its authority as the Public Service took over greater control of responsibilities. As a result the Board became more or less an advisory body and eventually folded by the end of the decade. Whatever the reasons for the loss of the Fisheries Research Board, the seasoned scientific staff, strong in the tradition of high-quality advancement of research activities under the Board, continued to contribute to the Biological Station's global reputation for excellence in scientific research.

The 1970s showed a strong surge of interest in pelagic species, particularly herring. In the early 1970s, herring stocks were in severe decline and an Atlantic Herring Management Board was established and directed out of St. Andrews that helped to revolutionize fisheries management over a 5-year period. In 1972, the efforts of the St. Andrews staff led ICNAF to establish fishing quotas and national allocations for three large herring stocks, a management measure not previously adopted in any international fishery. St. Andrews thus played an integral role in spearheading the international agreement for partitioning stock allocations among nations that, soon after, was universally applied to many fishery resources worldwide.

The year 1970 marked the beginning of annual groundfish random stratified surveys conducted from the Gulf of St. Lawrence to the Gulf of Maine. These time series remain and are critical to fisheries resource evaluation of Northwest Atlantic fish stocks.

A significant development of the decade pertained to aquaculture. Dr. R.H. Cook (Fig. 6) held the director's position from 1977 to 1992 and he exerted a tremendous amount of influence over the formation of a solid aquaculture program at St. Andrews to support the newly developing industry in the Bay of Fundy. Atlantic salmon culture and American lobster culture were evaluated, and in time, salmon culture was a success. Although the world's first in-

© 1999 NRC Canada

Fig. 7. Aerial view of the St. Andrews Biological Station and wharf in 1998. Behind the main laboratory (Penhallow Building) is the former residence (Ester Lord Building) now used for administration and scientific working space. To the left of the Penhallow Building are extensive wet laboratory facilities used in aquaculture research. On the top of the hill is the Lauzier Building (oceanography, nutrition, and histology), and below it and to the right are buildings housing the Atlantic Reference Centre and the Scott–Templeman Collection. The Hunstman Marine Science Centre (not shown) is located to the left of the station in Brandy Cove.

tegrated lobster culture facility was operated at St. Andrews for more than a decade, lobster culture proved to be an unprofitable venture for private industry, although invaluable information was gained on lobster holding practices and transferred to industry to reduce incidence of disease and death. Lobster landings remained high, whereas wild salmon stocks declined. The ban on commercial fishing of Atlantic salmon, begun in 1972, encouraged experimentation with cultured salmon. In 1978, a pilot salmonid sea cage culture project was initiated at Deer Island, Passamaquoddy Bay, and successfully produced 6 metric tons (t) of fish of market size (3–4 kg). Sea ranching experiments from the station and the Atlantic Salmon Federation's research facility (in nearby Chamcook) were also highly successful in 1978. From these early efforts, the station's finfish and invertebrate aquaculture research program began to develop a worldwide reputation.

During the 1970s, a collection of primarily marine organisms from Atlantic Canada was further developed and, in 1984, became the Atlantic Reference Centre (ARC), an arm of the HML, occupying offices at the station (after 1986, the HML became the Huntsman Marine Science Centre). The ARC provides identification services for aquatic biota, as well as curation and the development of a major reference, research, and teaching collection of aquatic organisms. The ARC houses the renowned Scott–Templeman Collection of aquatic organisms of Atlantic Canada.

Georges Bank, aquaculture, conservation, and the environment, 1980–1999

In October 1984, the International Court of Justice provided a ruling that divided Georges Bank into U.S. and Canadian sections. The Georges Bank boundary dispute before the World Court required considerable input from the station's researchers regarding these rich fishing grounds. Scientists evaluated the impact of the single maritime boundary on traditional fishing patterns and on the distribution of fisheries resources. Transboundary straddling fish stocks on Georges Bank led to strong collaborations between station scientists and U.S. scientists in both state and federal agencies. With the extension of jurisdiction in 1977 to 200 mi (320 km), many depleted stocks rebounded, and interest and participation in the commercial fishery were strong.

The widespread occurrence of acid rain in eastern North America prompted an extensive Acid Rain Program, which began at the station in 1981. Researchers in the program developed an understanding of the processes governing susceptibility of fish habitats to acid precipitation, the mechanisms by which acidification affects fish populations, and the ability to predict probable impacts on fish populations. Some of the findings included the effects of low pH on survival and recruitment of Atlantic salmon. An examination was made of the feasibility of renovating acidified fish habitats by the use of liming.

By 1981, the term "aquaculture" had made its way to top administrative levels in Ottawa. The principal mission of the Department became "stock assessment, habitat protection and resource enhancement, including aquaculture." In 1985–1986, the Biological Station established the Atlantic Salmon Demonstration and Development Farm in Lime Kiln Bay in the heart of the southwest New Brunswick aquaculture industry. This was an experimental-scale Atlantic salmon farm and served to develop and transfer aquaculture technologies to the private sector. By 1988, 34 salmon farms existed in the Bay of Fundy. These produced about

© 1999 NRC Canada

3000 t and were profitable. The high tides, deep water, and numerous protected coves provide ideal conditions for marine sea cages in the southwestern Bay of Fundy. A strong research program on factors controlling smoltification assisted industry tremendously, as many freshwater smolt hatcheries were established by the private sector. The Salmon Genetics Research Program, a joint effort between DFO and the Atlantic Salmon Federation, was continued at Chamcook. The program's original aim was to develop high-performance strains of salmon for sea ranching or replenishing depleted wild stocks. In 1982–1983, the program emphasis shifted and became vital in the development of salmon strains for the aquaculture industry. The Biological Station housed the editorial office of the World Aquaculture Society and currently holds the administrative and editorial offices of the Aquaculture Association of Canada. Three past presidents of the World Aquaculture Society and two past presidents of the Aquaculture Association of Canada are currently members of the Biological Station staff. In addition, St. Andrews is a venue for major aquaculture meetings, including the annual Atlantic Aquaculture Exposition, Conference, and Fair.

In 1992–1993, most of Atlantic Canada's groundfish fisheries were closed. This changed the atmosphere and kind of research conducted by personnel in many groups in eastern Canada. The southern stocks that St. Andrews was mandated to provide advice for, however, continued to sustain fisheries. However, by the late 1990s, annual quotas for many of these had diminished considerably. The crisis in the fisheries in Atlantic Canada led to the disappearance of the Canadian Atlantic Fishery Scientific Advisory Committee (CAFSAC), and in 1993, the Fisheries Resource Conservation Council (FRCC) was formed. A Regional Advisory Process (RAP) was created in which stock status reports were peer reviewed through an open and transparent process with information passed first to the FRCC (for groundfish) and to advisory committees (for all other species) and then to the Minister. Scientists and fishers also began to collaborate more. Joint DFO/industry resource surveys were developed to gain estimates of fish abundance (previously, CAFSAC deliberations on stock status were conducted in the absence of industry members). Herring resource assessment also became more integrated with industry through the Pelagic Research Group, and hydroacoustics was increasingly used to provide "real-time" assessments of abundance of individual herring stocks using industry vessels, including in-season management.

Research advances included newly developed underwater habitat mapping techniques using SCUBA diving and videorecording to better understand the behaviour and ecology of lobsters. The Atlantic Oceanographic Group, which was established at St. Andrews in 1946, was transferred to Halifax in 1961. However, a fisheries oceanography program continued at the Biological Station. This program has increased in importance in recent years and is focused on a number of regional and international issues in relation to both the harvest fisheries and aquaculture.

Aquaculture research at the Biological Station broadened as the industry grew and faced new challenges. With over 80 industry cage sites, salmon production in southwest New Brunswick in 1997 was 17 000 t, having a value of $110 million (over 94% of all Atlantic salmon sold commercially worldwide are now cultivated fish). Halibut and haddock aquaculture is believed to have the potential to diversify the salmon aquaculture industry. Different approaches will be required to culture these species compared with salmon, and as a consequence, wet and dry laboratory facilities at the Biological Station have been renovated and expanded (Fig. 7). A marine fish aquaculture program, begun in 1988, had by 1993 produced the first halibut reared to juvenile stages in Atlantic Canada. Haddock, a highly priced gadoid, was also first raised in 1993. By 1998, a pilot-scale haddock hatchery at the Biological Station had achieved considerable success. With support from the New Brunswick provincial government, industry partners have entered into joint partnerships with Biological Station staff to develop the new technologies of raising marine fish. Although none has reached commercial production by the late 1990s, future research will strive to expedite their commercial culture. Regarding invertebrates, significant efforts are being made towards the culture and enhancement of soft-shell clam and sea scallop. Sea urchin culture for roe consumption is also being explored and shows promise.

In 1996, the Biological Station was named DFO's Centre of Excellence for Finfish Aquaculture in Atlantic Canada. With the closing of the DFO-operated Halifax Fisheries Laboratory in 1998, some of these staff positions and facilities related to aquaculture were moved to St. Andrews, further strengthening the program with the addition of a fish nutrition laboratory, histology laboratory, quarantine disease facility, and electron microscope.

Paralleling the growing support for aquaculture is a nearly equal effort to evaluate and mitigate the negative impacts of aquaculture on the environment. These impact studies conducted by station scientists include nontarget effects of the use of therapeutants, overfeeding, use of noise to ward off seal attacks, overcrowding of sea pens, and the interaction of salmon escapees with disappearing native salmon river runs.

The Biological Station in the 1990s was led by three directors: Dr. R.H. Cook (1977–1992), Dr. W. M. Watson-Wright (1992–1997), and Dr. T.W. Sephton (1997–present) (Fig. 6), each strongly focused on aquaculture, although providing support for all groups at the station. It is this team spirit, together with competence in main areas of expertise, that has fostered the excellent reputation of aquatic research conducted in St. Andrews during the past 100 years. As the station enters the next millennium, the strength and legacy of achievements from the previous 100 years have created a solid foundation for future growth and development and the vision required to confront upcoming challenges in the aquatic sciences. Let the next 100 years be as pioneering and successful as the first.

Acknowledgements

The preparation of this historic perspective would not have been possible had it not been for the efforts of others to record the rich history of the St. Andrews Biological Station. These accounts and contributions are listed below. The Biological Station's annual reports were particularly useful and because of their quantity were not cited. Helpful comments were made on earlier manuscript drafts by D. Aiken, J.M. Anderson, B. Chang, R. Halliday, M. Rudi, M. Sinclair, J.

© 1999 NRC Canada

Stewart, S. Taylor, and two anonymous reviewers, for which the author is grateful. It is important to note, due to space limitations, that it was not possible to adequately highlight all of the major accomplishments made by the scientific staff during the station's first century. Since 1990, the author has been a research scientist at the St. Andrews Biological Station and has contributed to a variety of areas including groundfish stock assessments, aquaculture, and marine mammal conservation.

References

Historical sources

Carter, N.M. 1968. Index and list of titles, Fisheries Research Board of Canada and associated publications. Bull. Fish. Res. Board Can. No. 164.

Chang, B.D. (*Editor*). 1990. Scientific research activities at the St. Andrews Biological Station. Can. MS Rep. Fish. Aquat. Sci. No. 2054.

Chang, B.D. (*Editor*). 1994. St. Andrews Biological Station activity report 1990–1993. Can. MS Rep. Fish. Aquat. Sci. No. 2269.

Chang, B.D., and Watson-Wright, W.M. 1997. Aquaculture research at the St. Andrews Biological Station: past, present and future. Aquacult. Assoc. Can. Spec. Publ. No. 2. pp. 105–108.

Hart, J.L. 1958. Fisheries Research Board of Canada Biological Station, St. Andrews, N.B., 1908–1958: fifty years of research in aquatic biology. J. Fish. Res. Board Can. **15**: 1127–1161.

Johnstone, K. 1977. The aquatic explorers: a history of the Fisheries Research Board of Canada. University of Toronto Press, Toronto, Ont.

Needler, A.W.H. 1958. Fisheries Research Board of Canada Biological Station, Nanaimo, B.C., 1908–1958. J. Fish. Res. Board Can. **15**: 759–777.

Needler, A.W.H. 1984. The seventy-fifth anniversary of two Canadian biological stations. Can. J. Fish. Aquat. Sci. **41**: 216–224.

Parsons, L.S. 1993. Management of marine fisheries in Canada. Can. Bull. Fish. Aquat. Sci. No. 225.

Penhallow, D.P. 1912. Report on the Atlantic Biological Station of Canada, St. Andrews, N.B., for 1908. Contrib. Can. Biol. **1906–1910**: 1–21.

Prince, E.E. 1901. Marine Biological Station of Canada. Contrib. Can. Biol. **1901**: 1–8.

Rudi, M. 1999. The history of the St. Andrews Biological Station: a guide to sources of information. URL site: http://www.mar.dfo-mpo.gc.ca/

Sander, F. 1987. Activity report of the St. Andrews Biological Station (1986). Can. MS Rep. Fish. Aquat. Sci. No. 1948.

Sander, F. 1988. St. Andrews Biological Station publications 1977–86. Can. MS Rep. Fish. Aquat. Sci. No. 1960.

100 selected contributions

A representative overview of the Biological Station's scientific accomplishments is provided through a selection of 100 key contributions published during the twentieth century. The selected publications, clustered by decade, serve to illuminate the great breadth and depth of research interests, as well as the many recurring themes and motifs as they have emerged and subsided over the years.

1899–1909

Bensley, B.A. 1901. Report on the sardine industry in relation to the Canadian herring fisheries. Contrib. Can. Biol. **1901**: 59–62.

Fowler, J. 1901. Report on the flora of St. Andrews, N.B. Contrib. Can. Biol. **1901**: 41–48.

Knight, A.P. 1901. The effects of polluted waters on fish life. Contrib. Can. Biol. **1901**: 9–18.

Knight, A.P. 1907. The effects of dynamite explosions on fish life. Contrib. Can. Biol. **1907**: 21–30.

Macallum, A.B. 1903. On the inorganic composition of the Medusae *Aurelia flavidula* and *Cyanea arctica*. J. Physiol. **29**: 213–241.

Prince, E.E. 1907. The eggs and early life-history of the herring, gaspereau, shad and other clupeoids. Contrib. Can. Biol. **1907**: 95–110.

Scott, F.H. 1901. Food of the sea-urchin (*Strongylocentrotus dröbachiensis*). Contrib. Can. Biol. **1901**: 49–54.

Stafford, J. 1901. The clam fishery of Passamaquoddy Bay. Contrib. Can. Biol. **1901**: 19–40.

Stafford, J. 1905. The larva and spat of the Canadian oyster. Am. Nat. **39**: 41–44.

Wright, R.R. 1907. The plankton of eastern Nova Scotia waters, an account of floating organisms upon which young food-fishes mainly subsist. Contrib. Can. Biol. **1907**: 1–19.

1910–1919

Bailey, L.W. 1915. The plankton diatoms of the Bay of Fundy. Contrib. Can. Biol. **1915**: 11–23.

Cox, P. 1916. A supposed disease of quahaugs from New Brunswick. Contrib. Can. Biol. **1916**: 73–79.

Duff, D. 1916. Investigation of the haddock fishery, with special reference to the growth and maturity of the haddock (*Melanogrammus æglefinus*). Contrib. Can. Biol. **1916**: 95–102.

Gran, H.H. 1919. Quantitative investigations as to phytoplankton and pelagic Protozoa in the Gulf of St. Lawrence and outside the same. *In* Canadian fisheries expedition 1914–1915, in the Gulf of St. Lawrence and Atlantic waters of Canada. Department of the Naval Service, Ottawa, Ont. pp. 487–495.

Horne Craigie, E. 1916. Hydrographic section of the Bay of Fundy in 1914. Contrib. Can. Biol. **1916**: 163–167.

Huntsman, A.G. 1918. The scale method of calculating the rate of growth in fishes. Trans. R. Soc. Can. **12**: 47–52.

Huntsman, A.G. 1918. The effect of the tide on the distribution of the fishes of the Canadian Atlantic coast. Trans. R. Soc. Can. **12**: 61–67.

Knight, A.P. 1916. Lobster sanctuaries and hatching ponds: an investigation of the Long Beach lobster pond, Digby County, Nova Scotia in 1914. Contrib. Can. Biol. **1916**: 41–54.

Robertson, A.D. 1916. First report on the "barren oyster bottoms" investigation, Richmond Bay, P.E.I. Contrib. Can. Biol. **1916**: 55–71.

Wodehouse, R.P. 1916. Report on the life history of the cod as determined from the scales and other data. Contrib. Can. Biol. **1916**: 103–113.

1920–1929

Battle, H.I. 1929. Effects of extreme temperatures and salinities on the development of *Enchelyopus cimbrius* (L.). Contrib. Can. Biol. Fish. (New Ser.), **5**: 107–192.

Connolly, C.J. 1925. The larval stages and megalops of *Rhithropanopeus harrisi* (Gould). Contrib. Can. Biol. (New Ser.), **2**: 327–334.

Cox, P. 1924. Larvae of the halibut (*Hippoglossus hippoglossus* L.) on the Atlantic coast of Nova Scotia. Contrib. Can. Biol. (New Ser.), **1**: 409–412.

Huntsman, A.G. 1921. The fishes of the Bay of Fundy. Contrib. Can. Biol. **1921**: 49–72.

Knight, A.P. 1921. The histology of the flexor tendon in the crushing claw of the lobster. Contrib. Can. Biol. **1918–1920**: 185–188.

© 1999 NRC Canada

Leim, A.H. 1924. The life history of the shad (*Alosa sapidissima* (Wilson)) with special reference to the factors limiting its abundance. Contrib. Can. Biol. (New Ser.), **2**: 161–284.

Mavor, J.W. 1920. Drift bottles as indicating a superficial circulation in the Gulf of Maine. Science (Washington), **52**: 442–443.

McCormick, N.A., and Noble, E.C. 1924. The yield of insulin from fish. Contrib. Can. Biol. (New Ser.), **2**: 115–127.

Needler, A.W.H. 1927. Biological studies of fishery statistics. Contrib. Can. Biol. Fish. (New Ser.), **3**: 307–315.

White, H.C. 1924. A quantitative determination of the number of survivors from planting 5000 trout fry in each of two streams. Contrib. Can. Biol. (New Ser.), **2**: 135–150.

1930–1939

Battle, H.I. 1931. Rythmic sexual maturity and spawning of certain bivalve mollusks. Contrib. Can. Biol. Fish. (New Ser.), **7**: 255–276.

Hachey, H.B. 1934. The replacement of Bay of Fundy waters. J. Biol. Board Can. **1**: 121–131.

Hachey, H.B. 1935. Tidal mixing in an estuary. J. Biol. Board Can. **1**: 171–178.

Hachey, H.B. 1939. Temporary migrations of Gulf stream water on the Atlantic seaboard. J. Biol. Board Can. **4**: 339–348.

Huntsman, A.G. 1931. Biological and oceanographic conditions in Hudson Bay. 1. Hudson Bay and the determination of fisheries. Contrib. Can. Biol. Fish. (New Ser.), **6**: 455–462.

Huntsman, A.G. 1938. Sea movements of Canadian Atlantic salmon kelts. J. Fish. Res. Board Can. **4**: 96–135.

Medcof, J.C. 1939. Larval life of the oyster (*Ostrea virginica*) in Bideford River. J. Biol. Board Can. **4**: 287–301.

Needler, A.W.H. 1930. The migrations of haddock and the interrelationships of haddock populations in North American waters. Contrib. Can. Biol. Fish. (New Ser.), **6**: 241–313.

Smith, M.W. 1934. Physical and biological conditions in heavily fertilized water. J. Biol. Board Can. **1**: 67–93.

White, H.C. 1939. Factors influencing descent of Atlantic salmon smolts. J. Biol. Board Can. **4**: 323–326.

1940–1949

Elson, P.F. 1942. Effect of temperature on activity of *Salvelinus fontinalis*. J. Fish. Res. Board Can. **5**: 461–470.

Hachey, H.B. 1947. Water transports and current patterns for the Scotian shelf. J. Fish. Res. Board Can. **7**: 1–16.

Huntsman, A.G. 1945. Variable seaward migration of salmon. J. Fish. Res. Board Can. **6**: 311–325.

Kerswill, C.J. 1949. Effects of water circulation on the growth of quahaugs and oysters. J. Fish. Res. Board Can. **7**: 545–551.

McKenzie, R.A. 1940. Nova Scotian autumn cod spawning. J. Fish. Res. Board Can. **5**: 105–120.

Medcof, J.C. 1944. Structure, deposition and quality of oyster shell (*Ostrea virginica* Gmelin). J. Fish. Res. Board Can. **6**: 209–216.

Medcof, J.C. 1946. Effect of relaying and transferring on fatness of oysters. J. Fish. Res. Board Can. **6**: 449–455.

Needler, A.B. 1949. Paralytic shellfish poisoning and *Goniaulax tamarensis*. J. Fish. Res. Board Can. **7**: 490–504.

Smith, G.F.M. 1944. The catchability of lobsters. J. Fish. Res. Board Can. **6**: 291–301.

White, H.C. 1942. Atlantic salmon redds and artificial spawning beds. J. Fish. Res. Board Can. **6**: 37–44.

1950–1959

Dickie, L.M. 1955. Fluctuations in abundance of the giant scallop, *Placopecten magellanicus* (Gmelin), in the Digby area of the Bay of Fundy. J. Fish. Res. Board Can. **12**: 797–857.

Dickie, L.M., and McCracken, F.D. 1955. Isopleth diagrams to predict equilibrium yields of a small flounder fishery. J. Fish. Res. Board Can. **12**: 187–209.

Lauzier, L. 1953. The St. Lawrence spring run-off and summer salinities in the Magdalen shallows. J. Fish. Res. Board Can. **10**: 146–147.

McCracken, F.D. 1958. On the biology and fishery of the Canadian Atlantic halibut, *Hippoglossus hippoglossus* L. J. Fish. Res. Board Can. **15**: 1269–1311.

McKenzie, R.A., and Smith, G.F.M. 1955. Atlantic cod populations along the southern Canadian mainland as shown by vertebral count studies. J. Fish. Res. Board Can. **12**: 698–705.

McLeese, D.W. 1956. Effects of temperature, salinity and oxygen on the survival of the American lobster. J. Fish. Res. Board Can. **13**: 247–272.

Medcof, J.C. 1955. Day and night characteristics of spatfall and of behaviour of oyster larvae. J. Fish. Res. Board Can. **12**: 270–286.

Paloheimo, J.E. 1958. A method of estimating natural and fishing mortalities. J. Fish. Res. Board Can. **15**: 749–758.

Smith, M.W. 1955. Fertilization and predator control to improve trout angling in natural lakes. J. Fish. Res. Board Can. **12**: 210–237.

Wilder, D.C. 1953. The growth rate of the American lobster (*Homarus americanus*). J. Fish. Res. Board Can. **10**: 371–412.

1960–1969

Aiken, D.E. 1969. Photoperiod, endocrinology and the crustacean molt cycle. Science (Washington, D.C.), **164**: 149–155.

Beamish, F.W.H. 1966. Vertical migration by demersal fish in the Northwest Atlantic. J. Fish. Res. Board Can. **23**: 109–139.

Bourne, N. 1965. A comparison of catches by 3- and 4-inch rings on offshore scallop drags. J. Fish. Res. Board Can. **22**: 313–333.

Elson, P.F. 1967. Effects on wild young salmon of spraying DDT over New Brunswick forests. J. Fish. Res. Board Can. **24**: 731–767.

Halliday, R.G., and Scott, W.B. 1969. Records of mesopelagic and other fishes from the Canadian Atlantic with notes on their distribution. J. Fish. Res. Board Can. **26**: 2691–2702.

Leim, A.H., and Scott, W.B. 1966. Fishes of the Atlantic coast of Canada. Bull. Fish. Res. Board Can. No. 155.

Paloheimo, J.E., and Dickie, L.M. 1966. Food and growth of fishes. III. Relations among food, body size, and growth efficiency. J. Fish. Res. Board Can. **23**: 1209–1248.

Powles, P.M. 1965. Life history and ecology of American plaice (*Hippoglossoides platessoides* F.) in the Magdalen shallows. J. Fish. Res. Board Can. **22**: 565–598.

Scarratt, D.J. 1968. An artificial reef for lobsters (*Homarus americanus*). J. Fish. Res. Board Can. **25**: 2683–2690.

Tibbo, S.N., and Lauzier, L.M. 1969. Larval swordfish (*Xiphias gladius*) from three localities in the western Atlantic. J. Fish. Res. Board Can. **26**: 3248–3251.

1970–1979

Caddy, J.F. 1975. Spatial model for an exploited shellfish population, and its application to the Georges Bank scallop fishery. J. Fish. Res. Board Can. **32**: 1305–1328.

Carrothers, P.J.G., and Foulkes, T.J. 1973. Measured towing characteristics of Canadian east coast otter trawls. Int. Comm. Northwest Atl. Fish. Res. Bull. **9**: 11–19.

Doubleday, W.G. 1975. Harvesting in matrix population models. Biometrics, **31**: 189–200.

Hutzinger, O., Jamieson, W.D., and Zitko, V. 1970. Identification of polychlorinated biphenyls and DDT in mixtures by mass spectrometry. Nature (Lond.), **226**: 664.

Lett, P.F., Kohler, A.C., and Fitzgerald, D.N. 1975. Role of stock biomass and temperature in recruitment of southern Gulf of St.

© 1999 NRC Canada

Lawrence Atlantic cod, *Gadus morhua*. J. Fish. Res. Board Can. **32**: 1613–1627.

Paloheimo, J.E., and Elson, P.F. 1974. Reduction of Atlantic salmon (*Salmo salar*) catches in Canada attributed to the Greenland fishery. J. Fish. Res. Board Can. **31**: 1467–1480.

Scott, J.S. 1975. Geographic variation in incidence of trematode parasites of American plaice (*Hippoglossoides platessoides*) of the Northwest Atlantic. J. Fish. Res. Board Can. **32**: 547–550.

Sutterlin, A.M., and Gray, R. 1973. Chemical basis for homing of Atlantic salmon (*Salmo salar*) to a hatchery. J. Fish. Res. Board Can. **30**: 985–989.

Tyler, A.V., and Dunn, R.S. 1976. Ration, growth and measures of somatic and organic condition in relation to meal frequency in winter flounder, *Pseudopleuronectes americanus*, with hypotheses regarding population homeostasis. J. Fish. Res. Board Can. **33**: 63–75.

Wildish, D.J., and Kristmanson, D.D. 1979. Tidal energy and sublittoral macrobenthic animals in estuaries. J. Fish. Res. Board Can. **36**: 1197–1206.

1980–1989

Aiken, D.E., and Waddy, S.L. 1989. Interaction of temperature and photoperiod in the regulation of spawning by American lobsters *Homarus americanus*. Can. J. Fish. Aquat. Sci. **46**: 145–148.

Campbell, A. 1985. Application of a yield and egg-per-recruit model to the lobster fishery in the Bay of Fundy. N. Am. J. Fish. Manage. **5**: 91–104.

Gavaris, S. 1988. An adaptive framework for the estimation of population size. Can. Atl. Fish. Sci. Advisory Comm. Res. Doc. 88/29.

Iles, T.D., and Sinclair, M. 1982. Atlantic herring: stock discreteness and abundance. Science (Washington, D.C.), **215**: 627–633.

Lacroix, G.L. 1985. Survival of eggs and alevins of Atlantic salmon (*Salmo salar*) in relation to the chemistry of interstitial water in redds in some acidic streams of Atlantic Canada. Can. J. Fish. Aquat. Sci. **42**: 292–299.

Lawton, P. 1987. Diel activity and foraging behavior of juvenile American lobsters, *Homarus americanus*. Can. J. Fish. Aquat. Sci. **44**: 1195–1205.

Melvin, G.D., Dadswell, M.J., and Martin, J.D. 1986. Fidelity of the American shad, *Alosa sapidissima* (Cluepeidae), to its river of previous spawning. Can. J. Fish. Aquat. Sci. **43**: 640–646.

Saunders, R.L., Henderson, E.B., and Harmon, P.R. 1985. Effects of photoperiod on juvenile growth and smolting of Atlantic salmon and subsequent survival and growth in sea cages. Aquaculture, **45**: 55–66.

Waiwood, K.G., and Buzeta, M.-I. 1989. Reproductive biology of southwest Scotian Shelf haddock (*Melanogrammus aeglefinus*). Can. J. Fish. Aquat. Sci. **46**(Suppl. 1): 153–170.

Zitko, V. 1988. Multivariate classification of chlorobiphenyls according to enzyme induction. Chemosphere, **17**: 1111–1116.

1990–1999

Chambers, R.C., and Trippel, E.A (*Editors*). 1997. Early life history and recruitment in fish populations. Chapman and Hall, New York.

Haya, K., Martin, J.L., Burridge, L.E., Waiwood, B.A., and Wildish, D.J. 1991. Domoic acid in shellfish and plankton from the Bay of Fundy, New Brunswick, Canada. J. Shellfish Res. **10**: 113–118.

Hunt, J.J. 1996. Rates of sexual maturation of Atlantic cod in NAFO Division 5Ze and commercial fishery implications. J. Northwest Atl. Fish. Sci. **18**: 61–75.

Lough, R.G., Smith, W.G., Werner, F.E., Loder, J.W., Page, F.H., Hannah, C.G., Naimie, C.E., Perry, R.I., Sinclair, M., and Lynch, D.R. 1994. Influence of wind-driven advection on interannual variability in cod egg and larval distributions on Georges Bank: 1982 vs 1985. ICES Mar. Sci. Symp. **198**: 356–378.

Neilson, J.D., and Perry, R.I. 1990. Diel vertical migrations of marine fishes: an obligate or facultative process? Adv. Mar. Biol. **26**: 115–168.

Parsons, G.J., Robinson, S.M.C., Chandler, R.A., Davidson, L.A., Lanteigne, M., and Dadswell, M.J. 1992. Intra-annual and long-term patterns in the reproductive cycle of giant scallops *Placopecten magellanicus* (Bivalvia: Pectinidae) from Passamaquoddy Bay, New Brunswick, Canada. Mar. Ecol. Prog. Ser. **80**: 203–214.

Peterson, R.H., Martin-Robichaud, D.J., and Berge, Å. 1996. Influence of temperature and salinity on length and yolk utilization of striped bass larvae. Aquacult. Int. **4**: 89–103.

Porter, J.M., Stokesbury, M.J.W., Dickson, C.A., and Hogan,W.E. 1994. A mark–recapture experiment on bluefin tuna (*Thunnus thynnus* L.) from the Browns – Georges Bank region of the Canadian Atlantic: 1993 update. Int. Comm. Conserv. Atl. Tunas Coll. Vol. Sci. Pap. **42**: 150–153.

Stephenson, R.L., and Lane, D.E. 1995. Fisheries management science: a plea for conceptual change. Can. J. Fish. Aquat. Sci. **52**: 2051–2056.

Wildish, D., and Kristmanson, D. 1997. Benthic suspension feeders and flow. Cambridge University Press, Cambridge, U.K.

© 1999 NRC Canada

Canadian Journal of Fisheries and Aquatic Sciences

Author Index
Volume 56, 1999

Journal canadien des sciences halieutiques et aquatiques

Index des auteurs
Volume 56, 1999

Able, K.W., 222
Ackerman, J.D., 1551
Aiken, D.E., 2324
Alexander, R., 2087
Allen, A.P., 739, 2029
Allen, Y.C., 748
Allin, C.J., 670
Alsop, D.H., 2112
Amiard, J.-C., 1757
Aminot, A., 1801
Andrews, A.H., 1329, 1339
Angeli, N., 1437
Antrim, L.D., 711
Armstrong, D.E., 60
Arnott, S.E., 162
Ashley, K.I., 1011
Aubin-Horth, N., 1122
Auger, P., 994
Ault, J.S., S-4
Avendaño, 2444
Babcock, R., 1668
Balch, T., 2300
Baldwin, C.M., S-128
Balvay, G., 1437
Bannister, R.C.A., 1904
Barrowman, N.J., 2404
Bartels, A.D., 2282
Baxter, C.V., 915
Beacham, T.D., 297
Beamer, E.M., 377
Beamish, F.W.H., 1752
Beamish, R.J., 506, 516, 2062, 2340
Beauchamp, D.A., 1293, S-128
Béland, F., 1058
Belzile, C., 2120
Benoît, H.P., 785
Berejikian, B.A., 830
Bergman, H.L., 1471
Beyers, D.W., 814, 823
Bienert, R.W., 711
Bills, P.J., 925
Birtwell, I.K., 2087
Bishop, K., 1461
Bishop, T.D., 97
Black, K.P., 2271
Boisclair, D., 1122
Bonfil, R., 601
Booth, R.K., 2172
Borgmann, U., 1494
Bosley, K.L., 2181
Boulding, E.G., 2248
Bourne, N.F., 1978
Bourque, M.-C., 839
Boutillier, J.A., 1978
Bouvet, Y., 1659
Bowen, K.G., 2404
Bowen, W.D., 2224
Brand, D., 2087
Brandt, S.B., S-1
Brännäs, E., 1068
Brickman, D., 2350
Brill, R.W., 173
Brind'Amour, A., 2240
Brinkhurst, R.O., 739, 2029
Brodeur, J.C., 184
Brodeur, R., S-188
Brohon, B., 1659
Browman, H.I., 1058
Brown, E.D., 419
Brown, R., 1898
Buckel, J.A., 275
Bue, B.G., 888
Bult, T.P., 1298, S-180
Burgherr, P., 1452
Burnison, B.K., 407
Burton, E.J., 1329
Byström, P., 1285
Cacela, D., 1471
Cailliet, G.M., 1329, 1339
Campana, S.E., 1873
Campbell, D.H., 1856
Campbell, H.F., 1266
Campbell, P.G.C., 774
Caouette, J.P., 1600
Carey, J.B., 1649
Carignan, R., 339
Carolsfeld, J., 13
Carpenter, S.R., 53
Carrillo, P., 1809, 2227
Castonguay, M., 1818
Chafiq, M., 487
Chaloner, D.T., 1600
Chang, C.C.Y., 1856
Chanut, J.-P., 1631, 2120
Chapleau, F., 427, 2240
Charles, D.F., 131
Charles, S., 994
Charlton, M.N., 1351
Chase, B.C., 173
Chen, D.G., 2385
Chen, Y., 1525
Chételat, J., 560
Chouinard, G.A., 1873
Chow-Fraser, P., 1781
Ciereszko, A., 178
Claret, C., 487
Clark, W.G., 242, 1721
Clements, W.H., 814, 823
Coale, K.H., 1329, 1339
Cole, W.G., 496
Collins, G.B., 131
Comeau, M., 1088
Conan, G.Y., 1088
Conover, D.O., 275
Conway, J.D., 113
Cooney, R.T., 364
Corten, A., 2051
Couillard, Y., 774
Crosbie, B., 1781
Cuddington, K., 1964
Culp, J.M., 1624
Cummins, P.F., 839
Cunjak, R.A., 1649
Currie, D.J., 427
Currie, D.R., 539
Curtis, L.R., 642
Dabrowski, K., 178
Dagorn, L., 984
DeCicco, A.L., 1504
Deflandre, B., 2136
Demer, D., S-188
Demers, S., 2120

Note: Page numbers preceded by the letter "S" are articles published in the supplement.

Nota : Les numéros de pages précédés de la lettre «S». désignent les articles publiés dans le supplément.

de Mora, S.J., 1631
Dempson, J.B., 1649
De Robertis, A., 2000
Desrosiers, G., 2136
Devlin, R.H., 2340
Díaz, G.A., S-4
Dilworth-Christie, P., 427
Dixit, A.S., 1109
Dixit, S.S., 131, 739, 2029
Dixon, D.G., 1213, 1226, 2211
Dobson, E.P., 1213
Docker, M.F., 2340
Doucett, R.R., 2172
Downing, A., 679
Doyon, C., 1428
Drum, A.S., 711
Durand, J.D., 1659
Duston, J., 201
Dutil, J.-D., 1818
Dutilleul, P., 1437
Edwards, C., 661
Eisenmann, H., 1452
Eisenreich, S.J., 650
Elston, R.A., 711
Emmons, E.E., 661
Eriksson, T., 1068
Essington, T.E., S-52
Evans, R.D., 1981
Eveson, J.P., 1317
Fabrizio, M.C., 1409
Fahay, M.P., 222
Fahnenstiel, G.L., 1711
Felt, L., 1949
Ferguson, M.M., 2229, 2315
Fink, R., 2087
Finstad, B., 184
Fischer, J., 1949
Fisher Wold, A.K., 767
Fletcher, G.L., 1991
Fletcher, W.J., 907
Folkvord, A., 2099
Forney, J.L., 2148
Fortin, R., 1428
Foster, E.P., 642
Fournier, D.A., 925, 1525
Fowler, G.M., 1732
Fox, D.D., 590
Fox, M.G., 1362
Frank, K.T., 347, 356, 2350
Franks, P.J.S., 25
Fréchet, A., 1873
Frédou, T., 2069
Fréon, P., 6, 984
Frost, T.M., 162
Fry, B., 590, 2167
Fu, P., 1198
Fukushima, T., 1929
Fulton, E.A., 1096
Furgal, J.A., 1351
Gaertner, D., 394
Gaggiotti, O.E., 1376
Gagné, J.-P., 2136
Gal, G., 311
Gallagher, M., 1590
Gallagher, S.P., 570
Gangemi, J.T., 915
Gao, Y.W., 2062
Garcia, E., 339
Gard, M.F., 570
Gascon, D., 1818
Gerdeaux, D., 1437
Gerlotto, F., 6
Giannico, G.R., 2362
Gibert, J., 487
Gibson, R.J., 1298
Gilbert, D., 1818
Gilkinson, K., 1707
Gillis, D.M., 288
Gingras, N.J., 1122
Giske, J., S-26
Gíslason, D., 2229
Gislason, H., 629
Goddard, S.V., 1991
Goldman, C.R., 2331
González, M.J., 679
Gordon, D.C., 1707
Gorokhova, E., 2203
Gosselin, M., 1631, 2120
Gotceitas, V., S-180
Gould, W.R., 1234
Grahl-Nielsen, O., 2219
Gratton, M., 2120
Gratton, Y., 1832, 2420
Greenberg, B.M., 1351
Gregory, R.S., S-180
Gregory, T.R., 479
Grigorovich, I.A., 1
Gross, M.R., 1198
Guay, C., 1437
Gubala, C.P., S-128
Gudex, L.I., 1504
Guillard, J., 1437
Guinand, B., 1659
Guruge, W.A.H.P., 1241
Gutreuter, S., 2282
Guyette, R.P., 496
Haase, R., 1631
Haedrich, R.L., 1298, 1949
Haldorson, L.J., 1133
Hall, R.I., 1109
Hamilton, P.B., 560
Hampton, J., 925
Hand, A.J., 1266
Hanes, D., 419
Hansen, J.A., 1471
Hanson, J.M., 1873
Hansson, L.-A., 70
Hansson, S., 629, 2203
Hara, T.J., 13
Hard, J.J., 578
Hare, L., 1143
Hare, S.R., 242
Harley, S.J., 1278
Harris, L.R., 2463
Harrison, P.J., 2477
Harvey, B.C., 2161
Hatch, L.K., 2331
Hauer, F.R., 915
Haure, J., 1757
Havens, K.E., 590
Head, E.J.H., 2463
Healey, B.P., 1521
Healey, M.C., 2362
Heard, W.R., 578
Hearn, W.S., 1255
Hebert, C.E., 323
Hecky, R.E., 2193
Heggenes, J., 1298
Hennigar, A.W., 2300
Henry, C.J., 814
Herlihy, A.T., 739, 2029
Hershey, A.E., 767
Hesslein, R.H., 2193, 2211
Hewitt, R., S-188
Hilborn, R., 888
Hildén, M., 629
Hinch, S.G., 862, 1696
Hines, J.E., 1409
Hinton, D.E., 419
Hiriart, V., 1351
Hirvonen, H., 1891
Hobson, K.A., 323
Holland, D.S., 253
Holmes, R.M., 1801
Holomuzki, J.R., 2041
Holst, J.C., S-26
Hooker, B.A., 1801
Hopkins, G.J., 153
Horn, J.K., S-170
Houlihan, D.F., 231, 2019
Hovgård, H., 1307
Howey, P.W., 173
Hoyle, J.A., 1
Hrabik, T.R., 1534, S-35
Hruška, J., 1461
Hsieh, W.W., 2450
Hudson, J.J., 1679
Hudson, J.P., 1600
Hughes, N.F., 2292
Hughes, R.M., 131, 739, 2029
Humston, R., S-4
Hunt, G., S-188
Hurley, J.P., 60
Huse, G., S-26
Hutchings, J.A., 97, 1612, 1949
Huusko, A., 1420
Hyer, K., 364
Imai, A., 1929
Ings, D.W., S-180
Irons, K., 2282

Irvine, J.R., 1512
Ivanov, V.V., 516
Iverson, S.J., 2224
Jaffe, J.S., 2000
Jansson, H., 1766
Jennings, M.J., 661
Jeremiason, J.D., 650
Johannsson, O., 2211
Johnson, B.M., S-140
Johnston, N.T., 1011
Johnstone, R., 2019
Jolicoeur, P., 774
Jones, J.R., 124
Jørgensen, E.H., 1370
Jude, D.J., 1711
Kaan, J., 2262
Kallio-Nyberg, I., 853
Kanno, Y., 1585
Kao, M.H., 1991
Kaufmann, P.R., 739, 2029
Kault, D., 1096
Keesing, J., 1668
Kendall, C., 1856
Kérouel, R., 1801
Kerr, S.R., 1707
Kershner, M.W., 527
Khandwala, S.B., 2041
Kidd, K.A., 2193
King, J.R., 847
Kinnison, M.T., 1172
Kirkley, J., 2011
Kitamura, S., 13
Kitchell, J.F., S-52
Kline Jr., T.C., S-94
Klyashtorin, L., 516
Knapp, R.A., 1576
Knight, R.L., 527
Knudsen, C.M., 830
Köhler, S., 1461
Koljonen, M.-L., 1766
Kolok, A.S., 700
Koskiniemi, J., 1766
Kratz, T.K., 265
Kroglund, F., 2078
Kuikka, S., 629
Kulka, D.W., S-118
Kurashov, V., 516
Lake, R.G., 862
Lalonde, J.D., 2240
Lamon III, E.C., 53, S-71
Landry, F., 1916
Langness, O.P., 1031
Langston, J., 1856
Lapointe, M.F., 1046
Laroche, J., 1659
Larsen, D.P., 739, 2029
Lassen, H., 1307
Laurila, A., 1891
Lavoie, D., 1182
Leavitt, P.R., 1109, 1964
LeBlond, P.H., 839
LeBreton, G.T.O., 1752
Lee, P.A., 1631
Legendre, P., 1437
Leggett, M.F., 2211
Leising, A.W., 25
Leonard, J.B.K., 1159
Levine, S.N., 451
Lewis, D.B., 1687
Lin, F., 178
Lipton, J., 1471
Liu, L., 178
Loew, E.R., 311
Logerwell, E., S-188
Lohman, K., 124
Lowell, R.B., 1624
Luecke, C., S-162
Lundstrom, C., 1329
Lundvall, D., 1285
Luo, J., S-4
Lutcavage, M.E., 173
MacIsaac, H.J., 1
Mackas, D.L., 2477
MacKinnon, M.D., 1213, 1226
Mackinson, S., 686
MacRae, R.K., 1484
Madsen, N., 1307
Maest, A.S., 1484
Magnuson, J.J., 162, 1534, 1687, S-35
Mäki-Petäys, A., 1420
Mallet, J.P., 994
Mapstone, B., 1096
Maravelias, C.D., 437
Marcano, J., 394
Marchand, C., 1832
Markager, S., 388
Marr, J.C.A., 1471
Marschall, E.A., 527
Marshall, C.T., 347, 356
Marteinsdottir, G., 1882
Marty, G.D., 419
Marwood, C.A., 1351
Mason, D.M., S-1
Mather, M.E., 87
Matsuishi, T., 1585
Matsushige, K., 1929
Mayer, C.M., 2148
McAllister, C.D., 2087
McArdle, B.H.2, 1278
McCarthy, I.D., 231
McCormick, S.D., 1159, 1649
McFarlane, G.A., 506, 516
McGregor-Shaw, C.R., 97
McKinley, R.S., 184, 2172
McKown, K.A., 275
McLaren, I.A., 2444
McLay, H.A., 2019
Metcalfe, C.D., 1389
Metcalfe, N.B., 2397
Methven, D.A., S-180
Meyer, E.I., 1452
Meyer, J.S., 1471, 1484
Meyer, R., 37, 1078
Michener, R.H., 2186
Millar, R.B., 37, 1078, 1278
Millard, E.S., 2211
Miller, R.J., 897
Mills, E.L., 2148
Mitchell, M.J., 2186
Mohammadian, A.M., 311
Moksness, E., 231
Montgomery, D.R., 377
Morales-Baquero, R., 1809, 2227
Morin, A., 560, 1639, 1938
Morita, K., 1585
Morrison, H.A., 1389
Morrison, K.A., 760
Moser, E.B., 191
Mostajir, B., 2120
Moth-Poulsen, T., 1307
Mucci, A., 2136
Muir, D.C.G., 2193
Mumford, P.L., 590
Munehara, H., 1849
Muotka, T., 1420
Myers, R.A., 2404
Naish, K-A, 2248
Nakamoto, R.J., 2161
Napp, J., S-188
Narimatsu, Y., 1849
Nash, C.H., 1696
Neff, B.D., 1198
Neis, B., 1949
Newlands, N., 686
Nibbelink, N.P., S-43
Nicholls, K.H., 153
Nichols, J.D., 1409
Niimi, A.J., 1389
Nishimura, K., 1585
Noakes, D.J., 516
Nolan, C.P., 1590
Nolan, D.T., 947
Northcote, T., 1981
Norwood, W.P., 1494
Noto, M., 973
Nøttestad, L., S-26
Nowicki, J.L., 1329
Nozais, C., 2136
Nyhammer, G., 2099
O'Connor, R.J., 739, 2029
O'Dea, M.F., 1649
Ohman, M.D., 2000
Okihiro, M.S., 419
Oliveira, K., 795
Omair, M., 1711
Ostrovsky, I., 1001
Otterlei, E., 2099
Outridge, P.M., 105
Owen, J.S., 2186
Paaver, T., 1766

Pagavino, M., 394
Palacz, Z., 1329
Panov, V.E., 1
Paradis, A.R., 1562
Parent, S., 1639, 1938
Parkinson, E.A., 1916
Parma, A.M., 242
Parrish, D.L., 79, 87, 1543
Parry, G.D., 539, 2271
Paterson, M.J., 650, 2193
Patterson, K.R., 208
Paulsen, S.G., 131, 739, 2029
Pavlov, D.A., 231
Pazzia, I., 2235
Pearson, W.H., 711
Pelletier, É., 2120, 2136
Peltonen, H., 853
Pepin, M., 1562
Pepin, P., 785, 1562
Perrein-Ettajani, H., 1757
Perry, R.I., 2477
Persat, H., 994
Persson, A., 70
Persson, L., 1285
Pess, G., 377
Pet, J.S., 1241
Peterman, R.M., 1046, 1716
Peterson, B.J., 1801
Petrie, B., 2350, 2463
Petrosky, C.E., 1031
Peuhkuri, N., 1891
Phillips, R.B., 1504
Pick, F.R., 560
Piet, G.J., 1241
Piironen, J., 1891
Pillsbury, R.W., 2041
Pinel-Alloul, B., 1437
Planas, D., 1792
Planque, B., 2069
Playle, R.C., 407
Plourde, S., 2420
Poister, D., 60
Polacheck, T., 1255
Pollock, K.H., 1234, 1255
Poole, G.C., 915
Post, D.M., 1534
Post, J.R., 1916
Power, G., 2172
Power, J.H., 191
Power, M.V., 1213, 1226
Prajneshu, X., 1026
Preisler, H.K., 1576
Pyper, B.J., 1046, 1716
Quinlan, R., 1109
Quinn II, T.J., 1133
Quinn, T.P., 377, 1172
Rahel, F.J., S-43
Rakitin, A., 2315
Ramcharan, C.W., 748
Ranta, E., 1891
Rasmussen, J.B., 875, 2235
Reche, I., 1809, 2227
Reckhow, K.H., 1150
Reid, S.M., 1362
Reilly, P., 947
Reinhardt, U., 1206
Reiss, C.S., 2444
Renaud, C., 1757
Reuter, J.E., 2331
Rice, J.A., 814, 823
Richards, J.G., 407
Richardson, J.S., 1696
Ridgway, L.L., 2240
Riera, J.L., 265
Riessen, H.P., 2487
Riggs, M., 1856
Riis, T., 388
Riley, S.C., 1298
Rita, H., 853
Robichaud, G., 1088
Robinson, C.L,K., 2433
Rocha-Olivares, A., 803
Rodriguez, C.A., 1058
Rooper, C.N., 1133
Roper, B.B., 939
Rose, G.A., S-118
Rose, K.A., 2148,
Rosenau, M., 1981
Routledge, R.D., 1512
Rowan, D., 2235
Roy, I., 1143
Roy, S., 2120
Rudstam, L.G., 311, 2148
Runge, J.A., 2420
Rutherford, E.S., 2148
Ryding, K.E., 2374
Sánchez-Castillo, P., 1809, 2227
Sanderson, B.L., 1534
Sandheinrich, M.B., 2282
Sand-Jensen, K., 388
Saunders, R.L., 201
Scarnecchia, D.L., 939
Schael, D.M., 527
Schaller, H.A., 1031
Scheibling, R.E., 2300
Schindler, D.E., S-61
Schindler, D.W., 451, 1401, 1679
Schindler, J.E., 265
Schneider, D.C., 1949, S-170, S-180
Schneidervin, R.W., S-162
Schram, S.T., 1409
Schroder, S.L., 830
Schwarz, C.J., 551
Scott, B., 1882
Secor, D.H., S-86
Seppä, T., 1891
Serafy, J.E., S-4
Servos, M.R., 2211
Severin, K.P., 1898
Shackell, N.L., 2350
Sharr, S., 888
Sheaves, M., 1096
Sheehy, M.R.J., 1904
Shelton, P.A., 1521
Shelton, P.M.J., 1904
Shore, J., 2350
Shuter, B.J., 847
Shutt, J.L., 323
Sibert, J.R., 925
Silva, S.R., 1856
Simard, Y., 1182, 1832
Skalski, J.R., 2374
Skomal, G.B., 173
Skúlason, S., 2229
Smith, B.D., 960
Smith, P.E., S-170
Smith, R.E.H., 1351
Smith, R.J.F., 830
Smith, S.G., S-4
Smith, S.J., 2224
Smith, V.H., 2262
Smol, J.P., 131, 1109
Snorrason, S., 2229
Soria, M., 6
Sparholt, H., 629
Spear, P.A., 1428
Squires, D., 2011
Stamford, M.D., 1011
Standke, S.J., 153
Starr, M., 1088
Staurnes, M., 2078
Stead, S.M., 2019
Stefanski, L.A., 1234
Stefansson, S.O., 2099
Stein, R.A., 527
Steinberg, N.D., 275
Steinhart, G.B., S-152
Steinman, A.D., 590
Stemberger, R.S., 739, 2029
Stevens, J.D., 868
Stewart, A.R., 467
Stewart, R.E.A., 105
Stobo, W.T., 551, 1732
Stockwell, J.D., S-140
Stow, C.A., 53, S-71
St-Pierre, J.F., 1058
Strong, M.B., 113
Sullivan, P.J., 242
Sumner, N.R., 907
Sutinen, J.G., 253
Svanbäck, R., 1285
Swanson, B.L., 1409
Swartzman, G., S-188
Sylvestre, M., 1792
Takashima, Y., 1585
Tam, F., 590
Terhune, J.M., 113
Tezak, E.P., 830
Therriault, J.-C., 1088
Thibault, D., 2120

Thompson, B.A., 748
Thompson, P.A., 2477
Thomson, R.E., 506
Tita, G., 2136
Trippel, E.A., 113, 2315, 2495
Trumble, R.J., 242
Tsumura, K., 1011
Tucker, S., 875, 2235
Unwin, M.J., 1172
Valdimarsson, S.K., 2397
van den Heuvel, M.R., 1213, 1226
van Densen, W.L.T., 1241
Vanderploeg, H.A., 1711
Vanier, C., 1792
Van Meer, T., 1213
Varis, O., 629
Vasconcellos, M., 686
Vasin, O., 1766
Veinott, G., 1981
Venugopalan, R., 1026
Vetter, R.D., 803, 1376
Vijverberg, J., 1241
Vincent, W.F., 388
Vogel, J.L., 1293, S-128
Waddy, S.L., 2324
Wahlström, E., 1865
Wainright, S.C., 2181
Wallace, R.G., 1752
Walsh, D., S-188
Walters, C.J., 601, 1046
Wang, D., 774
Wang, J.D., S-4
Ware, D.M., 2385, 2433
Warren, G.L., 590
Watras, C.J., 760
Welch, D.W., 1317
Wendelaar Bonga, S.E., 947
Wengert, M.W., S-162
Weseloh, D.V.C., 323
West, G., 868
Westman, E., 1865
Westrich, K.M., 1504
Whalen, K.G., 79, 87, 1543
Whillans, T.H., 1362
White, J.L., 2161
Whitelaw, W., 1255
Whittier, T.R., 739, 2029
Whittle, D.M., 1389
Wickins, J.F., 1904
Wileman, D., 1307
Wilhelm, F.M., 1401, 1679
Willette, T.M., 364
Wilson, A.B., 2248
Wilson, R.W., 670
Wipfli, M.S., 1600
Witting, D.A., 222
Wolkers, J., 1370
Wood, C.C., 297
Wood, C.M., 479, 2112
Wright, P., 1882
Wu, J.Q., 2450
Wurtsbaugh, W.A., S-152
Xiao, Y., 868
Yacobi, Y.Z., 1001
Yamamoto, T.S., 1585
Yan, N.D., 1, 162
Yasuda, I., 973
Yelland, D.R., 2477
Young, K.A., 1700
Youson, J.H., 2340
Ytrestøyl, T., 184
Zakardjian, B.A., 2420
Zimmerman, A.P., 847
Zlokovitz, E.R., S-86

The index and/or table of contents has been removed and photographed separately within this volume year.

For roll film users, this information for the current volume year is at the beginning of the microfilm. For a prior year volume, this information is at the end of the microfilm.

For microfiche users, the index and/or contents is contained on a separate fiche.

ASSIGNMENT OF COPYRIGHT

Ms. No. _____

To: NATIONAL RESEARCH COUNCIL OF CANADA ("NRC") Research Press

From: _____

_____

_____

_____

(name and address of author signing this form)

This refers to the manuscript entitled: _____

_____

written by myself and the following additional author(s): _____

_____

for publication in: _____

1. I declare that the list of authors fairly conforms to academic conventions about who should be listed. I declare that the manuscript, or its equivalent, has not been submitted for publication elsewhere. If it is accepted for publication by the National Research Council of Canada, I will ensure that it, or its equivalent, is not submitted for publication elsewhere.

2. I declare that I am (check ONE):

☐ (a) the sole owner of the copyright relating to the manuscript,	and →	I **assign** to NRC the entire copyright.
☐ (b) a part owner of the copyright, in conjunction with interests held by co-authors or their employers,	and →	I **assign** to NRC my entire interest in the copyright, and I expect the co-authors to also sign a form like this one.
☐ (c) an agent of my employer with authority to assign the copyright owned by the employer, who is: _____,	and →	I **assign** to NRC, on behalf of my employer, my employer's entire interest in the copyright relating to the manuscript, and I expect the co-authors to also sign a form like this one.
☐ (d) a public servant in Canada (federal, provincial or territorial) or the United Kingdom, so that the copyright is owned by Her Majesty,	and →	I have obtained the approval of my employer, according to the terms of my employment, to grant NRC **non-exclusive permission** to publish the manuscript and administer the copyright.
☐ (e) a public servant of the United States of America, and subject to the law that creates no U.S. copyright for the manuscript,	and →	I **assign** to NRC, on behalf of my employer, my employer's entire interest in any copyright that may exist outside the U.S., and I expect the co-authors to sign a form like this one.

3. I understand that my submission of this document does not guarantee publication, and that publication will not occur until **all authors** have provided a copyright transfer. If the manuscript is not published within 2 years after I sign this, the assignment is revoked.

Signed at _____ on _____

(City and Province/State) (Date)

_____

(Signature)

[Standard NRC form; alterations not acceptable.]

Comments on Copyright Transfer
(with extracts from the *Copyright Act*, Revised Statutes of Canada 1985, chapter C-42, as amended)

The publisher is not permitted to publish the manuscript without permission or an assignment of ownership of copyright. For greatest flexibility, and to be prepared to deal with future uses of the published material, the publisher requires ownership.

The owner may assign the right, but that assignment must be in writing:

13.(4) The owner of the copyright in any work may assign the right, either wholly or partially, and either generally or subject to territorial limitations, and either for the whole term of the copyright or for any other part thereof, and may grant any interest in the right by licence, but no assignment or grant is valid unless it is in writing signed by the owner of the right in respect of which the assignment or grant is made, or by his duly authorized agent.

The owner may be the author, but in many cases, the owner is the author's employer:

13.(3) Where the author of a work was in the employment of some other person under a contract of service or apprenticeship and the work was made in the course of his employment by that person, the person by whom the author was employed shall, in the absence of any agreement to the contrary, be the first owner of the copyright, but where the work is an article or other contribution to a newspaper, magazine or similar periodical, there shall, in the absence of any agreement to the contrary, be deemed to be reserved to the author a right to restrain the publication of the work, otherwise than as part of a newspaper, magazine or similar periodical.

The only exception to taking ownership arises when the manuscript is covered by Crown copyright owned by a Canadian government.

12. Without prejudice to any rights or privileges of the Crown, where any work is, or has been, prepared or published by or under the direction or control of Her Majesty or any government department, the copyright in the work shall, subject to any agreement with the author, belong to Her Majesty and in that case shall continue for the remainder of the calendar year of the first publication of the work and for a period of fifty years following the end of that calendar year.

Governments, and in particular the federal government, do not have a simple mechanism for assigning ownership of this particular type of Crown asset. Therefore, when an author is a public servant so that there is Crown copyright in the manuscript, a simple permission to use is acceptable to the publisher, if it is granted by a person with appropriate authority.

CESSION DU DROIT D'AUTEUR

Document n° _____

Au : CONSEIL NATIONAL DE RECHERCHES DU CANADA («CNRC») - Presses scientifiques

De : _____

_____

_____

_____

(nom et adresse de l'auteur qui signe le présent formulaire)

La présente cession porte sur le document intitulé : _____

_____

rédigé par moi, en collaboration avec l'auteur/les auteurs suivant(s) : _____

_____

aux fins de publication dans : _____

1. Je déclare que la liste des auteurs ci-dessus respecte les pratiques usuelles de rédaction savante quant aux personnes dont le nom doit être cité. Je déclare que le document ou son équivalent n'a pas été soumis à quelque autre organisme aux fins de publication. Si le CNRC accepte de publier le document, je m'assurerai que celui-ci ou son équivalent n'est soumis à aucun autre organisme aux fins de publication sans en obtenir la permission préalable du CNRC.

2. Je déclare être (UN SEUL choix) :

☐ (a) le seul titulaire de droit d'auteur afférent au document,	et →	je **cède** le droit d'auteur intégral au CNRC.
☐ (b) un titulaire partite du droit d'auteur, de concert avec des coauteurs ou leurs employeurs,	et →	je **cède** ma part du droit d'auteur au CNRC et m'attends à ce que les coauteurs signent une entente comparable.
☐ (c) un agent de mon employeur ayant l'autorité de céder le droit d'auteur appartenant à l'employeur, nommément : _____,	et →	je **cède** au CNRC, au nom de mon employeur, la part entière du droit d'auteur afférent au document appartenant à mon employeur, et m'attends à ce que les coauteurs signent une entente comparable.
☐ (d) un fonctionnaire du Canada (fédéral, provincial ou territorial) ou du Royaume-Uni, donc le droit d'auteur appartient à Sa Majesté,	et →	j'ai obtenu de mon employeur, en vertu de mes conditions d'emploi, l'autorisation d'accorder au CNRC la **permission non exclusive** de publier le document et de gérer le droit d'auteur.
☐ (e) un fonctionnaire des États-Unis d'Amérique, donc sujet à la loi qui n'associe aucun droit d'auteur américain au document,	et →	je **cède** au CNRC, au nom de mon employeur, la part entière de quelque droit d'auteur en vigueur ailleurs qu'aux É.-U. appartenant à mon employeur, et m'attends à ce que les coauteurs signent une entente comparable.

3. Je comprends que la soumission du document ne garantit aucunement sa publication et que la publication ne pourra être réalisée tant que **tous les auteurs** n'auront pas signé une cession du droit d'auteur. Si le document n'est pas publié dans les deux années suivant ma signature des présentes, la cession sera automatiquement révoquée.

Signé à _____, le _____

(ville et province/état) (date)

_____

(signature)

[Formulaire normalisé du CNRC; aucune modification permise.]

Commentaires sur la cession du droit d'auteur
(accompagnés d'extraits de la *Loi sur le droit d'auteur*, Lois révisées du Canada 1985, chapitre C-42 modifié)

L'éditeur ne peut publier un document sans la permission ou une cession du droit d'auteur. Pour des raisons de souplesse et en vue de l'utilisation future du document publié, l'éditeur doit devenir titulaire du droit d'auteur.

Le titulaire peut céder le droit, mais cette cession doit être faite par écrit :

13.(4) Le titulaire du droit d'auteur sur une oeuvre peut céder ce droit, en totalité ou en partie, d'une façon générale, ou avec des restrictions territoriales, pour la durée complète ou partielle de la protection; il peut également concéder, par une licence, un intérêt quelconque dans ce droit; mais la cession ou la concession n'est valable que si elle est rédigée par écrit et signée par le titulaire du droit qui en fait l'objet, ou par son agent dûment autorisé.

Le titulaire peut être l'auteur, mais dans plusieurs cas, le titulaire est l'employeur de l'auteur:

13.(3) Lorsque l'auteur est employé par une autre personne en vertu d'un contrat de louage de service ou d'apprentissage, et que l'oeuvre est exécutée dans l'exercice de cet emploi, l'employeur est, à moins de stipulation contraire, le premier titulaire du droit d'auteur; mais lorsque l'oeuvre est un article ou un autre contribution, à un journal, à une revue ou à un périodique du même genre, l'auteur, en l'absence de convention contraire, est réputé posséder le droit d'interdire la publication de cette oeuvre ailleurs que dans un journal, une revue ou un périodique semblable.

La seule exception dans la cession du droit d'auteur est lorsque le document est associé au droit d'auteur de la Couronne, qui appartient au gouvernement du Canada .

12. Sous réserve de tous les droits ou privilèges de la Couronne, le droit d'auteur sur les oeuvres préparées ou publiées par l'entremise, sous la direction ou la surveillance de Sa Majesté ou d'un ministère du gouvernement, appartient, sauf stipulation conclue avec l'auteur, à Sa Majesté et, dans ce cas, il subsiste jusqu'à la fin de la cinquantième année suivant celle de la première publication de l'oeuvre.

Les gouvernements, en particulier le gouvernement fédéral, ne disposent pas d'un mécanisme simple de cession de droit d'auteur pour ce genre de biens de la Couronne. C'est pourquoi lorsqu'un auteur est un fonctionnaire et que, par conséquent, le droit d'auteur appartient à la Couronne, une simple permission d'usage est suffisante pour l'éditeur, pour autant que celle-ci ait été octroyée par une personne jouissant de l'autorité nécessaire pour ce faire.

CALL FOR NOMINATIONS

HERZBERG MEMORIAL

Prize and Fellowship

Description

The Herzberg Memorial Prize and Fellowship is a prestigious distinction that was created in 1999 by the National Research Council of Canada (NRC), in commemoration of Gerhard Herzberg, the renowned NRC scientist and Nobel laureate. It provides the recipient with an opportunity to work for a period of time in an NRC institute.

Eligibility

The award is open to Canadian and foreign applicants. Nominees should be active researchers with an exceptional record of achievements in a field that is relevant to NRC's programs. They must also be committed to working for a period of up to one year, on a full-time basis, in an NRC institute.

Nominations

Candidates may apply on their own behalf. They can also be nominated by other persons. In both cases, candidates must provide a curriculum vitae and a statement containing the following information: an outline of their major scientific achievements; their interest in working in an NRC laboratory for a specific period of time; their availability; the nature of the research activities they would like to pursue at NRC; and their current research relationship, if any, with NRC.

Candidates applying on their own behalf should provide the names of at least three referees from whom NRC can solicit comments on a confidential basis. Nominations for the first competition must be received by 29 February 2000.

Value

The financial value of the Prize is $25,000. It will be paid as a lump sum to the successful candidate upon the signing of a fellowship agreement with NRC. That amount is taxable. The financial value of the Fellowship will be subject to negotiations with the selected candidate and, where appropriate, with the candidate's current employer. Other financial considerations such as relocation and travel expenses will also be negotiated on a case by case basis.

To submit an application or to ask for additional information, please contact:

Serge Hamel, Corporate Services
National Research Council,
Building M-58, Montreal Road
Ottawa, Ontario
Canada KIA OR6
Tel.: (613) 993-3656
Fax: (613) 991-0398

APPEL DE CANDIDATURES

Prix et Bourse HERZBERG

Description

Le Prix et la Bourse Herzberg ont été établis en 1999 par le Conseil national de recherches du Canada (CNRC) en mémoire de Gerhard Herzberg, chercheur émérite du CNRC et prix Nobel. Ils permettent au lauréat de venir effectuer un stage de travail dans un institut du CNRC.

Admissibilité

Les candidats peuvent être soit du Canada soit d'autres pays. Ils doivent avoir à leur actif des réalisations exceptionnelles dans un domaine de recherche pertinent aux programmes du CNRC. Ils doivent aussi s'engager à travailler à temps plein dans un institut du CNRC pour une période pouvant aller jusqu'à un an.

Candidatures

Les candidats peuvent soit soumettre eux-mêmes leur candidature soit être proposés par d'autres personnes. Dans les deux cas, ils doivent soumettre leur CV ainsi qu'un dossier de présentation renfermant les informations suivantes : un résumé de leurs principales réalisations scientifiques; une déclaration de leur intérêt à venir travailler dans un laboratoire du CNRC; leur disponibilité à cet égard; la nature des activités de recherche qu'ils aimeraient poursuivre au CNRC; et les liens de recherche actuels qu'ils peuvent avoir avec le CNRC.

Les candidats qui posent eux-mêmes leur candidature doivent fournir les noms d'au moins trois personnes auxquelles le CNRC pourra demander des références en toute confidentialité. Les candidatures doivent parvenir au CNRC avant le 29 février 2000.

Valeur

La valeur financière du Prix est de 25 000 $. Le Prix sera remis sous forme d'un montant forfaitaire au lauréat au moment de la signature de l'entente avec le CNRC pour son affectation à titre de boursier. Ce montant est imposable. Quant à la valeur financière de la Bourse, elle sera négociable selon les conditions dans lesquelles le boursier effectuera son stage au CNRC.

Pour soumettre des candidatures ou demander des renseignements supplémentaires, s'adresser à :

Serge Hamel, Services intégrés
Conseil national de recherches du Canada
Édifice M-58, chemin Montréal
Ottawa, Ontario
Canada KIA OR6
Tél. : (613) 993-3656
Téléc. : (613) 991-0398

NRC · CNRC

National Research Council Canada | Conseil national de recherches Canada

Canada

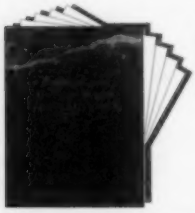

Perspectives on Canadian Marine Fisheries Management

L.S. Parsons and/et W.H. Lear
(*Editors/Directeurs scientifiques*)

446 pages
Hardcover/Édition reliée
November/Novembre1993
ISBN 0-660-15003-4
ISSN 0706-6503
NRC/CNRC 36176
$55.00/55,00 $

This volume, Canadian Bulletin of Fisheries and Aquatic Sciences 226, is a collection of 15 articles describing management approaches in different fisheries arising from the diversity and complexity of Canada's marine fisheries. Visit http://www.nrc.ca/cisti/journals/books/perspe_e.html at the NRC Research Press Web site to view the Table of Contents.

On décrit dans ce document, le Bulletin canadien des sciences halieutiques et aquatiques 226 (un recueil des 15 articles), des approches de gestion de diverses pêches axées sur la diversité et la complexité des pêches maritimes canadiennes. Visitez http://www.nrc.ca/cisti/journals/books/perspe_f.html au site Web des Press scientifiques du CNRC pour consulter la table des matières.

To order copies of this publication/Pour commander des exemplaires de ce livre

- Telephone: (613) 993-0151
- Fax: (613) 952-7656
- Mail orders: Monograph Orders, NRC Research Press, National Research Council Canada, Ottawa, Ontario K1A 0R6, Canada
- Internet e-mail: research.journals@nrc.ca
- World Wide Web: http://www.nrc.ca/cisti/journals/formmono.html

Canadian customers please add 7% GST. Orders from Quebec add a further 6.5% QST to the total price including GST. Make cheque or money order payable to "Receiver General for Canada, credit NRC". Note that for all orders outside Canada, rates are in U.S. Dollars. All sales are final.

- Téléphone : (613) 993-0151
- Télécopieur : (613) 952-7656
- Par la poste : Monographies, Presses scientifiques du CNRC, Conseil national de recherches Canada, Ottawa (Ontario) K1A 0R6, Canada
- Courrier électronique : research.journals@nrc.ca
- World Wide Web : http://www.nrc.ca/cisti/journals/formmofr.html

Les clients canadiens doivent ajouter la TPS de 7 %. Les clients du Québec doivent ajouter 6,5 % de TVQ au montant total, une fois la TPS additionnée. Libellez le chèque ou le mandat à l'ordre du «Receveur général du Canada, au crédit du CNRC». Pour les clients non canadiens, les prix sont en dollars américains. Aucun remboursement.

Please send me ____ copies of/Veuillez me faire parvenir ____ exemplaire(s) de *Perspectives on Canadian Marine Fisheries Management.*

NRC Research Press

Monograph Program

Presses scientifiques du CNRC

Programme de monographies

NRC·CNRC

PLEASE PRINT/LETTRES MOULÉES

☐ Payment enclosed/Paiement inclus ☐ Charge to/Imputer à ☐ Visa ☐ MasterCard

Account number/ N° de compte | | | | | | | | | | | | | | | | | | Expiry date/ Date d'expiration ____

Name/Nom

Signature/Signature

Address/Adresse

City/Ville Province/Province

Postal code/Code postal Country/Pays

Telephone/Téléphone Fax/Télécopieur

e-mail/Courrier électronique Date of order/Date de la commande

Guide to the Parasites of Fishes of Canada. Part IV. Trematoda

David I. Gibson

373 pages
Softcover/Édition brochée
March/mars 1996
ISBN 0-660-16403-5
ISSN 0706-6481
NRC/CNRC 40083
$42.95/42,95 $
Canadian Special Publication of Fisheries and Aquatic Sciences/ Publication spéciale canadienne des sciences halieutiques et aquatiques 124

More than 80 keys leading to the identification of more than 220 species of trematode parasites of Canadian fishes and diagnoses of more than 80 family–group taxa and 130 genera are given. Each genus is illustrated. For each species a Canadian host list, locality data, and any relevant remarks are included. Visit http://www.nrc.ca/cisti/journals/40083/133to136.html at the NRC Research Press Web to view a short chapter of this book.

On retrouve plus de 80 clefs qui permettent d'identifier quelque 220 espèces de trématodes parasites des poissons du Canada et la description de plus de 80 taxums de famille/groupe et de 130 genres. Chaque genre y est illustré. À chaque espèce sont associées des données sur l'emplacement et des remarques particulières. Visitez http://www.nrc.ca/cisti/journals/40083/f133to6.html au site Web des Presses scientifiques du CNRC pour afficher un court chapitre du livre.

To order copies of this publication/Pour commander des exemplaires de ce livre

- Telephone: (613) 993-0151
- Fax: (613) 952-7656
- Mail orders: Monograph Orders, NRC Research Press, National Research Council Canada, Ottawa, Ontario K1A 0R6, Canada
- Internet e-mail: research.journals@nrc.ca
- World Wide Web: http://www.nrc.ca/cisti/journals/formmono.html

Canadian customers please add 7% GST. Orders from Quebec add a further 6.5% QST to the total price including GST. Make cheque or money order payable to "Receiver General for Canada, credit NRC". Note that for all orders outside Canada, rates are in U.S. dollars. All sales are final.

- Téléphone : (613) 993-0151
- Télécopieur : (613) 952-7656
- Par la poste : Monographies, Presses scientifiques du CNRC, Conseil national de recherches Canada, Ottawa (Ontario) K1A 0R6, Canada
- Courrier électronique : research.journals@nrc.ca
- World Wide Web : http://www.nrc.ca/cisti/journals/formmofr.html

Les clients canadiens doivent ajouter la TPS de 7 %. Les clients du Québec doivent ajouter 6,5 % de TVQ au montant total, une fois la TPS additionnée. Libellez le chèque ou le mandat à l'ordre du «Receveur général du Canada, au crédit du CNRC». Pour les clients non canadiens, les prix sont en dollars américains. Aucun remboursement.

Please send me ____ copies of/Veuillez me faire parvenir ____ exemplaire(s) de *Guide to the Parasites of Fishes of Canada: Part IV. Trematoda.*

NRC Research Press

Monograph Program

Presses scientifiques du CNRC

Programme de monographies

NRC·CNRC

PLEASE PRINT/LETTRES MOULÉES

☐ Payment enclosed/Paiement inclus ☐ Charge to/Imputer à ☐ Visa ☐ MasterCard

Account no./ N° de compte | Expiry date/ Date d'expiration

Name/Nom

Signature/Signature

Address/Adresse

City/Ville | Province/Province

Postal code/Code postal | Country/Pays

Telephone/Téléphone | Fax/Télécopieur

e-mail/Courrier électronique | Date of order/Date de la commande

PERSPECTIVES

Howard P. Riessen 2487–2494 Predator-induced life history shifts in *Daphnia*: a synthesis of studies using meta-analysis

PERSPECTIVES

Edward A. Trippel 2495–2507 The first marine biological station in Canada: 100 years of scientific research at St. Andrews

Author Index for Volume 56 / Index des auteurs pour le volume 56 **AI-1**
Contents for Volume 56 / Sommaire pour le volume 56 **C-1**

© 1999 NRC Canada

S.L. Waddy and D.E. Aiken	**2324–2330**	Timing of the metamorphic molt of the American lobster (*Homarus americanus*) is governed by a population-based, photoperiodically entrained daily rhythm
Lorin K. Hatch, John E. Reuter, and Charles R. Goldman	**2331–2339**	Relative importance of stream-borne particulate and dissolved phosphorus fractions to Lake Tahoe phytoplankton
Margaret F. Docker, John H. Youson, Richard J. Beamish, and Robert H. Devlin	**2340–2349**	Phylogeny of the lamprey genus *Lampetra* inferred from mitochondrial cytochrome *b* and ND3 gene sequences
Nancy L. Shackell, Kenneth T. Frank, Brian Petrie, David Brickman, and Jennifer Shore	**2350–2361**	Dispersal of early life stage haddock (*Melanogrammus aeglefinus*) as inferred from the spatial distribution and variability in length-at-age of juveniles
Guillermo R. Giannico and Michael C. Healey	**2362–2373**	Ideal free distribution theory as a tool to examine juvenile coho salmon (*Oncorhynchus kisutch*) habitat choice under different conditions of food abundance and cover
Kristen E. Ryding and John R. Skalski	**2374–2384**	Multivariate regression relationships between ocean conditions and early marine survival of coho salmon (*Oncorhynchus kisutch*)
D.G. Chen and D.M. Ware	**2385–2396**	A neural network model for forecasting fish stock recruitment
Sveinn K. Valdimarsson and Neil B. Metcalfe	**2397–2403**	Effect of time of day, time of year, and life history strategy on time budgeting in juvenile Atlantic salmon, *Salmo salar*
Ransom A. Myers, Keith G. Bowen, and Nicholas J. Barrowman	**2404–2419**	Maximum reproductive rate of fish at low population sizes
GLOBEC CANADA		GLOBEC CANADA
Bruno A. Zakardjian, Jeffrey A. Runge, Stephane Plourde, and Yves Gratton	**2420–2432**	A biophysical model of the interaction between vertical migration of crustacean zooplankton and circulation in the Lower St. Lawrence Estuary
Clifford L.K. Robinson and Daniel M. Ware	**2433–2443**	Simulated and observed response of the southwest Vancouver Island pelagic ecosystem to oceanic conditions in the 1990s
C.S. Reiss, I.A. McLaren, and P.A. Avendaño	**2444–2449**	Utility of storage lipid volumes in inferring recent trophic history of copepods
Julia Qiuying Wu and William W. Hsieh	**2450–2462**	A modelling study of the 1976 climate regime shift in the North Pacific Ocean
Erica J.H. Head, Leslie R. Harris, and Brian Petrie	**2463–2476**	Distribution of *Calanus* spp. on and around the Nova Scotia Shelf in April: evidence for an offshore source of *Calanus finmarchicus* to the central and western regions
R. Ian Perry, Peter A. Thompson, David L. Mackas, Paul J. Harrison, and Douglas R. Yelland	**2477–2486**	Stable carbon isotopes as pelagic food web tracers in adjacent shelf and slope regions off British Columbia, Canada

Contents (continued) / Table des matières (suite)

National Research Council Canada
Ottawa, Canada K1A 0R6

Conseil national de recherches Canada
Ottawa, Canada K1A 0R6

Postage paid at Ottawa
Publications mail
Registration No. 1240579

Port payé à Ottawa
Poste-publication
Enregistrement n° 1240579

Canadian Journal of Fisheries and Aquatic Sciences

Volume 56, Number 12, December 1999

Journal canadien des sciences halieutiques et aquatiques

Volume 56, numéro 12, décembre 1999

RAPID COMMUNICATIONS

Davíð Gíslason, Moira M. Ferguson, Skúli Skúlason, and Sigurður S. Snorrason 2229–2234
Rapid and coupled phenotypic and genetic divergence in Icelandic Arctic char (*Salvelinus alpinus*)

Strahan Tucker, Ivano Pazzia, David Rowan, and Joseph B. Rasmussen 2235–2239
Detecting pan-Atlantic migration in salmon (*Salmo salar*) using ^{137}Cs

ARTICLES

Janick D. Lalonde, François Chapleau, Anik Brind'Amour et Lara Louise Ridgway 2240–2247
Les métaux (Mn, Cu, Cd, Zn et Hg) des meuniers noirs (*Catostomus commersoni*) et des grands brochets (*Esox lucius*) de l'amont et de l'aval du barrage Moses-Saunders sur le fleuve Saint-Laurent près de Cornwall (Ontario) et Massena (New York)

A.B. Wilson, K-A Naish, and E.G. Boulding 2248–2261
Multiple dispersal strategies of the invasive quagga mussel (*Dreissena bugensis*) as revealed by microsatellite analysis

Jacob Kann and Val H. Smith 2262–2270
Estimating the probability of exceeding elevated pH values critical to fish populations in a hypereutrophic lake

Kerry P. Black and Gregory D. Parry 2271–2281
Entrainment, dispersal, and settlement of scallop dredge sediment plumes: field measurements and numerical modelling

Steve Gutreuter, Andrew D. Bartels, Kevin Irons, and Mark B. Sandheinrich 2282–2291
Evaluation of the flood-pulse concept based on statistical models of growth of selected fishes of the Upper Mississippi River system

Nicholas F. Hughes 2292–2299
Population processes responsible for larger-fish-upstream distribution patterns of Arctic grayling (*Thymallus arcticus*) in interior Alaskan runoff rivers

Robert E. Scheibling, Allan W. Hennigar, and Toby Balch 2300–2314
Destructive grazing, epiphytism, and disease: the dynamics of sea urchin – kelp interactions in Nova Scotia

Ana Rakitin, Moira M. Ferguson, and Edward A. Trippel 2315–2323
Sperm competition and fertilization success in Atlantic cod (*Gadus morhua*): effect of sire size and condition factor on gamete quality

Continued on inside back cover / Suite au verso

Canada

Printed in Canada by / Imprimé au Canada par
University of Toronto Press Inc.
Typesetting by / Typographie par
NRC Research Press / Presses scientifiques du CNRC

0706-652X(199912)56:12;1-J